DYNAMIC STABILITY ASSESSMENT OF DAMAGED PASSENGER SHIPS USING A TIME SIMULATION APPROACH

by

OSMAN TURAN, BSc, MSc

A Thesis Submitted for the Degree of Doctor of Philosophy

Department of Ship and Marine Technology
Faculty of Engineering
University of Strathclyde
GLASGOW

February 1993

SUMMARY

In the transition from deterministic to probabilistic approaches to assessing the damage survivability of passenger ships this PhD study seeks to draw attention to the key need in regard to loss prevention - the need to address damage survivability by taking full account of vessel dynamics in realistic environments.

The thesis begins by critically reviewing the development of sub-division and damage stability requirements, emphasising the inherent weaknesses in the existing approaches to assessing damage survivability. The approach adopted in this thesis is then described. This is based on real time simulation of the dynamic behaviour of the damaged vessel in realistic wind and wave conditions. The mathematical model comprises coupled sway-heave-roll motions in beam seas while taking into consideration progressive flooding as well as water accumulation. A series of comprehensive model experiments have been specifically designed and undertaken to investigate the nature and magnitude of couplings in the above modes of motion in upright and inclined conditions. The damage survivability of the vessel is examined by considering a number of damage scenarios, chosen on the basis of maximising the danger of potential capsize (or sinkage) while taking into account actual accident records.

The practical applicability of the proposed procedure is demonstrated by means of a parametric investigation aimed at identifying the effect of a number of key parameters on the damage survivability of a modern car/passenger ferry. These include: wave height; wave length; wind speed; flooding; water accumulation; location and extent of flooding; loading. The results of the investigation are presented and discussed. On the basis of these results boundary stability curves are proposed as a substitute for existing still-water damage stability criteria. These curves involve relationships between design and environmental parameters and inherent stability-related parameters.

ACKNOWLEDGEMENTS

This work has been carried out under the supervision of Dr. Dracos Vassalos in the Department of Ship and Marine Technology, University of Strathclyde. I would like to express my deep gratitude to Dr Dracos Vassalos for his continuous encouragement, very valuable stimulating discussions and guidance throughout this research.

I also wish to thank to Dr. Philip Sayer, Head of Department, for giving me the opportunity to carry out this research in the Department of Ship and Marine Technology.

I am also very specially indebted to Dr Mehmet Atlar for his constructive discussions and help in terms of valuable knowledge and material.

The financial support in the form of a scholarship from the Ministry of Education of Turkey is most appreciated.

I would also like to thank:

- David Clelland and the laboratory staff, Bill, Charlie and Jack for their great help during the preparation of experimental set-up and tests.

- Research colleques in the department for their help and discussions on the problems encountered.

- DOT people for providing valuable material used in this research.

- The Basketball crowd who are great friends, made my social life very colourful and eased the strain of the PhD study.

I would like to express my sincere thanks to my family in Turkey who gave endless support and encouragement throughout this study.

Finally, I would like to express my deepest gratitude to Lesley, who shared the side effects of this research and gave support and encouragement.

NOMENCLATURE

ADW(t)	:	Instantaneous amount of water on deck
A_{ii}, A_{ij}	:	Added mass coefficients
A_{iind}, A_{ijnd}	:	Non-dimensional added mass coefficient
A_p	:	Lateral projected area of vessel above the free surface(m^2)
B	:	Breadth
B_{ii}, B_{ij}	:	Damping coefficient
B_{iind}, B_{ijnd}	:	Non-dimensional damping coefficient
C_d	:	Drag coefficient(1.22)
C_r	:	Coefficient to calculate radius of gyration for roll
d	:	Draught
D_{bh}	:	Depth to bulkhead deck deck
F_{iwave}, M_{iwave}	:	Wave excitation force and moment
F_{iwind}, M_{iwind}	:	Wind excitation force and moment
FRAO(ω)	:	Force for per unit amplitude at a given
FREAL(t)	:	Random force realisation in time domain frequency and mode of motion
FS(ω)	:	Force spectrum
G	:	Pulsating source potential of unit strength at a point (ζ,η) in the strip contour [40, 41]
g	:	Gravitational acceleration
H_{wm}	:	Wind moment arm between the centre of lateral area and half the mean draught
i,j	:	Indices for motion, i,j: 2, 3, 4 corresponds to sway, heave and roll respectively
i_{44}	:	radius of gyration for roll
I_{ij}	:	Mass moment of inertia
KG	:	Vertical centre of gravity
L_{bp}	:	Length between parpendiculars
lcg(t,X_4,θ)	:	Longitudinal centre of gravity of water on deck
L_{OA}	:	Length(Loa)
M	:	Mass of ship
n	:	Direction cosines of the normal vector

p	:	Hydrodynamic sectional pressure
p_S	:	Sectional hydrostatic pressure
RES_i	:	Restoring force and moments
s	:	Wetted contour of the strip section
$S(\omega)$	:	JONSWAP spectrum
$SRM(t,X_4,\theta)$	:	Instantaneous static heeling moment due to water on deck
$SSF(t)$	:	Instantaneous static sinkage force due to water on deck
$STM(t,X_4,\theta)$	:	Instantaneous static trimming moment due to water on deck
$S_W(\omega)$	:	Sea spectrum component at a given frequency
$TCB(t,X_3,\theta,X_4)$	:	Transverse centre of buoyancy of the ship
$tcg(t,X_4,\theta)$	:	Transverse centre of gravity of water on deck
$TCGs$	:	Transverse centre of gravity of the ship
T_{sh}	:	Heave natural period of a ship
T_{sr}	:	Roll natural period of a ship
V_w	:	Relative wind velocity(m/sec)
$WA(\omega_i)$	:	Average wave amplitude calculated using sea spectrum for a given frequency
$WREAL(t)$	:	Random wave realisation in time domain
X_2	:	Sway motion
X_3	:	Heave motion
X_4	:	Roll motion
$\Delta(t,X_3,\theta,X_4)$	:	Instantaneous displacement
$\Delta(t_0)$	:	Initial displacement at time $t = t_0$
ε	:	Phase angle
Φ_D	:	Incident wave potential
Φ_I	:	Incident wave potential
Φ_R	:	Incident wave potential
θ	:	Instantaneous trim
Q_d	:	Unknown source strength
ρ	:	Density of water
ω_e	:	Excitation frequency (rad/sec)
ω_m:	:	Modal frequency
ω_{nd}	:	non-dimensional frequency ($\omega_{nd} = \omega_e \sqrt{\frac{B}{2g}}$)

ω_o	:	Oscillation frequency
ω_{sh}	:	Heave natural frequency of a ship
ω_{sr}	:	Roll natural frequency of a ship
ω_w	:	Wave frequency
ρ_w	:	Density of air

CONTENTS

CHAPTER 1: INTRODUCTION

1.1 GENERAL

The safety of ships is of paramount importance to ship designers, operators and regulatory bodies. Coupled with its importance, the safety of passenger ships is a complex matter involving different aspects such as the specific mission of the vessel, design, passengers, navigation, cargo handling, profits etc.

The safety of passenger vessels has always been the prime concern of regulatory bodies because of the human factor. The purpose for building a ship influences its safety standards. Ships built for a specific duty such as research or defence have safety as their prime concern, while commercial vehicles take economical viability as their prime concern. The safety standards of commercial vehicles always conflict with their economical viability and their operational efficiency, and it becomes a compromise between what is socially desirable and what is economically viable. The arguments which arise, concern changes on design and regulations, which bring extra cost or low operational efficiency. It is obvious that this conflict increases the potential risk of ship losses. One must realize that total safety can only be achieved in an immobile world [1], therefore improvements on the safety of vessels must be practical but at the same time must offer a substantially improved standard.

1.2 PROBLEMS WITH SURVIVABILITY STANDARDS

The survivability of a ship is related to intact and damage stability requirements. In general it can be said that intact ship survivability has received more attention than damage survivability of ships. The introduction of compartmentation standards for cargo ships as well as significant amendments in residual stability criteria for both cargo (it did not exist before) and passenger ships in as recent as 1990 are suitable for illustrating the lack of understanding with regard to the survival criteria for damaged vessels.

Existing mandatory damage stability criteria and compartmentation standards for passenger vessels were evaluated and implemented originally during the 1910's and have not been improved substantially since then. However, the modern passenger ship design has changed completely and substantial differences are apparent. For instance, increased passenger capacity, the location of sleeping cabins and entertainment areas, higher superstructure, and smaller machinery space with powerful engines. All these changes in modern ship design are not reflected in current damage stability criteria, and therefore realistic stability standards for modern passenger ships are not currently available.

There is also a strong common view that existing stability criteria (Deterministic Approach) are inadequate, because of the simplified mathematical modelling which neglects too many important factors involving physical phenomena. In addition, regulations are mainly for the final equilibrium position of damaged ships without any firm criteria for the intermediate stages of flooding.

Realizing the inadequacy of these criteria, the International Maritime Organisation (IMO) has carried out extensive studies and adopted new stability criteria [2] based on a "Probabilistic Approach". The new approach accounts for the probability of damage statistics and considers modern designs as well as some other important parameters affecting stability. However, the existing criteria have not been replaced by the new criteria because of the complexity in applying the latter and the Probabilistic Approach was accepted only as an equivalent to the existing Deterministic Approach.

However, the criteria from both approaches are based totally on the residual stability at the final equilibrium position in a still water environment, and neither of them address the consequences of non-survival incidents in which flooding above the bulkhead deck and rapid capsize can result. Evaluating damage stability in static conditions is too simplistic, and both approaches ignore reality since still water is the exception rather than the rule during the operation of a ship in open sea. The presence of waves and winds in a real

environment spoils the main assumption of the existing criteria and the importance of these environmental parameters are emphasized by both experimental and theoretical studies [3, 4, 5].

1.3 RO-RO CONCEPT AND PASSENGER/VEHICLE FERRIES

Increasing trade volume in the world and improvements on road transportation affected ship design. Roll on-Roll off type ships, which make the transportation of cargo and vehicles very flexible, have been developed and improved. Improved road networks which include ports, increased the demand substantially and in addition, longer holidays and greater car ownership increased the demand for passenger/car ferries. In response to this demand ferries have grown in size and now have the standards of comfort and service equal to the luxury passenger vehicles.

The main characteristic of the Ro-Ro type ship is the undivided vehicle deck which makes these type of ships very flexible and popular but at the same time much more vulnerable to flooding and water accumulation. The type of cargo that Ro-Ro ships can carry varies from passengers and private cars to trailers and trains. Until 1992, like other cargo ships vehicle Ro-Ros had not been subject to any subdivision regulations either below or above the main deck. Due to the nature of cargos, most cargo ships have subdivisions above or below the bulkhead deck. However, pure Ro-Ro vessels do not have any subdivisions above or below the bulkhead deck, since they carry mainly road transportation vehicles. However, following the introduction of SOLAS 90 rules [6] all cargo ships including Ro-Ros must now comply with the new subdivision requirements below the bulkhead deck as well as with the residual damage stability standards. The Ro-Ro vessels carrying more than 12 passengers are also subject to the subdivision standards but only below the bulkhead deck. Of course the main vehicle deck is not subject to the subdivision regulations and this makes Ro-Ros prone to capsizing as was experienced with the Herald of Free Enterprise disaster.

1.4 THE NEED FOR NEW DAMAGE STABILITY REGULATIONS

It goes without saying that so long as the assumptions inherent in present day regulations are violated, accidents will continue to happen.

The majority of research so far has been expended in intact stability, the usual argument being made that damage stability is too complicated to deal with before full understanding of intact stability can be achieved.

It is questionable, however, that vessels ever capsize in what might be termed "pure" intact mode since progressive flooding, shifting of cargo, wetness and so on are likely to play a part during any capsize sequence.

Furthermore, the shipping industry must have learned its lesson by now in the light of the plethora of disasters during the recent past.

The treatment of damage stability of ships based on the dynamic behaviour of the vessel in realistic environmental conditions and derivation of damage stability and subdivision requirements deriving from this is long overdue.

This thesis represents the first attempt towards achieving this goal.

Sea accidents, caused by collision, shifting cargo, foundering etc., may lead to different results like capsizing or sinkage and loss of ship, with a high number of deaths. The potential risk of capsizing for passenger ships, especially passenger/vehicle ferries, is very high. Moreover capsizing could occur within a very short time which is not long enough to enable evacuation of the ship. Ships also capsize as a result of water accumulation in the vehicle deck and as a result of dynamic excitations due to the environmental conditions such as waves and wind. Transient dynamic effects such as shifting of cargo and accumulation of flood water are also possible causes of capsizing or loss of ship.

Studies carried out e.g. Kummerman's 1st international conference, also prove that, during a ship's operation, vessel parameters play a crucial part on its static and dynamic stability. The vertical position of the centre of gravity(KG), trim, heel, freeboard, progressive flooding and draught are some of the vital parameters that can change the responses of a ship to the environmental excitations. Recent accident records show that most of the losses and capsizes occurred during the intermediate stages of flooding [9]. However, the present regulations do not comprehensively take into account the effects and parameters mentioned above, nor is it possible to account for these influential parameters in the present form of the criteria. Before more accidents such as that of the Herald of Free Enterprise are experienced, new dynamic damage stability regulations which consider environmental effects as well as progressive flooding, must be developed and used.

In order to improve the stability standard of a ship, the reasons for capsizing or loss of passenger ships must be investigated by considering the dynamic effects of the environmental conditions as well as of the vessel parameters. This investigation can be best carried out by a time simulation approach supported by model experiments. Time simulation is the best approach to investigate the instantaneous behaviour of a ship under different external effects in a certain period of time, while progressive flooding takes place. This kind of investigation can be repeated by considering different environmental conditions, different damage scenarios, which are also not considered by present regulations, and different loading conditions. The results of such investigations can help significantly to devise more realistic damage stability criteria.

1.5 METHODS FOR INVESTIGATING THE DYNAMIC STABILITY

The main purpose of this research work is to examine the ship motions during and after flooding in order to understand the physical problems behind the capsizing phenomena. By using the results of the analysis, an approach for more realistic residual and intermediate damage stability criteria can be developed.

For such an investigation the most important motion(s) have to be studied. It is common knowledge that roll motion, which is the most important motion for the dynamic stability of ships is normally taken into consideration when studying capsizing. In addition however, the sway and heave motions have to be considered due to their strong coupling with roll. Heave motion can also increase the possibility of water ingress as the damaged part may immerse further in the water.

The waves and wind are the main external excitation sources, therefore they must be taken into account in any realistic modelling. The hydrodynamic coefficients in these equations of motion must also be determined, especially the coupling coefficients, and since the focus is on large amplitudes, the non-linearity of the coefficients may become more important, especially due to the additional effects deriving from the inclined position of the ship. As there is not any established theoretical method for calculating the coefficients for large motions, experiments may have to be carried out for comparison purposes. Non-linear effects must be considered as much as possible, in particular instantaneous restoring.

Since the accumulation of water on a large deck appears to be a very important factor, this problem has to be investigated by looking into the accumulation and sloshing effects, and the possibility of incorporating these effects into the ship motions may have to be sought.

In addition, different damage scenarios should be modelled by examining accident records as well as by considering a number of potential flooding scenarios. A parametric study must consider a number of influential environmental and ship design parameters. Based on the result of these investigations a methodology for deriving limiting criteria could be put forward involving relationships between the most important ship design and environmental parameters, in a way that is both meaningful and practical.

1.6 STRUCTURE OF THE THESIS

The work presented here begins by stating the overall aims to be achieved, followed by a critical review of existing damage stability criteria and literature. The critical review also includes a detailed account of the recent theoretical and experimental research activities in the subject. After defining the problem of damage stability, the adopted approach, including a number of fundamental aspects is explained. The mathematical modelling then follows where the solution of the motion equations, the calculation of the excitation/restoration for regular and irregular waves as well as for wind, water ingress, water accumulation and sloshing are detailed.

Chapter 6 addresses the model experiments, undertaken in the course of this research, where the experimental technique and the design of the experimental mechanism used to determine the hydrodynamic coefficients, are explained. The experimental results are then analysed and compared with theoretical results.

Chapter 7 describes in detail an extensive parametric study. In this study, the general static and quasi-dynamic stability trends are investigated using 10 different ships at intact and damaged conditions. The parametric study is then continued by investigating the dynamic behaviour of a sample ferry. For this investigation, different wave heights and lengths, different loading conditions and different damage scenarios are taken into account.

In the light of the information obtained from the parametric study, a new approach to assessing damaged stability is put forward. By using the proposed approach, a methodology for deriving new limiting damage stability criteria which include environmental effects, freeboard, loading conditions whilst considering the intermediate stages of flooding, is put forward. Finally, the results are discussed, recommendations for future research are put forward and conclusions are drawn.

CHAPTER 2: AIMS OF THE THESIS

The main aims of the thesis are as follows:

i) To review critically the existing damage stability criteria of passenger ships with a view to identifying where these criteria fall short in safeguarding life and property at sea. Additionally, to investigate research efforts into damage stability in order to enhance understanding of capsizing phenomena and survivability of ships.

ii) To develop a mathematical model and computational procedure to investigate the physical problems behind the dynamic damage stability of passenger ships in a realistic environment.

iii) To carry out a parametric study to identify the influential parameters on capsizing and damage stability.

iv) To develop a damage stability assessment procedure which takes into account dynamic effects and progressive flooding.

v) To propose a methodology for deriving realistic damage stability criteria, which account for environmental and ship design parameters.

vi) To apply the proposed methodology on an existing ship and compare the results with criteria currently in operation.

CHAPTER 3:

CRITICAL REVIEW OF PASSENGER VESSEL DAMAGE STABILITY

3.1 HISTORICAL BACKGROUND OF DAMAGE STABILITY REQUIREMENTS

The idea of having damage stability requirements on an international basis goes back to the 1910's, with the loss of the Titanic stimulating the process to reach agreement. However, the agreement reached at the SOLAS (Safety of Life at Sea) conference 1913, never came into effect because of World War 1. Following the war, studies of subdivision were renewed because shipowners insisted that the 1914 Convention requirements were too penalising. During the 1920's several informal conferences were held and a number of studies and tests were carried out.

In 1929 a full international conference on Safety of Life at Sea was convened and as a result the criterion of service and factorial system of subdivision were adopted to draw distinction between vessels in the carriage of cargo and those dedicated to the carriage of passengers. This procedure was concerned essentially with the sinkage of vessels as a result of flooding and did not put forward any stability regulations for the intermediate and final stages of flooding.

In 1948, another SOLAS conference was held but since there had not been any major sea disaster between 1929 and 1948, regulatory bodies were not forced to make major changes. However, a few new damage stability regulations were included which improved standards. The capsizing of the Andrea Doria, built under the 1948 Convention, raised discussions on the inadequacies in practical applications of the 1948 Convention and consequently substantial changes were proposed in the 1960 SOLAS conference. Since time was insufficient to reach any agreement for major changes, it was decided to form a sub-

committee to carry out a study for the new rules. In 1960, despite the raised standards, the principal regulations remained the same.

The sub-committee (SOLAS Sub-committee on stability, subdivision and load lines) started its research in 1961. Its purpose was to review the existing criteria concerning the subdivision and damage stability of passenger certified ships and to consider the relevant part of these criteria in comparison with other possible criteria based on probabilistic studies, from the point of view of stability and feasibility of application. The sub-committee carried out an extensive study on new requirements which involved collecting and analysing sea accidents and the stability of ships in a damaged condition, as well as an evaluation of new methods in dealing with the subdivision of ships. These new regulations on subdivision and stability for passenger ships were drawn up to the last form in 1974 and adopted as new regulations. Due to the complexity of the new subdivision requirements and the need for specific computer programs for their application, the new regulations were adopted as being equivalent to and a total alternative to the provision of part B of chapter II of the 1960 convention [2] and this decision remains the same to date.

With such recent tragedies as the European Gateway and the Herald of Free Enterprise, strong common views expressed that the 1960 Convention, which refers to the current mandatory criteria, had to be replaced by a more realistic and updated damage stability assessment. Regulatory bodies studied the problems and, for the first time, they introduced in 1990 extensive residual stability standards, for both passenger and cargo ships. They are based on righting levers (GZ), area under the GZ curve and limiting angles of inclination, all calculated in calm water and came into effect at the beginning of 1992.

3.2 REVIEW OF EXISTING CRITERIA

Since the main aim is to improve the damage survivability of ships, it is important to examine the bases of the existing criteria, which are derived from deterministic and probabilistic approaches.

3.2.1 Deterministic Approach: 1960 Convention

The principle of the deterministic approach is to divide the ship into floodable compartments by watertight transverse bulkheads. The deterministic approach is based on the criterion service (Cs) and factor of subdivision (F), and takes into account the number of passengers, accommodation area below the bulkhead deck, and the volume of machinery space. The factor of subdivision shows the compartment standard of the ship as indicated below:

$F > 0.5$	Ship must have one-compartment standard
$0.5 > F > 0.33$	Ship must have two-compartment standard
$F < 0.33$	Ship must have three-compartment standard

F depends on the criterion service number and the length of the ship. The floodable length (L_f) at each location along the ship length is calculated and multiplication of this value by the factor of subdivision gives the permissible compartment length (L_p) at each point. In this way, a floodable length curve along the ship is derived and is used in deciding the actual location of transverse watertight bulkheads. The checking calculations are carried out based on the actual compartment length curve (Fig 3.1). Details of the deterministic approach can be found in [7].

As was explained earlier, the modern passenger ship design is completely different from that of the 1920's for which the principal requirements of the deterministic approach were evaluated. The calculation of the criterion service(C_S) is dependent on some ship design parameters which either do not exist or are completely different in modern ship designs. For instance, the trend in modern ship designs is to accommodate all the passengers and crew above the bulkhead deck (especially ferries) in contrast to the old passenger ship designs. Improvements in machinery design reduced the size of the engine compartments and increased the power of the engine. Modern passenger ships have a very high capacity with improved service standards, but trade conditions force the designers to create popular and more economical ships. Modern multi-purpose ferries

reflect the recent trends to accommodate a high number of passengers and commercial vehicles in the same ship and offer very high accommodation standards. All these changes, which require different safety standards, are not included in the current approaches. Therefore existing safety standards are not suitable for modern passenger ships or are inadequate.

3.2.2 Probabilistic Approach

The probabilistic approach has been developed as an alternative to the deterministic approach when the inadequacy of the latter was realised.

The most important and principal distinction of the new regulations is the use of the probabilistic approach. The calculation of the probability of damage is based on information contained in various IMO documents, which includes collision casualty reports giving dimensions, location of damage in the ship, sea state, voyage reports pertaining to operating draughts and permeabilities, as well as stability.

An index of subdivision is evaluated as a criterion of the degree of safety. "A" is a measure of the ship's ability to survive after damage and this index reflects the effect of bulkhead spacing, stability and other features relevant to stability. Calculation of "A" includes:

a- The probability of flooding each single compartment and each possible group of two or more compartments.

b- The probability that the residual buoyancy after flooding will be sufficient.

c- The probability that the stability after flooding will be sufficient to prevent capsizing or dangerous heeling due to loss of stability or large heeling moment.

The principles of the probabilistic approach are illustrated schematically in Figure 3.2.

According to the new approach, the subdivision of a ship is sufficient if the attained subdivision index "A" is not less than the required subdivision index "R", which is calculated by taking into account the ship's length and number of persons carried on board. Details of the probabilistic approach can be found in [2].

All these analyses, observations and considerations of different parameters, as well as taking into account modern ship designs, make the probabilistic approach more realistic, having inbuilt better physical understanding. In addition, it allows for a flexible watertight subdivision arrangement. However, the complexity of the probabilistic approach in comparison with the deterministic approach raises difficulties on the practical application and as a result it was adopted only as an equivalent and alternative to the mandatory regulations, which are based on the deterministic approach. Having said this, the complexity of practical application may not be a valid reason any longer, since advanced technology and computers can deal with the complex problems involved without any difficulty.

One disadvantage of this approach is the absence of experience gained from applications and therefore safety standards offered from the approach may not be as reliable as they should. This experience and reliability can only be gained by making it mandatory. In so doing, it should not be forgotten that the damage stability requirements derived from the probabilistic approach are also based on static conditions which is never the case in a realistic environment. Waves, wind, progressive flooding, shifting of cargo, etc. are factors which are neglected, despite their recognised effects on a ship's stability.

The common view including that of IMO is that existing mandatory criteria must be replaced by more realistic criteria which will consider the environmental conditions as well as recent changes in passenger ships design. Since the probabilistic approach is based on firm statistical facts it would be very useful to make these criteria mandatory, whilst attempting to improve this approach extensively by

including the dynamic effects of the environment as well as the intermediate stages of flooding.

3.2.3 Recent Amendments and their Effects

Recent accidents as well as overall accident statistics, forced official bodies to improve the rules by adopting a more realistic approach. As an immediate result of this, they introduced some measures on damage stability not only for passenger ships but also for cargo ships.

In May 1990, IMO decided to introduce new and extensive regulations regarding both the intermediate as well as the final stages of flooding [6]. They can be highlighted as follows:

a- The positive residual righting lever curve to have a minimum range of 15 deg. beyond the angle of equilibrium (Fig 3.3).

b- The area under the righting lever curve to be at least 0.015 rad.m measured from the angle of equilibrium to the lesser of :

  i- The angle at which progressive flooding occurs

  ii- 22 deg. (measured from upright) in the case of one compartment damage

  iii- 27 deg. (measured from upright) in the case of the simultaneous flooding of two or more adjacent compartments

c- A residual righting lever is to be obtained within the range specified above by taking into account the greatest of the following heeling moments:

  i- The crowding of passengers at one side

  ii- The launching of all fully loaded Davit-Karmel survival craft at one side.

  iii- Heeling due to the wind pressure

However in no case is this righting lever to be less than 0.1 m.

d- In intermediate stages of flooding the maximum righting lever to be at least 0.05 m and the range of positive righting lever to be at least 7 deg.

As seen from the regulations the main objective is to restrict the heeling during and after the flooding while requiring minimum residual restoring ability. This is a very positive step towards improving the stability of ships, and the immediate effect of these rules on the existing ships has already been seen. For example, as a result of introducing the new rules, a number of ships which failed the regulations have had to be modified structurally to provide extra buoyancy and residual stability. Of course, these compulsory modifications paved the way for research aimed at identifying the optimum applications which satisfy safety, economical and operational needs.

3.3 INVESTIGATION OF STABILITY PROBLEMS

Being a popular subject, safety and survivability of ships is of interest to everyone. A considerable amount of studies on this subject have been carried out and others are still ongoing. The interest for researchers in understanding the reasons for the different problems of survivability such as capsizing and loss of stability lead some of them to focus on different factors. Some investigators focus on the effect of the environmental aspects and findings from these investigations have resulted in conclusions and solutions to some of the problems.

In order to achieve a realistic safety standard there is a need for establishing a relation between the state of sea surface and minimum values of damage stability characteristics, which may allow the ship to avoid capsizing in the given environmental conditions. Establishing this relation, however, is a difficult problem since capsizing is a highly non-linear problem and a function of many parameters. It is also unlikely that appropriate damage stability characteristics can be arrived at on the basis of full scale data alone

(accidents or full scale experiments). Therefore, there remain two principal methods in establishing a relation between sea states, ship stability and residual buoyancy namely, model experiments and theoretical studies.

Pioneering damage stability experiments were carried out in the early 1970s [3, 4]. From the damage stability experiments carried out in 1973 [3], it can be concluded that capsizing is definitely related to environmental parameters. In this study the model used was a typical Passenger/Vehicle ferry and the experiments were carried out for different sea states, loading conditions and freeboards. In each case, where capsizing occurred, the primary cause was considered to be the accumulation of water on the main deck due to spillage of water and roll motion. These experiments also revealed that wave height is a very significant factor affecting capsizing. The findings suggest that significant increases in initial stability are required in order to resist capsize, as freeboard decreases and wave height increases.

Research in [8] supports the commonly held view that the probability of capsizing of a vessel increases at higher sea states and for longer periods of stay in given conditions. When the deck is flooded (especially the car deck) the static stability becomes worse due to the dramatic decrease in the waterplane area. The combination of low GM and accumulation of water leads the ship to rapid capsizing as was experienced in the Herald of Free Enterprise disaster [9].

Another observation is that the critical GM (metacentric height to avoid capsizing) is very sensitive to initial heel. The experiments carried out by Adee and Pantazopoulos [10] indicated that most of the capsizing cases were related to the large static or pseudo-static heel due to trapped water on the ship's deck. For intermediate and low metacentric height cases the presence of water on deck results in a larger roll oscillation and leads to dangerous conditions including capsizing [10].

The static and dynamic effects of water on deck is an important effect to be considered. It was found from experiments and confirmed by theoretical studies that the dynamic behaviour of water on deck has an adverse effect on ship motions when the natural rolling period of the ship is close to that of the motions of shipping water [11]. It was also claimed that the motion of water on deck sometimes works as a damping mechanism against the ship's motion [12]. This problem is highly non-linear and is difficult to model analytically. Most of the results concerning the effect of water on deck have been derived from model experiments, and the studies are mainly on small ships such as fishing vessels and on liquid tanks of LNG ships. Therefore, it is important to investigate the static and dynamic effects of water on the vehicle deck of ferries.

A ship with static heel can be excited easily by a large range of sea states, as static heel changes the hydrostatic and hydrodynamic characteristics of the ship [17, 28]. Kobayashi [13] concluded from his theoretical and experimental work that heel, waves, wind and their direction, are very important parameters influencing ship motions and stability. He also claimed that the effect of heaving motion on roll motion cannot be ignored for an inclined ship. His experimental and theoretical results showed that the roll amplitude for heeled conditions is greater than that for the upright condition, especially at around the resonant frequency. Since the hydrodynamic characteristics of a ship at an inclined condition change, it would be necessary to determine these at inclined conditions. In considering this point Kobayashi [13] applied strip theory to calculate the hydrodynamic forces and moments for asymmetrical sections and compared some of his results with experiments. However, strip theory is based on small amplitude oscillations, therefore it is worthwhile to investigate the validity of this method for large amplitudes or to look for an alternative method.

Although theoretical methods used to calculate the hydrodynamic coefficients are well established, they cannot predict most of the non-linearities such as viscous effects and non-linear couplings. This is important for motions such as roll which is affected significantly by

these non-linearities, especially when the excitation frequency is close to the natural roll frequency. Therefore, probably the best way to determine the hydrodynamic coefficients is by means of model experiments. Non-linear effects which cannot be modelled theoretically can also be measured by means of experiments.

Pioneering experiments for the determination of hydrodynamic coefficients were carried out in the late 1950's and early 1960's [14, 15]. Vugts [15] carried out experiments for different cross-sectional shapes, draughts and frequencies and his results have been the major reference for most researchers. However, his results are for small amplitude motions and include only two-dimensional effects. Beukelman [16] also carried out experiments for a whole ship in shallow waters and measured the coefficients at predefined sections. By using these experimental results he tried to improve strip theory calculation for shallow water. However all these experiments were carried out for ships at upright conditions and for small amplitudes. As mentioned above, coefficients may change for an inclined ship due to the new underwater geometry and there may be new coupling coefficients caused by static heel. In addition, for large amplitudes, the underwater volume of the ship and hence the restoring force and moments, can change significantly. This can be included in the analysis of experimental results so that hydrodynamic coefficients can be measured more realistically.

Another study attempted to develop an analytical method for predicting the wave-excited motions of ships with static heel due to asymmetrical flooding [17]. This method is based on linear wave excitation formulated in the frequency domain and takes into account 5 degrees of freedom coupled motions. The hydrodynamic coefficients are obtained again by using strip theory. In order to predict the roll motion correctly around the resonant condition, viscous damping and wave drag forces are included in the mathematical model. In this study, while it was accepted that the ship motions at an inclined condition may be non-linear, the linear method is claimed to provide most of the essential features of the motion characteristics of the ship. Based on this method it was found that a ship with a static heel

can be excited to large roll amplitudes in the case of head waves. It was also claimed that for a ship at neutral heel, waves coming from the opposite direction to heel could excite larger roll motion than waves coming from the heeling side. However, this model is formulated in the frequency domain and the static inclination is modelled by assuming asymmetric weight distribution. Therefore, the method cannot provide any information on water accumulation or the behaviour of a ship during progressive flooding.

The idea of directional instability due to sway-roll-yaw coupling was one of the reasons behind capsizing as put forward by Bishop, Price and Temarel [18]. A combination of other effects (flooding, water on deck, waves, heel, trim etc.) with forward speed, can cause directional instability and may lead to rapid capsizing. Although it would not be the primary cause for capsizing or instability of a damaged ship, it surely has a contributory effect on capsizing and must be considered in the case of forward speed.

One of the important reasons for sea disasters is the shifting of cargo due to environmental excitation. 60% of reported accidents for Roll on-Roll off ships are due to shifting of cargo which is believed to be caused by either insufficient or non-existent lashing points. Ship motions at sea affect the cargo in the form of an acceleration which causes stresses in the lashing equipment which may lead to failure, resulting in shifting of cargo.

3.4 METHOD TO CALCULATE SHIP RESPONSE

In order to calculate ship motions, there are two main approaches depending on whether a solution is sought in the frequency or the time domains.

Frequency domain analysis is a very good approach for engineering purposes when a wide range of information is required. General information on sea state, hydrodynamic coefficients or ship responses can be obtained immediately by looking at one graph. Another advantage is that results can be obtained very quickly with short

computing time. However, it is difficult to obtain explicit results especially if there are time dependent parameters, non-linearities and large amplitude motions. Today, frequency domain analysis is widely used for preliminary calculations of hydrodynamic forces [19, 20, 21, 22] and ship Response Amplitude Operators (RAO). By obtaining the relevant information from these preliminary calculations, the next stage, which refers to time explicit calculations, can be carried out.

In order to obtain an exact solution, one must observe the changes in parameters and responses, and reflect these changes immediately on other parameters, as well as including the non-linearities and large amplitude motions. Time simulation seems the only option for modelling such detailed calculations.

The development of time simulation has been linked to computer technology. Almost 20 years ago, the majority of studies were undertaken in the frequency domain due to the limitation on computer technology and its availability. However, as computer technology has advanced, the time simulation approach gained more ground. Today, very fast computers at very affordable prices, even for individuals, enforce most of the research activities to utilise simulation techniques.

In spite of this improvement, there are only a few research studies on damage stability by using the time simulation approach. On the other hand, there are a lot of time simulation applications which investigate intact stability. The biggest contribution of time simulation is that non-linear effects can be included in the study. The instantaneous changes in the underwater volume of a ship was proven to be very important on ship motions and included in the calculations [23, 24, 25]. Time simulation also showed that hydrostatic coupling, especially between roll and heave, is very strong [26, 28]. This was further improved when the effects of the instantaneous wave profile were included [23, 29, 30]. This approach which provides non-linear restoring/excitation has gained some ground for head and following waves but not for beam waves [31, 32].

In order to model flooding, the best approach is the time dependent added weight method which allows the water to be added at specified time steps while the ship motions are calculated at that instantaneous moment [27]. The same approach can be used to investigate water accumulation.

Recent research, using a time domain approach investigates the capsizing due to transient behaviour [33, 34]. This is done by examining the safe basins in the phase space (Roll and Roll Velocity) constructed by simulating all possible initial conditions. Transient capsizes can occur at a wave height that is a small fraction of the wave height at which the final steady state motions become unstable and capsize occurs [33]. Similar work is shown by Umeda [35] in his analysis of surf-riding situations.

Another very important benefit that time simulation provides is the modelling of random waves. In time simulation the ship can experience waves which have different frequencies and heights. Of course there are still points that are not really well established such as time dependent hydrodynamic coefficients and forces. De Kat [23] tried to introduce time dependence on hydrodynamic coefficients so that different coefficients for different frequencies can be employed during the time simulation. It is quite likely that as time simulation attracts more researchers and computers become faster these problems will be gradually solved.

3.5 CONSIDERING THE DESIGN ASPECTS

High operational efficiency is desired by the owners of commercial ships and is attained by neglecting some design factors which are related to ship survivability. This, however, simply increases the potential risk of disaster. For instance, short-range ferries which have a high passenger capacity have capsized or sunk in Bangladesh and in the Philippines with a large number of deaths. These ferries are designed for shallow waters, and have very low freeboard and high superstructure which reduce their seakeeping characteristics and seaworthiness. In addition, most of these boats do not meet the

existing stability criteria at some operating conditions and are usually overloaded.

In the regions such as North Sea, Baltic Sea, English Channel, and European Continent where the economic standards of the countries are similar, large trade volume, hence busy transportation, exists. This factor makes Passenger/Vehicle ferries very popular, therefore the ferries serving in these areas are the most advanced ferries with very high standards of service. However, despite the improved standards of service they do not have good safety standards in realistic terms and the recent ferry disaster (Herald of Free Enterprise) focused everyone's attention on the potential capsizing risk of ferries.

As mentioned above, car decks in ferries are not divided by any transverse bulkheads (Fig 3.4). This, of course, increases the risk of capsizing or loss in the case of flooding. Subdividing the vehicle deck transversely is probably the most reliable approach when considering safety, but the least viable when considering the initial cost, and the resulting low capacity and low efficiency. Recently, some designs which divide the vehicle deck transversely were proposed. These designs use mainly partial or full height retractable barriers (Fig 3.5a, Fig 3.5b). Fitting portable barriers seems a reasonable idea considering their flexibility and better economic efficiency compared to fixed barriers. However, they may not be viable economically for short haul ferries and although these designs prevent water accumulating and covering the whole deck area, several drawbacks have been identified. Partial bulkheads can restrict water flooding up to 10-15 degrees of heel but beyond this heel other parts of the vehicle deck can be flooded. It was suggested that regardless of the type of bulkheads, a minimum of three have to be installed [36]. Furthermore, partial bulkheads are not structurally as strong as fixed bulkheads, therefore, they may be damaged very easily in the case of shifting cargo or collision. Therefore, before rushing into fitting these bulkheads without knowing the consequences, extensive investigations must be carried out by taking into account effects of different structural bulkhead designs, compartment lengths etc.

A recent trend in designs is to have a double skin below the bulkhead deck to prevent flooding against minor damages and this can be designed along the whole ship length or part of it. This type of design is also recommended by the probabilistic approach, as long as the depth of the double skin is not less than 20% of the beam at each side. This is a very efficient arrangement to keep flooding in the small side tanks, as long as the inner hull is not penetrated. It would cause heel only due to the asymmetric flooding of the side tanks, but, this permanent heel may cause a problem if the side structure above the bulkhead deck is damaged. Another and probably the worst problem may result following penetration of the inner skin which will flood the inner hull. Since the probabilistic approach allows ships to have an undivided inner hull, any damage would inevitably sink the ship.

In order to minimise sinkage and heeling of a vessel by the amount of water entering, it is logical to reduce the permeability of the flooded compartment especially below the waterline. This can be done by storing empty drums inside the wing tanks (Fig 3.6). Polythene drums or balls seem to be suitable in wing spaces because they cannot corrode and can be removed very easily [37].

As mentioned before, in order to comply with the new damage stability rules, existing ferries have to be modified to increase their residual stability. To meet these standards some ships had to be fitted with side sponsons to increase the residual buoyancy (Fig 3.7, [36]). In order to create enough residual buoyancy as well as stability for new designs, the side tank arrangement above the bulkhead deck has been proposed, together with possible flares (Fig 3.8, [36]) which may be more economically viable.

Again all these ideas have to be combined with realistic safety regulations which are yet to be devised.

3.6 RECENT RESEARCH ACTIVITIES

In the wake of the Herald of Free Enterprise disaster, The UK Department of Transport (DTp) set up the Ro-Ro/Ferry Safety Research Programme to investigate the problems and to develop minimum dynamic stability requirements. The program was divided into two phases. Phase 1 covered:

- Physical model tests of damaged Ro-Ros in realistic sea conditions.

- Theoretical studies into the practical benefits (damage stability performance) and penalties of applying various devices to Ro-Ros. This latter work was further divided into three separate projects:

  i- Collision Resistance
  ii- Hull Form and Superstructure
  iii- Internal Arrangements

- Risk Analysis involving a theoretical study of hazards and their consequences.

Phase 1 of the research work was based on model tests and confirmed that even in modest sea conditions the new generation of conventionally designed vehicle ferries with small freeboards can survive only with unacceptably high metacentric heights (GM) [38]. In order to improve this condition, the following alternatives were proposed:

- Increase the freeboard to provide much greater freeboard in flooded conditions
- Subdivide the vehicle deck
- Provide side buoyancy

Phase 2 which is to determine the minimum stability requirements covers the following stages:

- Damage stability model experiments to investigate the effects of trim, static heel, wind, forward speed and partial bulkheads.

- Development of a mathematical model of dynamic capsize of passenger ferries by including the environmental effects as well as progressive flooding and water accumulation.

Successful completion of this programme (Phase 2) will contribute substantially towards achieving realistic damage stability requirements for Ro-Ro ships. However the second phase may take longer than expected, due to difficulties in the mathematical modelling of the associated complex phenomena.

3.7. SUMMARY

In the preceding sections, the review of existing criteria and literature draws attention to a number of key facts which are highlighted next.

The existing damage stability criteria are inadequate and do not reflect the true standard of safety since they ignore the changes in modern ship designs. The effect of waves and other external forces are neglected in the existing criteria, and reliance is based only on the reserve stability of the intact vessel.

Although the probabilistic approach is more realistic compared to the deterministic approach, it is more complex and lacks experience in its application. Furthermore, it does not include the effect of waves and other external forces.

The research carried out in the past gives some clear ideas about the problems with ship stability. Review of existing studies leads to the conclusion that external forces such as waves, wind, and accumulation of water on deck are prime causes of capsizing or loss of damaged ships. It is also concluded that the initial permanent heel due to asymmetric flooding affects the ship's stability considerably.

It is very clear that there is a need for a more comprehensive approach to the damage stability assessment of passenger ships. For this reason, the damaged ship motions, under the effect of external forces, must be investigated as a first step to help in the development of a dynamic damage stability assessment.

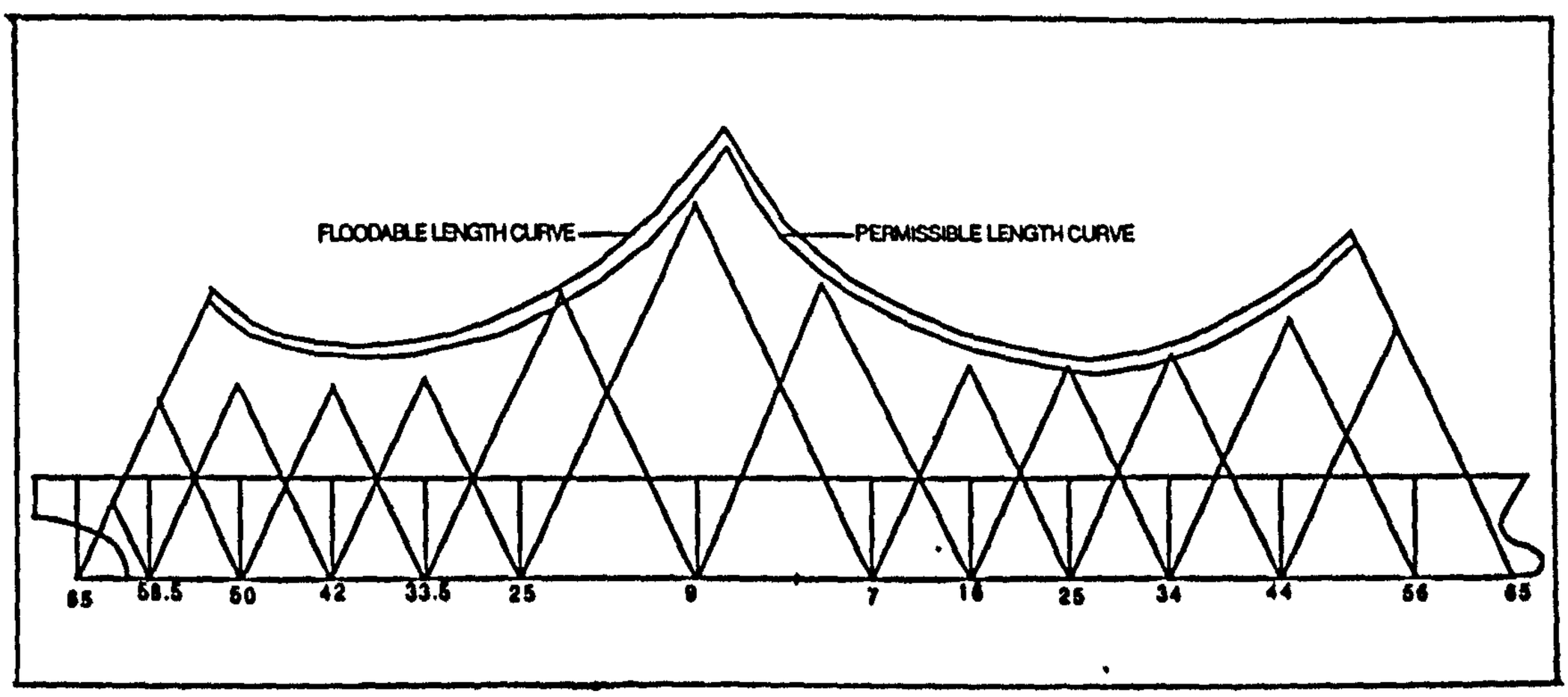

Fig 3.1 Floodable and permissible compartment length curves

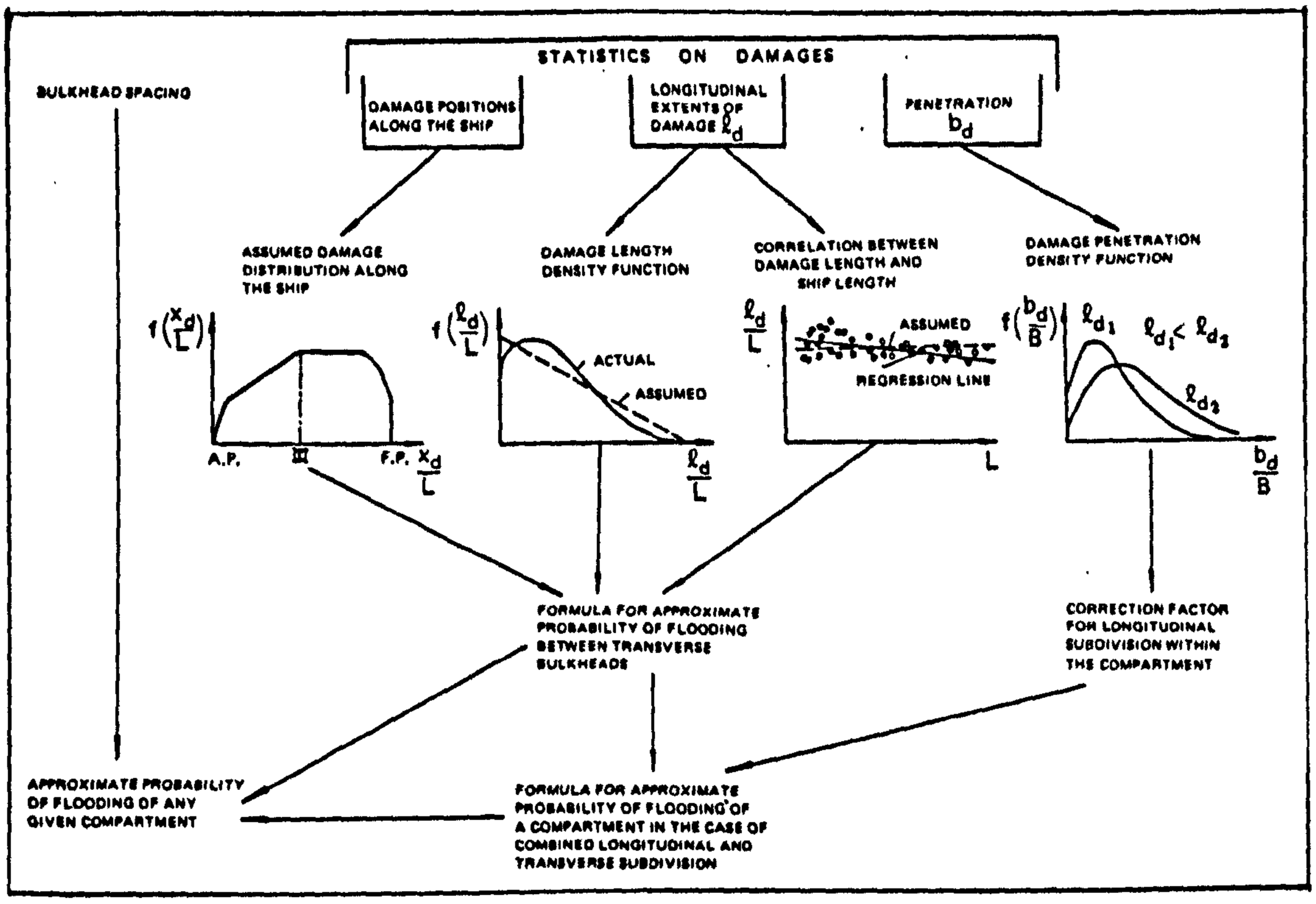

Fig 3.2A Principles of calculation of probability of flooding of any given part of ship's hull according to the probabilistic approach [2]

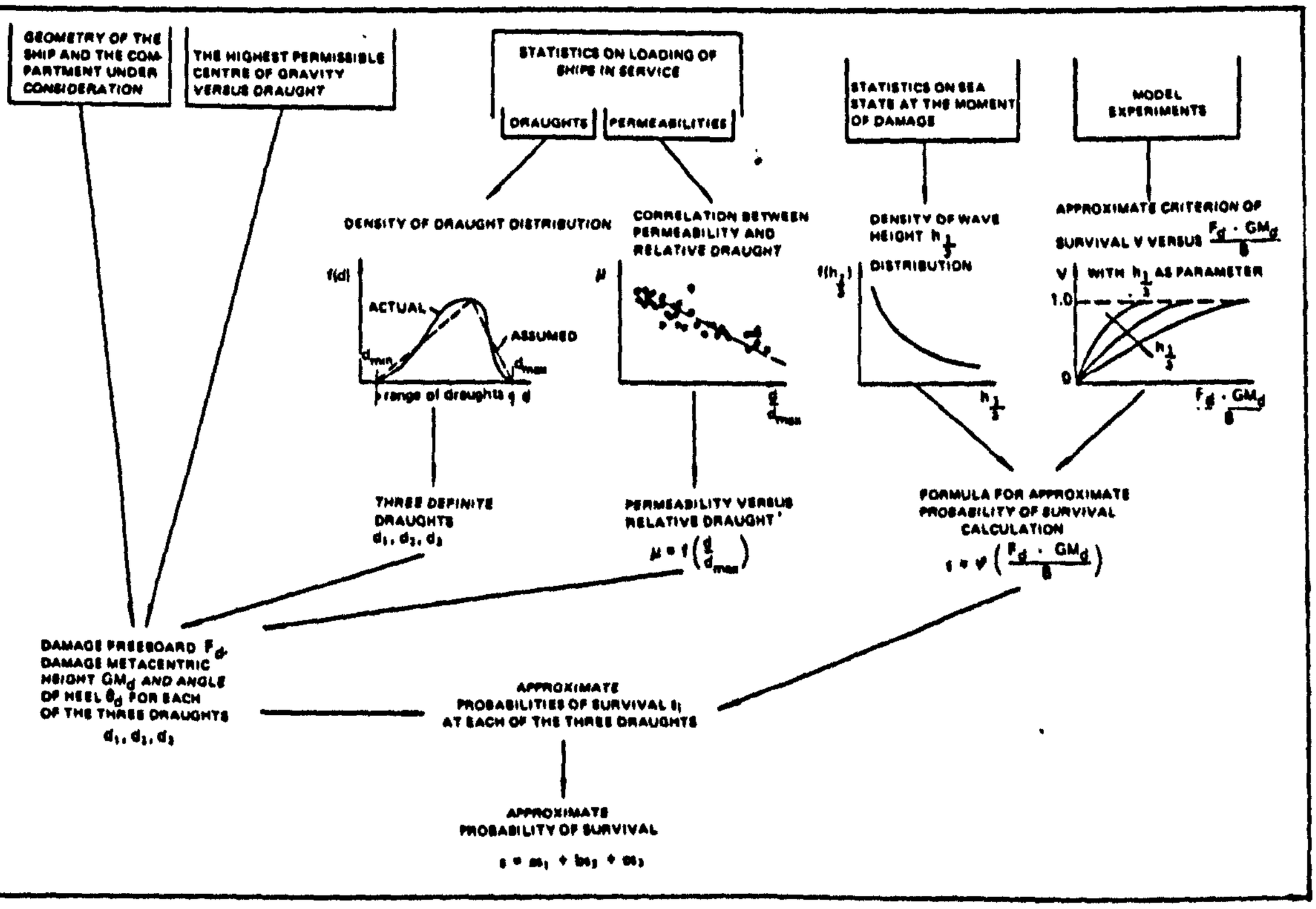

Fig 3.2B Principles of calculation of probability of survival of flooding of any given part of ship's hull according to the probabilistic approach[2]

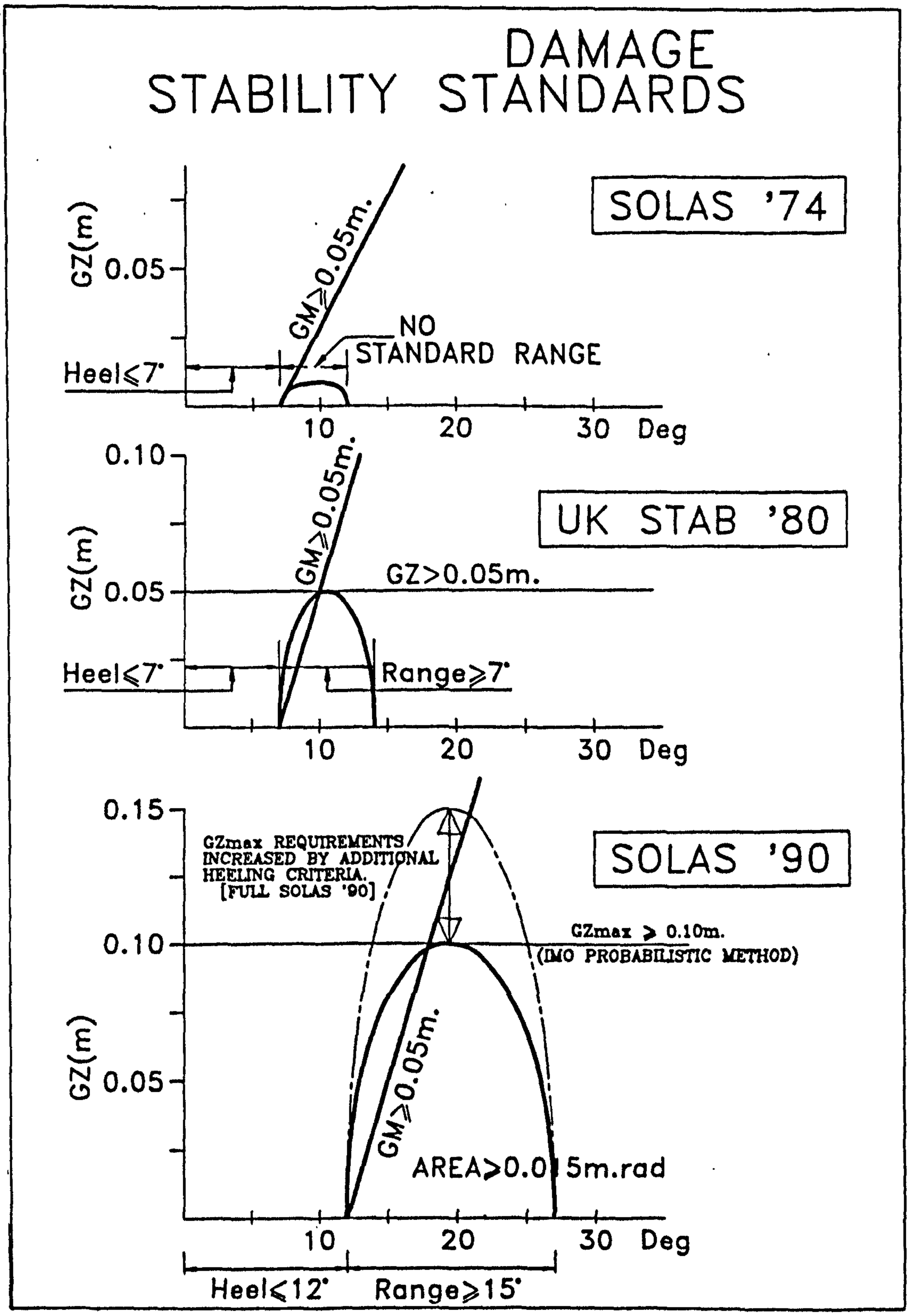

Fig 3.3 Changes in residual stability standards for damaged passenger ships [36]

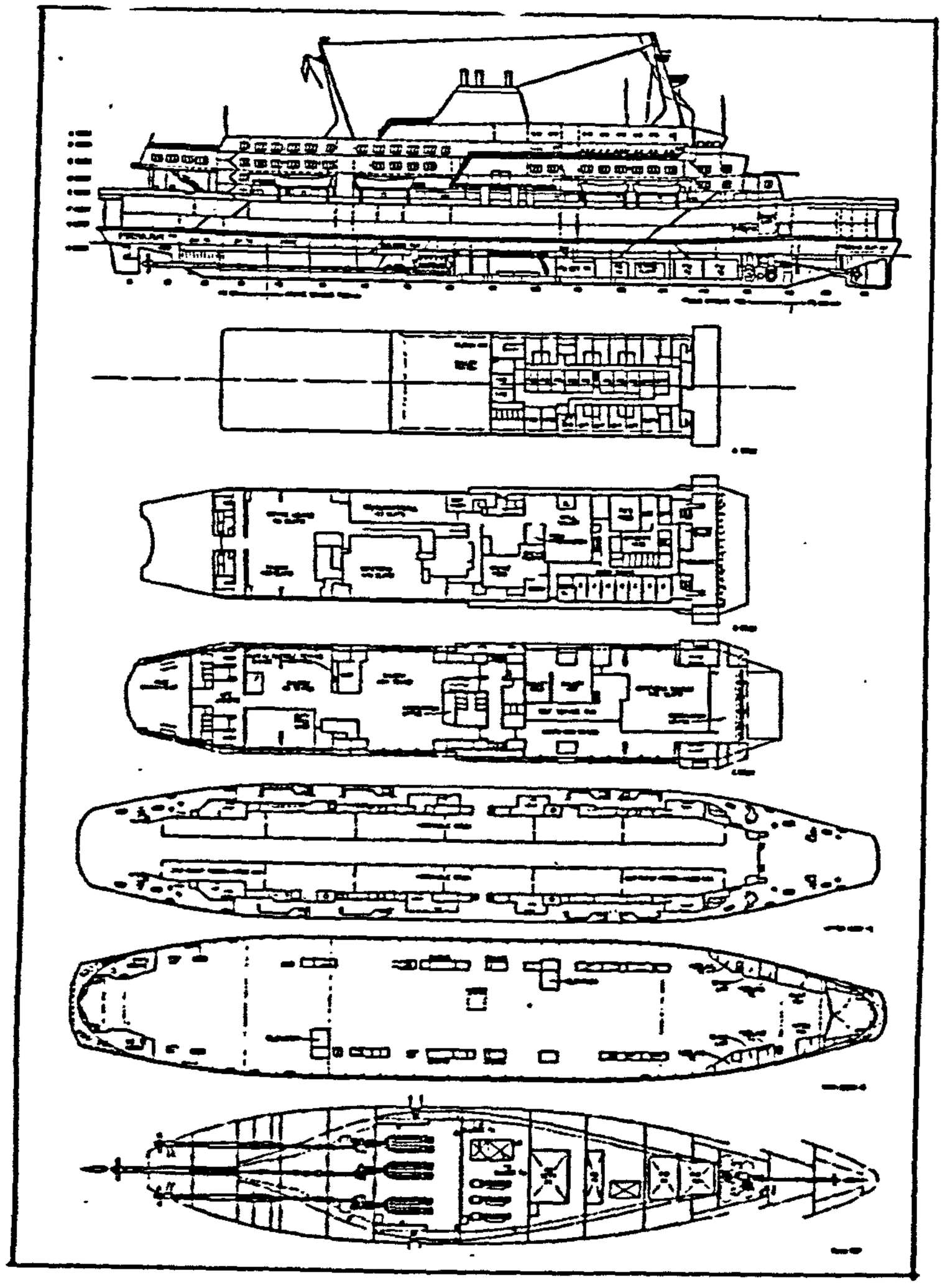

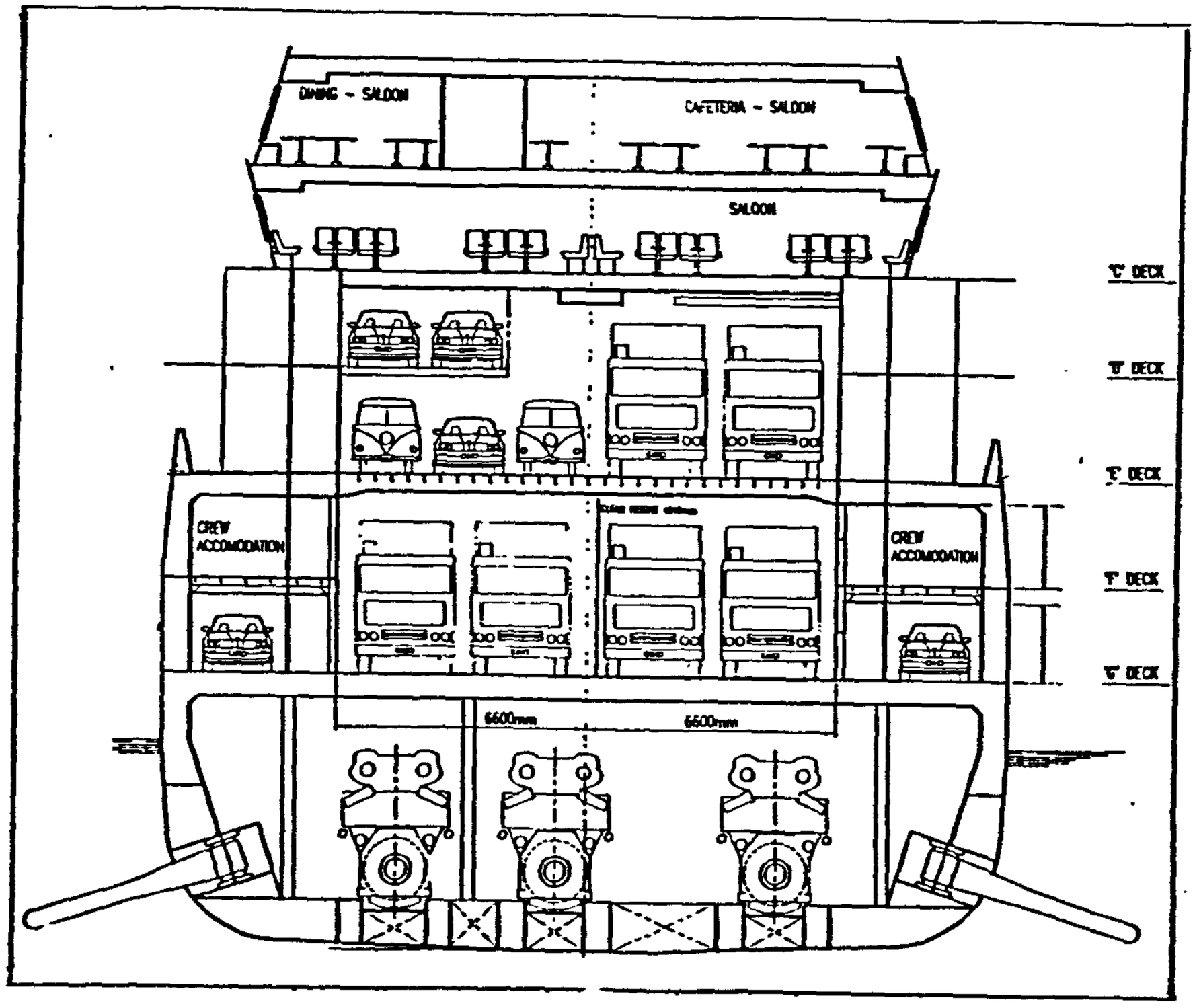

Fig 3.4 General arrangement of a typical short crossing ferry

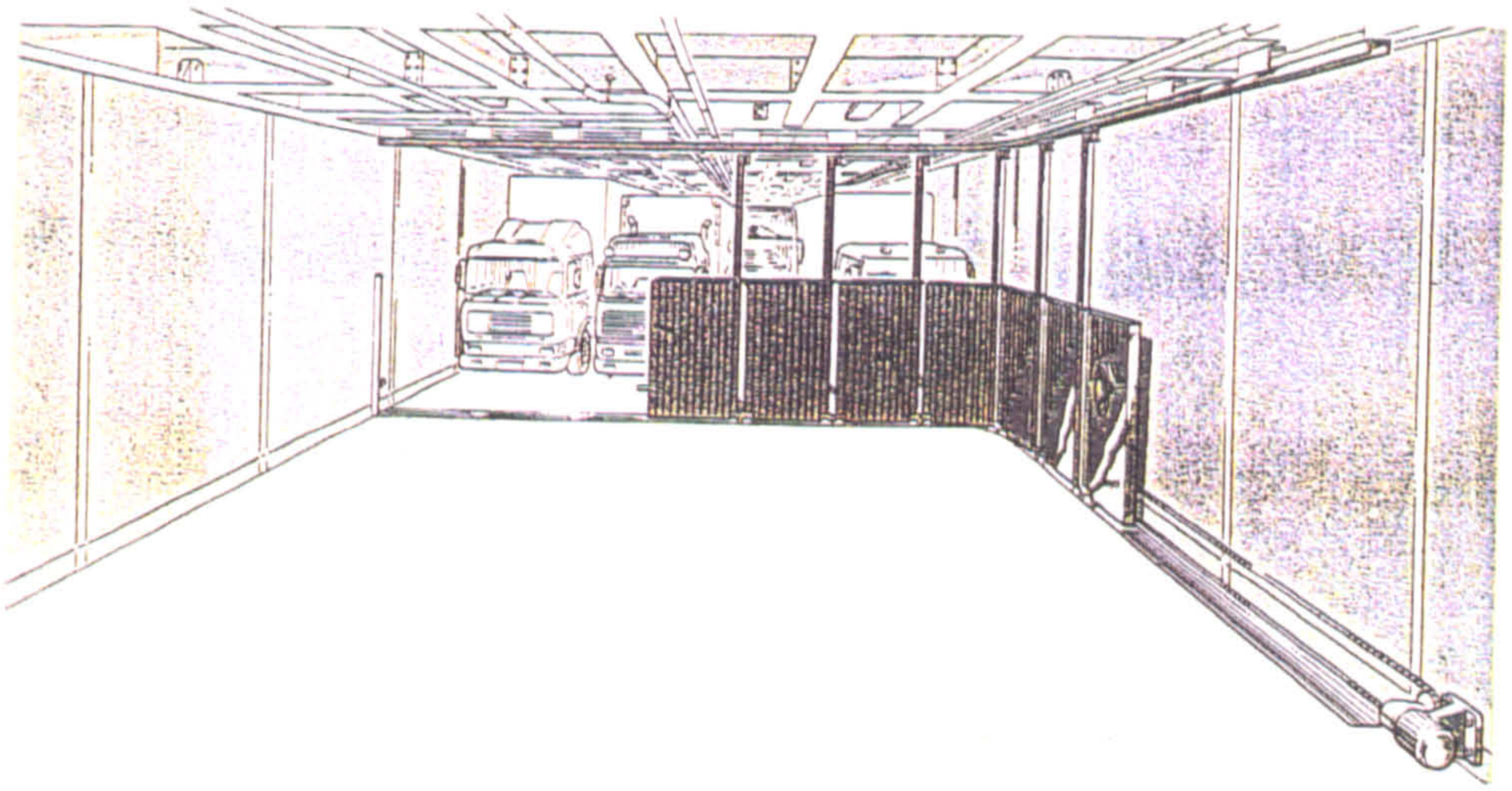

Fig 3.5A Retractable transverse barrier [36]

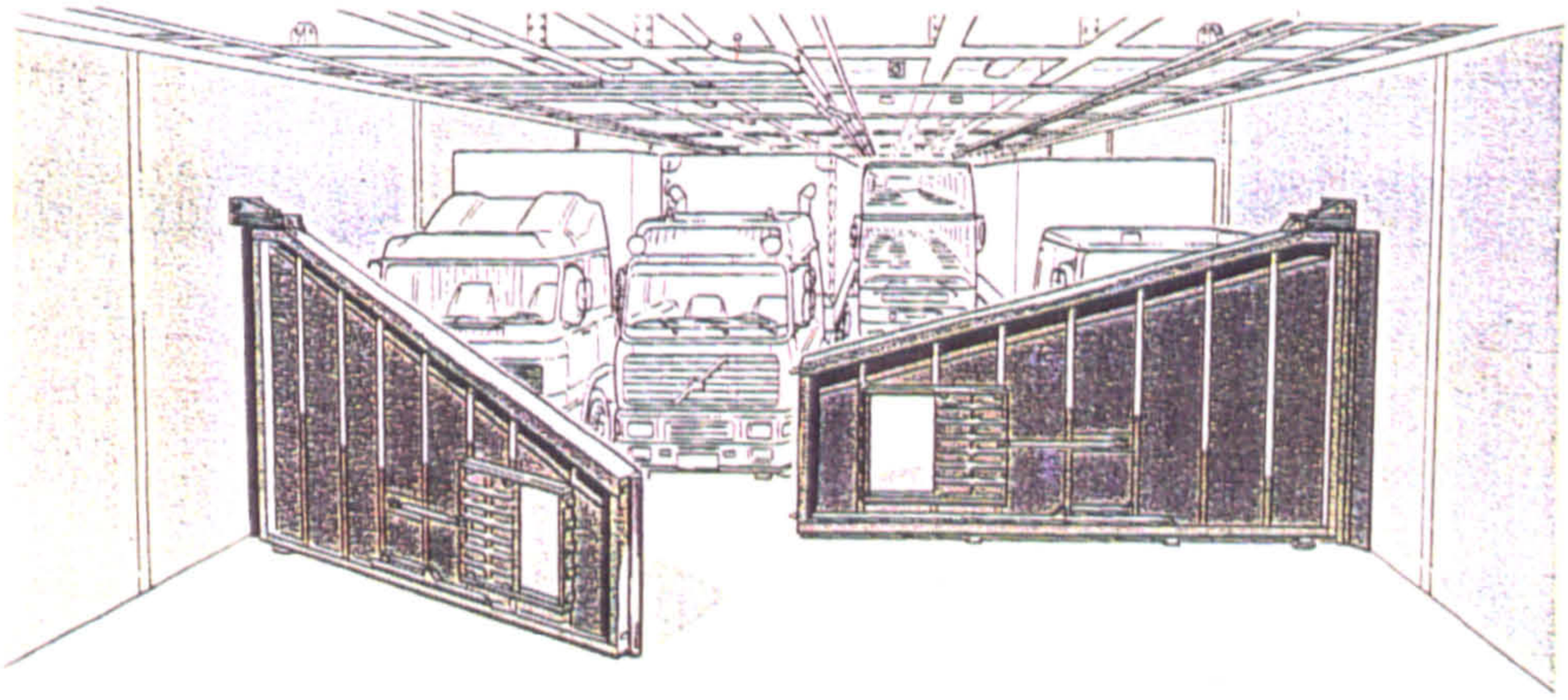

Fig 3.5B Retractable transverse barriers [36]

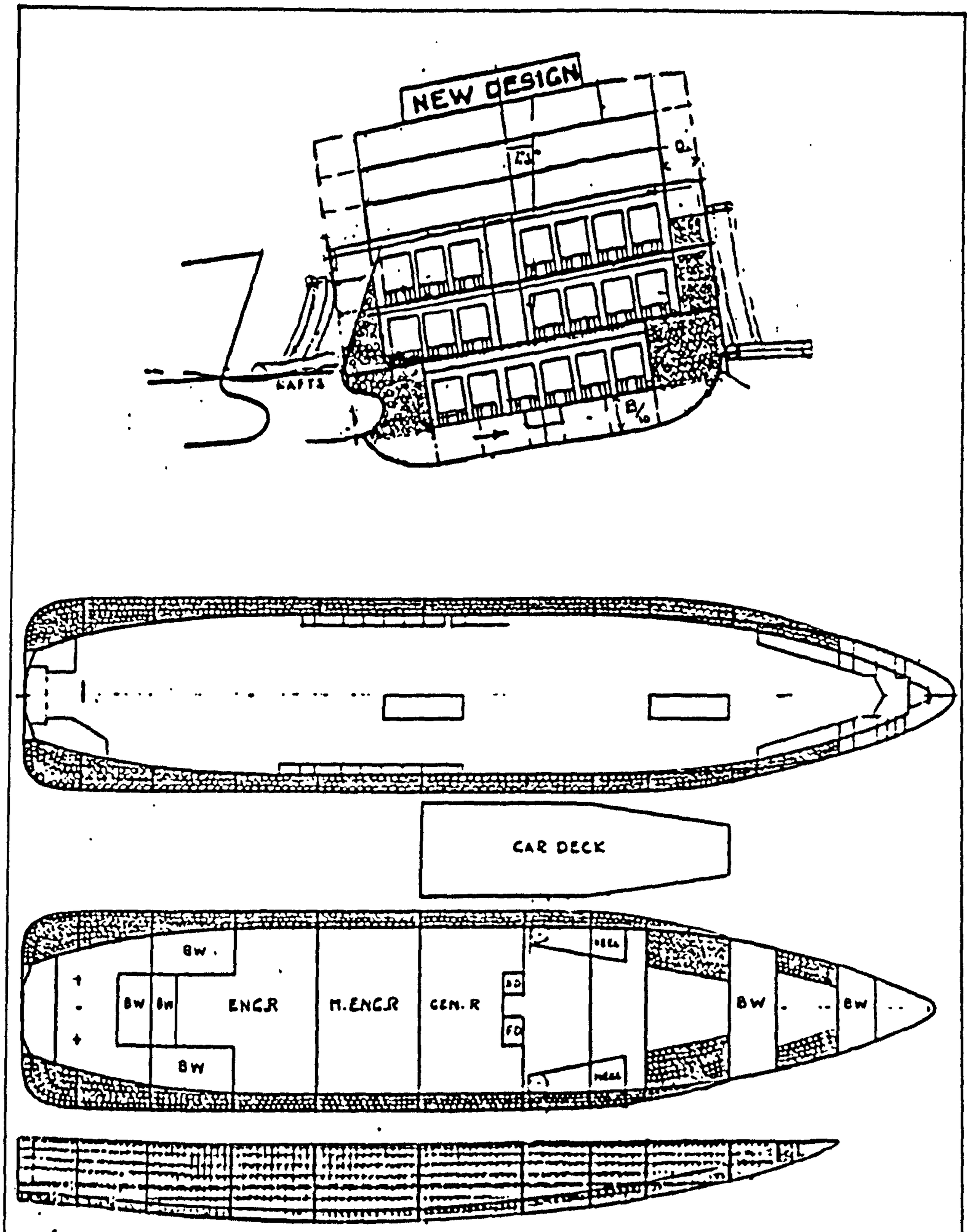

Fig 3.6 Side tanks filled with polythene drums to provide permanent buoyancy against flooding [37]

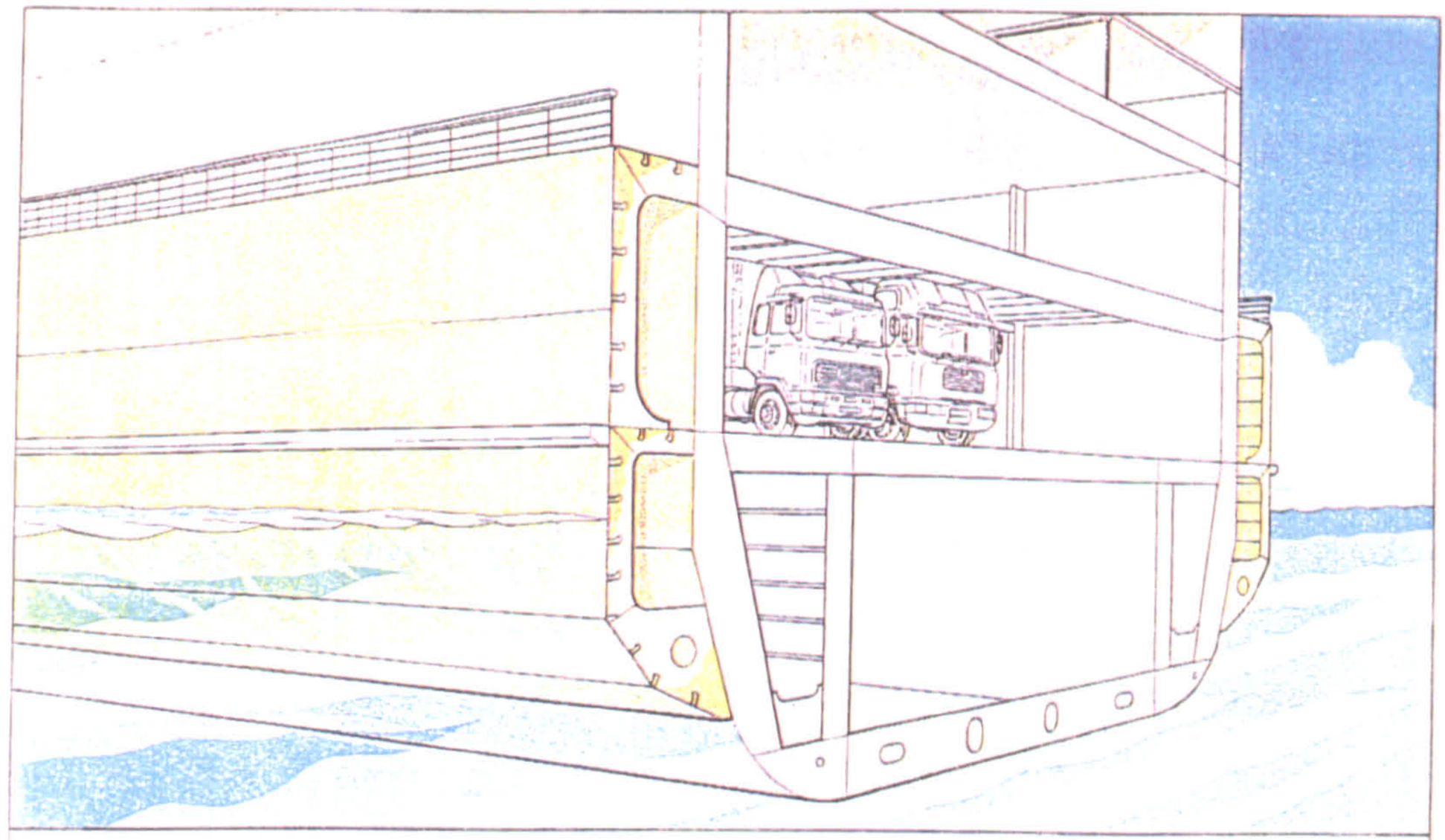

Fig 3.7 Structural side sponsons [36]

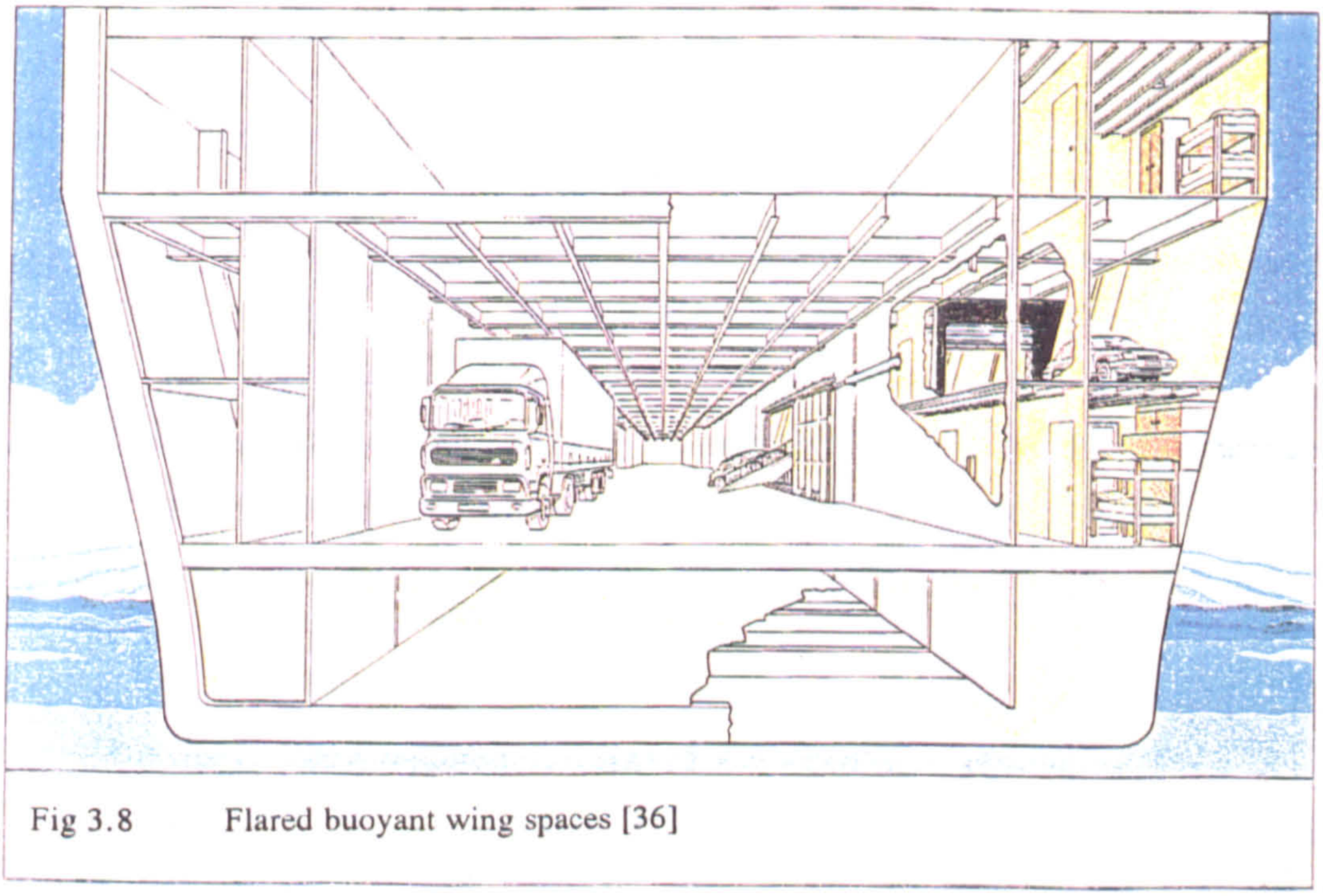

Fig 3.8 Flared buoyant wing spaces [36]

CHAPTER 4: ADOPTED APPROACH

4.1 GENERAL

Present damage stability assessment is concerned with only residual static stability represented by residual GM, GZ, as well as freeboard. Damage statistics, however, show that passenger ships, especially Roll on-Roll off ships (ferries), capsize or sink within a very short time even though their stability parameters meet damage stability requirements. This proves that there are other parameters which affect ship stability. Research carried out also shows that the environmental parameters which create dynamic excitations are very dominant on ships, and suggests that the damage stability of ships should be considered as a dynamic problem instead of a static one.

In addition, there are some parameters other than environmental which are found to have an effect on damage stability. These include progressive flooding, asymmetric flooding, flooding of the main vehicle deck, accumulation of water and shifting cargo.

In order to achieve success in developing realistic damage stability regulations for ships, the first step is to adopt a new approach to investigate the capsizing and damage stability. This approach must include all the important parameters influencing dynamic damage stability in the most meaningful way. Secondly, an extensive investigation must be carried out to identify the key parameters and to form new stability regulations. For this purpose representative damage scenarios must be modelled and a computational procedure developed.

4.2 DYNAMIC ANALYSIS

In order to develop a realistic model which includes the dynamic effects mentioned above, it is not just a matter of including everything, but also most importantly how to incorporate and combine all these effects in the most meaningful way. For the

dynamic analysis, the approach adopted and the parameters taken into account in the modelling, are explained below.

4.2.1 Time Simulation Approach

Damage and flooding are continuous phenomena which may lead to different results depending on the parameters used. Investigating the behaviour of ships in different conditions would certainly help to provide a better understanding of the capsizing phenomenon and to develop a realistic damage stability assessment procedure. In order to take into account non-linearities, changes in excitation forces, progressive flooding and responses of the ship in time, there is a need to adopt time simulation modelling. Time simulation with small steps gives a very clear picture of what is happening.

The time simulation process starts from the beginning of flooding when the initial condition of the ship is known. At each time step, different parameters such as the amount of water inflow, heel, displacement, excitation forces and response amplitude of the ship's motions can be examined in detail. This process continues until either capsizing occurs or the total time allowed for simulation is used up.

4.2.2 Motions

As is common knowledge, the static and dynamic stability of a ship depend on its heeling or rolling motion. This heel or roll angle is itself used as a criterion which is considered by intact and damage ship stability assessments. However, in a real environment there are other motions which effect the ship's stability and roll motion, directly or indirectly.

For a ship at the upright condition, there is no dynamic coupling between roll and heave motion, but at an inclined condition there may be a strong coupling between the same motions due to asymmetry. However, the most important effect of heave motion is the non-linear coupling between roll and heave due to changes in restoring forces and moment. This occurs due to the significant changes on the instantaneous underwater volume of the ship which becomes more vital in the case of large amplitudes. Another effect of heave is that it

may cause water to flood in if the ship's main deck submerges due to large heave amplitudes.

The coupling between sway and roll is well known and this may be strong enough to exacerbate the ship's roll. Especially in a damaged condition, even a few degrees of roll amplitude due to sway may be enough to flood the areas above the waterline.

Of course there are other motions which may affect roll motion, however, it is believed that these effects are small enough to be ignored. The only other effect may come from pitching or more precisely trim due to the water flooding the ship. In the case of beam seas, pitching is usually small and thus it can be ignored, but trim is considered to be vital for stability and its effect is taken into account.

Due to the reasons explained above the mathematical model is developed by taking into account coupled sway, heave and roll motions together with instantaneous sinkage and trim.

4.2.3 Forces and Moments

It is assumed that the cause of ship motions derives from wave and wind excitation, as well as the internal conditions of the vessel and its cargo such as flooding, water accumulation on deck or shifting of cargo. The latter excitations originate of course, from wave and wind effects. In response to these excitation forces the ship produces reaction forces such as hydrostatic (restoring), hydrodynamic (added mass and damping) and inertial which depend mainly on characteristics of the ship. The following sections explain how these parameters are determined.

i- Wave and Wind Excitation Forces

Waves may be considered as regular or irregular, but in this thesis regular waves are taken into account in the investigations undertaken. In addition, although the mathematical model can handle waves from any direction, only beam waves are considered in this study. Wave excitation forces and moments (Froude-Krylov and Diffraction) are calculated by using a two dimensional method using integral

equations. Firstly, sectional forces are calculated and these are then integrated along the ship's length to obtain the total forces and moment.

Wind force and moment are calculated by using the wind pressure over the projected area, the pressure changing as the square of the wind speed. It is assumed that wind is coming from the beam and that wind speed is constant during the simulation time for each case examined.

ii- Hydrodynamic Coefficients

The hydrodynamic coefficients are very important in estimating ship motions by theoretical and experimental methods. The theoretical method used in this thesis to estimate the hydrodynamic coefficients (added mass and damping) is based on two dimensional linear potential theory and thus it does not include viscous effects. In addition, the ship is assumed to oscillate with small amplitudes to satisfy the linear theory requirements. This may affect the prediction of ship motions, especially the roll motion significantly. The estimation of roll damping, in particular, is quite difficult because it is significantly affected by fluid viscosity. Ikeda's semi-empirical roll damping calculation method, which includes viscous effect and has been shown to give good results for symmetric ships and moderately large amplitudes, is used for the estimation of roll damping [39].

However, since the aim should be to include non-linearities as much as possible, it is necessary to investigate the effect of large amplitude motions and static heel on hydrodynamic coefficients, especially coupling coefficients. If the experimental and the theoretical results differ, the difference may be accounted with empirical formulae, so that the theoretical approach can be used for all types of ships. In order to investigate the validity of the theory for an asymmetric ship oscillating with large amplitudes, an experimental technique is presently developed. An experimental mechanism is designed and the analysis carried out by considering the non-linearity in the restoring

forces due to large amplitude motions. This investigation is explained in detail in Chapter 6.

iii- Restoring Forces

In order to take into account the non-linearity in the restoring forces, which result from large amplitude motions, they are calculated instantaneously at each time step. This is accomplished by calculating the underwater volume of the ship up to the free surface at each time step and by taking into account instantaneous roll and heave motions. Free surface in the calculations can be defined either by taking into account the calm water or the wave profile.

When the wave profile is taken into account, the resultant force is not purely the restoring force but the combination of restoring and hydrostatic wave excitation force, which is called static Froude-Krylov force [23, 30]. This force is a result of the undisturbed wave profile.

Application of restoring force together with static Froude-Krylov force is still fraught with problems, which may be due to the limitation with the mathematical modelling. Furthermore it creates inconsistency between the calculation approaches of hydrodynamic properties of the ship (i.e Wave excitation forces are calculated up to the exact free surface, but added mass and damping properties of the ship can be calculated only up to the calm water surface).

Application of the integration of the pressure up to the exact free surface proves to be giving good results for following waves [23, 24, 30] but seems to fail for beam seas since the results of ship motions appear to be overestimated [32], [further discussion is given in Chapter 5]. Due to the uncertainties and limitations during the analysis, the free surface is presently defined by considering the calm water level.

4.2.4 Flooding

Flooding can be defined in two ways, each serving a different purpose. Firstly, by assuming that there is a constant rate of flooding

at each time step and that the total amount of water can be predefined. Secondly, by taking into account the instantaneous relative water elevation at the damage location, which is probably the more realistic method. For certain environmental and loading conditions, the second method determines whether water floods in or not and continues until the ship either capsizes or the predefined period for time simulation period is used up.

The main aim of this thesis is to study the effects of water on ship rather than determining the possibility of water inflow, which is determined by the second method. In addition, although the second option is the more realistic for water ingress, there are still a number of uncertainties associated with the second method such as the effects of wave, its direction and height, and ship motions on the water ingress, location and extent of damage etc. Considering the first option of water ingress is presently used in the parametric investigations.

4.2.5 Accumulation of Water and Sloshing

The entrapped water on deck poses stability problems and contributes substantially to capsizing, especially on a large deck like those found on Roll on-Roll off ships. The effect of water could be of either static or dynamic nature. A limited investigation of water sloshing is carried out by using a two dimensional potential flow theory in a rectangular tank [Appendix A.2]. At present the accumulation of water is included in the equations of ship motions in a static sense, by taking into account the instantaneous amount of water on deck, roll and trim. Sloshing, which may be important, depends on the frequency of the ship roll motions and can be considered within certain limits if the preliminary investigations prove it is an important factor, within the usual frequency range where large motions of ferries occur.

4.3 PARAMETRIC STUDY

The parametric study is a most essential part in developing a new approach, aimed at understanding the reasons behind capsizing, damage stability problems or at establishing relationships between

different parameters, leading to the proposal of an alternative solution to the existing damage stability problems.

The parametric study comprises two parts. The first part consists of an investigation on static and quasi-dynamic stability analyses of 10 ships at both intact and damaged conditions. The purpose of this investigation is to group similar problems which can be identified by using these assessments, to examine the inadequacies of these assessments and finally to compare the proposed dynamic assessment against these. To carry out this study, existing static and quasi-dynamic assessments for intact ships are modified to accommodate damage stability calculations.

The second part of the parametric study consists of dynamic damage stability analyses. This part investigates the effects of certain parameters which are assumed to be relevant to the damaged ship stability. These parameters are mainly related to the excitation sources and to ship particulars, as well as to the loading condition of the ships.

The investigation addresses a range of parameters known or expected to play a key role, including: wave height and length, wind, progressive flooding, accumulation of water, ship motions, coupling effects and the ship and damage particulars, such as location and extent of damage, length of compartment flooded and loading conditions. Both excitation and ship parameters are investigated systematically over a wide range, so that the most important parameters and their limiting values can be identified. The information obtained from the investigation, using a time domain procedure forms the basis for developing the stability assessment procedure.

4.4 JUSTIFICATION OF THE ADOPTED APPROACH

Most of the theoretical approaches developed in ship stability research are concerned with examining the stability of the developed equations of motion with little success having been achieved so far in linking mathematical stability to practical ship stability.

In addition, recent advances in non-linear system dynamics have demonstrated quite clearly that in many cases in examining the dynamic behaviour of non-linear systems, it is more important to include all the factors known to be important, even approximately, than aiming at improving the accuracy of a limited number of factors.

Based on the above two arguments, the present approach attempts to incorporate all the key factors known or expected to play an important role in affecting the dynamic behaviour of a damaged ship in realistic environmental conditions, each one estimated as accurately as the state of the art allows. Furthermore, emphasis is placed on practical ship stability; in understanding how capsizing occurs, what causes it, which conditions are dangerous, how ship survivability can be enhanced and how it can be assessed.

In other words what might be termed rigorous approach is substituted by a vigorous approach where engineering intuition and experience, as well as understanding of the physical phenomena involved in extreme vessel behaviour, are called upon to pave the way for progress in the subject of ship damage stability.

CHAPTER 5: MATHEMATICAL MODELLING

For ease of approaching the modelling of a complex problem, such as the dynamic behaviour of a damaged ship in a realistic environment, the mathematical modelling is structured on the basis of the main contributing effects which can be grouped as follows:

1- Hydrodynamic effects (wave excitation and hydrodynamic reaction).

2- Hydrostatic effects (restoring forces and moment).

3- Flooding effect (water ingress and flooding).

4- The above effects are incorporated in the formulation of the ship motions in the time domain, which comprises coupled sway, heave and roll.

First, however, the co-ordinate systems used in the above calculations are defined.

5.1 CO-ORDINATE SYSTEMS

In the development of the mathematical modelling three different co-ordinate systems are used and these together with the associated sign conventions are defined as follows:

The first, is the ship co-ordinate system (oxyz), which is used to define the ship's hull and is located at the keel level of the centreplane amidships as shown in Fig 5.1a. In this system, x is positive forward; y is positive to starboard; and z is positive upwards.

The second co-ordinate system ($O_eX_eY_eZ_e$), the earth co-ordinate system, is used to calculate the underwater volume and parameters related to it. $O_eX_eY_eZ_e$ is located at the calm water level of the centreplane amidships as shown in Fig 5.1a. When there is no heel or

trim, the wave co-ordinate system has the same directions as those for the ship co-ordinate system.

The third co-ordinate system ($O_{ge}X_{ge}Y_{ge}Z_{ge}$) is located at the centre of gravity G and the directions are parallel to the earth system. The third co-ordinate system is used to measure ship motions. Since it is assumed that the ship rotates around the centre of gravity, all rotational motions, excitation and restoring moments are calculated with reference to it (Fig 5.1b). Anti-clockwise roll motion, upwards heave in the z direction and starboard sway in the y direction are defined as positive motions.

5.2 HYDRODYNAMIC FORCES

Within the context of linear theory, the hydrodynamic oscillatory forces of a ship in waves can be represented by the linear summation of the wave excitation forces, Fw, due to wave motion and radiation forces, F_R, due to the vessel's motion response.

Although three dimensional effects are anticipated, it is assumed that the length of the ship is much greater than the beam and draught such that the hydrodynamic interaction in the longitudinal direction can be neglected. Under this assumption strip theory is used to formulate the above mentioned force components for a number of ship sections, and then integrated along the ship length to obtain the total component force.

The wave excitation forces can be separated into two: Firstly, the Froude-Krylov forces which are caused by the undisturbed incident wave when it passes through the ship, assuming that the ship is not there; secondly, the diffraction forces which are caused by the hydrodynamic disturbance due to the presence of the ship.

Motion induced hydrodynamic forces (Radiation) are assumed to consist of two components which are in phase with the acceleration and velocity of oscillations, the added mass and damping terms, respectively.

In evaluating the above mentioned forces, the strip theory was utilised in combination with the two-dimensional wave source distribution technique known as Frank-Close-Fit Method. The theory, development and computational application of this well established solution can be found in detail in published literature [20, 40, 41, 70].

The total velocity potential of the fluid motion, generated by regular waves with the stationary ship section undergoing small amplitude oscillation, can be described by the time dependent potential

$$\Phi(x,y,z,t)=\Phi_I(x,y,z,t)+\Phi_D(x,y,z,t)+\Phi_R(x,y,z,t) \quad \text{[Eq 5.1]}$$

Φ_I, Φ_D and Φ_R are the incident, the diffracted and the radiated wave potentials, respectively.

In order to define the above mentioned potentials, certain boundary conditions are imposed and the problem is solved as a boundary value problem in the presence of these conditions. The solution can be separated into well known problems in association with the diffraction and radiation components which would yield the wave excitation forces and added mass/damping coefficients respectively.

Definition of these boundary conditions and solution of the potentials are summarised in Appendix A.1 for completeness.

5.2.1 Wave Excitation Forces.

i- Regular Waves

As mentioned above, the two dimensional source and sink method is based on sinusoidal waves. Having obtained the velocity potential for the incident and diffracted waves, the pressure distribution around a cross section can be calculated from the linearised Bernoulli equation as follows:

$$p^{(i)}=-\rho\frac{\partial\Phi}{\partial t} \quad \text{[Eq 5.2]}$$

where :

p : Hydrodynamic sectional pressure

ρ : Density of water

i : Mode of motion, 2,3 and 4 are for sway, heave and roll, respectively

Sectional excitation forces can be obtained by integrating the pressure as shown below:

$$f^{(i)} = \int_s p^{(i)} n^{(i)} ds \qquad \text{[Eq 5.3]}$$

where

$n^{(i)}$: Direction cosines of the outward normal vector for each mode of motion, i

If these sectional forces are integrated along the ship length the total wave excitation forces for the particular condition (frequency, wave direction, height) can be evaluated. Details of this application can be found in Appendix A.1, while development of the theory and the computational solution can be found in [20, 42, 70].

ii- Irregular Waves

In order to represent the North Sea wave environment, the JONSWAP spectrum is used. This spectrum is introduced in an attempt to take into account the higher peaks of spectra in a storm situation for the same total energy as compared to the Pierson-Moskowitz spectrum [71]. The JONSWAP spectrum represents the wave condition in a fetch-limited sea. The incorporation of the peak enhancement factor, γ, helps to model the worst case spectra encountered during a typical storm. The JONSWAP spectrum can be represented as shown next:

$$S(\omega) = \alpha\, g^2\, \omega^{-5}\left(-1.25\left(\frac{\omega}{\omega_m}\right)^{-4}\right)\gamma^a \qquad \text{[Eq 5.4]}$$

In order to generate the force spectrum for a given sea state and frequency range, firstly the maximum excitation force amplitude per

unit wave amplitude for each mode of motion is calculated at a number of frequency intervals within the frequency range considered. Maximum force amplitudes are calculated using exactly the same method, which is used for the calculation of the excitation force for regular waves, as explained in the previous section.

The discrete component of a force spectrum at a given frequency and sea state can be calculated by using spectral techniques i.e.

$$FS(\omega) = (FRAO(\omega))^2 \; S_W(\omega) \qquad \text{[Eq 5.5]}$$

where:

$S_W(\omega)$: Sea spectrum component at a given frequency

$FRAO(\omega)$: Force for per unit amplitude at a given frequency and mode of motion

In order to generate the force spectra for the specified range of frequencies, the same calculations must be repeated for each frequency interval, which is chosen as 0.05 rad./sec. For a given sea state, the force amplitude at a particular frequency is obtained by using the following expression:

$$FAMP(\omega) = \sqrt{2 \; FS(\omega) \; d\omega} \qquad \text{[Eq 5.6]}$$

$d\omega$: Frequency interval

Having obtained the force amplitudes over the frequency range of interest, wave height and mode of motion, the force amplitudes in the frequency domain are transformed to a random wave realisation in the time domain. This is done by using standard Fourier Analysis techniques as indicated below:

$$FREAL(t) = \sum_{i=1}^{k} FAMP(\omega_i) \; Cos(\omega_i t + \varepsilon_i) \qquad \text{[Eq 5.7]}$$

k : Number of frequency intervals

ε : Random phase angle

This calculation is carried out for each time step for the predefined simulation time. Random wave realisations (WREAL) used in time simulation are derived in a similar manner.

$$WA(\omega_i) = \sqrt{2\, S_W(\omega)\, d\omega} \qquad \text{[Eq 5.8]}$$

$$WREAL(t) = \sum_{i=1}^{k} WA(\omega_i)\, Cos(\omega_i t + \varepsilon_i) \qquad \text{[Eq 5.9]}$$

Details of this procedure can be found in [43].

5.2.2 Hydrodynamic Coefficients

In order to calculate motion induced forces (added mass and damping), the radiation velocity potential (Φ_R) is calculated at each section using again the Frank-Close-Fit method as in the estimation of diffraction forces. Finally, sectional added mass and damping are integrated along the ship to obtain the corresponding coefficients for the vessel. Details are given in Appendix A.1, while the theory and application of this method can be found in [20, 41, 42, 70].

i- Roll Damping

Because of its geometry and relatively weak restoring characteristics in the roll mode, a conventional ship is sensitive to the excitation in this mode. In particular, when the roll motion is large, the estimation of roll damping becomes difficult due to other effects eg. the fluid viscosity, presence of the bilge keels etc. Therefore, the method for the estimation of roll damping based on only potential theory is not satisfactory. The necessity for a correct prediction of roll motion urged researchers to find better methods for estimating roll damping leading to different approaches, which can be found in the literature. Amongst these, the method used to predict equivalent linear roll damping which was developed by Ikeda [39] is one of the most commonly used. This method is a semi-empirical solution taking the characteristics of the vessel into account and is reported to be

reasonably accurate up to moderately large amplitudes. According to this method, which is used in this study, the total roll damping can be represented as follows:

$$B_{44} = B_f + B_e + B_w + B_{b\text{-}k} + B_l \qquad \text{[Eq 5.10]}$$

Where:

B_f : Frictional damping
B_e : Eddy making damping
B_w : Wave damping
$B_{b\text{-}k}$: Bilge keel damping
B_l : Lift damping

Since the calculation is carried out at zero speed, lift damping is neglected. However, Ikeda's method was originally developed for symmetric ship hulls, therefore the damping value may have to be corrected if the static heel due to damage is very large. This may be done by applying a correction factor which may be evaluated by means of model experiments.

ii- Estimation of the Mass Moment of Inertia for Roll

A moment of inertia is the sum of all the component parts comprising ship mass, such as machinery, structural parts, etc., each multiplied by the square of its distance from the axis about which the moment is taken. However, it is very difficult to calculate inertia in this way and it involves too much work. As an approximation the roll inertia can be described as the total ship mass times the square of an ideal distance called radius of gyration. This can be estimated by carrying out rolling experiments. It is also customary that, in the literature the radius of gyration for roll (i_{44}) is expressed as a percentage of the ship's breadth i.e.

$$i_{44} = C_r \; B \qquad \text{[Eq 5.11]}$$

The coefficient for radius of gyration (C_r) value is almost constant for a great variety of ship types [44]. For practical applications the value of C_r values gained from experience as reported in [44], attains the following values :

$0.335 < C_r < 0.425$ i.e.

For large passenger ships $C_r = 0.425$

For warships $C_r = 0.38–0.40$

Therefore, for calculations in this study the moment of inertia of the intact ship is taken as:

$$I_{xx} = (i_{44})^2 \Delta \qquad \text{[Eq 5.12]}$$

where:

$i_{44} = 0.42\ B$

In the case of a damaged ship the inertia of the flooded water has to be included in the total inertia term. This can be done as shown:

$$I'_{xx} = I_{xx} + M_f\, DC^2 \qquad \text{[Eq 5.13]}$$

where:

M_f : Mass of flooded water

DC : Distance between the centre of volume of the flooded water and the centre of rotation.

In this approximation, the moment of inertia of the flooded water with respect to its own axis is neglected. The roll mass moment of inertia is calculated according to the co-ordinate system, which is passing through the centre of gravity and is fixed to earth ($O_{ge}X_{ge}Y_{ge}X_{ge}$). In the case of a static heel angle, the roll mass moment of inertia will not change due to the static heel.

iii- Ship Mass

The ship mass changes instantaneously in case of flooding and the total amount of water inflow in the damaged compartment is added to the total mass of the ship.

5.2.3 Wind Forces

The wind heeling force and moment exciting the ship, due to the wind pressure, is expressed in the same form recommended by the weather criteria [45]. The wind heeling force and moment in the upright position is therefore,

$$F_{wind} = 0.5\ \rho_w\ C_d\ A_p\ V^2_w \qquad \text{[Eq 5.14]}$$

$$M_{wind} = 0.5\ \rho_w\ C_d\ A_p\ H_{wm}\ V^2_w \qquad \text{[Eq 5.15]}$$

where;

ρ_w : Density of air($1.25\ 10^{-4}$ t/m^3)

C_d : Drag coefficient(1.22)

A_p : Lateral projected area of vessel above the free surface(m^2)

V_w : Relative wind velocity(m/sec)

H_{wm}: Wind moment arm between the centre of lateral area and half the mean draught

A constant wind speed of 26 m/sec is taken, corresponding to the value at the reference height of 10 m above the calm water surface. In reality the wind velocity varies as a function of height above the sea level and this can be accommodated in the calculation.

The ship profile above the waterline is divided into a suitable number of horizontal strips and the wind pressure is calculated for each strip and integrated along the ship height to find the total wind pressure. This calculation can be formulated as follows:

$$F_{wind} = 0.5\ \rho_w\ C_d \sum_{i=1}^{n} A_{pi}\ V^2_{wi} \qquad \text{[Eq 5.16]}$$

$$M_{wind} = 0.5\ \rho_w\ C_d \sum_{i=1}^{n} A_{pi}\ H_i\ V^2_{wi} \qquad \text{[Eq 5.17]}$$

where:

$$V_{wi} = V_w \left(\frac{H_{wmi}}{H_{wm}}\right)^{1/m} \qquad \text{[Eq 5.18]}$$

$$m = H_{wm}\left(\frac{\sqrt{H_{wmi}^{\,2}}}{Z_0}\right)$$

$$Z_0 = 7.31\ 10^{-7}\ V_w^2 + 8.68\ 10^{-8}\ V_w^3 \qquad \text{[Eq 5.19]}$$

V_w : The wind velocity at the reference height

However, research carried out on wind effects indicate that the wind moment decreases as the heel angle increases. Therefore the roll dependent wind moment can be expressed as recommended by Wendel [46], Kinoshita [47] and applied by Strathclyde University [30, 31] :

$$M_{wind}(\phi) = M_{wind}\ (0.25 + 0.75\ \mathrm{Cos}^3\phi) \qquad \text{[Eq 5.20]}$$

and the force

$$F_{wind}(\phi) = F_{wind}\ (0.25 + 0.75\ \mathrm{Cos}^3\phi) \qquad \text{[Eq 5.21]}$$

where ϕ is the heel angle.

5.3 RESTORING FORCES AND MOMENT

These forces and moment are hydrostatic in nature with a tendency to bring the ship back to its original position after a disturbance, and are related to the underwater volume of the ship. They are calculated by integrating the hydrostatic pressure up to the relative free surface as shown below:

$$F(t) = \int_L \int_s p_S\ n\ ds\ dx \qquad \text{[Eq 5.22]}$$

where

p_S : Hydrostatic pressure

n : Direction cosines of the normal vector

In linear theory, the heave restoring force is represented as a function of waterplane area, while the roll restoring moment is represented as a function of the transverse metacentric height (GM) in the static

equilibrium condition (calm water). However, in a non-linear approach, these parameters are calculated by using the actual instantaneous underwater volume of the ship and the pressure can be integrated either up to calm water level or up to the instantaneous water surface (wave elevation). If integration is done up to the wave surface the force obtained, which contains not only restoring force but also static wave excitation force, is called the static Froude-Krylov force [23, 30]. The pressure and associated limits are as shown.

$$p = \rho g z \quad ; \quad \infty < z < 0 \text{ or } \eta \qquad \text{[Eq 5.23]}$$

where z is water depth and η is wave elevation.

In recent years integrating the pressure up to the instantaneous water surface has been reported to produce more realistic results when the ship with forward speed is in following waves and wave length/ship length ratio is around 1 [23, 24, 30]. However, certain researchers report that this approach does not give satisfactory results for all conditions especially in beam waves and there is an uncertainty regarding the appropriate expression of the pressure above the calm water plane [32, 48]. Furthermore, Kobylinski emphasizes that in beam seas, as the non-linearity increases and because of incomplete definitions of some effects, the problem becomes more complex and the reliability of complex solutions becomes questionable [49]. Some preliminary investigations regarding the effect of integration up to exact free surface in this study also indicated that in beam seas the response of the ship, in the case of restoring force, calculated up to exact free surface, is overestimated considerably compared to the experimental results, while calculation of the restoring force up to calm water produced good results compared with the experimental results.

In a fully dynamic solution an equation of motion in time domain can be written as:

$$(I_i + A_i)\, x_i(t)'' + B_i x_i(t)' + C_i x_i(t) = F_i(t) \qquad \text{[Eq 5.24]}$$

Usually in this equation, added mass(A) and damping(B) coefficients are calculated in calm water and kept fixed during the simulation, while the restoring parameter, Cx, can be replaced with a non-linear restoring term which is calculated up to the calm water or the free surface instantaneously. However, calculation of restoring force up to instantaneous water surface may lead to inconsistencies and inaccurate results for some conditions unless certain non-linearities and some other effects (higher order wave excitation, non-linear coefficients) are fully taken into account. Moreover, within the limits of linear theory or other methods, inclusion of such effects even if this is possible, may become very complex, difficult and unreliable [32, 49]. Therefore, unless the same approach is used for the calculation of all relevant effects, and all non-linearities are included, it is believed that calculations must be carried out based on more established methods which provide more consistent and reliable results for achieving the objectives of this study.

If it is decided to calculate these forces up to the free surface, one has to face the complexities of these calculations, since linear theory limits may have to be violated or stretched. For instance, Fujino [50] calculated the hydrodynamic coefficients for the time varying submerged portions at each time step by using the extended strip theory synthesis. In his approach, wave profile is included in the calculations by defining average wave surface, which is a straight line across the section and at the midpoint between the instantaneous wave crest and trough. A similar approach was suggested and applied by Söding and Böttcher [72, 73]. In addition, they also tried to implement the hydrodynamic coefficients independent of frequency for irregular seas in time simulation, however they found that preparing the input data for these applications in the time simulation program was a very lengthy and difficult task.

Denise [32], who tried to introduce high order wave effects to estimate the large amplitude motions of an ocean-going barge, finds that especially near natural roll frequency of ship, integration up to exact free surface overestimates the roll motion. He indicates that,

unless consistency is provided for the calculation of all hydrodynamic forces (excitation and radiation forces), introducing higher order wave theory may not improve the accuracy of the results. He also feels that radiation and diffraction forces based on small motions theory cannot be applied to large amplitude motions and suggests that these forces must be varied with regard to instantaneous submerged volume. He applied this approach by varying the radiation and diffraction as the ratio between the instantaneous underwater volume of the ship (V) and the submerged volume of the ship at rest (V_0), and indicated that this approach improves the results considerably.

Since only beam waves are considered in this study, and the inclusion of the wave profile in the restoring calculation is not well established, hence it may lead to some inconsistency and inaccuracy, in order to include the non-linear restoring forces and moments, which result from the large amplitude motions, restoring terms are calculated instantaneously up to the calm water by taking into account the instantaneous heave and roll motions. Although integration up to the exact water surface is available in the developed computational model, it is excluded from the calculations in this study. Thus, the non-linear restoring is calculated as shown.

$$RES\_HEAVE(t,X_3,\theta,X_4) = g\,[\Delta(t,X_3,\theta,X_4)-\Delta(t_0)] \qquad \text{[Eq 5.25]}$$

$$RES\_ROLL(t,X_3,\theta,X_4) = g\,\Delta(t,X_3,\theta,X_4)\,[TCG_s-TCB(t,X_3,\theta,X_4)] \qquad \text{[Eq 5.26]}$$

Where:

$\Delta(t,X_3,\theta,X_4)$	: Instantaneous displacement
$\Delta(t_0)$	: Initial displacement at time $t = t_0$
X_3	: Heave motion
X_4	: Roll motion
θ	: Instantaneous trim
g	: Gravitational acceleration
TCGs	: Transverse centre of gravity of the ship
$TCB(t,X_3,\theta,X_4)$	: Transverse centre of buoyancy of the ship

5.4 MODELLING THE DAMAGE SCENARIOS

In order to investigate the motions of a damaged ship, first of all a method has to be adopted to include the effect of damaged compartments in the calculations.

There has been a number of sea accidents whereby ships have been lost before they reached the final stage of flooding. Due to lack of information and of extensive studies, as well as the ignorance of official bodies, important achievements have not been gained regarding intermediate stages of flooding. However, following recent sea accidents, the behaviour of damaged passenger ships has become a very popular subject and as a result intermediate stages of flooding have also started to receive a lot of attention.

The main aim is to analyse the motions of the damaged ship during the intermediate stages of flooding and after the final stage of flooding in the time domain. Therefore, the method employed must be flexible enough to accommodate the following requirements:

- Capability to define more than one damaged compartment independently at any location along the ship and at different decks at the same time.

- Capability to create temporary asymmetric flooding and water transfer from one compartment to another.

- Capability to control and change the amount of water and flooding time in each compartment, separately.

- Capability to model water ingress by considering the wave elevation relative to the damage location.

- Capability to calculate the effect of water inside each compartment, instantaneously.

5.4.1 Damage Calculation Methods

In classical Naval Architecture, there are two main methods to evaluate the stability of a damaged ship:

i- Lost Buoyancy Method

In this method, it is assumed that the damaged compartments are opened to the sea and the ship has lost the buoyancy in these compartments. This assumption represents the final equilibrium position of the damaged ship. Calculations can only be carried out for the final stage of flooding. Although the lost buoyancy method is suitable for the equilibrium position, intermediate stages of flooding cannot be analysed. Moreover, the damage and flooding of the compartments above the waterline cannot be modelled by this method.

ii- Added Weight Method

In this approach, water is added to the compartment which is assumed to be flooded. Using the intact hydrostatic values of the ship sinkage, heel and trim can be calculated for each time step when extra water is added. This method is suitable to model the intermediate stages of flooding as well as the flooding of compartments above the waterline.

iii- Combination of Time Dependent Added Weight Method and Accumulation of Water

The entrapped water on deck poses stability problems and contributes substantially to capsizing, especially on a large deck like that found on Roll on-Roll off ships. The accumulated water will induce both static and dynamic effects [51]. Modelling the dynamic effects however, is very difficult from a mathematical point of view [11]. Nowadays, this can be modelled within a certain accuracy for limited conditions with regard to boundary conditions, motion amplitude, viscosity, shape of tanks etc, while calculations are carried out using numerical solution techniques such as finite difference, finite elements etc, together with powerful computing [52, 53] (details can be seen in Appendix A.2).

The sloshing and accumulation of water can be important from a dynamic point of view when the excitation frequency is close to the natural frequency of water in the tank [11, 51, 54, 55]. Although this is possible in smaller ships, it is not common in the case of ferries, to meet resonant conditions, since the roll frequency in the latter is in general very low. In order to attain resonance the water depth in the tank must be very low, thus the effect of sloshing will naturally be small. On the other hand, progressive flooding would not allow resonant conditions since the water depth changes continuously. The other effect is that water in a very large compartment may flow to the corner of the deck and create static heel. As a result, the effective breadth of the tank would be very small and water depth high, so the natural frequency of the water in the tank, which depends on the depth and breadth, would be very high. This would reduce the effect of sloshing drastically [55]. On the other hand, some experiments and a number of studies [10, 56] suggest that the effect of the water on deck can be represented by a pseudo-static heel angle. A computer program has been developed by the author to investigate the behaviour of water in a compartment. This non-linear model has some limitations regarding the amplitude of the oscillations, and the water depth, and viscosity is not included [Appendix A.2]. A limited parametric study showed that the dynamic pressure due to sloshing is very small compared to the hydrostatic pressure. However, it is suggested that more investigations must be carried out to identify the precise effect.

Considering the difficulties of modelling the dynamic effect of the accumulated water and that the static effect of the water is dominant, the effect of water accumulation is included in the time simulation by taking into account the instantaneous amount of water on deck, roll angle and trim. The formulation of the effect of water on deck is thus taken into account as follows:

Instantaneous amount of water on the deck,

$$ADW(t) = ADW(t-\Delta t)+DW(\Delta t) \qquad \text{[Eq 5.27]}$$

Instantaneous static force to sink the ship,

$$SSF(t) = g\ ADW(t) \qquad \text{[Eq 5.28]}$$

It is assumed that the ship rotates around the initial centre of gravity and hence the instantaneous static heeling moment becomes,

$$SRM(t,X_4,\theta) = g\ ADW(t)\ [TCG_S - tcg(t,X_4,\theta)] \qquad \text{[Eq 5.29]}$$

Instantaneous trim moment,

$$STM(t,X_4,\theta) = g\ ADW(t)\ [LCG_S - lcg(t,X_4,\theta)] \qquad \text{[Eq 5.30]}$$

Where:

$ADW(t)$	:	Instantaneous amount of water on deck
$lcg(t,X_4,\theta)$	:	Longitudinal centre of gravity of water on deck
$tcg(t,X_4,\theta)$	:	Transverse centre of gravity of water on deck
$SSF(t)$	:	Instantaneous static sinkage force due to water on deck
$SRM(t,X_4,\theta)$	:	Instantaneous static heeling moment due to water on deck
$STM(t,X_4,\theta)$	:	Instantaneous static trimming moment due to water on deck

These forces and moments are included in the equations of motion, following appropriate transformations.

5.4.2 Modelling the Water Ingress

Water ingress is modelled in two different ways and each option serves different purposes.

i- Option 1

This option is based on predefined water flow for each damaged compartment and modelling is done as follows:

1- A maximum of three damaged compartments can be defined independently from each other. These compartments are defined according to the ship co-ordinate system, vertically or horizontally at any location in the ship.

2- Flooding and damage for each compartment can be specified by defining:

- The **TOTAL AMOUNT OF WATER**, which is expected to flow into each compartment between the initial and final stages of flooding.

- The **INITIAL AMOUNT OF WATER**, which is the amount already having flooded in before the time simulation starts.

- The **FLOW RATE** which is the amount of water flowing in to a particular compartment per unit time.

- The **FLOODING TIME**, which is the length of time that progressive flooding takes place.

- The **STARTING TIME** which controls the starting time of flooding for each compartment.

All these parameters for each compartment are defined separately and thus enabling total control on the mode of flooding. This flexibility provides the opportunity for extensive analyses over a wide range of parameters.

ii- Option 2

This option of water ingress is based on the relative position of the water level (wave elevation) and the damage location. This instantaneous relative position is calculated by taking into account the instantaneous wave elevation and ship motions. Option 2 of water ingress provides more realistic modelling of the progressive flooding of the compartments, especially the decks above the waterline as water ingress depends on the wave height and ship motions.

As stated before, damage can occur vertically and longitudinally anywhere in the ship. The damage opening due to collision, grounding etc. may occur below, or above the water surface or a combination of these. It has been found from experiments and theoretical studies that the flow rate of water is mainly related to the pressure head, which changes depending on the location of the hole relative to the water surface. Experimental results also indicate that the flow rate is related to the shape and area of the opening and empirical formulae are based on these parameters as well as on the static pressure head.

The empirical formulations have generally been derived for civil engineering applications such as dam design, river flooding or canal flow etc. Therefore all the empirical formulations about water flow are based on calm water surface. If damage is below the water surface the existing formulation can estimate the water flow with good accuracy. However, in the case of damage at or especially above calm water surface, the existence of waves may affect the water flow considerably. At the moment empirical formulae are available for the steady water flow through an opening at calm water surface such as flow over a notch or weir [57, 58], but there is no formulation for the water flow in a wave environment through, an opening above the calm water surface. In such cases, pressure is entirely dependent on the wave particulars such as wave height, direction and steepness. Therefore, the existing formulation which is for water flow over a notch may not give very accurate results. It has been found from damage stability experiments that water ingress is considerably affected by the wave direction [38], thus existing formulations may have to be correlated for this kind of problem. Bearing in mind these problems, the emphasis here is placed upon the hydrostatic effect including the wave height, edge effect and location of damage. Formulations for different damage conditions are attended as follows.

Flow for a damage below the waterline (Fig 5.2a)

The water ingress model for this condition is based on the empirical formula developed for the steady water flow through an orifice, and

static pressure head is calculated by using Bernoulli's equation [57], [Appendix A.3]:

$$U = K\sqrt{2\,g\,H} \qquad \text{[Eq 5.30]}$$

Flow rate,

$$Q = U\ A_{op} \qquad \text{[Eq 5.31]}$$

where:

U : Velocity of the water

H : The distance between the water level and the centre of damage hole (Fig 5.2a)

K : Flow coefficient

A_{op} : Area of the damaged hole or opening

Flow above the water surface (Fig 5.2b)

For this condition, the static pressure head is calculated by considering the water elevation but by using the formulation developed for flow over a notch or weir, which is the most suitable for the modelling of this problem.[57] [Appendix A.3].

Flow rate:

$$Q = U\ A_{op} \qquad \text{[Eq 5.32]}$$

$$U = K\sqrt{g\,H} \qquad \text{[Eq 5.33]}$$

The K value (Flow coefficient or discharge coefficient) changes depending on the shape of the damaged area, while at the same time it may also be affected by the thickness and the roughness of the hole edges. In civil engineering applications, K is generally taken between 0.45 and 0.58 [57, 58]. The existing empirical formulae and coefficients for the water flow over a notch are approximated by using the calm surface and free discharge conditions, with these formulae being based on the static pressure head. However, in the

case of flooding of the compartments of a ship above the waterline, the other effects such as wave height, direction, velocity of wave and orbital velocity of water particles, which would influence the water flow, are not included in any empirical formula. Moreover, the amount of water, which may flow out back to sea due to ship motions is unknown and this makes the scenario more complex to model.

Since there is no relevant empirical formula for estimating the water inflow and outflow for this particular condition, the net water ingress at each time step can be approximated by using the existing formulae but with an adjusted flow coefficient(K). A calibration study to approximate K (as a result of flow in and out at each time step) was undertaken based on a limited set of experiments for a single ship model [38]. These experiments were undertaken with a view to investigating the effect of waves and progressive flooding of the vehicle deck on the capsizing of a ship. By simulating the same roll and heeling behaviour of the ship at the same conditions as the experiments, the K value was varied until simulation and experimental results were reasonably close to each other. Based on this calibration, the K values for damage into and away from waves were found to be in the region of 0.40 - 0.45 and 0.20, respectively.

It must be emphasized that these values are approximate values based on limited experiments whose objectives were different. Therefore, in order to establish an accurate estimation, specifically designed experiments for different wave directions and wave heights must be carried out.

5.5 MOTIONS

For the analysis of vessel dynamic behaviour, the following non-linear coupled system of equations is used for the calculation of sway, heave and roll motions of the damaged ship. Subscripts i and j (X_i, A_{ij}) show the mode of motion. i,j=2 denotes sway motion, i,j=3 heave motion, and i,j=4 roll motion.

Eq 5.34:

$$(M + A_{22})\, X_2'' + B_{22}\, X_2' + A_{23}\, X_3'' + B_{23}\, X_3' + A_{24}\, X_4'' + B_{24}\, X_4' = F_{2wind} + F_{2wave}$$

$$(M + A_{33})\, X_3'' + B_{33}\, X_3' + RES_3(t,X_3,\theta,X_4) + A_{32}\, X_2'' + B_{32}\, X_2' + A_{34}\, X_4'' + B_{34}\, X_4' = F_{3wave} + F_{3wod}$$

$$(I_{44} + A_{44})\, X_4'' + B_{44}\, X_4' + RES_4(t,X_3,\theta,X_4) + A_{42}\, X_2'' + B_{42}\, X_2' + A_{43}\, X_3'' + B_{43}\, X_3' = M_{4wind} + M_{4wave} + M_{4wod}$$

Where:

M	: Mass of ship
A_{ij}	: Added mass
B_{ij}	: Damping coefficient
RES_i	: Restoring force and moments
I_{ij}	: Mass moment of inertia
F_{iwind}, M_{iwind}	: Wind excitation force and moment
F_{iwave}, M_{iwave}	: Wave excitation force and moment
F_{iwod}, M_{iwod}	: Excitation force and moments due to water on deck.

The solution of these equations in the time domain is carried out by using NAG [59] routines, based on the RUNGE-KUTTA method [Appendix A.4].

5.6 VALIDATION OF THE COMPUTATIONAL METHOD

i- Intact Case

In order to check the accuracy of the developed computational method, two different sets of calculations are carried out and compared with available results published in the literature.

The first comparison is based on a 140m tanker whose motion characteristics were studied at upright and at inclined conditions [17]. The second comparison is based on a 19m Canadian fishing vessel whose motions were examined by means of theory and experiments [60].

There are different reasons for using these two published results for comparison purposes. First of all, both studies provide results based on certain conditions, such as beam waves, without forward speed, and coupled motions which are also those conditions on which the study in the thesis is based. Moreover, details of the models and conditions, as well as the results for a wide range of frequencies, are available.

In addition, in both studies computational calculations of excitation forces and hydrodynamic coefficients (except for roll damping which is calculated by using non-linear methods) are based on strip theory, which is also used by the present author to calculate the excitation forces, damping and added mass coefficients (except roll damping). Both models are different in size which should provide additional support of the validity of the computational method for different ship sizes. Furthermore, the availability of experimental results for all motions of the second model makes it an ideal choice for comparison purposes.

The first comparison is done with Lee's computational results [17] for a tanker. As Figure 5.3a shows, the predicted heave motions of both methods are in very good agreement over a large range of Wl/Sl ratios, but at some Wl/Sl ratios (high frequencies) results differ slightly. For the roll motion (Fig 5.3b), agreement is good between the two methods except in the region of natural roll frequency. Time simulation shows that roll motion is larger than that in LEE's method. This difference is due to the different damping values, since both computational methods use different formulations to estimate roll damping. However overall, it can be said that the general agreement between the two methods is satisfactory.

The second comparison is made with Karppinen's experimental and computational results [60] for a Canadian fishing vessel. As seen from Figure 5.4a the time simulation results for sway motion agree well with experimental results, even better than Karppinen's theoretical results. In the case of heave motion (Fig 5.4b), the agreement between the three results is good, except around

W_{nd}=2.5, at which both theoretical methods overestimate the heave motion when compared to the experiments. In the case of roll, all three methods agree well [Fig 5.4c]. The small shift in the response curves is probably due to the difference in the estimation of mass moment of inertia and this was also put forward as the reason by Karppinen for the small shift between his theoretical and experimental results.

ii- Damaged Case

As far as the author is aware, the research in this thesis is the first theoretical study to investigate the damage stability and flooding of a ship dynamically, thus no results exist with which a direct comparison can be made. The only results which are available, are the experimental results which were carried out by BMT [38] as part of the damage stability of Ro-Ro passenger ships programme, Phase 1. A similar study for the same ship, which was used by BMT, was carried out by the Department of Ship and Marine Technology [62], using the computational methods described in this thesis. The ship is assumed to be damaged below and above the bulkhead deck and simulation is carried out to investigate the flooding of the vehicle deck and capsizing of the ship, which is under the effects of irregular waves coming from the beam. For this study, the effect of wave height, freeboard and loading conditions are investigated. The results of simulation at different conditions were plotted and then the average stability boundary curve between capsize and non-capsize regions is defined (Fig 5.5). Both experimental and theoretical results are in close agreement. This comparison proves that the adopted model predicts the motions and flooding of a damaged ship exceptionally well.

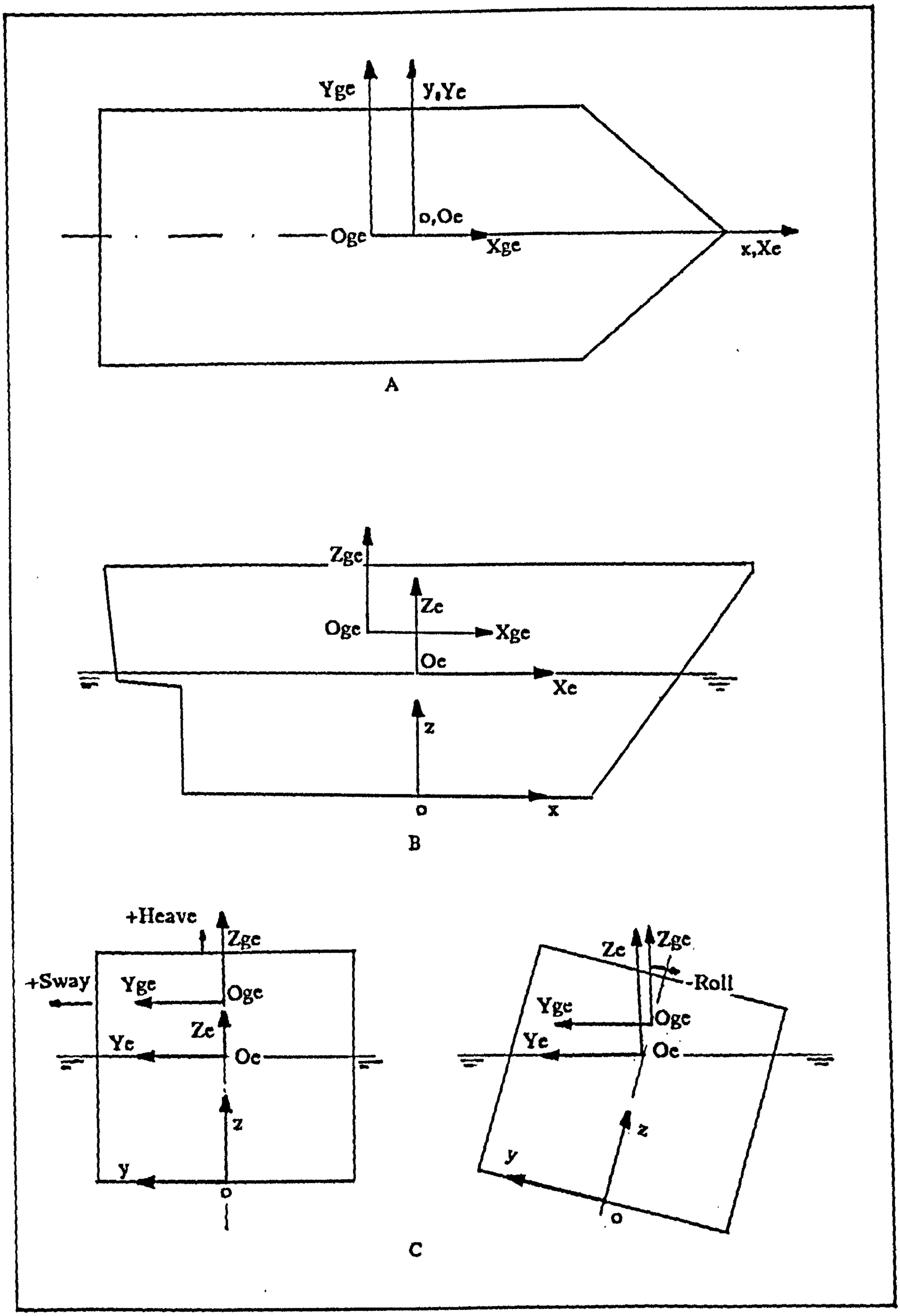

Fig 5.1 Co-ordinate systems

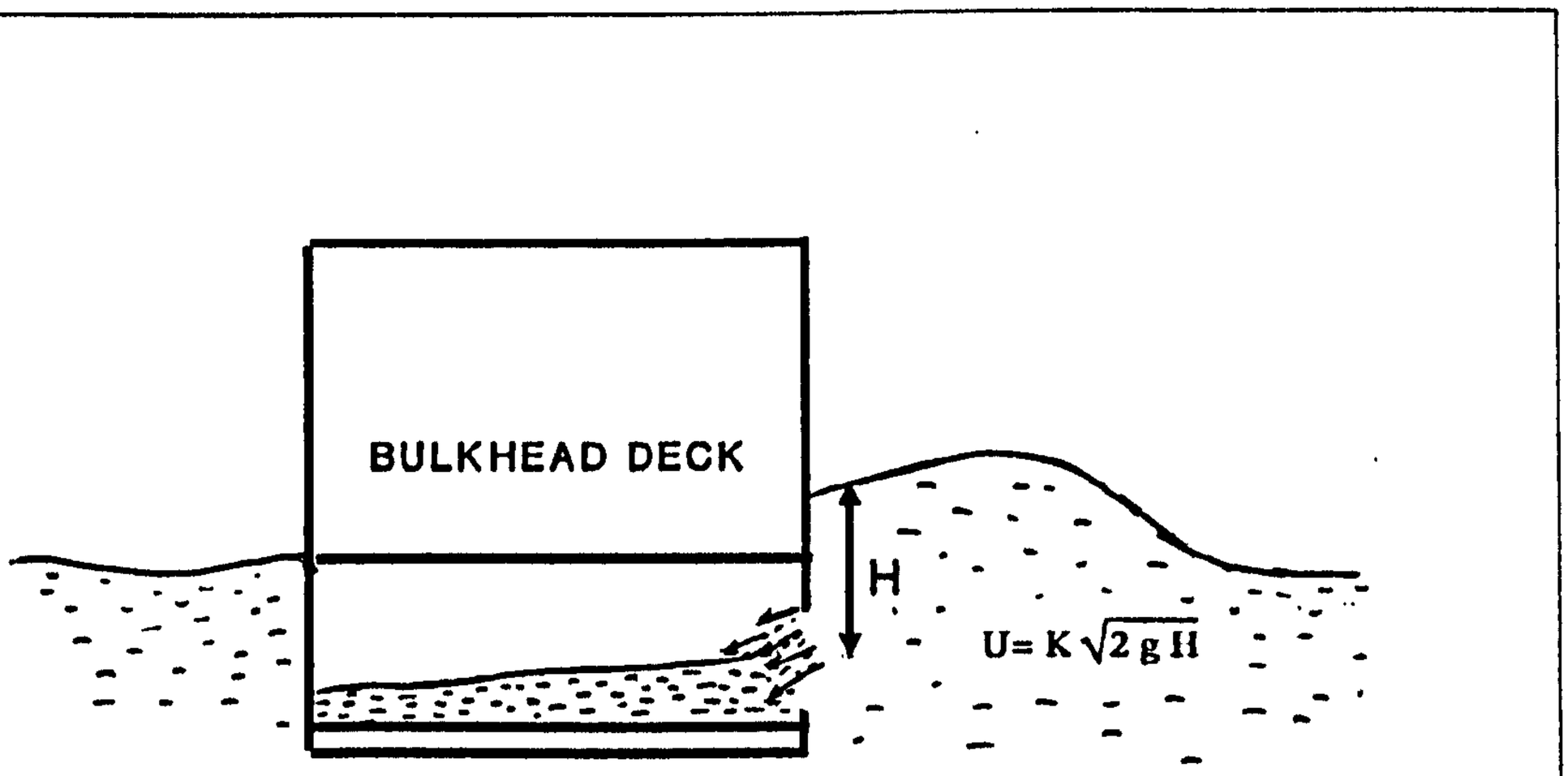

A Flow for a damage below the waterline

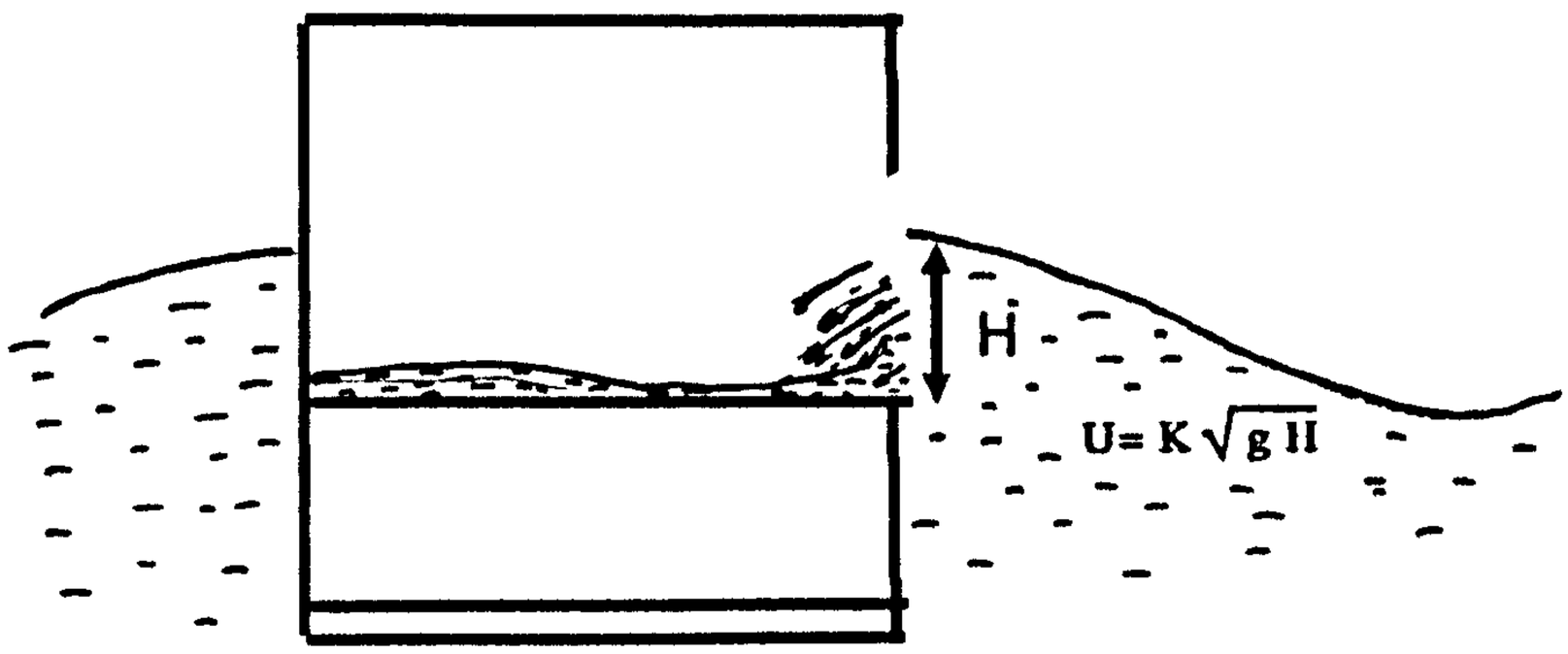

B Flow over a deck above the waterline

Fig 5.2 Modelling of water ingress

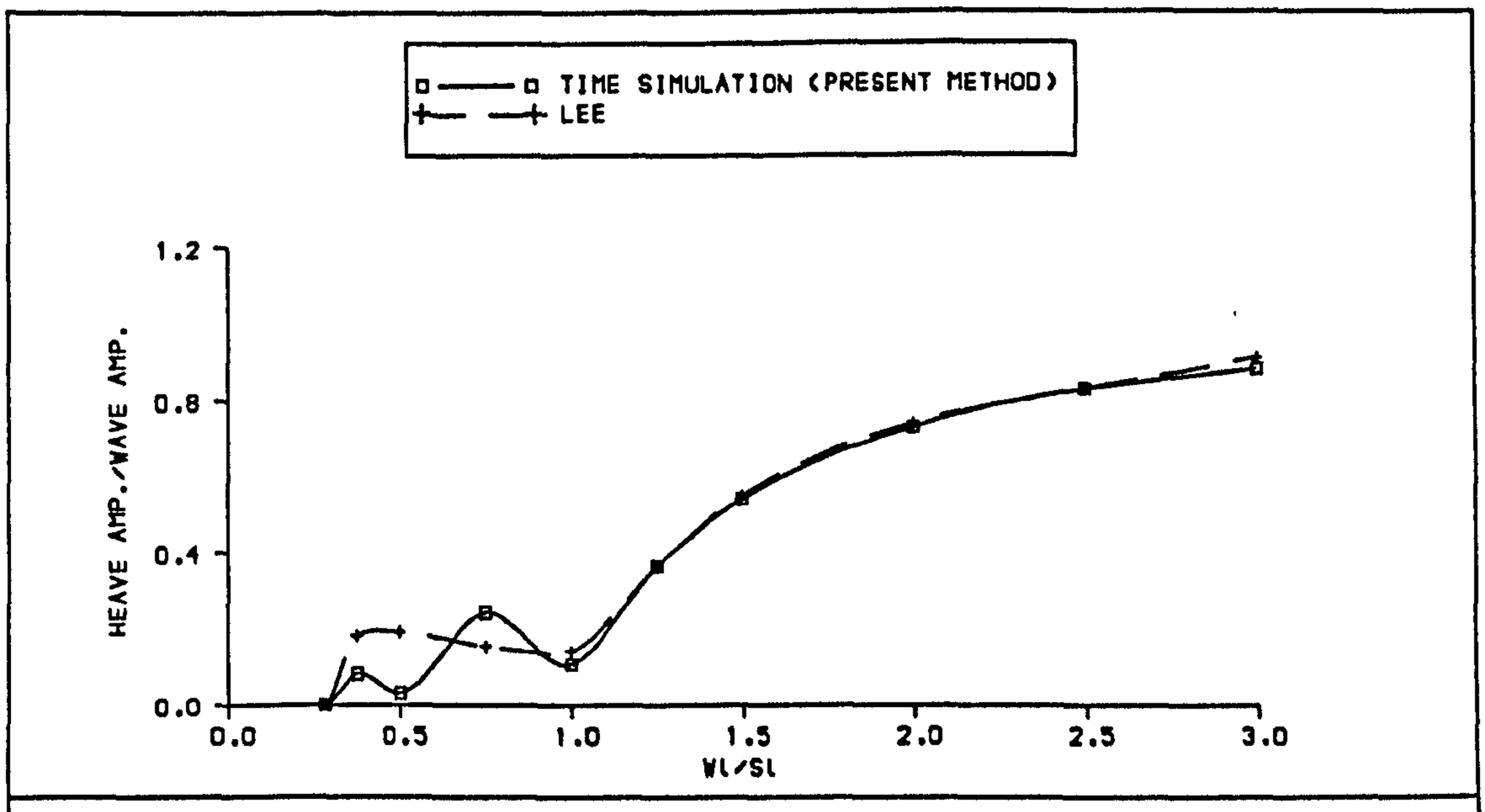

Fig 5.3A COMPARISON OF DIFFERENT METHODS FOR HEAVE RESPONSES OF A TANKER
WAVE DIRECTION = 180. DEGREES

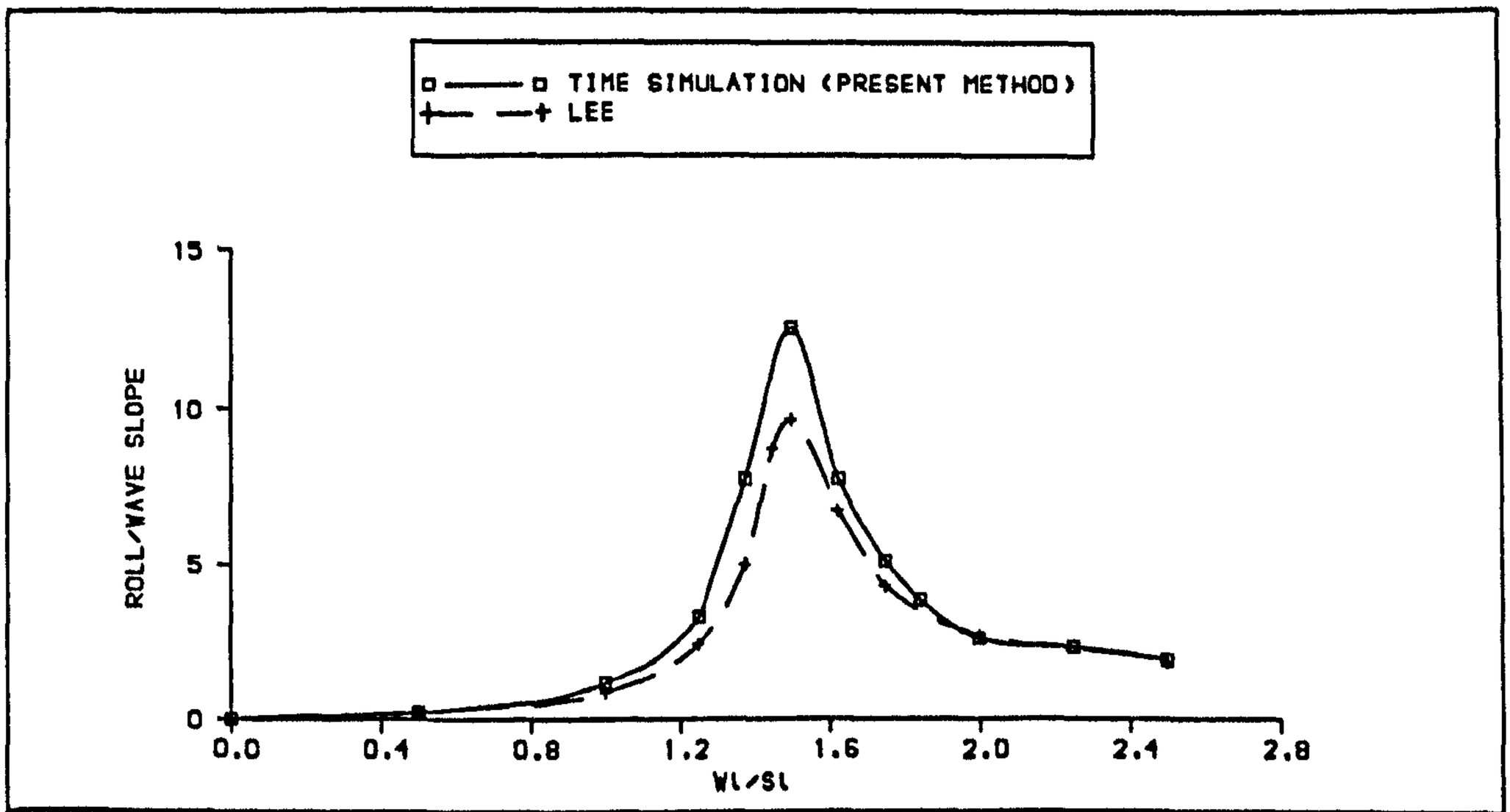

Fig 5.3B COMPARISON OF DIFFERENT METHODS FOR ROLL RESPONSES OF A TANKER
WAVE DIRECTION = 90. DEGREES

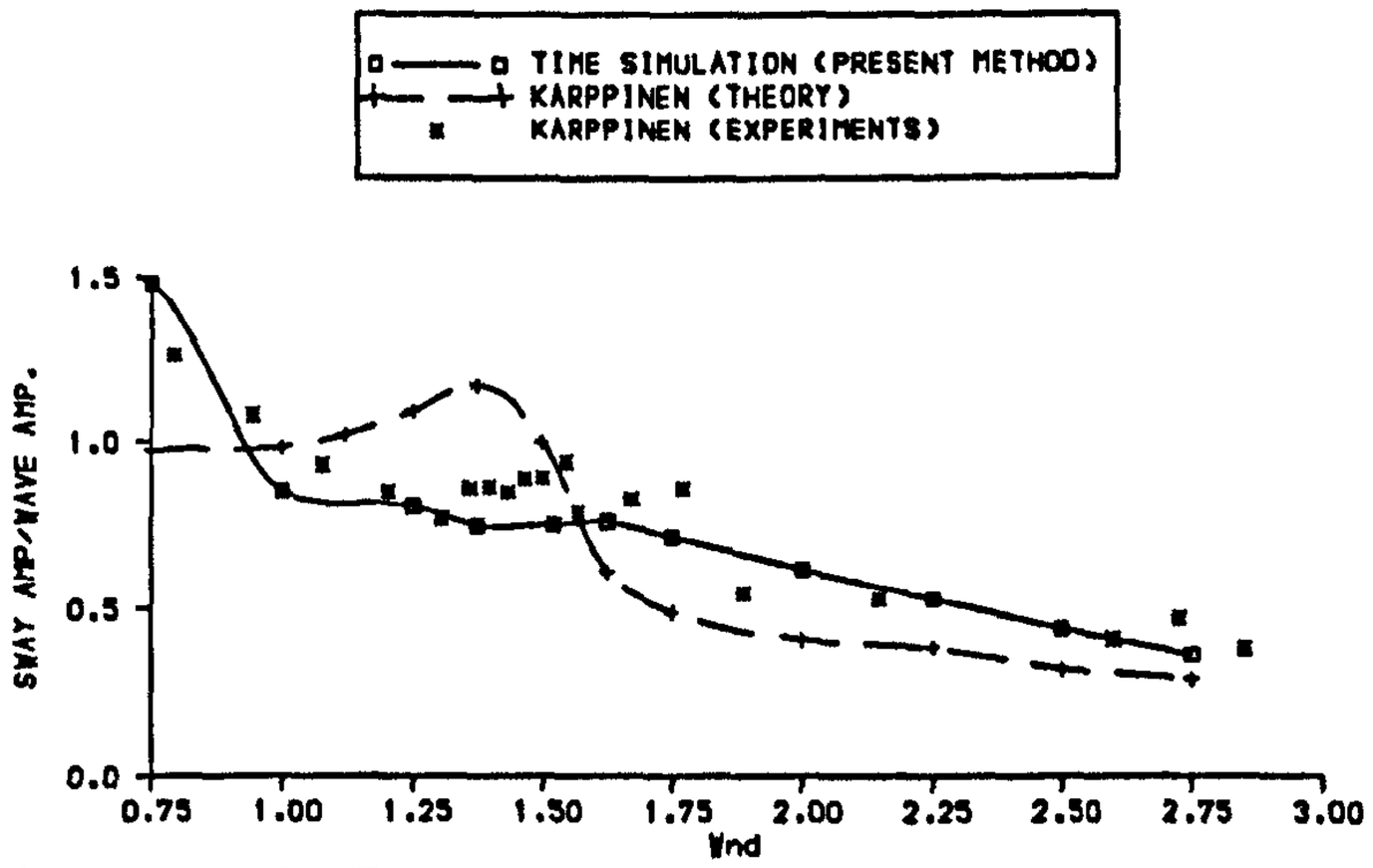

Fig 5.4A COMPARISON OF DIFFERENT METHODS FOR SWAY RESPONSES OF A FISHING BOAT
WAVE DIRECTION = 90. DEGREES

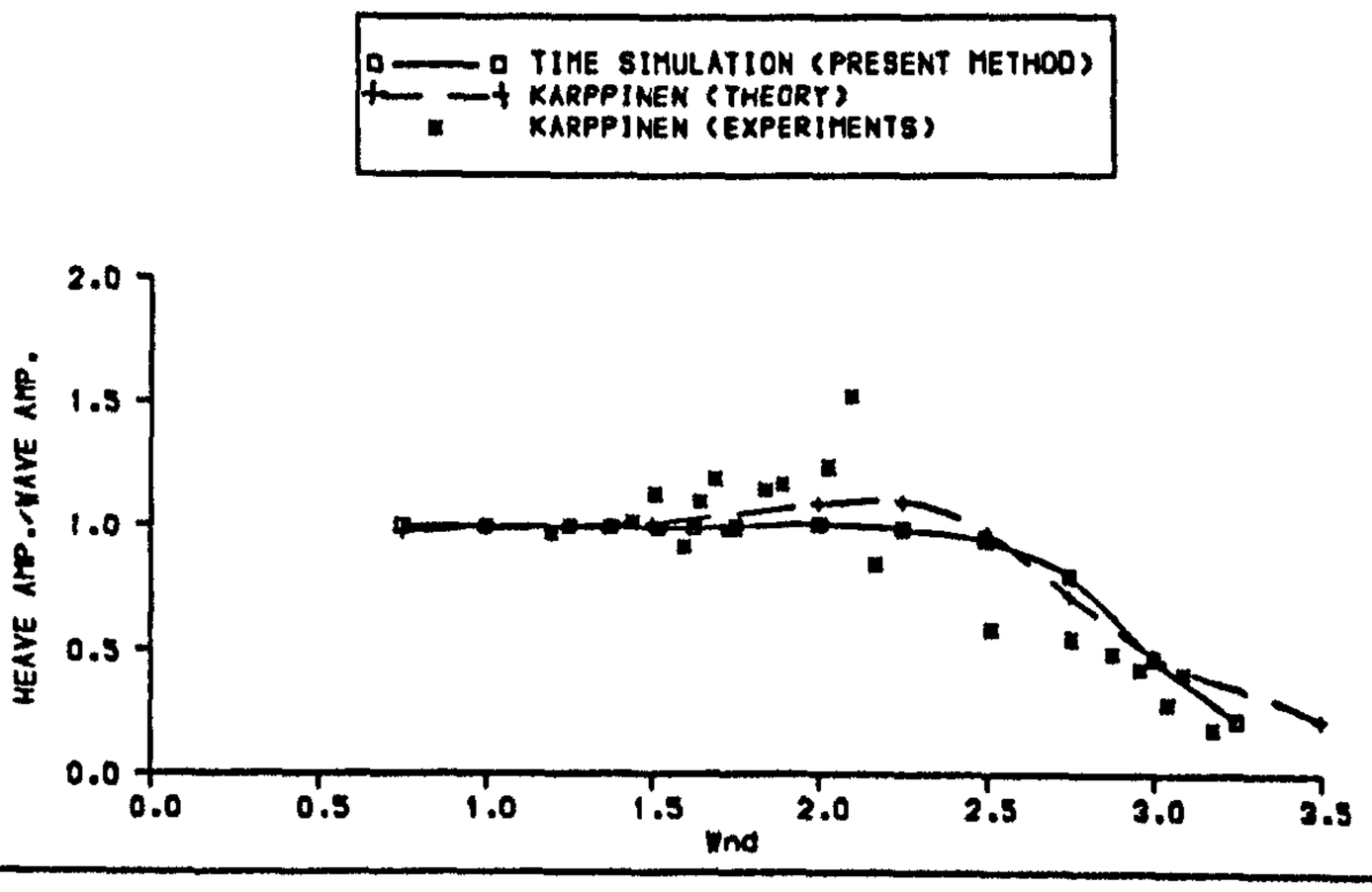

Fig 5.4B COMPARISON OF DIFFERENT METHODS FOR HEAVE RESPONSES OF A FISHING BOAT
WAVE DIRECTION = 90. DEGREES

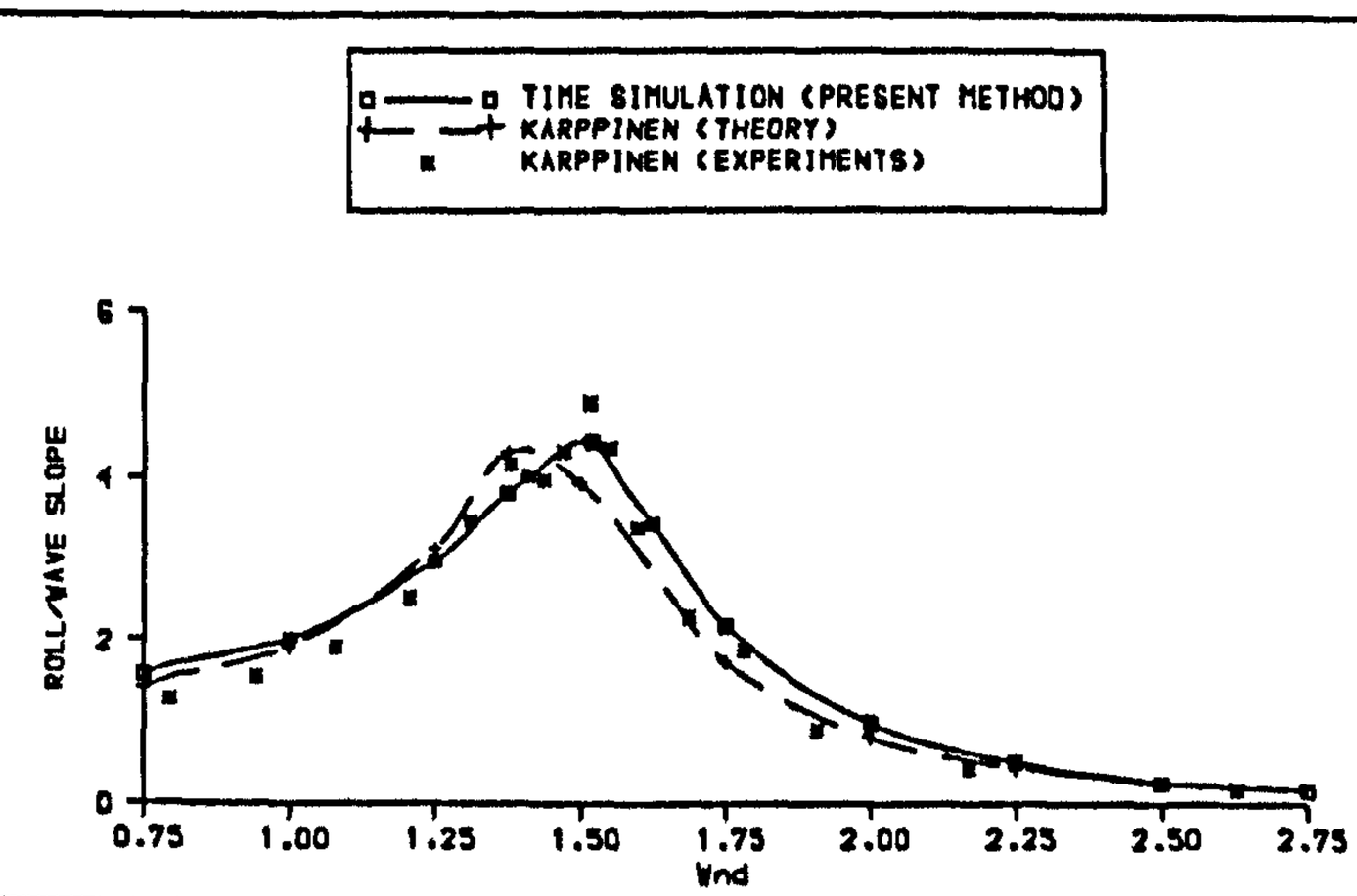

Fig 5.4C COMPARISON OF DIFFERENT METHODS FOR ROLL RESPONSES OF A FISHING BOAT
WAVE DIRECTION = 90. DEGREES

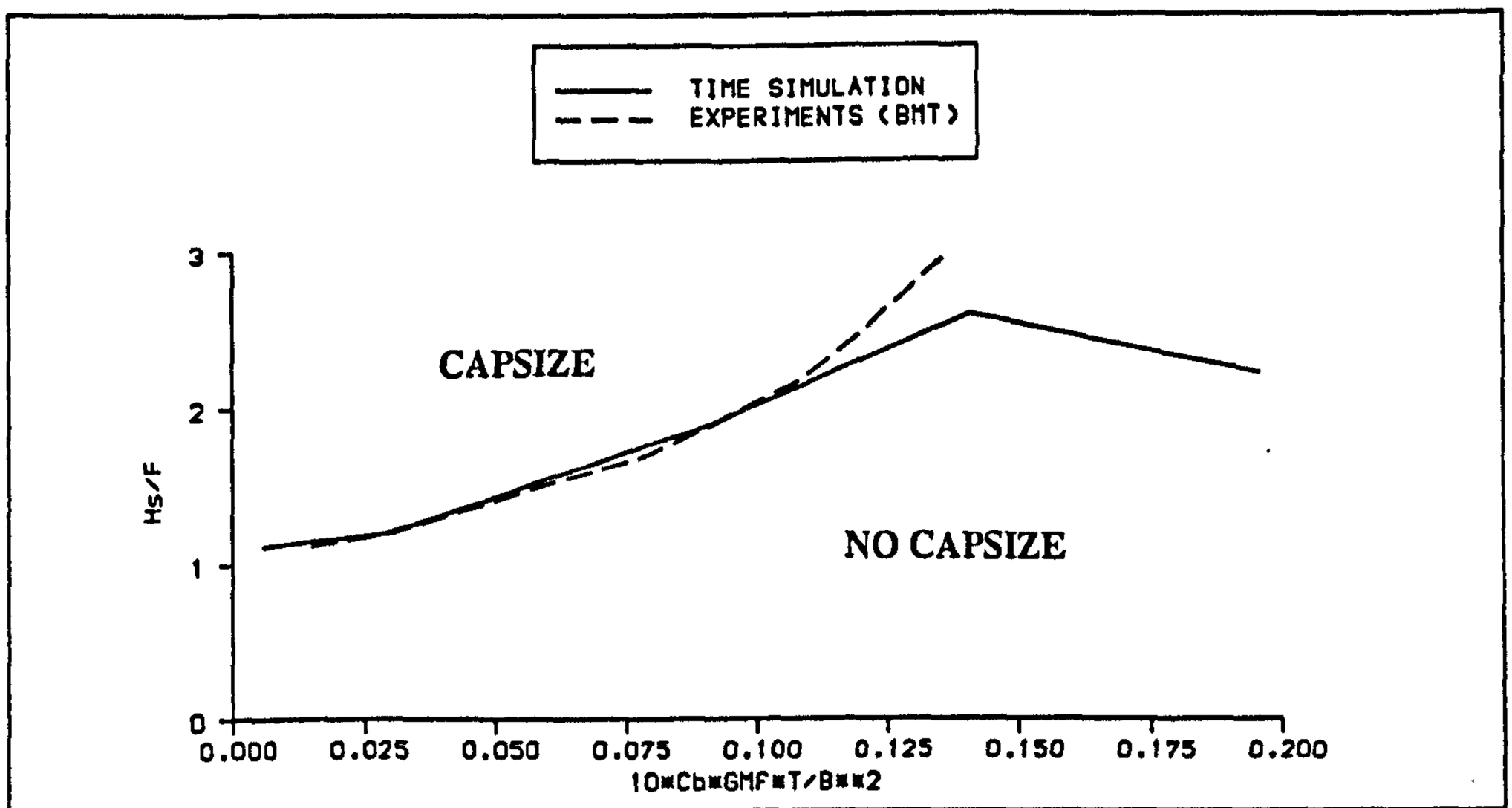

Fig 5.5 COMPARISON OF EXPERIMENTAL AND THEORETICAL RESULTS ON BOUNDARY CURVES BETWEEN CAPSIZE AND NO CAPSIZE ZONES. FREEBOARD: ALL, WAVE DIR: INTO

H_s : Significant wave height

F :Damaged freeboard

GM_f: Metacentric height in damage condition

T :Draught

CHAPTER 6: MODEL EXPERIMENTS

6.1 INTRODUCTION

Although considerable progress has been made in analytical studies of ship motions, experimental investigations of seakeeping cannot yet be dispensed with. In addition, controlled experiments are a valuable method to determine the usefulness of theories. They are also very valuable in attempting to improve the theoretical prediction of ship behaviour in a seaway as well as to determine the optimum hull form, hydrodynamic coefficients, resistance etc.

In order to estimate the ship motions, the hydrodynamic coefficients have to be known. Two methods are mainly used for this: experiments and theoretical calculations. Several theories exist to determine these coefficients mainly using two dimensional and three dimensional methods based on potential flow theory in which no viscous effect is taken into account. Two dimensional methods make use of diffraction and strip theories. Forward speed can also be included. In general, three-dimensional methods are based on source distribution techniques, with the ship surface defined by panels rather than by segments as in the two-dimensional case (16, 63).

However, there are certain problems with theoretical approaches, such as absence of viscous effects, effect of large amplitudes, three dimensional effects etc. Therefore, experiments are necessary in order either to calibrate the results obtained from theoretical approaches or to determine the coefficients directly for particular ships where exact theory cannot be applied. On the other hand, it is important to have a knowledge of the magnitudes of the various coefficients as well as of the influence of the hull modifications on these coefficients.

In the literature there are only a few systematic experimental studies carried out for measuring hydrodynamic coefficients. Gerritsma (14) carried out forced experiments to measure the added mass and damping coefficients as well as coupling coefficients of heave and

pitch motions for a series 60 model with forward speed in calm water. Along the same lines Gerritsma and Beukelman [64] tried to determine the distribution of damping and added mass coefficients along the ship length by carrying out forced heave experiments using a segmented model with forward speed. Results were compared to the whole model results and it was concluded that the influence of slits between the sections is very small. Gerritsma [65] applied the same technique to calculate the force distribution along the ship in waves. Motora [66] also carried out experiments to determine hydrodynamic coefficients. Very detailed experiments have been carried out by Vugts [15] for different segmented blocks which have the same sectional dimensions along the length and on whole models. Experiments were carried out for small amplitude motions. His results have been used very widely and are still being used for comparison purposes as well as for specific applications. Another set of experiments was carried out by Gerritsma and Beukelman [16, 67] for a ship travelling in shallow waters, and they concluded that strip theory can be used to determine the coefficients for shallow water.

6.2 OBJECTIVE OF EXPERIMENTS

Passenger ships and ferries have different hull forms from other conventional ships. They have a slender hull form with very fine water-lines and small block coefficient. The stern, due to the twin propeller, is very close to the surface providing less buoyancy while the ship towards the bow forms a V shape. Therefore, these ships may have different motion characteristics than cargo ships and as a result, the existing experimental results may not be used for these type of ships. On the other hand, inclined ships due to asymmetric damage may have different motion characteristics. Therefore, particular coefficients may be needed for asymmetrically damaged ships especially in large motions which may create non-linear effects that may influence the hydrodynamic coefficients. If the effect of large amplitude motions as well as ship asymmetry are found to be important it is essential to include these effects in the motion calculations by using appropriate coefficients. In order to derive coefficients for passenger type ships, experiments have to be carried out and compared with the theoretical results. If possible, by using

experimental results, theoretical calculations of coefficients can be correlated for general use. This would allow more accuracy on the prediction of ship motions and in modifying the ship forms for better and safer designs. However, as stated in Chapter 2, the main aim of the research in this thesis is different from those of the experimental and theoretical work for producing the general hydrodynamic coefficients for passenger ships. In order to achieve the main aims of the thesis, the experimental work for obtaining the hydrodynamic coefficients must be limited in scope, as follows:

- To develop an experimental technique to determine the hydrodynamic coefficients as well as to measure the coupled motions of ships.

- To calculate the hydrodynamic coefficients for intact and asymmetrically damaged ships at large amplitude motions.

- To compare the results with available theoretical results and identify the main differences.

Of course, in order to come up with a solution for general use, it is essential to achieve in the long term the following aims of the research regarding the determination of hydrodynamic coefficients.

- To carry out extensive experimental work on different types of passenger ships and establish the differences between the experimental and theoretical results

- To derive empirical factors for adjusting accordingly the theoretically derived results.

- To produce curves of hydrodynamic coefficients for general passenger type ships at intact and damaged conditions.

When all the stages mentioned above are completed in the long term, they will provide a useful contribution towards predicting the hydrodynamic coefficients, hence the motions of passenger type

ships. By achieving this, important progress can be made in the course of developing more sound stability standards.

6.3 SELECTION OF MODEL AND EXPERIMENTS

Since the focus of the research is on the behaviour of Passenger and Passenger/Car ships it was decided to choose a typical passenger ship, designed to work in the Mediterranean Sea. Since some model experiments of this particular ship have already been carried out in the Department, a 1/30 scale wood model was already available. Her body form and profile are shown in Fig 6.1a and b.

The main dimensions of the ship and model are as follows:

	Ship	Model
Length(Loa)	= 75.8 m.	Loa = 2.56 m
Length(Lbp)	= 63.0 m.	Lbp = 2.163 m.
Breadth	= 12.5 m.	B = 0.417 m.
Draught	= 2.8 m.	d = 0.093 m.
Δ	= 1216 tonnes	Δ = 0.044 tonnes
KG	= 5.17 m.	KG = 0.172 m
Depth bulkh. deck	= 4.6 m	D_{bh} = 0.153 m
Lcg	= -3.15 m	LCG = -0.105 m.
Heave Period	= 3.95 sec	T_{sh} = 0.721 sec
Roll Period	= 8.1 sec.	T_{sr} = 0.676 sec
Capacity	= 530 crew & pas.	

In the time simulation analysis, the coupled sway, heave and roll motions are considered without forward speed at symmetric and asymmetric damaged conditions. Therefore, the focus is on these motions and their interactions, indicated through the coupling coefficients. At the upright condition, the non-existence of hydrodynamic coupling between heave-roll, heave-sway, and vice-versa, are known. However, in the case of asymmetric damage conditions there may be coupling. Part of the overall aim is to clarify which coupling effects are present between these motions and to quantify the magnitude of the coupling effects as well as the effect of the static heel on them.

In order to determine the hydrodynamic coefficients for asymmetrically damaged ships, the ship is inclined at around 6 and 12 degrees. These values might change slightly due to the different ballast conditions used for different experiments.

Another aim is to measure the coefficients at large amplitudes as well. Therefore, it was decided that sway and heave experiments be carried out at two different amplitudes: 2 cm and 4 cm. In full scale these correspond to 0.6 and 1.2 m. respectively. For heave motion, the maximum amplitude of only 4 cm (1.2 m. in full scale) could be used, considering the limitations of the experimental mechanism and the particulars of the model. Large amplitude motion is a relative definition and its limits can change depending on the size of the ship, hull form etc. The model has 9 cm (2.8 m in full scale) draught and 15 cm depth which corresponds to 6 cm freeboard (4.6 m depth and 1.8 m freeboard in full scale). In the case of the model coming out of water by 4 cm relative to water level at equilibrium position, the quarter of the model length from the stern was slightly out of water because of the shallow draught of the ship towards the stern (Fig 6.1a). On the other hand the model had very small freeboard when it re-entered the water by 4cm relative to the water level at the equilibrium position. At this amplitude, the model was slamming slightly when it was re-entering the water. If the maximum amplitude was increased further, more serious slamming would be faced and distort the recorded signals while the deck would be flooded. In addition the hull form changes considerably with depth, therefore, 4 cm heave amplitude is large enough to cause substantial changes in underwater form and hence, non-linear motion. Therefore, 4 cm heave amplitude can be accepted as large.

In the case of roll motion the amplitude could not be fixed because of the roll excitation force mechanism used. This will be explained later. Full details of the range of experiments carried out can be found in Table 6.1.

6.4 EXPERIMENTAL SET UP

6.4.1 Experimental Tank

For the experiments described above the DENNY tank in Dumbarton (Glasgow) was used. This tank is one of the oldest tanks in the world and is designed particularly for resistance tests. Its rails are on the tank rather than on the side walls (Fig 6.2a and Fig 6.2b). The main dimensions of the tank are:

Length = 100 m
Breadth = 7 m
Depth = 2.5 m

6.4.2 Experimental Set Up for Heave and Heave Coupled Motions

i- Heave

The heave excitation force is obtained by using a (DC) motor placed on the carriage. The excitation force is transmitted by using a disk and arm arrangement. The disk is connected to the motor so that the amplitude of motion is changed by connecting the arm to different holes on the disk (Fig 6.3a). The force from the arm is transmitted to the ship by using roller guides, linear bearings and a steel bar connected to the ship at the centre of gravity. The motor and roller guides are connected to the aluminium plate frame, to which the main parts of the experimental set-up are attached (Fig 6.3a). The heave motion is measured by using a Linear Variable Differential Transformer (LVDT) which is also connected to the aluminium box. There is in addition a roller guide and an aluminium bar connected to the front of the model as a yaw preventer. Heave forces are measured by using a load cell connected between the arm and the steel bar.

ii- Heave-Roll

In the case of coupled heave-roll motions, the heave mechanism is modified by connecting the main steel driving bar and the model with a steel rolling shaft. A universal joint is added to the yaw preventer mechanism to allow roll motion. Roll motion is then measured by using a potentiometer which is connected to the roll shaft. The centre of the roll shaft and the universal joint are situated at the centre of gravity of the model.

iii- Heave-Sway

For this condition, the heave mechanism is modified by adding a horizontal linear bearing in the sway direction and rolling carriage, between the model and the main driving bar. A linear bearing and carriage are also added to the yaw preventing mechanism to allow the boat to sway. Sway is measured by installing a potentiometer to the rolling carriage at the sway direction (Fig 6.3.b).

6.4.3 Experimental Set Up for Sway and Sway Coupled Motions

i- Sway and Sway-Heave

The sway forcing mechanism is exactly the same as in heave. In order to force the ship in the sway direction, the heave forcing mechanism is rotated by 90 degrees (Fig 6.4a and Fig 6.4b). The driving bar is connected to the steel bar and the yaw preventer by using rolling carriages. In the case of sway only motion, rolling carriages are clamped to the yaw preventer and steel bar. In the case of sway-heave these clamps are released so that the model can heave. Sway motion is also measured by an LVDT, and the force by a load cell as in heave motion. In the case of sway-heave, the heave motion is measured with a second LVDT installed.

ii- Sway-Roll

In the case of sway-roll, the sway mechanism is modified by placing the roll shaft between the model and the steel bar. The yaw preventer is also modified by installing a universal joint to allow the model to roll. Again the centre of shaft and universal joint are situated at the centre of gravity of the model.

6.4.4 Experimental Set Up for Roll and Roll Coupled Motions.

i- Roll

In order to excite the model into roll motion, a roll moment mechanism is used, based on the centrifugal force principle (Fig 6.5a). As Fig 6.5 shows, the roll moment mechanism has two L shaped arms and an equal weight is attached to the bent edge of each arm. Each arm is then connected vertically to a shaft, which is passing through the motor of the roll moment mechanism. Therefore,

there is a distance between the vertical centre of the weight and the centre of the shaft, r, which can be varied depending on the requirements. Each arm faces the opposite direction to each other, having 180 degrees of an angle between them. The roll moment mechanism is then placed at the centre line of the model, so that each arm can be at each side of the centreline of the model. Thus a shaft rotation, at a chosen frequency, creates a centrifugal force for each arm but at opposite directions. The horizontal distance between the centre of the roll moment mechanism, which is at the centre line of the model and the centre of weight, l, causes the roll excitation moment.

The roll moment mechanism is attached to the model with the centre of the roll mechanism at the same level as the centre of gravity. The rolling shaft mechanism, which allows the model to roll, and the steel bar are attached to the model as described previously, with the bar clamped to the aluminium frame (Fig 6.5b).

The roll motion is measured by a potentiometer. The force is estimated by using the following expression, which gives the same value as that obtained from the experiments [Appendix B.1].

$$M = 2\,l\,F \qquad \text{(Eq 6.1)}$$

$$F = \omega_e^2\, m\, r \qquad \text{(Eq 6.2)}$$

Where:

ω_e: Excitation frequency (rad/sec)
m : Mass attached to the arm of the roll mechanism
r : Vertical distance between centres of shaft and mass
l : Horizontal ,, ,, ,, ,, ,, ,, ,,

In order to obtain the rotational signal of the roll moment mechanism another potentiometer is used and is connected to the shaft of the roll moment mechanism. The phase angles between the roll moment and roll motion are measured for the analyses.

ii- Roll-Heave

In the case of roll-heave experiments the same system is used but instead of clamping the steel bar, it is freed under the control of rolling guidance, connected to the aluminium box. Heave is measured by an LVDT.

iii- Roll-Sway

In the case of roll-sway, a linear bearing and rolling carriage are connected to the rolling shaft mechanism and to the other steel bar, which is clamped to the aluminium box. Sway motion is measured using a potentiometer, which is rolling with the carriage.

6.4.5 Data Acquisition

The signal measurement apparatus can be described briefly as follows. The linear motions are measured by LVDTs, forces by load cells, and angular motions by potentiometers, which were also used to measure the coupled sway motion caused by the forced heave and roll motions. All devices have a signal feeder which is also connected to the signal converter. All data is transferred to the A/D converter which converts analogue signals to digital signals. The converted signals are sent to the computer for analysis. There is an oscilloscope to observe the signals during the experiments and it helps to decide whether test signals are suitable, and when it can be sampled. Force is created by DC motor which is connected to the AC/DC converter. A schematic diagram and a photograph of the experimental set up can be seen in Fig 6.6a and Fig 6.6b.

6.5 PREPARATION OF EXPERIMENTS

6.5.1 Ballasting the Ship

In order to obtain the right displacement, weights were located mainly at the locations (Fig 6.3a) where the bars are installed. However the final adjustment of weights is done by considering the three draft marks at forward, aft and middle sections. The vertical centre of gravity is then adjusted by carrying out inclining experiments. Ideally, the displacement of the model for all the test conditions must be the same. However, because different equipment, which are sometimes part of the ballast, are used for different

conditions, the final mass of the model may be slightly different for each test. To attain a static inclination for modelling the asymmetric damage conditions, weights on the bars are transferred to one side until the required heel is obtained. Since weights are shifted at the same level, the vertical centre of gravity is not changed. Even though the static heel would cause a slight shift of the transverse centre of gravity, throughout the experiments the centre of rotation is not changed.

6.5.2 Determination of Mass Moment of Inertia

In order to determine the mass moment of inertia (I_{xx}), a mechanism, which is a singular suspension system (Fig 6.7), was used to measure it.

The model is connected to the steel bar which is also connected to the rolling shaft mechanism at the other end. The rolling shaft mechanism is clamped to the frame so that the ship can be suspended. This system allows measurement of the natural roll period of the model by displacing the model to the one side and letting it oscillate freely. The total oscillation time and total number of cycles are recorded. This gives the average roll period of the system from which Ixx is calculated. Details of the determination of the roll mass moment of inertia is given in [Appendix B.2].

6.5.3 Calibrations

Before the measurements, a calibration of the different equipment used for measuring the experimental results is carried out. The roll mechanism and its voltage control box are calibrated to find the corresponding frequency for each voltage mark on the control button, as well as the excitation moments for different weights. The load cell measuring heave and sway excitation forces and the LVDTs, which are used to measure the sway and heave motion amplitudes, are also calibrated. The final calibration is carried out for the potentiometer which is used to measure the roll angle. Details are given in [Appendix B.3].

6.6 DETERMINATION OF THE STIFFNESS VALUES

i- Roll Stiffness

In the case of linear restoring, the restoring coefficient of roll (K) is determined from knowledge of the gradient of the righting arm curve at small angles. Since the righting arm curve is a function of body geometry and the centre of gravity, the restoring coefficient becomes non-linear as the roll amplitude becomes larger. In this case, the restoring coefficients derived for small angles cannot be used.

The average work done on the fluid during a cycle by inertial and restoring moments is zero. However, the ship does work on the fluid during the first half of the cycle and the fluid does an equivalent amount on the body during the second half of the cycle. Only damping forces do a net amount of work and therefore take the energy out of the body and dissipate it into the fluid.

Therefore, the nonlinear nature of restoring moment can be taken into account by examining the restoring energy present during a half cycle. This can be done by calculating the area under the restoring curve for each motion amplitude. Dividing the area by the maximum amplitude would give the stiffness coefficient.

$$K_R(\phi) = \int_{\phi_1}^{\phi_2} \frac{RES_R(\phi)\, d\phi}{\phi_m} \qquad \text{(Eq 6.3)}$$

The above equation would give the linearised equivalent restoring coefficient for roll. The equivalent coefficient for this model is determined by carrying out experiments. The model arranged for roll experiments, is inclined by shifting different weights, and for each weight shifted the inclination is recorded. Details are given in [Appendix B.4].

ii- Heave Stiffness

The heave stiffness coefficient may change significantly with large heave amplitude due to appreciable changes in the waterplane area.

Therefore, it is important to use accurate values for each of the different experiments. Details are in [Appendix B.4].

iii- Heave into Roll Coupled Stiffness

This coupling may be very important for large amplitude motions especially with a hull form changing significantly with depth. In case of asymmetry, this coupling may have a more substantial effect on the motions and it is important therefore to include it in the analysis and to calculate it accurately. This is explained in [Appendix B.4].

6.7 MEASUREMENTS AND OBSERVATIONS OF EXPERIMENTS

6.7.1 Heave, Heave-Roll and Heave-Sway

During the heave motion experiments, it was observed that the effect of free surface on the force signals was appreciable especially when the frequency was very low, even though at these frequencies the wave amplitude was very small and hence difficult to observe. This is due to the change in the buoyancy of the model caused by surface movement, which cannot be detected by the eye. Therefore, some experiments had to be repeated whilst waiting sufficiently until the water had calmed down completely before another run was carried out. Since it was not easy to control this problem repeatability tests showed some differences at low frequencies.

As mentioned in the foregoing, the rails of the carriage are suspended on the tank by using girders, therefore the rails are very sensitive to vibration. In addition, since the forcing mechanism is fixed to the rails and to the model, this caused problems during the heave motion experiments at low frequencies. The sensitive load cell used could pick up the vibrations and in order to reduce this, the carriage was made stiffer. The other vibration source, motor noise, is not big enough to influence the results. At higher frequencies these problems disappeared but a backlash problem which caused distortion on the signals appeared instead. Although its effect on the maximum force amplitude can be ignored, it affects the position of the peak in the response which in turn could affect the calculation of the phase angles.

Heave experiments could not be carried out for frequencies higher than 1.6 hertz. The heaving model was affected by the free surface whilst the model itself started to affect the experimental mechanism, causing vibration or even deflection of the rails. At 4 cm amplitude the maximum frequency had to be further reduced since bigger amplitudes started causing larger vibrations and deflections at lower frequencies. Heave experiments were carried out for 2 cm and 4 cm amplitudes, and at the latter amplitude the stern was coming out of water and was slamming upon re-entry (Fig 6.8a and Fig 6.8b)), hence it had to be the maximum amplitude which was used for the experiments. However, this slight slamming did not affect the results. The radiating waves created from the heaving model, were reflected from the side walls of the tank, and although their effect was not measured, these waves may have affected the results at certain frequencies.

Measurements were carried out after the motion of the ship became steady and 15 consecutive force and response periods were recorded. As frequency was increased, the measuring time decreased. Measurements had to be started as soon as motion became steady to avoid the reflected waves. This was due to the fact that at high frequencies, the radiated waves by the heaving ship were very large in amplitude (Fig 6.8c) and when they returned they could have distorted the recorded signals. Although, at low frequencies, reflected waves travel faster, they are very small in amplitude, therefore returning waves did not distort the recorded signals. During the experiments it was observed that radiated waves at the same side of static heel were higher and more regular than the waves at the side opposite to the static heel. The reason for this is that, the inclined side of the ship, which has outward flare like a paddle type of wavemaker, pushes the water on the surface away from the ship when the ship moves downwards and as a result big waves are created. On the other hand, the other side of the ship which has inward flare, cannot push the water outwards, hence waves created by the ship water interaction are small. When the ship moves upwards, the inward flare side pushes the water outwards, but the push, which is coming from the underwater, does not affect the water surface

substantially, and as a result, the inclined side of the ship causes bigger and more regular waves.

As was expected, roll motion induced by heave was not observed for the upright condition, however, when the ship was inclined (6 and 12 deg. respectively), the ship started rolling as a result of heave induced excitation. This confirmed the existence of coupling between heave and roll for asymmetrical bodies.

In the case of coupled heave-sway experiments, no sway motion was observed or recorded for both the upright and the inclined positions.

6.7.2 Roll, Roll-Heave and Roll-Sway

Since maximum roll amplitude is frequency dependent, for small frequencies, roll motion was too small to measure and even if there was a signal it was not very clear. Therefore, results for frequencies (f) less than 0.38 hertz could not be measured. Overall the roll response curve for the frequency range of interest was similar to those found in published reports. Outside the resonance area, the roll amplitude was small but near resonance the amplitude increased drastically (Fig 6.8d). Since the roll excitation mechanism is controlled manually to set the frequency, it was difficult to balance the frequency for small changes. This caused some difficulty especially at frequencies near resonance, since small differences in frequency changed the amplitude considerably, and as a result the peak of some response curves could not be defined accurately.

During the roll motion the waves generated by the model were very small compared to other motions. In the case of coupled motions, neither sway nor heave motions, induced by forced roll at either inclined or upright conditions, were observed or recorded.

At high frequencies the ship tended to yaw because of the excitation force, and as a result the yaw preventer mechanism had to be used.

6.7.3 Sway, Sway-Roll and Sway-Heave

Since sway can couple with yaw very easily, the yaw preventer

mechanism had to be fixed. Despite the yaw preventer at high frequencies, yaw coupling could be observed, this being exacerbated by the tolerance between guiding rail and rollers.

Since there is no sway restoring, the excitation forces recorded were very small, especially at low frequencies. Due to the presence of waves, as a result of the sway motion, sway force amplitudes were not symmetrical especially at lower frequencies. Again backlash created problems in the calculation of phase angles and because of these problems some of the low frequency results had to be abandoned.

In the case of coupled motions, strong coupling was observed from sway into roll when the model was excited in the sway direction. At inclined positions some water splashed into the model because of the low stern and again results at very high frequencies could not be obtained. Since surface waves did not affect the sway motion due to the non-existence of restoring, repeatability was very good.

6.8 ANALYSIS OF EXPERIMENTS

6.8.1 Co-ordinate System

Measurements were carried out in the earth coordinate system whose origin is at the centre of gravity (Fig 6.9). The roll centre is located at the centre of gravity of the intact ship. For both intact and damage cases the centre of rotation is not changed. Stiffness and moment of inertia values are all calculated in the earth coordinate system.

6.8.2 Mathematical Model for Analysis

The most general way of describing the motion of a linear system is as a set of three coupled equations of motion as follows:

Sway: (Eq 6.4)

$$(M+A_{22})\,X_2''+A_{22}\,X_2'+A_{23}\,X_3''+B_{23}\,X_3'+A_{24}\,X_4''+B_{24}\,X_4'=F_2$$

Heave: (Eq 6.4)

$$(M+A_{33})\ X_3"+B_{33}\ X_3'+C_{33}\ X_3+A_{32}\ X_2"+B_{32}\ X_2'+A_{34}\ X_4"+B_{34}\ X_4'+C_{34}\ X_4= F_3$$

Roll: (Eq 6.4)

$$(I_{44}+A_{44})\ X_4"+B_{44}\ X_4'+C_{44}\ X_4+A_{42}\ X_2"+B_{42}\ X_2'+A_{43}\ X_3"+B_{43}\ X_3'+C_{43}\ X_3= M_4$$

However, only two degrees of freedom at a time are required for the derivation of coefficients. Accordingly, the single degree of freedom experiments are carried out to obtain the corresponding added mass and damping coefficients. Then experiments for two-degrees-of freedom are undertaken to determine the coupled coefficients. Therefore, the solution of equations up to two degrees of freedom is required. The solution for the single degree of freedom system leads to the following expressions for the calculation of added mass and damping coefficients [Appendix B.5].

$$A_{jj}=\frac{1}{\omega_e{}^2}\left(K_{jj}-\frac{F_{j0}\cos\varepsilon_j}{X_{j0}}\right)-M_{jo} \qquad \text{(Eq 6.5)}$$

$$B_{jj}=\frac{F_{j0}\sin\varepsilon_j}{X_{j0}\,\omega_e} \qquad \text{(Eq 6.6)}$$

where:

A_{jj} : Added mass coefficient
B_{jj} : Damping coefficient
K_{jj} : Restoring force or moment
M_{j0} : Mass or mass moment of inertia of the model.
ε_j : Phase angle between force and response
X_{j0} : Maximum amplitude of motion
ω_e : Frequency (rad/sec)
F_{j0} : Maximum excitation force amplitude

In order to determine the coupled coefficients, the following expressions are used [Appendix B.5]:

Eq 6.7 :

$$A_{ij}=\left(\frac{-(M_i+A_{ii})\,X_{i0}\,\omega_e^2\cos(\varepsilon_i-\varepsilon_j)+B_{ii}\,X_{i0}\,\omega_e\sin(\varepsilon_i-\varepsilon_j)+K_{ii}\,X_{i0}\cos(\varepsilon_i-\varepsilon_j)+K_{ij}\,X_{j0}}{X_{j0}\,\omega_e^2}\right)$$

Eq 6.8 :

$$B_{ij}=\left(\frac{(M_i+A_{ii})+X_{i0}\,\omega_e^2\,\mathrm{Cos}\varepsilon_i-B_{ii}\,X_{i0}\,\omega_e\,\mathrm{Sin}\varepsilon_i-K_{ii}\,X_{i0}\,\mathrm{Cos}\varepsilon_i+A_{ij}\,X_{j0}\,\omega_e^2\cos\varepsilon_j-K_{ij}\,X_{j0}\cos\varepsilon_j}{X_{j0}\,\omega_e\,\mathrm{Sin}\varepsilon_j}\right)$$

Where:

- j : Index of the forced motion
- i : Index of the coupled motion
- K_{ij} : Coupled restoring (n into m)
- ε_j : Phase angle of forced motion
- ε_i : Phase angle of coupled motion
- X_{i0} : Maximum amplitude of coupled motion

i- Phase Angles

Phase angles are measured between zero crossings of force and motions. If force is leading, the phase angle is taken as positive and if it is lagging it is taken as negative.

ii- Forces

Maximum force amplitudes are determined as half the average double amplitude from the force record. Because of the asymmetry in amplitude which is either due to the damage condition or sudden change of form, the force amplitude is calculated in this manner.

iii- Results

The results are presented in graphical form. Before they are plotted, all values are non-dimensionalised in order to use them in real application and for comparison purposes. The procedure of non-

dimensionalising is as follows:

All parameters are plotted against non-dimensional frequency(ω_{nd}).

$$\omega_{nd} = \omega_e \sqrt{\frac{B}{2\,g}} \qquad \text{(Eq 6.9)}$$

Where:

ω_e : Frequency (rad/sec)
B : Ship breadth
g : Gravitational acceleration

Non-dimensionalised Force

$$F_{nd} = \left(\frac{F_0 \text{ x } B}{\text{Amp x g x Mass}} \right)$$

F_0 : Maximum force amplitude
Amp : Amplitude of motion(m)
Mass : Model mass

Non-dimensionalised Roll Moment

$$MR_{nd} = \left(\frac{MR_0}{\text{Amp x Mass x B x g}} \right)$$

where:

MR_0 : Maximum amplitude of moment
Amp : Amplitude of roll motion (Rad)

Non-dimensionalised Added Mass

$$A_{jjnd} = \frac{A_{jj}}{\text{Mass}} \qquad \text{For Heave and Sway}$$

$$A_{jjnd} = \frac{A_{jj}}{Mass\ B^2} \qquad \text{For Roll}$$

Non-dimensionalised Damping

$$B_{jjnd} = \frac{B_{jj}}{Mass} \sqrt{\frac{B}{2\ g}} \qquad \text{For Heave and Sway}$$

$$B_{jjnd} = \frac{B_{jj}}{Mass\ B^2} \sqrt{\frac{B}{2\ g}} \quad \text{For Roll}$$

Non-dimensionalised Coupling Coefficients

Sway into roll, Heave into roll

$$A_{ijnd} = \frac{A_{ij}}{Mass\ B} \qquad \text{Added Mass}$$

$$B_{ijnd} = \frac{B_{ij}}{Mass\ B} \sqrt{\frac{B}{2\ g}} \quad \text{Damping}$$

6.9 RELIABILITY OF THE EXPERIMENTAL RIG

In all experiments there are always errors, which may be small or vital. Therefore it is important to examine the source and degree of errors. However, probably the most important element in experiments is the reliability of the experimental rig. If consistent results are obtained by using the designed mechanism, then results can be trusted and improved by identifying and eliminating other errors that might exist.

In order to carry out error analysis according to the statistical rules, a sufficient amount of data is needed for the same condition. However to obtain a large enough sample of data for error analysis would be difficult due to the limited time and availability of the experimental facilities. As a result only specific conditions are repeated to check the reliability of the mechanism and to identify the source and importance of errors.

During the experiments some conditions are repeated three times, over a wide range of frequency. It is believed that the collected data is sufficient to provide enough information on the reliability of the experimental mechanism and errors.

After the completion of the experiments, it can be concluded that the design of the mechanism is a success, as it carried out all its planned duties without failure and provided consistent results. However, there are some differences between the repeated results as expected and it is believed that these are due to a combination of human errors, wrong timing of the measurements as well as uncontrollable environmental errors. These are explained next.

6.9.1 Forced Sway Experiments

The repetition of sway experiments is quite good at almost all frequencies. If the added mass is examined, this agreement can be seen clearly (Fig 6.10). The small differences between the results may be due to the measured excitation forces which also show small differences [Appendix B.6]. If the damping is examined, there is a good agreement in the frequency range of 0.75 - 1.5 (non-dimensional, ω_{nd}), but at low frequencies the agreement worsens. One of the main reasons is probably the small differences in phase angles which renders estimates of damping difficult. The other parameter, sway excitation force is so small at low frequencies that it is usual to have small differences in real values, but these small differences can become large in relative terms. Therefore, these small differences may change the damping results considerably.

In the case of coupled sway-roll experiments, results are in good agreement except again at low frequencies (Fig 6.11a and Fig 6.11b). At this range, there is a large difference in added mass which also shows small disagreement at the non-dimensional frequency (ω_{nd}) range 0.75-1.0. At low frequencies, the main reasons can again be found in the roll and sway phase angles. Roll phase angles at low frequencies differ between 20% and 100% (Fig 6.12c). Sway phase angles at all frequencies fluctuate at just under 180 degrees (Fig

6.12b) and a few degrees of difference in phase can change the coupled coefficients considerably. At low frequencies roll amplitudes are also very small, so that small spikes in the recorded signal, due for example to vibration of the motor or rails, can change the phase angle a few degrees, which is sufficient to affect the results. Therefore, at low frequencies it is very difficult to obtain very good agreement between the results of the repeated experiments for identical conditions. However, overall, the results of the repeated experiments can be said to be in sufficiently good agreement.

6.9.2 Forced Heave Experiments

Repetition of heave experiments is very good, except at low frequencies where restoring forces are dominant. At low frequencies, the heave phase angle is less than 5 degrees and the small effect of restoring force may create small differences in the phase angle as well as in the excitation force, but this small change creates a large difference in the added mass (effect of force), while damping coefficients (effect of phase angle) differ more than 100% (Fig 6.13). Since the water surface can be disturbed very easily and this disturbance cannot be noticed very easily by naked eye, the heave force signal may be affected slightly in terms of its amplitude and phase angle. However, it is difficult to eliminate this effect completely.

6.9.3 Forced Roll Experiments

Again, repetition of the experiments is good (Fig 6.14) with the exception of results at the low frequency range. Again phase angles at low frequency fluctuate due to small roll amplitudes and spikes due to the presence of noise. The same problem is also present at high frequencies. In addition, since the experimental rig is fixed to the tank rails, which obviously vibrate at high frequencies, vibration of the rails may be the second reason for the small fluctuation of the phase angle. However, the results of repeated experiments for identical conditions are still reasonably consistent.

6.10 PRESENTATION OF THE RESULTS

6.10.1 Single Degree of Freedom

i- Effect of Amplitude

In order to investigate the effect of amplitude on the hydrodynamic coefficients, two different amplitudes, 2 cm and 4 cm, are considered. They correspond to 0.6 m and 1.2 m of amplitude in full scale. Results are presented for each motion as follows. For the repeated tests first set of the results is used for the presentation

Sway

Experiments are carried out for different frequencies. However, the maximum frequency changes, depending on the amplitude, which creates unacceptable vibration in the experimental mechanism, which in turn seems also to break down under this kind of excessive dynamic loading. Therefore, for 4 cm amplitude no results could be obtained beyond 1.20 hertz (7.54 rad/sec).

According to the results, the change in the amplitude does not affect significantly the added mass and damping coefficients of sway motion (Fig 6.15). This small difference is probably due to the small changes in phase angles as well as the excitation forces.

Heave

Except at low frequencies, the added mass coefficients for both heave amplitudes follow the same trends and are of similar magnitude (Fig 6.16). At low frequencies, the effect of different amplitudes can be seen. At the low frequency range, the heave excitation force which is dominated by the stiffness force is slightly larger at 4 cm amplitude compared with the 2 cm case (Fig B.6.5 in Appendix B.6). Because of the hull form, the buoyancy force, which is a function of the waterplane area (WPA) changes considerably and so does the heave excitation force. Although it is less likely, the water surface disturbances at low frequencies which may affect the excitation forces and phase angles slightly, cannot be discarded completely as another possibility for the observed difference. If the expression for the added mass (Eq 6.5) is examined, it can be concluded that the change in the force can affect the results considerably.

In the case of damping, the same conclusions can be drawn (Fig 6.16b). If the expression for damping is examined it can be seen that in Equation 6.6, $\sin\varepsilon$ is very sensitive to phase angle changes, especially at low and very high frequencies, where phase angles are just above 0 and just below 180 degrees, respectively.

When the frequency is around 0.45 hertz (0.41 in non-dimensional form) there is a sudden change in added mass and damping coefficients. The reason for this change is probably due to the non-linear effect of heave stiffness. In the case of heave, although it is not normal to have appreciable non-linear effects, which are generally observed with roll motion, this particular ship has a strongly draught-dependent hull form. A small analysis indicated that the waterplane area curve of this ship changes with draught non-linearly (cubic or higher). Therefore, it is believed that, the sudden change of the experimental results at this particular frequency is due to the non-linear stiffness.

Although there is not a lot of information available due to the limited experimental results, some suggestions can be put forward regarding the sudden change at the frequency of 0.45 hertz. This sudden change can be due to what is known as the jump phenomenon, which may be described as a jump to higher motion amplitudes within a certain frequency range. This phenomenon can be analysed by using a Duffing's type equation [68], which defines the stiffness in a cubic form. The WPA of this model is a cubic function of the draught and this may provide a base for making this argument. Further support for this is provided by observing the decrease in the force amplitude at this particular frequency for a constant motion amplitude.

Another possibility may be superharmonic motion, which has also been related to roll motion due to its high non-linearity in the stiffness term. Superharmonic motion occurs when the excitation frequency/motion frequency (ω_e/ω_0) ratio is around 0.33 [69], again with a cubic form of stiffness. The way that experiments were carried out, the excitation frequency was also the motion frequency. Therefore, it is difficult to come to a conclusion with regard to the

above, but calculated natural heave frequency for the model was around 1.2 hertz, which gives ω_e/ω_o ratio around 0.3.

It must be emphasized that all these observations on the different non-linearities mentioned above are related to roll motion. Therefore, caution must be exercised before arriving at the same conclusion, with regard to heave motion, without any further study. However, certain parameters and observations mentioned above suggest that this sudden change in the heave force and hydrodynamic coefficients at this frequency is due to non-linear effects.

Roll

Because of the forcing mechanism used to excite the model in roll, the roll amplitude cannot be fixed. As can be seen in Fig 6.19c the roll response of the ship changes with frequency for a mass of 1.4 kg at each side of the arm. As Fig 6.19c shows, the roll amplitude of the ship increases drastically in the resonant region, while it is very small just outside this region. Therefore, the coefficients are very much dependent on the roll amplitude.

An examination af the added mass in the upright condition reveals that added mass, which is large at low frequencies, reduces as frequency increases. However, it increases suddenly near the natural roll frequency and then continues to decrease as frequency increases beyond the natural frequency. The sudden increase of the added mass at the resonance region is due to the sudden large increase in the roll amplitude of the model (Fig 6.16c). This effect of large roll amplitude on added mass can be seen in Eq 6.5. The damping coefficient is also very high at low frequencies compared to the values at high frequencies (Fig 6.19).

ii- Effect of Static Heel

In order to investigate the effect of static heel on the hydrodynamic coefficients, which is normal with damaged ships, the ship is considered at different heeling conditions. This investigation helps to identify whether the coefficients in the upright condition can be used when referring to heeled conditions. For this purpose 6 and 12

degrees of static heel are considered for the investigation. However these values may change slightly when considering different motions.

Sway

Static heel affects the sway added mass and this effect depends on frequency and static heel (Fig 6.17a). At low to moderate frequencies, the added mass of the upright ship is small and increasing, while the added mass of the inclined ship is large and decreasing. However, as frequency increases, all the added mass curves have the same trend. At high frequencies the added mass of the ship with small inclination does not differ from the one at the upright condition, but for a larger heel the added mass differs noticeably from the one at the upright condition.

Sway damping has a similar trend in all conditions but changes considerably with static heel (Fig 6.17b). Again at high frequencies the damping in the upright and small static heel conditions does not change significantly, but for lower frequencies important changes are observed. For larger static heel, the damping again differs from the values in the upright and small static heel conditions but follows a similar trend. These results show that the added mass and damping coefficients for sway are dependent on static heel. The dependency of sway motion on a static heel can be explained by the different and asymmetric underwater hull form created by the static heel. This asymmetry creates different radiation forces on the two sides of the model. As a result the sway force values and phase angles change and even if these changes are small they can cause large differences on the coefficients. Lack of buoyancy force in sway motion probably renders sway radiation forces and phase angles more dependent on the changes of the hull form.

At the inclined condition the ship has a different underwater form which affects the phase angle and force values, and these changes, even if they are small, cause larger differences on the coefficients.

Heave

Except at low frequencies, heave added mass does not show

significant differences between the different static heel conditions (Fig 6.18a and Fig 6.18b). As mentioned in the foregoing, the difference at low frequencies may be due to small differences in the force measurements, which are affected by small disturbances in the free surface. In the case of damping, there is a good agreement between the curves throughout the frequency range. The reason for such a small effect of the static heel is due to the fact that heave stiffness does not change significantly with static heel [Appendix B.4], so that the excitation force and phase angle do not change significantly either. However, the non-linear effect of heave stiffness at the frequency of 0.45 hertz can still be observed for all the test conditions tried, although this effect changes slightly depending on these conditions.

Roll

Static heel changes the added mass moment of inertia coefficient of roll significantly, compared to the upright condition (Fig 6.19a). However, the difference between the added mass moment at different static heels (6 and 12 degrees) is small enough to be ignored. The reason for the difference between the upright and inclined conditions can be attributed to the differences in the roll stiffness values. The roll restoring curves between upright and inclined conditions change significantly but the stiffness curves between the two inclined conditions do not [Appendix B.4]. The phase angles which change slightly between these conditions may also be another reason for the observed differences.

In the case of damping, there are differences between the upright and inclined conditions as well as between the two inclined conditions (Fig 6.19b). The source of these differences is possibly phase angles and the amplitudes which change with static heel angle (Fig 6.19 and Appendix B.6). Damping at low frequencies appears to be high but decreasing drastically as the frequency increases. Therefore it is difficult to identify the differences between different conditions at higher frequencies. Considering this point, the differences between different conditions must be investigated for particular frequencies, rather than looking at the overall trends.

6.10.2 Two Degree of Freedom

i- Sway into Roll (Forced Sway)

Strong coupling between sway and roll is known to exist but it is important to know whether static heel changes this effect and hence the coupling coefficients. It seems that the roll response curve for each condition changes, more precisely it shifts as static heel changes [Appendix B.6]. Of course this shift changes the roll amplitude and phase angle for a particular frequency and these in turn affect the added mass and damping coefficients. The differences become significant near the resonant region where large roll angles are observed (Fig 6.20a and Fig 6.20b).

ii- Roll into Sway (Forced Roll)

Unlike sway into roll coupling, no roll induced sway motion could be observed. There may be coupling from roll into sway but it was not strong enough to excite the model in the sway direction.

iii- Heave into Roll (Forced Heave)

Effect of Static Heel

For a ship in the upright condition, no coupling between heave and roll was observed as expected. However, for an inclined ship, strong coupling from heave into roll was observed, and when the heave excitation frequency was near the roll natural frequency, the roll amplitude of ship was measured at approximately 9 degrees. This heave into roll coupling, however, does not change significantly for different static heel angles, especially for the added mass (Fig 6.21). The larger change is observed for the heave into roll damping coefficient for different static heels, but again it was not big enough for it to be taken into account.

Effect of Amplitude

A ship at 10.3 deg inclined condition is tested for 2 cm and 4 cm heave amplitudes and it was found that the effect of the heave amplitude on heave into roll coupling is very strong. This effect can be seen in Fig 6.22c, which shows the roll response due to heave motion. The same difference is observed with the heave into roll

added mass (Fig 6.22a), however, the difference observed with heave into roll damping was smaller (Fig 6.22b).

iv- Roll into Heave (Forced Roll)

As in the case of sway into roll experiments, no heave motion due to roll is observed. These experiments also show that roll motion cannot affect other motions but can be affected by them very easily.

v- Heave into Sway and Sway into Heave

Both in the upright and inclined conditions no coupling in either way is observed. This experimental finding suggests that coupling between heave and sway in all conditions is almost impossible.

6.11 COMPARISON BETWEEN EXPERIMENTALLY AND THEORETICALLY DERIVED COEFFICIENTS

In order to verify the experimental results and identify the experimental errors as well as the differences and the reasons behind these, it was considered appropriate to carry out a comparative study between experimental and theoretical results. This kind of comparison is not to conclude whether experimental or theoretical results are right or wrong but to identify weaknesses in each method and to attempt to improve upon them.

Theoretical calculations are based on two dimensional velocity potential at each section (strip theory) and solved by using the Frank-Close-Fit Method as explained in Chapter 5.

6.11.1 Single Degree of Freedom

Although theoretical and experimental results of sway added mass in the upright condition show similar trends (Fig 6.23a), they differ considerably at low frequencies. However, as frequency increases agreement between theory and experiments becomes better. Especially in the inclined condition the agreement is very good (Fig 6.24a).

The damping curves, which are obtained from experiments and theory for both upright and inclined conditions, show a similar trend for all frequencies. However, values at inclined conditions differ

considerably (Fig 6.23b), while agreement between theory and experiments in the upright condition can be said to be reasonable (Fig 6.24b).

In the case of heave added mass, for both upright and inclined conditions, experiments and theory are in very close agreement (Fig 6.25a and Fig 6.26a). There is only one particular frequency where there is a large difference, which is assumed to be due to the non-linear heave stiffness force. An examination of the heave damping values reveals the same trend between theory and experiments, but despite the reasonably good agreement there are some differences at certain frequencies (Fig 6.25b and Fig 6.26b). Again the subharmonic motion at low frequencies can be the reason, while the combination of non-linear effects as well as the sensitivity of the damping with phase angle at high frequencies may be the possible cause for the differences.

For roll motion, the situation is completely different. Roll added moment values from theory and experiments in the upright condition have similar trends towards the high frequency range but different magnitudes. Although this difference may be within acceptable limits, near the natural roll frequency this difference may affect the responses considerably. In addition, the trend of the experimental results at low frequencies is significantly different (Fig 6.27a). This may be due to the experimental set up which could only excite the model at very small roll motion at low frequencies. Theoretical results at the inclined positions do not change appreciably compared with the upright conditions, but experimental results at inclined condition change drastically and have a different trend compared to the experimental results in the upright condition (Fig 6.27a), as well as theoretical results in the inclined condition (Fig 6.28a). The reason for these can be due to the changes in the non-linear effects such as viscosity and non-linear stiffness on the inclined ship which are not taken into account by the theory. The effect of roll amplitude also seems to be more significant at the inclined conditions. Of course the non-linear restoring which is taken into account in the analysis of experiments may be another important parameter

influencing added moment. In the case of damping coefficients from medium to high frequencies, the damping values for theoretical and experimental results show similar trends for both the upright and the inclined conditions (Fig 6.27b and Fig 6.28b) but the same is not true at low frequencies. In the low frequency range, theory estimates damping to be almost zero but in contrast the experimental results show very large damping. However, in general, damping values derived from experiments ought to be higher than those derived from potential theory, which does not include the viscous effects, which constitute the main damping contribution. The opposite finding of the experimental results at high frequencies may be related to the lack of high sensitivity of the experimental mechanism as well as some parameters such as roll phase angle and roll amplitude.

Since varying roll amplitude is very small and there is a noise problem at high frequencies, measurement of roll and phase angles may be distorted. The experimental damping is significantly dependent on roll amplitudes and phase angles while potential theory, which is based on small amplitude assumption, is independent of amplitude and phase angle. If experimental results are examined, it can be seen that roll amplitudes are small and more importantly phase angle fluctuates just under 180 degrees. Slight distortion of these measurements which may seem unimportant can cause magnified effect on roll damping. For instance, $\sin\varepsilon$ from damping equation (Eq 6.5) is very close to zero when phase angle is just under 180 degrees and can increase the damping by 200% if phase angle is measured two degrees less. A few degrees of distortion is quite normal considering the noise level, small amplitude and especially sensitivity of potentiometer, which is used for measurement of roll and phase angles.

The roll experimental mechanism used in this thesis may not be the best for high frequencies and very small amplitudes, therefore, it may be necessary to increase the accuracy by including very sensitive measurement tools. Furthermore, in order to establish trends and identify the differences and reasons between theory and experiments it is obvious that more experiments and more comparisons are

required.

6.11.2 Coupling Coefficients

An upright ship which rolls, does not experience dynamic coupling from heave motion. However this changes if symmetry is lost due to static heel. This coupling between heave and roll has not been investigated theoretically in detail (Conceiçao et al [69], calculated the coefficients for asymmetric ship using potential theory), and it is believed that no experimental investigation has been carried out before. Fig 6.29 shows a comparison between experiments and theory, and as is clearly seen they give completely different results although the added mass values have a similar trend. However, heave into roll damping values differ completely both in magnitudes and trends. Theory predicts small values and results change slightly with frequency, while experiments show a drastic change with frequency. Although this proves that theory and experiments give different results, again more experimental results are needed to establish any solid trends and conclusions.

In the case of sway into roll coupling coefficients, there are also large differences although the trend can be said to be similar. However, the added mass values are completely different and this difference changes depending on frequency (Fig 6.30a and Fig 6.31a). Similar observations are valid for both upright and inclined conditions. Again sway into roll damping values have similar trends but values differ significantly at some frequencies. Especially at the roll natural frequency the difference reaches a maximum (Fig 6.30b, Fig 6.31b) since at the natural frequency the model rolls with large amplitudes due to the coupling from sway. At high frequencies the trend of the sway into roll damping curves (Fig 6.30b and Fig 6.31b) follow opposite directions.

The differences between theory and experiments for sway into roll coefficients are also observed by Vugts [15] but at a lesser degree since his results are based on two-dimensional cylinders.

Although some differences are observed, comparisons prove that the

experimental set up gives reasonably good results and also that coupling coefficients differ considerably between theory and experiments. However, it is useful to investigate the effect of these differences on ship (full scale) responses and this is discussed in the following section.

6.12 EFFECT OF EXPERIMENTAL AND THEORETICAL COEFFICIENTS ON SHIP RESPONSE

As shown in the previous section, experimentally derived hydrodynamic coefficients are in good agreement with some theoretically derived coefficients, while in disagreement with others. Some coefficients even appear to have different trends. However, these differences may not have an effect on the ship responses since there is no linear relation between coefficients and ship motions. In order to improve the accuracy of the theoretical calculation method of the hydrodynamic coefficients, it is important to identify which coefficients, including the coupling coefficients, affect ship motions and how important their effect is. For this purpose a small parametric study for comparison is carried out on some coefficients and their effects on the full scale ship are studied. This comparison is based on the assumption that the experimental results are reasonably accurate, although it was mentioned earlier that some errors might be expected. These results and conclusions are given next.

As mentioned above this study was carried out for the same ship whose 1/30 scale model was used in the experiments. For this study three frequencies are chosen: one in the low frequency range (0.506 rad/sec), one near the natural roll frequency (0.785 rad/sec.) and the third in the high frequency range (1.438 rad/sec.). Results are presented for coupled sway, heave and roll motions.

6.12.1 Roll

i- Upright Condition

At the low frequency (0.506 rad/sec) the coupled roll motion obtained by using experimentally derived coefficients, shows a steady response without any transients, while the motion obtained using theoretically derived coefficients, appears to be unsettled (Fig 6.32b). Therefore,

results do not agree although responses for both methods are small. Obviously the large difference in damping values (Fig 6.27b) is reflected in the response.

Near the natural roll frequency, roll oscillations for both conditions are much larger compared to the oscillations at the lower frequency, and moreover, the difference between the theoretical and experimental methods is also large (Fig 6.32b). Although both methods show steady responses, a large difference exists and is believed to be due to the small roll added moment derived from experiments as well as the large difference between sway into roll coupling values (Fig 6.27a, Fig 6.30a and Fig 6.30b). Since these coefficients can change both the roll response and the natural roll frequency, small changes in the added moment and damping values may affect response considerably near the natural roll frequency.

At the high frequency, the roll response is again typically small and despite a difference between theoretical and experimentally derived coefficients the difference in roll response is very small, thus proving that coefficients do not affect ship response proportionally.

ii- Inclined Condition (10.3 deg.)

At the low frequency, despite the fact that both methods provide completely different roll added moment and damping values (Fig 6.28a and Fig 6.28b), the roll response for both methods is in good agreement (Fig 6.33a). It must be noted that coupling damping coefficients at this particular frequency and inclined condition are similar in both methods (Fig 6.29b and Fig 6.31b). Again roll oscillations are small at this condition.

Near the natural roll frequency, experimentally derived coefficients again cause very large amplitudes (15 deg, Fig 6.33b), while roll response for both methods differs considerably. Since near the natural roll frequency, roll motion coefficients from experiments and theory are similar (Fig 6.28a and Fig 6.28b), the only reason for the large motions and the difference in response may be due to the coupling coefficients. Since heave into roll coefficients exist due to static

heel, and both experimentally and theoretically derived coefficients differ greatly (Fig 6.29a and Fig 6.29b), this coupling may also be another reason for the large difference observed in motions. Sway into roll coupling coefficients for this frequency differ considerably as well (Fig 6.31a and Fig 6.31b). It can be said that roll response is very sensitive to all the coefficients near the natural frequency.

Fig 6.33c reveals that at the high frequency, again after the transient period, both methods give similar results with a small difference in amplitude despite the large differences in the coefficients.

Overall it can be said, that outside the resonant roll region, large differences in the coefficients may cause only small differences in the response, but around the natural frequency region the opposite is true.

6.12.2 Heave

For both upright and inclined conditions, at low and medium frequencies, heave motion is not affected by the differences in hydrodynamic coefficients between theory and experiments. At the high frequency the results are affected only slightly (Fig 6.34, and Fig B.6.12 in Appendix B.6). The main reason for this good agreement between both responses, is that both theoretically and experimentally derived coefficients, especially added mass are in good agreement. The slight difference between theoretical and experimental results at high frequencies is due to differences in damping coefficients.

6.12.3 Sway

At low and medium frequencies, for both upright and inclined conditions, the sway oscillations of the ship do not change significantly between theoretical and experimental methods. However, in the case of theoretical coefficients being used, the ship drifts considerably before it starts oscillating steadily (Fig 6.35a and Fig 6.35b), while when using experimental coefficients the ship starts oscillating without any significant drift. The main reason for this drift is due to the sway damping which, if calculated theoretically, is

almost zero at the low frequency whilst having a small value at the medium frequency (Fig 6.23b and Fig 6.24b). However, at high frequencies both theoretically and experimentally derived damping coefficients are high (Fig 6.16b and Fig 6.17b) and hence the drift is small with only a small difference in the amplitudes (Fig 6.35c, and Fig b.6.13 in Appendix 6).

6.12.4 Effect of Heave into Roll Coefficient on Ship Response

This coupling is not common since it is only encountered if there is static heel, and this may be very important during progressive flooding, which in turn may cause asymmetric flooding. Therefore, it is important to find out the effect of this coupling on roll motion. For this purpose the roll response of the ship is examined firstly by including and secondly by excluding heave into roll coupling coefficients as obtained from experiments. In both conditions hydrostatic coupling between heave and roll is present.

At low frequencies the effect of heave into roll coupling can be seen to be insignificant since, in general, roll amplitude is small at low frequencies. However, near the natural roll frequency heave into roll coupling becomes very significant as roll amplitude is three times larger, compared to the roll amplitude with no heave into roll coupling (Fig 6.36). The main reason for this difference is due to the fact that both coupled added mass and damping coefficients are large, and thus they may cause a shift in the natural roll frequency, causing resonance (Fig 6.29). Furthermore near natural roll frequency, roll motion can be affected significantly by small changes or additional influences.

At the high frequency the response of the ship is not affected by the heave into roll coupling coefficients. The main reason for this derives from the fact that heave into roll added mass value which is almost zero at the high frequency (1.438 hertz) does not create any shift in the natural roll frequency. In addition, since this excitation frequency is far from the natural roll frequency, the roll amplitude is small and the large heave into roll damping does not have any effect.

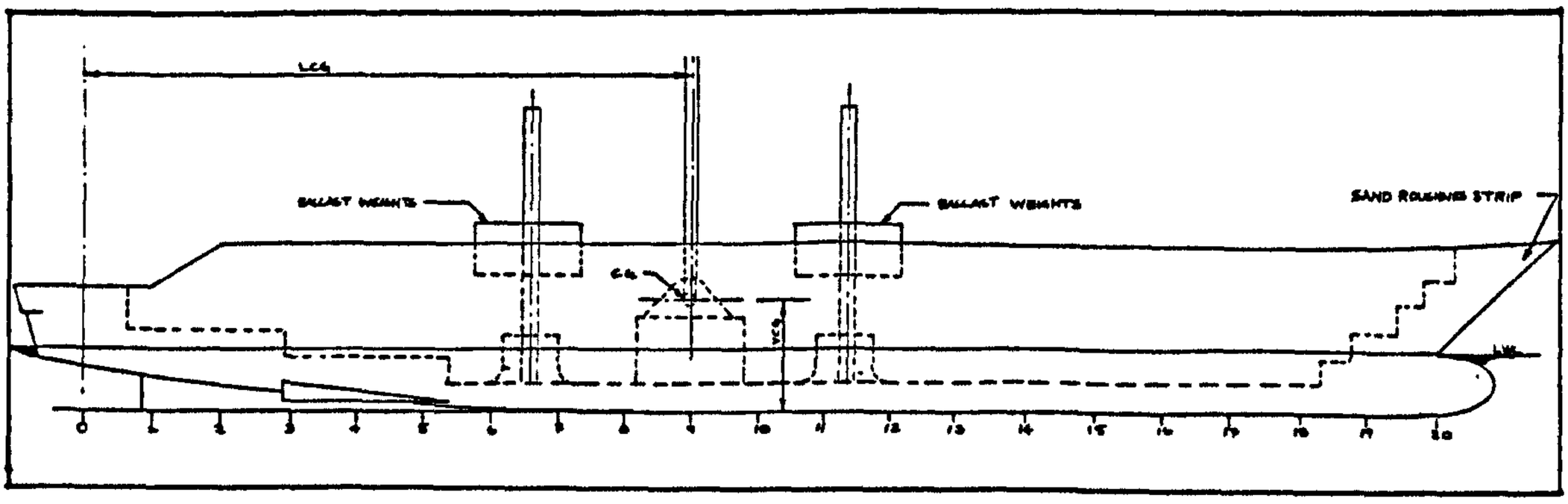

Fig 6.1A Model ship used in the experiments

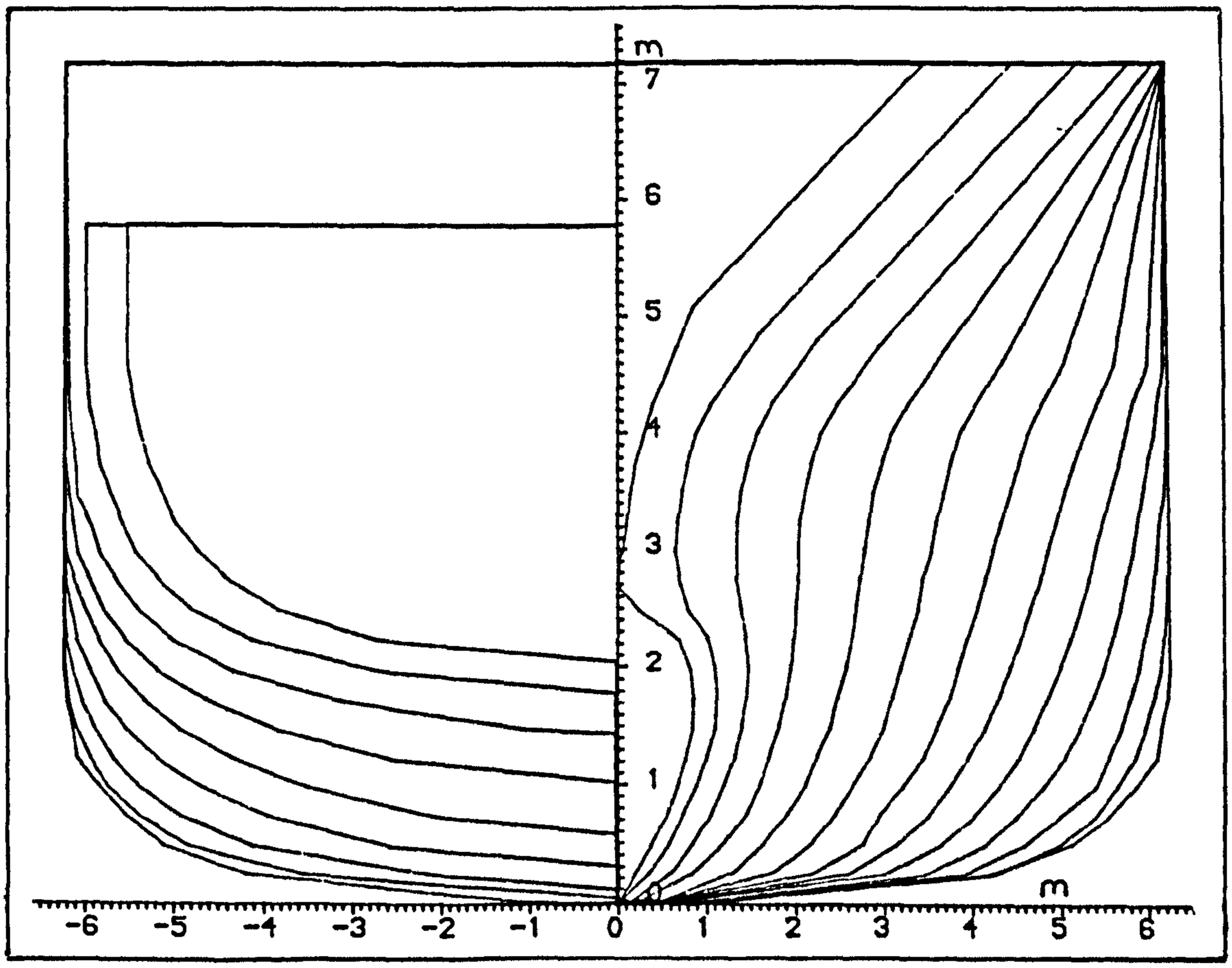

Fig 6.1B Hull form used in the experiments

	UPRIGHT CONDITION	INCLINED CONDITION	
FORCED SWAY EXPERIMENTS		Static Heel 6 Deg	Static Heel 12 Deg
Mode of Experiment	Sway Amplitude [cm]	Sway Amplitude [cm]	Sway Amplitude [cm]
SWAY	2 and 4	2	2
SWAY-HEAVE	4	4	4
SWAY-ROLL	4	4	4

	UPRIGHT CONDITION	INCLINED CONDITION	
FORCED HEAVE EXPERIMENTS		Static Heel 6 Deg	Static Heel 12 Deg
Mode of Experiment	Heave Amplitude [cm]	Heave Amplitude [cm]	Heave Amplitude [cm]
HEAVE	2 and 4	2	2
HEAVE-SWAY	4	4	4
HEAVE-ROLL	4	2 and 4	2 and 4

	UPRIGHT CONDITION	INCLINED CONDITION	
FORCED ROLL EXPERIMENTS	Roll amplitude is not fixable	Roll amplitude is not fixable	
Mode of Experiment		Static Heel 6 Deg	Static Heel 12 Deg
ROLL	yes	yes	yes
ROLL-SWAY	yes	yes	yes
ROLL-HEAVE	yes	yes	yes

Table 6.1 Experiments carried out

Fig 6.2A General view of the experimental tank

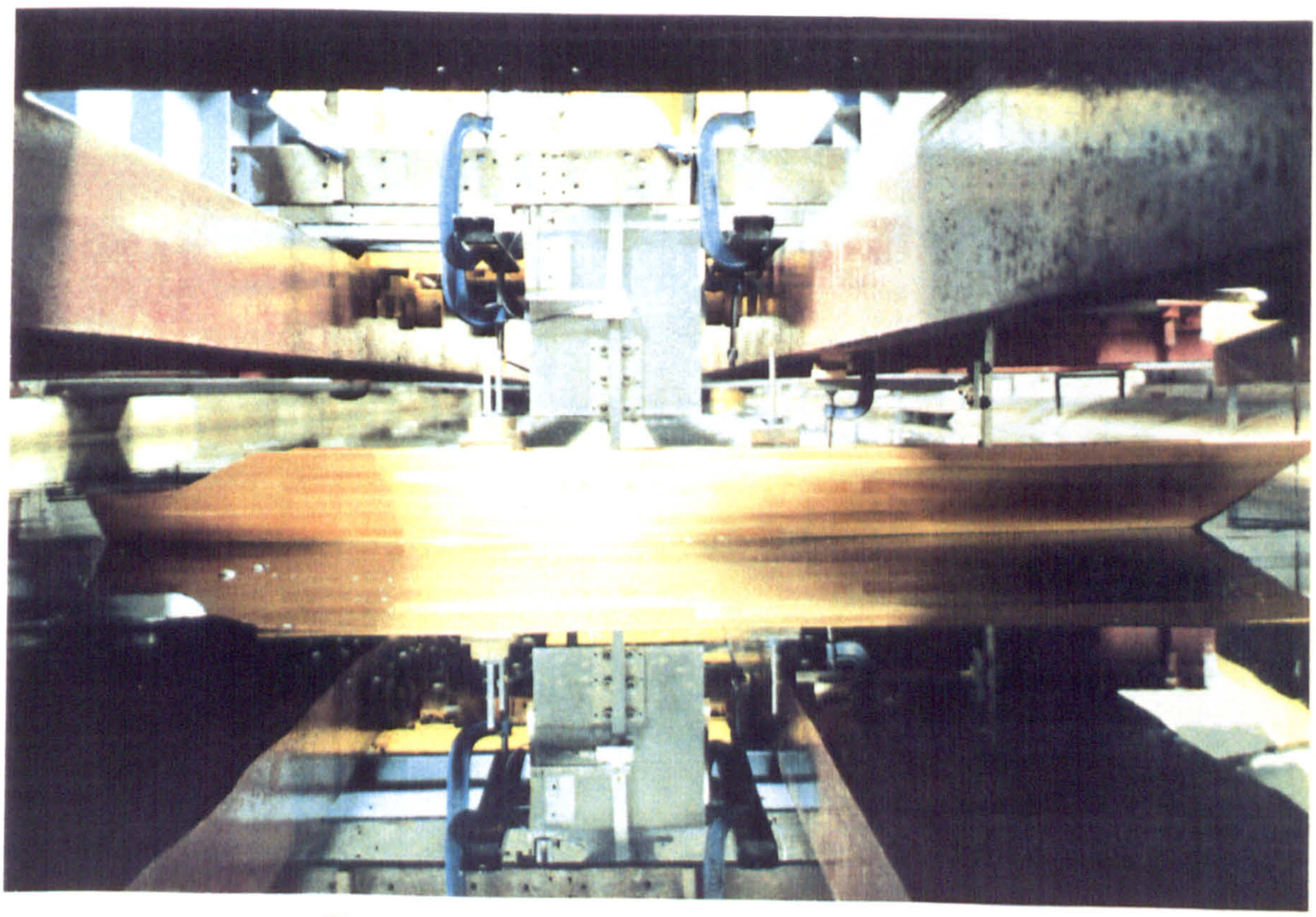

Fig 6.2B General set up of the experimental rig

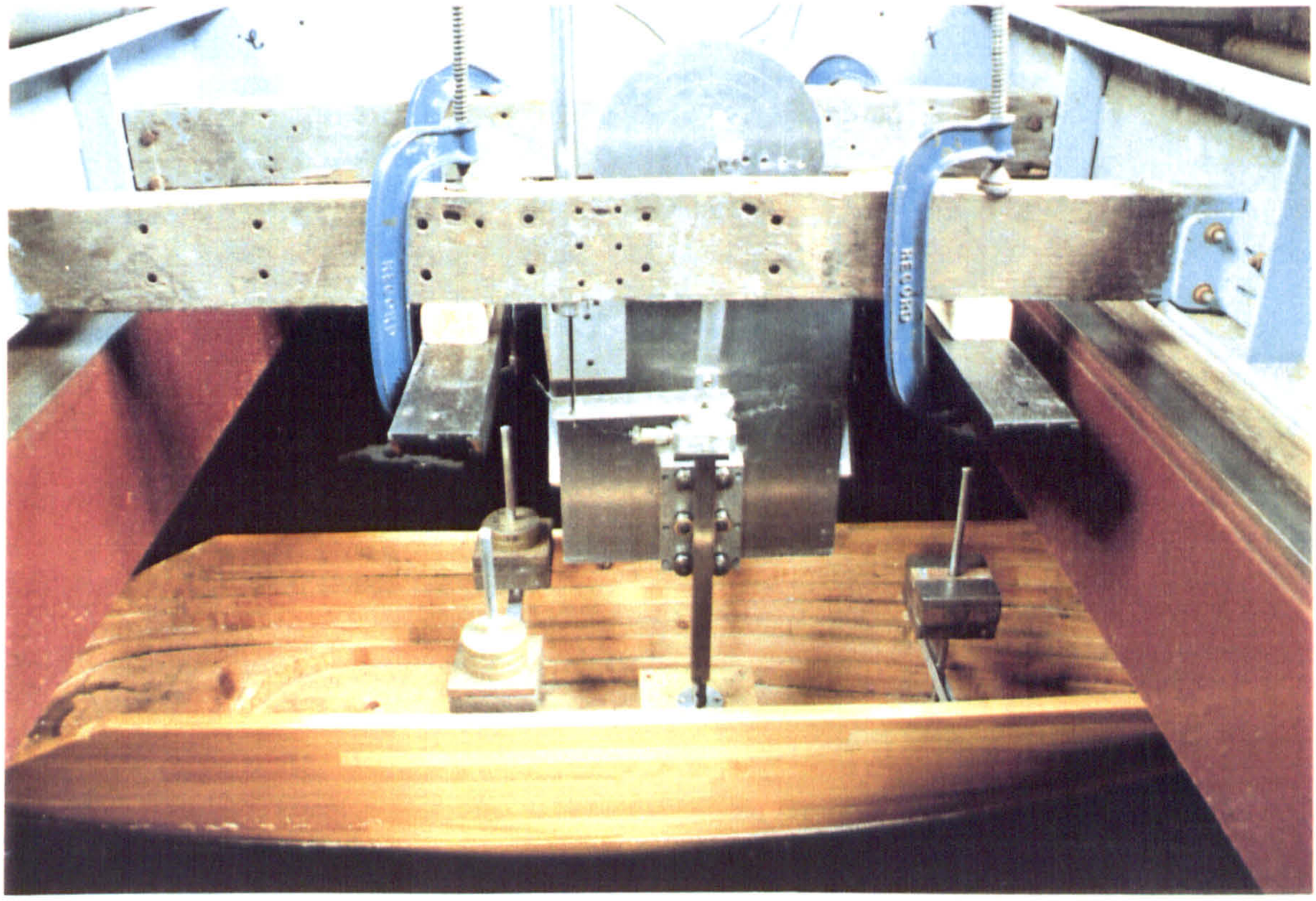

Fig 6.3A Experimental set up to determine the hydrodynamic coefficients of heave motion [Forced heave]

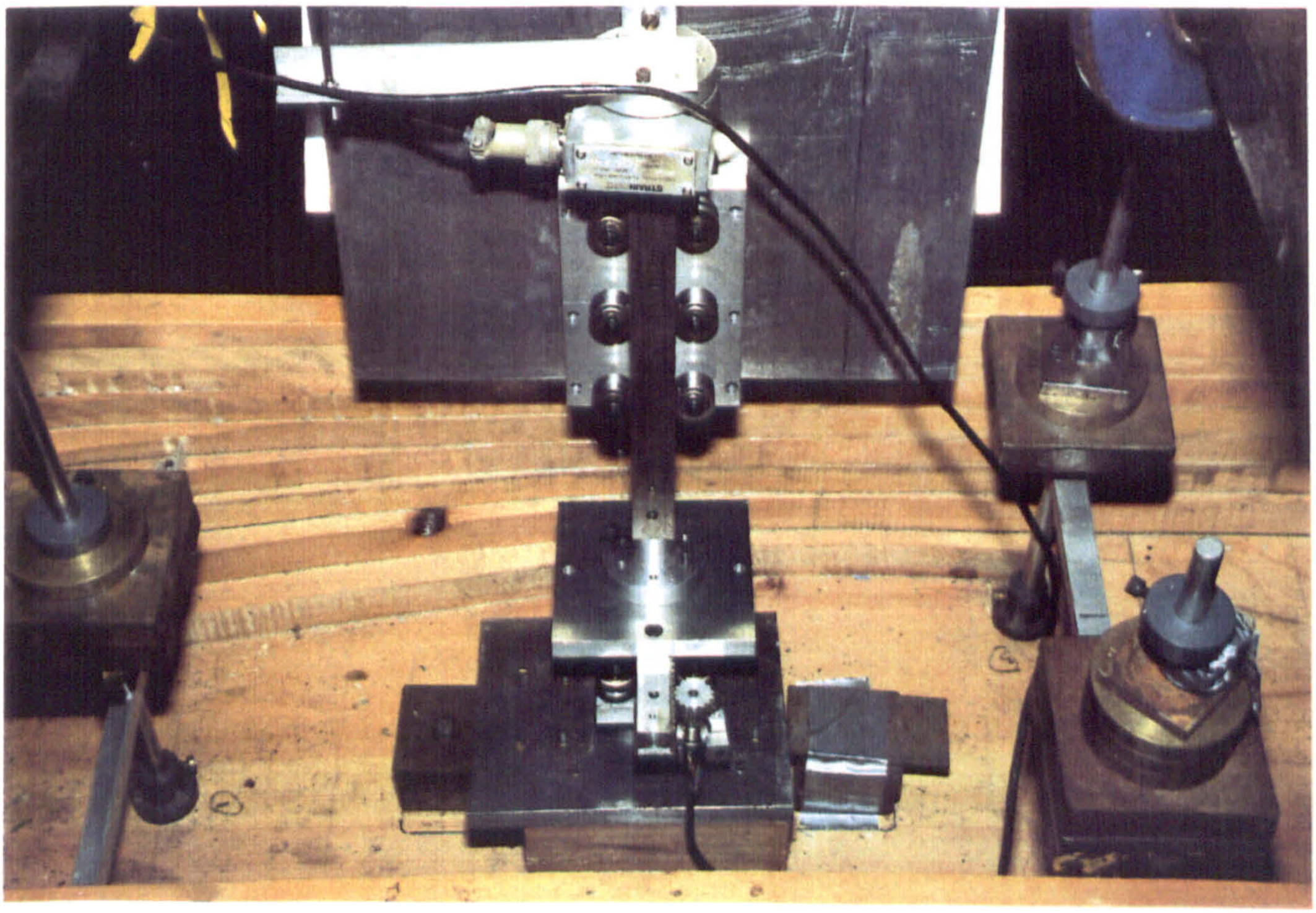

Fig 6.3B Experimental set up to determine the hydrodynamic coupling coefficients of heave into sway [Forced Heave]

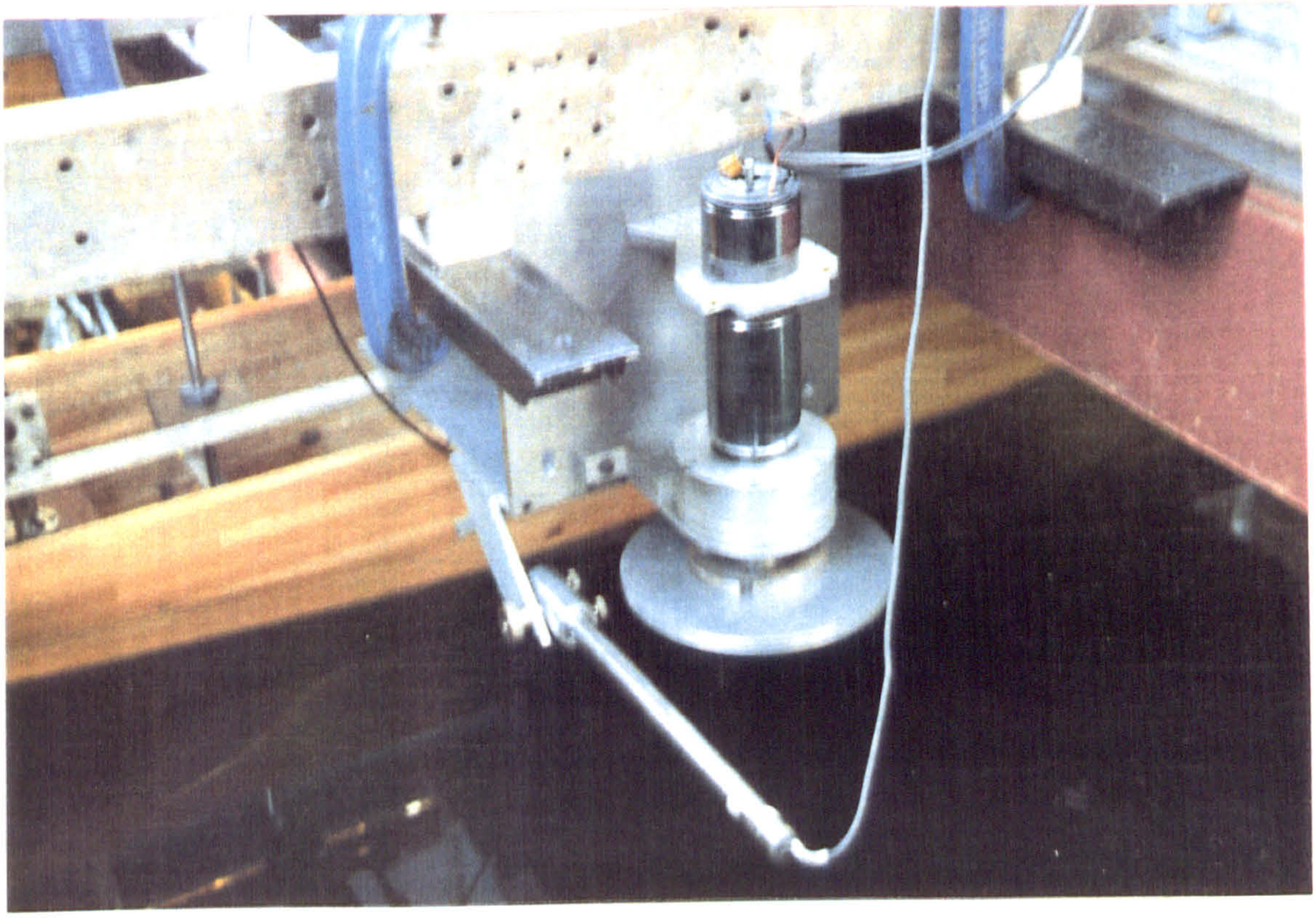

Fig 6.4A Experimental set up to determine the hydrodynamic coefficients of sway motion [Forced sway]

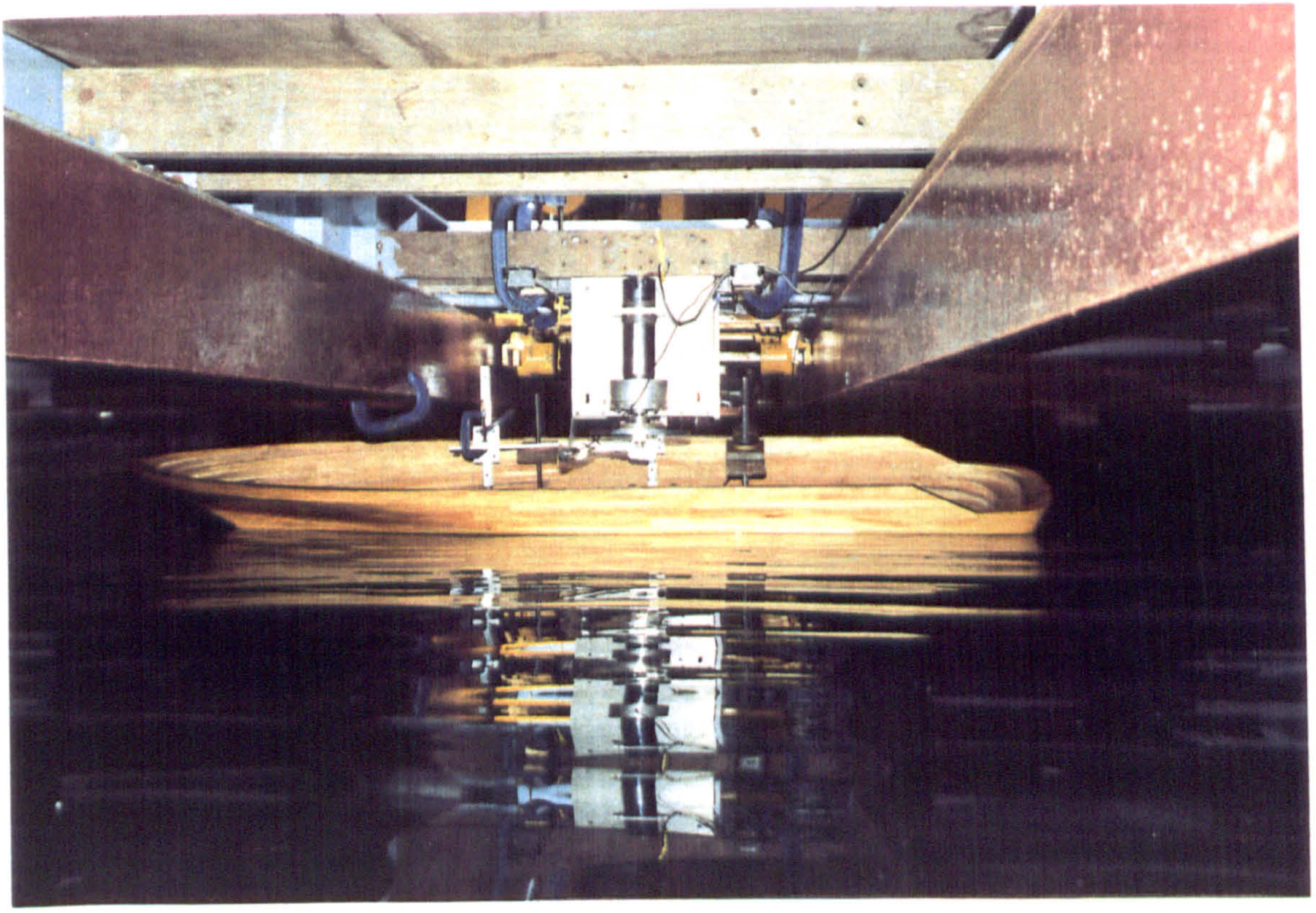

Fig 6.4B Experimental set up to determine the hydrodynamic coupling coefficients of sway into roll [Forced sway]

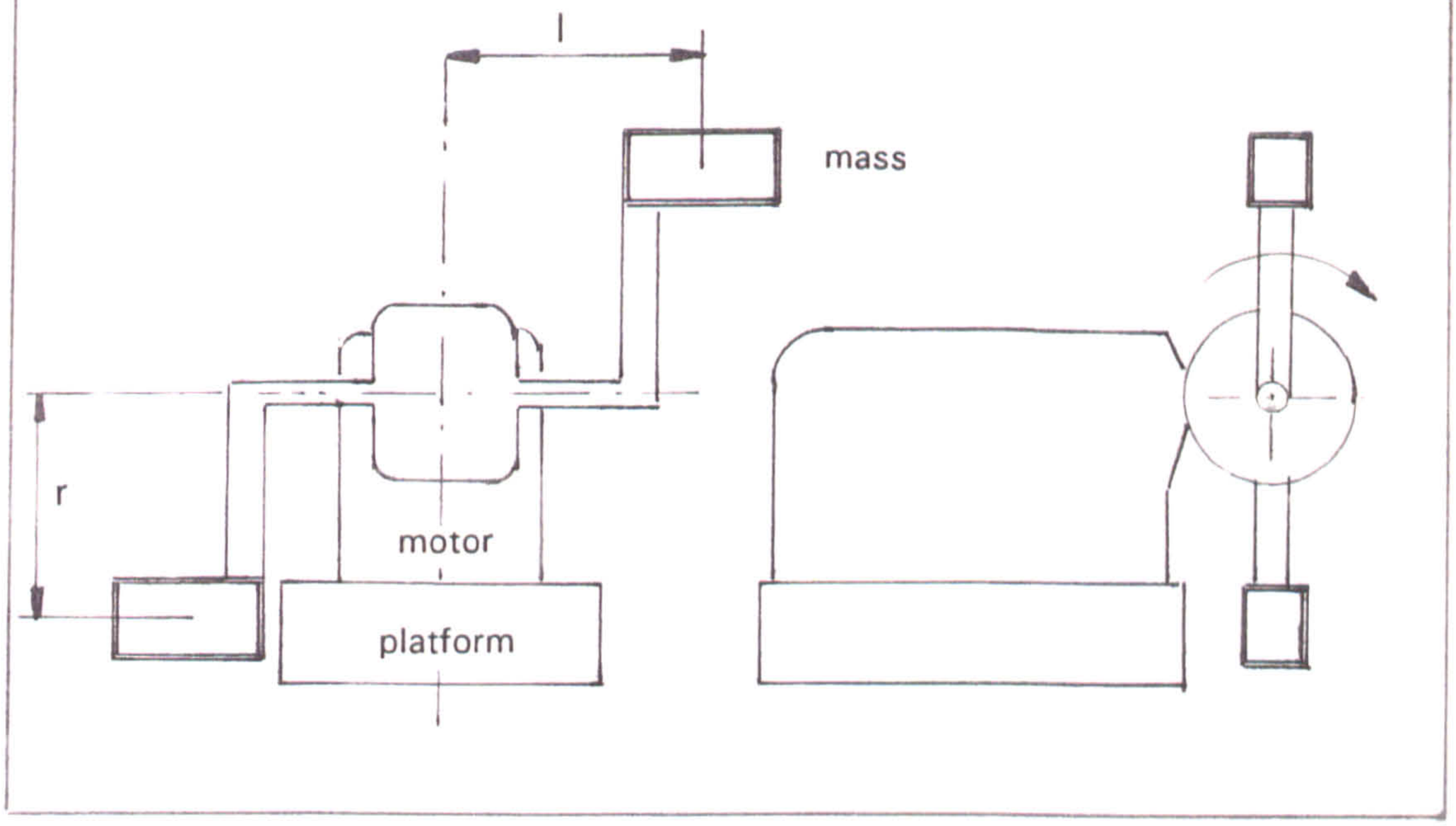

Fig 6.5A Roll moment mechanism

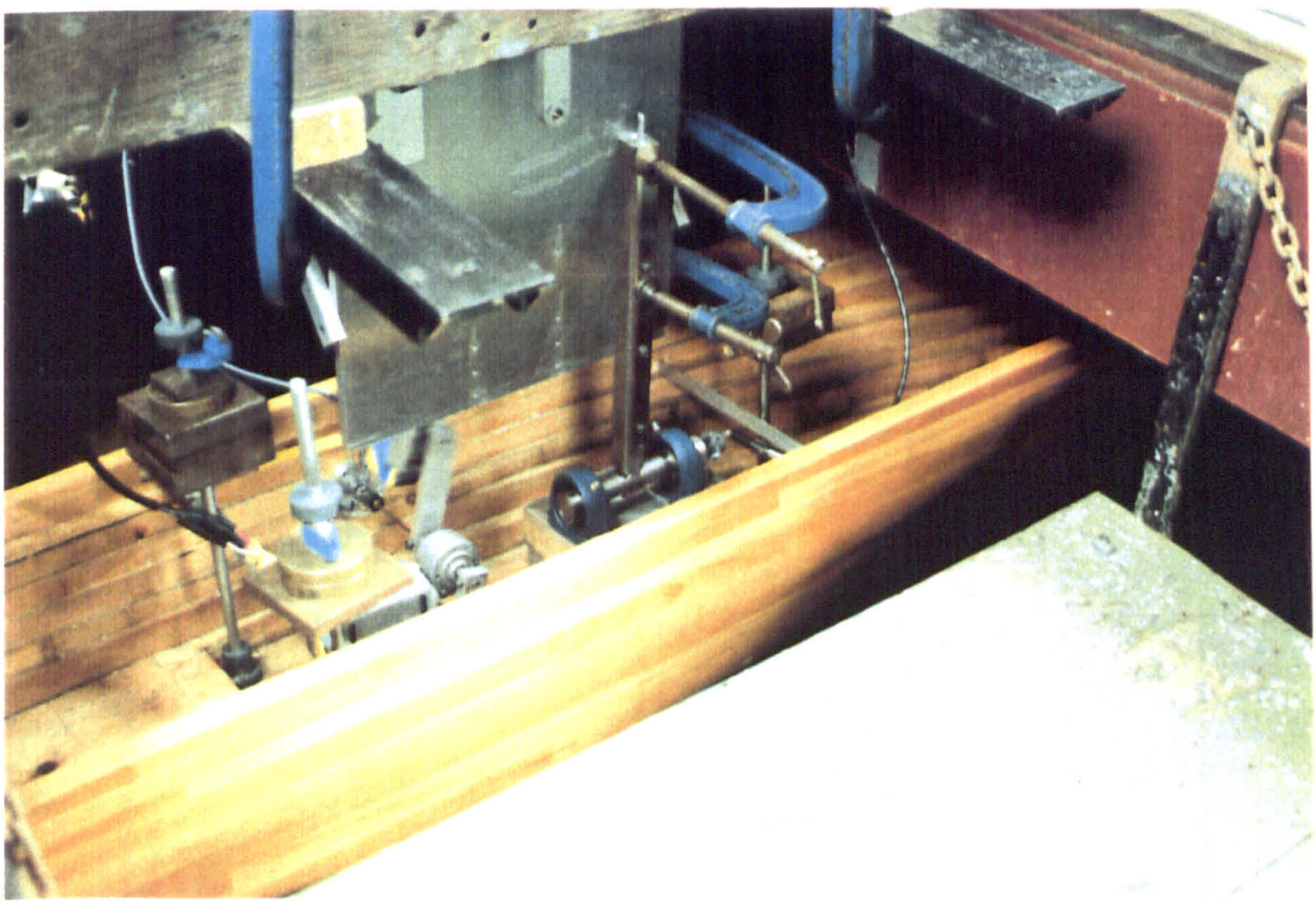

Fig 6.5B Experimental set up to determine the hydrodynamic coefficients of roll motion [Forced roll]

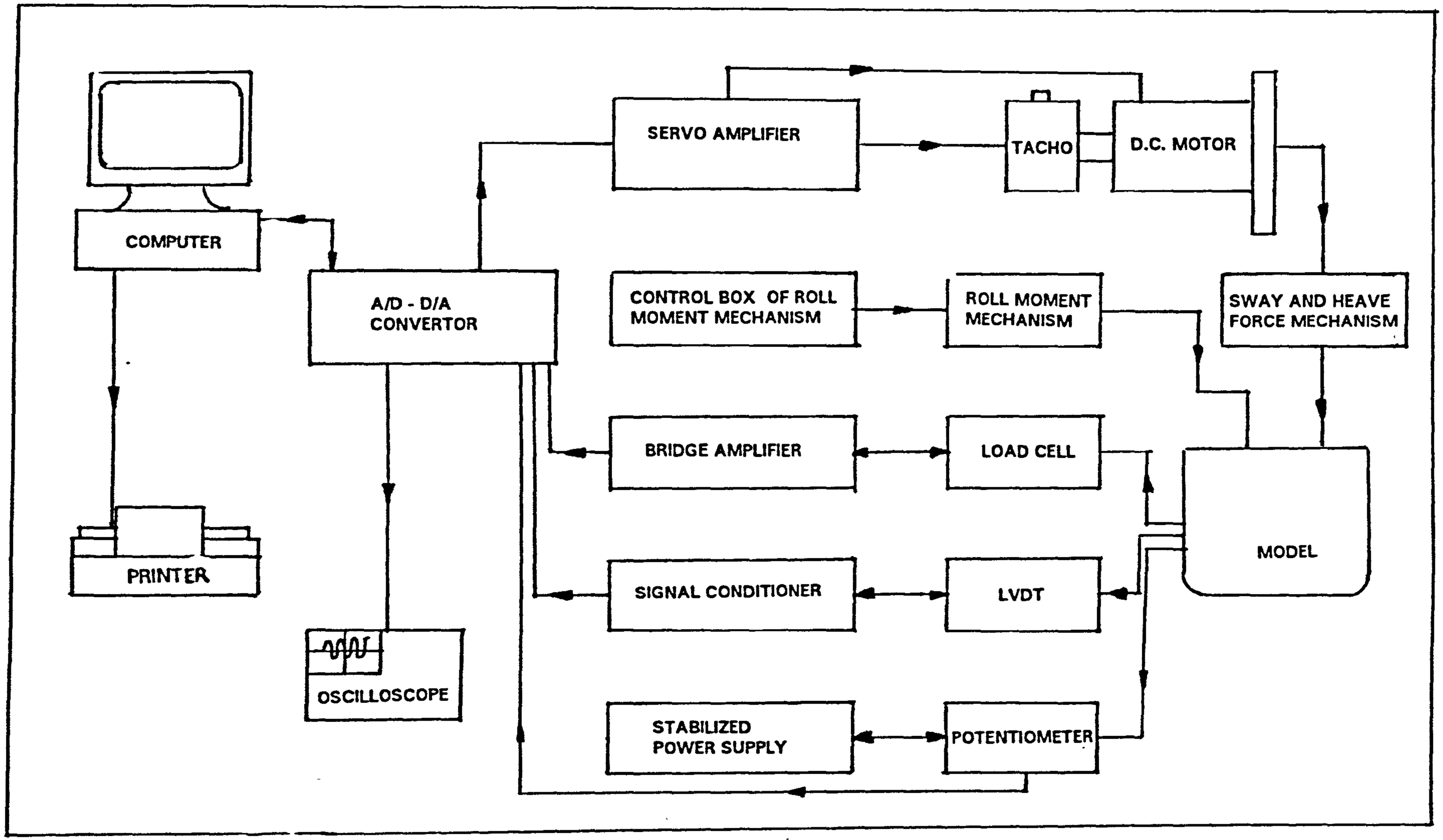

Fig 6.6A Schematic diagram of the experimental set up

Fig 6.6B A view of the experimental rig

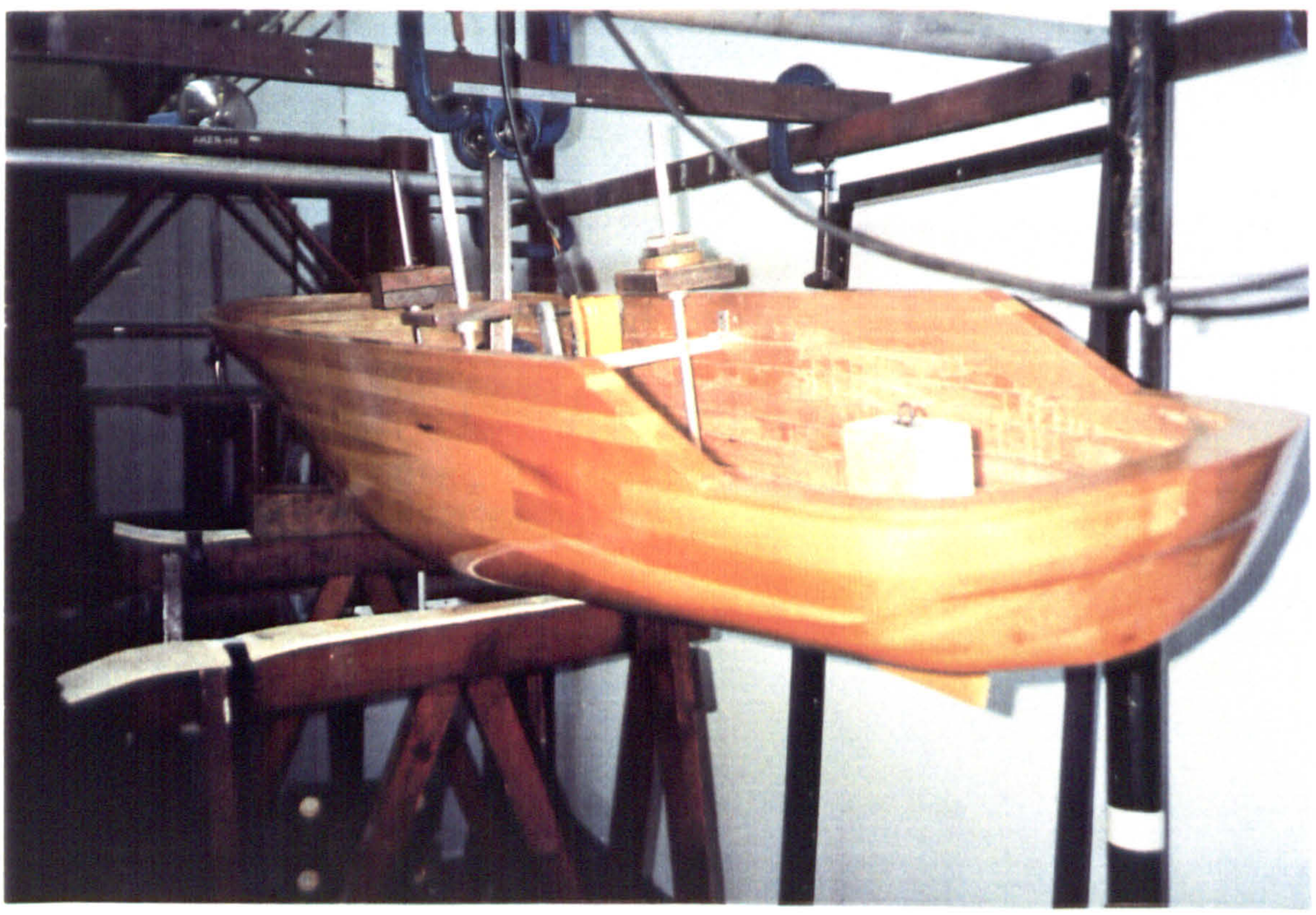

Fig 6.7 Experimental determination of roll mass moment of inertia (Ixx) of the model

Fig 6.8A Light slamming of the stern during the 4 cm amplitude heave experiments

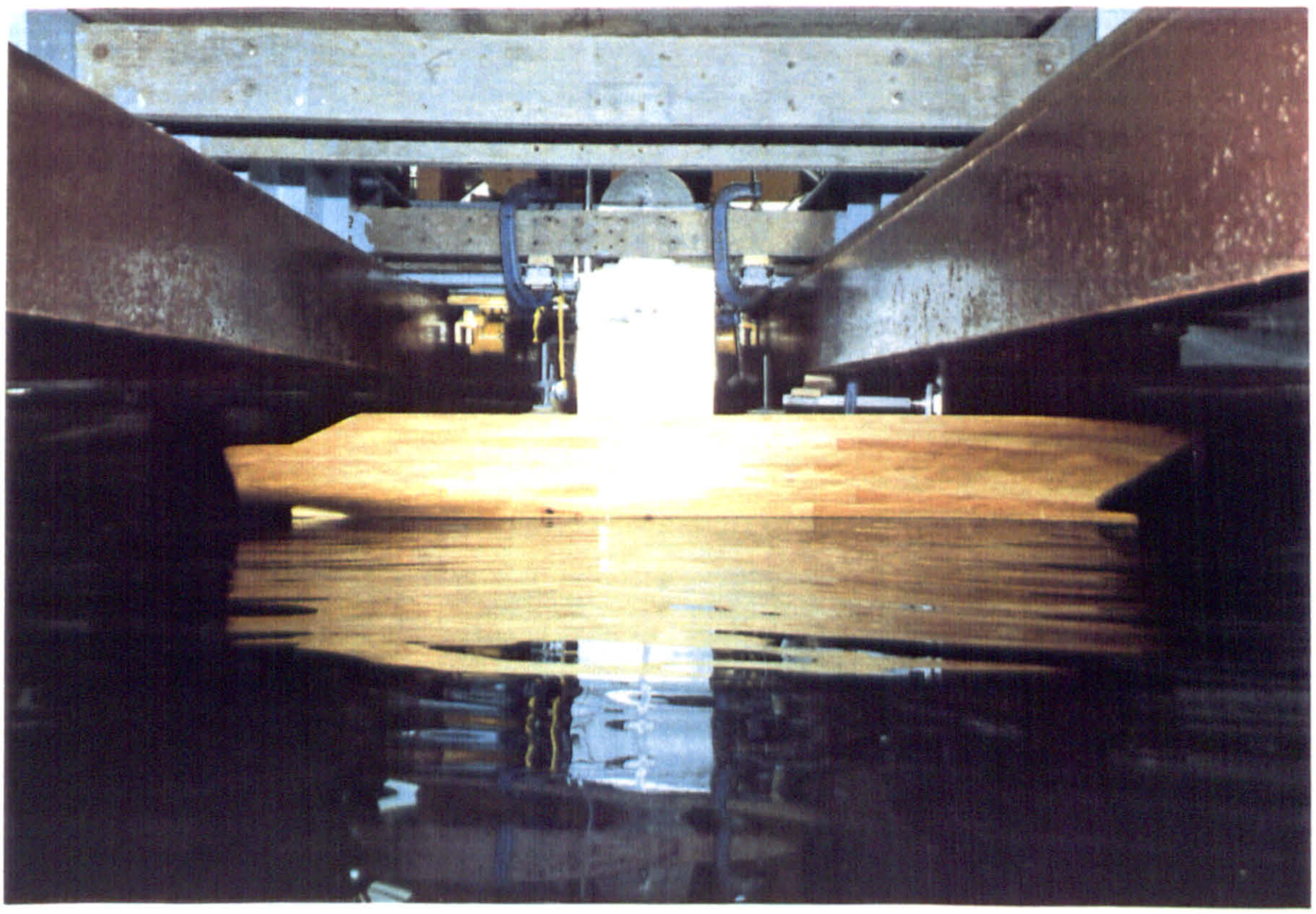

Fig 6.8B Heave experiments at low frequency [4 cm amplitude]

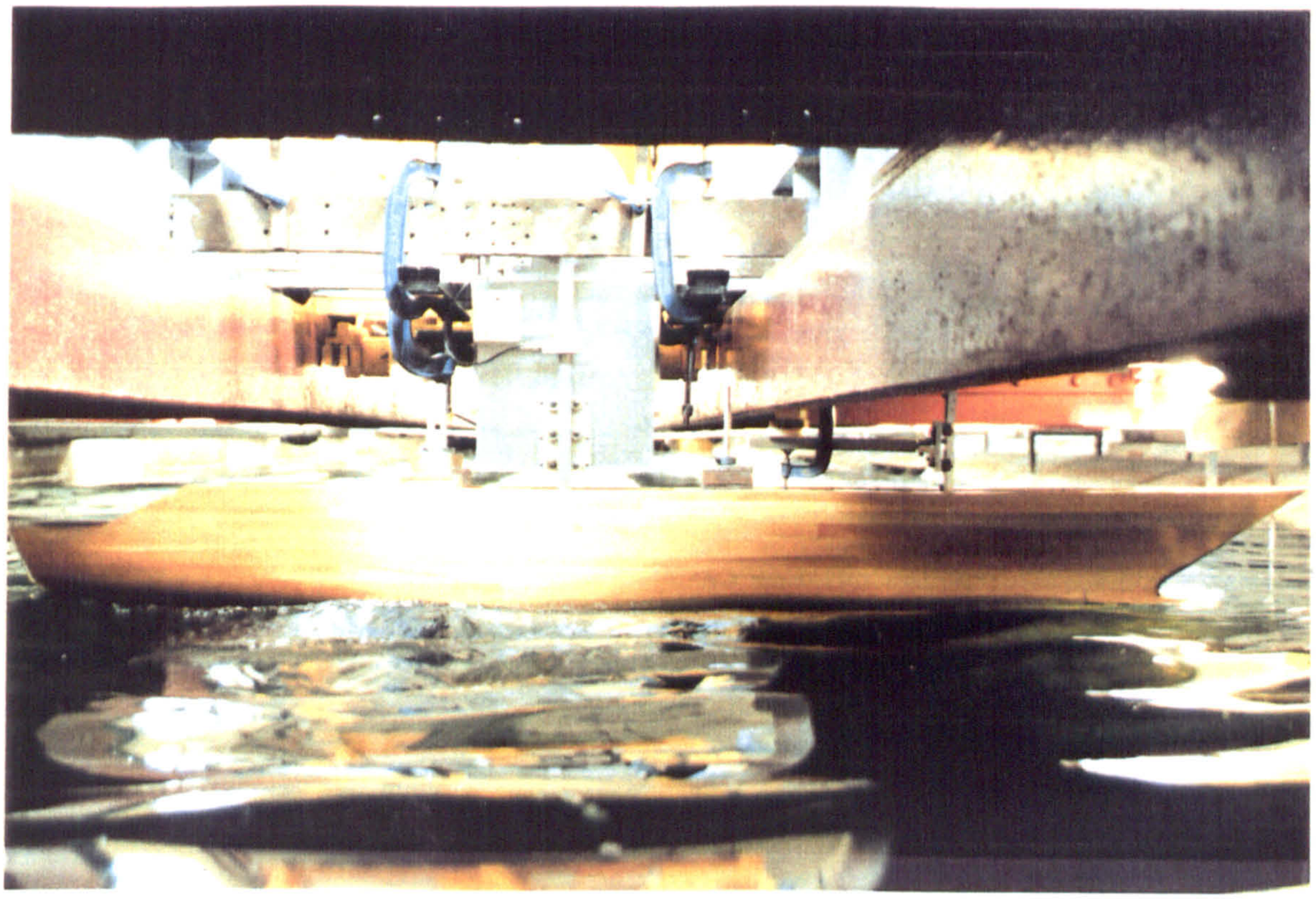

Fig 6.8C Heave experiments at high frequency: Radiated waves created by the heaving model

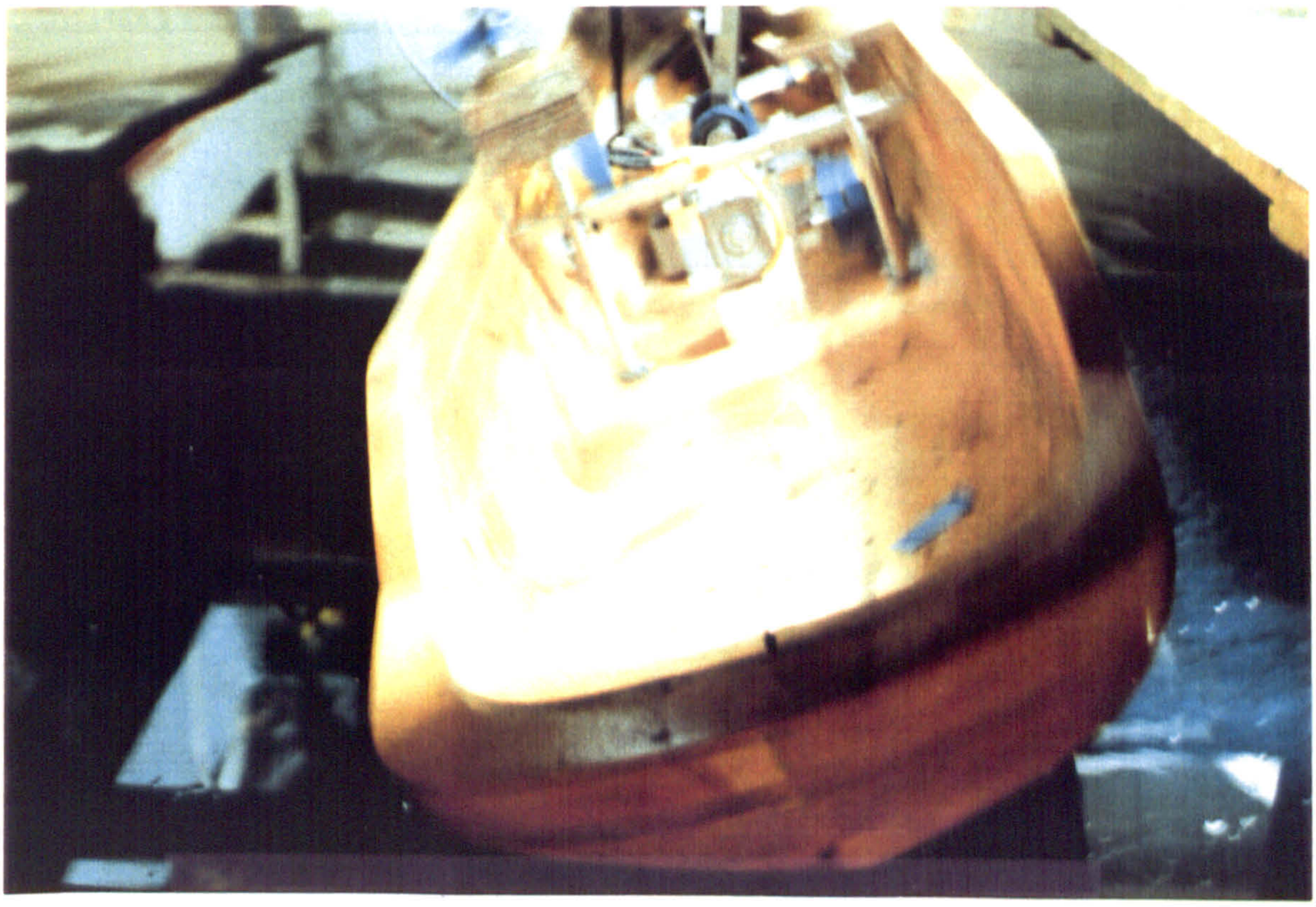

Fig 6.8D Large roll motion near resonance

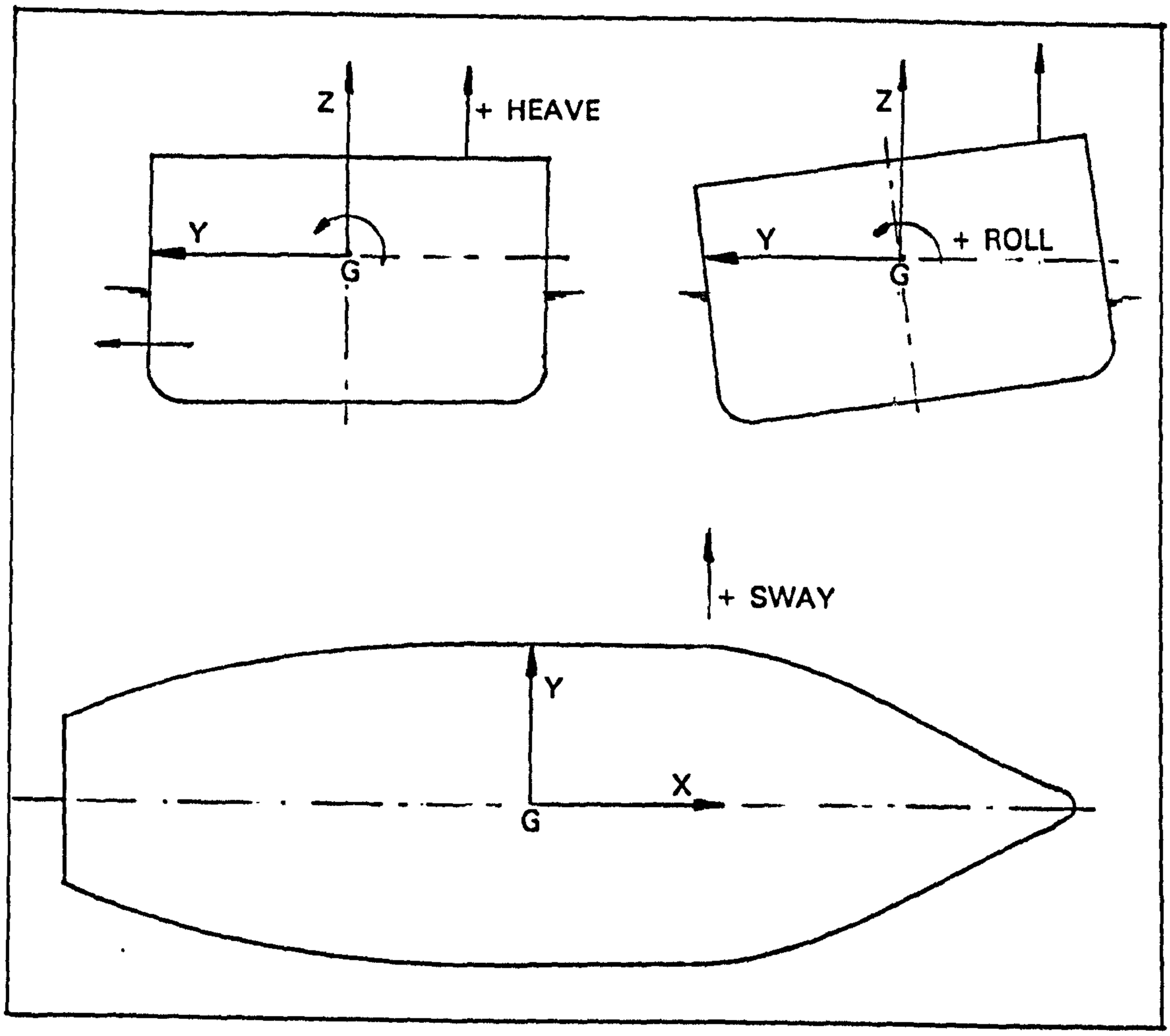

Fig 6.9 Co-ordinate system and sign convention used for the experiments.

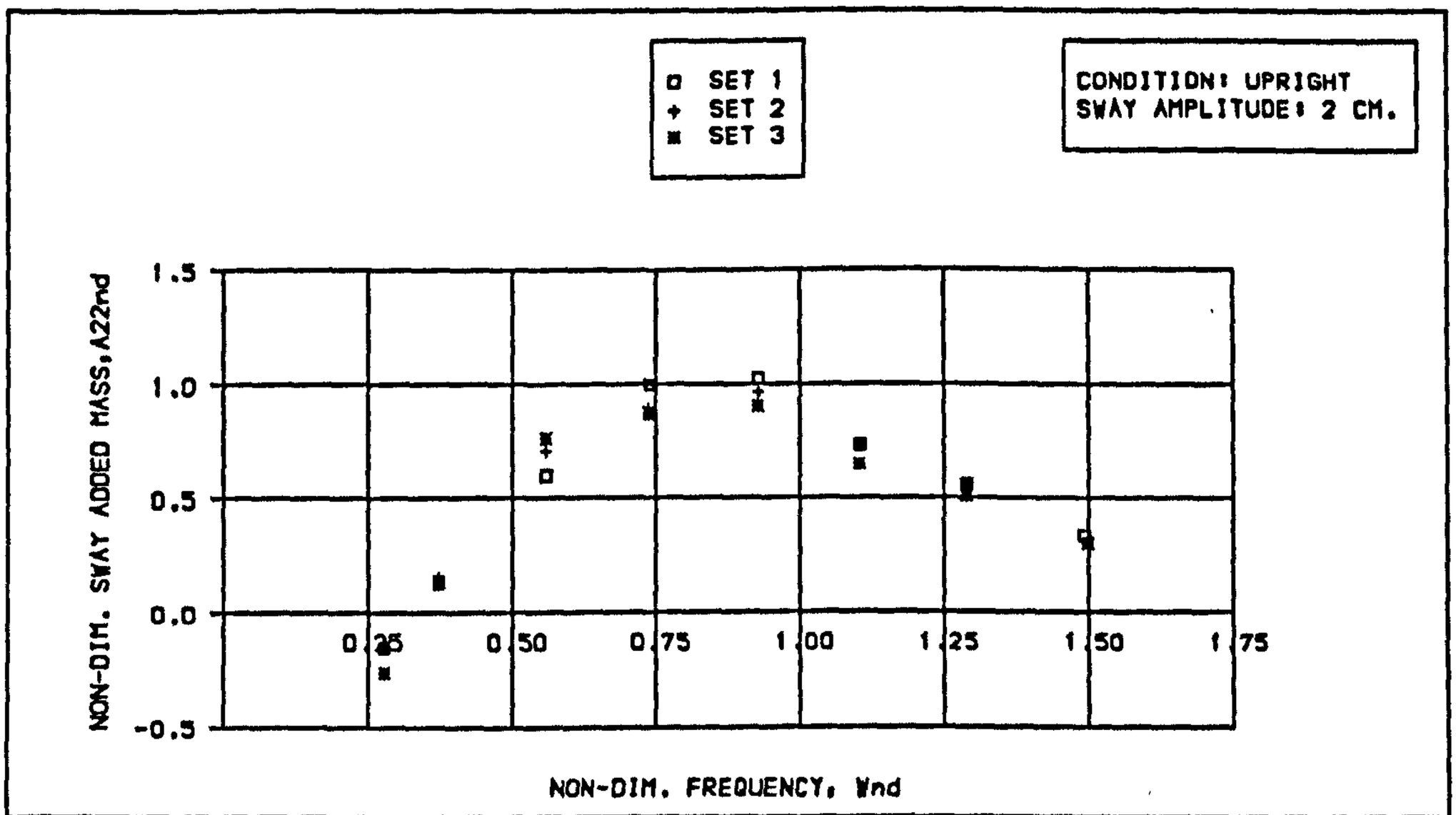

Fig 6.10A REPETITION OF EXPERIMENTS FOR SWAY MOTION [ADDED MASS]

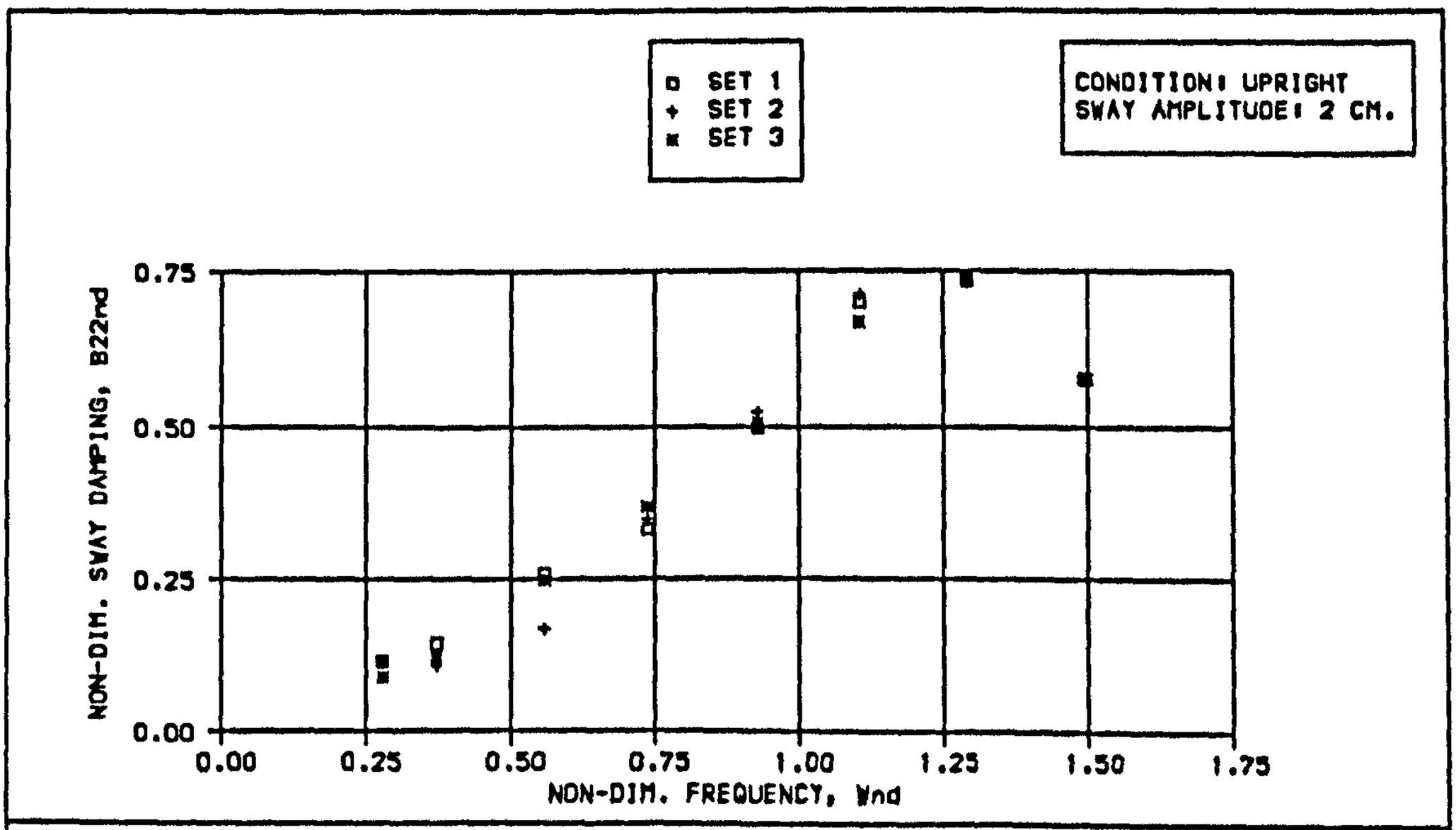

Fig 6.10B REPETITION OF EXPERIMENTS FOR SWAY MOTION [DAMPING]

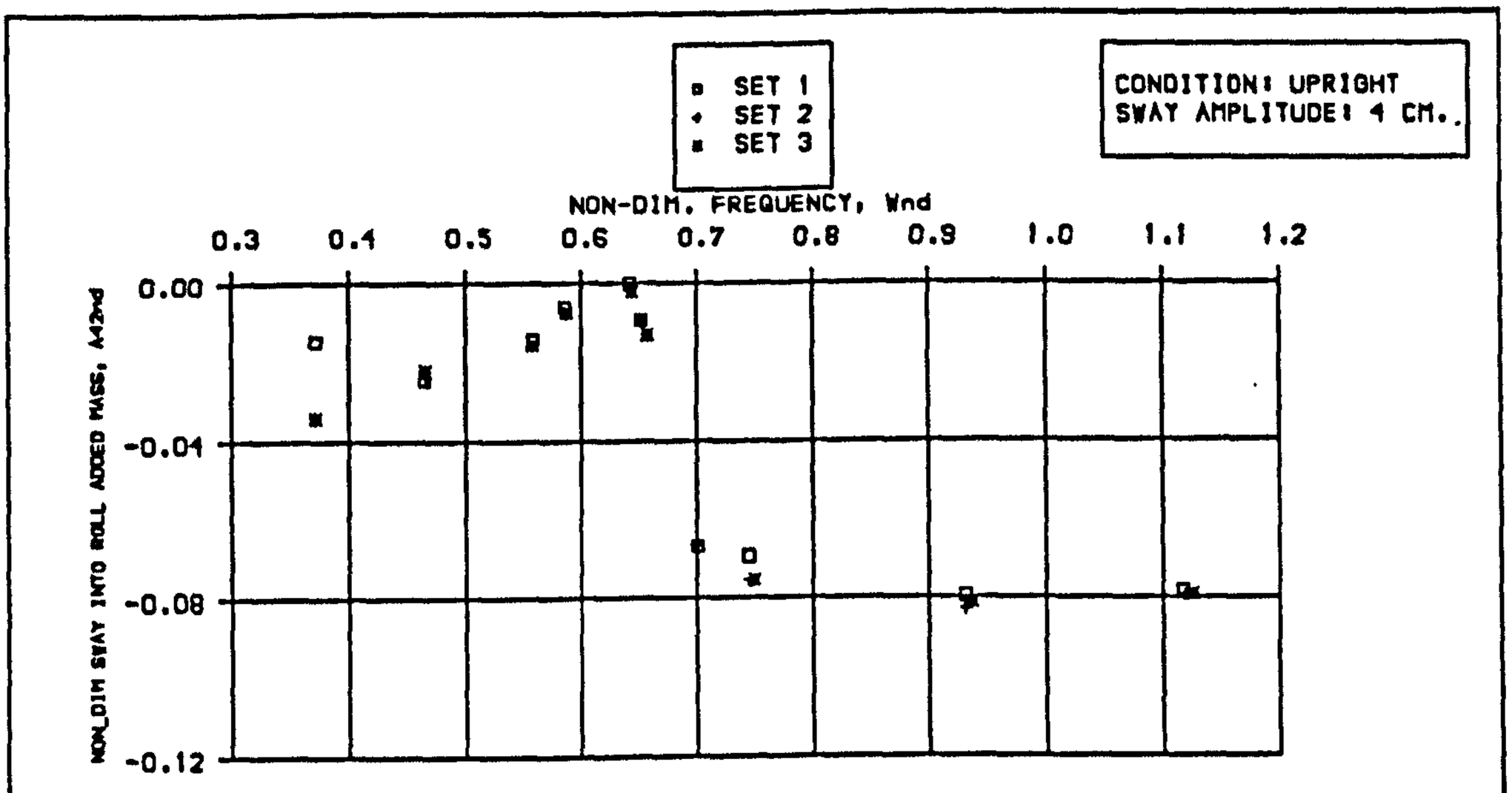

Fig 6.11A REPETITION OF EXPERIMENTS FOR COUPLED SWAY AND ROLL MOTIONS (ADDED MASS)

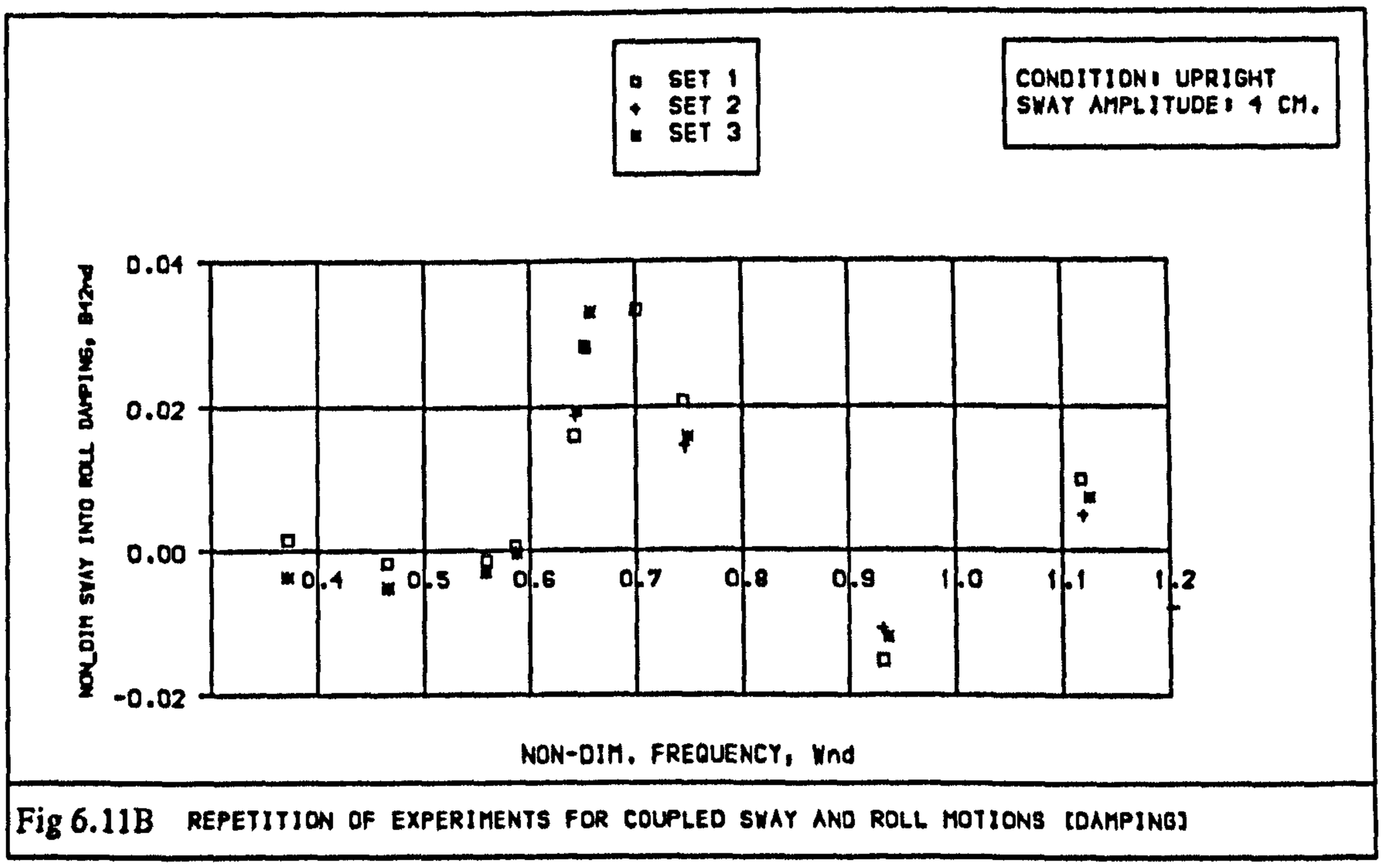

Fig 6.11B REPETITION OF EXPERIMENTS FOR COUPLED SWAY AND ROLL MOTIONS (DAMPING)

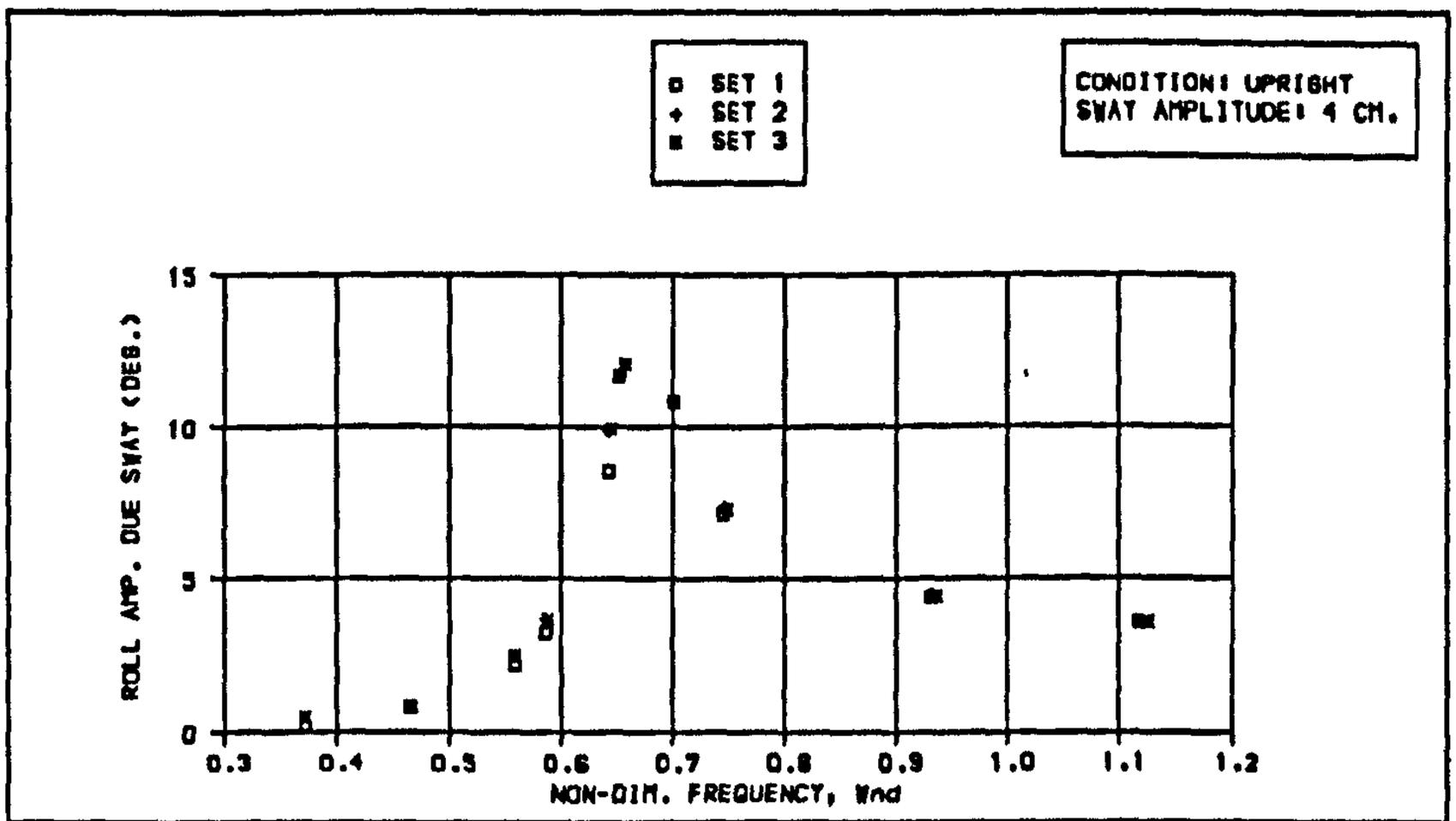

Fig 6.12A REPETITION OF EXPERIMENTS FOR COUPLED SWAY AND ROLL MOT. (ROLL AMP.)

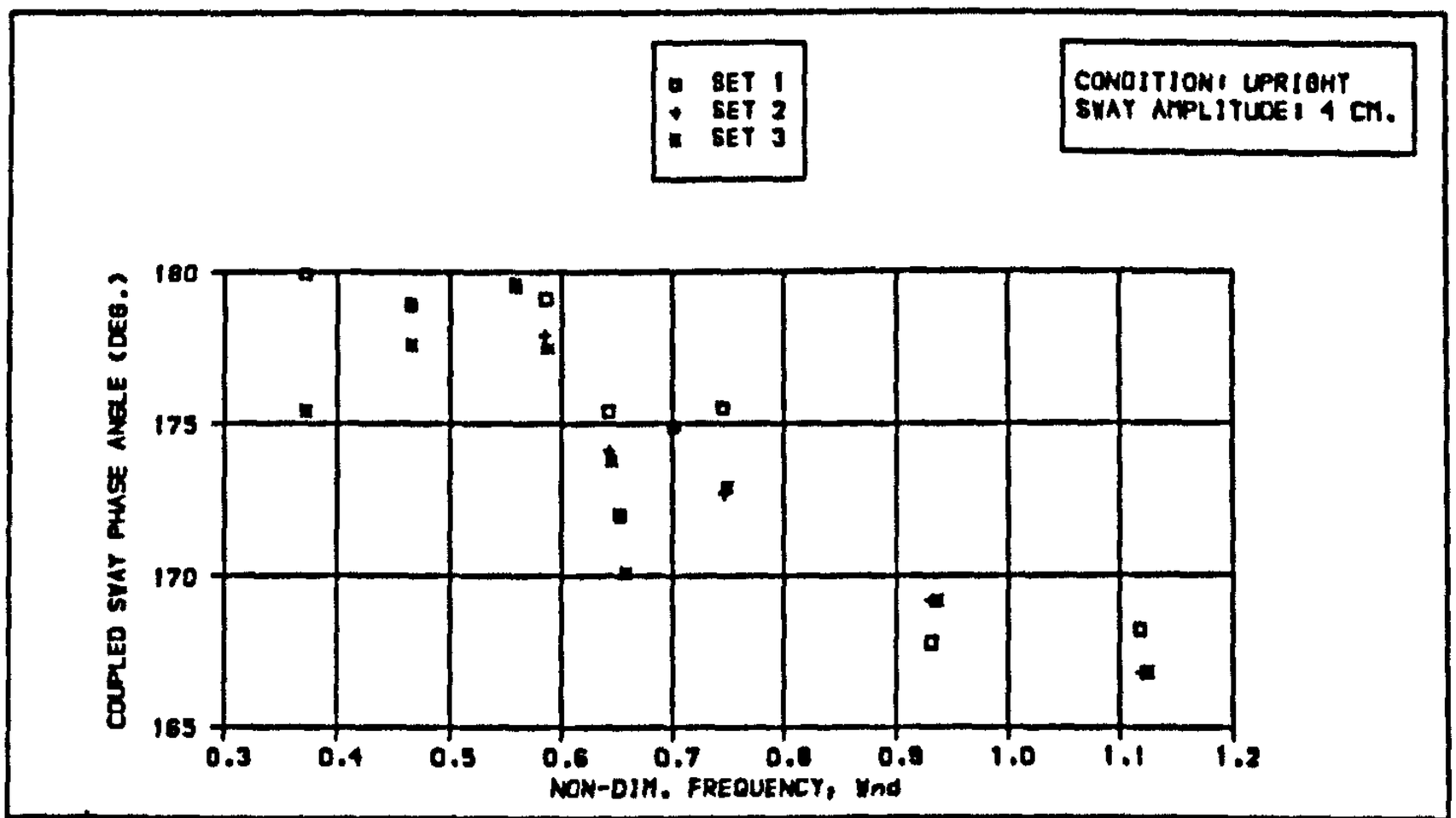

Fig 6.12B REPETITION OF EXPERIMENTS FOR COUPLED SWAY AND ROLL MOT. (SWAY PHASE)

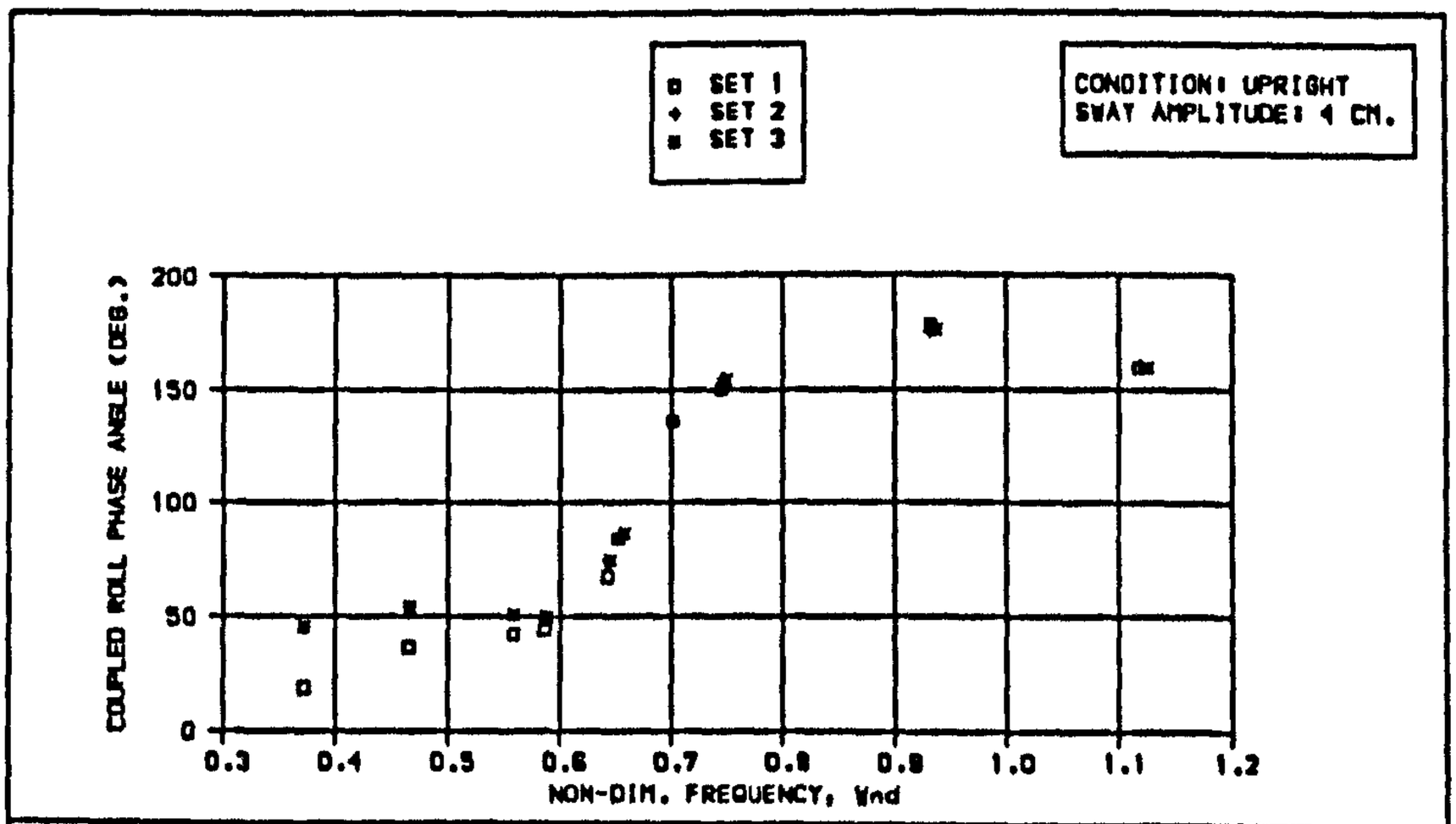

Fig 6.12C REPETITION OF EXPERIMENTS FOR COUPLED SWAY AND ROLL MOT. (ROLL PHASE)

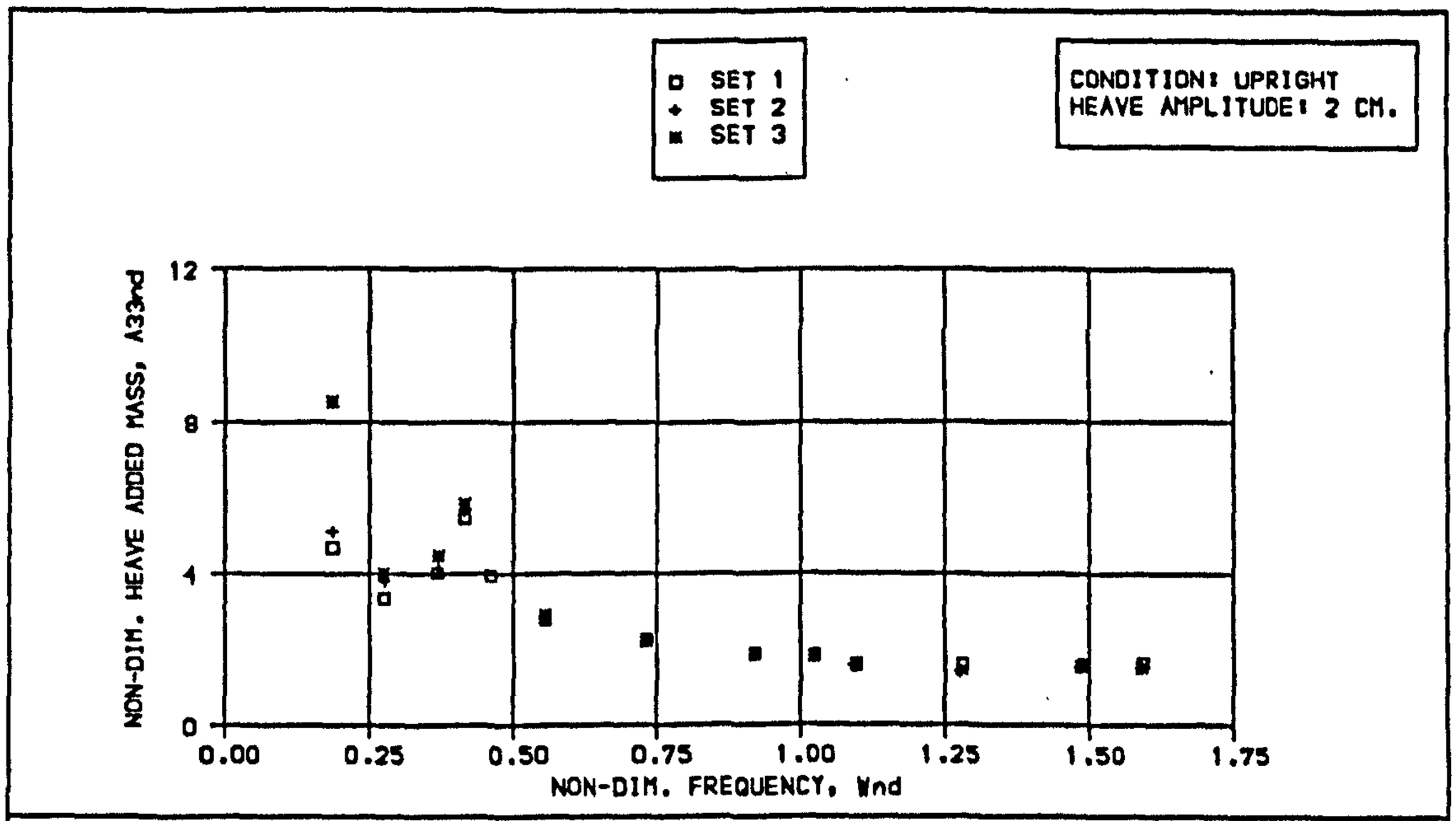

Fig 6.13A REPETITION OF EXPERIMENTS FOR HEAVE MOTION

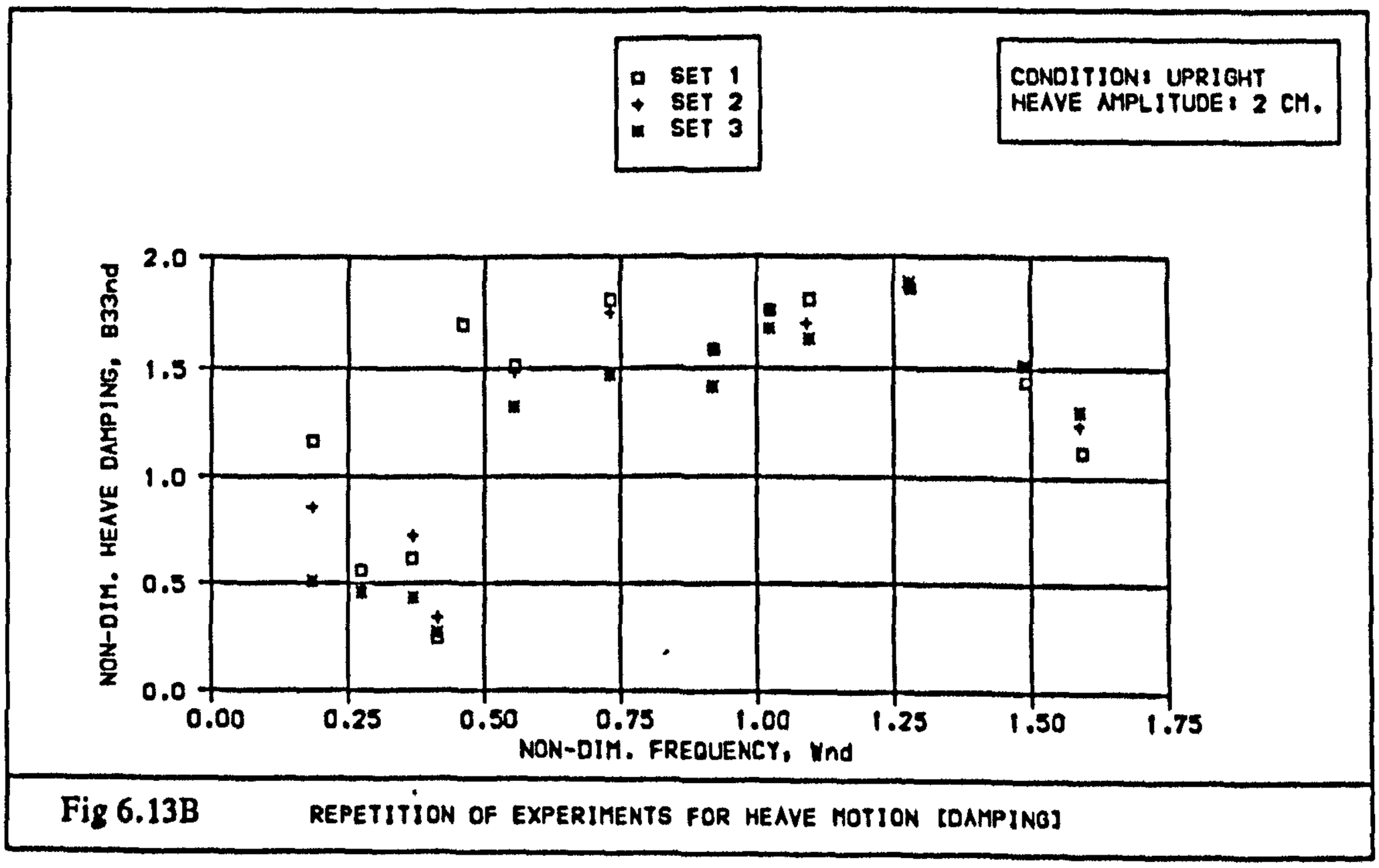

Fig 6.13B REPETITION OF EXPERIMENTS FOR HEAVE MOTION [DAMPING]

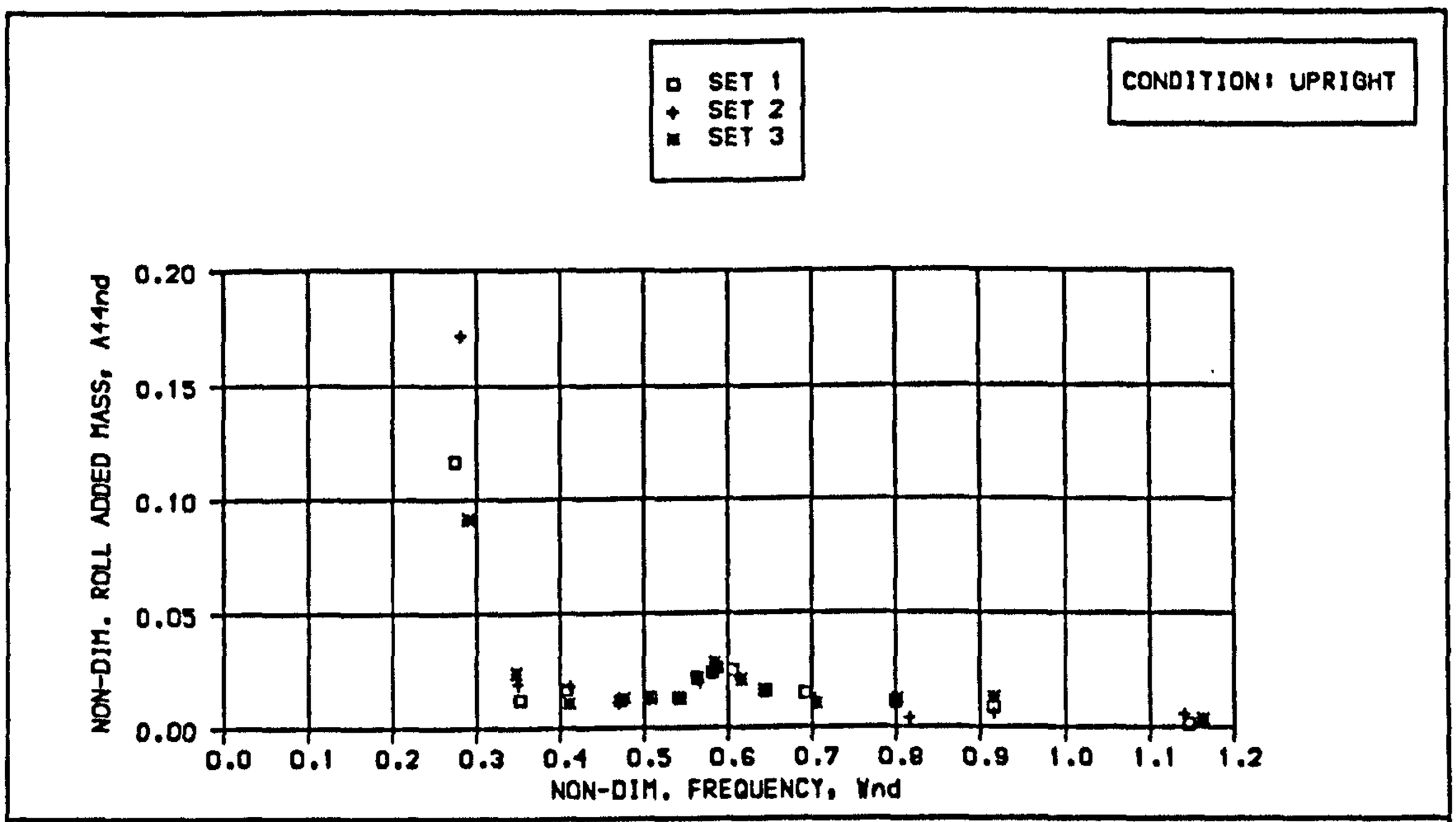

Fig 6.14A REPETITION OF EXPERIMENTS FOR ROLL MOTION [ADDED MASS]

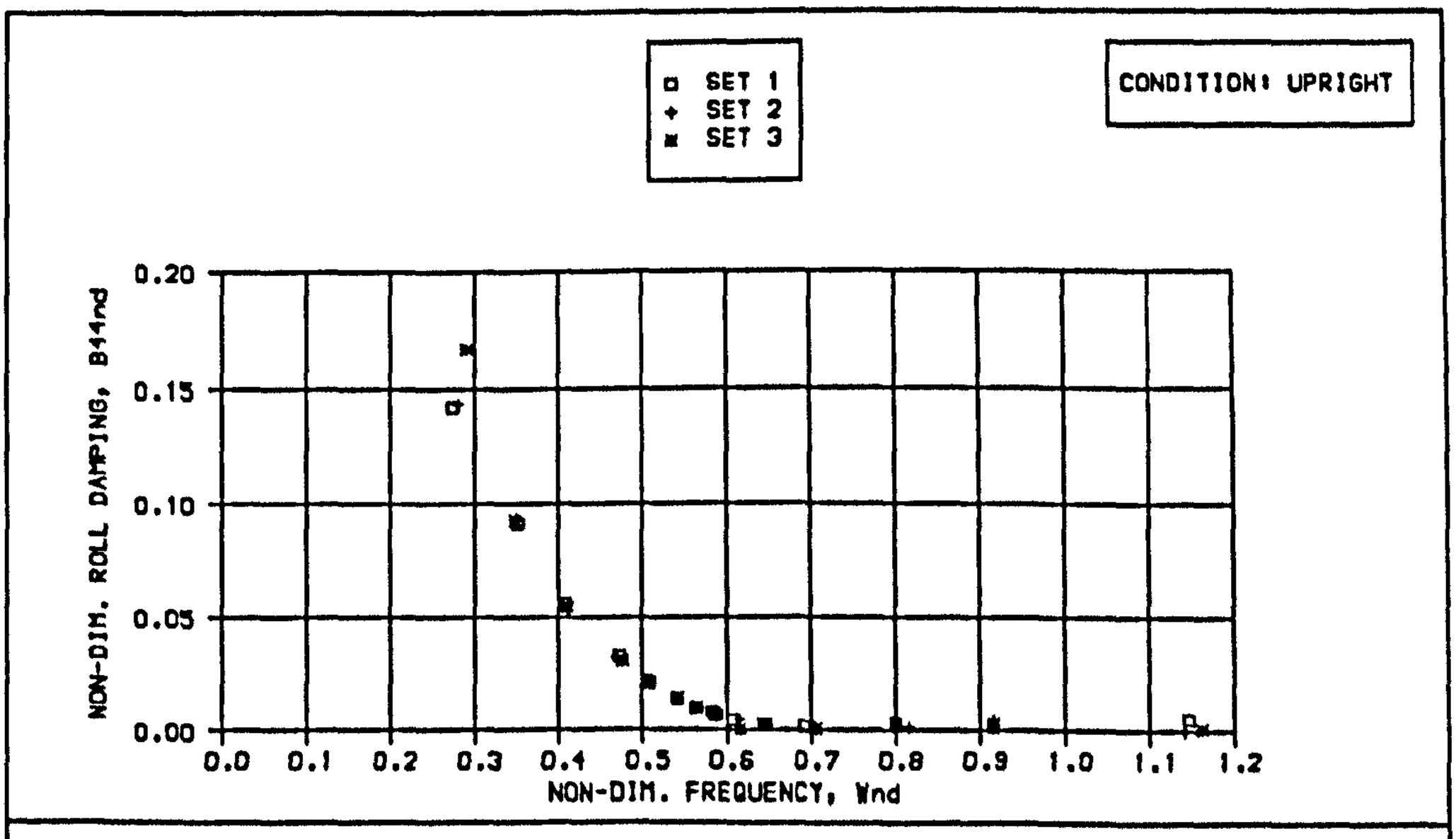

Fig 6.14B REPETITION OF EXPERIMENTS FOR ROLL MOTION [DAMPING]

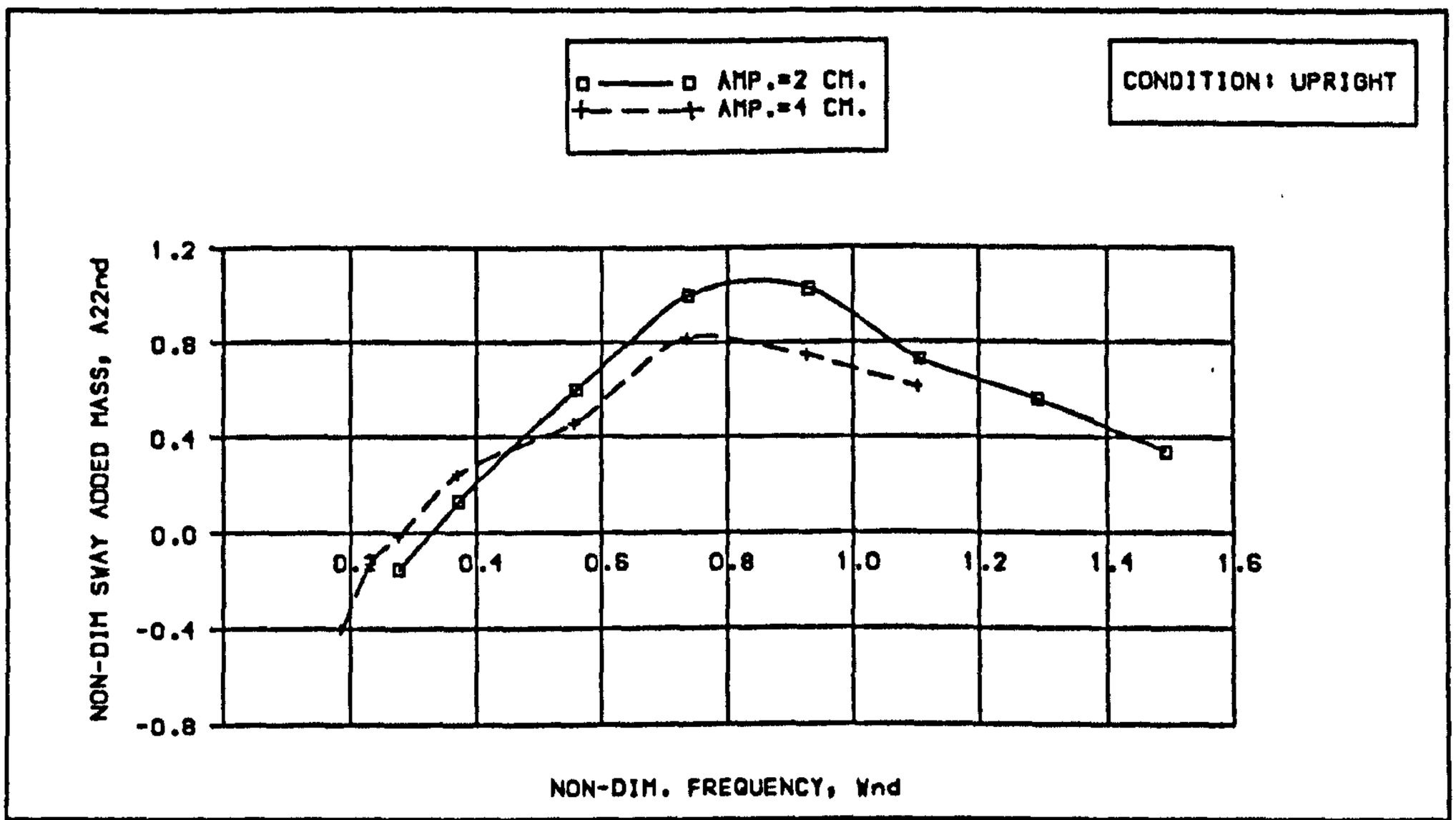

Fig 6.15A EFFECT OF AMPLITUDE ON SWAY ADDED MASS

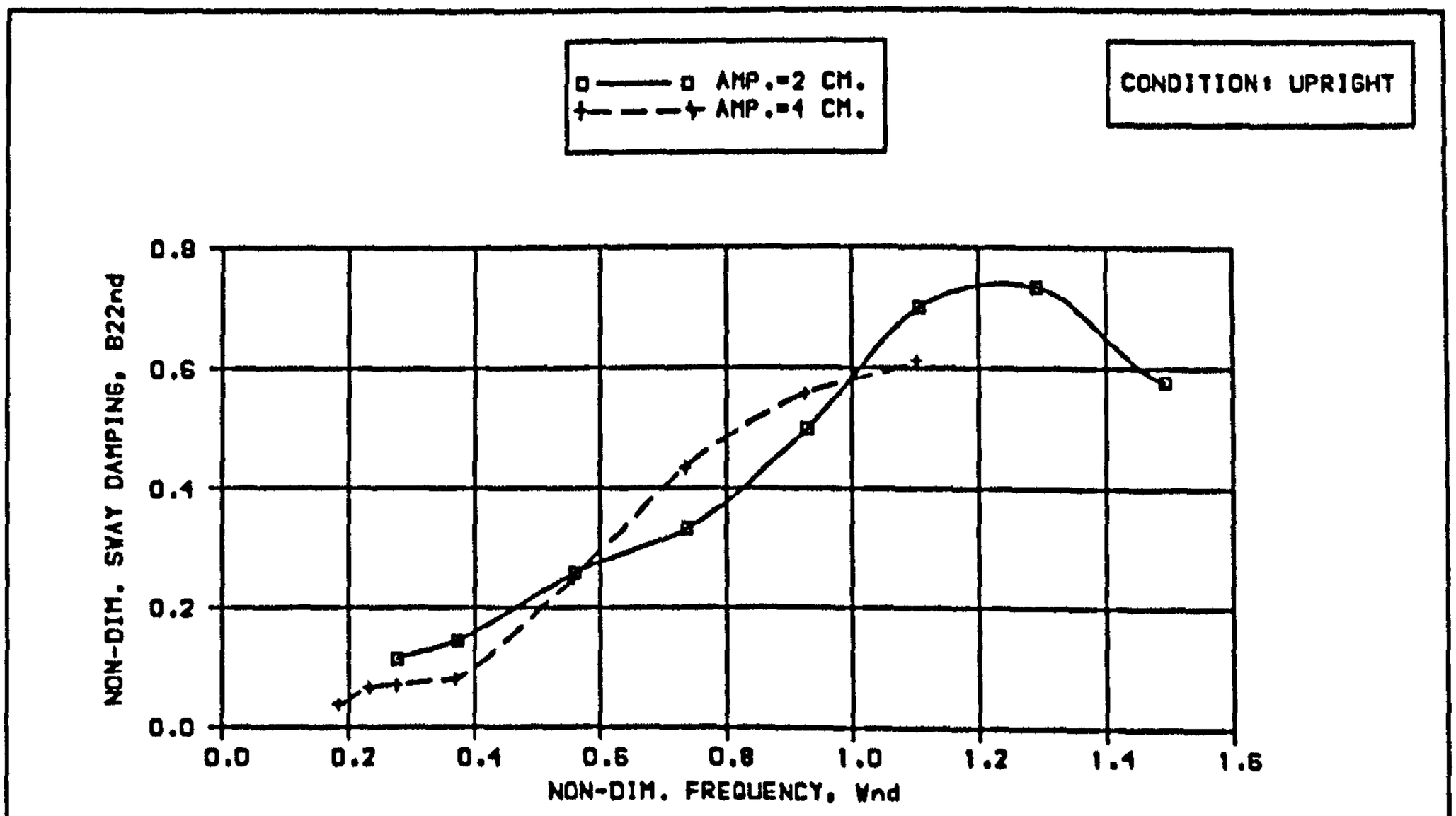

Fig 6.15B EFFECT OF AMPLITUDE ON SWAY DAMPING

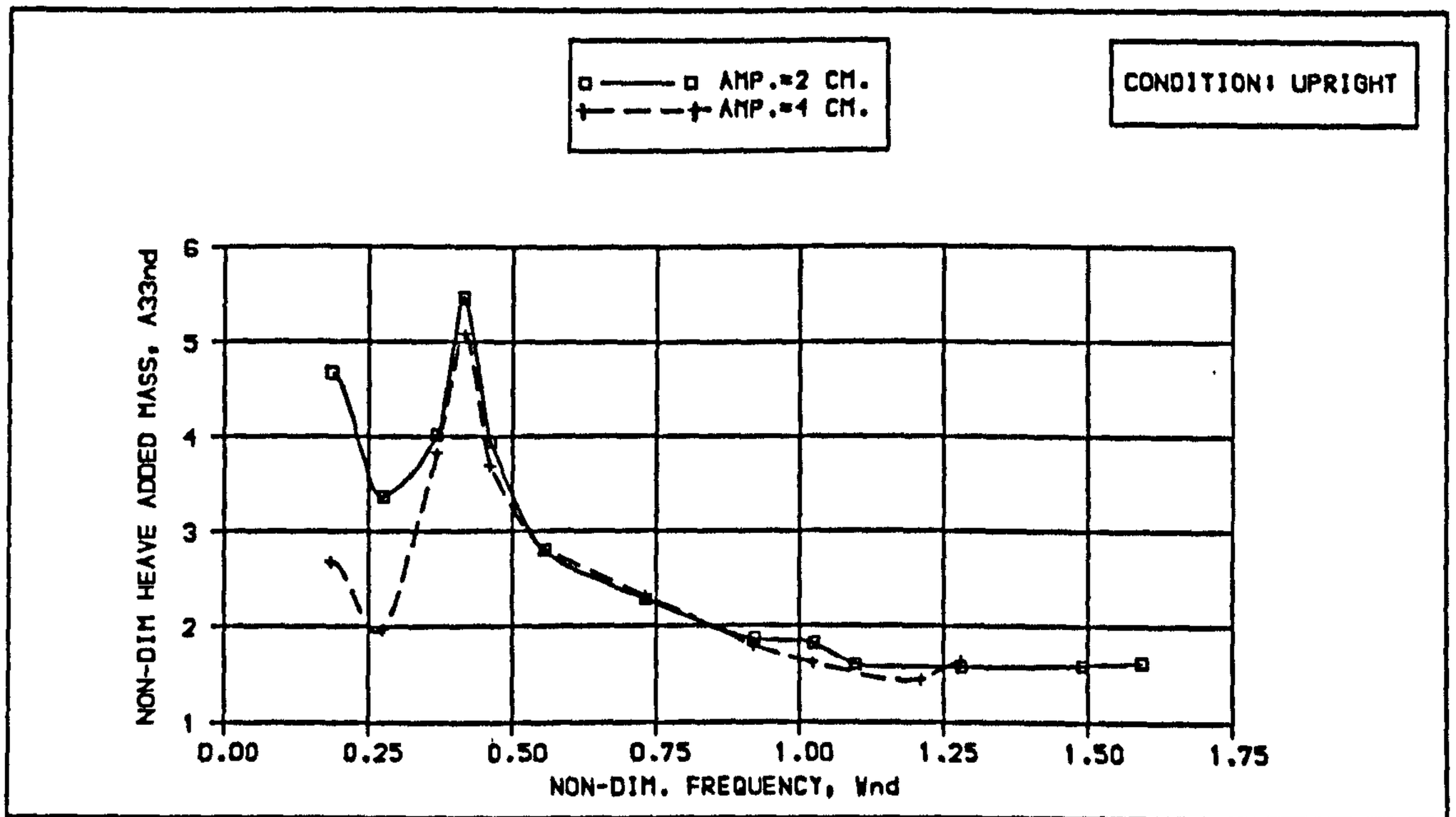

Fig 6.16A EFFECT OF AMPLITUDE ON HEAVE ADDED MASS

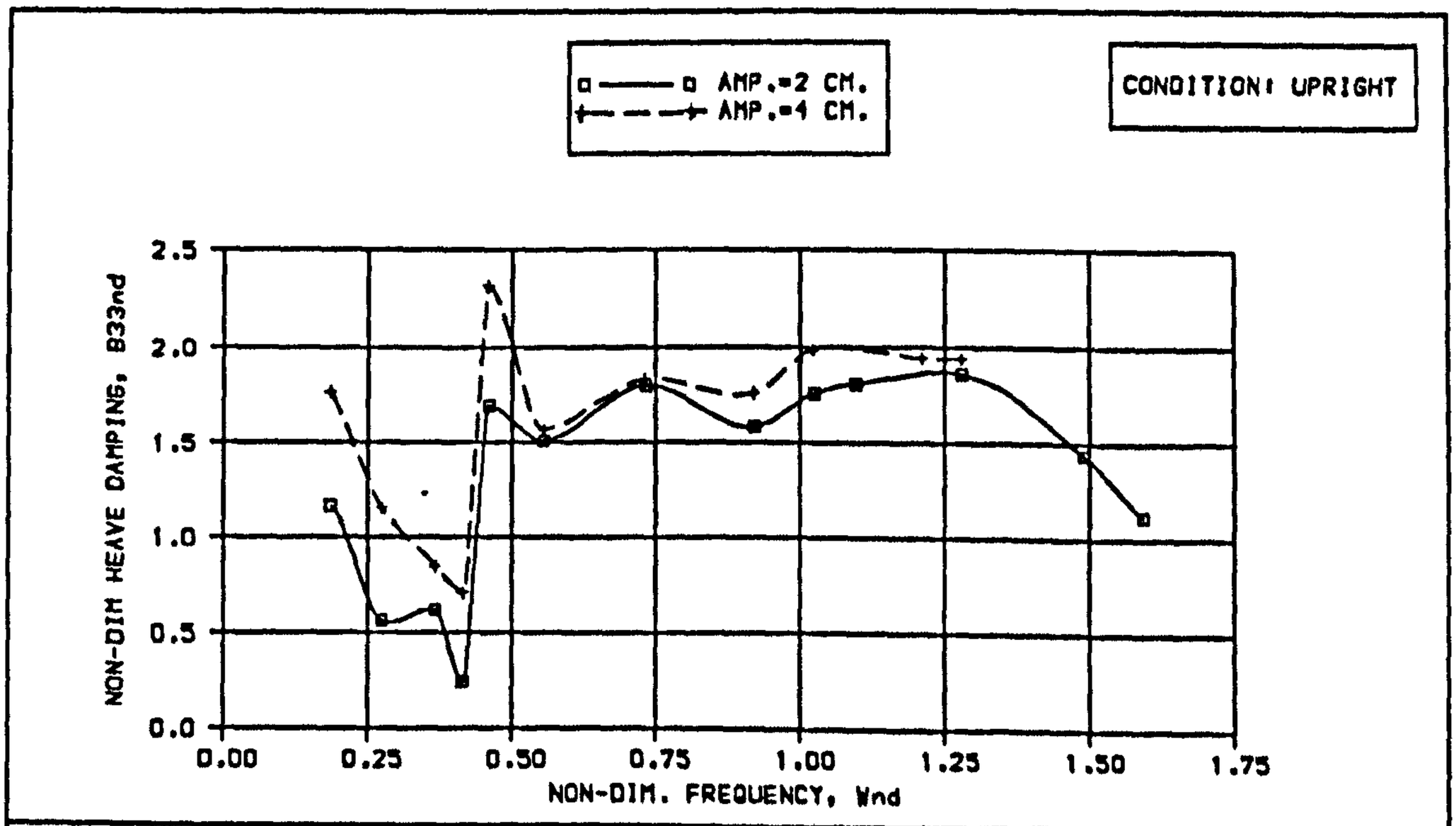

Fig 6.16B EFFECT OF AMPLITUDE ON HEAVE DAMPING

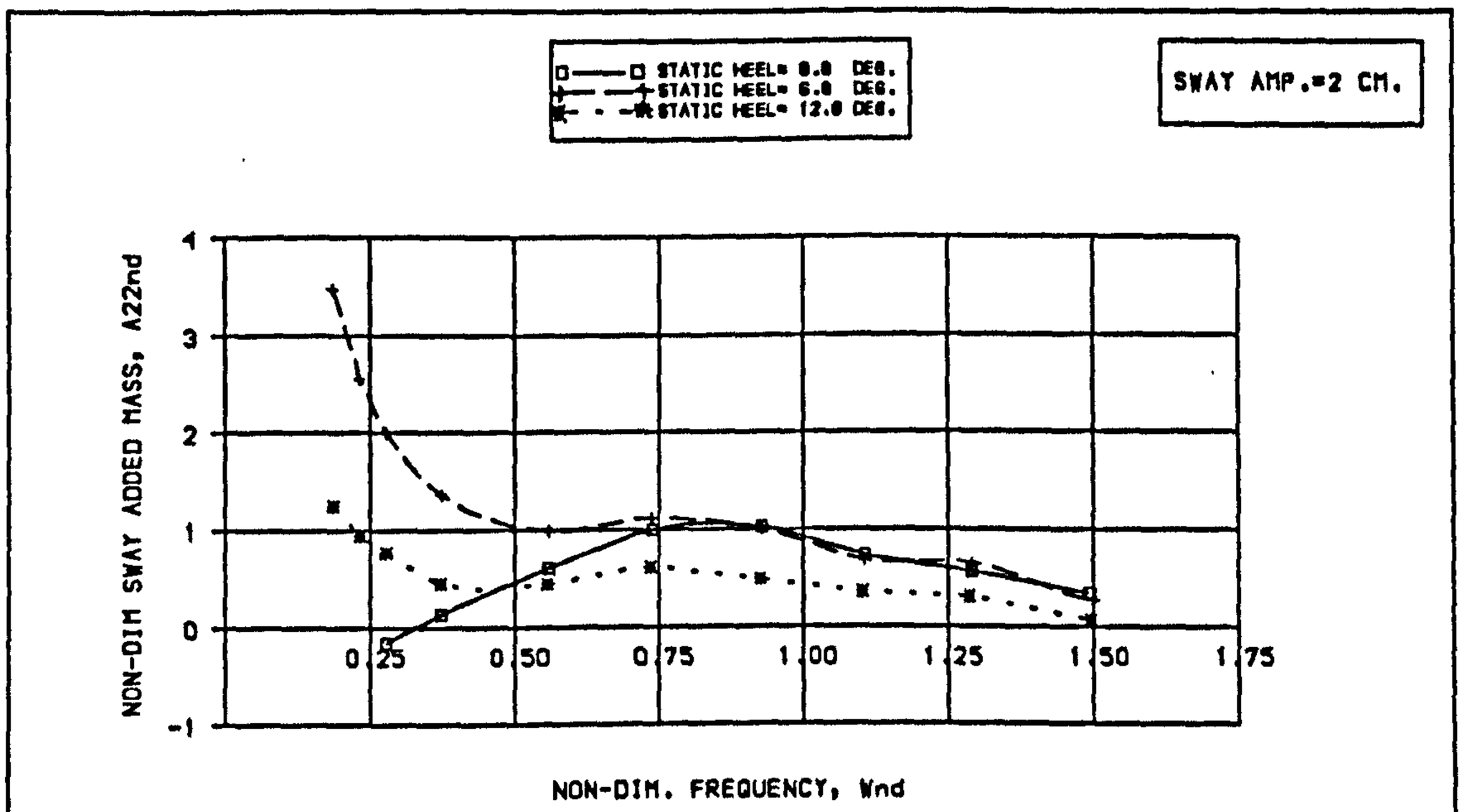

Fig 6.17A EFFECT OF STATIC HEEL ON SWAY ADDED MASS

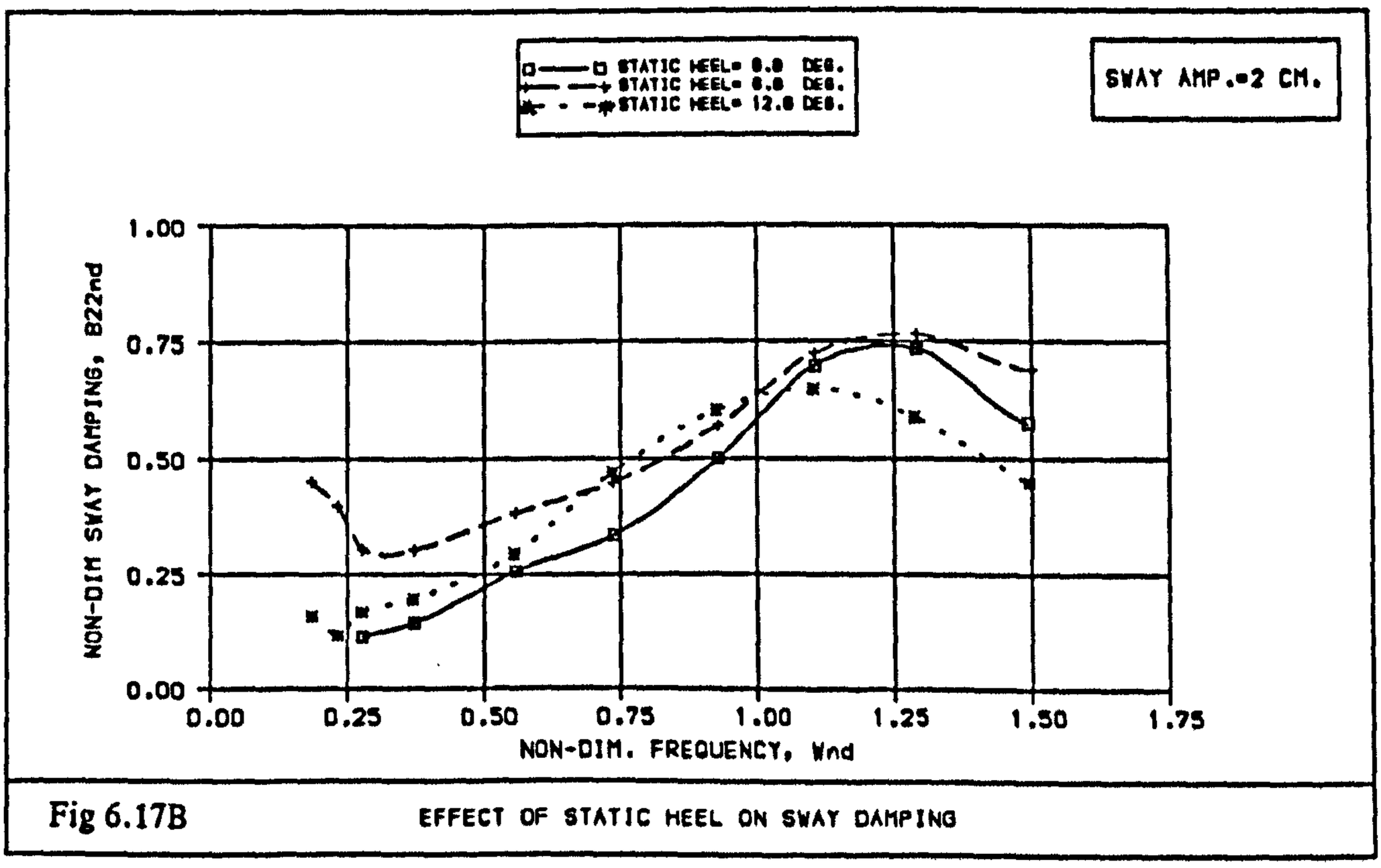

Fig 6.17B EFFECT OF STATIC HEEL ON SWAY DAMPING

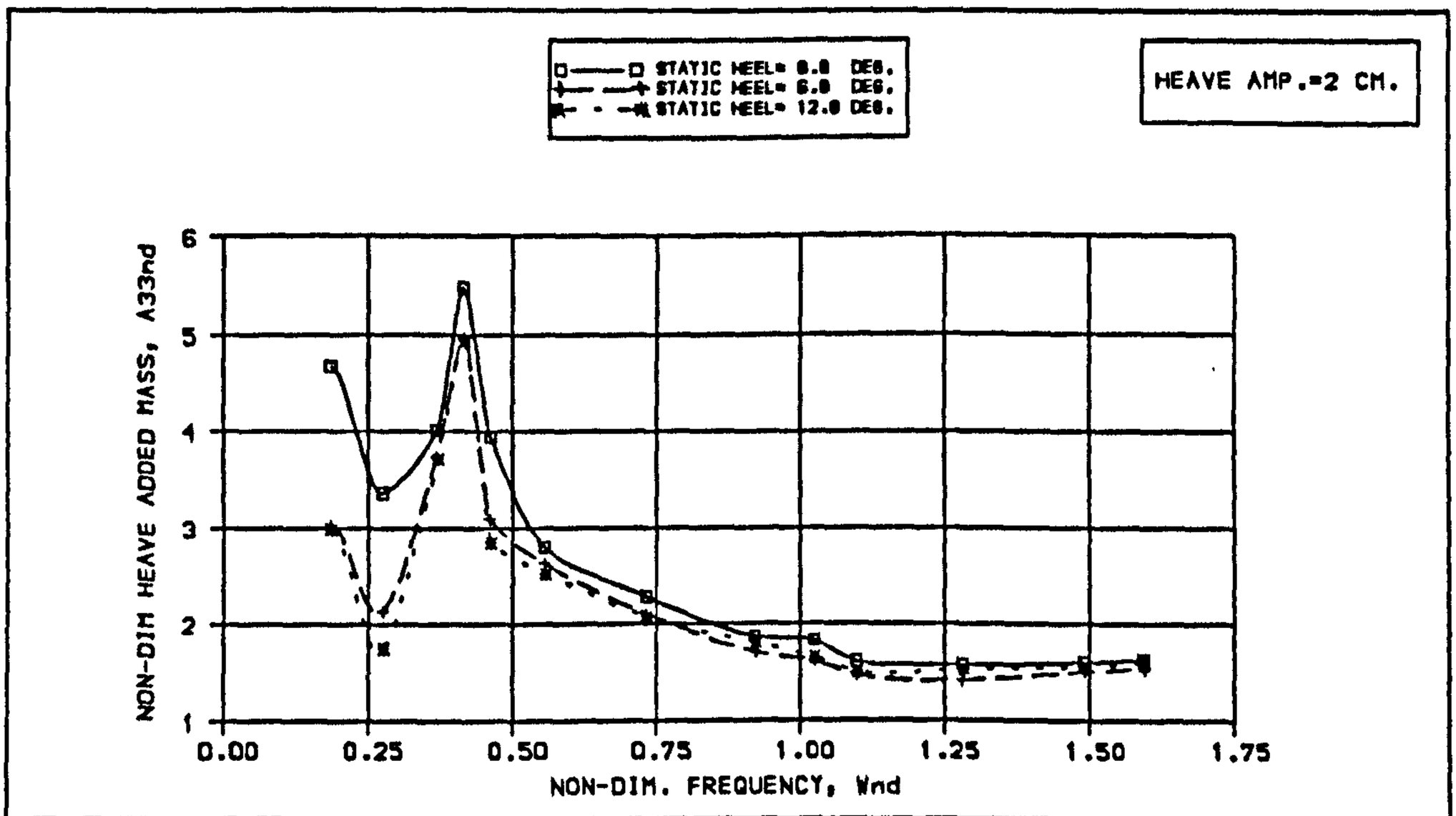

Fig 6.18A EFFECT OF STATIC HEEL ON HEAVE ADDED MASS

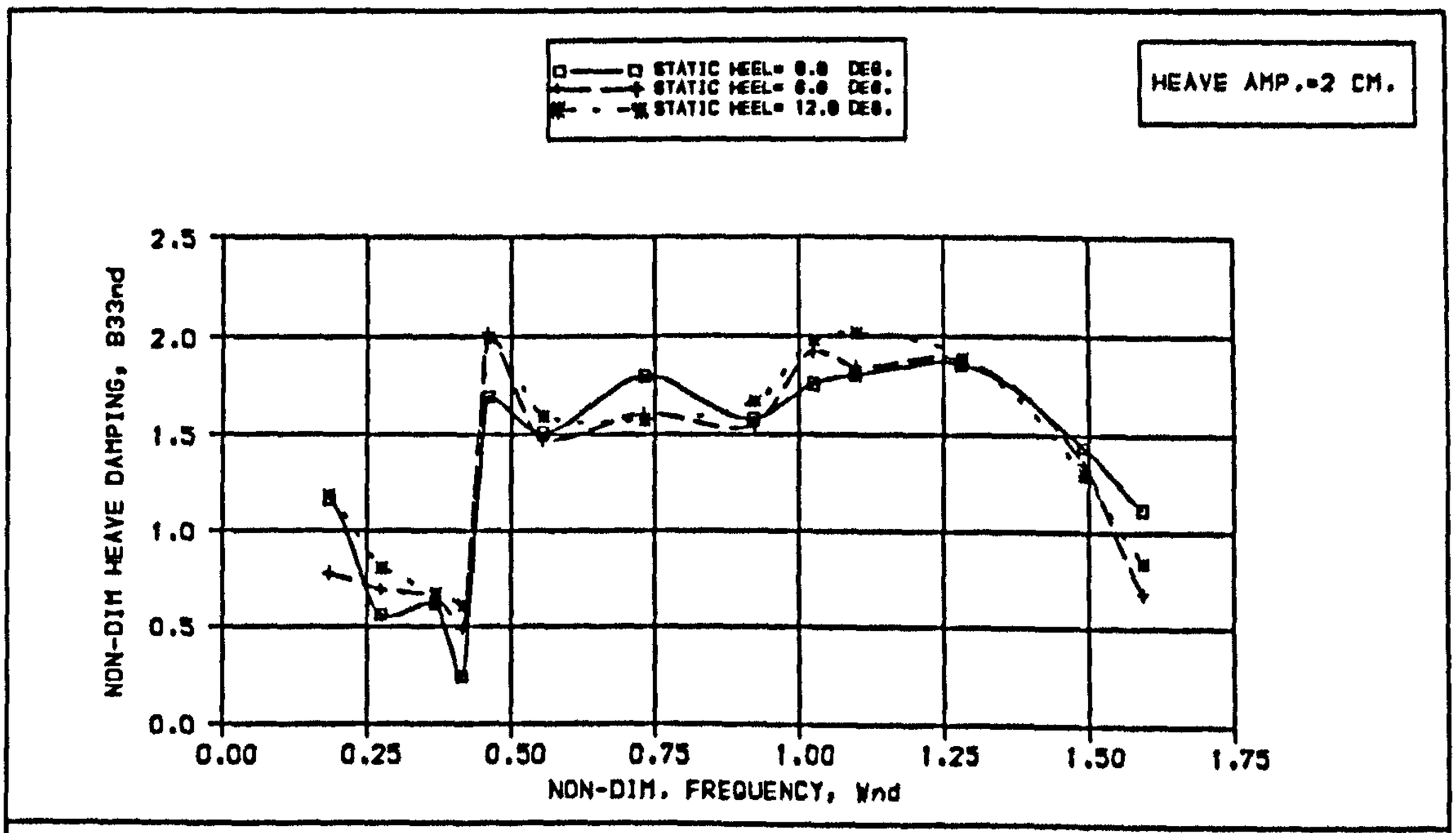

Fig 6.18B EFFECT OF STATIC HEEL ON HEAVE DAMPING

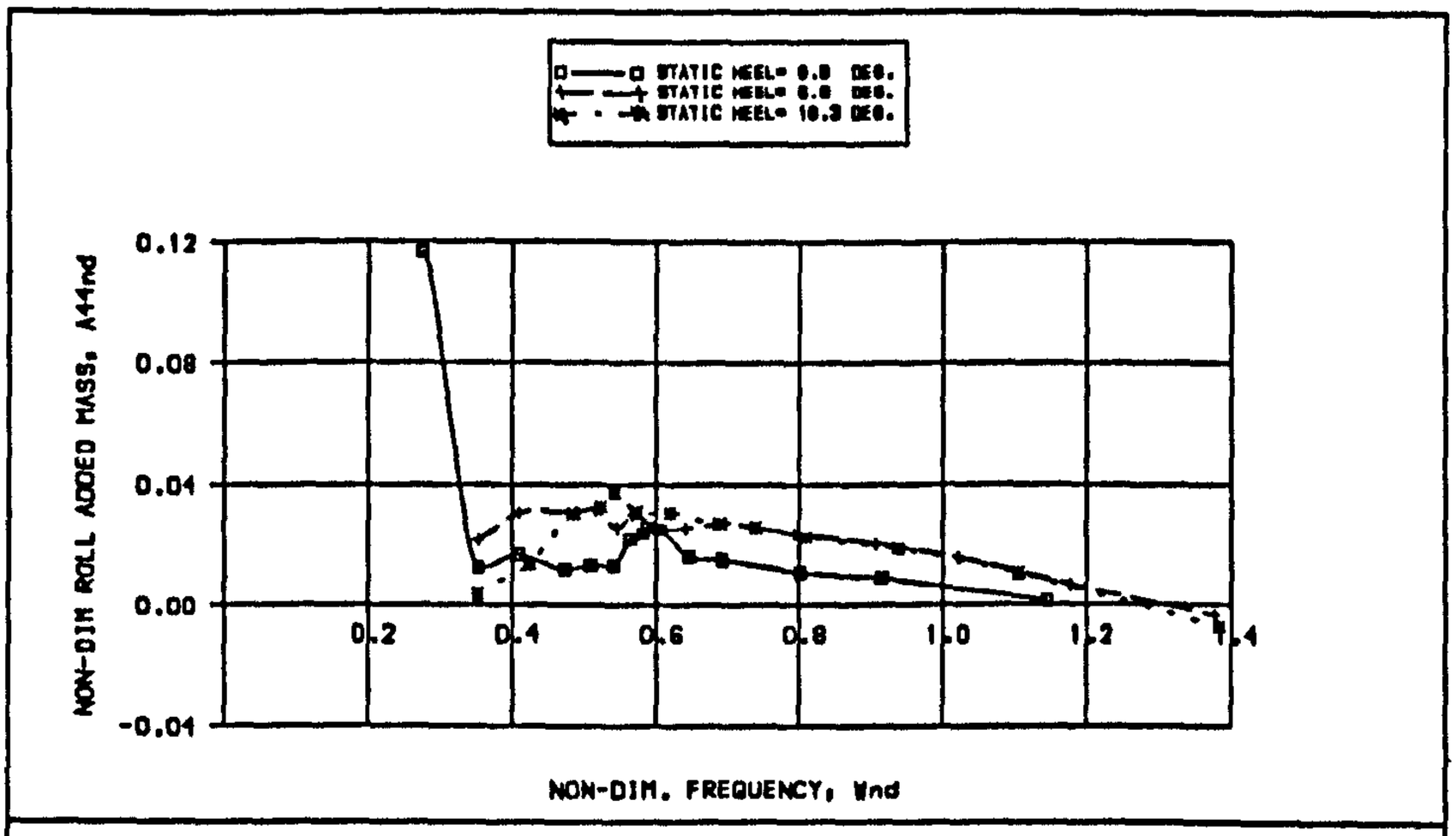

Fig 6.19A EFFECT OF STATIC HEEL ON ROLL ADDED MASS

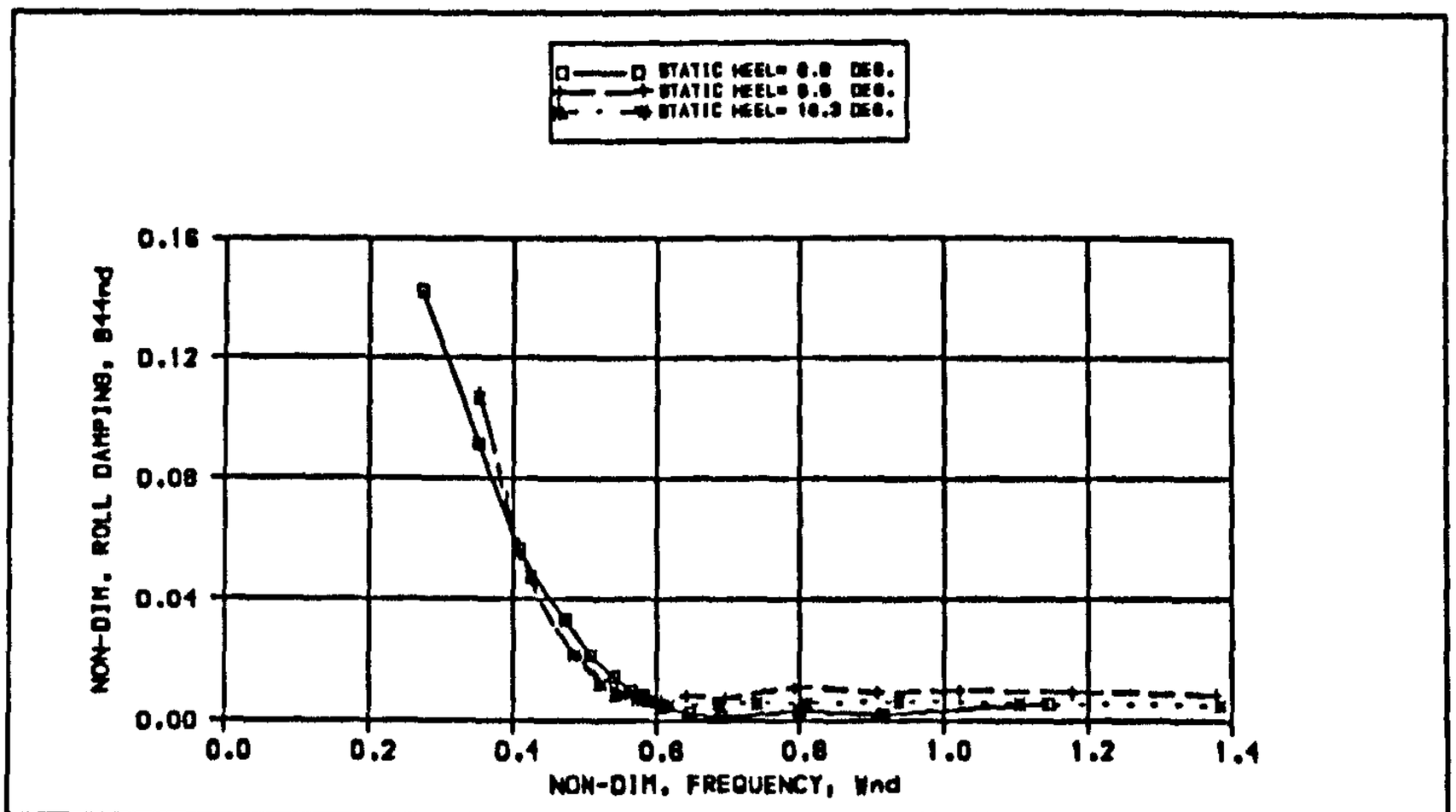

Fig 6.19B EFFECT OF STATIC HEEL ON ROLL DAMPING

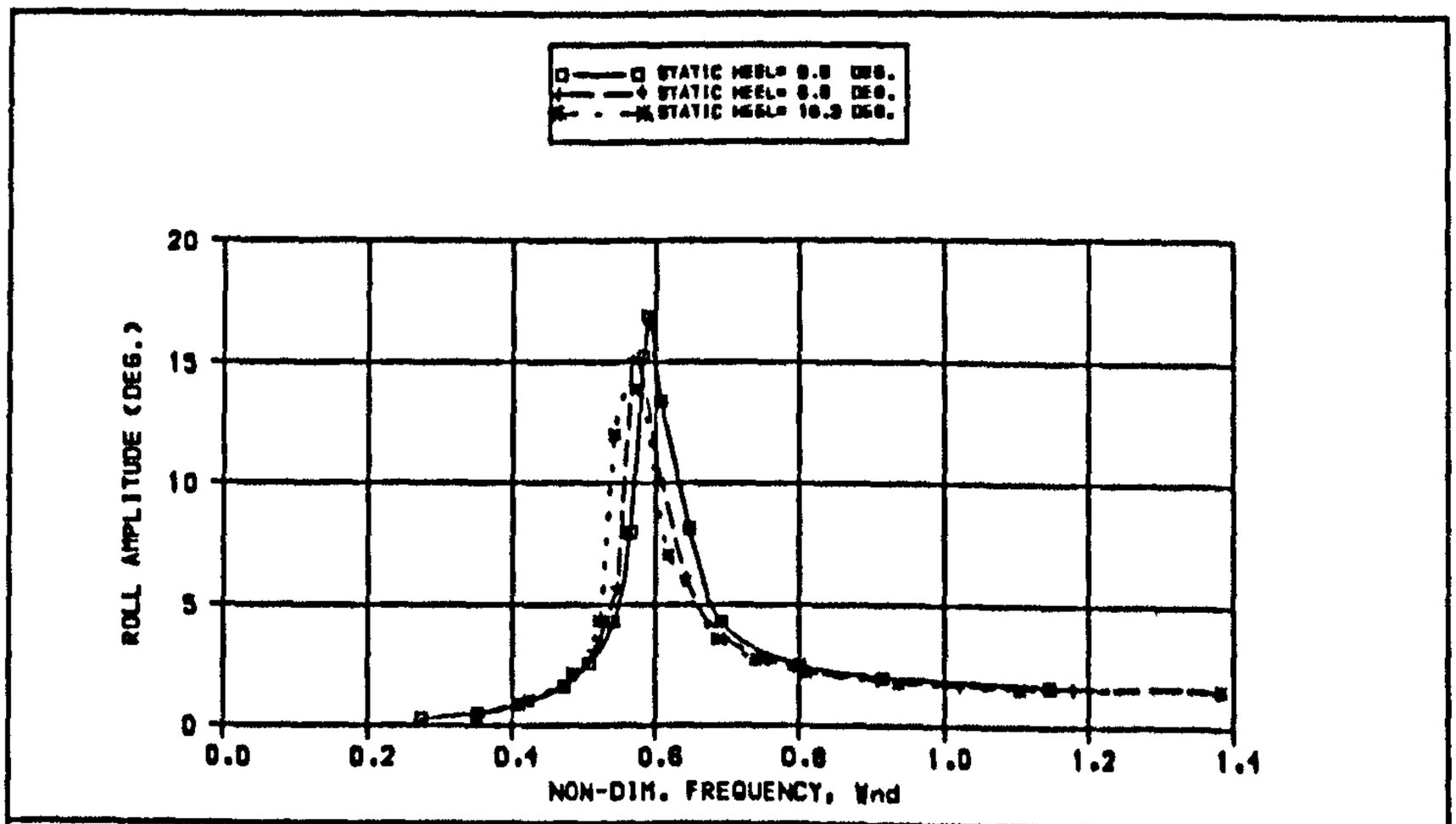

Fig 6.19C EFFECT OF STATIC HEEL ON ROLL MOTION OF THE SHIP

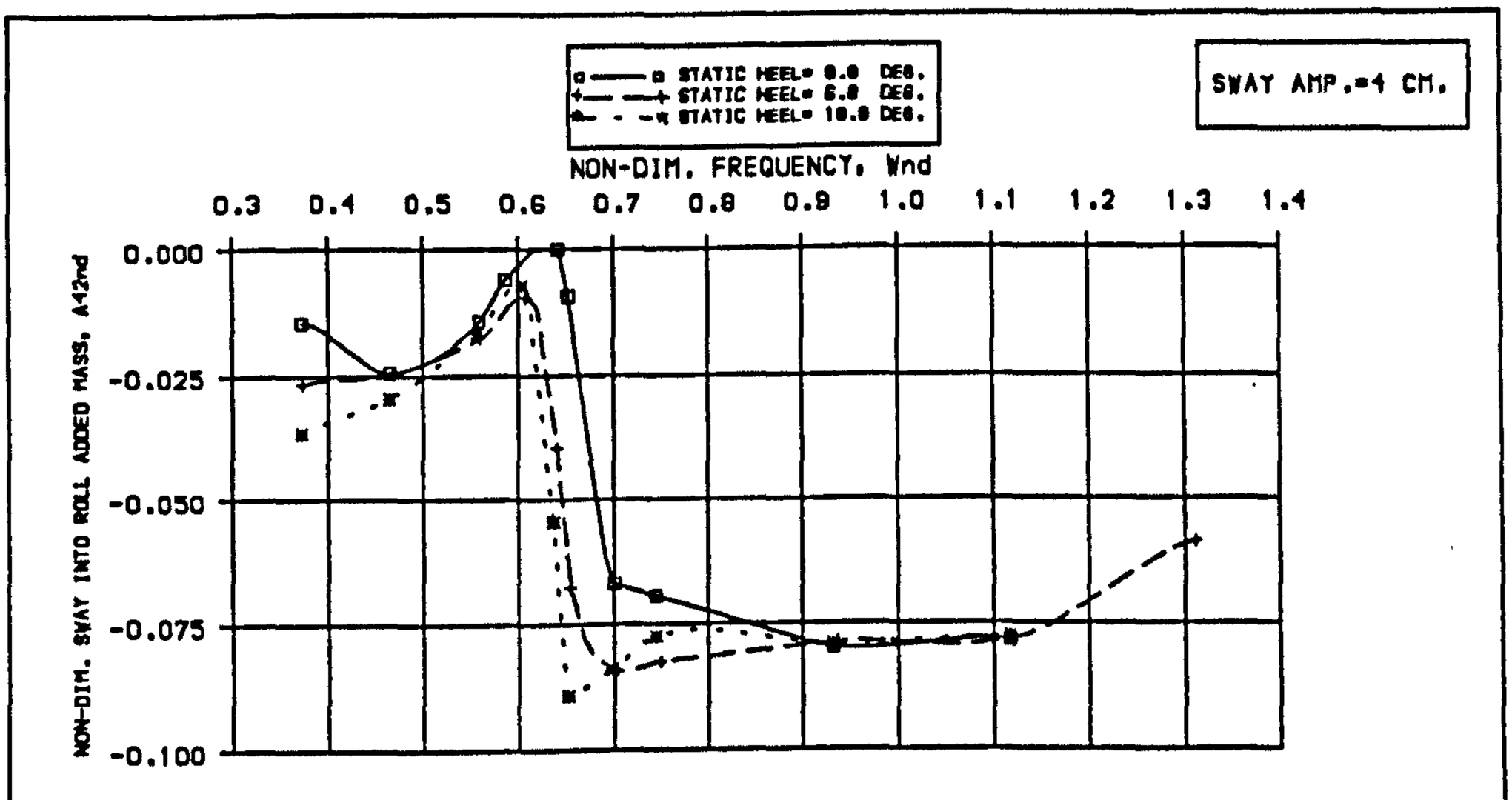

Fig 6.20A EFFECT OF STATIC HEEL ON SWAY INTO ROLL ADDED MASS

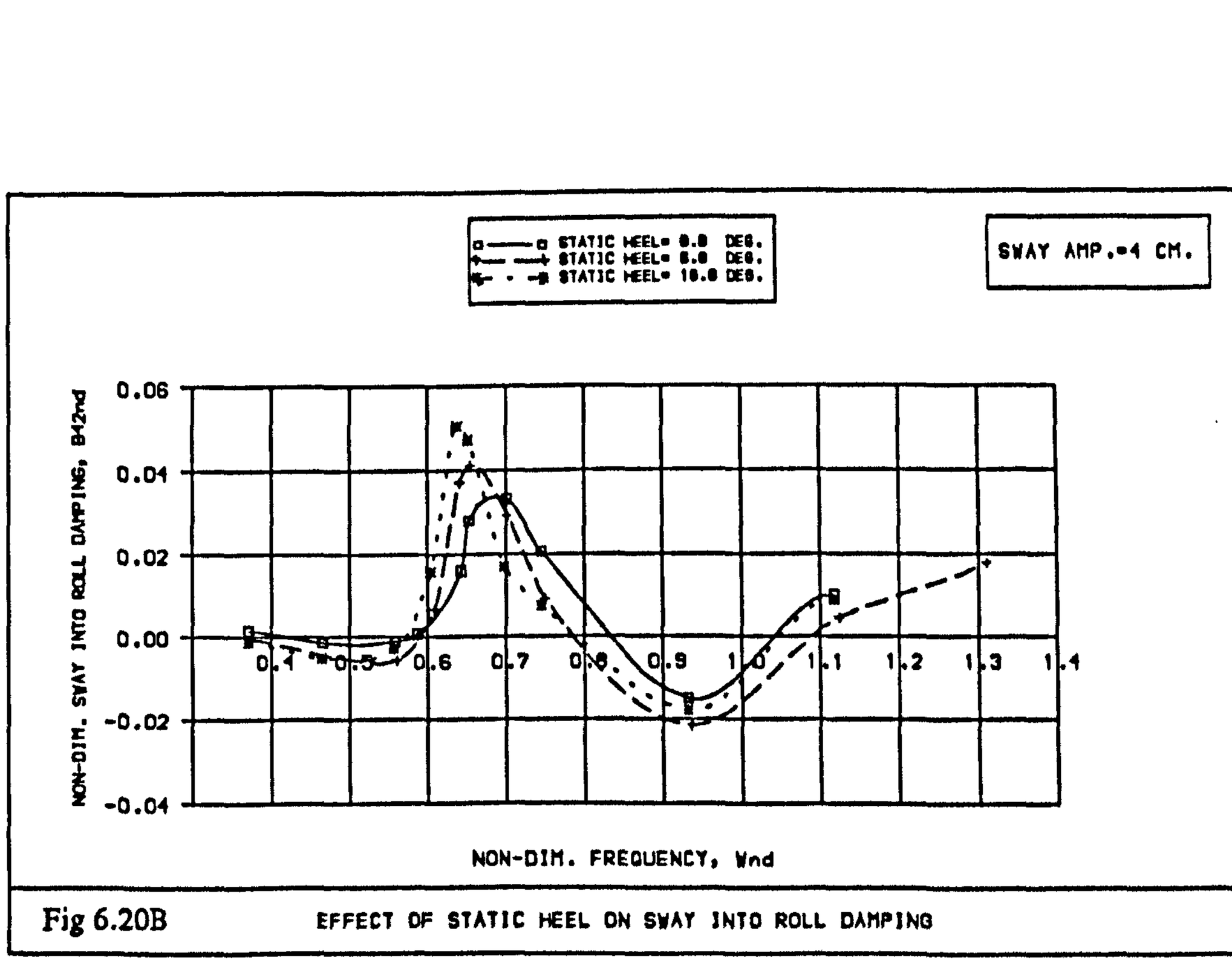

Fig 6.20B EFFECT OF STATIC HEEL ON SWAY INTO ROLL DAMPING

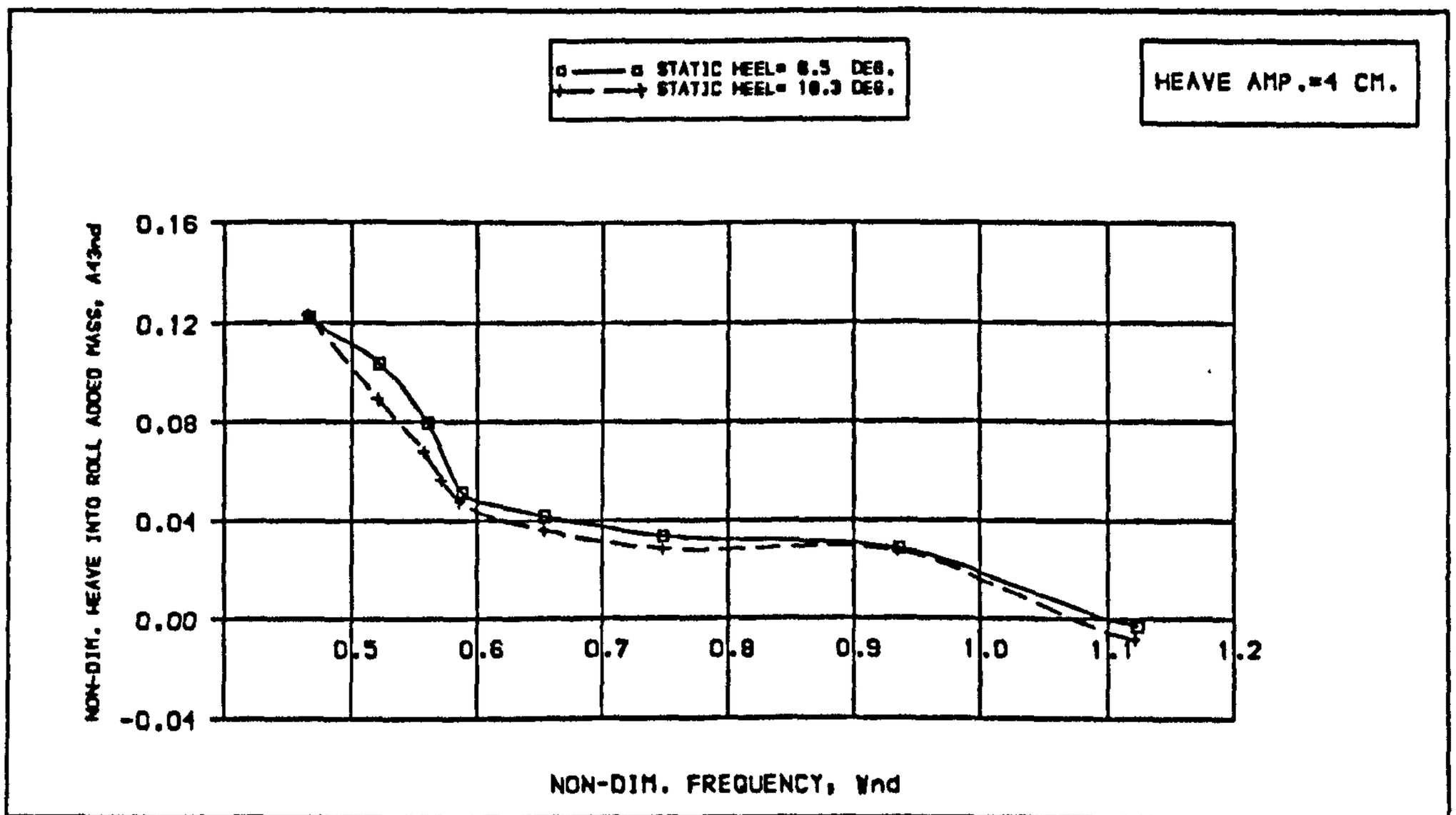

Fig 6.21A EFFECT OF STATIC HEEL ON HEAVE INTO ROLL ADDED MASS

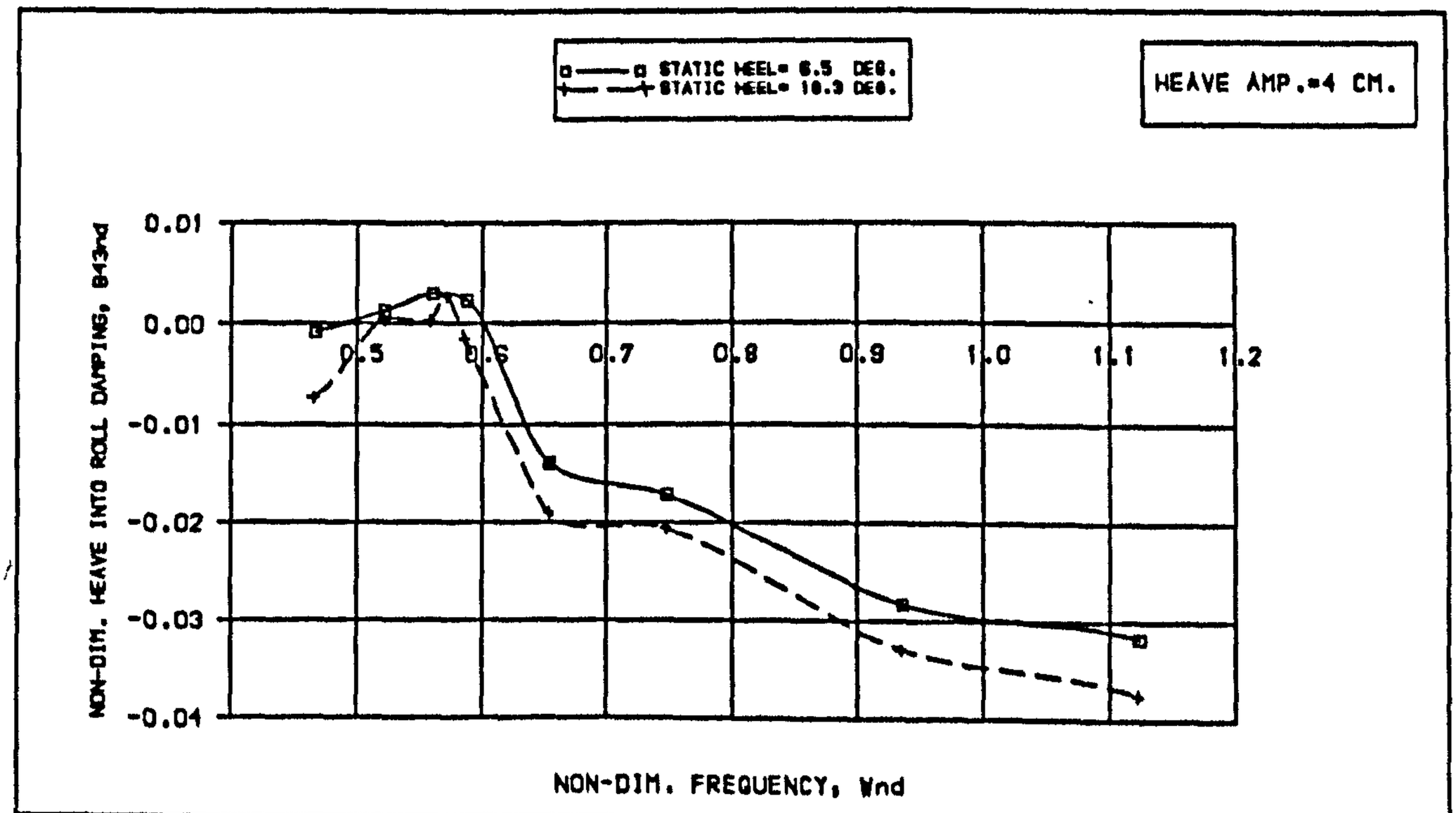

Fig 6.21B EFFECT OF STATIC HEEL ON HEAVE INTO ROLL DAMPING

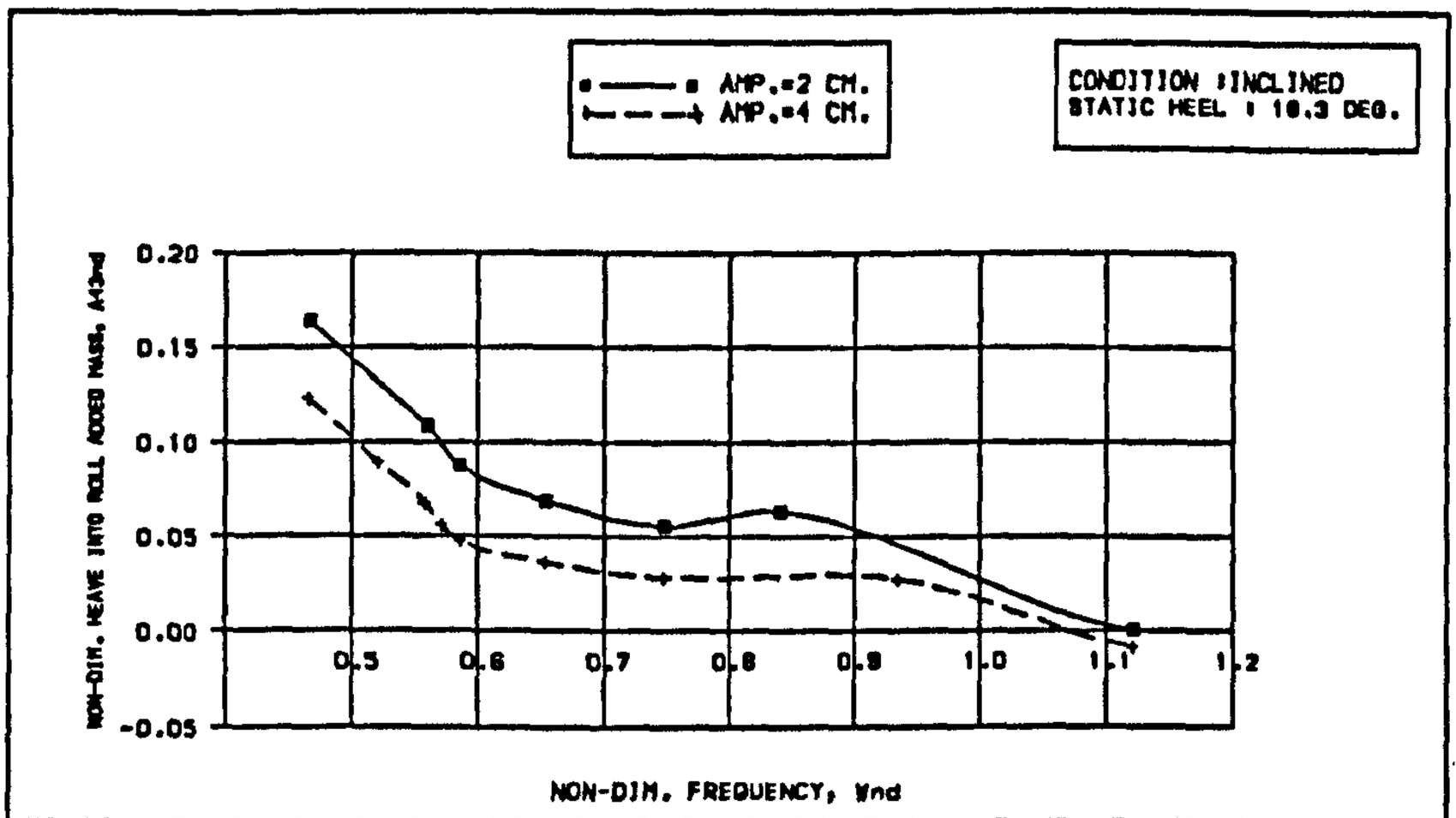

Fig 6.22A EFFECT OF HEAVE AMPLITUDE ON HEAVE INTO ROLL ADDED MASS

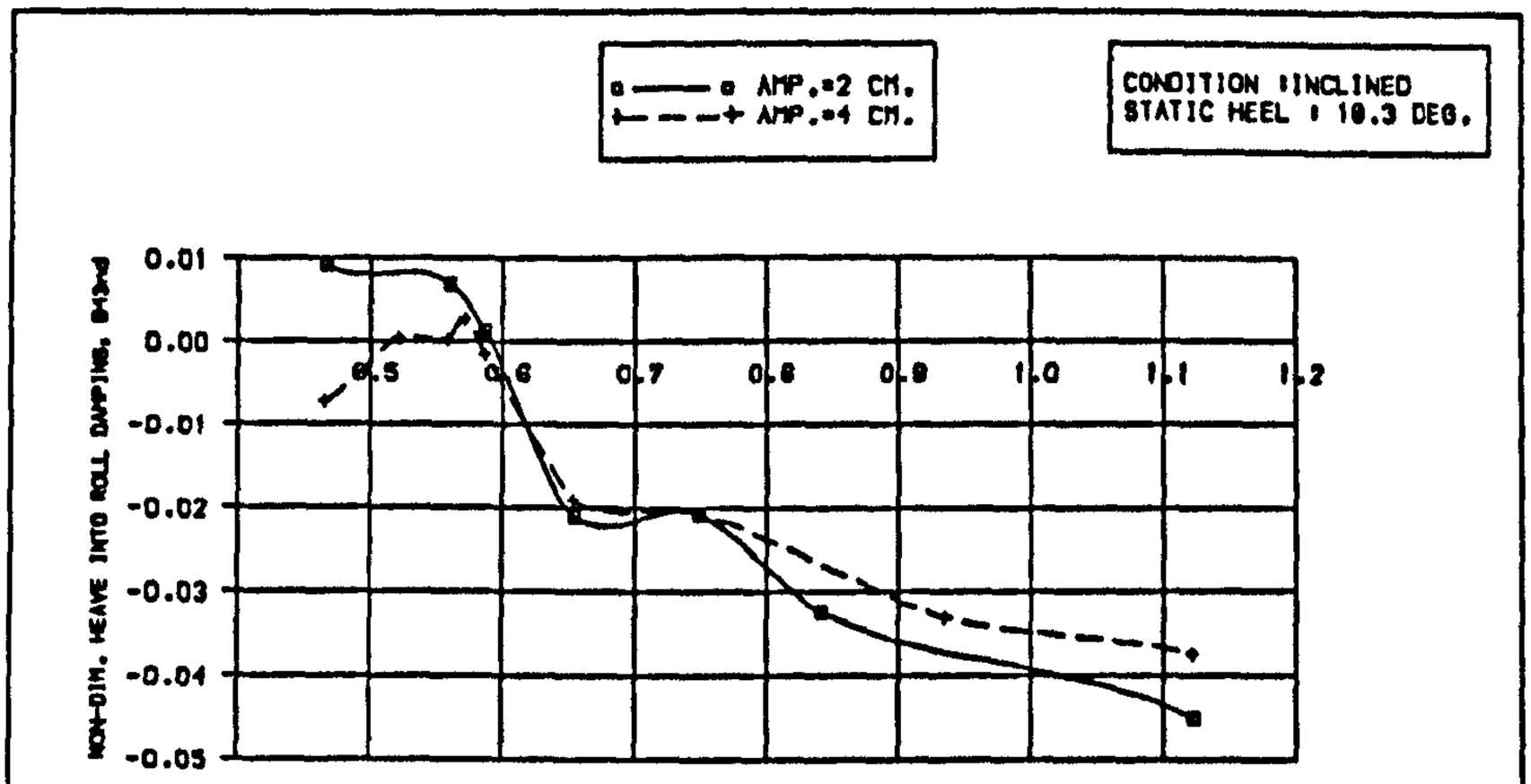

Fig 6.22B EFFECT OF HEAVE AMPLITUDE ON HEAVE INTO ROLL DAMPING

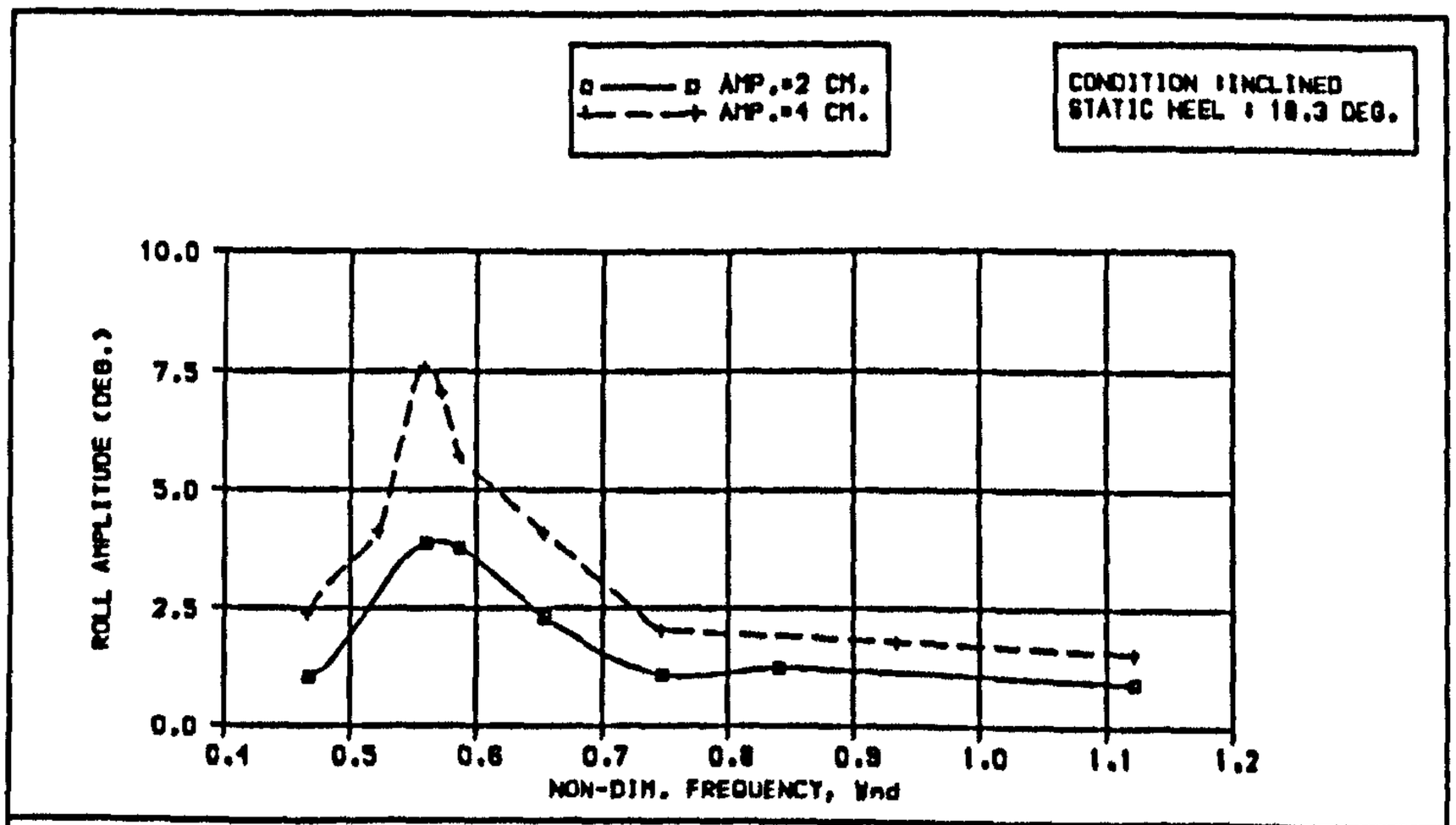

Fig 6.22C EFFECT OF HEAVE AMPLITUDE ON ROLL MOTION DUE TO COUPLING

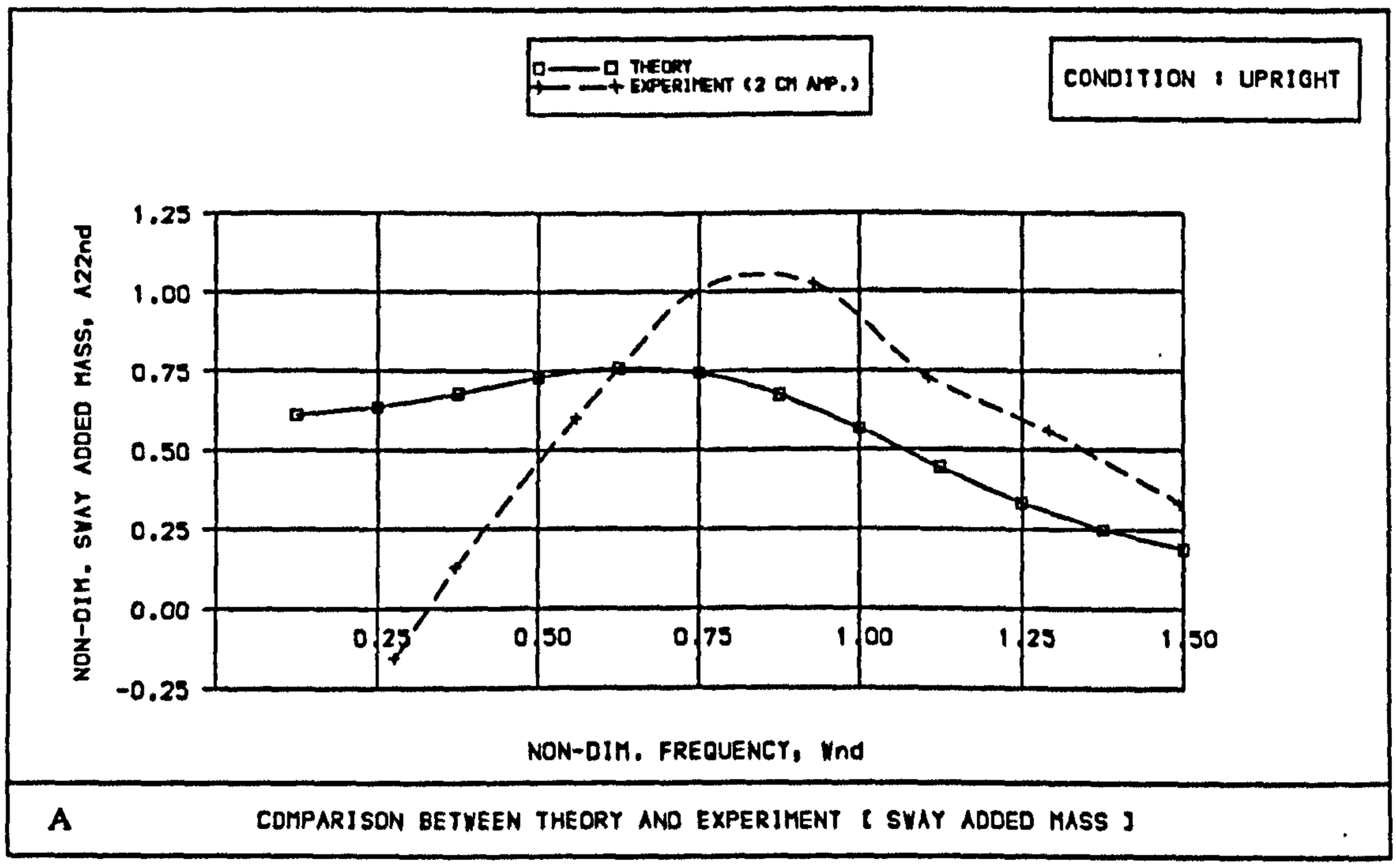

A COMPARISON BETWEEN THEORY AND EXPERIMENT [SWAY ADDED MASS]

Fig 6.23 Comparison between experimentally and theoretically derived coefficients of SWAY motion with ship at the UPRIGHT condition

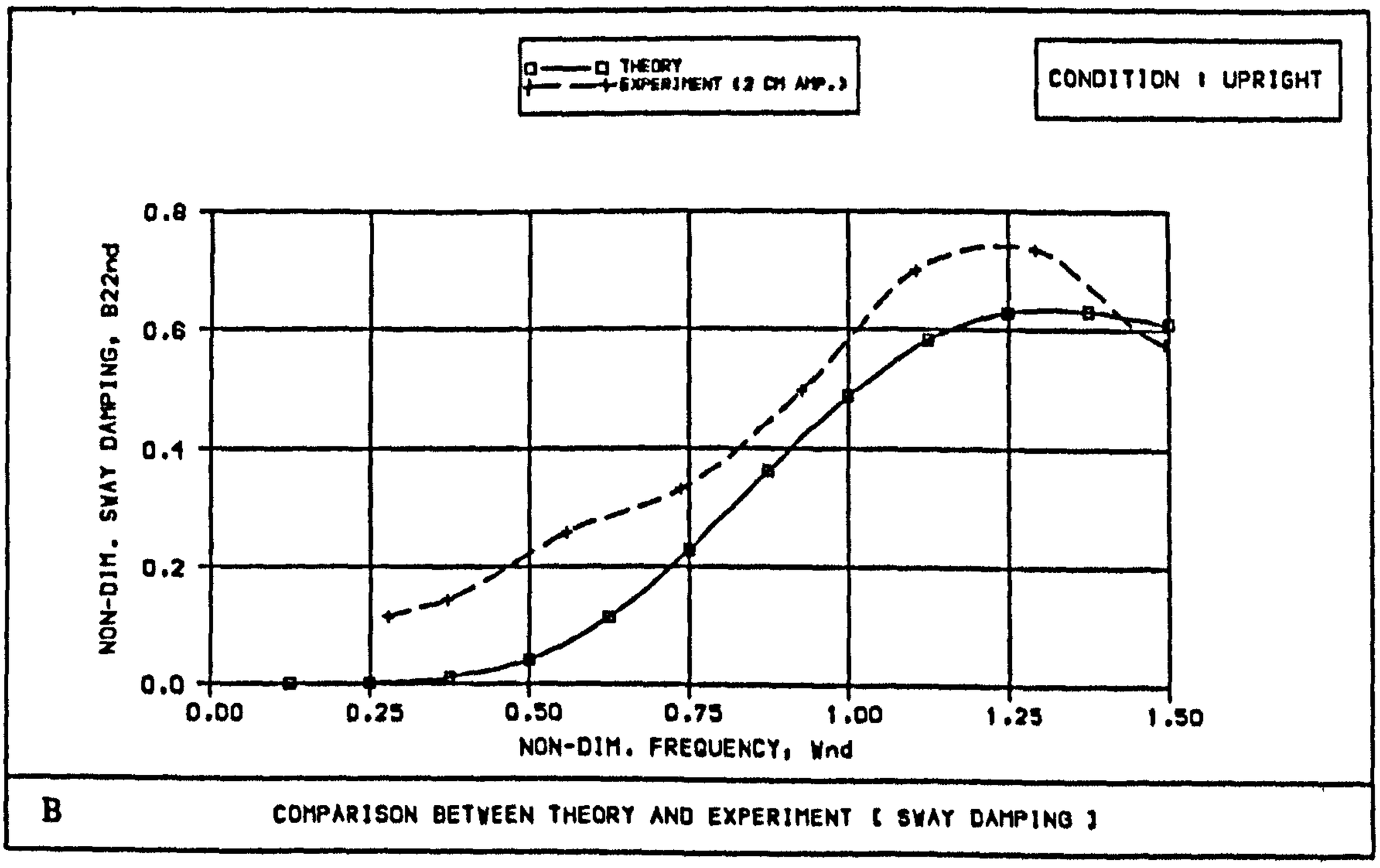

B COMPARISON BETWEEN THEORY AND EXPERIMENT [SWAY DAMPING]

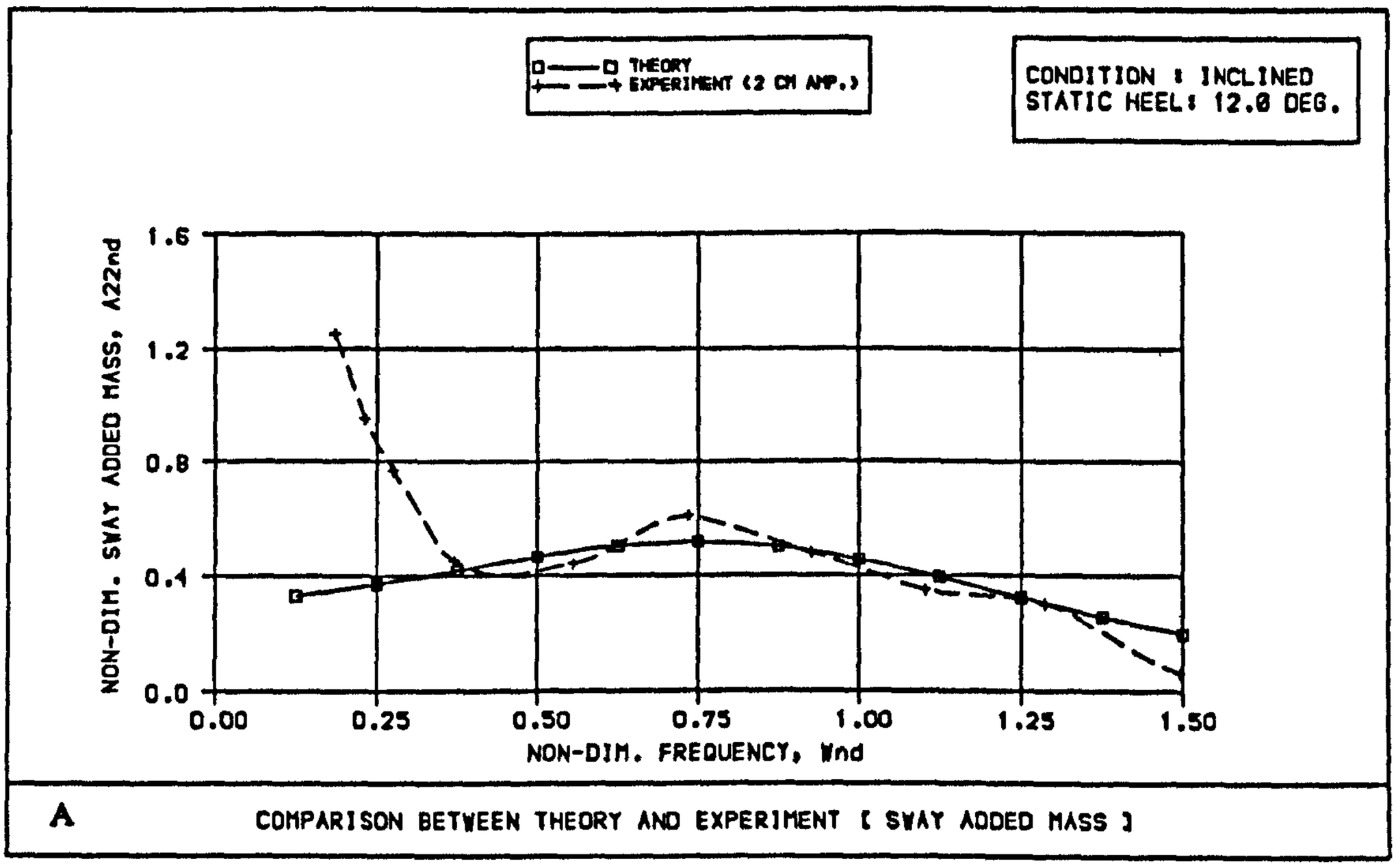

A COMPARISON BETWEEN THEORY AND EXPERIMENT [SWAY ADDED MASS]

Fig 6.24 Comparison between experimentally and theoretically derived coefficients of SWAY motion with ship at an INCLINED condition

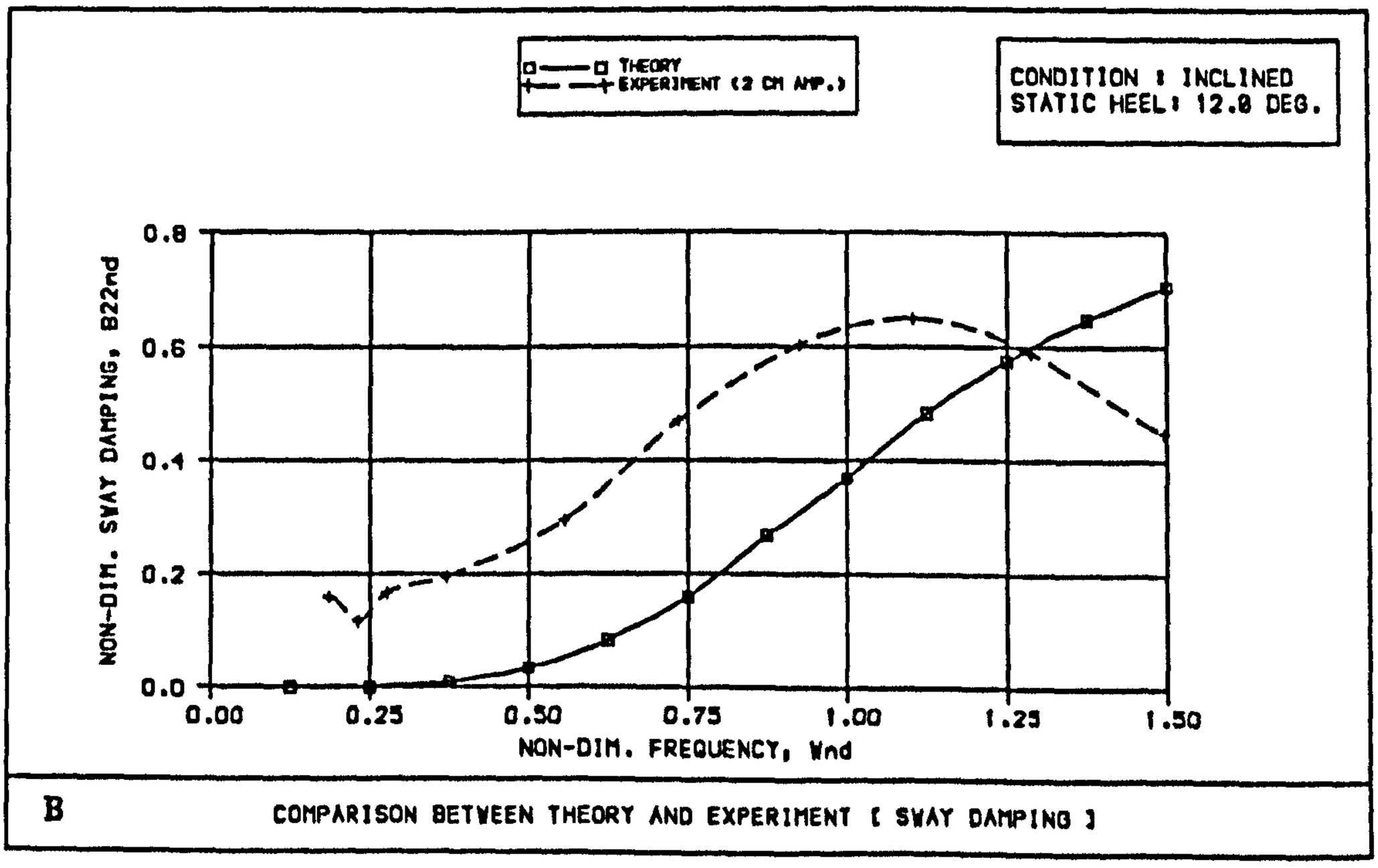

B COMPARISON BETWEEN THEORY AND EXPERIMENT [SWAY DAMPING]

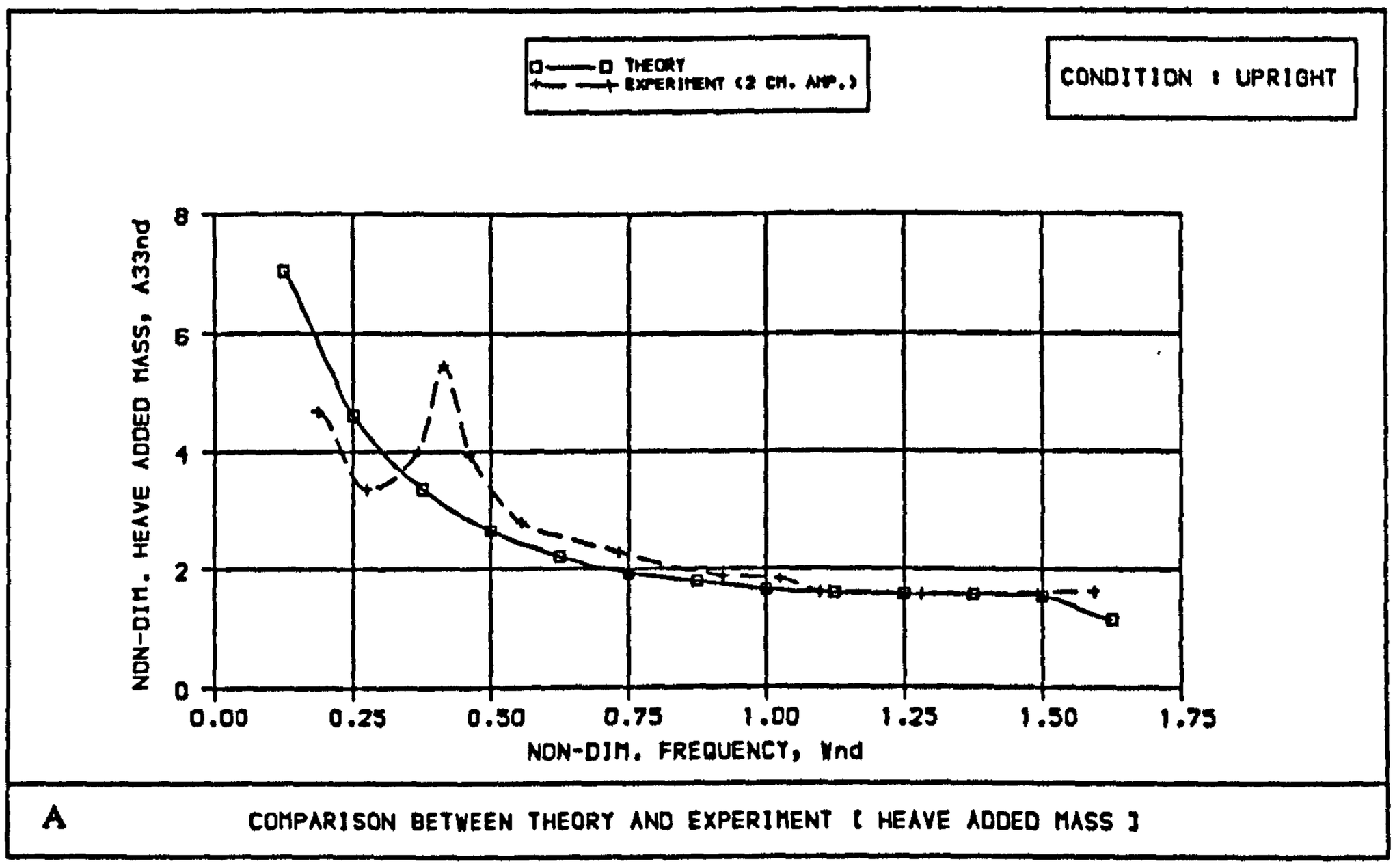

Fig 6.25 Comparison between experimentally and theoretically derived coefficients of **HEAVE** motion with ship at the **UPRIGHT** condition

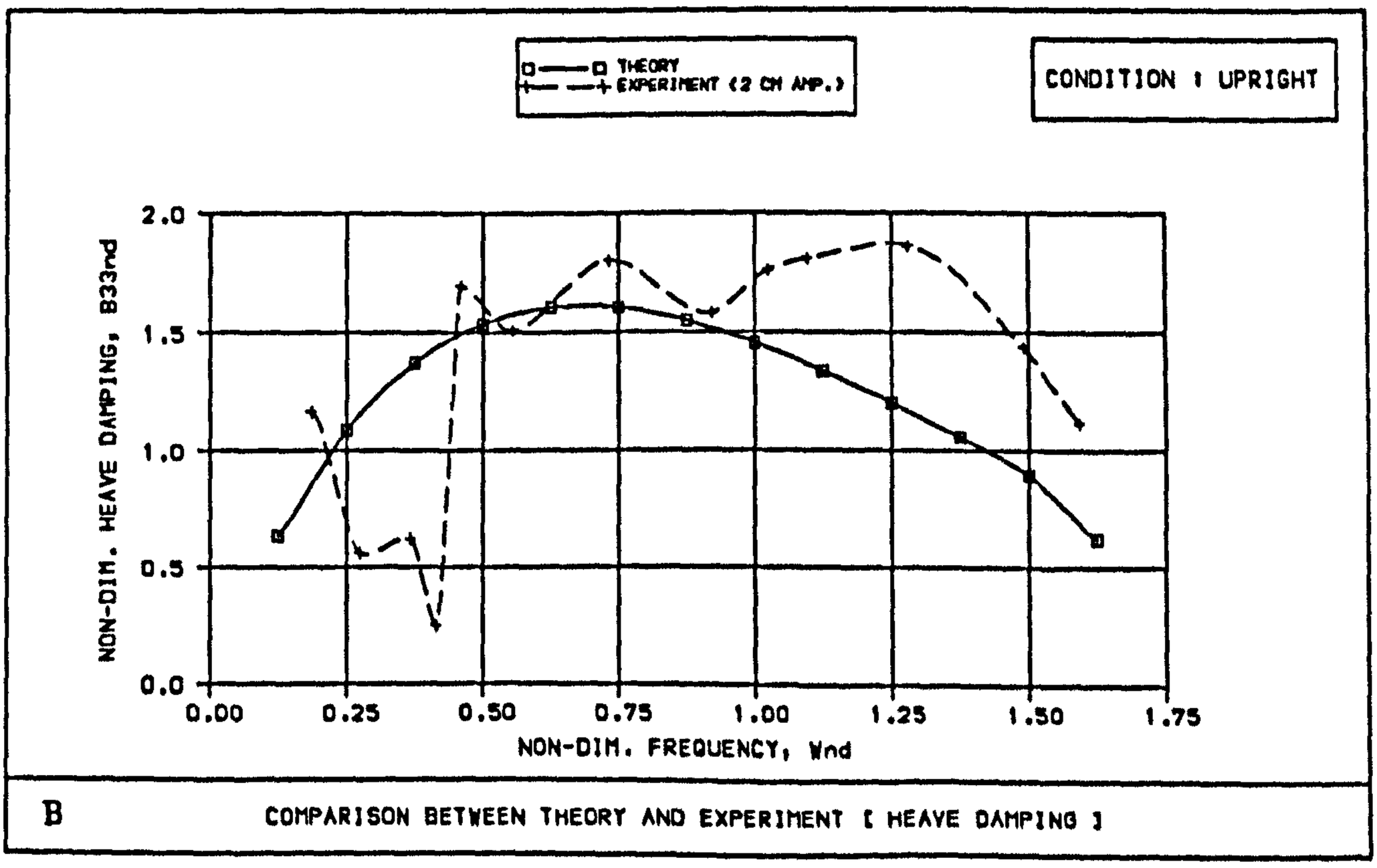

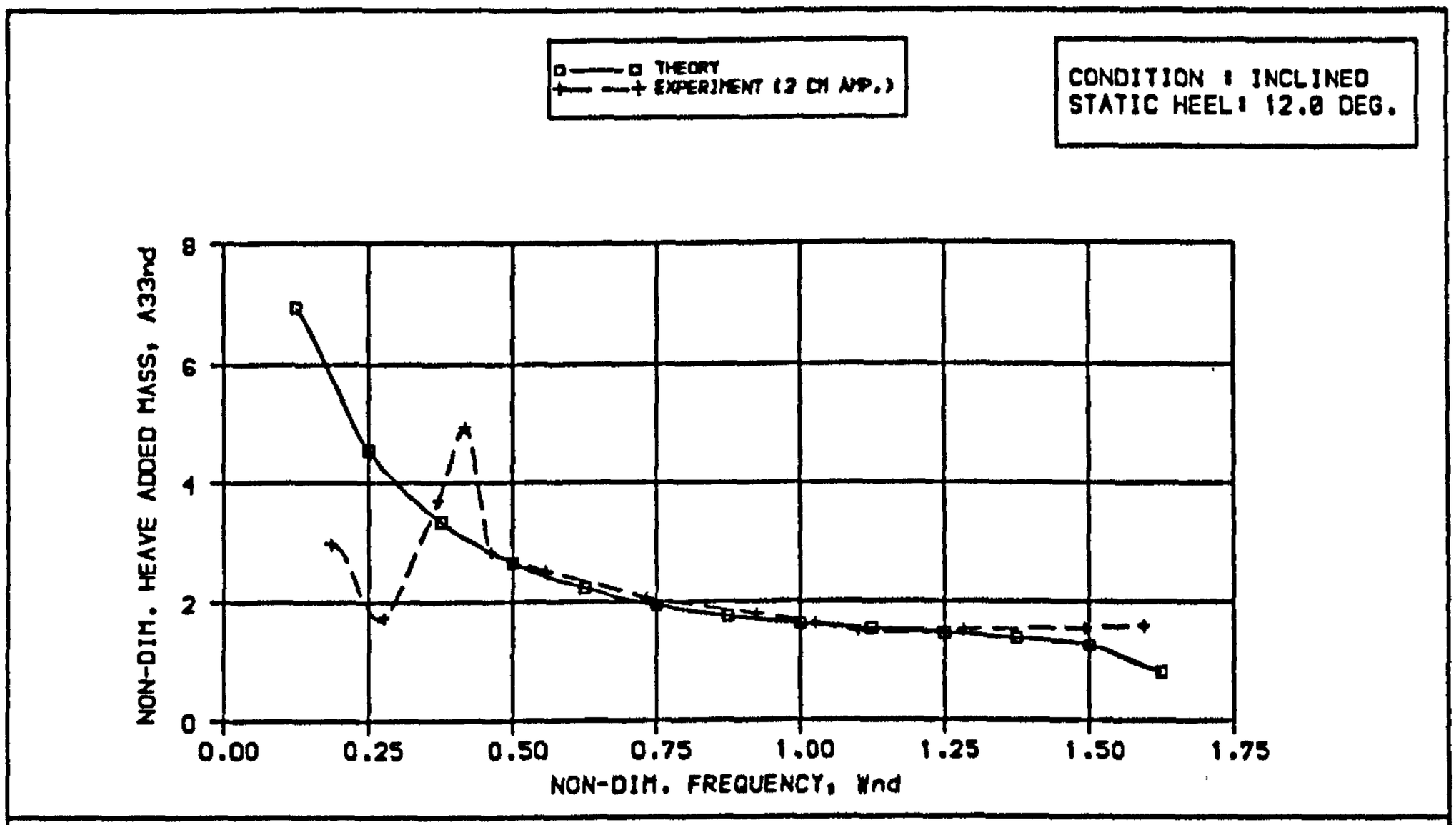

A COMPARISON BETWEEN THEORY AND EXPERIMENT [HEAVE ADDED MASS]

Fig 6.26 Comparison between experimentally and theoretically derived coefficients of HEAVE motion with ship at an INCLINED condition

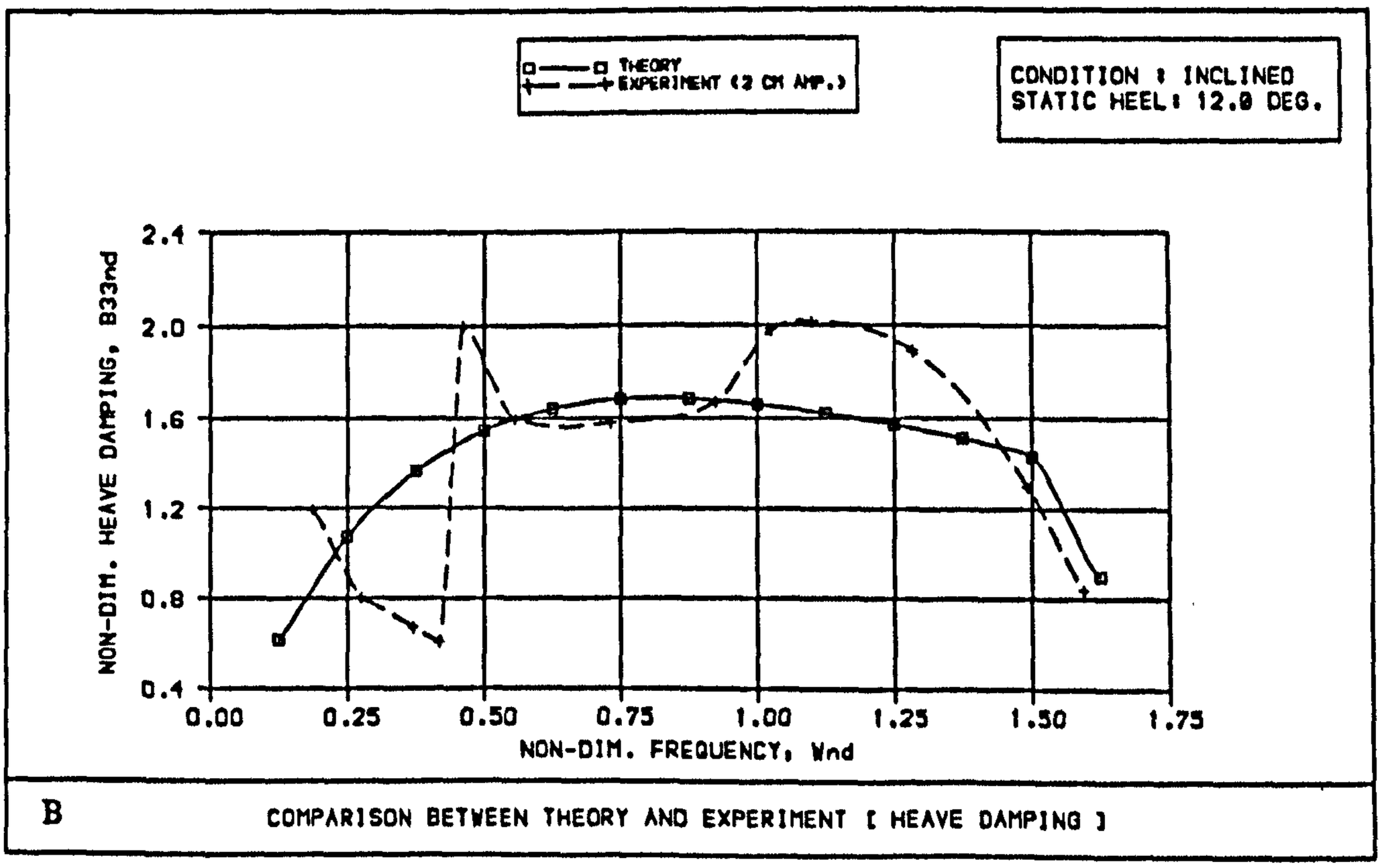

B COMPARISON BETWEEN THEORY AND EXPERIMENT [HEAVE DAMPING]

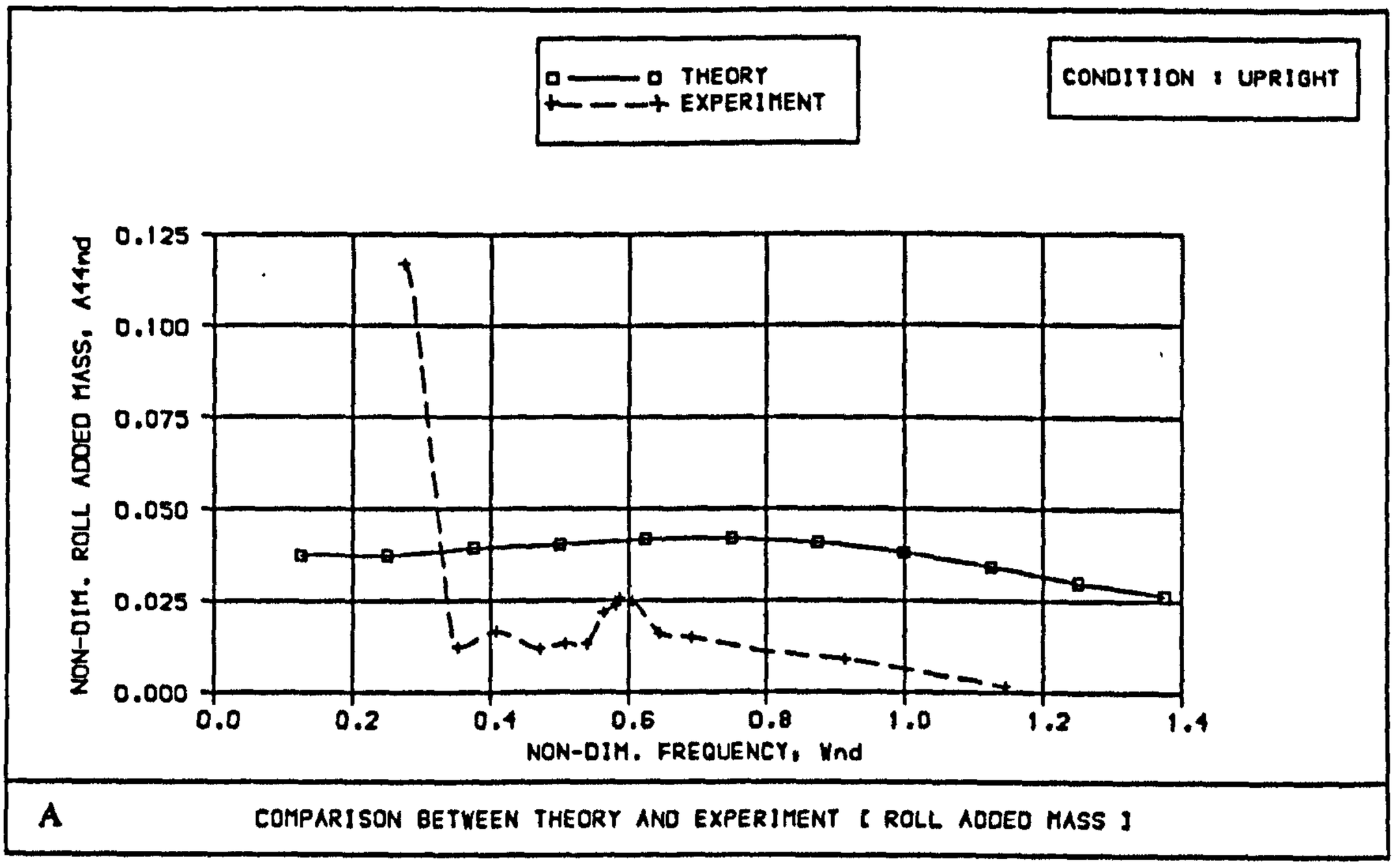

A COMPARISON BETWEEN THEORY AND EXPERIMENT [ROLL ADDED MASS]

Fig 6.27 Comparison between experimentally and theoretically derived coefficients of ROLL motion with ship at the UPRIGHT condition

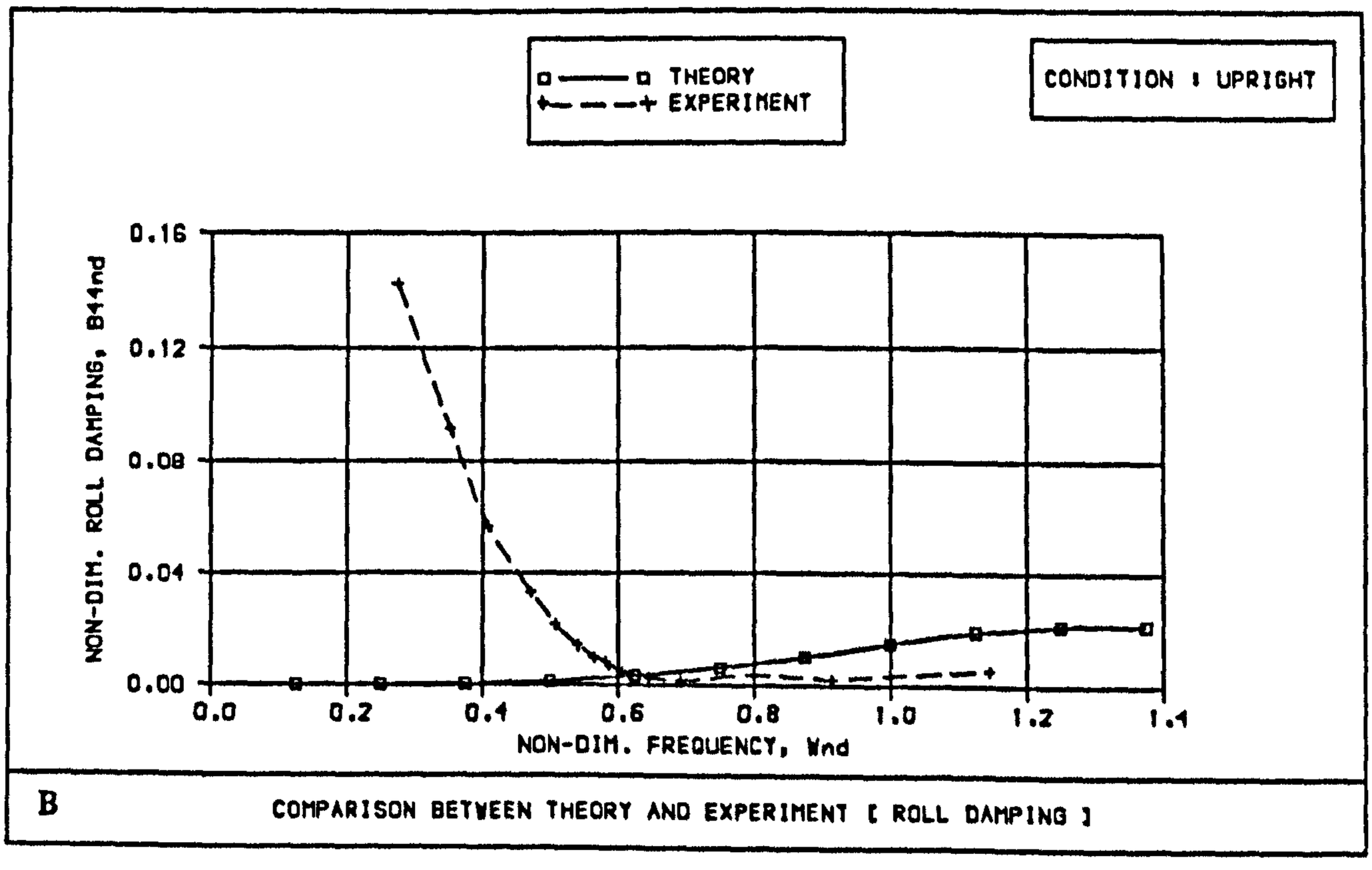

B COMPARISON BETWEEN THEORY AND EXPERIMENT [ROLL DAMPING]

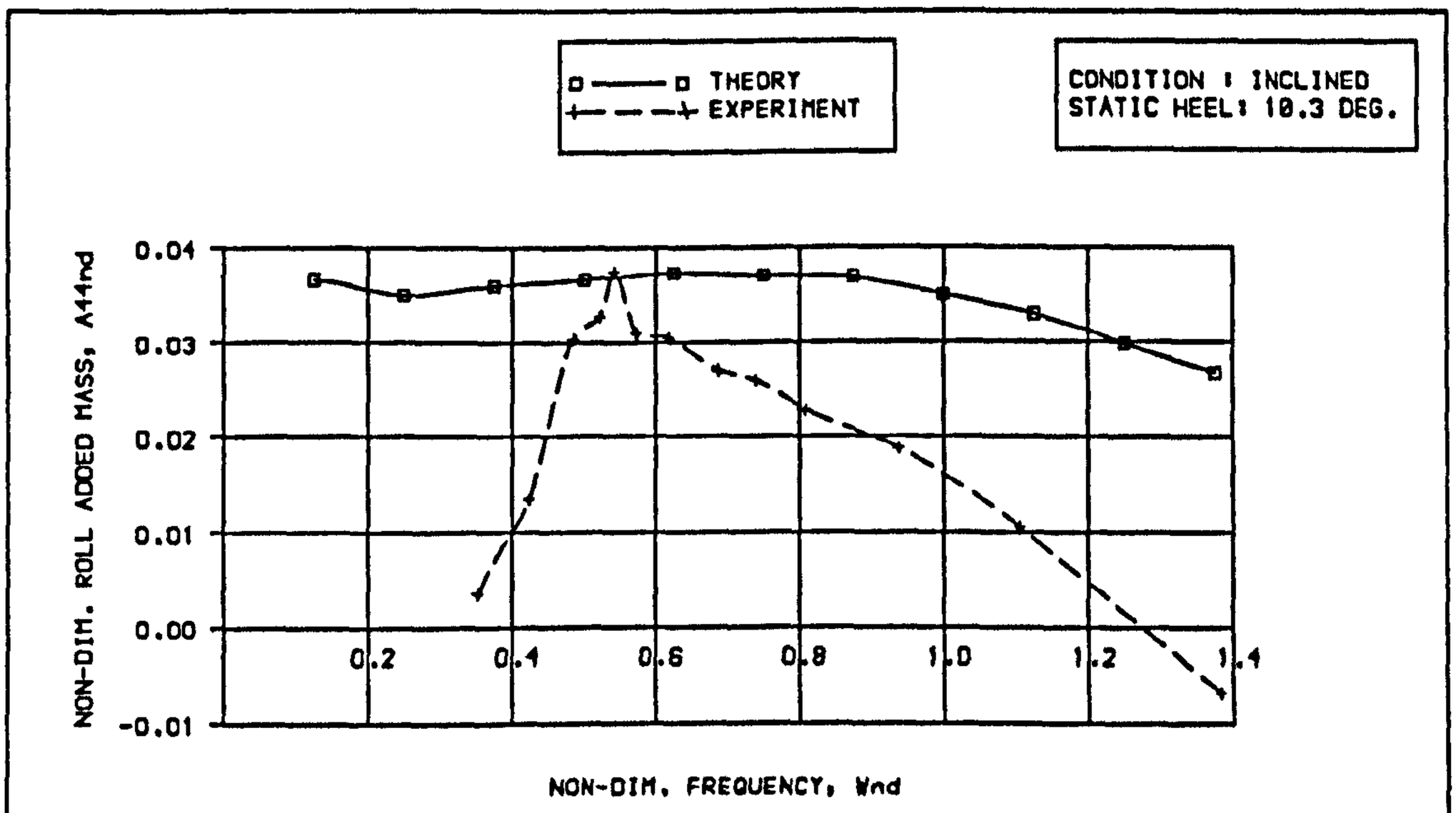

A COMPARISON BETWEEN THEORY AND EXPERIMENT [ROLL ADDED MASS]

Fig 6.28 Comparison between experimentally and theoretically derived coefficients of ROLL motion with ship at an INCLINED condition

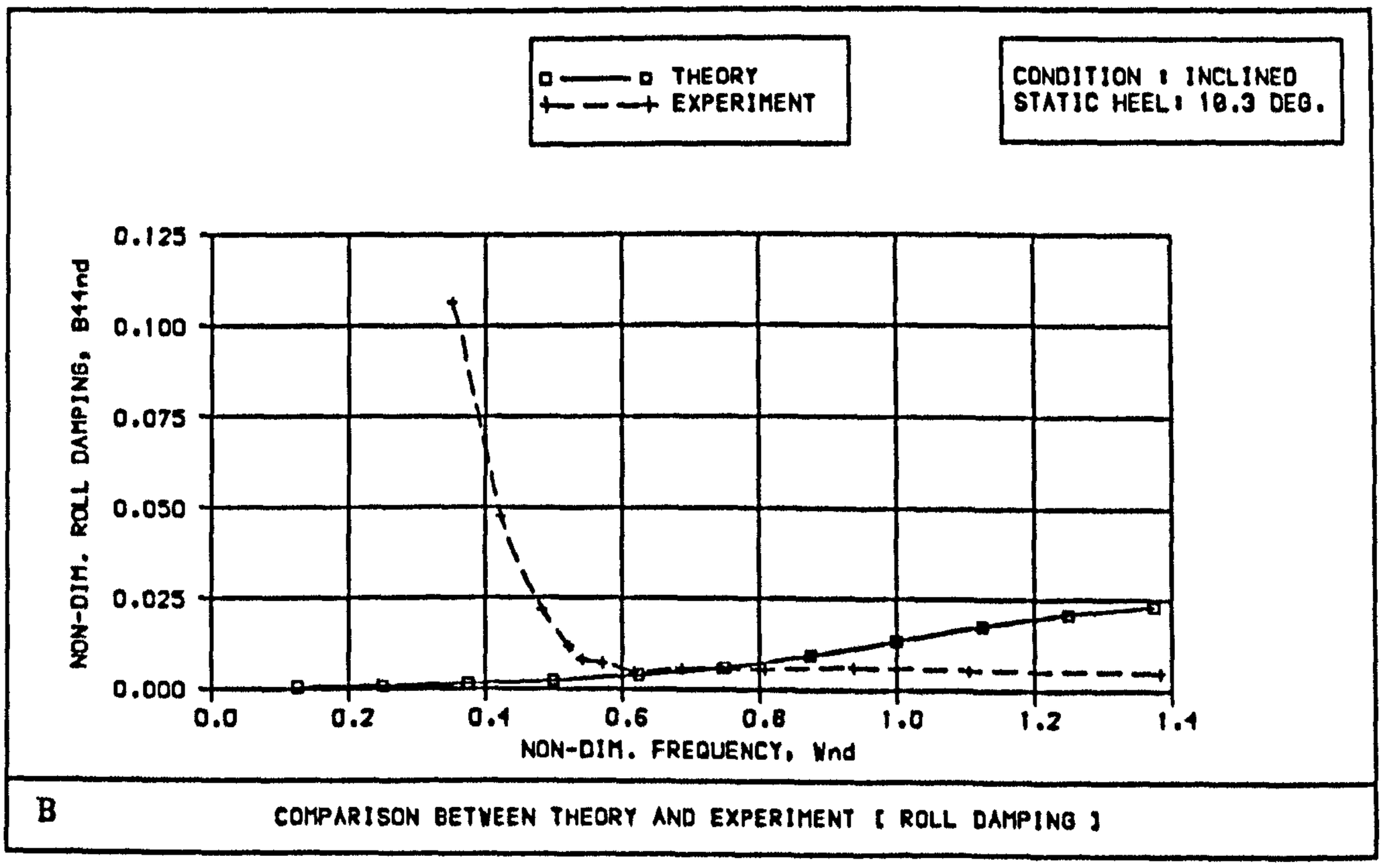

B COMPARISON BETWEEN THEORY AND EXPERIMENT [ROLL DAMPING]

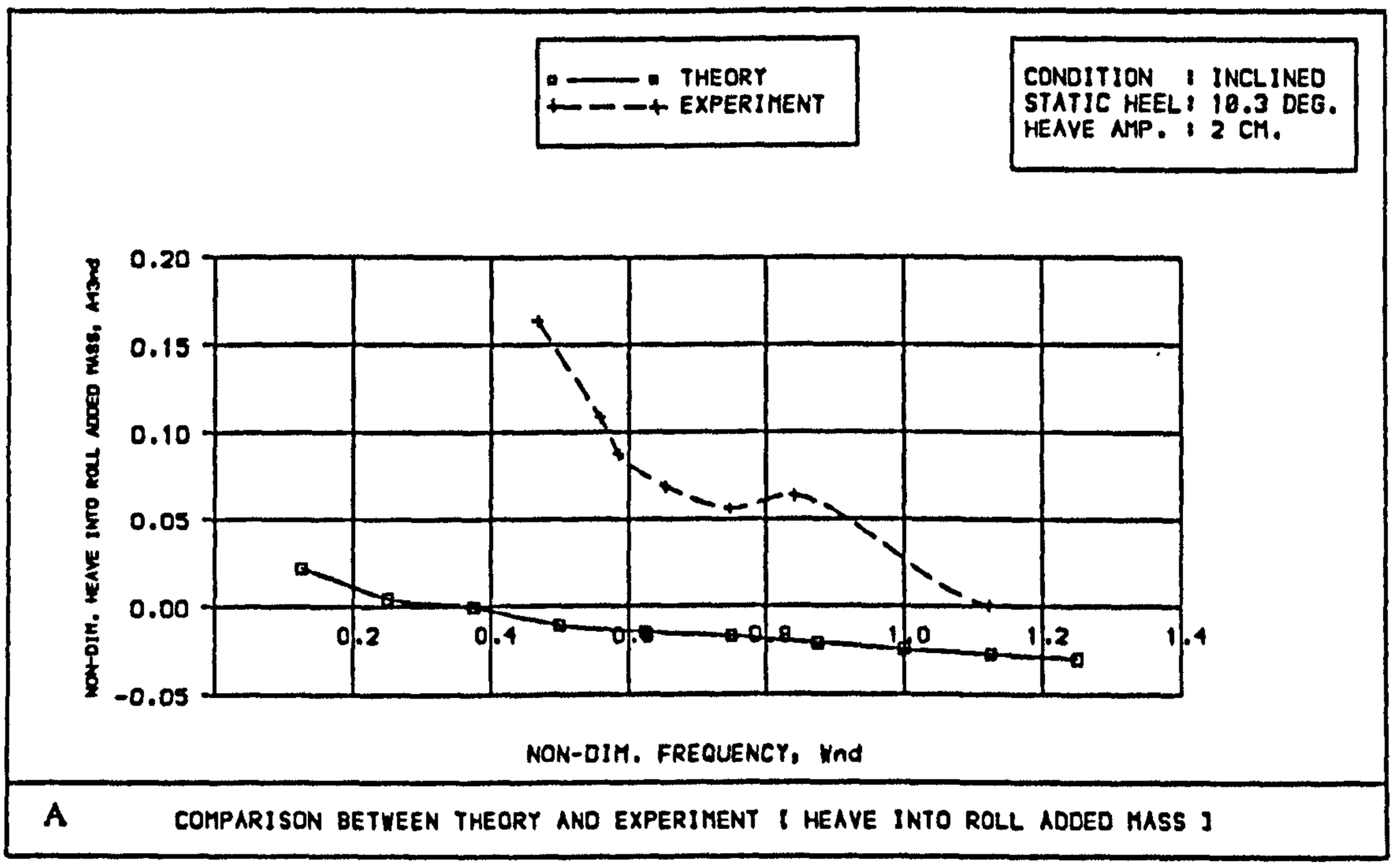

A COMPARISON BETWEEN THEORY AND EXPERIMENT [HEAVE INTO ROLL ADDED MASS]

Fig 6.29 Comparison between experimentally and theoretically derived coupling coefficients, induced by **HEAVE** into **ROLL** with ship at an **INCLINED** condition

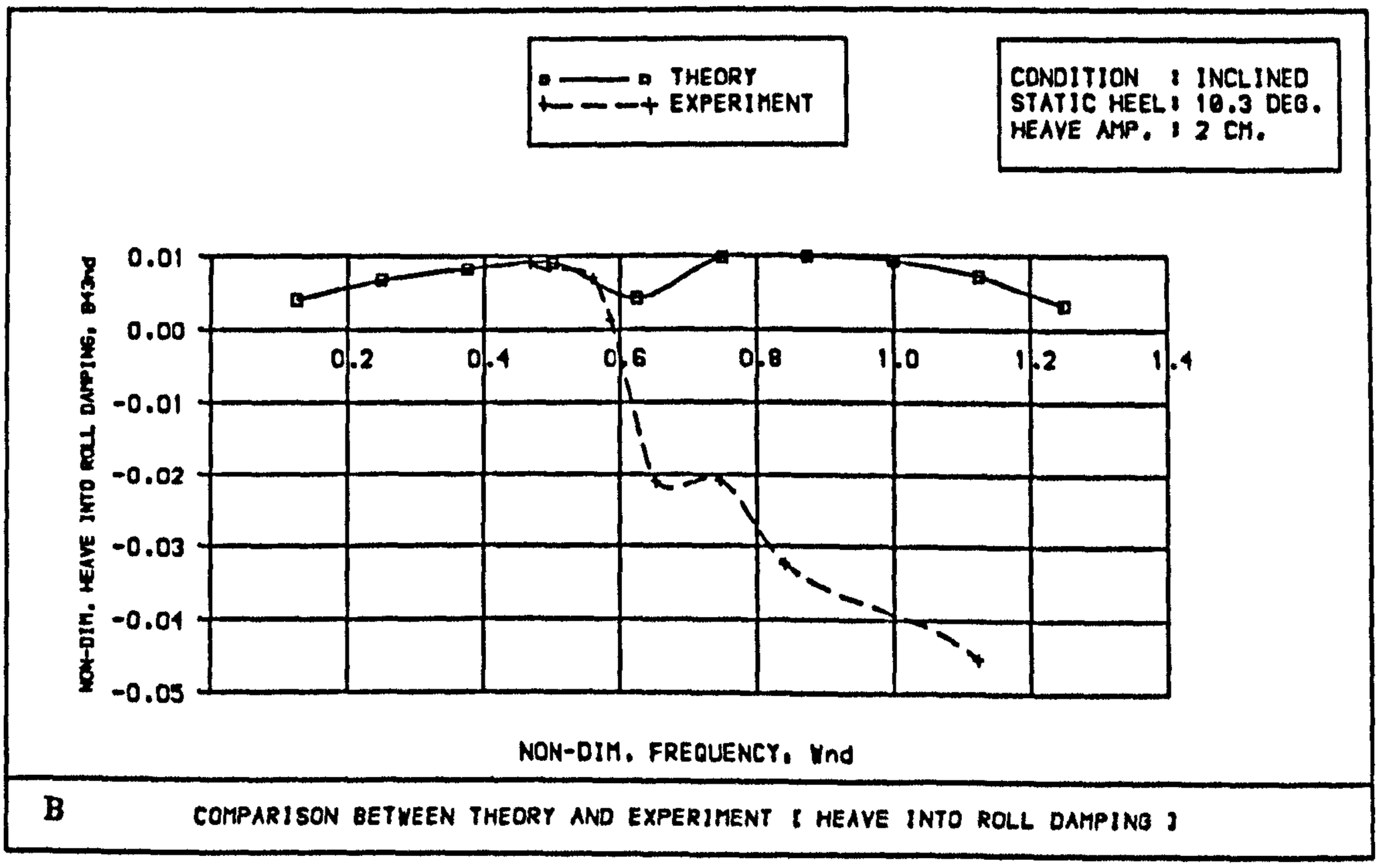

B COMPARISON BETWEEN THEORY AND EXPERIMENT [HEAVE INTO ROLL DAMPING]

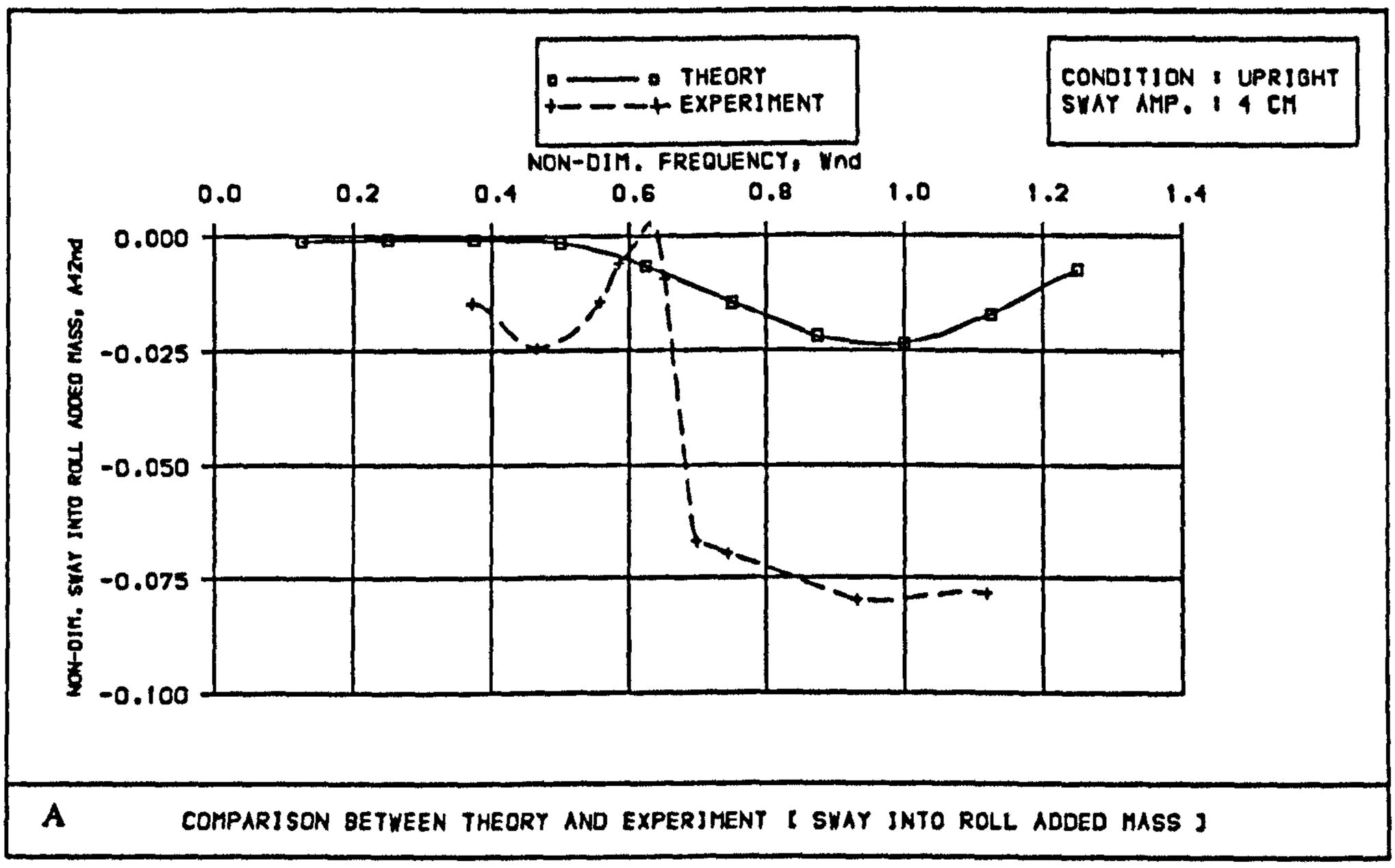

A COMPARISON BETWEEN THEORY AND EXPERIMENT [SWAY INTO ROLL ADDED MASS]

Fig 6.30 Comparison between experimentally and theoretically derived coupling coefficients, induced by SWAY into ROLL with ship at the UPRIGIIT condition

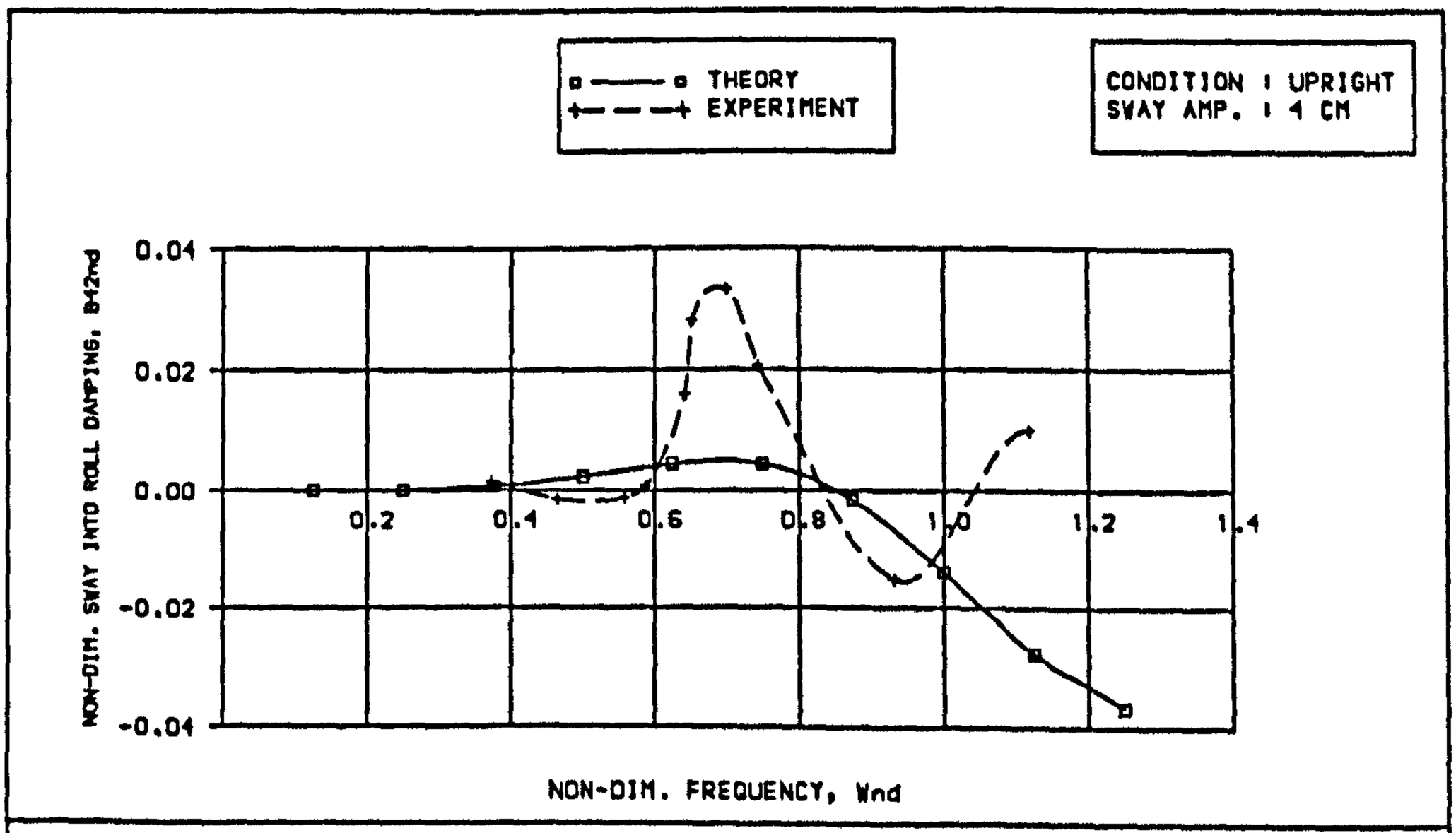

B COMPARISON BETWEEN THEORY AND EXPERIMENT [SWAY INTO ROLL DAMPING]

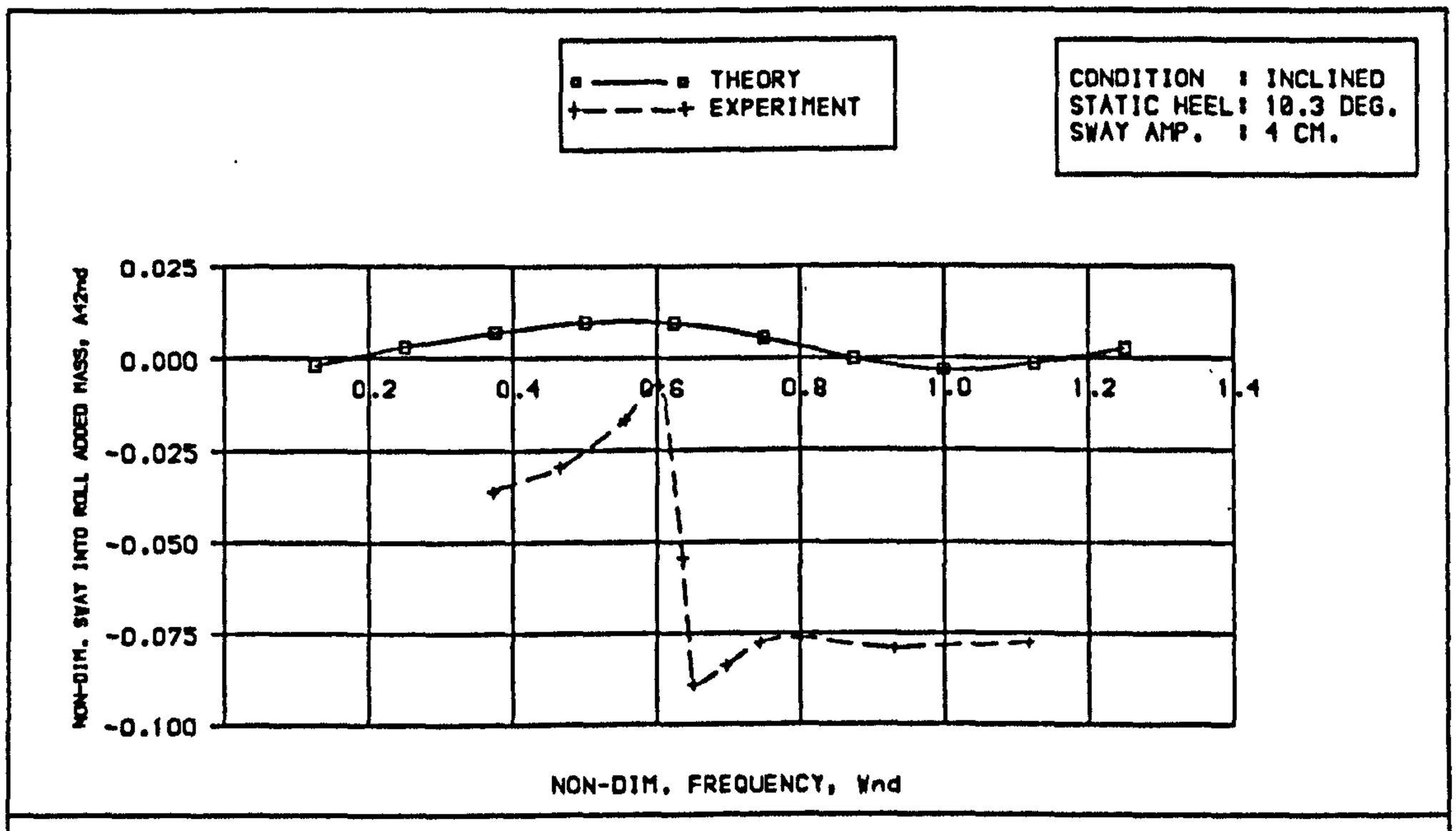

A COMPARISON BETWEEN THEORY AND EXPERIMENT [SWAY INTO ROLL ADDED MASS]

Fig 6.31 Comparison between experimentally and theoretically derived coupling coefficients, induced by SWAY into ROLL with ship at an INCLINED condition

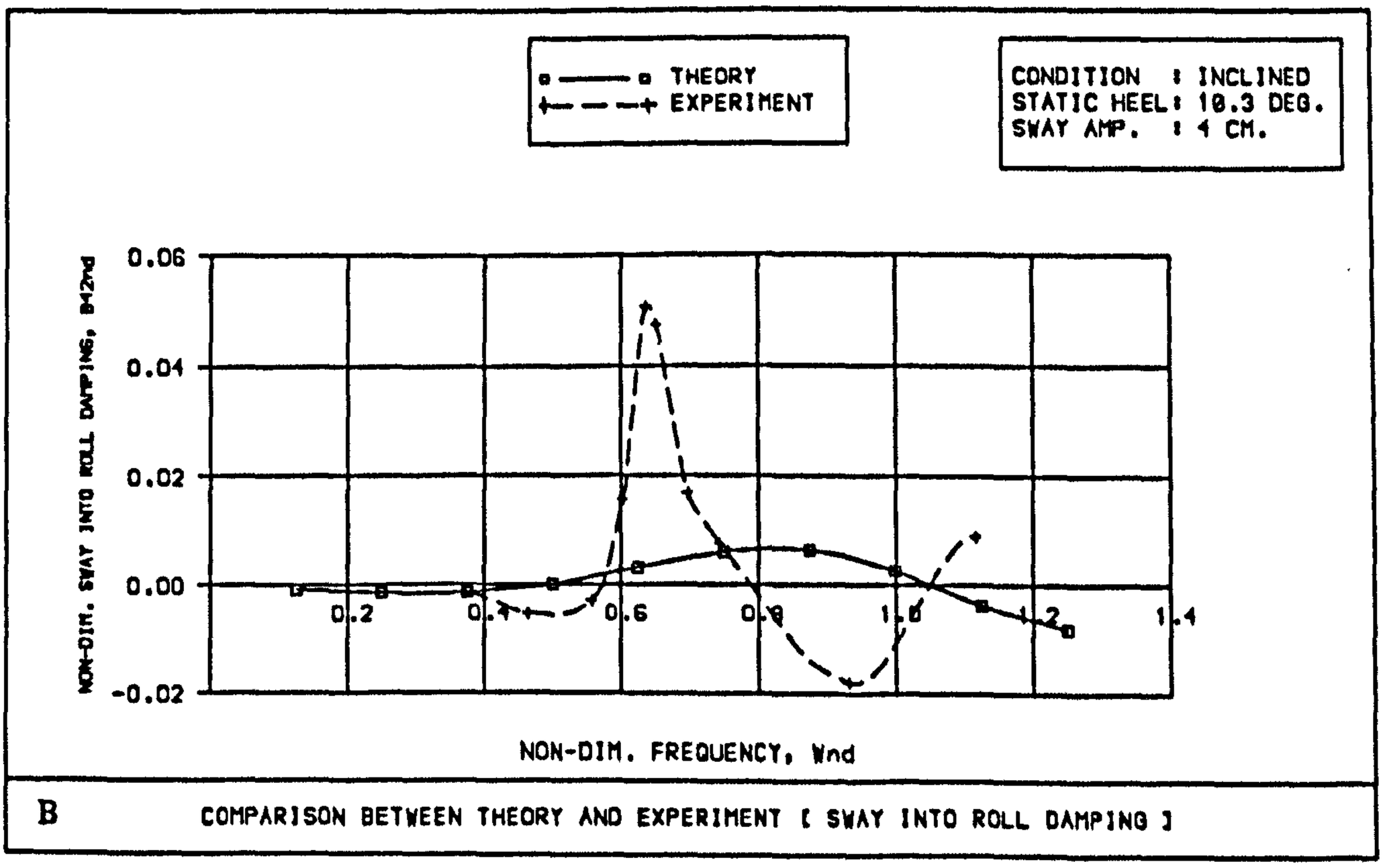

B COMPARISON BETWEEN THEORY AND EXPERIMENT [SWAY INTO ROLL DAMPING]

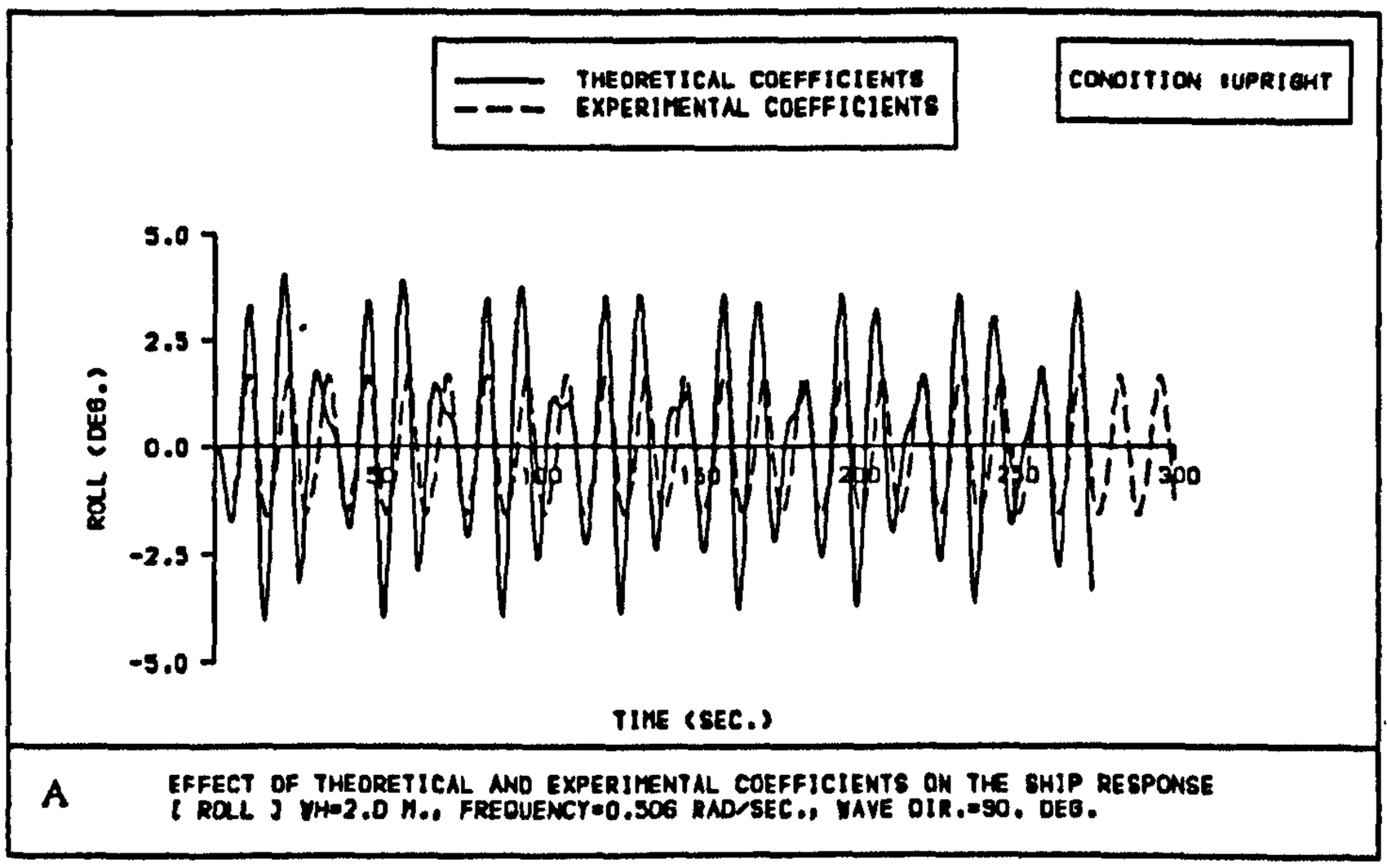

A EFFECT OF THEORETICAL AND EXPERIMENTAL COEFFICIENTS ON THE SHIP RESPONSE
[ROLL] WH=2.0 M., FREQUENCY=0.506 RAD/SEC., WAVE DIR.=90. DEG.

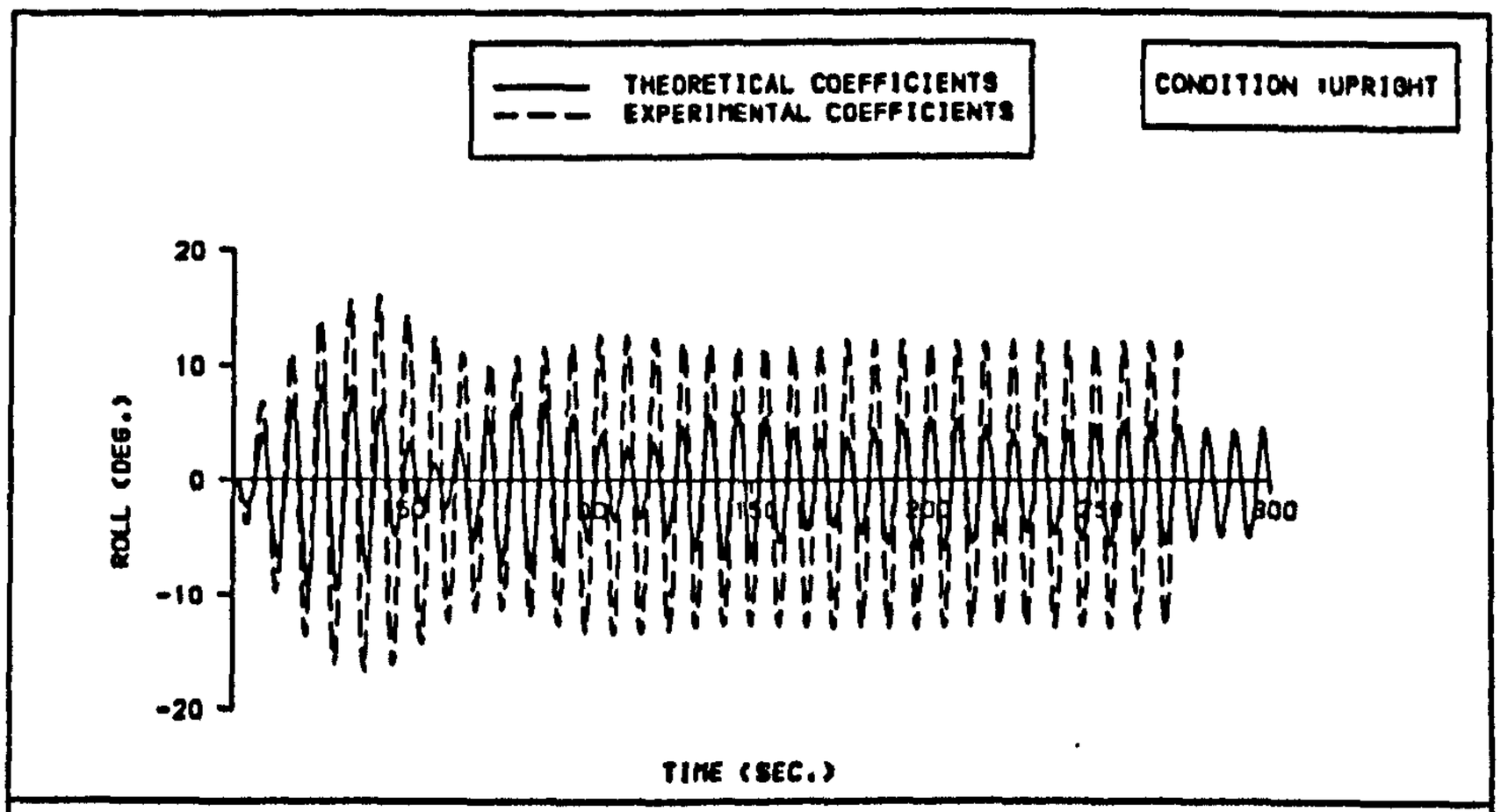

B EFFECT OF THEORETICAL AND EXPERIMENTAL COEFFICIENTS ON THE SHIP RESPONSE
[ROLL] WH=2.0 M., FREQUENCY=0.785 RAD/SEC., WAVE DIR.=90. DEG.

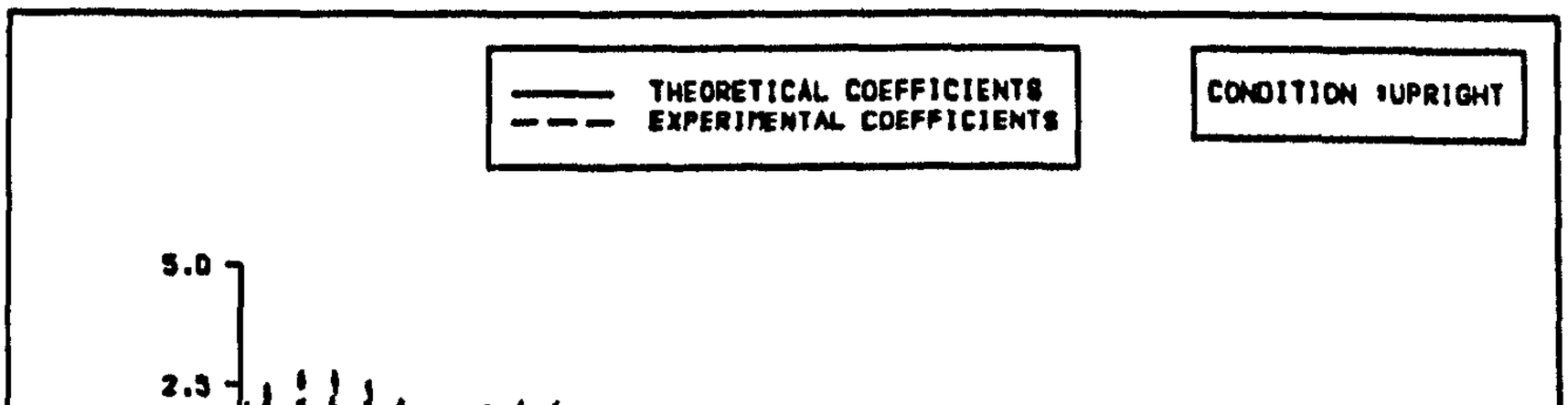

C EFFECT OF THEORETICAL AND EXPERIMENTAL COEFFICIENTS ON THE SHIP RESPONSE
[ROLL] WH=2.0 M., FREQUENCY=1.430 RAD/SEC., WAVE DIR.=90. DEG.

Fig 6.32 Comparison between the effect of experimentally and theoretically derived coefficients on ROLL motion [UPRIGHT CONDITION]

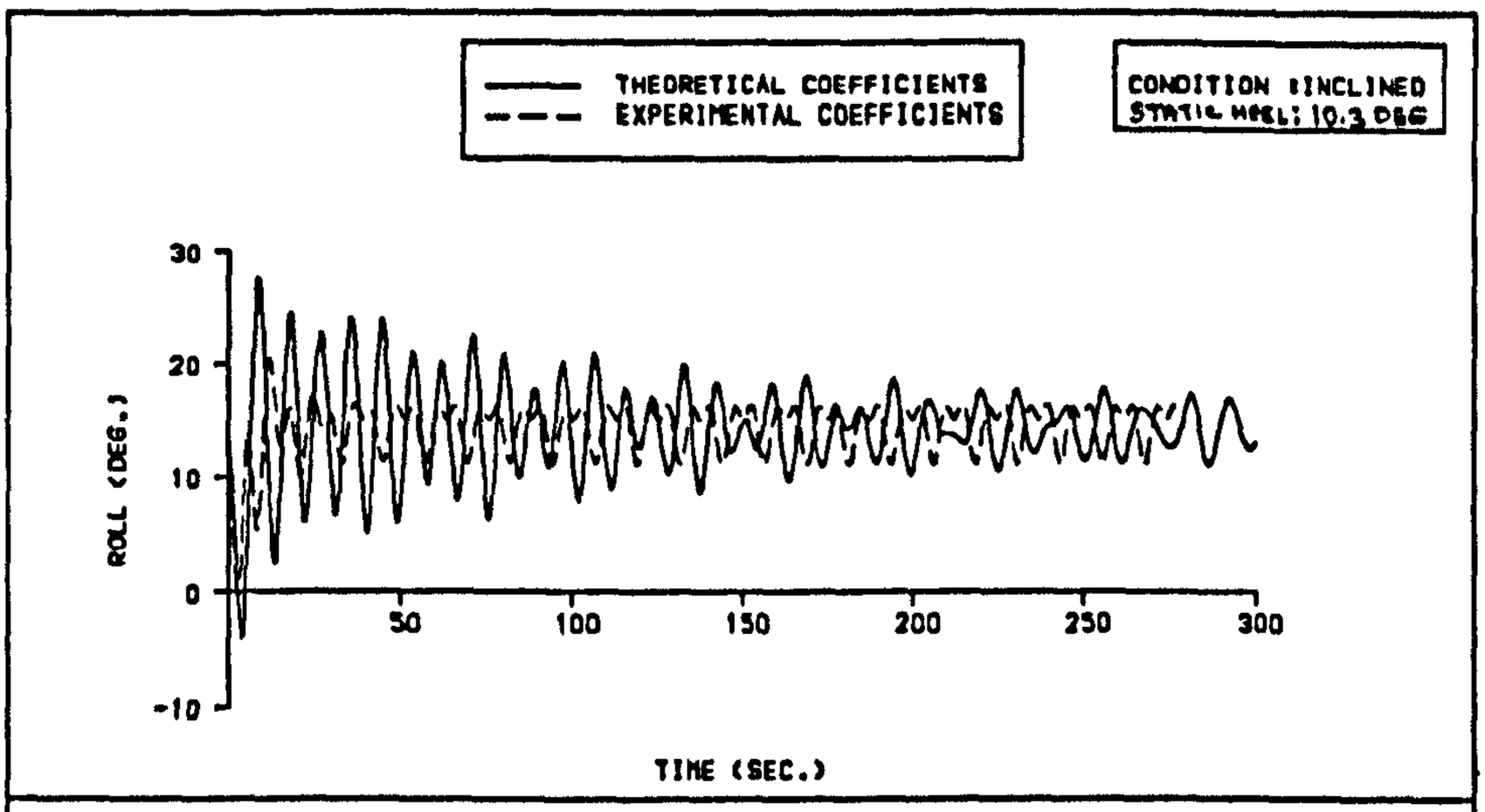

A EFFECT OF THEORETICAL AND EXPERIMENTAL COEFFICIENTS ON THE SHIP RESPONSE
[ROLL] WH=2.0 M., FREQUENCY=0.506 RAD/SEC., WAVE DIR.=90. DEG.

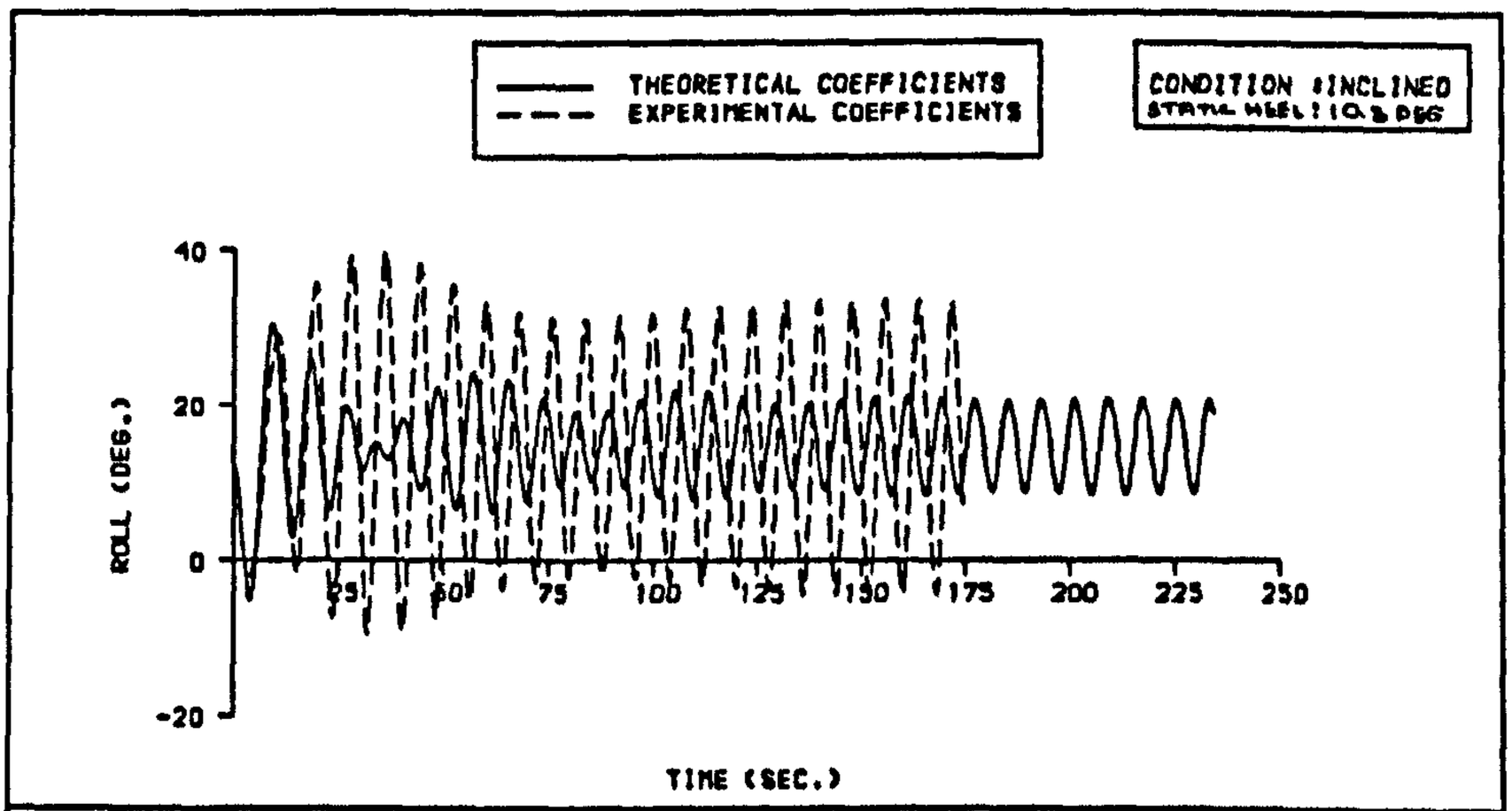

B EFFECT OF THEORETICAL AND EXPERIMENTAL COEFFICIENTS ON THE SHIP RESPONSE
[ROLL] WH=2.0 M., FREQUENCY=0.785 RAD/SEC., WAVE DIR.=90. DEG.

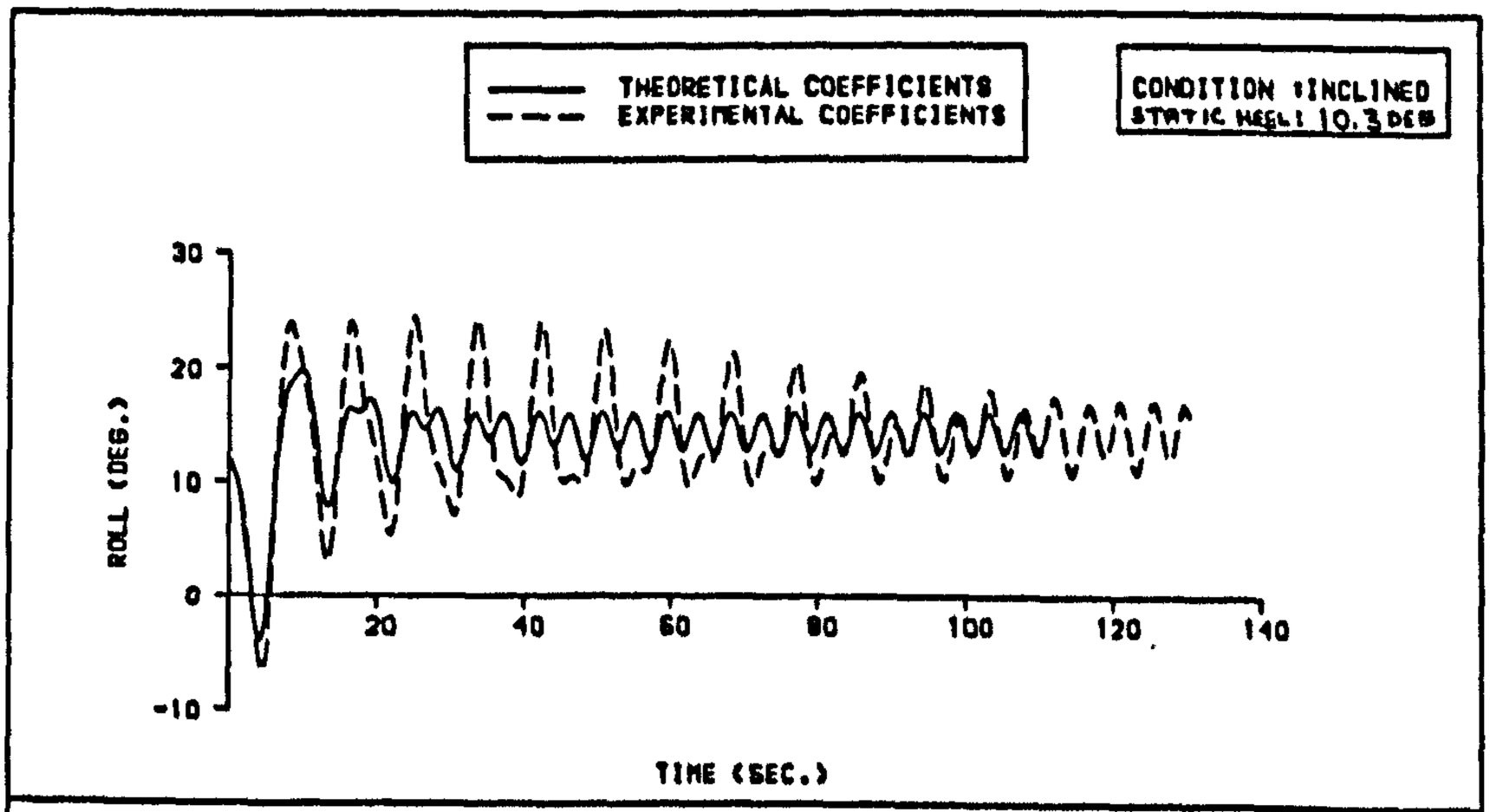

C EFFECT OF THEORETICAL AND EXPERIMENTAL COEFFICIENTS ON THE SHIP RESPONSE
[ROLL] WH=2.0 M., FREQUENCY=1.439 RAD/SEC., WAVE DIR.=90. DEG.

Fig 6.33 Comparison between the effect of experimentally and theoretically derived coefficients on ROLL [INCLINED CONDITION]

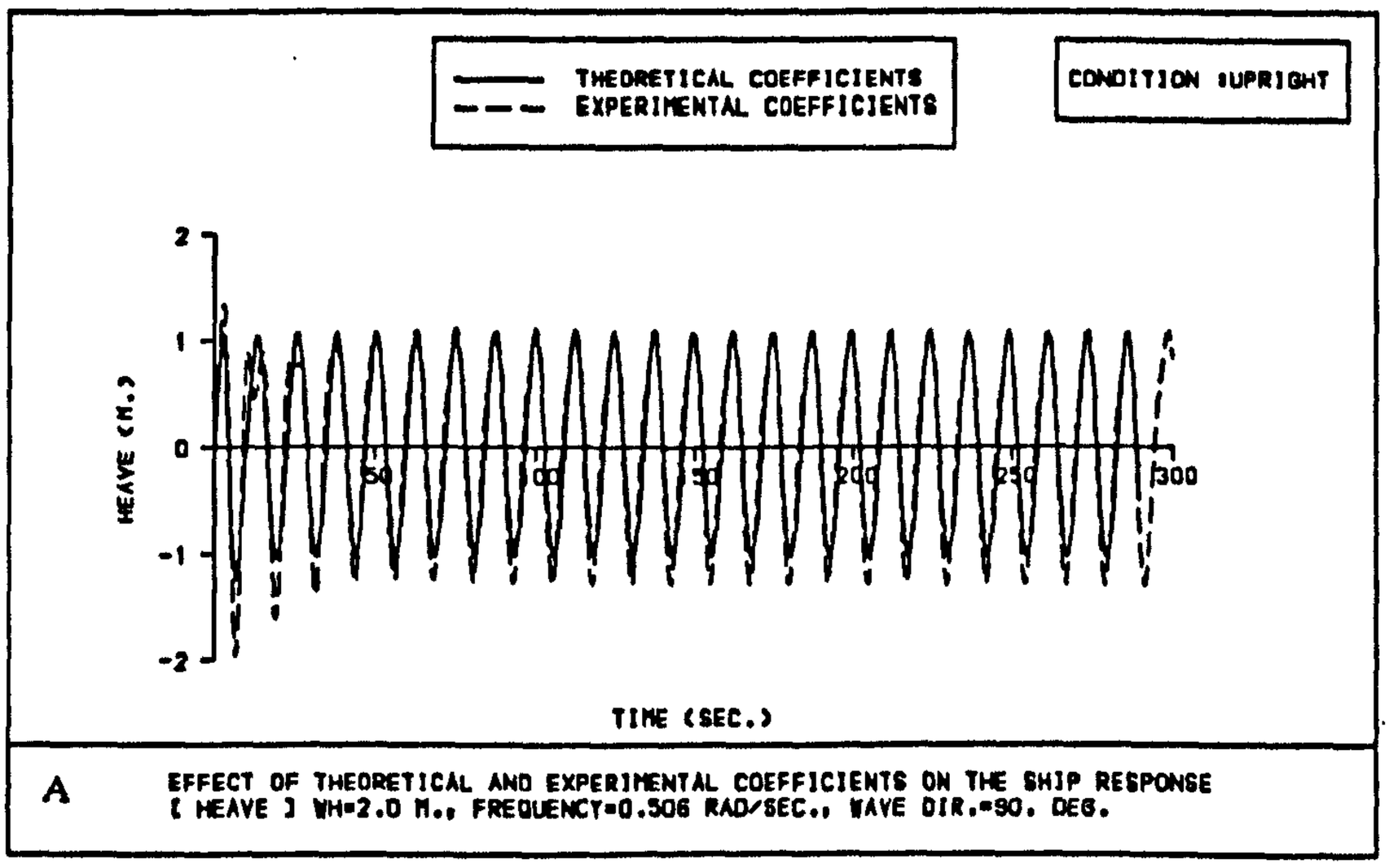

A EFFECT OF THEORETICAL AND EXPERIMENTAL COEFFICIENTS ON THE SHIP RESPONSE
[HEAVE] WH=2.0 M., FREQUENCY=0.506 RAD/SEC., WAVE DIR.=90. DEG.

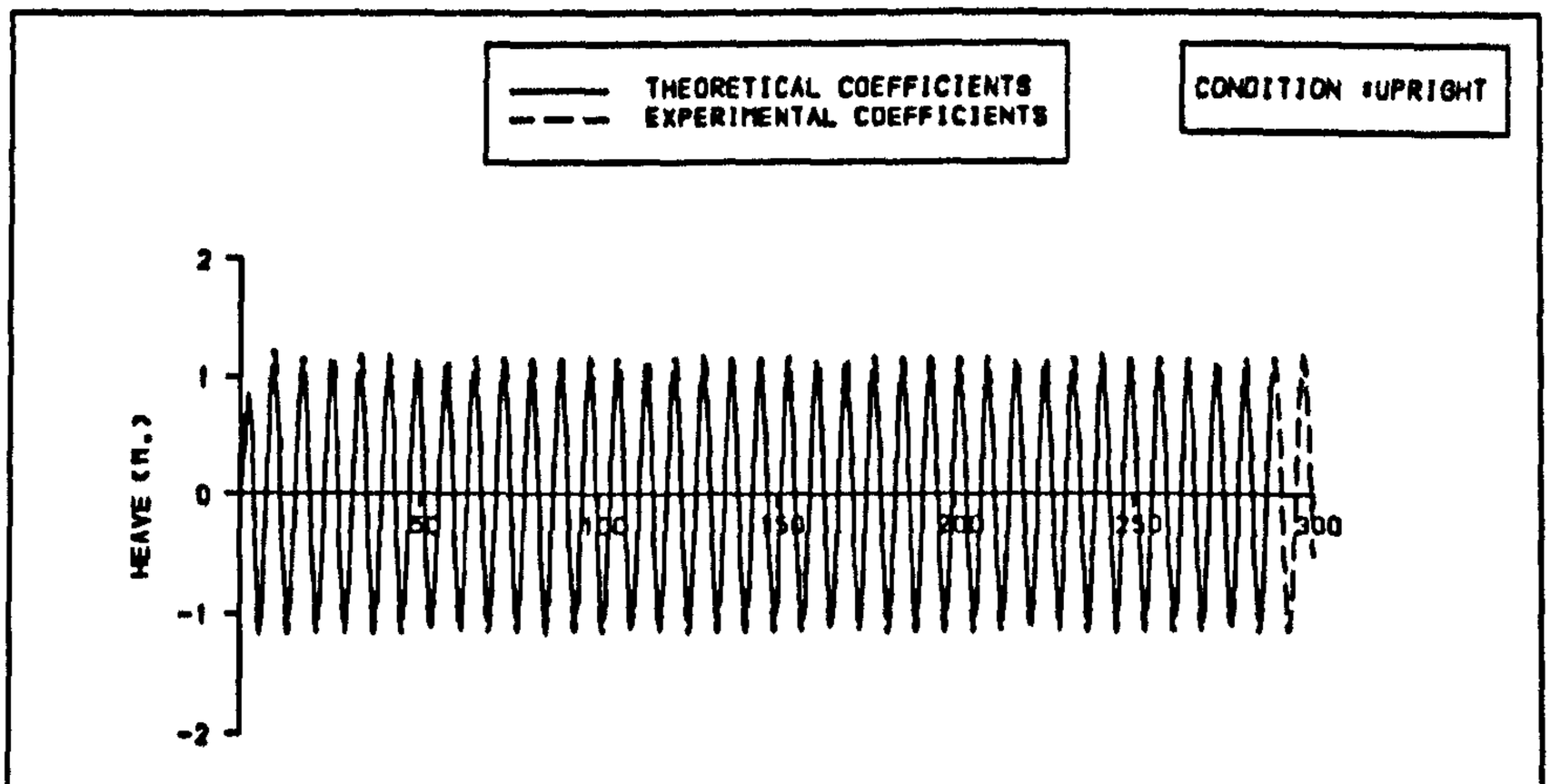

B EFFECT OF THEORETICAL AND EXPERIMENTAL COEFFICIENTS ON THE SHIP RESPONSE
[HEAVE] WH=2.0 M., FREQUENCY=0.785 RAD/SEC., WAVE DIR.=90. DEG.

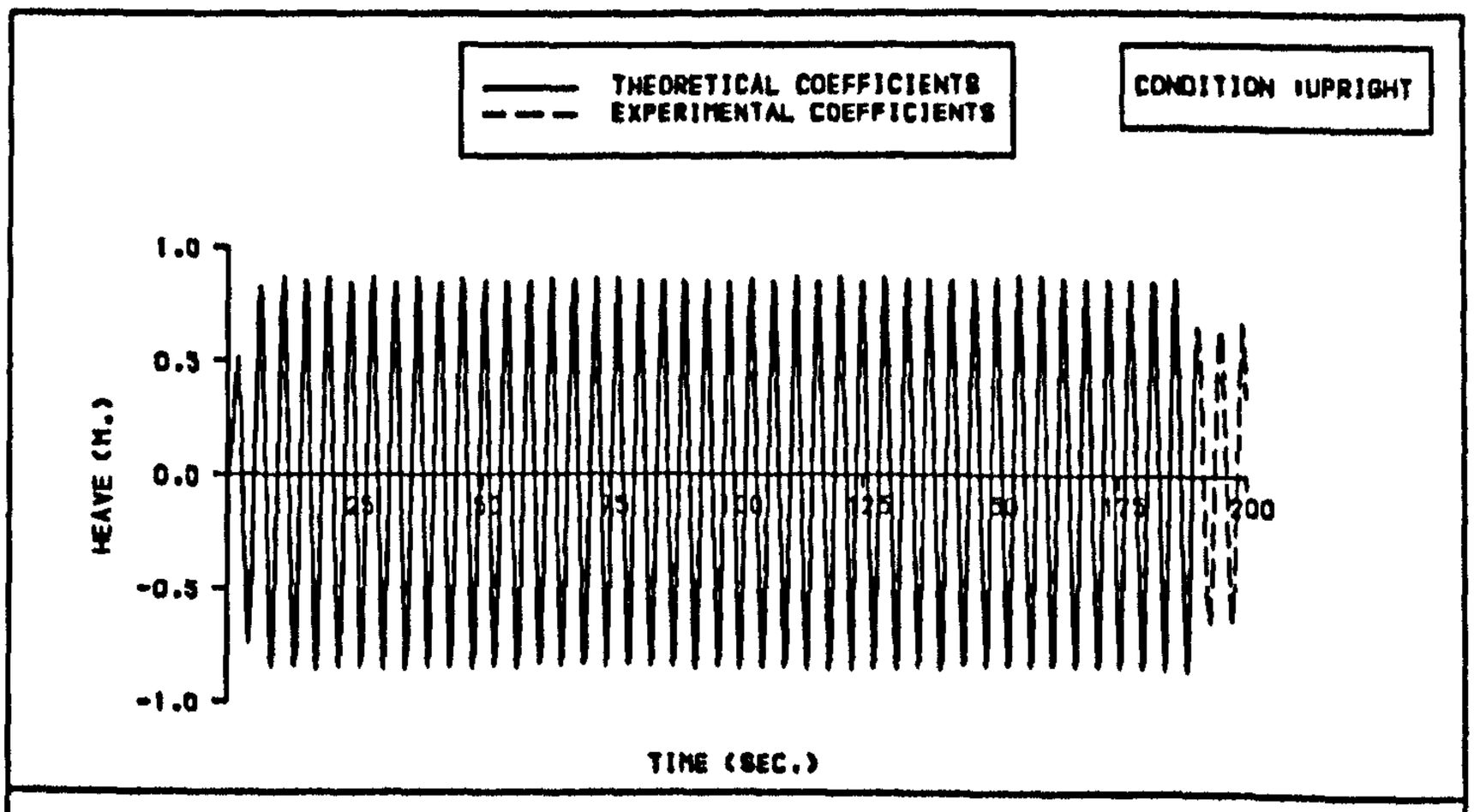

C EFFECT OF THEORETICAL AND EXPERIMENTAL COEFFICIENTS ON THE SHIP RESPONSE
[HEAVE] WH=2.0 M., FREQUENCY=1.430 RAD/SEC., WAVE DIR.=90. DEG.

Fig 6.34 Comparison between the effect of experimentally and theoretically derived coefficients on HEAVE [UPRIGHT CONDITION]

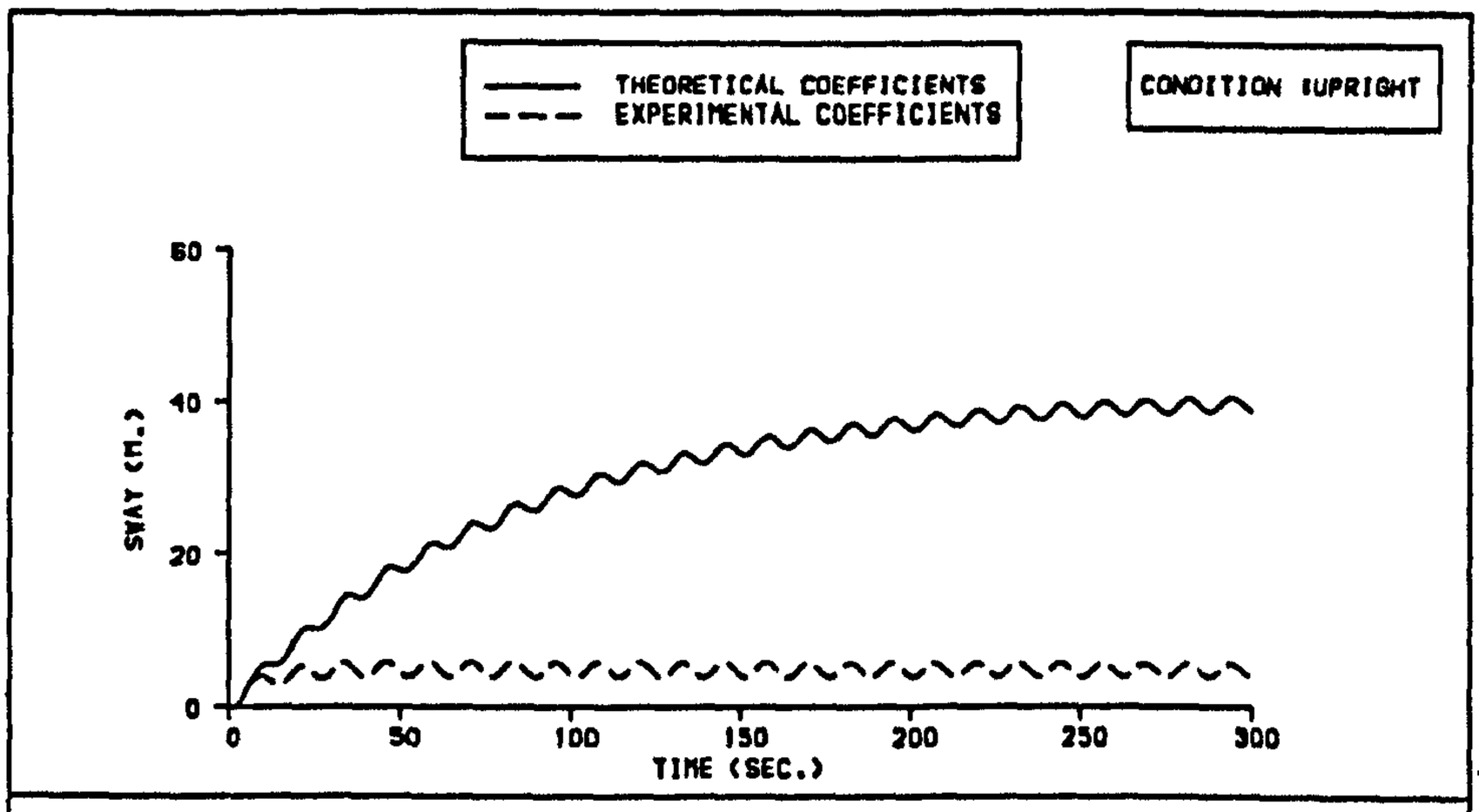

A EFFECT OF THEORETICAL AND EXPERIMENTAL COEFFICIENTS ON THE SHIP RESPONSE
(SWAY) WH=2.0 M., FREQUENCY=0.506 RAD/SEC., WAVE DIR.=90. DEG.

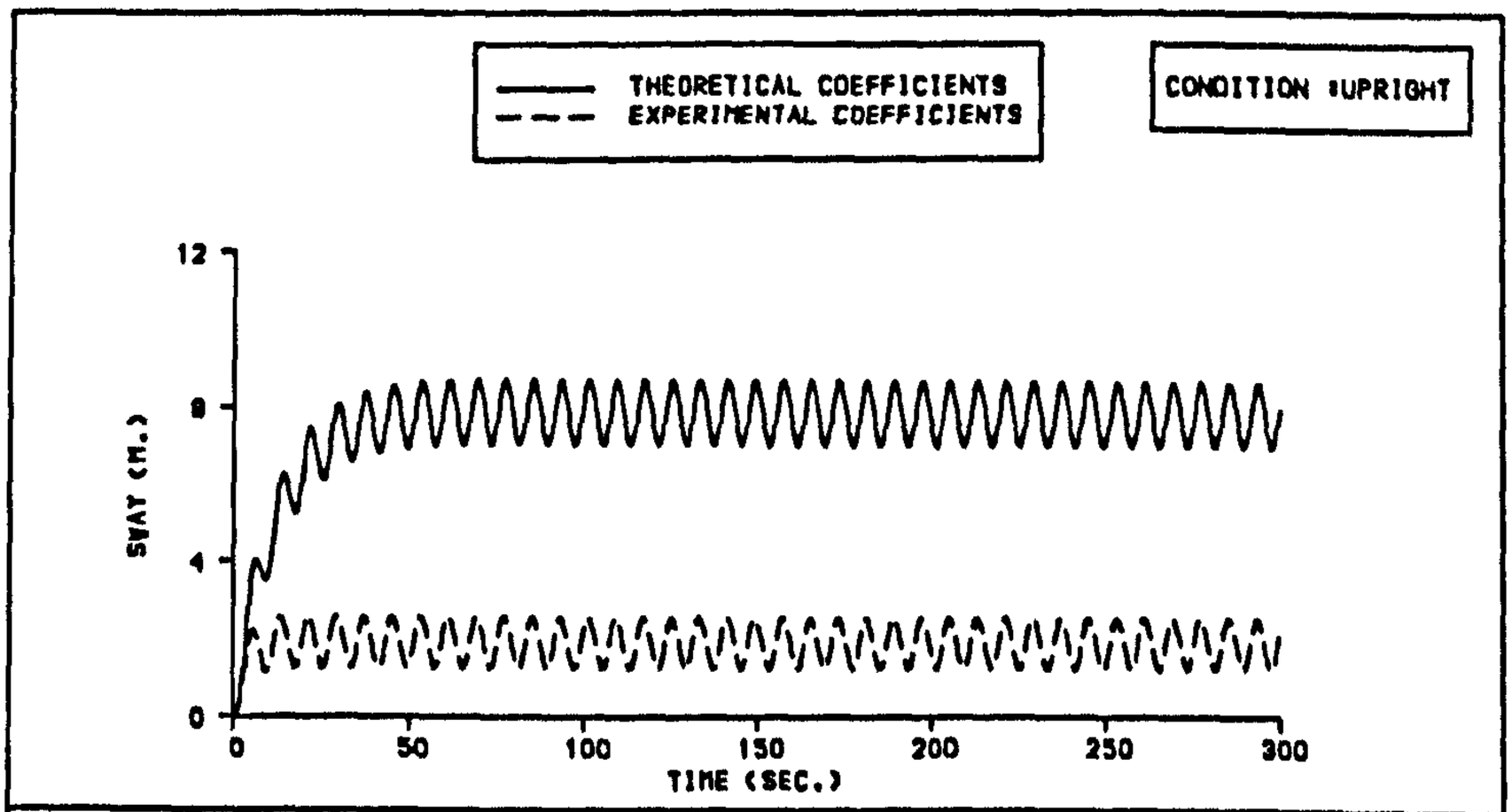

B EFFECT OF THEORETICAL AND EXPERIMENTAL COEFFICIENTS ON THE SHIP RESPONSE
(SWAY) WH=2.0 M., FREQUENCY=0.785 RAD/SEC., WAVE DIR.=90. DEG.

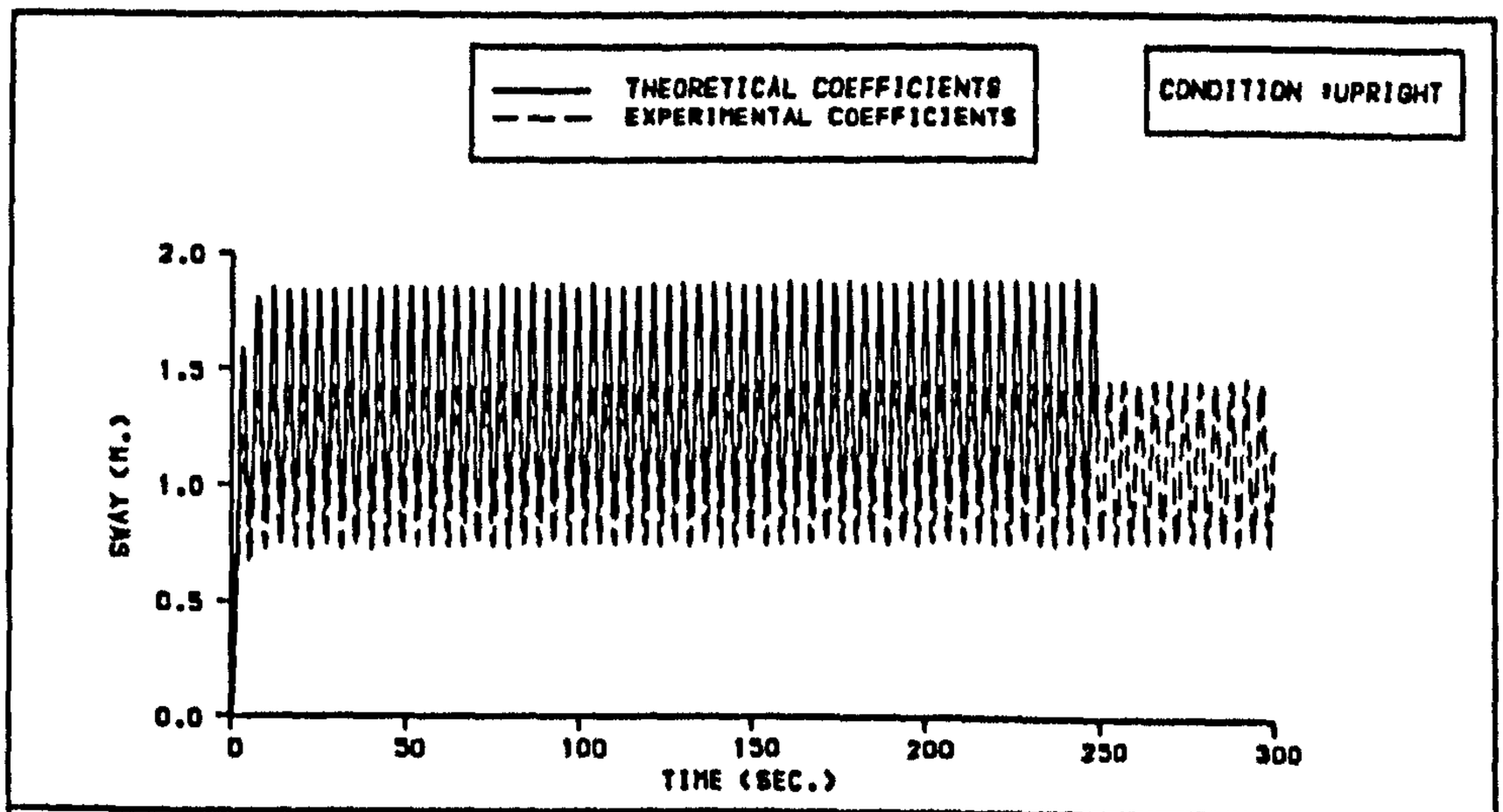

C EFFECT OF THEORETICAL AND EXPERIMENTAL COEFFICIENTS ON THE SHIP RESPONSE
(SWAY) WH=2.0 M., FREQUENCY=1.438 RAD/SEC., WAVE DIR.=90. DEG.

Fig 6.35 Comparison between the effect of experimentally and theoretically derived coefficients on SWAY motion [UPRIGHT CONDITION]

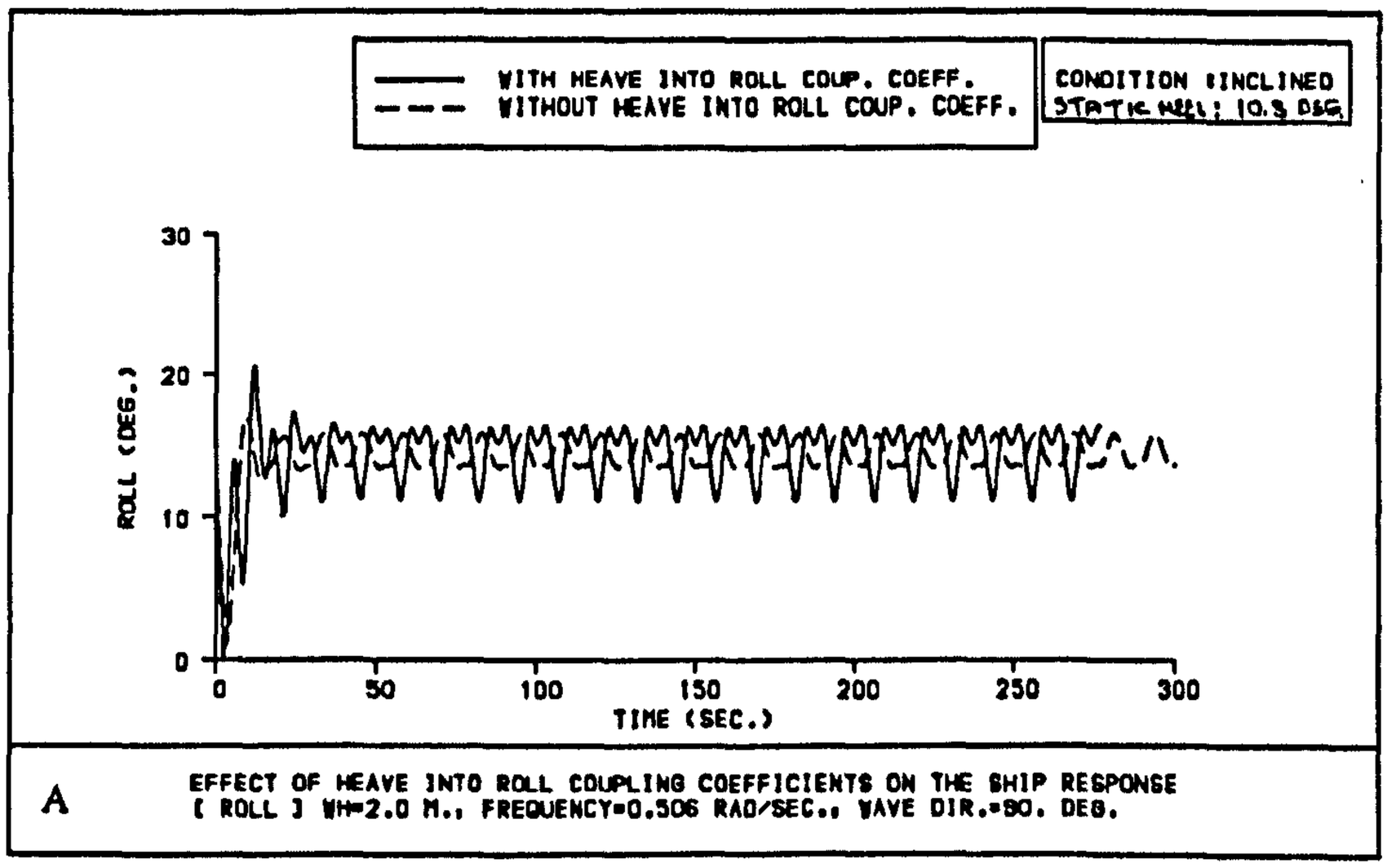

A EFFECT OF HEAVE INTO ROLL COUPLING COEFFICIENTS ON THE SHIP RESPONSE
[ROLL] WH=2.0 M., FREQUENCY=0.506 RAD/SEC., WAVE DIR.=90. DEG.

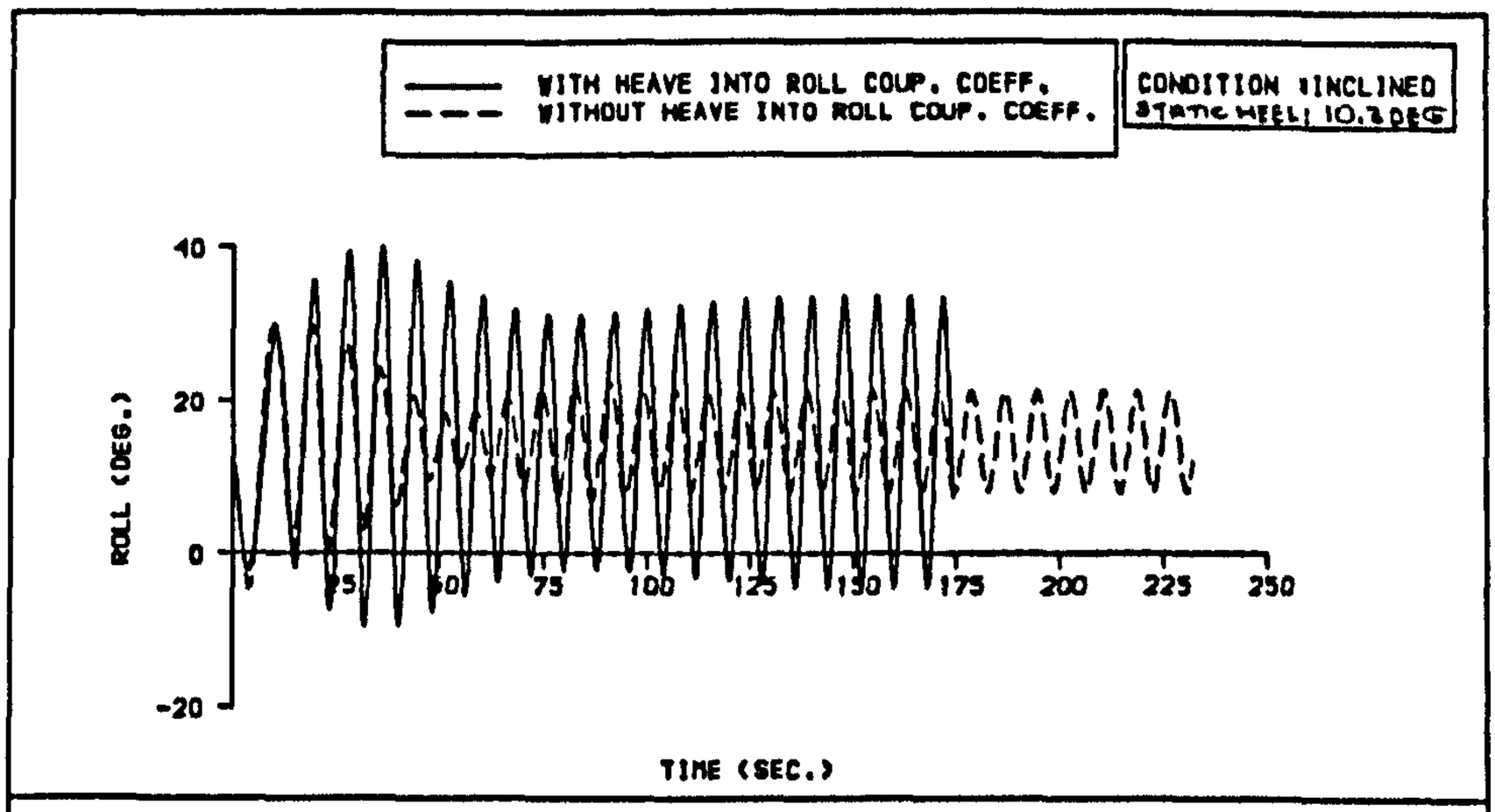

B EFFECT OF HEAVE INTO ROLL COUPLING COEFFICIENTS ON THE SHIP RESPONSE
[ROLL] WH=2.0 M., FREQUENCY=0.785 RAD/SEC., WAVE DIR.=90. DEG.

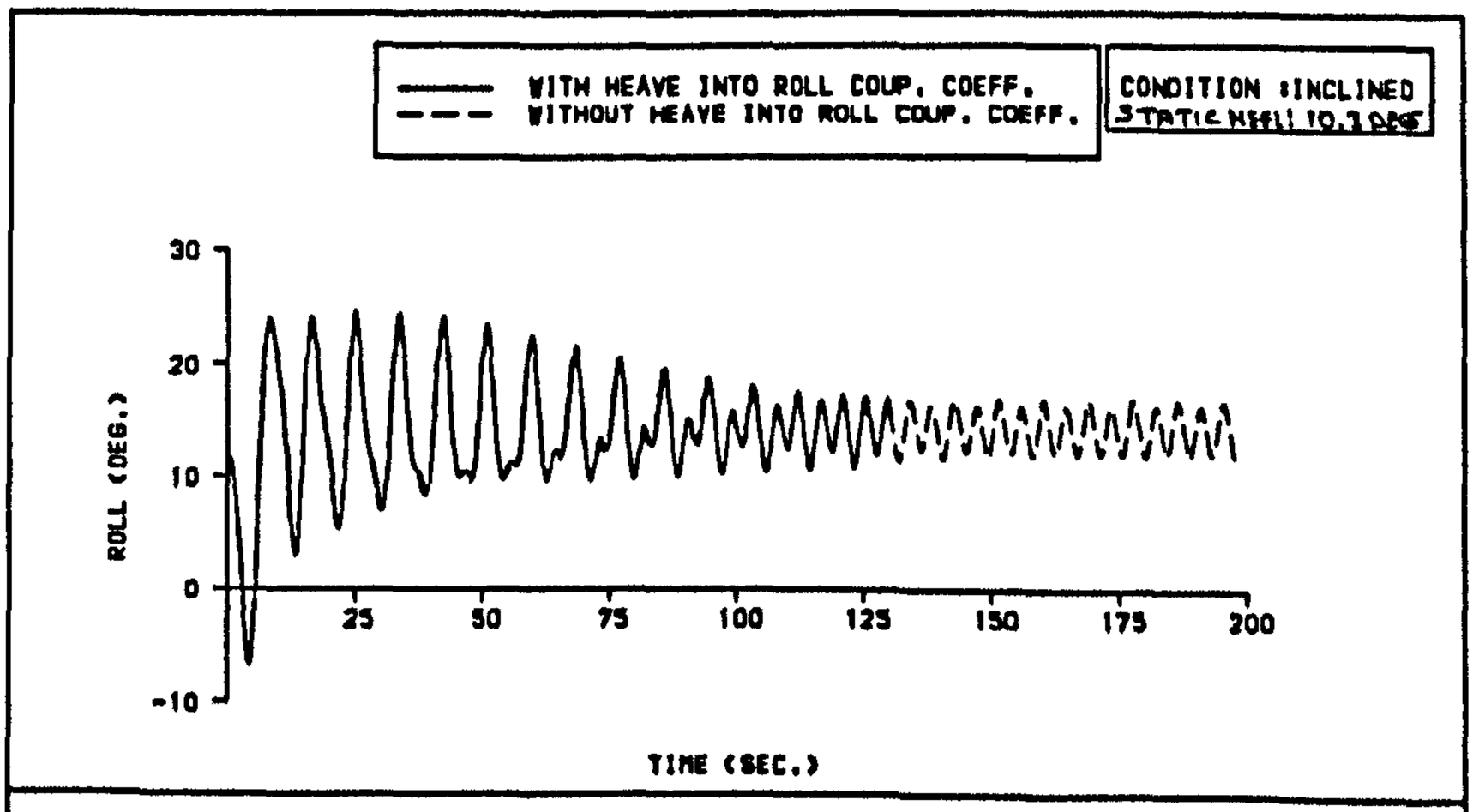

C EFFECT OF HEAVE INTO ROLL COUPLING COEFFICIENTS ON THE SHIP RESPONSE
[ROLL] WH=2.0 M., FREQUENCY=1.430 RAD/SEC., WAVE DIR.=90. DEG.

Fig 6.36 Effect of experimentally derived heave into roll coupling coefficients on ROLL motion with ship at an INCLINED condition

CHAPTER 7: PARAMETRIC INVESTIGATION

7.1 INTRODUCTION

A parametric investigation is generally regarded as an important approach in attempting to find general trends and the effects of changes of parameters on the quantity/quality being investigated, in this instance, damage stability. The need for this kind of study is clearly seen, if one reviews the amount of work which has been carried out in the past on damaged ships. For the study presently undertaken, available knowledge on both intact and damaged ships will be of value in guiding the investigation.

Until 1990 no mandatory limit had been set on any of the parameters known to affect damage stability of passenger ships except those related to the immersion of the margin line and the residual GM. Universally acceptable trends and limiting values as governing parameters would necessitate the use of a large number of passenger vessels. The resources, however, for doing so will be prohibitive. A feasible, yet well worthy, approach would be to consider a sample of selected ferries, representative of the vessels in operation.

This sample should then be provided to the scrutiny afforded by static and quasi-dynamic analyses. There are good reasons for proceeding in this way:

a) The majority of existing knowledge is based on static/quasi-static criteria.

b) A lot of information can be derived from straightforward calculating.

c) It would be necessary to prove the worth of any new criteria by comparing it to existing criteria.

The parametric investigation therefore, focuses initially on static and

quasi-dynamic approaches, before launching our investigation on the dynamic behaviour of the vessel and the parameters governing such behaviour.

For the static and quasi-dynamic stability analysis, ten passenger/car ferries are investigated in different conditions, namely intact, symmetric and asymmetric damage. The critical damage location for each ship is chosen according to IMO rules. Asymmetric damage is modelled by using B/5 depth for the side tanks. Design draught and KG are used for the calculations. For the quasi-dynamic damage stability calculations, different wave heights are chosen by considering North Sea wave statistics.

Following an examination of the static and quasi-dynamic stability analysis and of the design characteristics, SHIP 2 is chosen for the dynamic stability analysis. Her compartmentation and damage stability calculations are based on the probabilistic approach, therefore she has side tanks and a long inner compartment. A number of realisable damage scenarios are chosen for dynamic stability analysis by considering previous accident reports, as well as possible potential damages.

In addition, different wave heights, wave lengths, KGs and flow rates for water ingress are considered. The behaviour of the damaged ship under these conditions is investigated and findings are used to develop a methodology for proposing more soundly based damage stability criteria.

The three levels of analysis pertaining to static, quasi-static and dynamic stability are considered, in turn, in the following.

7.2 STATIC STABILITY

Static stability criteria which are currently in force are based on still water and involve no explicit use of external forces or motion characteristics.

Static stability criteria are developed on the basis of righting lever

curves because of their relation to hull form geometry. In general, there are three parameters which are considered to define the main requirements of the criteria. These are the minimum metacentric height (GM), minimum righting lever (GZ) within a given angle of heel, and minimum area under the righting curve within the given range of heel. As explained in Chapter 2 the last two parameters were introduced for assessing the stability of damaged passenger vessels in 1990 as mandatory regulations. The minimum range of positive righting lever beyond the equilibrium position is also another consideration. Although some rules along the same lines were introduced in 1980, the implication of these rules were left to individual governments rather than making them mandatory.

It is of course implied that any static stability requirements must satisfy the rule of 'no immersion of margin line in the case of damage'.

More specifically the minimum requirements of damage stability regulations are:

GM > 0.05 m
GZ > 0.1 m
Area > 0.015 rad m
ϕ_{min} for positive GZ range > 15 deg

However, in order to maintain consistency for the comparison between intact and damage conditions, the comparison refers to the area under the GZ curve up to 30 degrees of heel, which is the requirement of intact condition as well as the average downflooding angle for all the ships.

The static stability of ten different passenger/car ferries was investigated for intact, symmetric and asymmetric damage cases. The main parameters and damage locations(shaded areas) of these ships are given in [Appendix C]. Although in reality the ships do not have side tanks, for this parametric investigation side tanks were assumed in accordance with IMO. IMO rules specify that the tank depth must be B/5 and the double bottom depth B/10. This design alteration

provides information on the effect of asymmetric damage.

For the parametric study, the following assumptions are made:

- One loading condition at design KG
- Permeability is taken at 1.0
- For the asymmetric damage, the cross-flooding arrangement is assumed to be disabled.
- All damages are assumed to occur under the bulkhead deck.
- All damages are modelled as two compartment damages.
- The Lost Buoyancy Method is used in the calculation.
- The structure above the bulkhead deck is assumed to be intact

7.2.1 Results of Static Stability Analysis

Analysis of static stability can be undertaken by studying the effects of different ship parameters as indicated next.

i- Sinkage and Heel

Obviously symmetric damage causes more sinkage than asymmetric damage due to the flooding of a larger area. Initially it may seem that symmetric damage is worse when considering sinkage, but if the static heel due to asymmetric damage is considered, it may cause even greater problems. If static heel for different ships is examined (Fig 7.1a), it can be seen that the average is approximately 10 degrees, which actually may be enough to cause flooding of the vehicle deck if the side skin of the ship above the bulkhead deck is assumed to be damaged. Fig 7.1b shows the sinkage at the side of the vehicle deck. The combination of sinkage and heeling may cause even bigger problems. Therefore when there is damage at the bulkhead deck, it would be more logical to consider the level of vehicle deck in calculating the downflooding angle, rather than taking the uppermost continuous deck. Although new amendments require calculations of righting levers and area under the righting levers curve to be calculated up to the angle of inclination at which progressive flooding occurs, so far flooding of the vehicle deck has not been taken into account in the damaged stability calculations.

ii- Trim

The trim, another parameter which may affect stability, was also considered in the static stability calculations. Even though trim is not expected to affect the stability of the ship itself considerably, this parameter may cause the margin line to be immersed. Fig 7.1c shows that sinkage due to trim aft does not cause the bulkhead deck to immerse but residual freeboard is very small for some ships. The combination of trim and static heel may cause the vehicle deck to be flooded within a very short time.

iii- Metacentric Height (GM)

When the effect of damage on GM for each ship is examined, it can be seen that asymmetric damage results in higher GM values than intact and symmetric damage conditions (Fig 7.2). This means that the initial stability of the ship is improved due to the sudden increase of the waterplane area in the inclined position. However, high GM does not mean that the ship has better stability in real terms and this will be shown in the following section. In the case of symmetric damage, the GM is generally reduced. However in a few cases GM is increased with the increase taking place due to the change in the underwater hull form. Although the waterplane area decreases, KB increases and hence GM.

iv- Righting Lever (GZ)

The GZ values for all the cases satisfy the recent damage stability criteria which require a minimum of 0.1m GZ within the 15 degrees of positive GZ range, beyond the equilibrium position. It has to be remembered that the superstructure above the bulkhead is assumed to be intact and contributes to the buoyancy. When the entire GZ curves for each ship at intact and damaged conditions are examined, it is revealed that the maximum GZ value in both symmetric and asymmetric conditions is larger than the value at the intact condition (Fig 7.3). Fig 7.3 shows that in spite of what might be expected from the GM values the maximum GZ values in symmetric damage are in general larger than those in asymmetric damage.

However, if the heeling is limited by the immersion of the bulkhead

deck (margin line), most of the ships would not be able to satisfy the requirements, especially in the case of asymmetric damage, at which the bulkhead deck of most ships would be immersed. This is also another indication that GM should not be used as the only measure in judging damage stability.

v- Area Under the GZ Curve

An examination of the areas under the GZ curve reveals that although there is no considerable difference in the areas up to the downflooding angle between intact and symmetric damage cases, a bigger reduction is noticed in the case of asymmetric damage, implying a worsening of stability (Fig 7.4). This is due to the fact that because of the asymmetric damage, the positive range of the GZ curve is much smaller and hence the area under the curve. This, in turn, means that asymmetric damage is the worst which is completely the opposite to what is expected if GM is used as a yardstick. The worse case would be when the area under the GZ curve is calculated up to the angle at which the bulkhead deck immerses and progressive flooding occurs. In this case the positive range of stability or the area under the GZ curve would be an irrelevant requirement since the side of the bulkhead deck would already be under water, causing progressive flooding (Fig 7.1b).

The results of static stability calculations suggest that GM cannot be the main requirement. The minimum GM of 0.05 m is very unrealistic, thus causing problems in satisfying the requirement for minimum GZ. On the other hand, regulations do not include the flooding of vehicle deck and all other damage stability requirements mentioned above would be meaningless if flooding of the bulkhead deck is taken into account as it would limit the maximum permissible heel angle considerably and cause problems with regard to limiting the flooding on the vehicle deck. The existing requirements improve the standards of residual stability in case of damage below the bulkhead deck but fail again completely if there is a damage above the bulkhead deck.

7.3 QUASI-DYNAMIC STABILITY

One of the energy balance methods which is used in this study is developed by Strathclyde University within the SAFESHIP project [76] and it can be seen as a natural development of the Weather Criterion. This criterion is appropriate to the capsize mode known as "pure loss of stability" and the assessment procedure explicitly allows for the effect of wind, wave and roll motion in a quasi-dynamic manner. This criterion derives from the "butterfly diagram" where the outcome of an energy balance between excitation and restoring effects over an extreme half roll cycle is used to discriminate between "safe" and "unsafe" vessels.

Time varying roll restoring/excitation $GZ(\phi,t)$ is calculated at each prescribed time step, $t_i(i=1,n)$ for a period of time which is selected on the basis of the roll period, ship speed, heading angle and wave system in such a way as to maximise the potential of the vessel capsizing. An example of the computational procedure of the butterfly diagram is given in Fig 7.5, whilst details of the method is given in [30, 76].

Extreme roll cycle limits are defined by ϕ_1,(windward angle) calculated according to the weather criterion and ϕ_2 taken as down flooding angle(ϕ_f). The Strathclyde criterion has been developed for intact ships and tested for regular and random following waves in the presence of beam wind. The computational procedure of this method was extended by the author to damaged ships.

The stability criterion is the energy balance itself during a critical roll cycle expressed as the difference between excitation/restoring effects -NET AREA (NA). Positive net area implies a "safe ship". Furthermore, some qualitative features of the butterfly diagram provide additional information on the stability characteristics of a ship. For example, the width of the hysteresis loop of the butterfly diagram gives an indication of how prone the hull form is to parametric excitation. Although this parameter is primarily linked to the geometrical features of the ship, unfavourable loading (KG) also affects the shape of the hysteresis loop.

In general, the wider the loop is the less stable and more prone to environmental effects the vessel is.

For the Energy Balance Criterion, the same KG values and damage conditions as in the static stability calculations are used. Wind speed is taken as 20.0 m/sec. The wave heights considered are 3 m, 5 m and 7 m and the wave length for each ship is taken to be equal to the ship length. For this study the waves are assumed to be coming from the stern and the ship has zero forward speed. The following section gives a brief account of the results for each ship while Table 7.1 compares the results of the static and quasi-dynamic calculations.

Ship1 : The ship possesses good stability characteristics and a good restoring curve at intact condition up to medium wave heights. However, it loses her stability at a 7 m wave height. In the case of symmetric and asymmetric damage however, stability is poor due to the reduction in down flooding angle, as a result of sinkage and static heel.

Ship 2 : Positive net area decreases and hysteresis loop width gradually increases as wave height increases. Symmetric damage follows the same trend. In the case of asymmetric damage the restoring area becomes very small and the hysteresis loop becomes very wide indicating that the ship loses her stability due to static heel (Fig 7.6).

Ship 3 : The ship possesses good stability characteristics in waves at intact and symmetric damage conditions, even at high waves. She also has a narrow hysteresis loop but fails to satisfy the Strathclyde criterion by a big margin in the case of asymmetric damage. This sudden failure is due to the static heel, which reduces the range of positive heeling (between equilibrium position and downflooding angle) whilst increasing the range of heeling at negative side (between equilibrium position and windward roll angle).

Ship 4 : This ship has very good stability characteristics at intact as

well as at the symmetric damage conditions. Her restoring hysteresis loop at intact conditions is narrow and the loop increases only slightly at 7 m wave height (Fig 7.7), while at the symmetric damage the loop remains narrow and uneffected by the wave height. In the case of asymmetric damage she fails to satisfy the criterion only by a small margin despite the large static heel. This indicates that this vessel has better stability in comparison to other ships.

Ship 5 : This ship has a very small restoring area even at 3 m wave height, and as the wave height increases she loses her stability completely. As expected, stability in the case of asymmetric damage is very poor, however in the case of symmetric damage, her stability improves drastically despite the reduction in downflooding angle. This may be due to sinkage as a result of which the restoring ability of the ship increases.

Ship 6 : The ship has good stability characteristics with a narrow loop even in large waves. In the case of asymmetric damage her stability is better than in the intact case, despite the lower downflooding angle. However, stability becomes poor in the case of asymmetric damage and again the static heel is the main cause.

Ship 7 : This ship fails to fulfil the requirements in all conditions. This is due to the very small downflooding angle. This is indicative of the fact that this ship can only be used for short domestic crossings.

Ship 8: The ship has good stability characteristics although as the wave height increases her restoring ability decreases and the restoring hysteresis loop becomes wider. In symmetric damage, stability becomes even better and the hysteresis loop narrow in all the wave heights. This may be due to sinkage. In asymmetric damage the hysteresis loop becomes again very wide as the wave height increases, the restoring area smaller, and the ship loses her stability because of static heel (Table 7.1 and Fig 7.10).

Ship 9 : This is a stiff ship with good stability characteristics.

Therefore the hysteresis loop is very narrow in both the intact and symmetric damage conditions (Fig 7.8). The wave height does not affect it although the area under the curve becomes smaller. However, asymmetric damage changes the situation drastically and the net area becomes negative by a big margin while the loop progressively widens.

Ship 10: This ship has very good stability characteristics at intact condition and even better stability in the symmetric damage condition. The hysteresis loop is narrow even with the largest waves. This derives mainly from the very large downflooding angle, because the uppermost continuous deck is very high up (Fig C.10 in Appendix C). However in the case of asymmetric flooding, the net area becomes negative but retains a very narrow restoring loop characteristic.

Analyses of the results (Table 7.1 and Fig 7.9 and Fig 7.10) show that at the intact condition almost all ships can survive even in large waves. In general, as the wave height increases, the stability decreases and the hysteresis loop widens but this reduction is a gradual one (notable exceptions exist). In symmetric damage the ship characteristics do not change very much and stability is more or less similar to the intact case. However, in the case of asymmetric damage all ships fail, even at the most moderate seas, primarily because of the large static heel. The decrease in the downflooding angle also contributes to this. This general trend can be seen in Fig 7.9 and Fig 7.10 which show the variation of net area with wave height. Most of the ships survive at moderate seas and at intact or symmetric damage, but beyond 6 m wave height, the number of ships which become critical is increasing. In the case of asymmetric damage, all ships have negative net area.

Regarding the effect of the relative position of the wave with respect to the ship, at the intact condition, the most critical case occurs when the wave trough is approximately amidships where most of buoyancy is found. In the case of symmetric damage the most critical position is with the wave trough near the damaged location. This is due to the

fact that there is no buoyancy at this region and due to the shape of a ship, there is also little buoyancy available at both ends. In the case of asymmetric damage each ship has a negative net area, irrespective of the relative position of the wave.

An examination of the overall results reveals that, static heel and waves are the prime factors in affecting stability assessment on the basis of quasi-dynamic criteria. The downflooding angle also is an important parameter since it affects the net area. If the trim is substantial, it may cause some problems since it can cause either stern or forward submergence.

If static and quasi-dynamic results are compared it can be seen [Table 7.1] that in all conditions the trends from both methods are similar. However the effect of waves, which is not considered by static stability creates differences in the trends, especially at large waves. Both methods find asymmetric damage to be the most dangerous. However, there is a great controversy in that almost all ships (except ship 7) satisfy the static stability requirement at the asymmetric damage conditions, yet all fail the quasi-dynamic stability requirements. It is logical to accept that the effect of waves can affect stability considerably but such a drastic difference between the two methods raises questions as to the suitability of either method in assessing damage stability of ships. It is suspected that the reason for such a difference may be due to the way the windward angle is estimated, which affects the excitational area. According to the Strathclyde criteria, the windward angle is calculated from the upright position and derives from the vessel response in the relevant wind and wave environment. However in the case of asymmetric damage, the windward angle increases by the amount of static heel and this in turn increases the negative area prohibitively. Considering this point, the maximum windward roll angle must in future studies be calculated from the equilibrium position.

Although this parametric study of static and quasi-dynamic stability assessments provides some useful but limited information, it fails to represent the true picture of real damage scenarios. It is impossible to

obtain detailed information on the behaviour of ships since the effect of other motions, progressive flooding, flooding of the vehicle deck and accumulation of water cannot be modelled. Generally, in ferries, if there is an accident there is also damage above the bulkhead deck and static heel may cause the vehicle deck to be flooded very easily. In addition the effect of waves and wind are included to a very limited and approximate extent and these methods fail overall to give precise and detailed information. However, these findings help to emphasise the need for dynamic analysis in order to achieve a better understanding of the damage stability of ferries.

7.4 DYNAMIC STABILITY

In the light of the findings from the previous analyses, it was decided to select only one sample ship and carry out a dynamic stability analysis for a number of different conditions.

For this purpose Ship 2 was chosen since she works in international waters. She is a modern type of passenger/vehicle ferry with a big passenger and vehicle capacity and has 2.5 car decks, of which two are above the bulkhead deck and half below the bulkhead deck. Another interesting feature of this ship is that the compartmentation and damage stability calculations were carried out according to the probabilistic method. With this method, if the ship has side tanks at B/5 depth and the double bottom has a depth of B/10, the ship can have a very long inner compartment provided the relationship $A > R$ is maintained. This particular ship has a 60 m long inner compartment (Fig 7.11a). On the other hand she has good stability characteristics, therefore it was thought to be interesting to examine her performance in the presence of waves. In addition, it was thought that one ship would be sufficient to identify the general trends (in the behaviour of a damaged ship), which could be considered in proposing a methodology for developing damage stability criteria.

7.4.1 Conditions and Assumptions

The developed software allows for both irregular and regular waves in assessing a ship's dynamic behaviour. However, only regular waves were considered in the parametric investigation. Consideration

of regular waves allows better control in studying the effect of various parameters whilst saving substantially in computational time.

Taking into account North Sea wave statistics, a 6 m wave height can be taken as a representative maximum value. Two others were also considered, a 2 m and a 4 m. The wave length was chosen to be equal to the ship length and the wave direction 90 degrees. However, when necessary in the investigation (e.g. examining the effect of excitation frequency) different wave lengths are considered.

Considering the importance of loading condition of the ship, different KGs are used in the calculations. KGs vary between 10.2 m and 13.34 m, thus intact GM between 0.3 m and 3.44 m.

Water ingress is dealt with by adding a fixed amount of water in a particular tank at each time step (option 1 of water ingress). The flow rate and the total amount of water which can flood in are chosen depending on the location of the damage and the volume of the compartment. The interest focuses on examining the effect of water on ship behaviour, therefore, the water ingress assumption is based on the fact that water is flooding into the ship, rather than determining the possibility of water ingress.

It is worth mentioning that, although water ingress which depends on the wave elevation and damage location is modelled reasonably well in the developed software, its general application still needs detailed research with experimental verification. It is also very difficult to model a number of complicated phenomena associated with water ingress such as water inflow and outflow rates, venting effect from the main compartment, etc.

7.4.2 Damage Scenarios

The reasons and consequences of the accidents may vary greatly, therefore, considering different types of damages would help to view the full range of possible effects. Definitions must be done in a way that the most realistic and potentially most dangerous damage conditions would be examined. By defining and studying all the

possible worst damage conditions, the necessary information for taking the current precautions can be derived. This will also cater for effects due to less dangerous damages, which are not included in the investigations.

Along these lines, first of all the basis damage for the various scenarios was defined by considering the most dangerous damage location and its longitudinal extent in accordance with IMO's regulations. This damage was further extended in dealing with some of the potentially very dangerous scenarios considered in this study, which incidentally are not considered by the present damage stability regulations, such as flooding of an inner compartment.

Furthermore, considering other damages, which are not again considered by the regulations, but have been encountered in real sea accidents will be very important for the investigations. For instance, flooding of the vehicle deck (Herald of Free Enterprise), and combination of flooding at different levels at the same time (European Gateway) are probably the main examples from ferry accidents.

There are six different damage scenarios which are considered in the parametric study. The damage location shown in Fig 7.11a, is the most critical location according to IMO regulations. Damages can be defined as follows and are shown in Fig 7.11b.

1- Only the side tank is assumed to be flooded and cross-flooding arrangement is enabled to reduce static heel.

2- The side tank and vehicle deck are assumed to be flooded and cross-flooding arrangement is enabled to reduce static heel.

3- Only the side tank and inner compartment are assumed to be flooded and cross-flooding is assumed to be disabled.

4- Only the vehicle deck is assumed to be flooded.

5- Only the side tank and vehicle deck are assumed to be flooded. Again cross-flooding is assumed to be disabled.

6- The inner compartment, side tank and vehicle deck are assumed to be flooded. Cross-flooding is assumed to be disabled.

7.4.3 Parametric Investigation

i- Damage Scenario 1

In this condition it is assumed that the side tank (B/5) is damaged and water starts flooding in at 8 tonnes/sec, for 60 seconds, 480 tonnes of water in total. However it is also assumed that due to damage to the side of the vessel, there is cross-flooding which reduces the heeling. The cross-flooding rate is assumed to be 2.2 tonnes/sec, pumping a total of 480 tonnes of water into the second tank at the other side. As a result, the total amount of water in both tanks, after the final stage of flooding is 960 tonnes.

In calm water the ship inclines up to a static heel because of the progressive flooding of the tank, but returns to the upright condition as a result of the cross-flooding. The static heel, which occurs during the intermediate stages of flooding, varies depending on the KG of the ship. The static heel changes between 6 and 22 degrees. At low KGs the static heel is too small to cause any problem, but as KG increases progressively the static heel also increases significantly (Fig 7.12) and may cause problems if other effects are present, such as shifting of cargo. However, the ship will return to the upright condition because of the cross-flooding.

Small waves (2 m) do not affect the results significantly at low KGs (up to 11.84 m.), however with KG over 12 m, roll oscillations become significantly larger and when KG is approximately 12.5 m, the ship capsizes at low wave heights (Fig 7.13). This sudden increase in roll oscillations is probably caused by non-linear effects such as non-linear stiffness and heave coupling. Fig 7.13 shows the ship's sway, heave and roll motions, as well as sinkage and heel during and after progressive flooding. Fig 7.13 shows also the transverse centre of volume of flooded water. When KG is increased

beyond 12.59 m. the ship survives only at small waves(Fig 7.14). At big waves however, the ship capsizes systematically.

The reason for the sudden increase in roll oscillations at KG = 12.59 m is either due to subharmonic motion, which occurs when the forced roll period is a multiple of wave period (i.e. 2/1, 3/1,..), or due to parametric excitation which occurs when the wave period is half of the roll natural period. Another source might be the non-linear coupling due to heave which is also experienced when the heave period is half the roll period. In this case the wave period is 10.43 seconds and the ship's natural roll period is approximately 22 sec. The forced roll period is approximately 20 sec while the forced heave period is approximately 10 sec.

As wave height increases, the static heel effect becomes less important and oscillations due to excitation become more dominant. Fig 7.15 shows the change in the maximum roll amplitude as a function of KG and wave height. It is obvious that as KG increases, the ship's ability to survive in large waves decreases.

If the ship sinkage and heave motion are examined, the ship sinks around 0.25 m for this particular damage. As the wave height increases, heave motion increases, varying in the range between 1.0 m and 3.5 m. The static heel does not seem to be affecting the heave motion significantly.

Sway motion has small amplitudes ranging between 1 m and 3 m. The sway motion changes if there is a big static heel or a big roll motion and this is due to the change in underwater geometry.

Summarising, it can be said that this type of damage does not create any significant problem as long as KG and wave height are not very large.

ii- Damage Condition 2

In the second damage scenario, the side tank and the vehicle deck are assumed to be flooded. At first, the side tank is flooded at a rate

of 8 tonnes/sec, a total of 480 tonnes of water and then, because of the static heel, the vehicle deck starts flooding. In the mean time the cross-flooding arrangement starts pumping water into the tank at the other side, at a rate of 2.2 tonnes/sec, transferring 480 tonnes in total. The vehicle deck is flooded at a rate of 5 tonnes/sec, 1000 tonnes in total.

In calm water, the ship inclines again towards the one side and the vehicle deck starts flooding. The ship starts sinking as well as heeling. Although cross-flooding is used to balance the ship, because of the initial static heel the water on deck piles up at the one side. The distance of the transverse centre of gravity of this water from the centreline is large enough to create a static heeling moment. The ship therefore has a constant heel even after completion of cross-flooding (Fig 7.16). As Fig 7.16c shows, the transverse centre of gravity of water hardly changes as the amount increases, thus the static heeling moment continues to increase. Again the static heel varies depending on KG ; at low KGs the static heel does not create any problems (Fig 7.17), however at high KGs the ship capsizes, despite the relatively small amount of water on deck and the fact that calm water is being considered. This shows the danger of flooding the vehicle deck.

As Fig 7.17 shows, low KGs and a 2 m wave height do not effect the behaviour of the ship, compared with the calm water condition. This is due to the fact that wave excitation is not big enough to excite the inclined ship at large amplitudes. However, again at KG = 12.5 m the ship oscillates at very large amplitudes due to the non-linear excitation. At KG = 13.34 m, the ship capsizes with very small oscillations due to the flooding of the vehicle deck.

At 4 m wave height the ship's response does not change at low and medium KGs. However as KG is increased further, the ship starts capsizing within a very short time. At 6 m wave height, again there is no significant change in the ship response at low KGs (10.29 m and 11.04 m, Fig 7.17), but as KG is increased to 11.84 m, the ship starts oscillating at 40 degrees of amplitude (Fig 7.18) and at high KGs the ship capsizes within a very short time as expected.

The amount of water flooding the ship gives around 0.75 m of sinkage whilst the waves cause the ship to heave between 1 m and 3.5 m. The static heel and different amount of water do not change the heave response noticeably.

Generally the sway is small and the ship drifts initially a few metres, then starts oscillating. The amplitude of this oscillation varies between 1.25 m and 2.5 m, depending on the wave height.

Although in this study a water inflow of only 1000 tonnes is assumed, in reality the inflow can be significantly greater, so that the combination of sinkage, heave and roll can reduce the damaged freeboard significantly and increase the rate of progressive flooding.

iii- Damage Scenario 3

Here only the side tank and inner compartment below the bulkhead deck are assumed to be flooded with cross-flooding disabled. It is assumed that the side tank is flooded at a rate of 5 tonnes/sec, 480 tonnes in total, and the inner tank is flooded at a rate of 8 tonnes/sec, 4000 tonnes in total.

The ship initially inclines very quickly because of the flooding in the side tank. However the static heel gradually decreases as the amount of water in the main tank increases, with its transverse centre of gravity approaching progressively the centre line (Fig 7.19). The final static heel changes with KG. In calm water this damage case does not create any problem except for KG = 13.34 m, where the ship assumes a 25 degrees inclination. This heel may cause shifting of cargo and as a result the ship may capsize. In this scenario it is assumed that there is no damage above the bulkhead deck, therefore inclination does not cause any water ingress into the vehicle deck. However, 4,500 tonnes of flooded water causes a substantial 1.25 m sinkage.

If waves are present the behaviour of the ship does not change a great deal for small waves (2 m) and low KGs, but by increasing KG to

12.5 m the ship oscillates at very large amplitudes due to non-linear excitation (Fig 7.20). These large roll oscillations affect sway and heave motions. As KG is increased further, the roll oscillations become smaller again and static heel, which is approximately 25 degrees, becomes the dominant factor.

In waves of 4 m height and at low KGs, the behaviour of the ship does not change considerably compared to the calm water results. She rolls with small oscillations, while sway and heave do not change. However at KG = 11.84 m, the ship oscillates at large amplitudes (Fig 7.21) reaching approximately 25 degrees, but as the flooding continues the ship oscillation becomes smaller around the static heel. This is because the natural period of the ship changes due to the substantial amount of water flooding in, and also proves that a 4 m wave height does not excite the ship significantly at this KG. However, again at KG = 12.59 m, the ship oscillates at large amplitudes, and capsizes within a very short time (Fig 7.22). At higher KGs, the wave excitation is big enough to capsize the ship, since the ship has a very small restoring ability. The behaviour of the ship in 6 m high waves is similar to that in the 4 m wave height.

Fig 7.23 clearly shows that over a range of low KGs the response of the ship at different wave heights does not change significantly. However as KG increases the effect of wave height becomes more obvious.

When the amount of water flooded into the inner compartment is increased from 4,000 to 6,000 tonnes it does not make a significant change on the static heel, which reduces by a few degrees due to the distance of the transverse centre of gravity of water reducing further. However the most significant change occurs in sinkage, which increases to 1.75 m and causes the margin line to immerse a few centimetres which is both very dangerous and not permissible under the stability rules. It is concluded that this damage scenario, which is not considered by present regulations, can pose a threat to the ship's survivability.

iv- Damage Scenario 4

Here it is assumed that only the vehicle deck is flooded at a rate of 5 tonnes/sec, the total amount being 2,100 tonnes. It is also assumed that there is initial temporary heel due to collision or some other factor. In calm water, if there is no initial heel the ship does not really incline, but only sinks.

This amount of water causes the ship to sink by 0.75 m. In calm sea, when water starts flooding in, the ship starts oscillating due to the initial heel. However, when the static heeling moment, due to the water on deck equals the restoring moment, the ship stops oscillating and starts inclining with the static heel becoming progressively larger. Since the ship has a very long and wide vehicle deck, the amount of water flooding in piles up at the side of the deck. As seen in Fig 7.24, the transverse centre of gravity of the water on deck does not change despite the increasing amount of water during progressive flooding, but it creates a larger heeling moment. As more water comes in, the ship inclines more and remains inclined after flooding since there is no restoring moment to bring the ship back to the upright position (FIG 7.24B and Fig 7.24C). The inclination changes with KG: at low KGs (10.3 m and 11 m), the ship remains inclined around 20 degrees, however as KG increases (11.8 m), the ship inclines to a critical angle which is around 30 degrees. In this state the ship can capsize very easily if any other effects such as cargo shift are present. At KGs higher than 11.8 m the ship capsizes due to lack of restoring and the presence of static heeling moment (Fig 7.25).

A 2 m wave height does not change the behaviour of the ship, compared to the calm water behaviour. Oscillations are small at low KGs and the static moment is dominant. However, at KG = 11.84 m, the ship initially oscillates at large amplitudes reaching 45 degrees (which must be taken as capsize) but if simulation is allowed to continue, oscillations suddenly become smaller and flooding continues as the ship oscillates at small amplitudes. However after a while the ship starts rolling at large amplitudes again and capsizes (Fig 7.26). This change in the ship's behaviour can be due to the combination of

static heel, wave excitation and change in the natural roll frequency of the ship due to the water on deck as well as the change in the non-linear effect of heave on roll. These possibilities will be investigated later in this chapter.

At a wave height of 4 m, the behaviour of the ship changes drastically at moderate and high KGs. At KG = 10.29 m., and KG = 11.04 m the ship's roll oscillations, which are similar to those in a 2 m wave height and 11.84 m KG, become larger gradually and reach 40 degrees, but suddenly the oscillations become very small around the static heel. However, at high KGs (12.59 m, 13.34 m), wave excitation becomes very big and the ship capsizes very quickly.

At a 6 m wave height, at every KG there is a danger of capsizing. At low KGs (10.29 m and 11.04 m) the ship oscillates at large amplitudes which is clearly dangerous. However these big oscillations die out again, and beyond KG = 11.04 m, the ship cannot withstand the big wave excitation force and capsizes very quickly.

Fig 7.27 shows that apart from the region of low KG and very low wave height, all conditions cause a dangerous situation or capsize the ship even at calm water. This study shows clearly that flooding the vehicle deck is very dangerous and it is more than likely that the ship will capsize as was proved in the case of the Herald of Free Enterprise. Here, only a small amount of water (approximately 12% of displacement) is assumed to flood in, but if water ingress continues the ship could capsize or sink regardless of its KG.

v- Damage Scenario 5

Here only the side tank and vehicle deck are assumed to be damaged and cross-flooding to be disabled. The side tank is flooded at a rate of 8 tonnes/sec, a total of 480 tonnes, and the vehicle deck is flooded at a rate of 5 tonnes/sec, a total of 2,000 tonnes of water.

This damage causes the ship to sink approximately 0.75 m. The transverse centre of gravity of the flooded water is at a distance of approximately 10 m from the centre line and this does not change in

calm water. The ship inclines more as KG increases. At low KGs the inclination changes between 20 and 30 degrees which is a critical inclination. As KG is increased to 12.59 m, the ship capsizes following ingress of a considerable amount of water (Fig 7.28). When KG is further increased the ship ends up losing her restoring ability completely. Due to the very high KG, a small amount of water on deck is sufficient to capsize the ship within a very short time.

A 2 m wave height does not change the behaviour of the ship. Again the static heeling moment is a dominant factor and the ship oscillates only with small amplitudes of roll. At KG =12.59 m the ship inclines whilst undergoing moderate oscillations and when there is enough water on deck she capsizes. This shows the combined effect of static moment of water and dynamic moment of wave excitation. At KG = 13.34 m the ship capsizes within a very short time, as expected.

At 4 m wave height it can be said that the behaviour of the ship is the same as that at 2 m but the outcome is different in some cases. When KG is 11.84 m, the ship starts inclining with small amplitude oscillations, however after a while the ship starts oscillating at large amplitudes and capsizes (Fig 7.29). This may be due to the change in the natural frequency caused by the inclination of the ship and the non-linear heave coupling into roll. Again at higher KGs, the ship capsizes within a very short time (Fig 7.30).

At 6 m wave height the behaviour of the ship does not change at low KGs (10.29 m and 11.04 m), but as KG becomes approximately 11.84 m, the static heeling moment due to the water on deck loses its dominance on wave excitation and the ship starts oscillating at large amplitudes and eventually capsizes (Fig 7.31). Beyond this KG (12.59m, 13.34 m), the wave excitation is completely dominant and the ship capsizes very quickly, since her restoring ability is reduced considerably. Summarising this condition, it can be said that there is a clear line between wave excitation and static heeling moment. This line defines the limits between static heeling and wave excitation moments. The water on deck can prevent the ship from oscillating but

can capsize the ship very easily as well, if there is enough water on deck.

Fig 7.32 shows that in all conditions this damage gives critical stability, and between 11 m and 12.2 m of KG, wave excitation becomes a prime consideration for ship stability.

vi- Damage Scenario 6

Here it is assumed that the side tank, inner compartment and vehicle deck are flooded and that cross-flooding is disabled. The side tank is flooded at the rate of 5 tonnes/sec, 480 tonnes in total, the inner compartment at 8 tonnes/sec, a total 4,000 tonnes, and the vehicle deck 5 tonnes/sec, a total of 2,000 tonnes. In this damage case the ship sinks 1.75 m, which is very dangerous, since the margin line is immersed. This sinkage signifies the danger of the inner compartment being flooded (Fig 7.33A).

At calm water, the initial heel causes the water on the vehicle deck to pile up at one side of the ship. However, flooding of the inner compartment decreases the lever of the transverse centre of gravity of water, hence heeling increases slowly. At low KGs (10.29 m and 11.04 m) the ship attains a static heel of approximately 20 degrees which does not create a major problem. However at KG = 12.59 m, the static heel increases to 30 degrees (Fig 7.33b). The ship is then in a critical condition and could be lost with the substantial sinkage providing the additional incentive. At KG = 13.34 m the ship capsizes within a very short time with a very small amount of water on the deck.

A wave height of 2 m does not have any effect on the calm water results (Fig 7.37). Oscillations are very small and take place around the static heel. The wave excitation is obviously too small compared with the static heeling moment.

At 4 m wave height, oscillations become slightly larger at low KGs (10.29 m and 11.04 m) but do not create any major problem. However when KG is around 11.84 m the ship starts oscillating at

extreme amplitudes reaching 55 degrees (which of course, should be taken as a capsize) but as the flooding continues the oscillations die out and the ship rolls with only small oscillations around the static heel (Fig 7.34), while continuing to sink and heave. At KG = 12.59 m, due to the wave and parametric excitation as a result of coupling the ship capsizes within a very short time (Fig 7.35).

At 6 m wave height, the wave effect is insignificant at low KGs. At KG = 11.04 m the same roll behaviour which was observed at 4 m wave height and KG 11.84 m, can be seen (Fig 7.36). At KG = 12.59 m and 13.34 m the ship again capsizes within a very short time.

As shown in Fig 7.37, at low KGs the wave excitation does not affect the ship and she can be considered to be safe. However as KG increases there is a big difference between the effects at wave heights of 2m and those of 4 m and 6 m. This obviously provides an indications of the limiting wave height in the region of design KG. The probability of occurrence of this scenario is very high and potentially very dangerous (similar to that of the European Gateway), but unfortunately, like some other scenarios, this also is not considered by the present regulations.

7.5 EFFECT OF FREQUENCY

The behaviour of the ship is also related to the excitation frequency and its proximity to the natural frequencies of the ship. In linear theory, the ship oscillates at the same frequency as the wave frequency(ω_w). However in non-linear systems, due to the non-linear stiffness, it may not be the case and ship can oscillate at different frequencies(ω_o) from the wave frequencies as observed during the parametric study.

The ship natural frequency in each mode of motion is a function of basic ship properties, therefore the same wave affects different ships in a different way. Environmental conditions are changeable whereas the ship's parameters cannot be changed very easily. Therefore when a ship is designed to operate in a particular sea, all the possible

environmental conditions have to be taken into account, so that critical regions of environmental conditions can be avoided. The only parameter that can be changed on a ship whilst having some control over the damage is its loading condition which affects the natural roll frequency of the ship directly.

The roll natural frequency of a ship can be written as follows:

$$\omega_{sr} = 2\pi \sqrt{\frac{GM\ g\ \Delta}{(I_A + I_{xx})}} \text{ (rad/sec)} \qquad \text{[Eq 7.1]}$$

where I_A is added roll inertia.

Since GM=KM-KG, KG affects the natural roll period of the ship, and as KG increases (GM decreases) whilst keeping wave height constant, the ship becomes more sensitive to the excitation force.

Similarly, the heave natural frequency may be expressed as:

$$\omega_{sh} = 2\pi \sqrt{\frac{\rho\ g\ WPA}{(M + a)}} \text{ (rad/sec)} \qquad \text{[Eq 7.2]}$$

where WPA is waterplane area, M is the mass of the ship and a is the heave added mass coefficient. Excitation also changes with wave frequency and if it lies in the critical region, the response amplitude may become excessively large. Outside this region, the effect of wave excitation force becomes small.

The excitation force is also wave height dependent and this dependence becomes non-linear as the wave height progressively increases. However, within the range of wave heights considered a linear relationship is assumed.

Considering the effect of wave frequency on ship motions, the following possibilities are noteworthy:

a- When the ratio $\frac{\omega_{sr}}{\omega_w} = 1$ there is a resonant condition and the ship

can oscillate at very large amplitudes.

b- Due to the non-linear stiffness, some non-linearities in ship motions can be observed. If the natural roll frequency of a ship (ω_{sr}) or the roll response frequency of a ship (ω_o) is lower than the wave frequency (ω_w), there may be a subharmonic motion [68, 77, 78]. This can also cause the ship to oscillate at large amplitudes. The existence and magnitude of subharmonic motion are dependent on the degree of non-linearity of the stiffness. Generally a cubic form of roll stiffness is related to the subharmonic motion [68] as well as to jump phenomena [67]. Subharmonic motions can occur at different $\frac{\omega_{sr}}{\omega_w}$ or $\frac{\omega_o}{\omega_w}$. These ratios are mainly $\frac{\omega_o}{\omega_w}$=0.33 and 0.5 [68, 77]. As explained in Chapter 6, due to similar reasons, superharmonic motion can occur, if $\frac{\omega_o}{\omega_w}$=2, 3 or Jump phenomena can also be encountered.

c- If the natural roll frequency is lower than the wave frequency it is again possible for a subharmonic motion to occur [78] and this can cause the ship to oscillate at large amplitudes. The ratios to avoid are $\frac{\omega_{sr}}{\omega_w}$=0.5 and 0.33 [77].

d- If heave is coupled into roll motion, the ship may be subjected to parametric excitation if the ship roll natural frequency is half the heave natural frequency.

$$W_{sr} = 0.5\ W_{sh} \quad [79, 80] \qquad [Eq.\ 7.3]$$

This parametric excitation is the result of the nonlinear coupling of heave into roll motion. This nonlinearity derives from the nonlinear restoring creating instability and may cause large roll motion.

Taking into account these points, different loading conditions are tested at different wave frequencies. For this parametric study, damage scenario 3 is considered and five different loading conditions are used. Scenario 3 is common to occur in the case of an accident, as damage is confined below the bulkhead deck (under the waterline).

In addition, due to the substantial progressive sinkage, ship characteristics may change and this in turn affects significantly the ship motions during progressive flooding. The loading condition considered are KG = 10.29 m, 11.04 m, 11.84 m, 12.59 m, and 13.34 m. An investigation was carried out for a 2 m wave height and in order to cover a wide range of wave excitation frequencies, the wave length was varied between 40 m and 750 m.

In the parametric study, the heave natural frequency cannot be altered by changing the loading condition. It can only change if the waterplane area alters. Therefore, the change of heave frequency will be small. As expected the change in the ratio $\frac{\omega_{sr}}{\omega_w}$ affects ship behaviour. If the ratio $\frac{\omega_{sr}}{\omega_w}$ or $\frac{\omega_n}{\omega_w}$ is close to the critical ratios the ship oscillates at very large amplitudes. The results of the investigation can be seen in Fig 7.38. It can be observed that there are certain ratios $\frac{\omega_{sr}}{\omega_w}$ where large roll amplitudes are experienced or the ship capsizes. Generally maximum roll amplitudes occur when the ratio $\frac{\omega_{sr}}{\omega_w}$ is approximately 1, i.e at resonance. The natural roll frequency of the ship at the lowest KG is approximately 0.52 rad/sec. This means that a 225 m long wave is required for resonance and the roll motion at this KG is small. However, as KG increases, the natural roll frequency decreases whilst the maximum roll at resonance increases. Since the natural roll frequency decreases as KG increases, the possibility of encountering a wave at these frequencies is very low, therefore when the ratio becomes 1 there is no great danger.

From Fig 7.38 it can be seen clearly that at KG = 12.59 m and for $\frac{\omega_{sr}}{\omega_w}$ ratio at approximately 0.5, large roll is experienced. In order to investigate the real reason, the ship roll motion for the same condition is examined for pure roll without any coupling. As seen from Fig 7.39 the coupled roll motion oscillates at very large amplitudes whereas the single degree of freedom roll motion attains very small amplitudes with static heel, thus proving that the large roll

motion is due to the parametric excitation from heave coupling. The frequency of this wave is 0.62 rad/sec and the length is around 160 m. The possibility of encountering such a wave is higher even though it is not very common. Therefore this critical region must be studied with care.

If the frequency curves of roll excitation for different loading conditions (KGs) are examined, all loading conditions at 2 m wave height [Fig 7.40] show a maximum roll moment at around ω_W=0.9 rad/sec and this corresponds to wave length (WL) of 51 m. However the ship's response near this region is small even at high KG values, meaning that this particular frequency is not related to a $\frac{\omega_{sr}}{\omega_W}$ and the total force at 2 m is not big enough to excite the ship. Comparing the two results [Fig 7.41) at KG = 13.34 m, reveals that although at ω_W=0.88 rad/sec moment is much bigger than the moment at ω_W=0.37 rad/sec, the response of the ship indicates an opposite trend. At ω_W=0.88 rad/sec, the ship oscillates at 5-6 degrees amplitude, while the ship capsizes within a short time at ω_W=0.37 rad/sec. This proves that a large excitation force does not necessarily mean large motions. It also shows the effect of frequency on ship response.

7.6 EFFECT OF WATER ON DECK

The damage scenarios considered above lead to the clear conclusion that water on deck is a determining factor affecting damage stability. It is therefore of vital importance to identify the critical amount of water which can cause problems or capsize the ship. The amount of water, of course depends on the location and extent of damage, the ship's loading condition and wave height. Since it has been proved that flooding of the main vehicle deck is the critical form of flooding, damage scenario 4 is considered in this investigation.

The critical amount of water which can capsize the ship is principally a function of KG and it changes rapidly as KG is changing. As seen in Fig 7.42, the relationship between the critical amount of water on deck and KG is almost linear in calm water and moderate wave

heights, but the relationship becomes non-linear as the wave height increases. At large KGs however, the actual amount of water on deck is almost independent of wave height.

Depending on KG, the critical amount of water can drop from 7,500 tonnes to as little as 600 tonnes. In the region of operational KGs, the amount of water on deck that may cause the ship to capsize is estimated at approximately 15% to 20% of total displacement.

7.7 COMPARTMENT LENGTH

As is common knowledge, the main vehicle deck of the Ro-Ro's and Passenger/Car ferries is not divided by transverse bulkheads, and a very large area can therefore be flooded if water starts to enter. The Herald of Free Enterprise disaster provides the best example of this. Discussions are taking place and suggestions are being made whether to subdivide and how to subdivide the vehicle deck. As has been demonstrated, in these very large areas, water can flow freely and can very easily change the balance of the ship. It is therefore important to know the limiting compartment length on the vehicle deck which could restrict the dynamic motions and other harmful effects. This limiting compartment length would, of course, depend on wave height as well as loading condition. In order to find the critical length of a vehicle compartment a limited parametric study was carried out by using only the design KG and a range of wave heights. This provides a good idea on allowable compartment lengths which can be explored further in order to achieve optimum design modifications as well as for possible future regulations on this matter.

Fig 7.43a shows that the transient region between safe and unsafe compartment lengths is very narrow, especially in big waves. The critical value can, therefore, alter under the effect of environmental and ship parameters. In calm water, the static heel due to damage is almost constant if the compartment length is more than 56 m. This changes gradually when the compartment length is between 30 m and 56 m. However, when the compartment length is reduced to 25 m, the ship returns to the upright condition. When the ship has a long

compartment, the water on deck piles up at one side and even if the amount increases the transverse centre of gravity of water does not change significantly and the ship ends up with a static heel. This static heel exists until the compartment length is reduced to a critical point at which the ship returns to the upright condition very quickly as the amount of water increases. Fig 7.43b shows the time histories of transverse centre of gravity of water for compartment lengths of 25 m and 30 m, and illustrates the effect of a 5 m reduction in compartment length on the ship attitude. If the change of the transverse centre of gravity of the water with compartment length is examined, in calm water it can be seen that the trend is identical to the static heel curve.

In the case of waves, the ship survives in all the wave heights when the compartment length is reduced to 25 m. The transition region at 2 m wave height is broad enough to allow selection of the critical length which is between 40-45 m, but this region becomes narrower when the wave height is 4 m. The critical compartment length can be taken as 30 to 35 m, but at a wave height of 6 m the transition region almost disappears. The ship survives at 25 m but capsizes at 30 m.

Observation of the curves of transverse centre of gravity of water on deck [Fig 7.43c] reveals that the curve corresponding to a wave height of 2 m is identical to the calm water curve. This means that at 2 m wave height the static heel still dominates the ship's behaviour. However at 4m and 6 m, the dominant parameter is the ship oscillation caused by wave excitation as well as the accumulation of water. If the transverse centre of water for 4 m and 6 m is examined, it can be seen that there is no permanent tendency for it to be asymmetric. The transverse centre of water follows the roll motion instead and oscillates to either side around the centre line except when the compartment length is 30 m and the wave height reaches 4 m. At this particular point waves are not large enough to cause the ship to roll around the centre line, but water on deck is sufficient to create a static heel. When the compartment length reaches 40 m, however, the ship capsizes, but she returns to the upright condition and survives if the compartment length is reduced to 25 m [Fig

7.43d]. At 4 m and 6 m waves it can be said that the ship may either survive or capsize and that there is no discernible transition region.

It may be concluded that in a region near the design loading condition the ship may have to have a vehicle compartment with a length as small as 25 m. This length may be increased slightly if KG is reduced. This parametric study was based on the assumption that the centre of the compartment lies on the centreplane amidships. It may, therefore, be useful to examine the ensuing effects if the compartment centre is moved forward or aft.

7.8 FORCES AND COUPLING EFFECTS

Ship motions are the result of restoring and excitation forces, the effect of which changes depending on certain conditions. As the results show, capsizing or dangerous conditions may occur due to :

a- Static moment caused by water on deck [Capsizing Mode A]
b- Combination of wave excitation and static moment [Capsizing Mode B]
c- Wave excitation and coupling effects [Capsizing Mode C]

If the motions are examined it can be seen that a ship oscillating at large amplitudes suddenly starts oscillating at small amplitudes [Fig 7.34c] or the reverse may happen [Fig 7.29c). It is also observed that in the case of flooding the vehicle deck, static heel may suddenly change to the other side while large oscillations continue. In order to find the reasons behind this behaviour, it is worthwhile looking into the effects of forces and coupling.

The forces acting on rolling ships can be grouped as follows:

1- Wave excitation moment
2- Static moment due to water on deck
3- Restoring moment

Although 1 and 2 are the excitation and 3 is the restoring moment, depending on the frequency, they may have either the same or the

opposite effect on the ship.

Capsizing mode A is due to static heeling and it can be seen clearly in Fig 7.44b, where the ship capsizes without large oscillations as the water on deck increases. If the histories of the forces are examined, it can be seen that static moment dominates the behaviour of the ship [7.44b]. The wave excitation force is too small to excite the ship to large amplitudes, and the restoring and static moments balance each other until the ship's restoring ability cannot resist the static heeling moment and the ship capsizes. The restoring ability of the ship is weakened because of high KG values.

Capsizing mode B is the result of the combined effects of each force and moment. As seen in Fig 7.45a the ship is inclining while oscillating at moderate roll amplitudes and finally capsizes. If the forces are examined it can be seen that wave excitation is large but not large enough to capsize the ship, since restoring is almost twice the excitation moment. However as the water floods in the static heeling moment is gradually getting larger and changes the balance towards the excitation forces (Fig 7.45b). At the same time the increasing amount of water on deck changes the roll period of the ship so that an unfavorable phase angle develops between heave and roll motions which contributes to the ship oscillating at larger amplitudes, ending with the ship capsizing.

Capsizing mode C is the result of large roll motion where the wave effect is dominant. Wave forces are either too large on their own or in combination with coupling or the excitation frequency is near resonant. These large amplitude motions can be seen at a wide range of KGs (11.04 m - 13.34 m). In Fig 7.46a the ship with 11.84 m KG and encountering waves of 6 m high, capsizes within a short time as a result of very large oscillations. If the restoring forces are examined it can be seen that wave excitation is large and with a contribution from coupling the ship capsizes. The contribution of the static heel is small in this case. This type of capsizing is seen at high KG values but as the wave height increases the range of critical KGs widens as seen in this case and the ship becomes more vulnerable. If only the

roll oscillations (no static heel is included) for damage 6 are examined, the change of roll motion due to the different wave and loading conditions can be seen clearly [Fig 7.47].

The coupling effect of other motions on roll may be so strong that it may even become the dominant source of excitation. Therefore, it is important to examine the effect of coupling, so that some precautions may be taken. As stated before, the mathematical model pertains to coupled sway, heave and roll motions and it is common knowledge that there is no hydrodynamic coupling between heave and roll unless there is asymmetry which causes coupling between the two motions mentioned above. On the other hand, there is non-linear restoring coupling between roll and heave and it is a function of the under water volume of the ship. This coupling may be very strong and depends on the frequencies of forced roll and heave motions, on heave amplitude as well as on the form of the ship's hull.

Since sway does not have a restoring ability there is only hydrodynamic coupling between sway and roll. Especially sway into roll coupling is more obvious and proven by the experiments which were carried out in this research.

If the coupling effect on the dangerous conditions mentioned above is examined, the hydrostatic coupling due to heave can be clearly seen. If the results are examined it can be seen that the effect of hydrodynamic coupling due to sway changes depending on the wave and natural roll frequencies. For instance, in the case of damage case 2 and for KG = 12.59 m, the effect of coupling from heave and sway motions is small enough to be ignored (Fig 7.48). However in the case of damage condition 6 and KG = 11.84 m, although sway into roll coupling does not change the results, when heave motion is taken into account, the roll response of the ship changes drastically (Fig 7.49). When the roll and roll coupled with sway responses are examined, it can be seen that the ship oscillates at small amplitudes whilst inclining due to progressive flooding (Fig 7.49a and Fig 7.49 b). However, in the case of roll motion coupled with sway and heave motions, the ship starts oscillating at very large amplitudes (Fig

7.49c) reaching 50-55 degrees, but as more water floods in, the large oscillations start dying down, and eventually the ship oscillates at small roll amplitudes around the static heel.

In the case of damage condition 4, sway into roll coupling does not change the roll response of the ship from that of the single degree of freedom roll response (Fig 7.50a and Fig 7.50b), but in the case of roll motion coupled with sway and heave motions, the ship starts oscillating at large amplitudes which become small as progressive flooding continues. However, eventually the ship's oscillations start getting larger gradually and the ship ends up capsizing (Fig 7.50c).

In the case of damage condition 3, the effect of sway into roll coupling becomes significant, and this coupling, in the presence of 6 m waves, are double the single degree of freedom roll amplitudes (Fig 7.51a and Fig 7.51b). When heave motion is also taken into account, the response of the ship changes drastically and the ship capsizes within a very short time (Fig 7.51c).

In general, the heave coupling effect derives from the change in the restoring forces and moments as a result of the underwater volume of the ship varying. The scale of the change and non-linearity depend on the hull form, frequency and heave amplitude. In general, this parametric excitation occurs when the roll period is around twice the heave period. However, if the overall results are analysed it can be seen that this behaviour is observed over a range of KGs (as shown in Fig 7.47) which affect the natural roll period of the ship.

The wave height is also affecting the heave coupling effect. For the damage case 6 and KG = 11.84 m, Fig 7.47 shows that for a 2 m wave height the ship oscillates with small amplitudes around the static heel, while for a 4 m wave height the ship oscillates at large amplitudes. This has to be due to the heave amplitude which increases with wave height, thus changing the restoring forces and moments significantly.

7.9 LIMITING STABILITY ZONES

Following the parametric investigation, the next task is to identify the most effective way of using the results in the development of survival criteria for a damaged passenger ship. Probably the first and main step is to define the safe zone limits in the light of the environmental and loading conditions in association with the possible damage scenarios. However, for the representation of the stability, it is impossible to take into account every parameter which may effect the stability of the damaged ship. For this purpose, the most important and least inter-dependent parameters have to be chosen for the representation of safety zones while other parameters are involved indirectly during the calculations.

Results showed that loading condition and wave height are the most influential ship and environmental parameters, respectively, affecting the damage stability. Of course the heeling or the roll motion is the main parameter which decides whether the ship is safe or not for a given condition. KG, wave height and maximum roll motion including static heeling are therefore used in the derivation of the safety zones for ship survivability. The effects of other important parameters such the amount of water ingress, wind, heave motion and sinkage, are included indirectly during the calculation of the roll angle experienced by the ship under given conditions.

In the derivation, rather than using exact roll angles to define these zones, they were formed by considering safe, critical and unsafe zones taking into account the allowable roll or heeling angle during progressive flooding resulting from existing rules, dynamic analysis, as well as other effects not considered in the present calculations. It was decided that if the heel or roll motion lies between 0 and 20 degrees the ship is assumed to be safe, if the roll angle is between 21 and 40 degrees it was taken as critical and if the angle exceeds 40 degrees the ship is assumed to capsize.

Such survivability zones were produced for each damage condition and it appears that the boundary curves change significantly with the damage scenario considered (Fig 7.52 - Fig 7.57). If the figures are

examined it can be seen that if the damage is below the bulkhead deck the ship has a better chance to survive in most conditions such as scenarios 1 and 3 (Fig 7.52 and Fig 7.54). The critical region seems very narrow and dangerous zones appear only when the KG is very large. This limits the maximum allowable KG. However, when the vehicle deck is flooded, the dangerous zone extends to the lowest KG value (Fig 7.53). In the case of damage scenario 2 (Fig 7.53) it appears that at large waves the ship may not survive even at the smallest KG, despite the fact that the amount of water at the vehicle deck is as small as 1000 tonnes. With more water on deck the critical wave height would be much smaller. Although, in scenario 2 the safe zone covers most of the possible conditions this safe region is drastically reduced when only the vehicle deck is flooded with more water on deck (scenario 4, Fig 7.55). Of course the amount of water also plays a very important role as it can flow freely in a very large area. As a result the limiting wave height for damage scenario 4 appears to be as small as 2.5 m at KG = 11 m (Fig 7.55). Damage scenario 5 gives an even smaller safe zone but a larger critical zone (Fig 7.56). This larger critical zone is the result of the combination of static heel and the flooding of the vehicle deck, causing larger roll oscillation over a wide range of KGs even at modest wave heights. For damage scenario 6 the ship has a larger safe zone over a wide range of KGs when the wave height is small (Fig 7.57). At low KGs the limiting wave height is also increasing considerably and again there is a large critical zone which may be caused by the same factor as in damage case 5.

With the limiting zones for each scenario defined it became clear that there can be two boundary curves for all the cases. The first refers to flooding below the bulkhead deck and the second to flooding of the vehicle deck above the bulkhead deck. When damage is below the bulkhead deck, the limiting KG and wave height are large and increase the chance of surviving in poor conditions near the operating loading condition. However, these limiting KGs become smaller when the vehicle deck is flooded and the chance of surviving becomes very low when KG is around the operating value.

Since in the parametric study the effect of flooding, rather than the possibility of flooding, is examined, the results for damage above the bulkhead deck are obtained by assuming a certain amount of water is flooded in without the effect of damaged being taken into account. If simulations are carried out using damaged freeboards and option 2 of water ingress, the survival zones could be even worse.

The results presented here address the key influencing factors in a way that helps to demonstrate an approach for the assessment of damage stability and for the development of survival criteria. However it is obvious that more analyses have to be carried out on different ships to establish more detailed quantitative criteria.

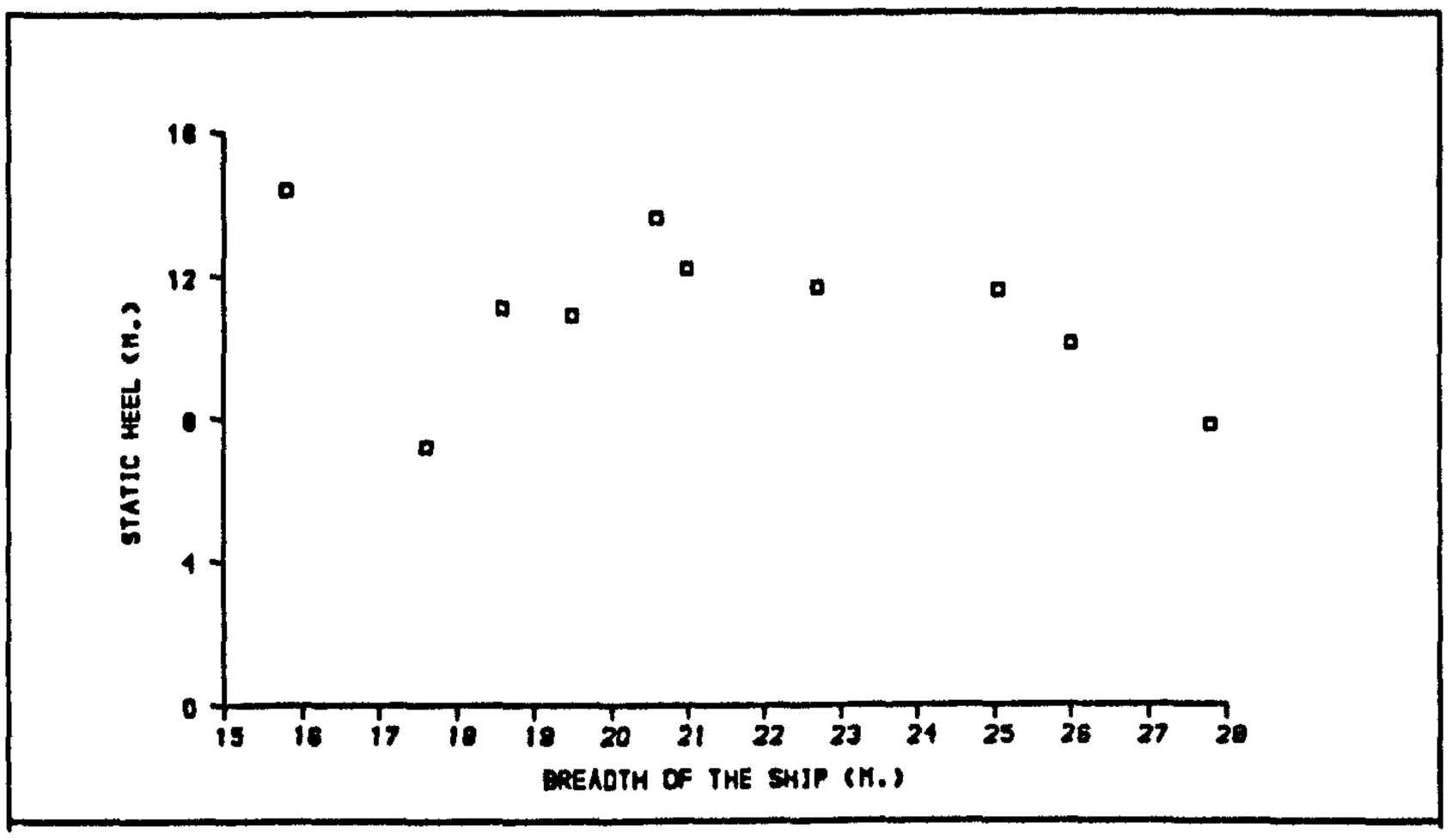

Fig 7.1A Effect of breadth on static heel due to asymmetric damage

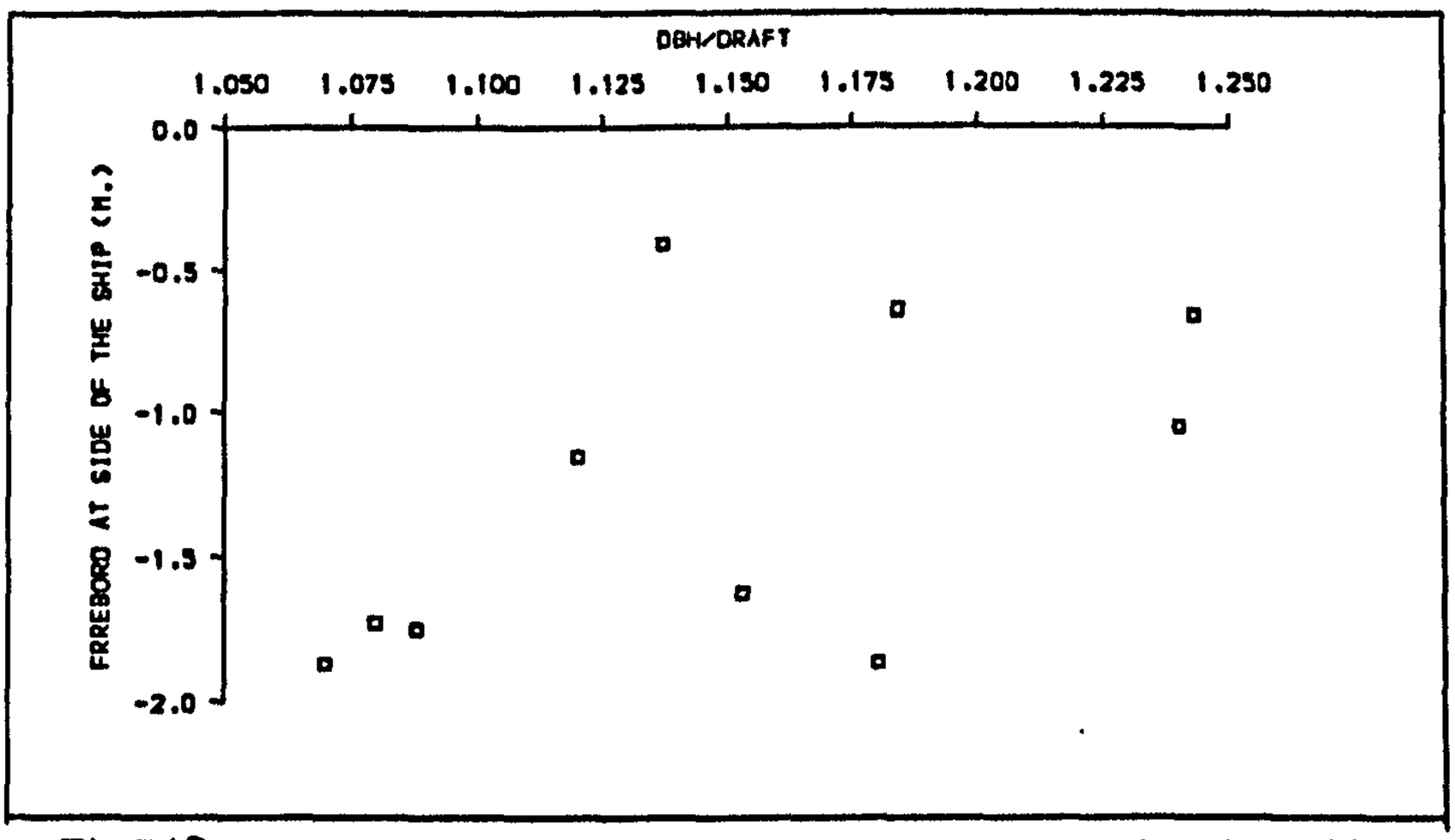

Fig 7.1B Damaged freeboard and immersion of bulkhead deck at side due to asymmetric damage

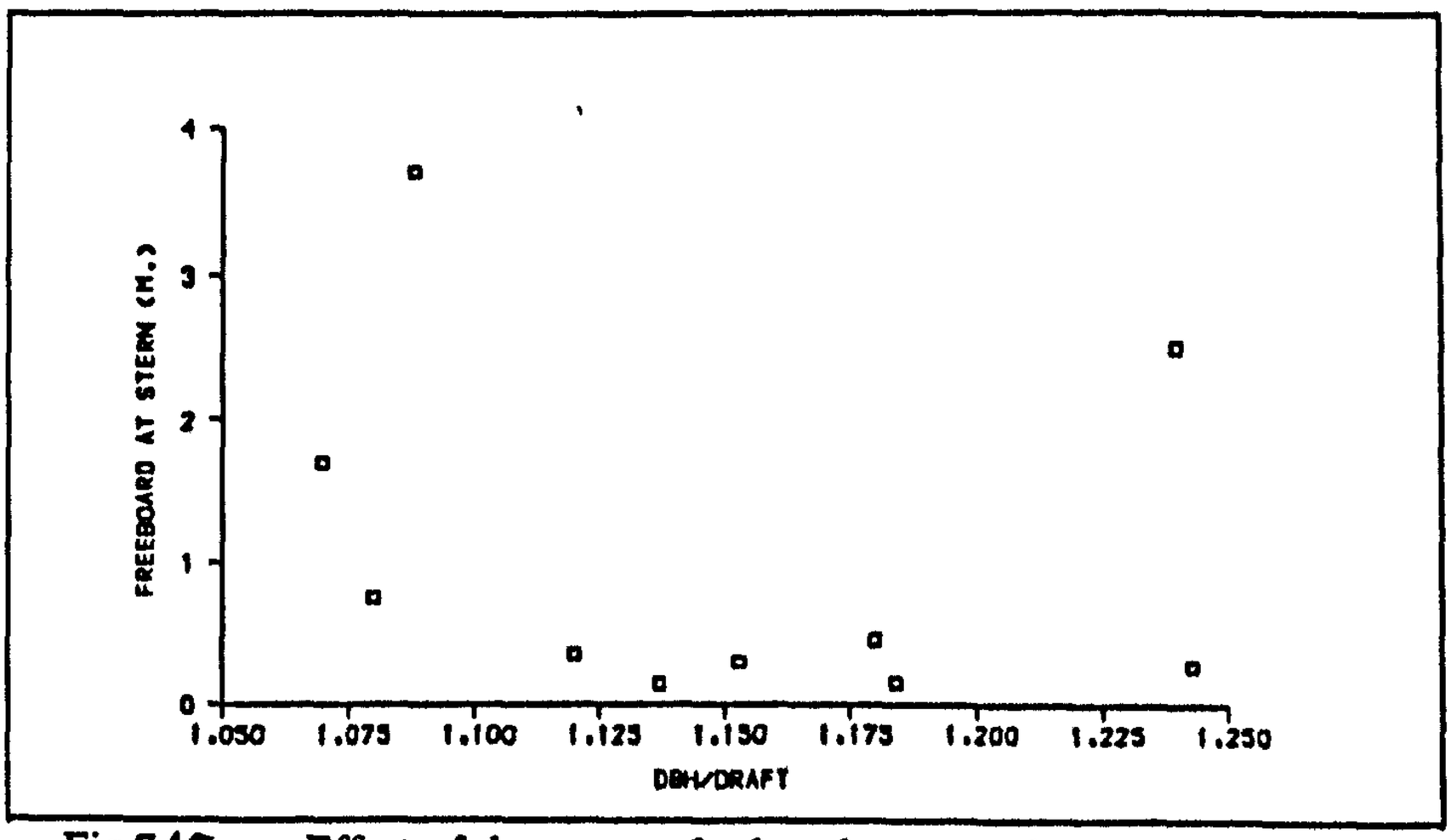

Fig 7.1C Effect of damage on freeboard at stern due to trim, caused by the flooding of damaged compartments

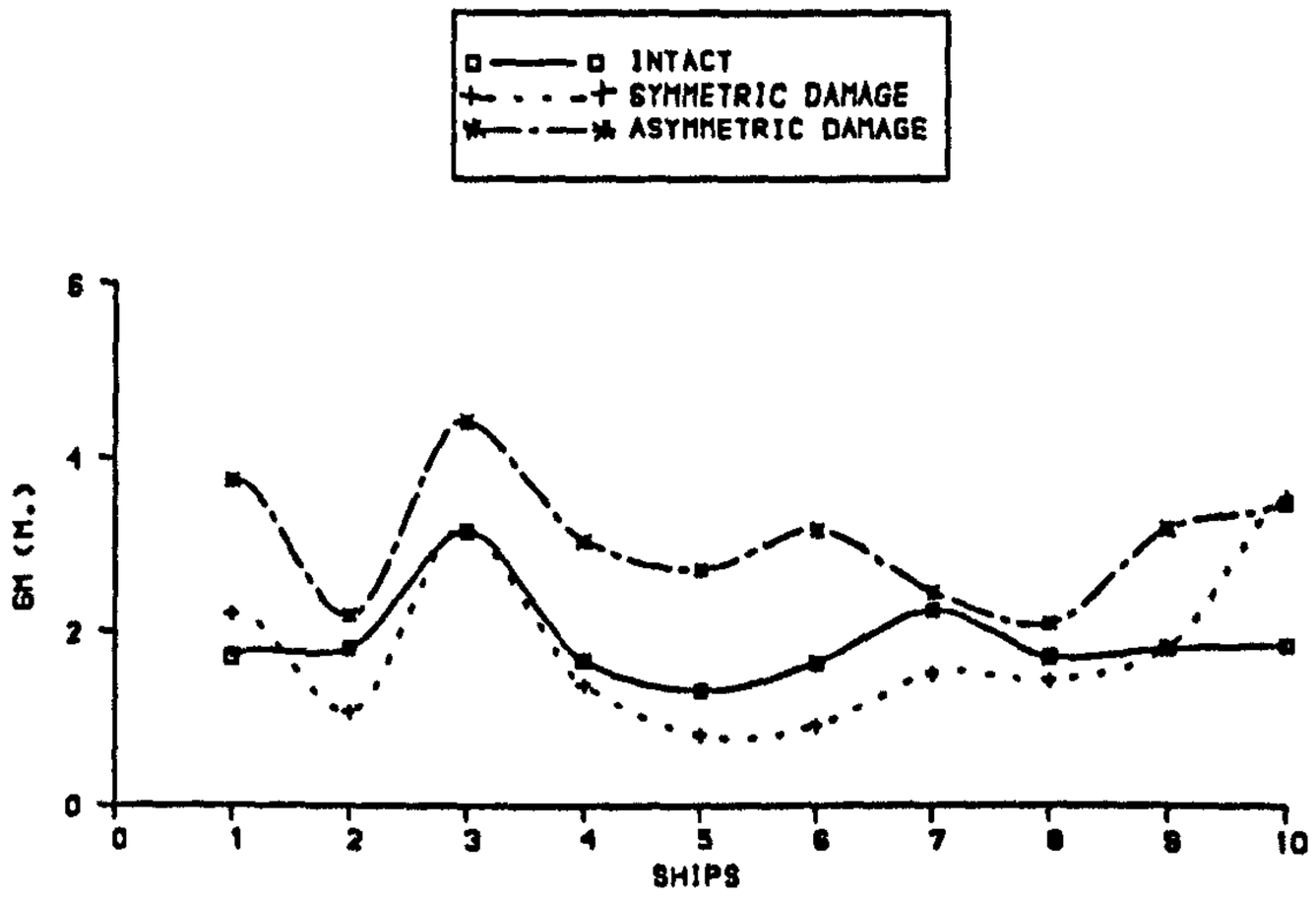

Fig 7.2 EFFECT OF DAMAGE ON GM FOR DIFFERENT SHIPS

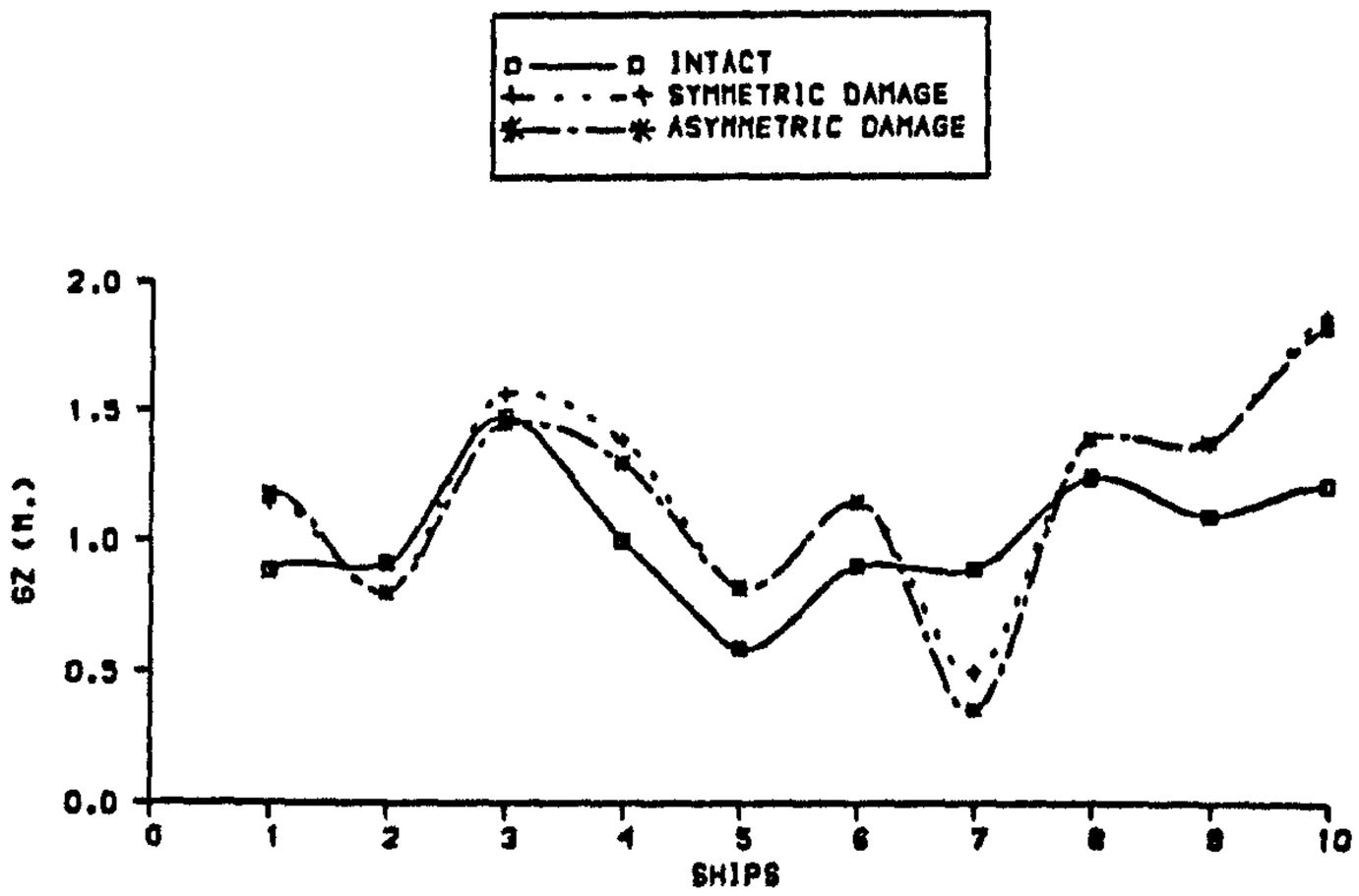

Fig 7.3 EFFECT OF DAMAGE ON MAXIMUM GZ FOR DIFFERENT SHIPS

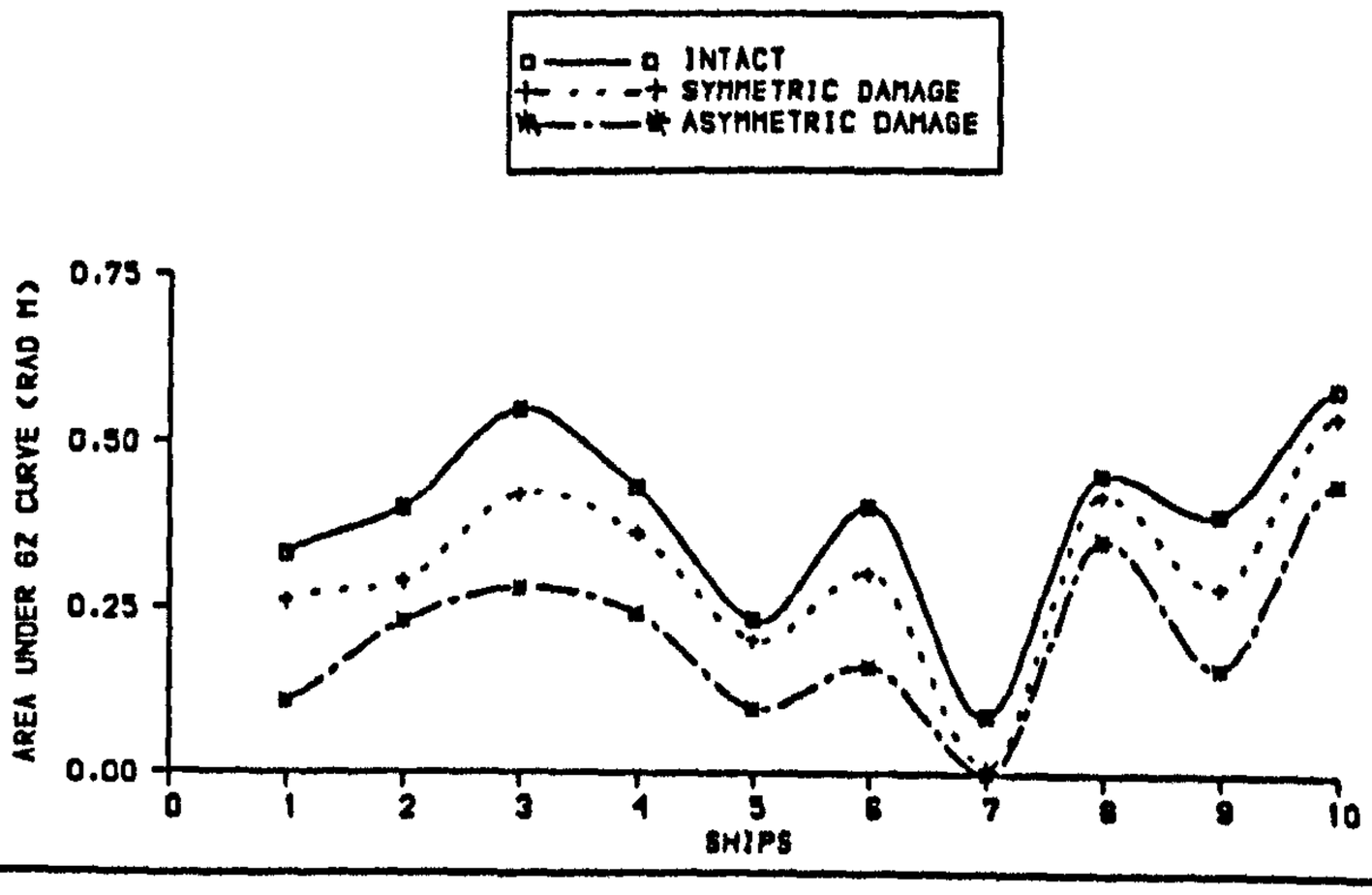

Fig 7.4 EFFECT OF DAMAGE ON AREA UNDER THE GZ CURVE UP TO DOWNFLOODING ANGLE FOR DIFFERENT SHIPS

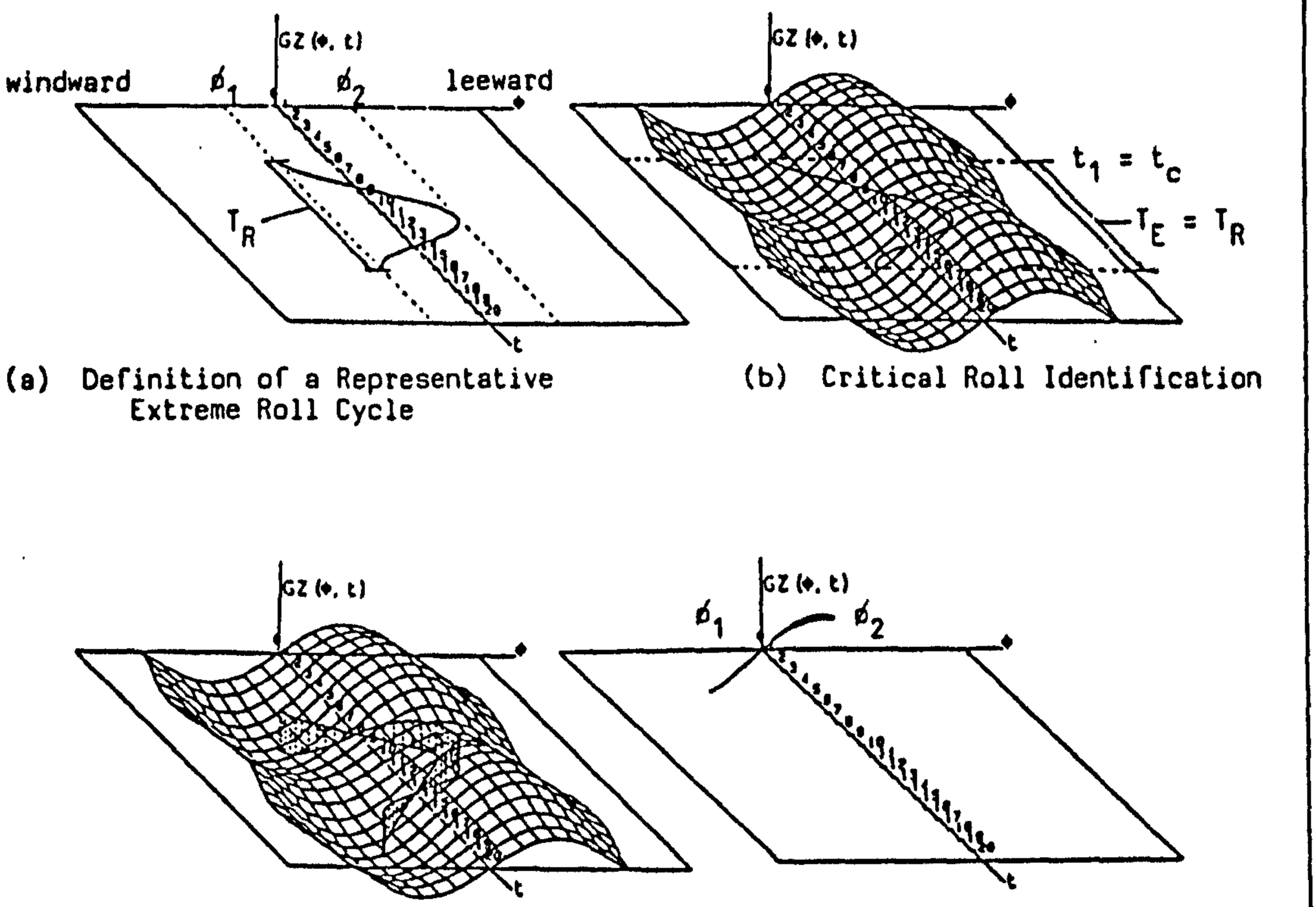

(a) Definition of a Representative Extreme Roll Cycle

(b) Critical Roll Identification

(c) Definition of GZ(ϕ,t) During the Critical Roll Cycle

(d) Representation of (c) on the Traditional GZ - ϕ Plane

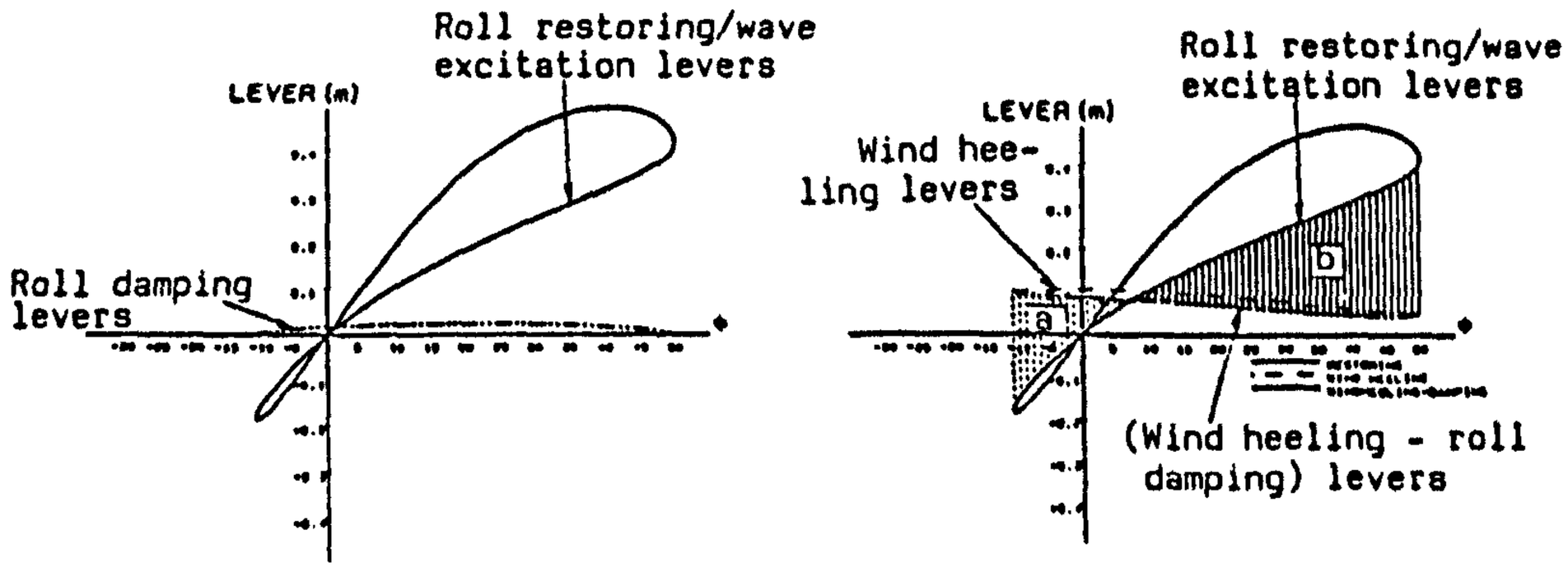

(e) Introduction of Other Time-varying Terms

(f) Introduction of Wind Heeling Excitation, and Energy Balance

Fig 7.5 Computational procedure of the Butterfly Diagram [30]

INTACT

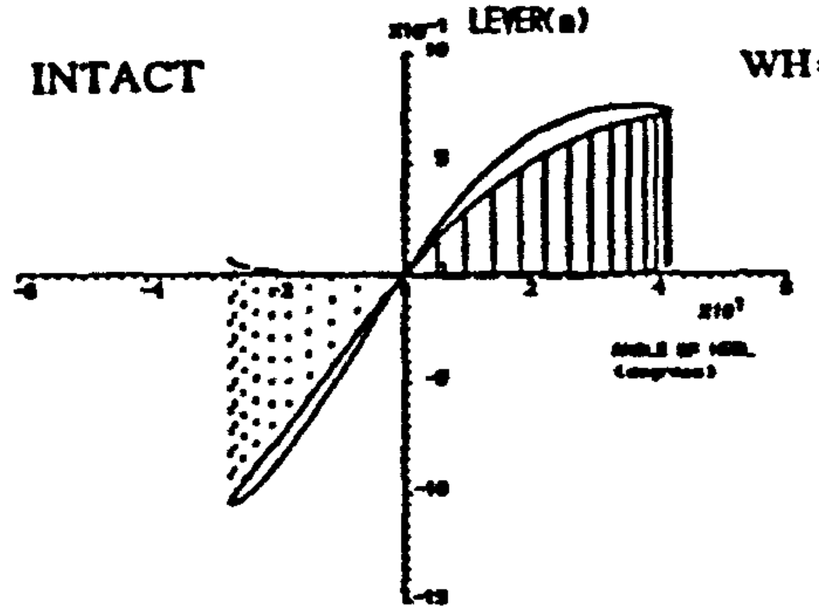

WH=3.0 m

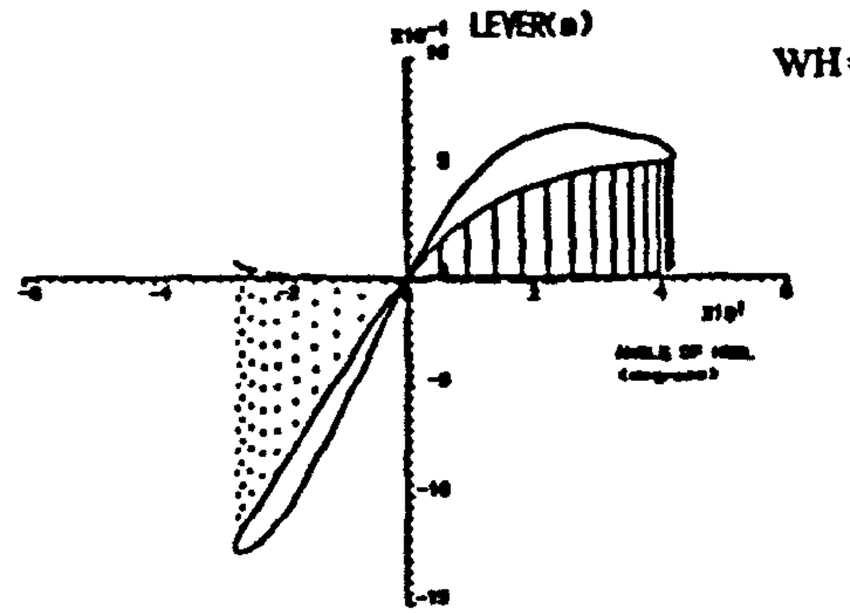

WH=5.0 m

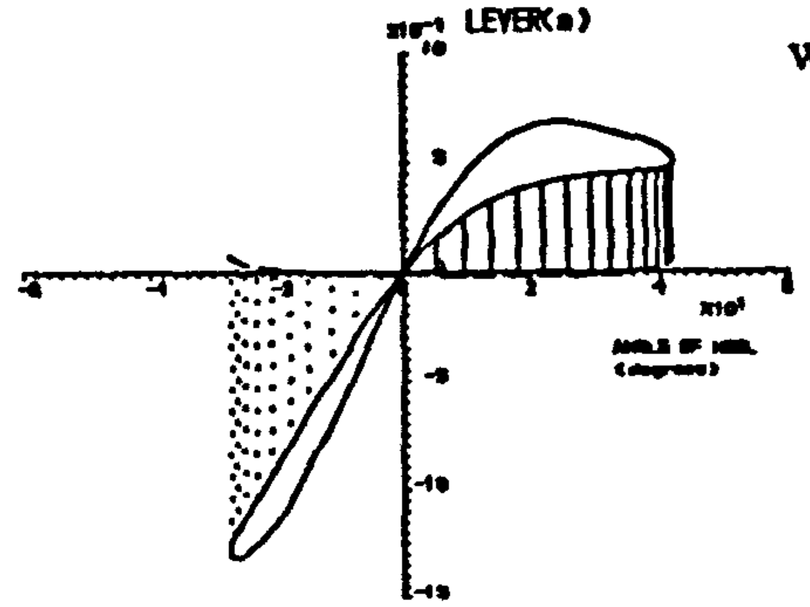

WH=7.0 m

SYMMETRIC DAMAGE

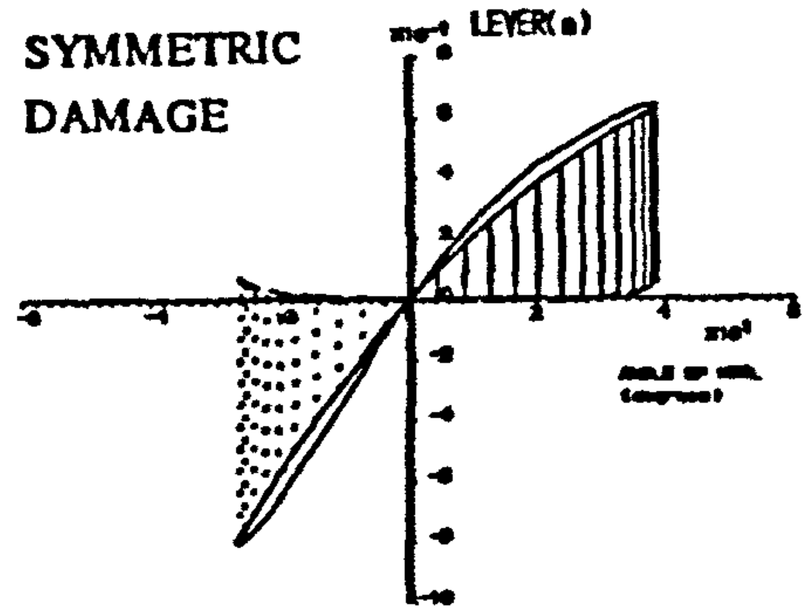

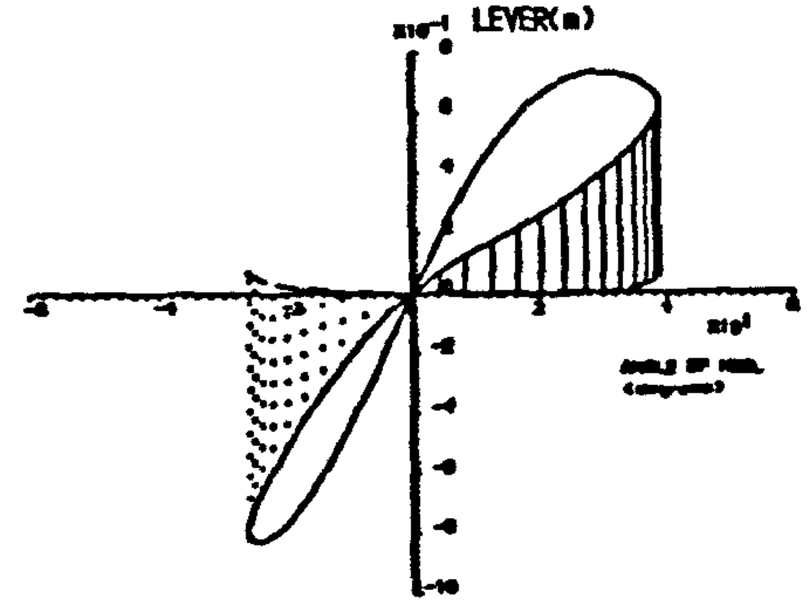

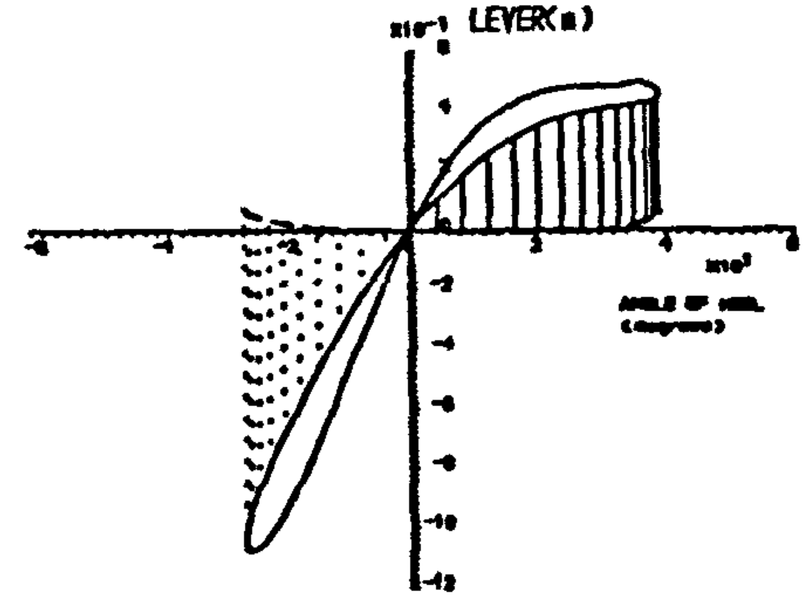

ASYMMETRIC DAMAGE

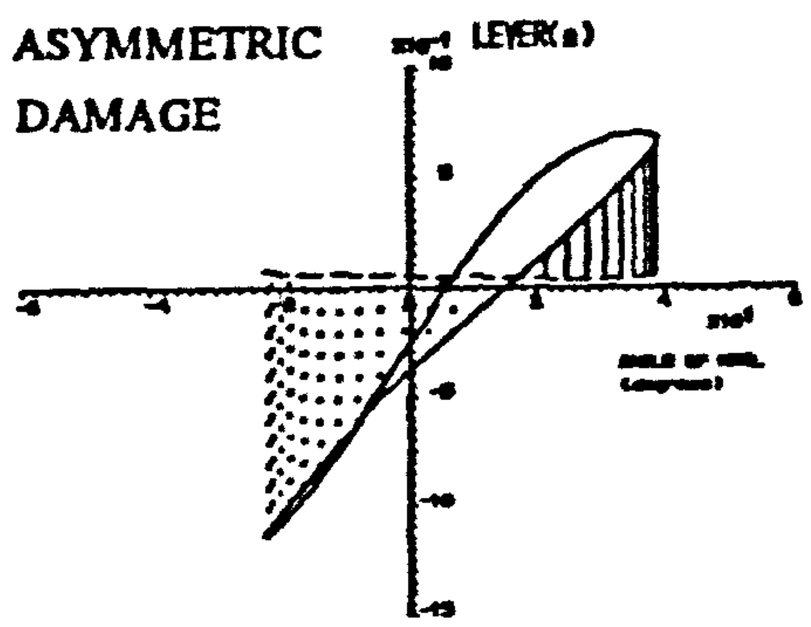

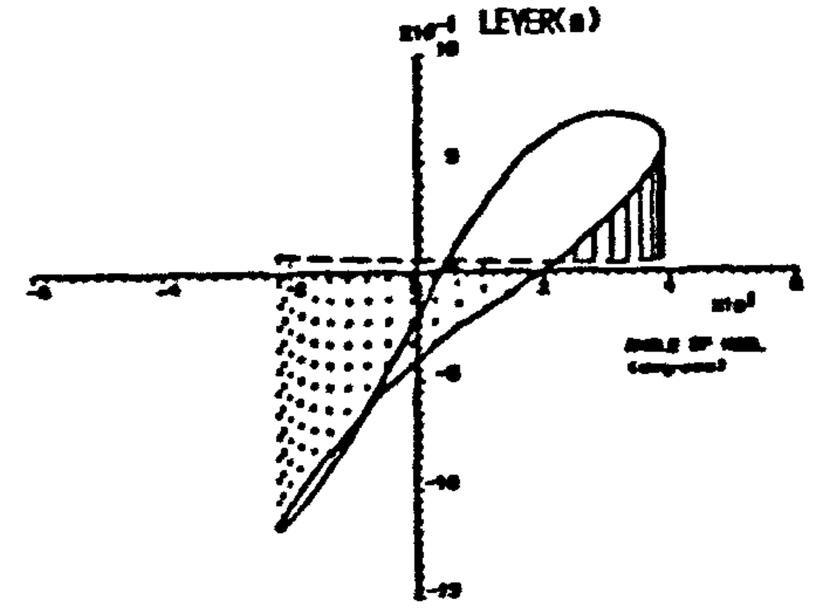

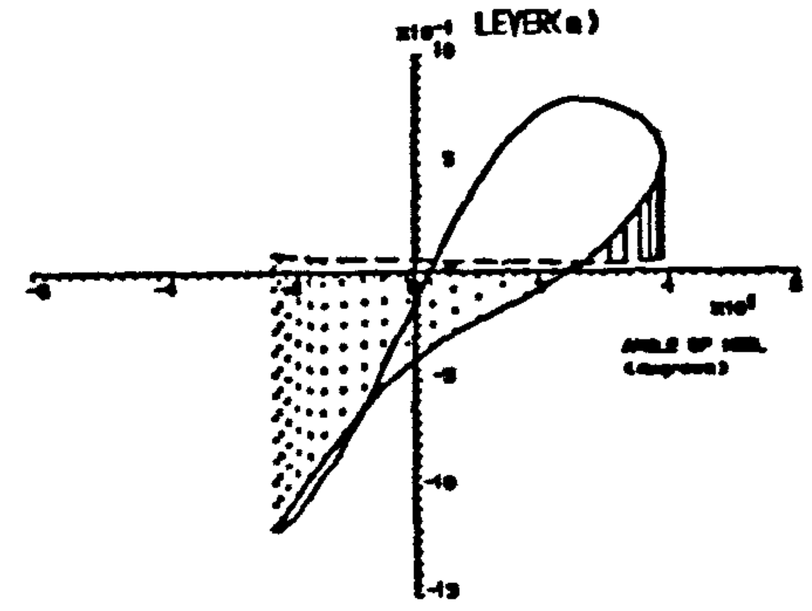

Fig 7.6 Stability of intact and damaged ship in waves [Strathclyde energy balance method, Ship 2]

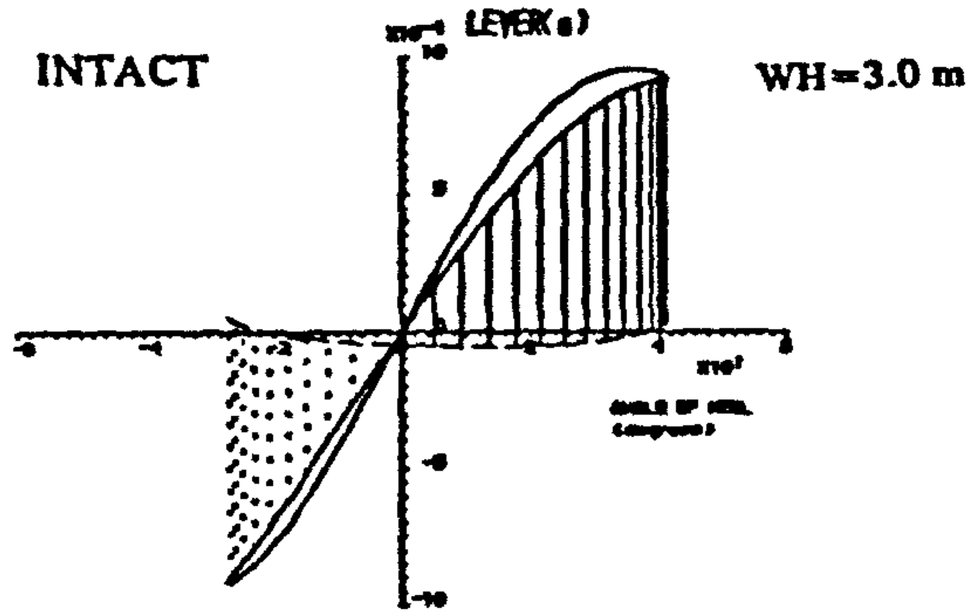

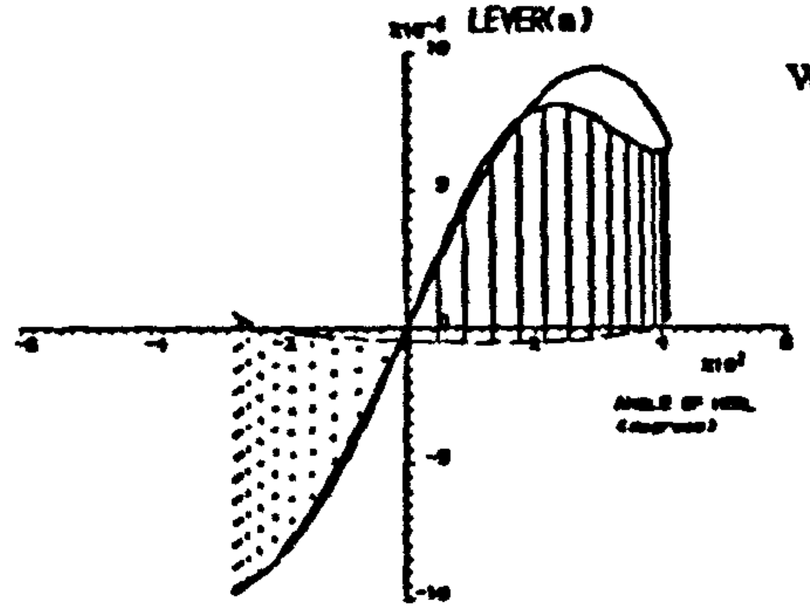

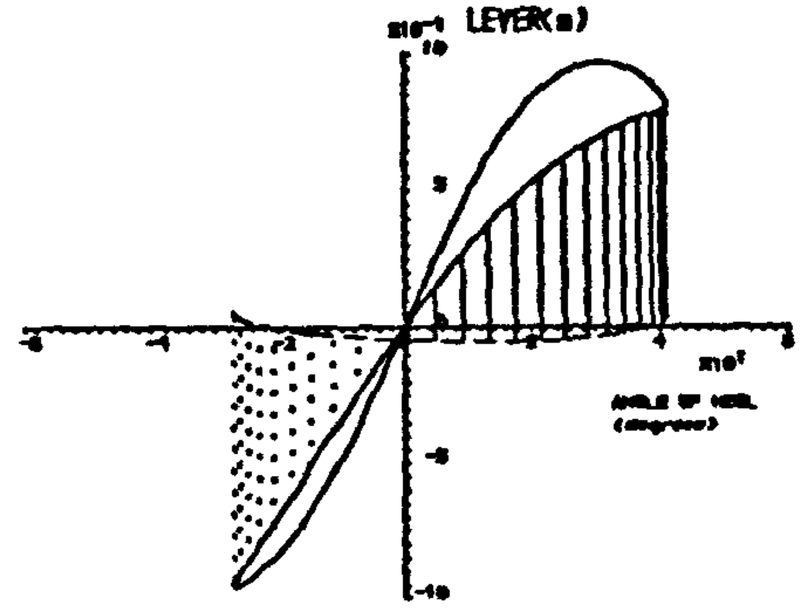

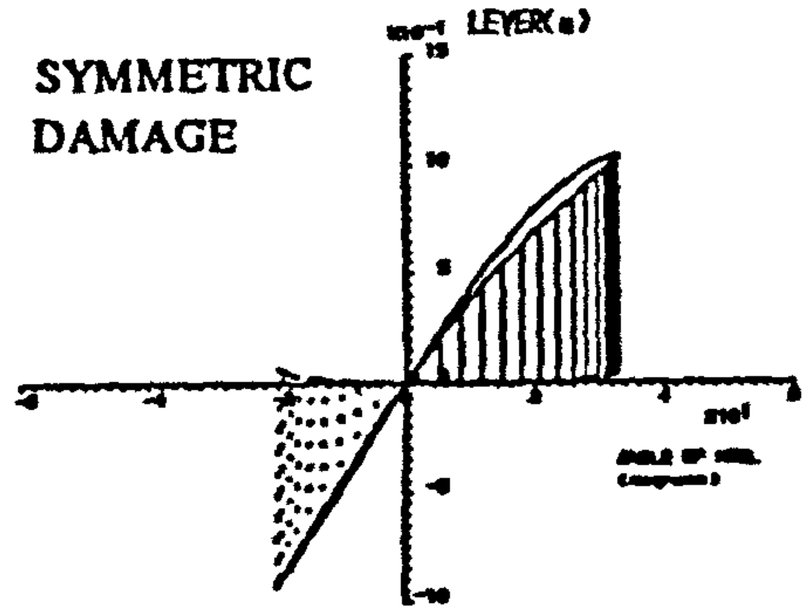

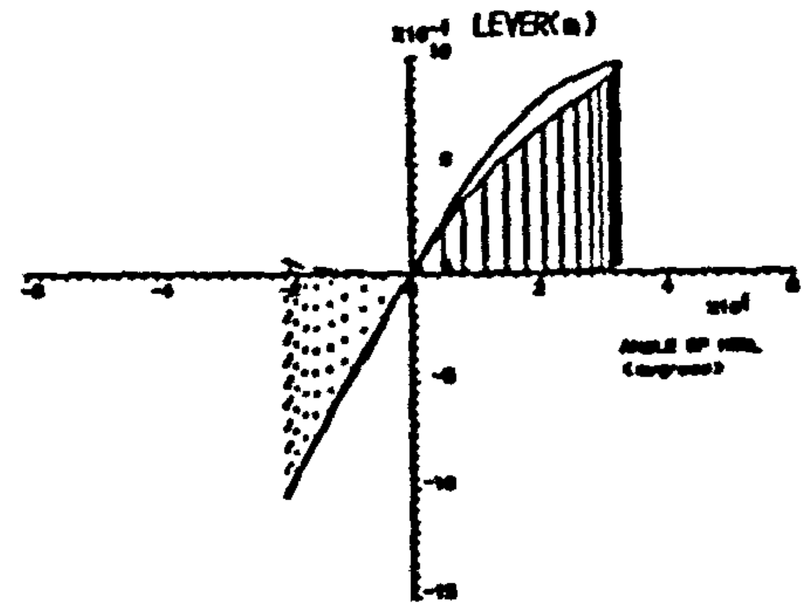

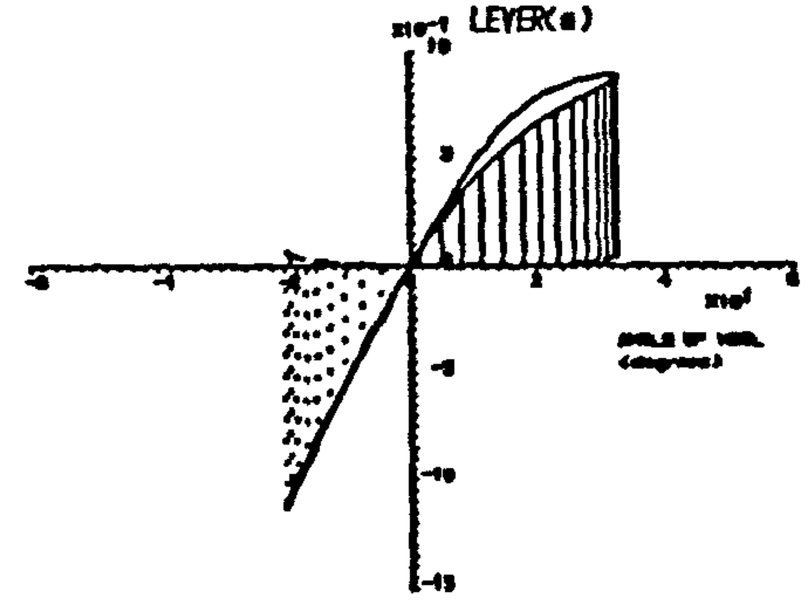

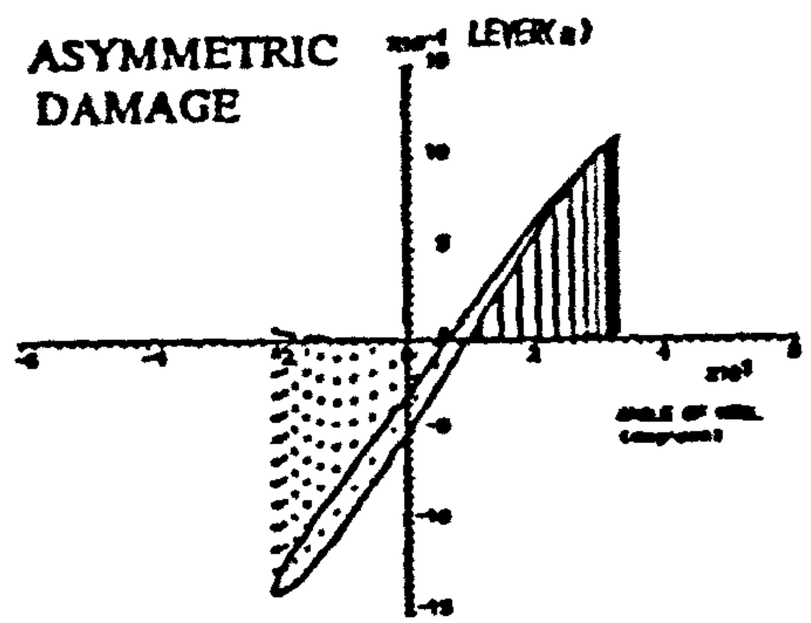

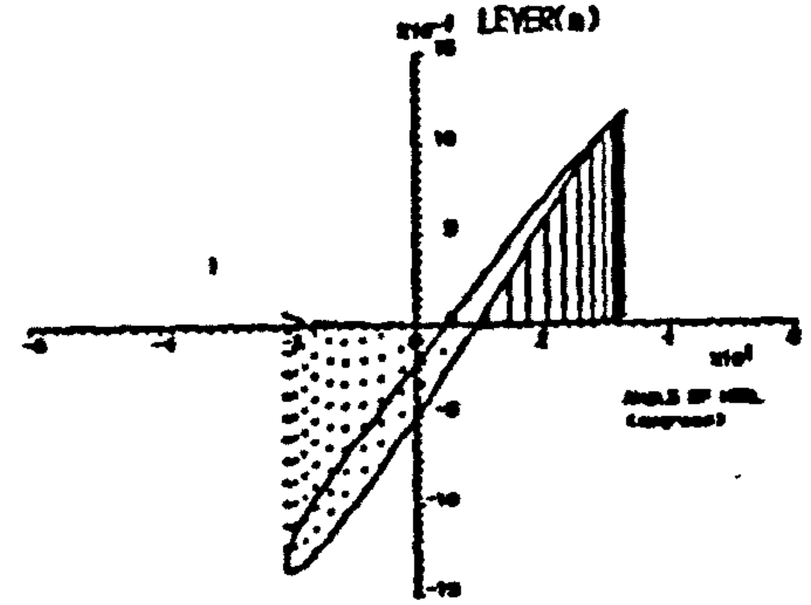

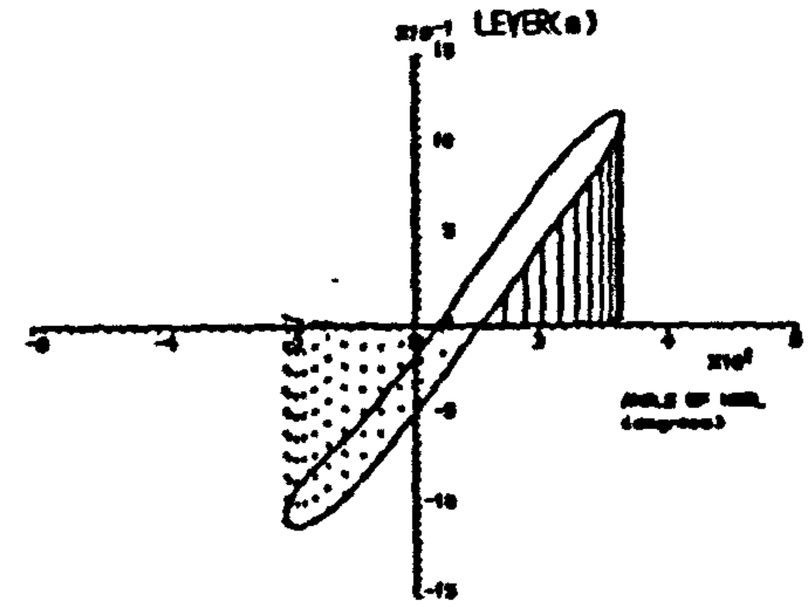

Fig 7.7 Stability of intact and damaged ship in waves [Strathclyde energy balance method, Ship 4]

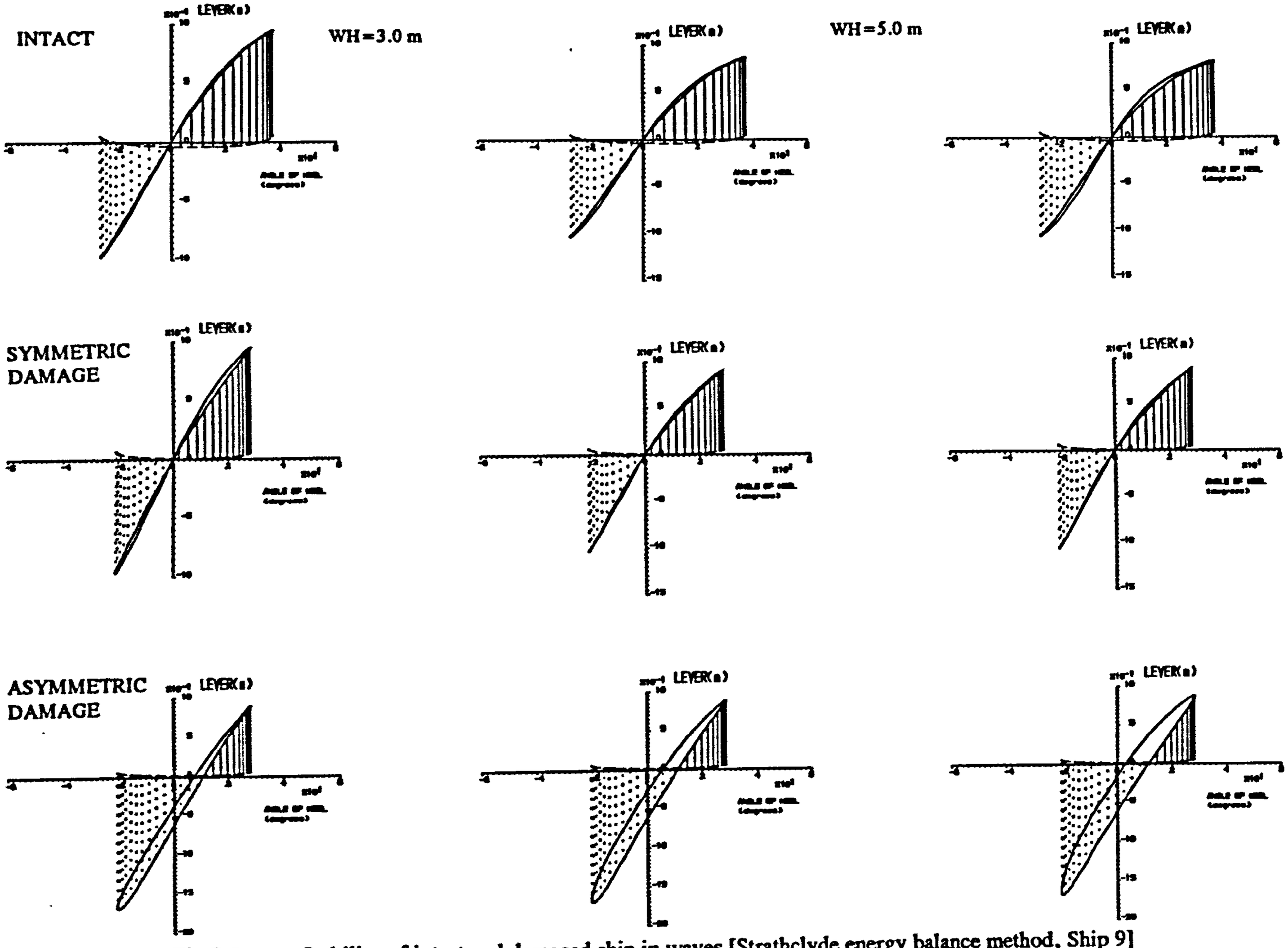

Fig 7.8 Stability of intact and damaged ship in waves [Strathclyde energy balance method, Ship 9]

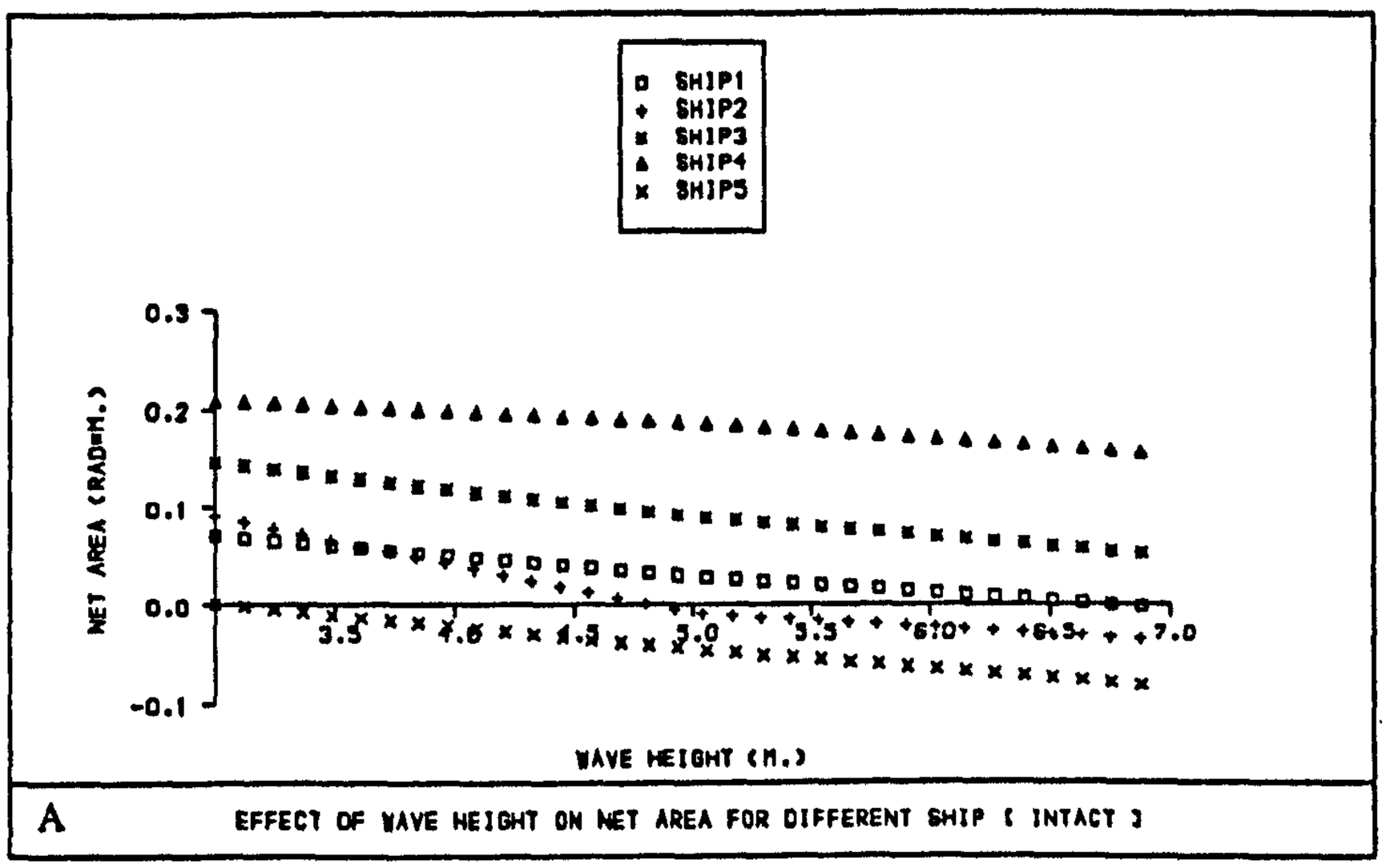

A EFFECT OF WAVE HEIGHT ON NET AREA FOR DIFFERENT SHIP (INTACT)

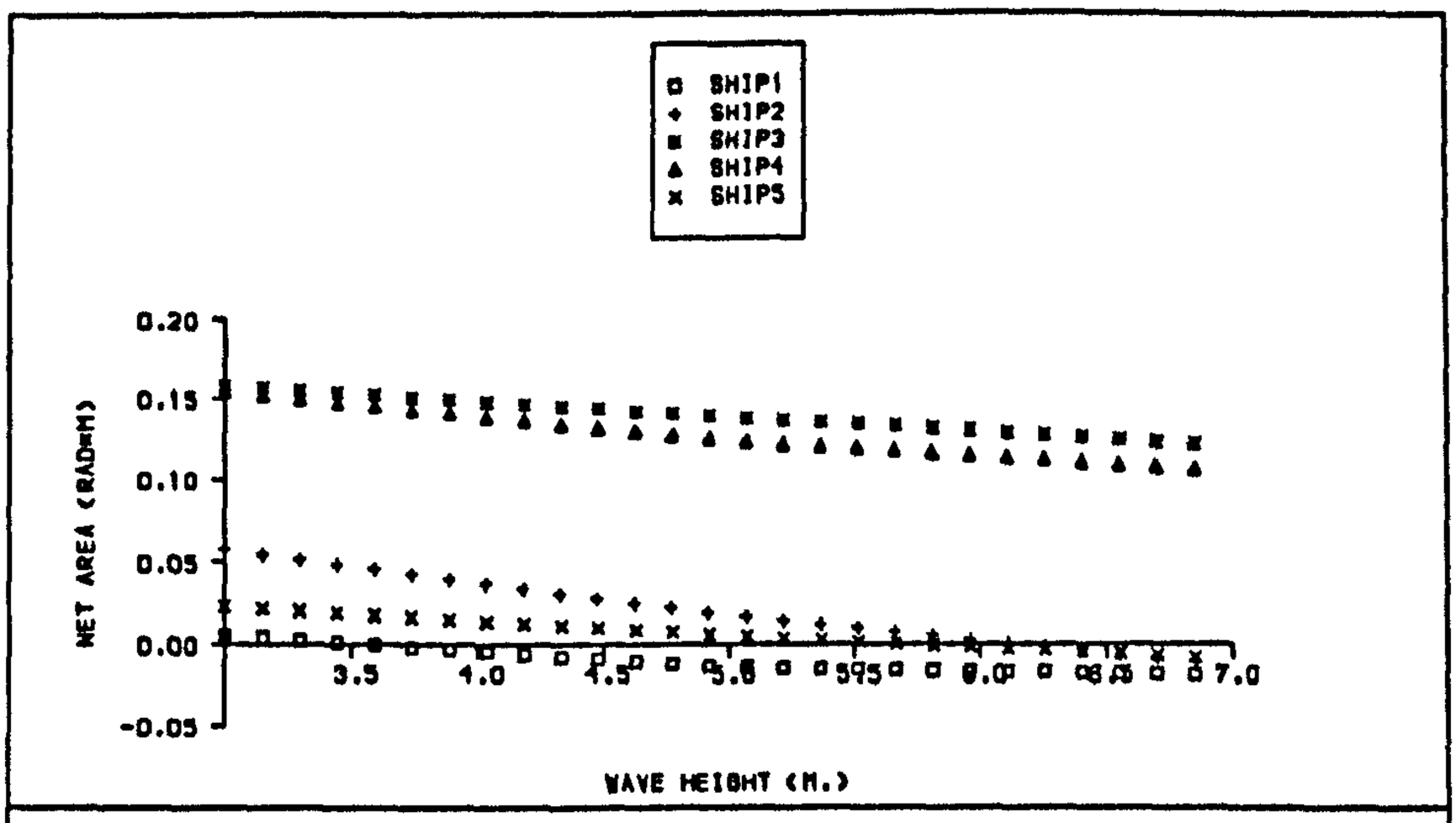

B EFFECT OF WAVE HEIGHT ON NET AREA FOR DIFFERENT SHIPS (SYMMETRIC DAMAGE)

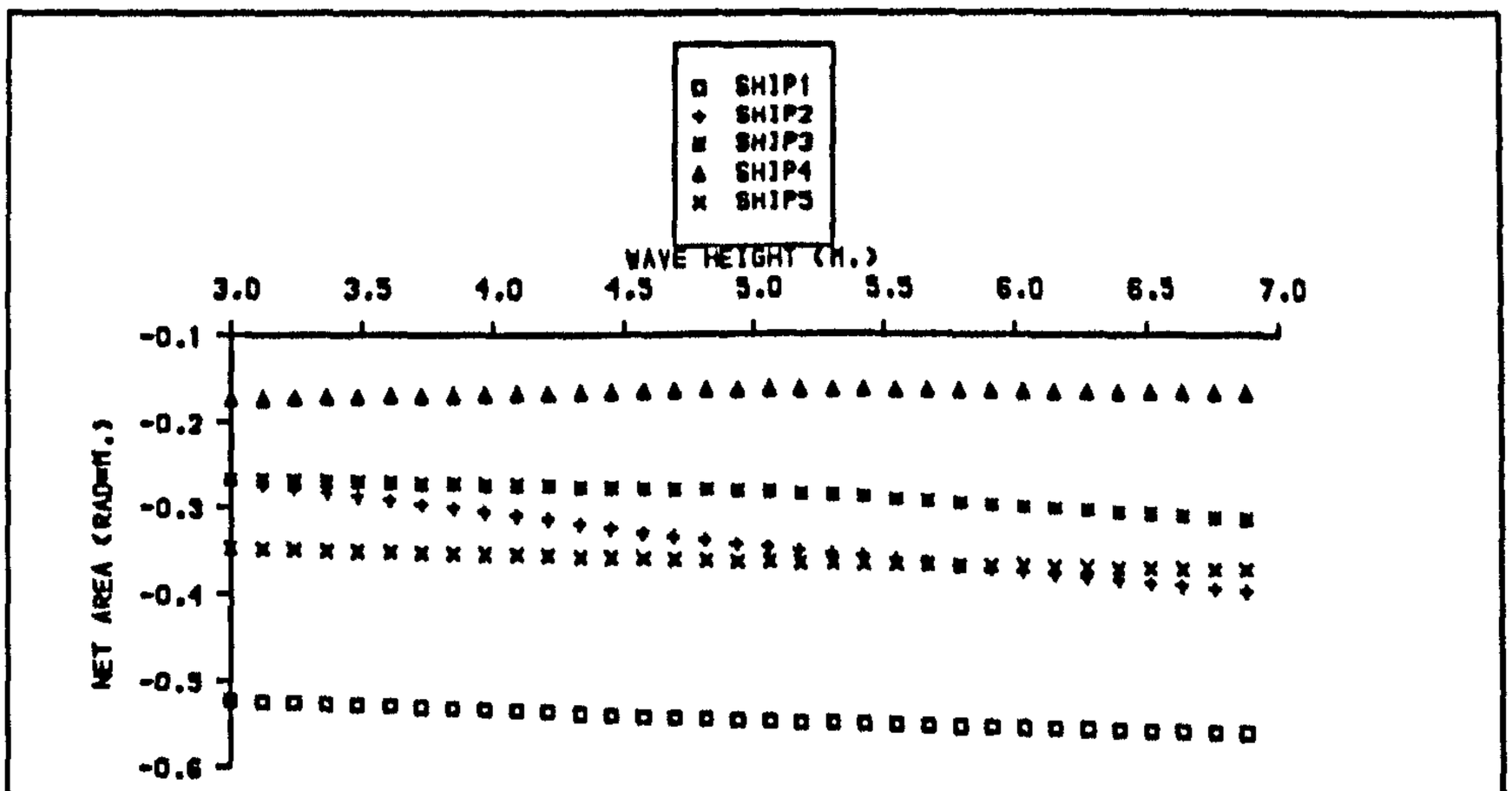

C EFFECT OF WAVE HEIGHT ON NET AREA FOR DIFFERENT SHIPS (ASYMMETRIC DAMAGE)

Fig 7.9 Effect of wave height on net area [Strathclyde Method, Ships 1-5]

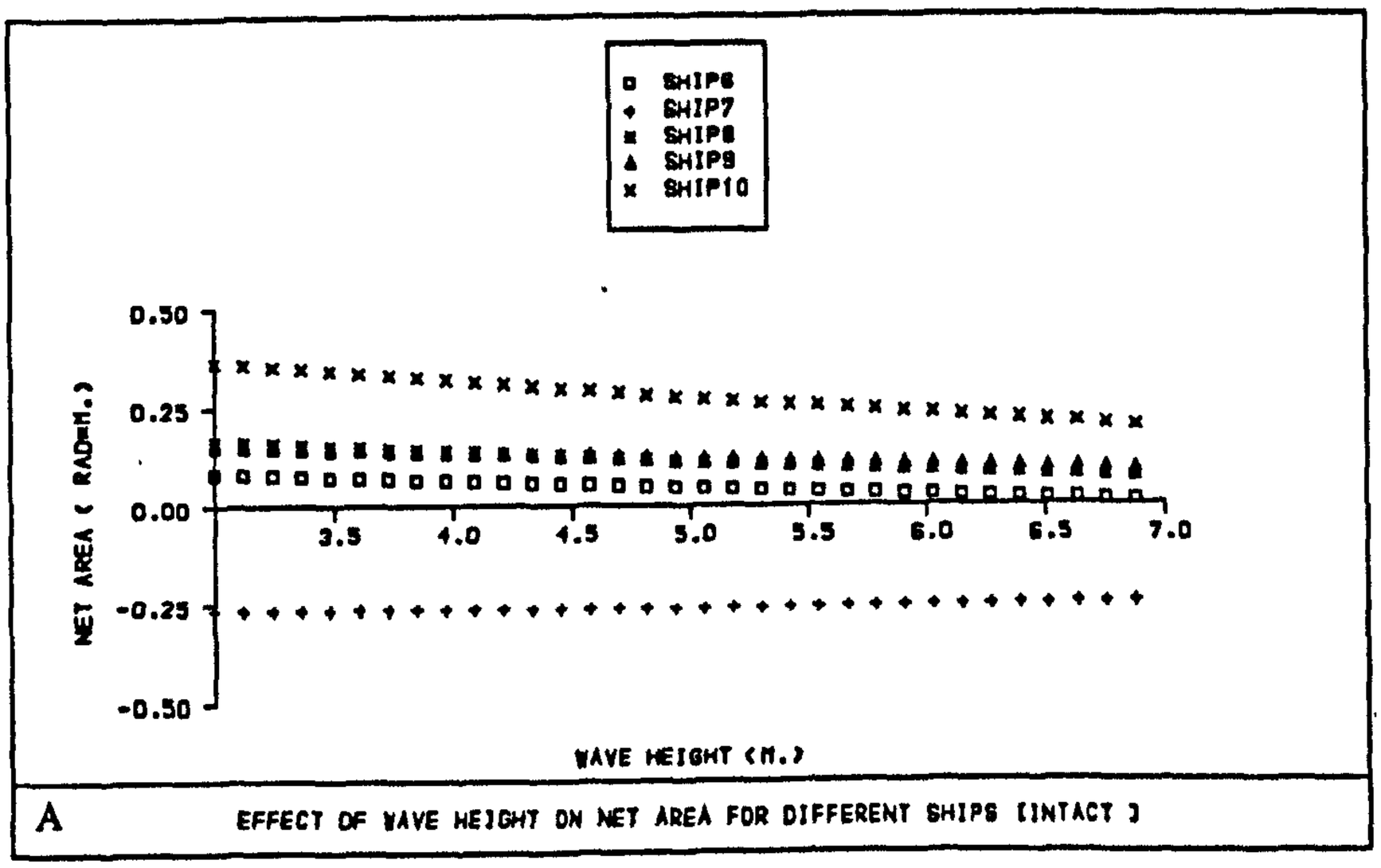

A EFFECT OF WAVE HEIGHT ON NET AREA FOR DIFFERENT SHIPS (INTACT)

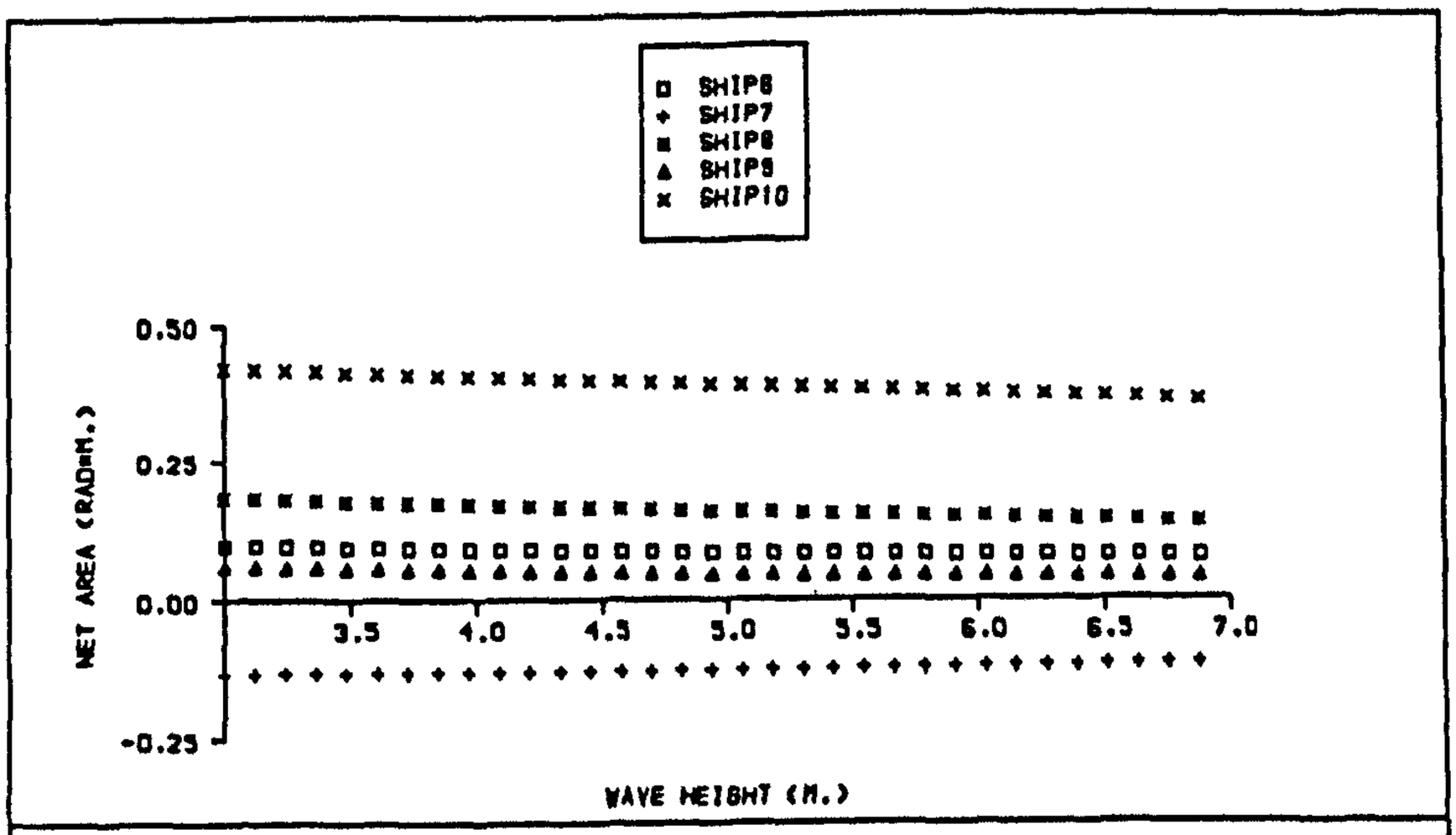

B EFFECT OF WAVE HEIGHT ON NET AREA FOR DIFFERENT SHIPS (SYMMETRIC DAMAGE)

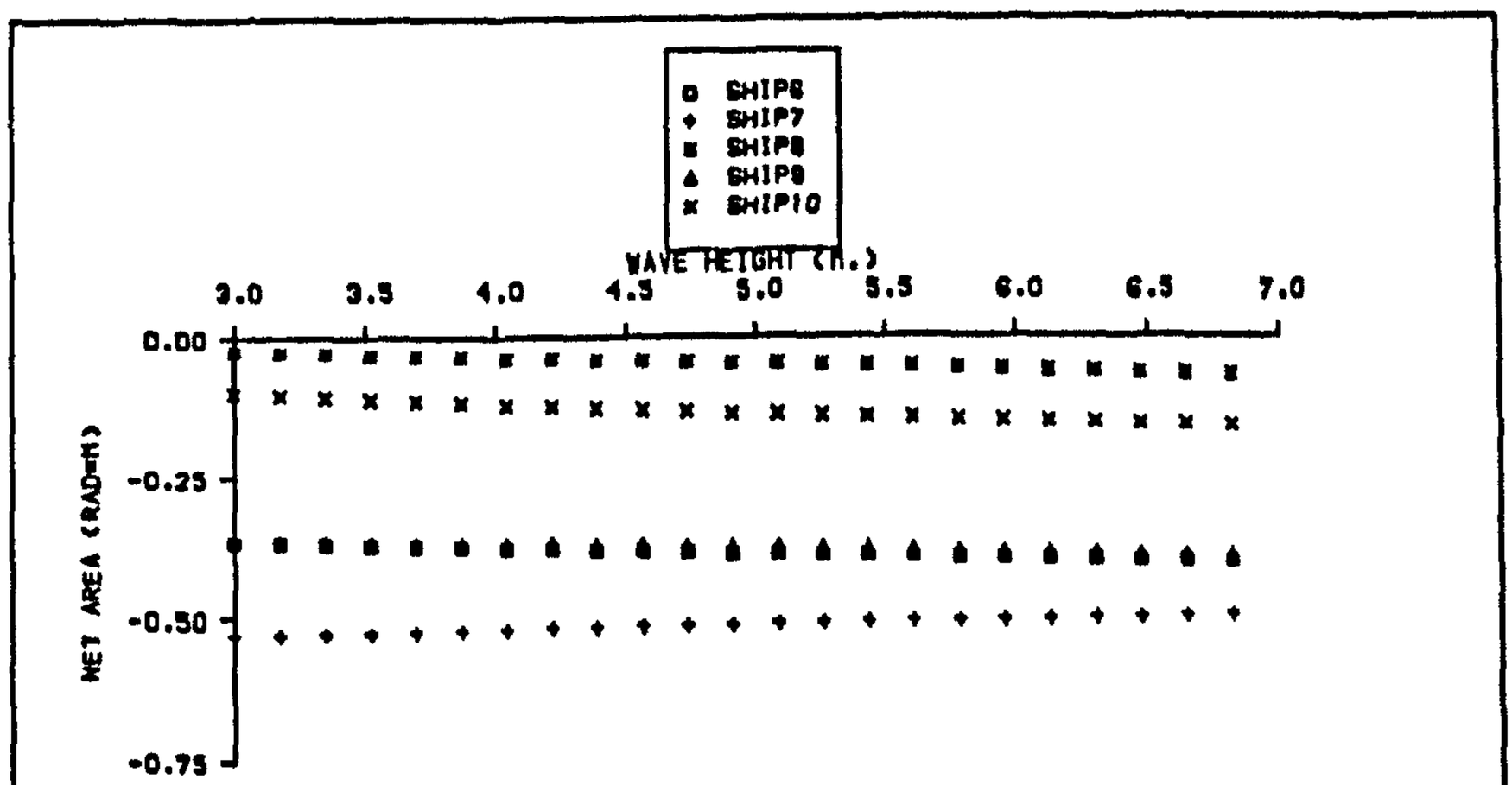

C EFFECT OF WAVE HEIGHT ON NET AREA FOR DIFFERENT SHIPS (ASYMMETRIC DAMAGE)

Fig 7.10 Effect of wave height on net area [Strathclyde Method, Ship 6-10]

	INTACT CONDITION				SYMMETRIC DAMAGE				ASYMMETRIC DAMAGE			
	STATIC STABILITY	QUASI-DYNAMIC STABILITY			STATIC STABILITY	QUASI-DYNAMIC STABILITY			STATIC STABILITY	QUASI-DYNAMIC STABILITY		
		NET AREA UNDER GZ CURVE BETWEEN ϕ_w AND ϕ_f				NET AREA UNDER GZ CURVE BETWEEN ϕ_w AND ϕ_f				NET AREA UNDER GZ CURVE BETWEEN ϕ_w AND ϕ_f		
	Area Under curve up to ϕ_f rad m	WH=3 m	WH=5 m	WH=7 m	Area Under curve up to ϕ_f rad m	WH=3 m	WH=5 m	WH=7 m	Area under curve up to ϕ_f rad m	WH=3 m	WH=5 m	WH=7 m
SHIP 1	0.330	0.071	0.028	-0.004	0.260	0.005	-0.011	-0.018	0.110	-0.530	-0.540	-0.550
SHIP 2	0.400	0.090	-0.009	-0.030	0.290	0.057	0.017	-0.013	0.224	-0.260	-0.345	-0.397
SHIP 3	0.550	0.146	0.090	0.050	0.420	0.150	0.130	0.120	0.279	-0.267	-0.280	-0.310
SHIP 4	0.430	0.208	0.185	0.153	0.367	0.153	0.125	0.105	0.240	-0.173	-0.160	-0.160
SHIP 5	0.230	0.001	-0.040	-0.083	0.200	0.023	0.005	-0.008	0.100	-0.340	-0.360	-0.370
SHIP 6	0.400	0.084	0.045	0.010	0.300	0.097	0.083	0.075	0.160	-0.360	-0.380	-0.400
SHIP 7	0.088	-0.266	-0.266	-0.240	0.010	-0.130	-0.120	-0.114	-	-0.530	-0.510	-0.490
SHIP 8	0.450	0.162	0.109	-0.068	0.420	0.184	0.158	0.137	0.355	-0.025	-0.048	-0.070
SHIP 9	0.390	0.148	0.117	0.090	0.285	0.061	0.046	0.041	0.160	-0.360	-0.370	-0.390
SHIP 10	0.500	0.363	0.270	0.190	0.54	0.420	0.380	0.357	0.440	-0.099	-0.130	-0.1612

Table 7.1

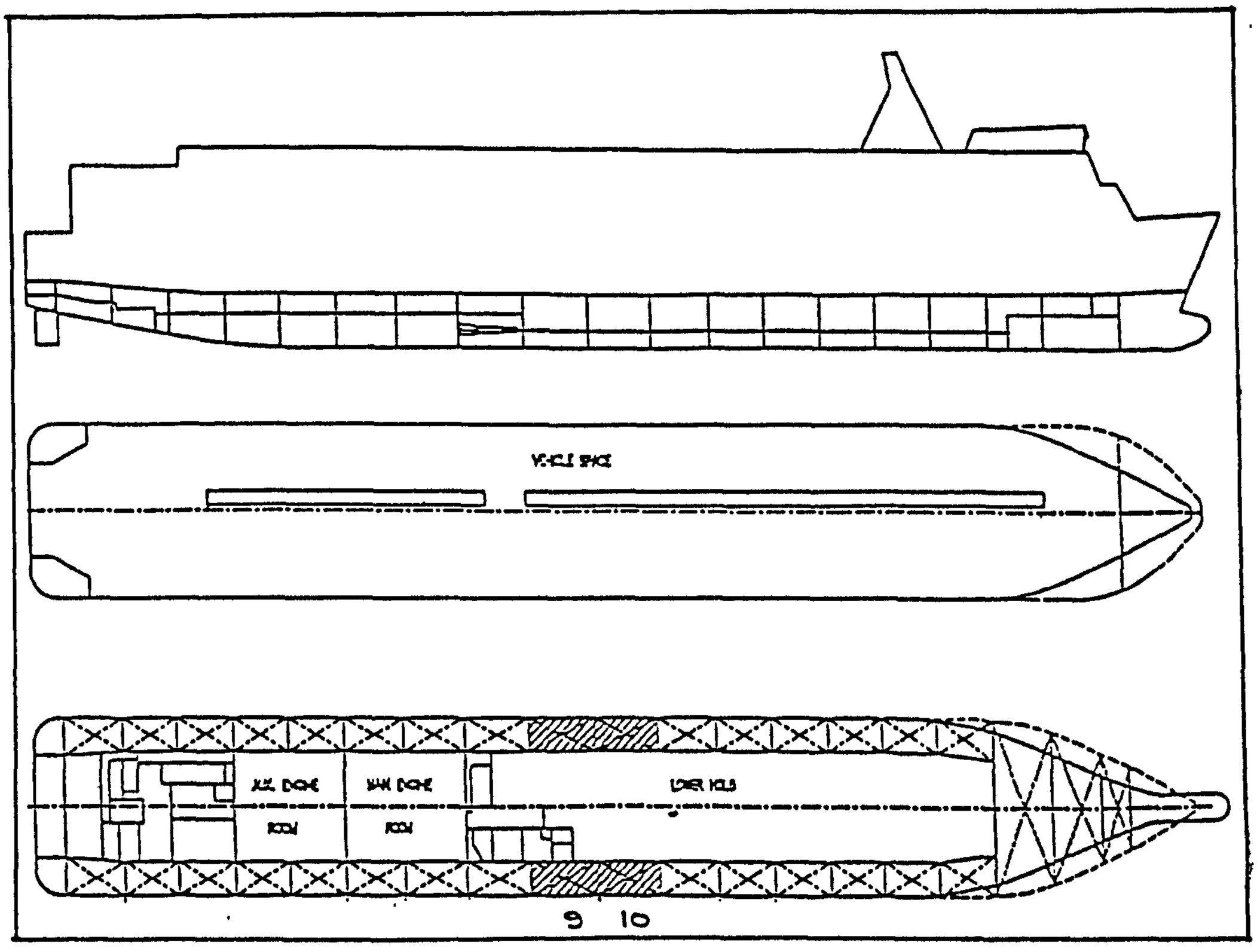

Fig 7.11A General and subdivision arrangement of sample ship. Shaded area(9, 10) shows the most critical damage according to stability regulations

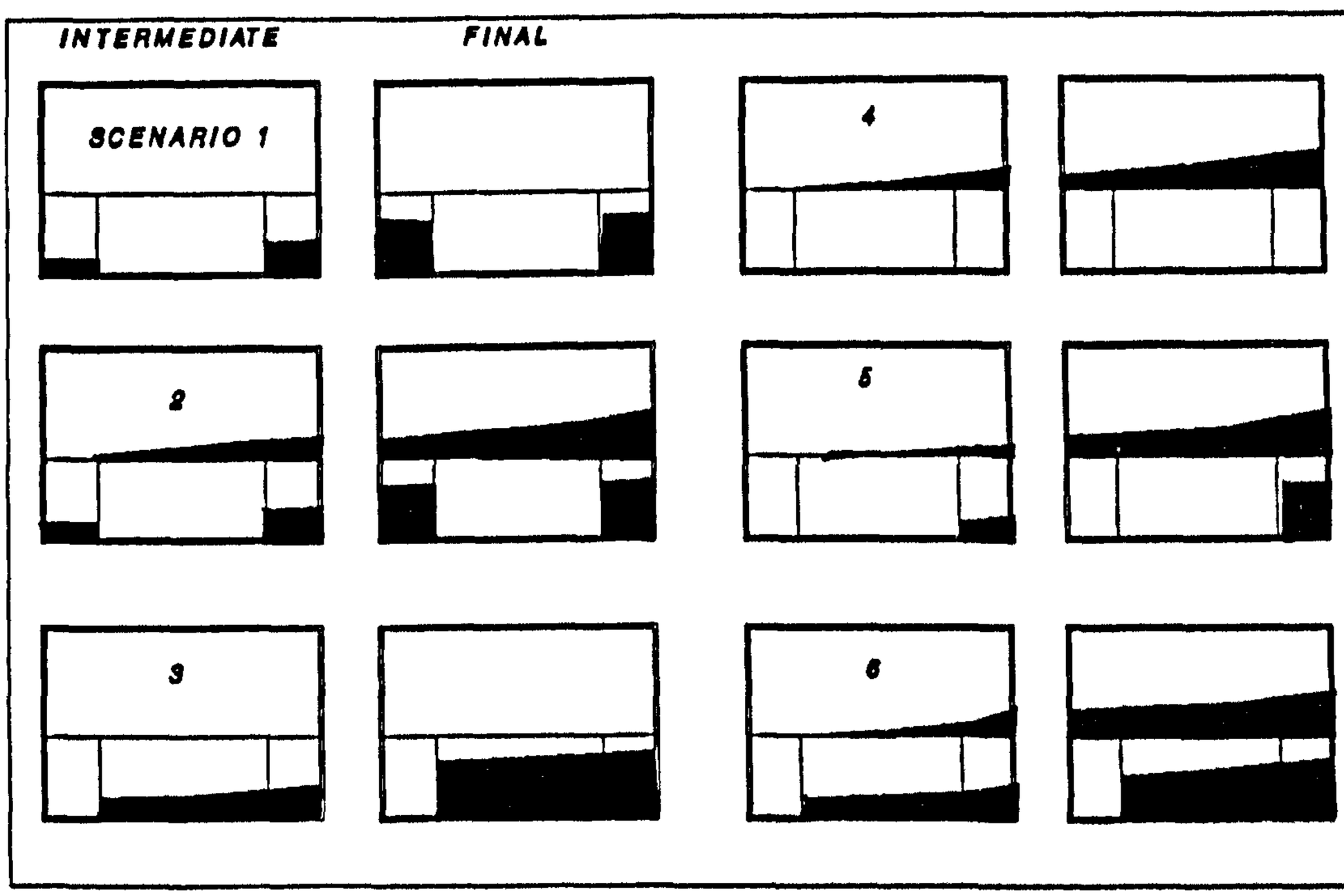

Fig 7.11B Damage scenarios at intermediate and final stages of flooding

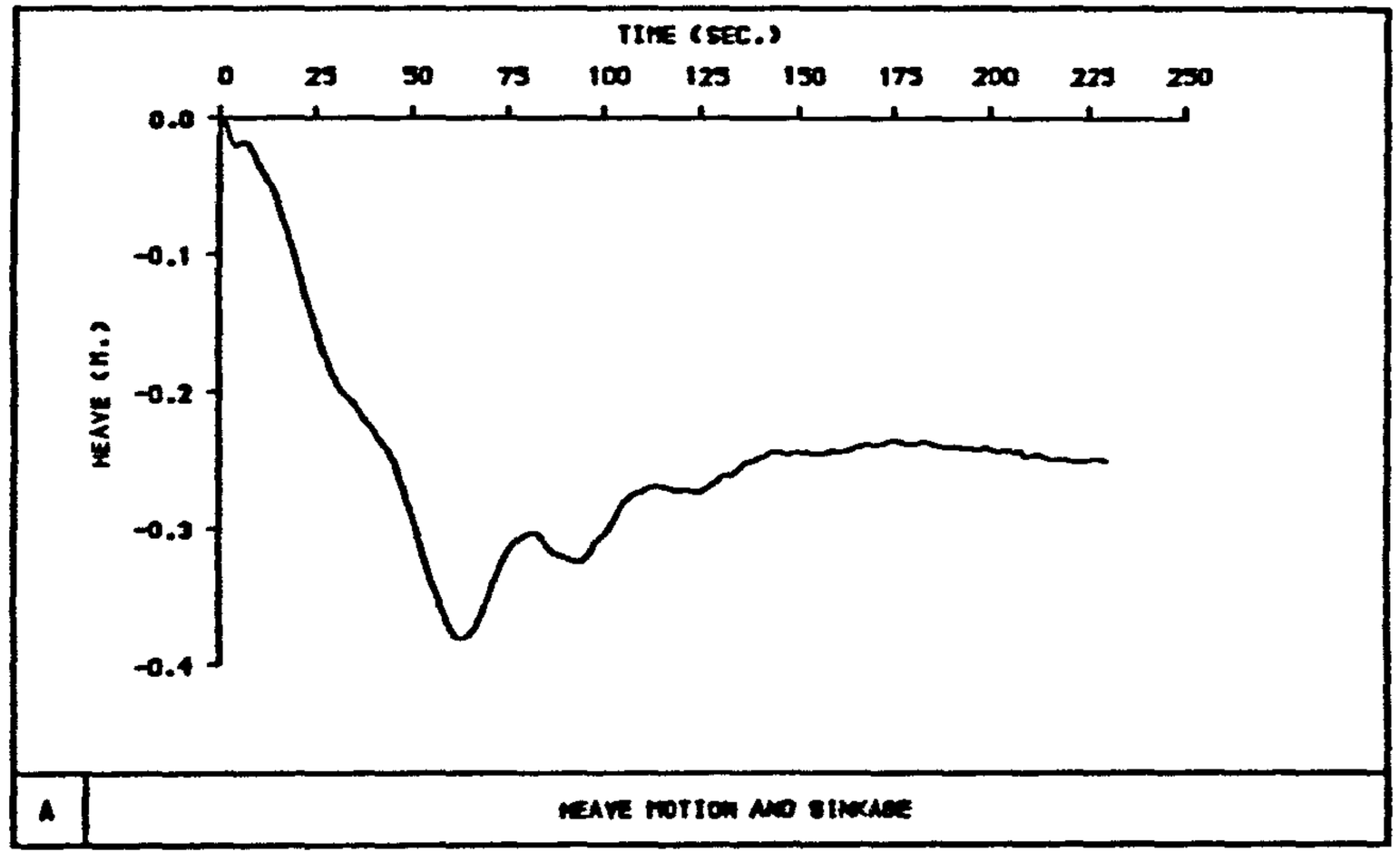

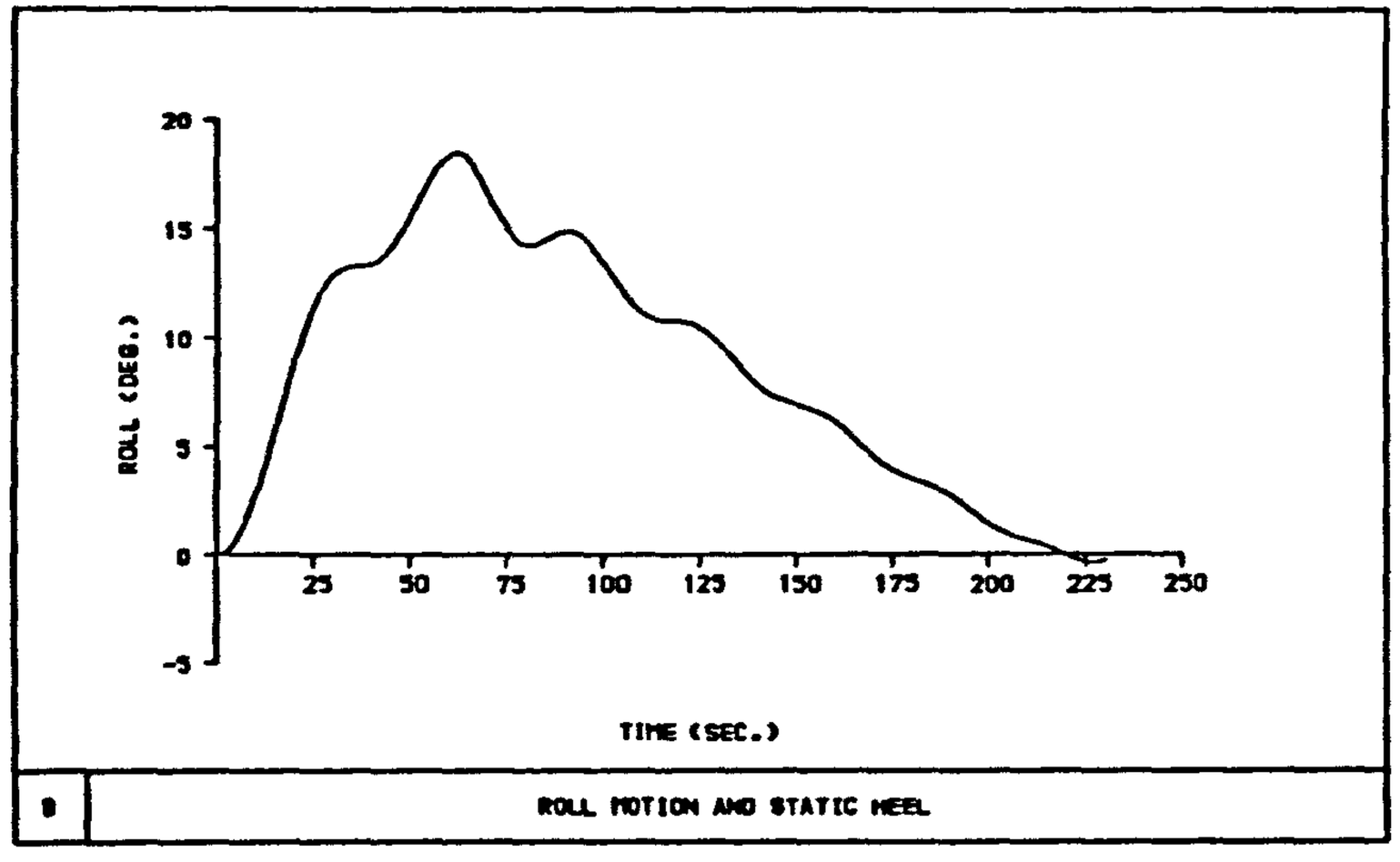

Fig 7.12 Time histories of ship motions and transverse centre of gravity of water on deck during progressive flooding, KG= 13.34 m, calm water [DAMAGE SCENARIO 1]

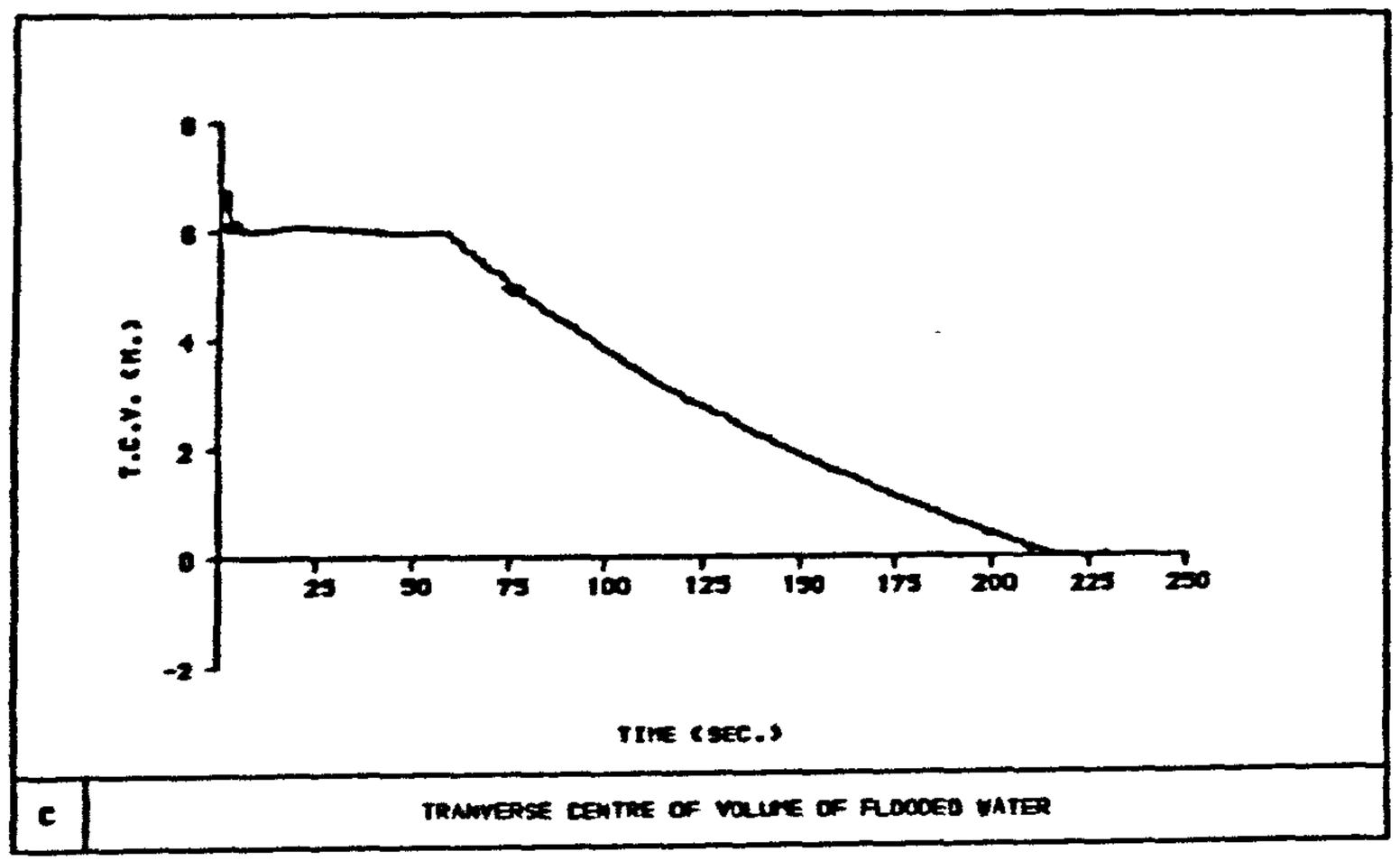

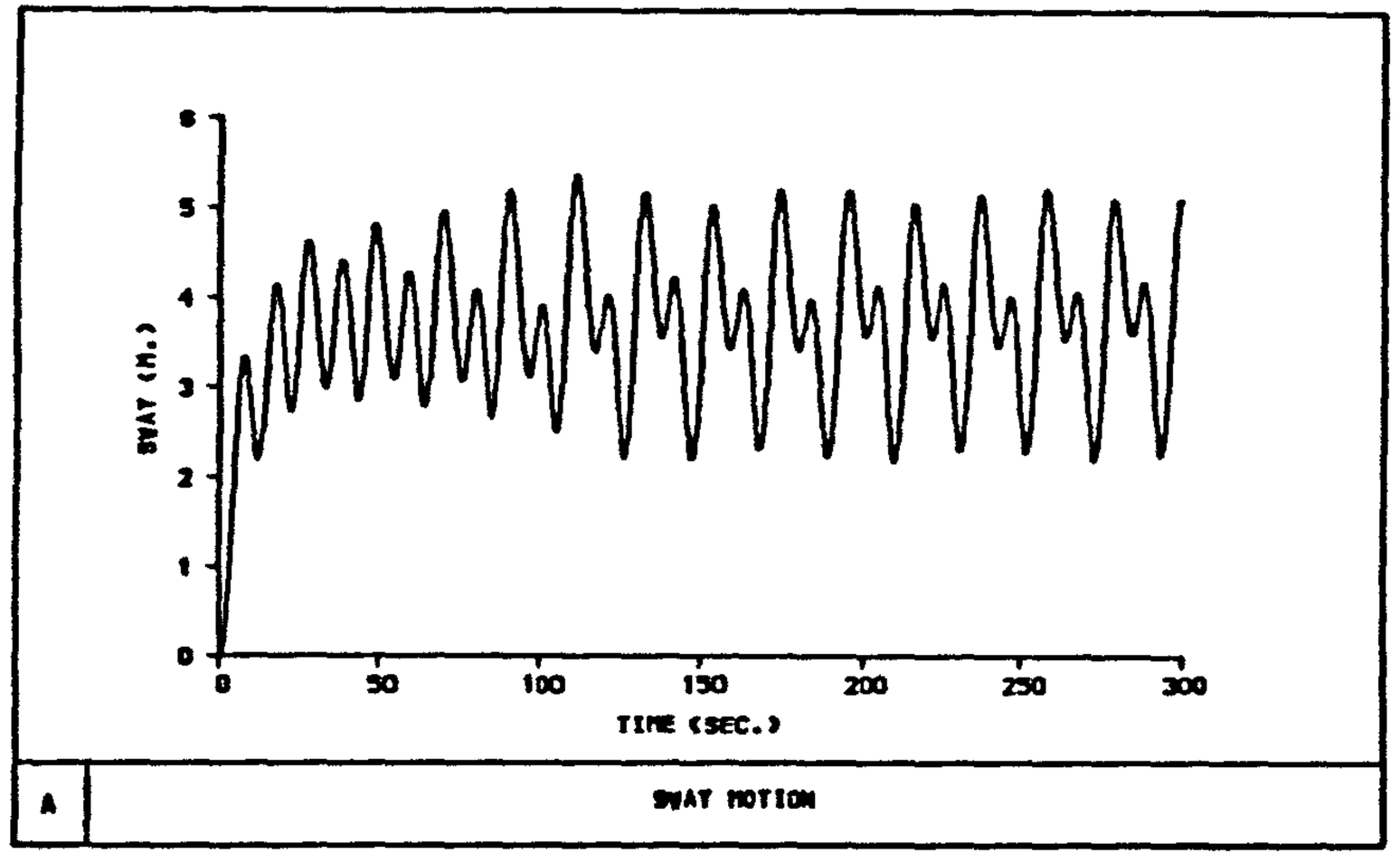

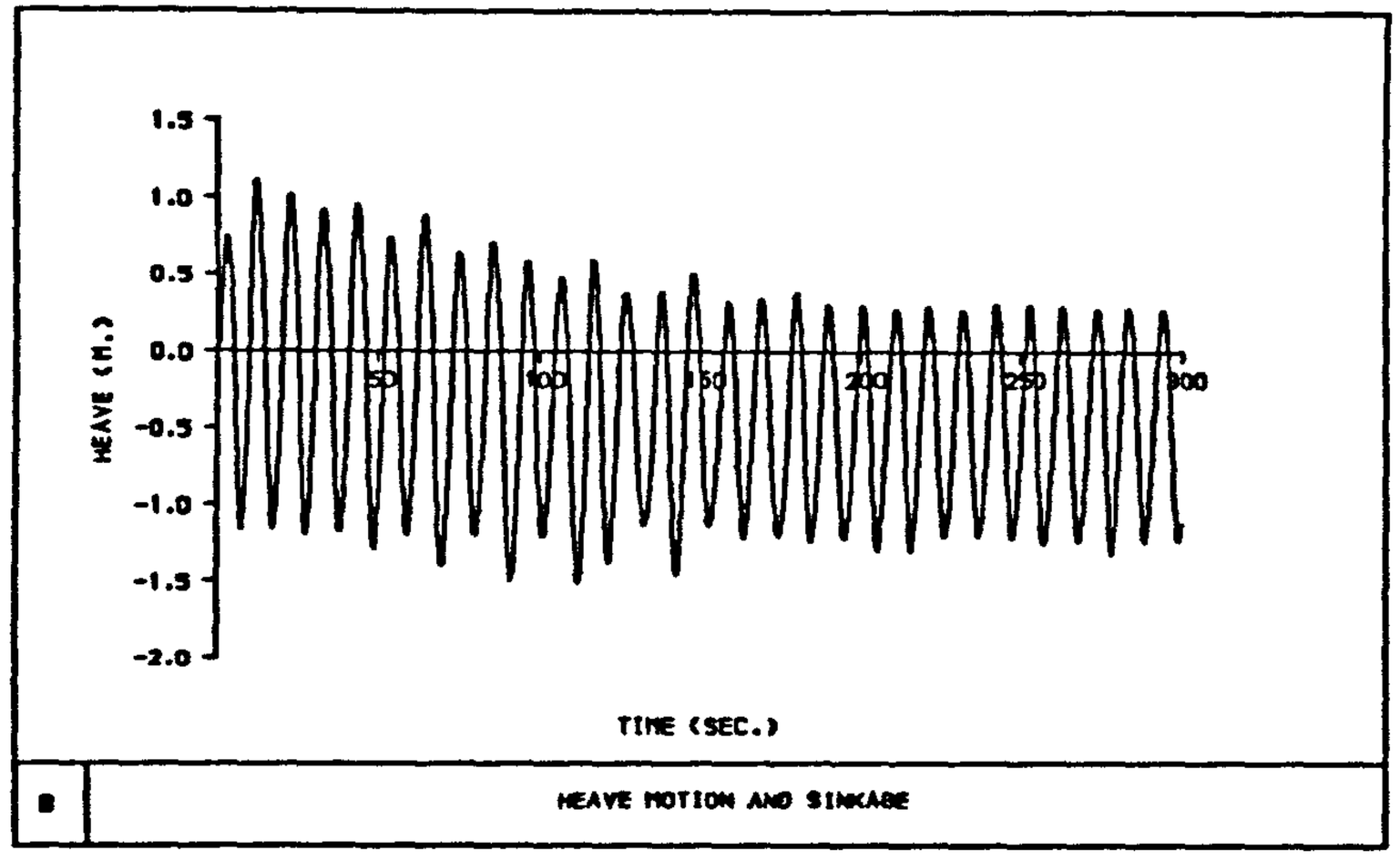

Fig 7.13 Time histories of ship motions and transverse centre of gravity of water on deck during progressive flooding, KG= 12.59 m, WH= 2.0 m [DAMAGE SCENARIO 1]

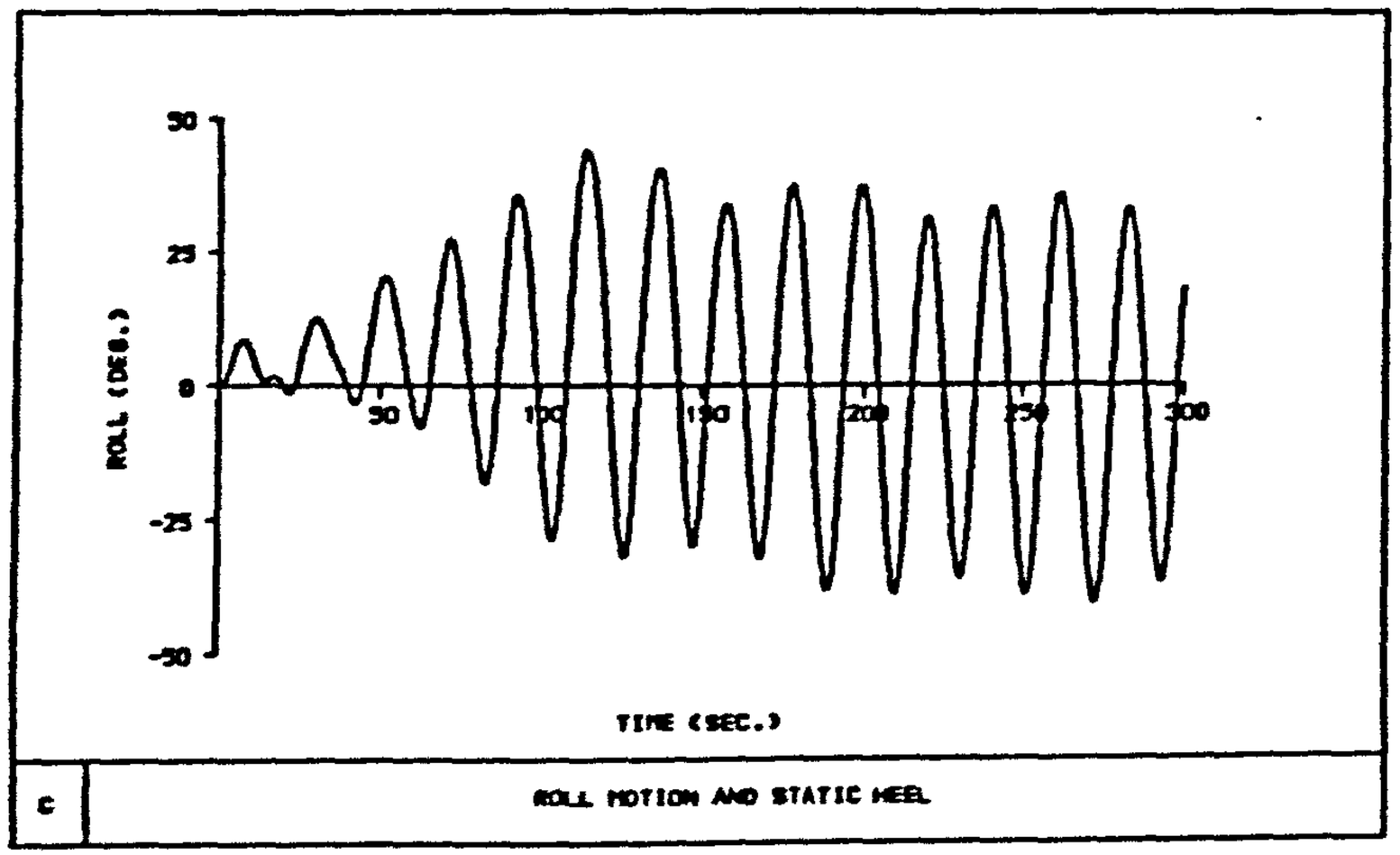

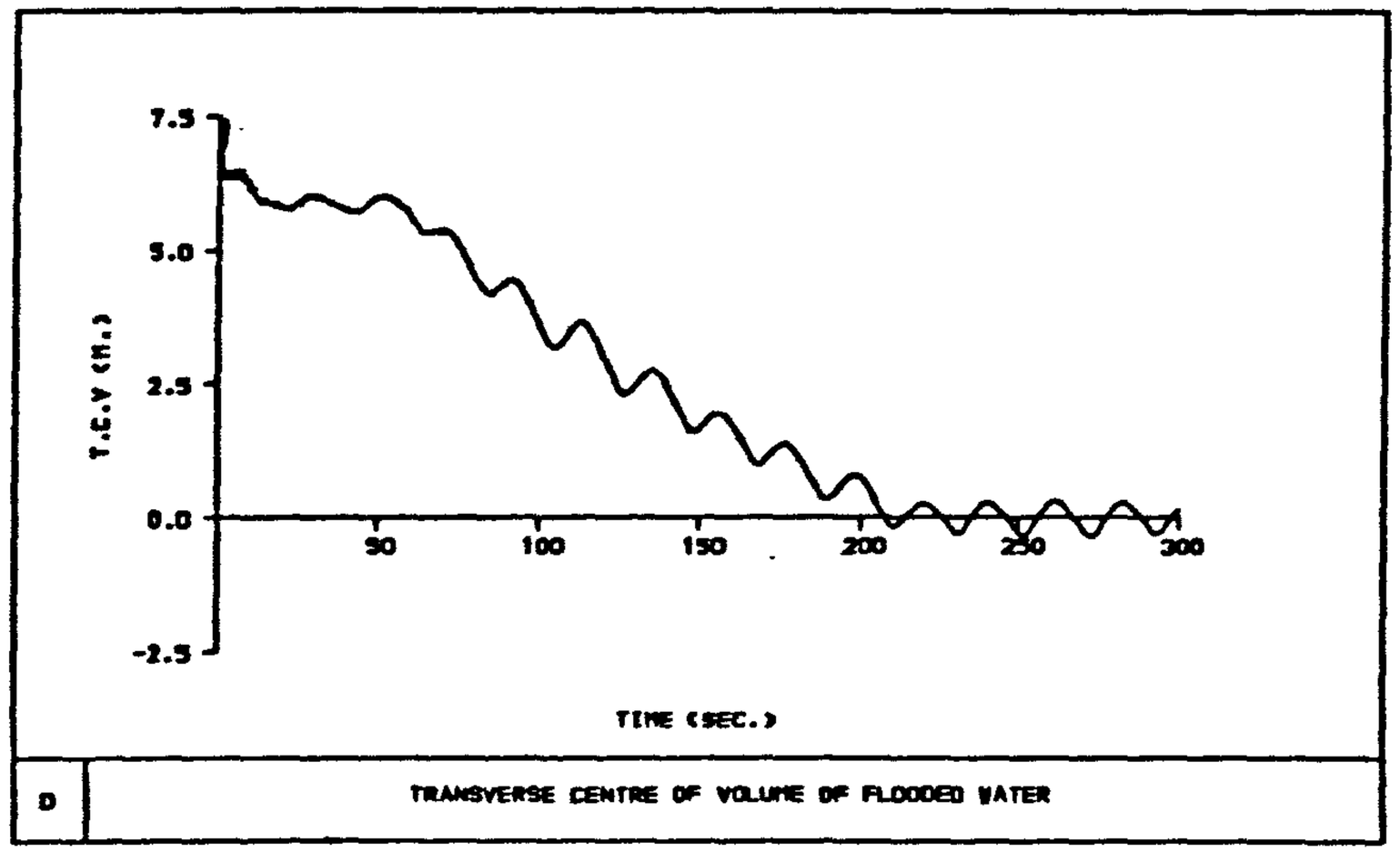

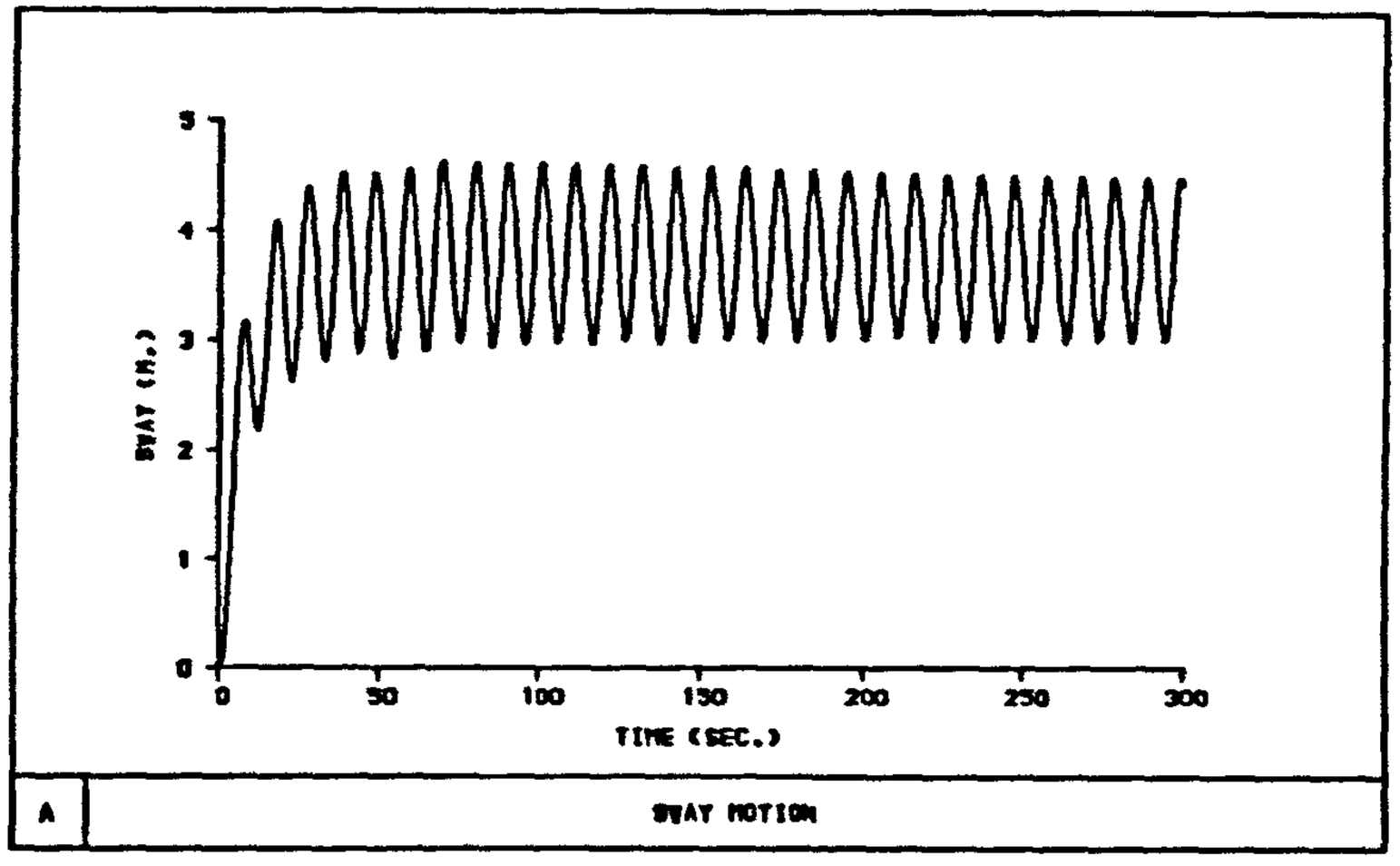

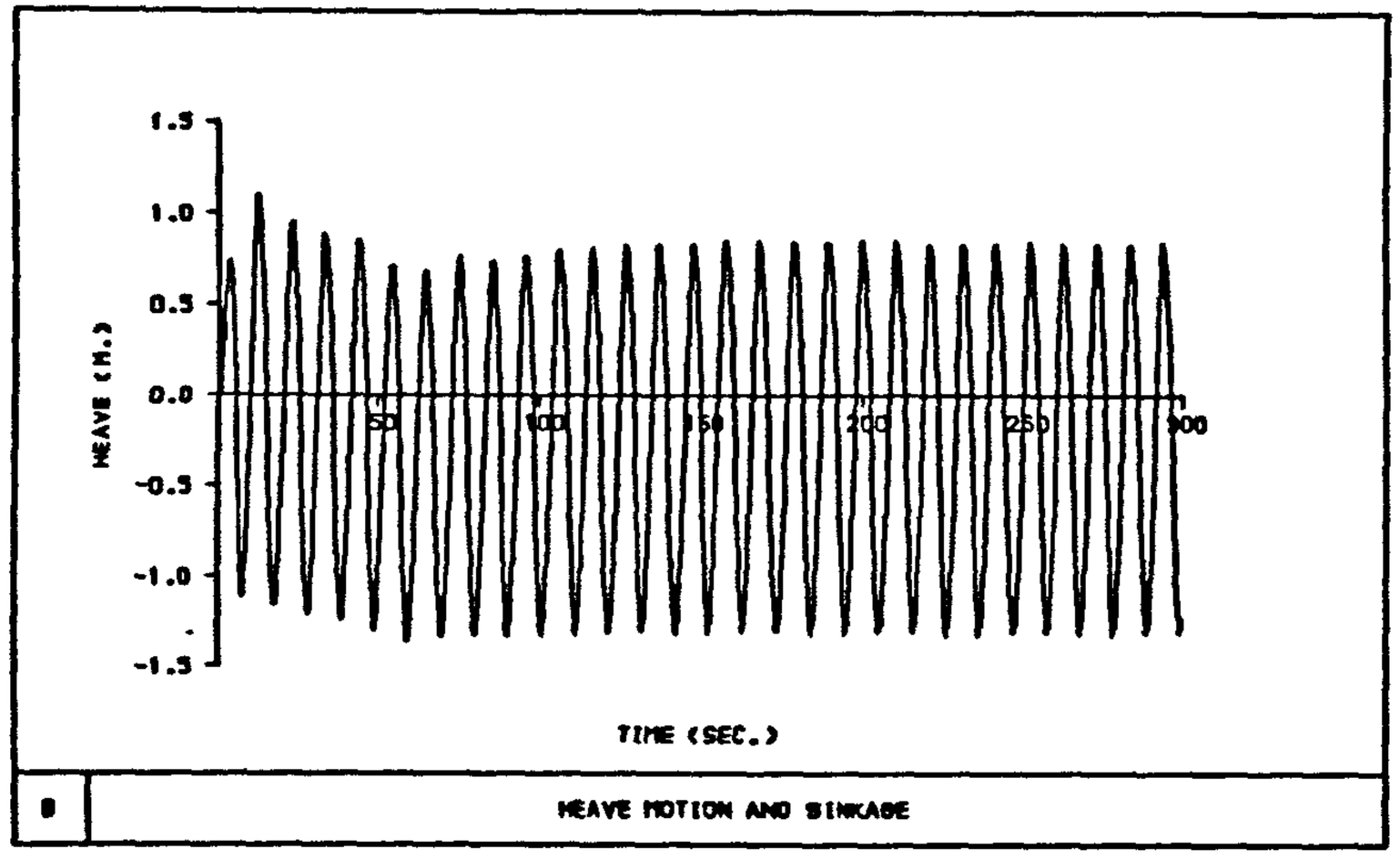

Fig 7.14 Time histories of ship motions and transverse centre of gravity of water on deck during progressive flooding, KG= 13.34 m, WH= 2.0 m [DAMAGE SCENARIO 1]

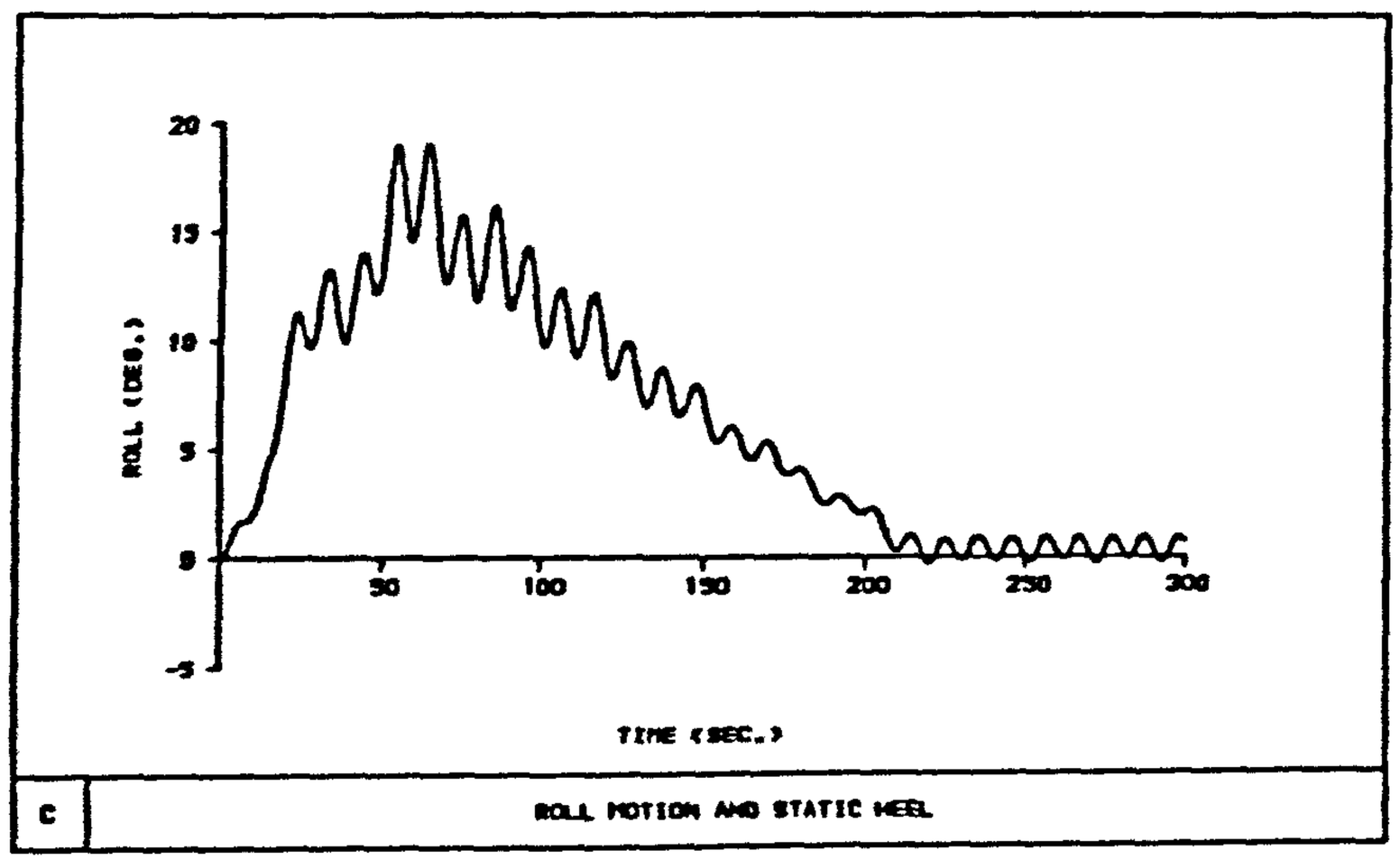

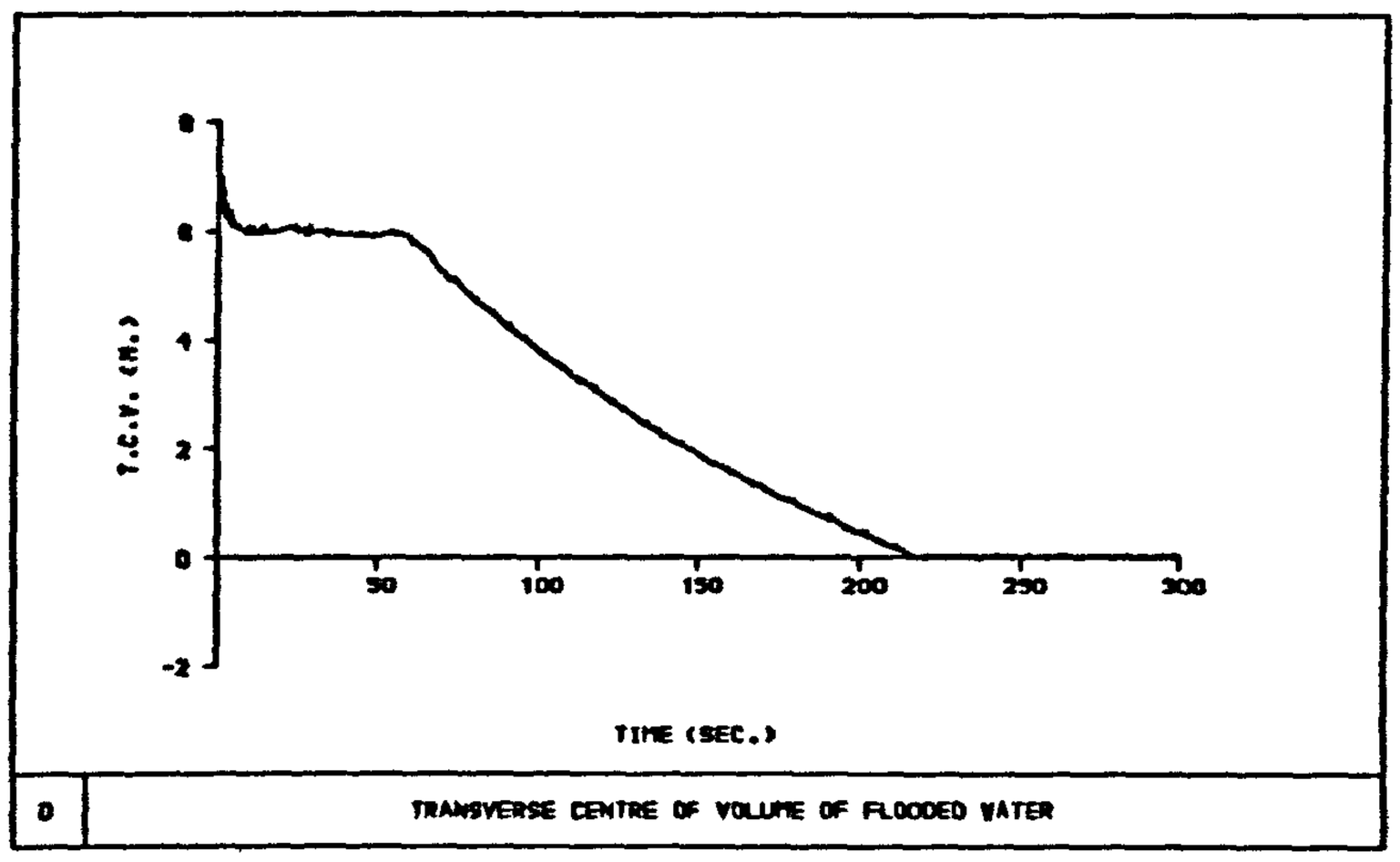

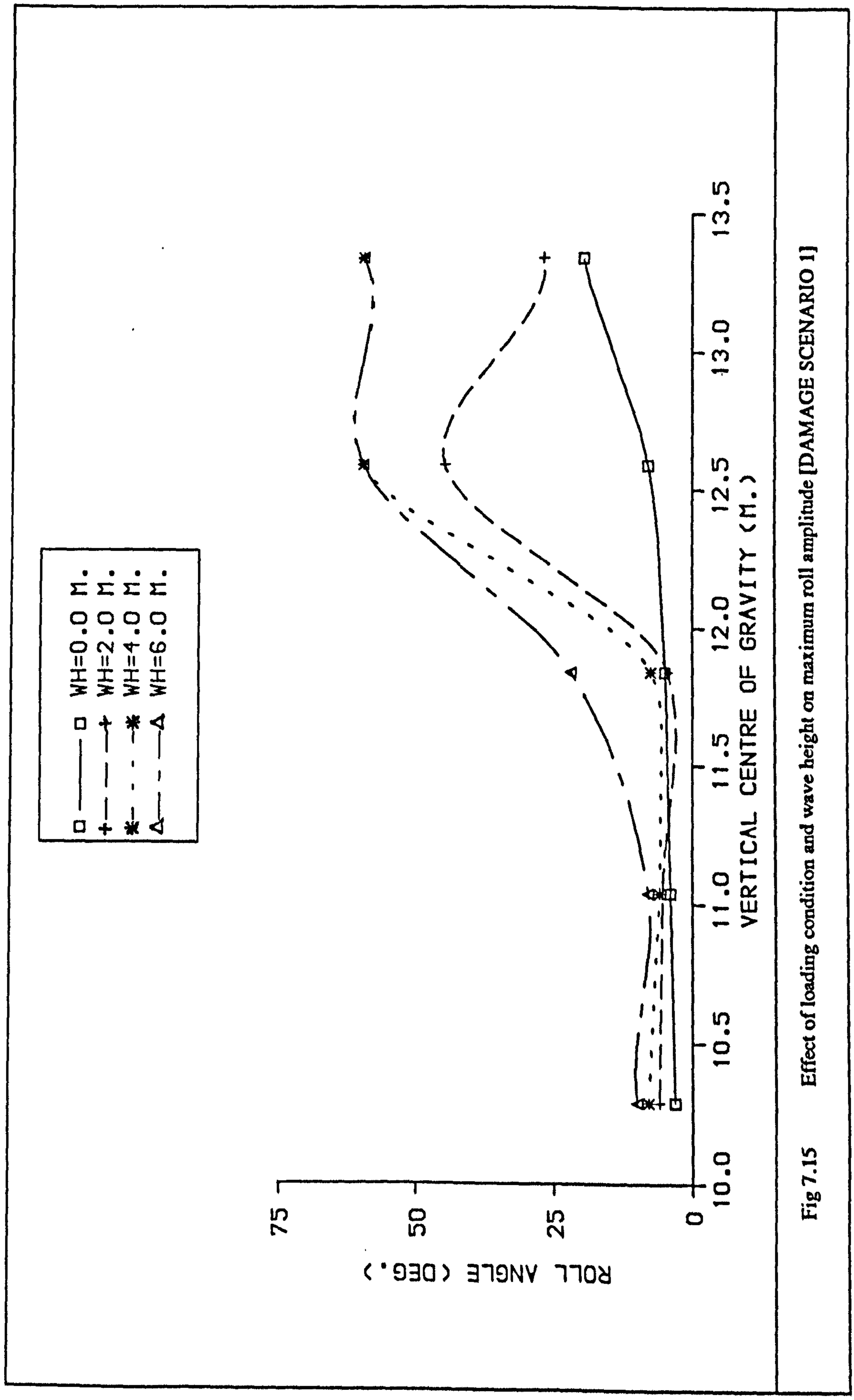

Fig 7.15 Effect of loading condition and wave height on maximum roll amplitude [DAMAGE SCENARIO 1]

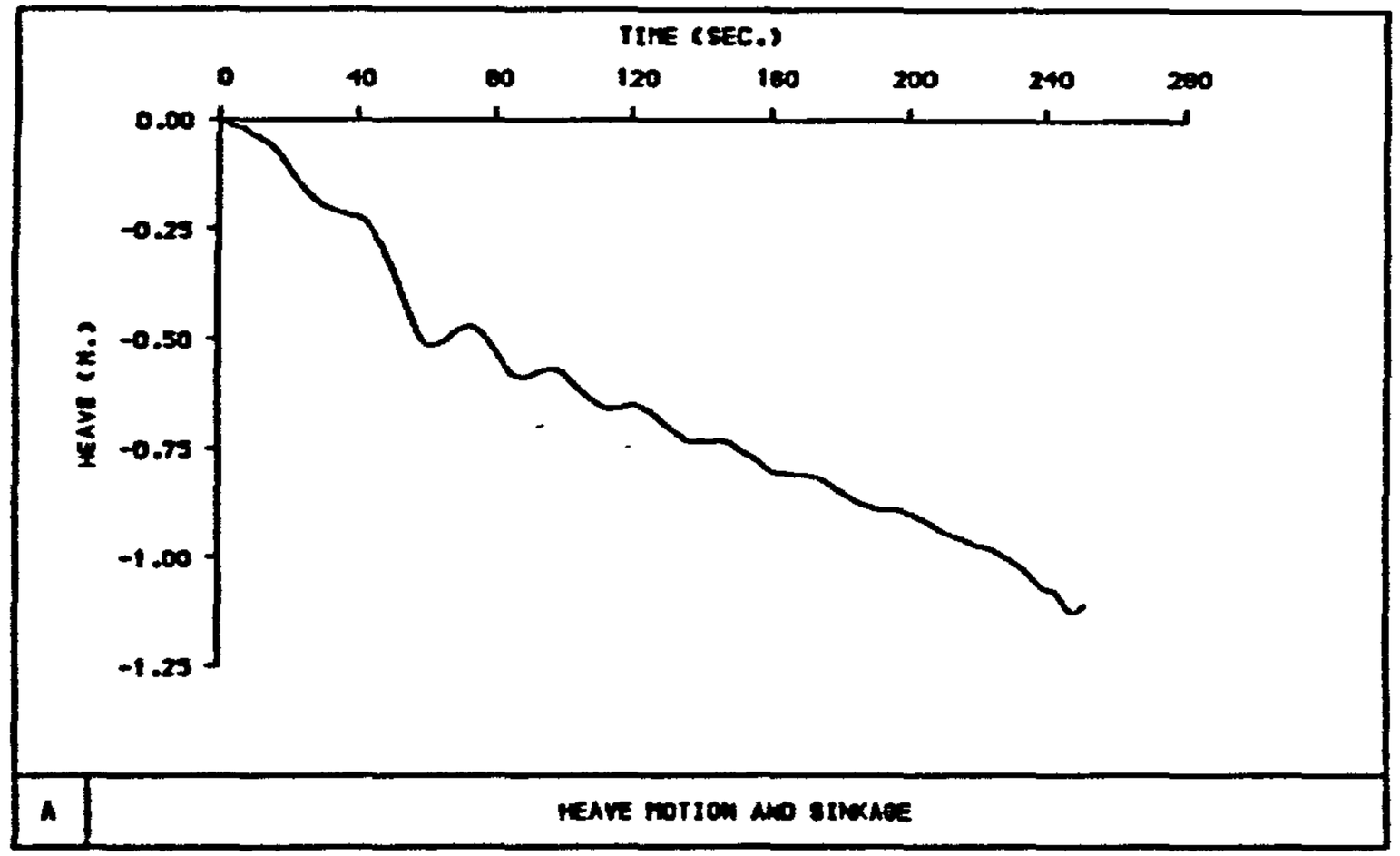

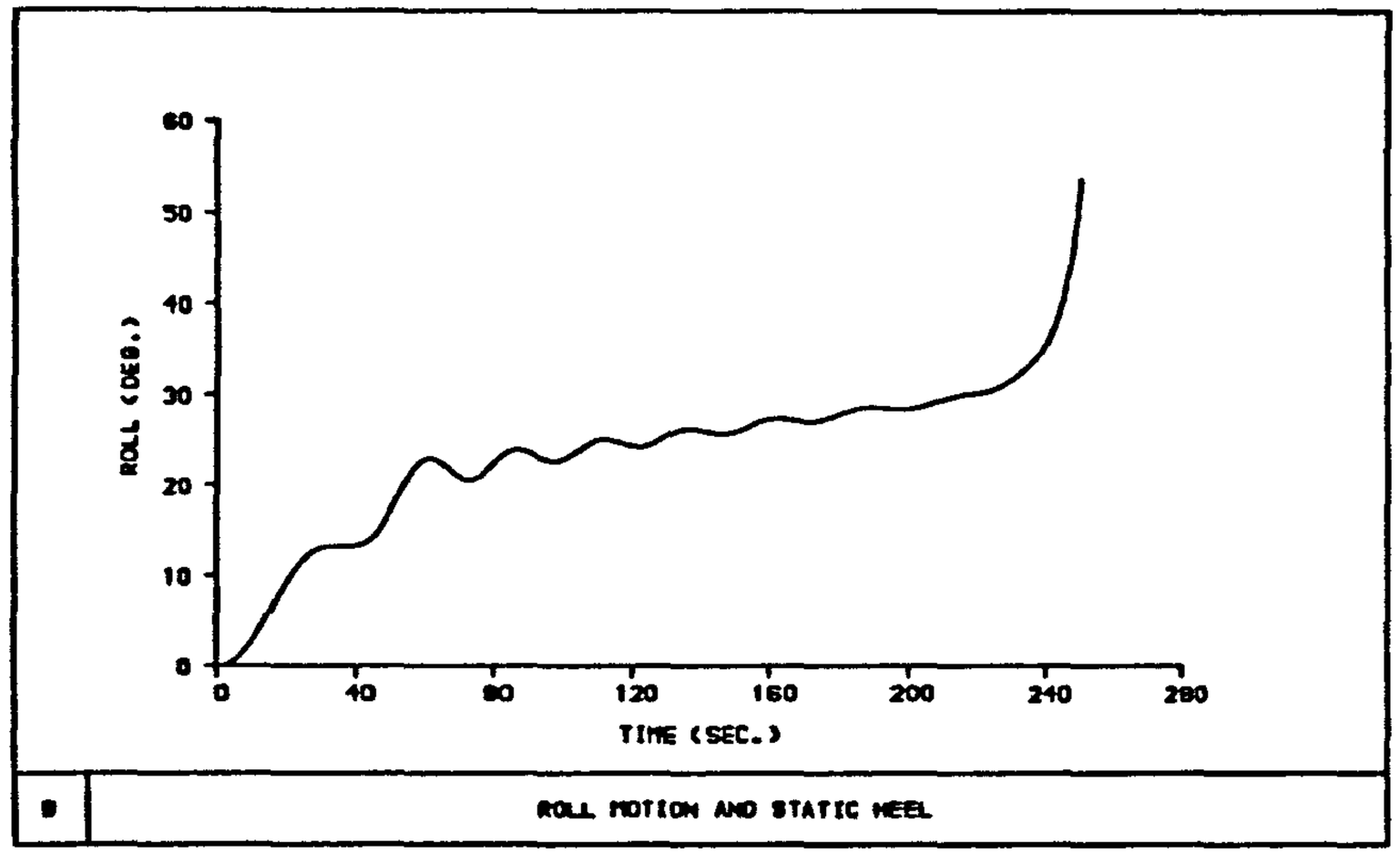

Fig 7.16 Time histories of ship motions and transverse centre of gravity of water on deck during progressive flooding, KG= 13.34 m, calm water [DAMAGE SCENARIO 2]

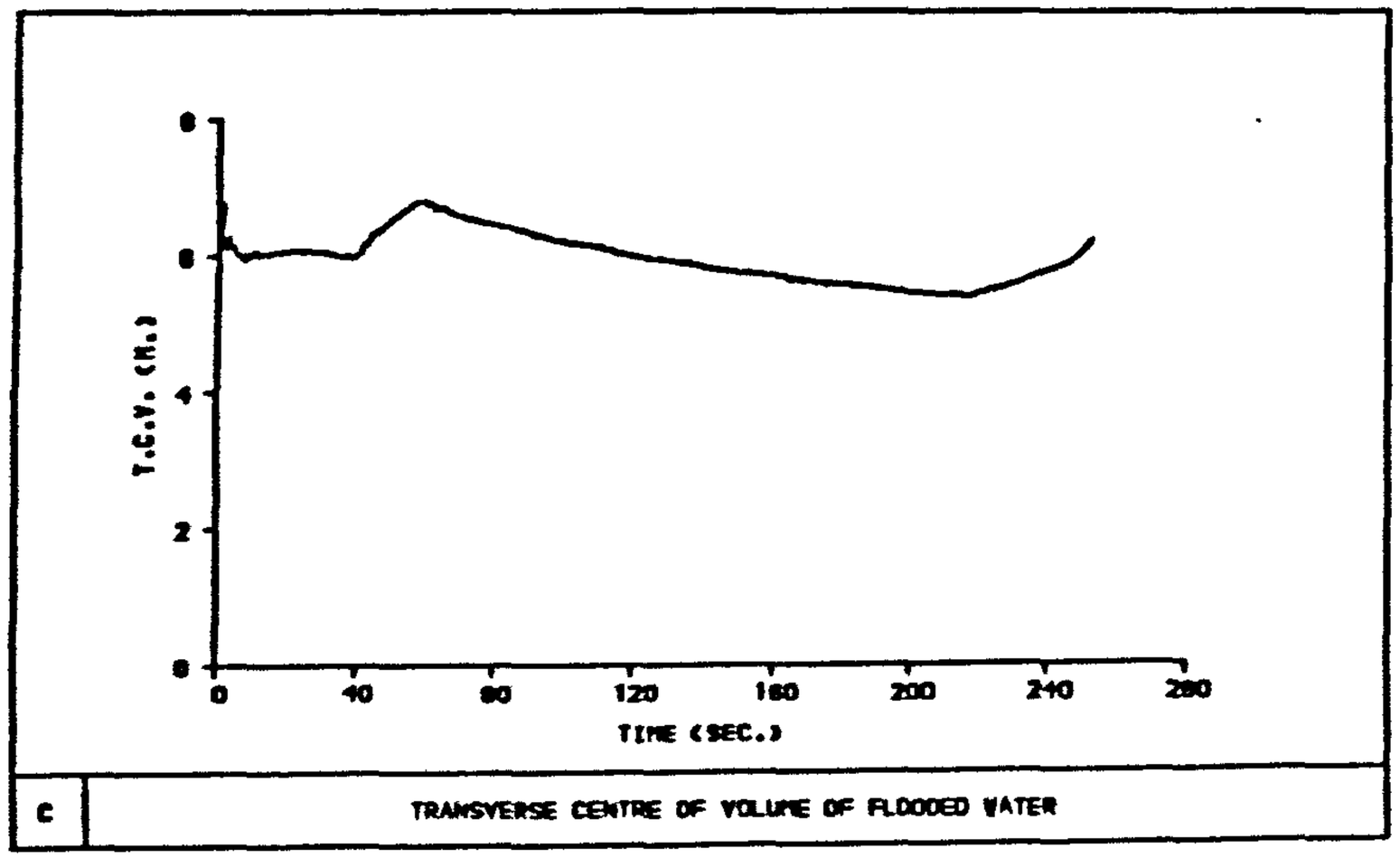

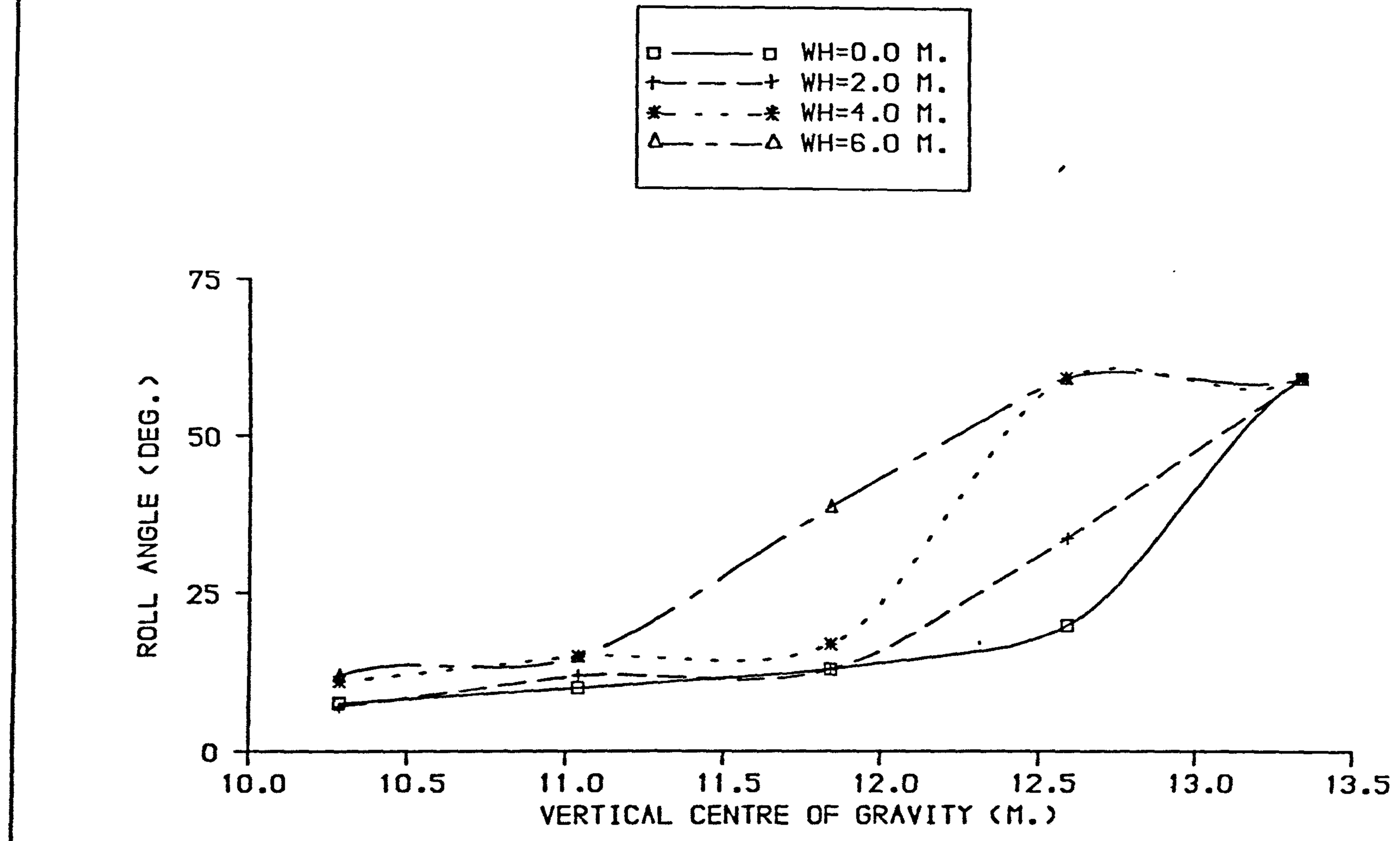

Fig 7.17 Effect of loading condition and wave height on maximum roll amplitude [DAMAGE SCENARIO 2]

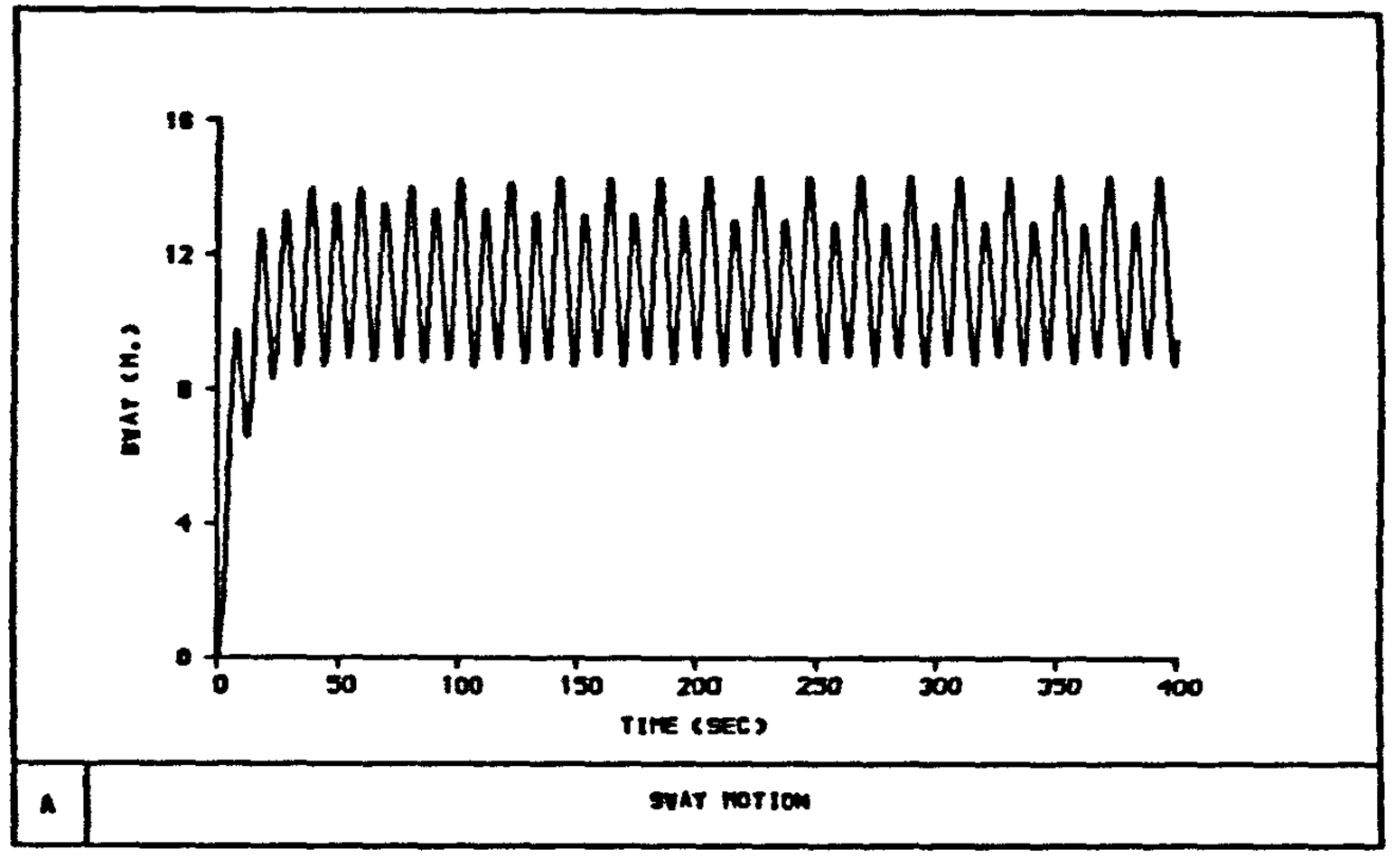

A SWAY MOTION

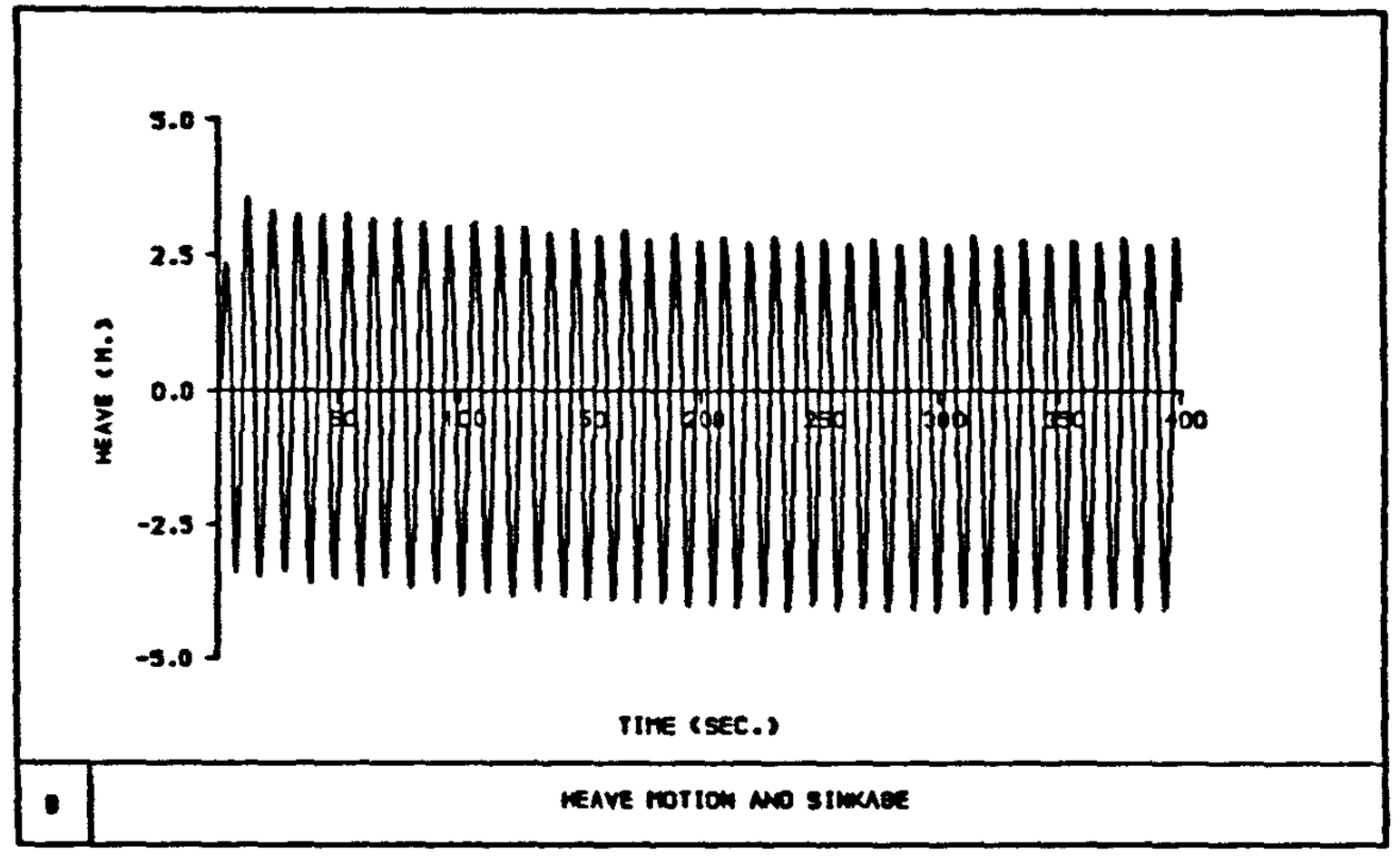

B HEAVE MOTION AND SINKAGE

Fig 7.18 Time histories of ship motions and transverse centre of gravity of water on deck during progressive flooding, KG= 11.84 m, WH= 6.0 m [DAMAGE SCENARIO 2]

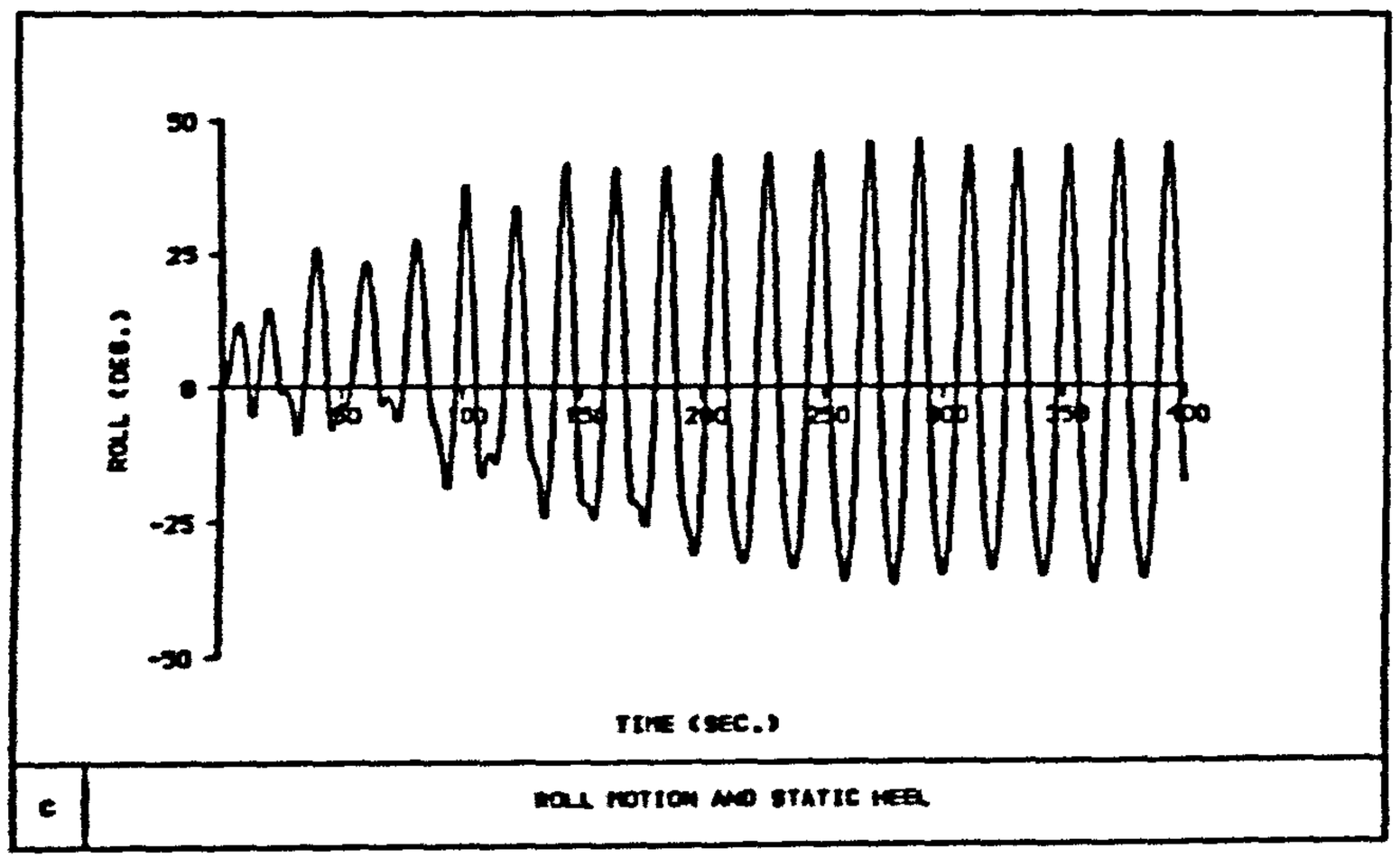

C ROLL MOTION AND STATIC HEEL

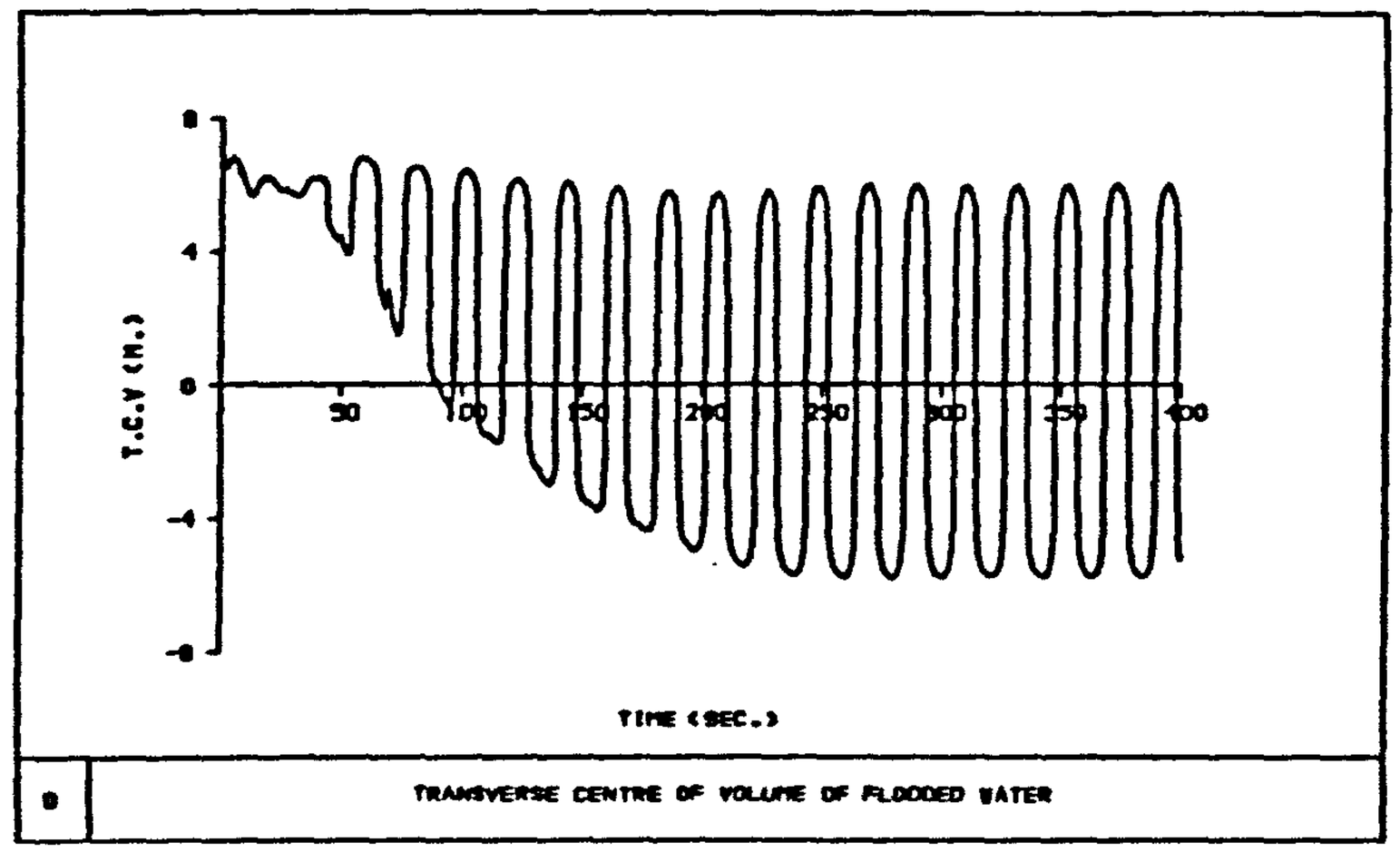

D TRANSVERSE CENTRE OF VOLUME OF FLOODED WATER

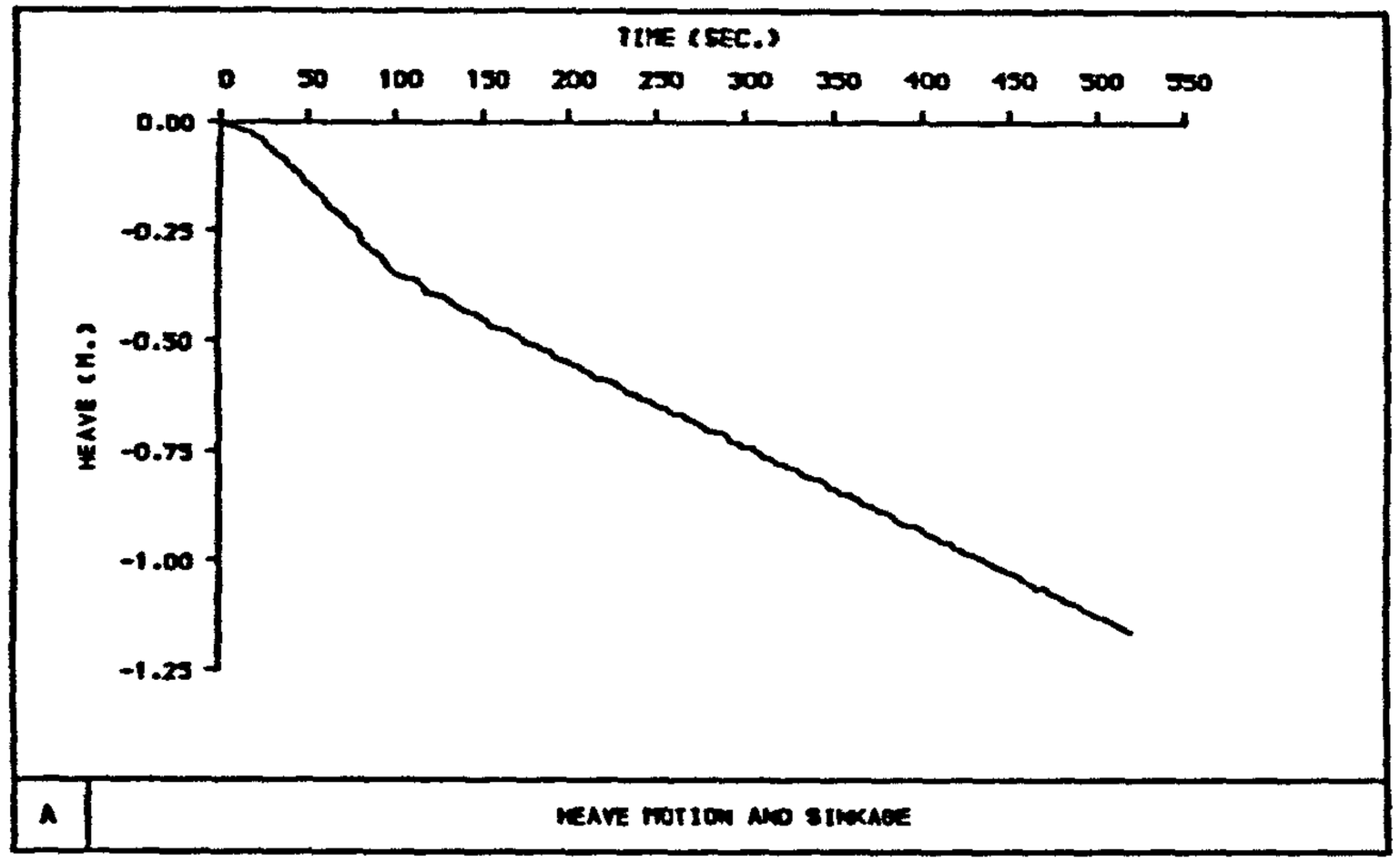

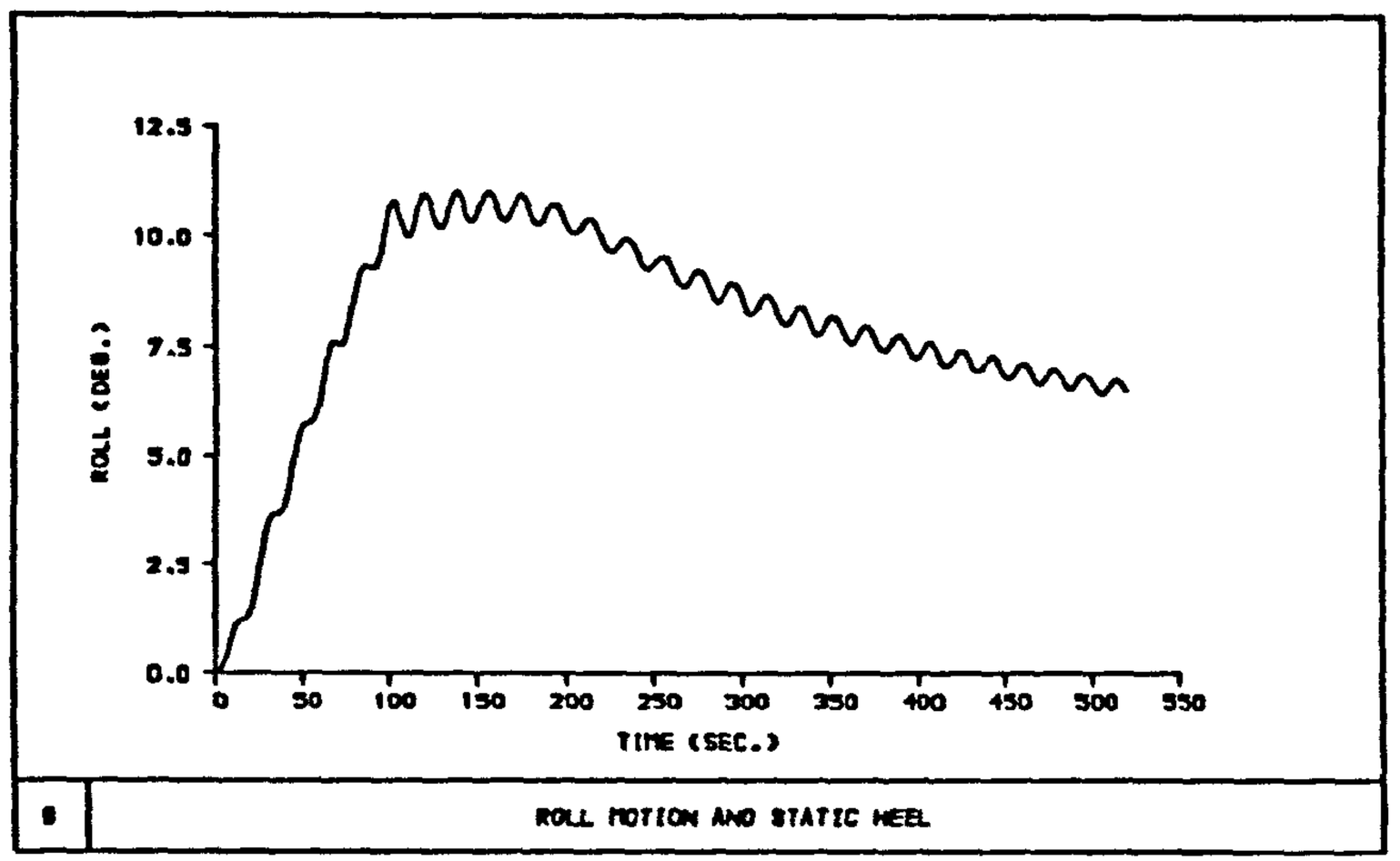

Fig 7.19 Time histories of ship motions and transverse centre of gravity of water on deck during progressive flooding, KG= 11.84 m, calm water [DAMAGE SCENARIO 3]

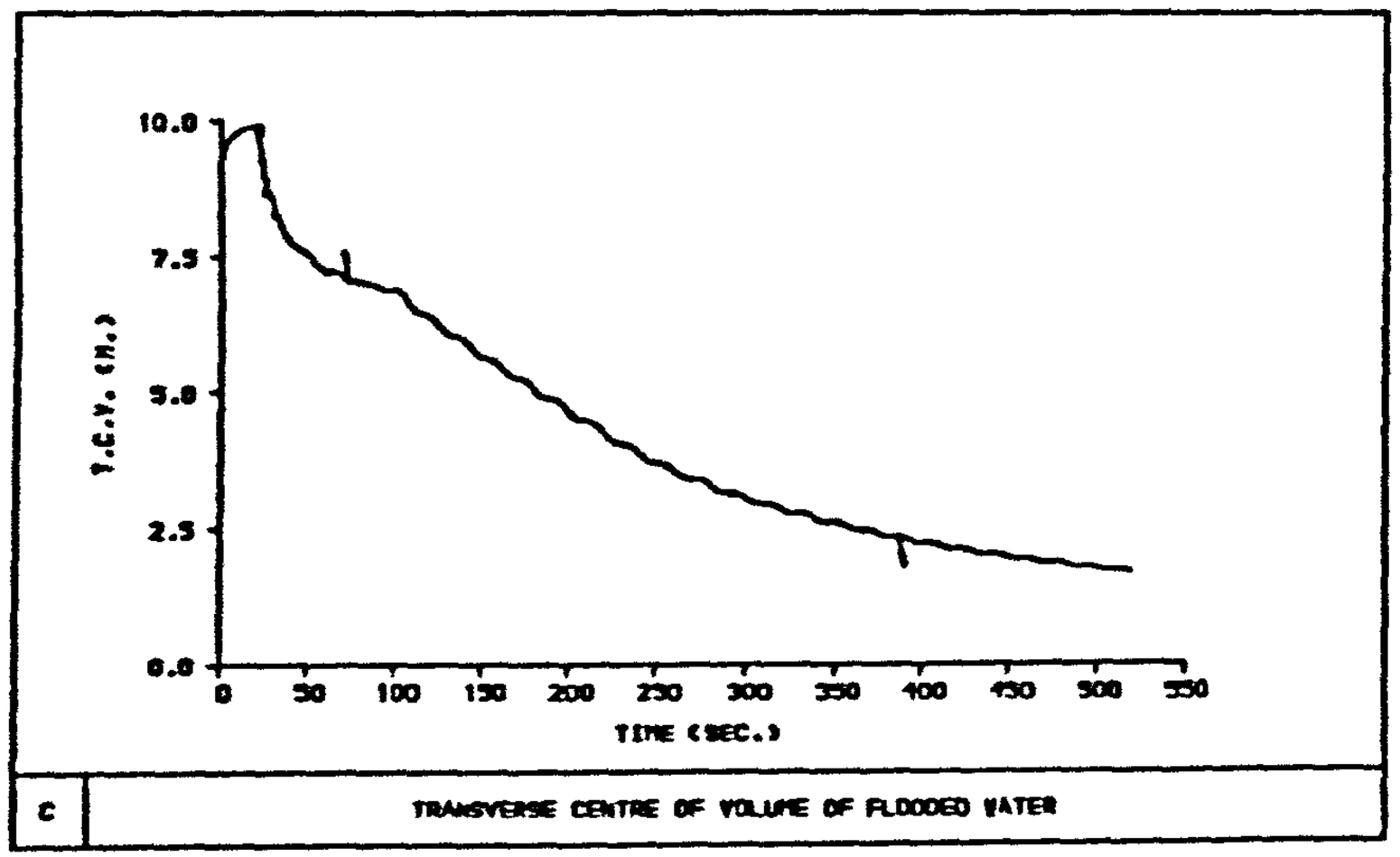

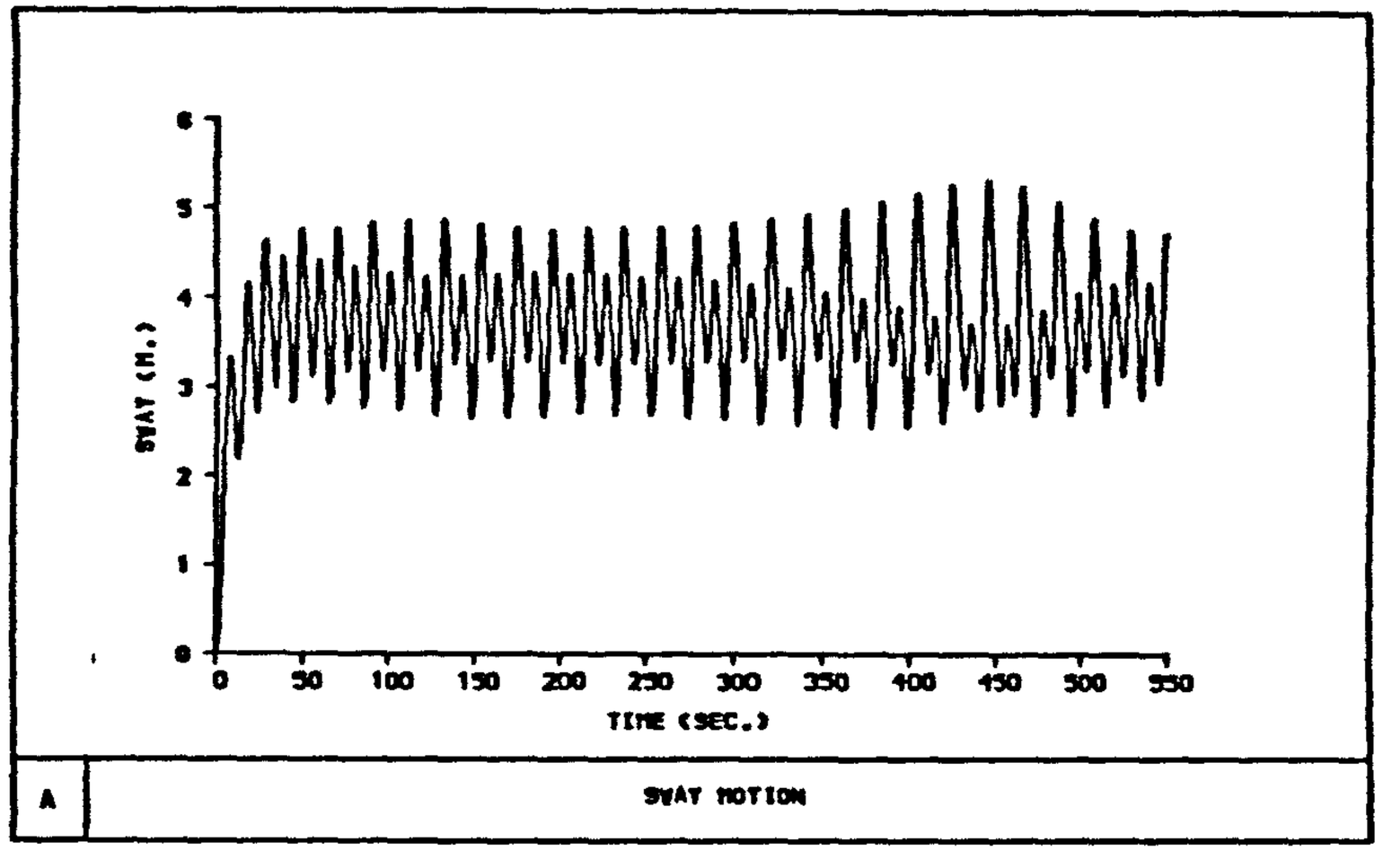

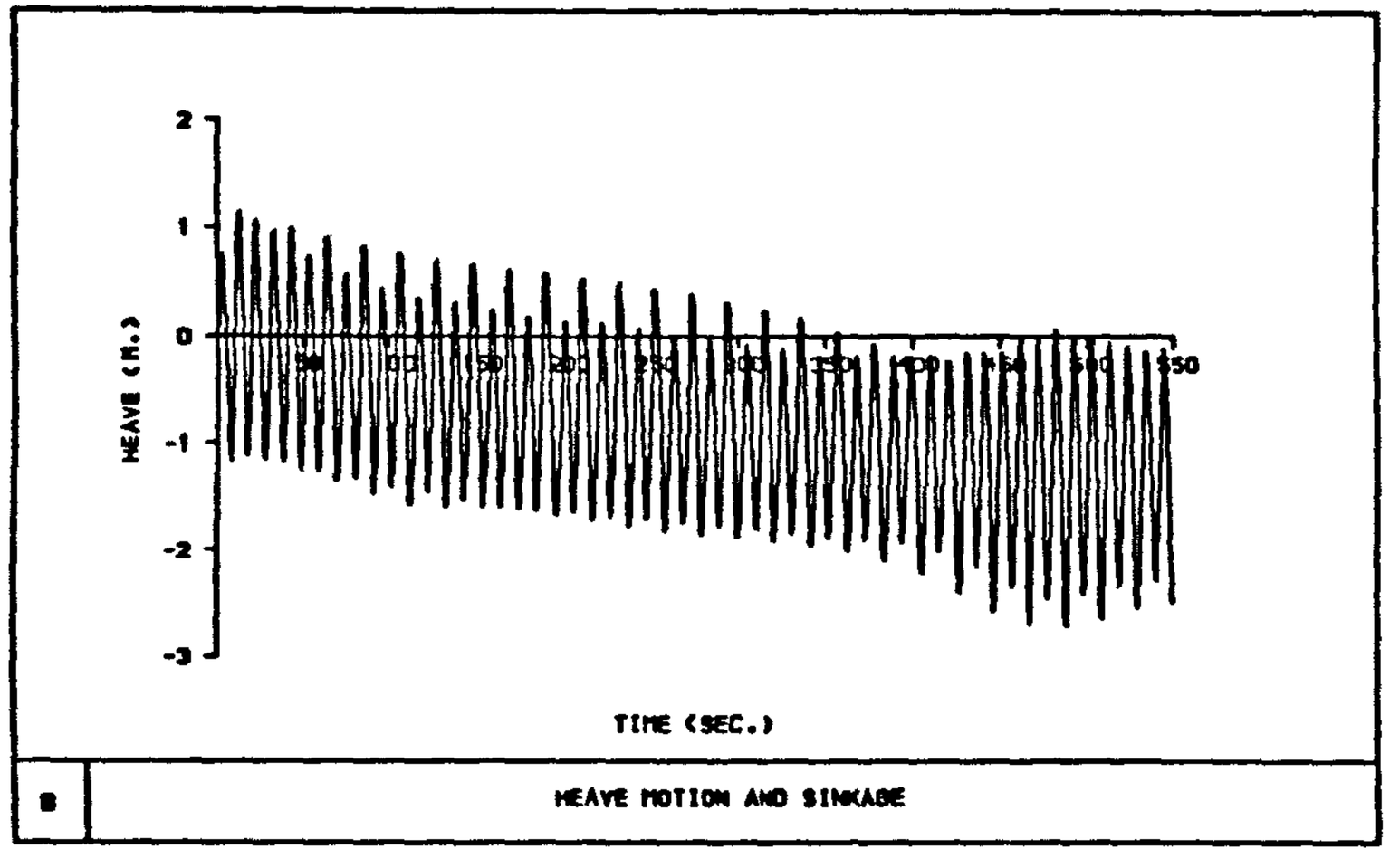

Fig 7.20 Time histories of ship motions and transverse centre of gravity of water on deck during progressive flooding, KG= 12.59 m, WH= 2.0 m [DAMAGE SCENARIO 3]

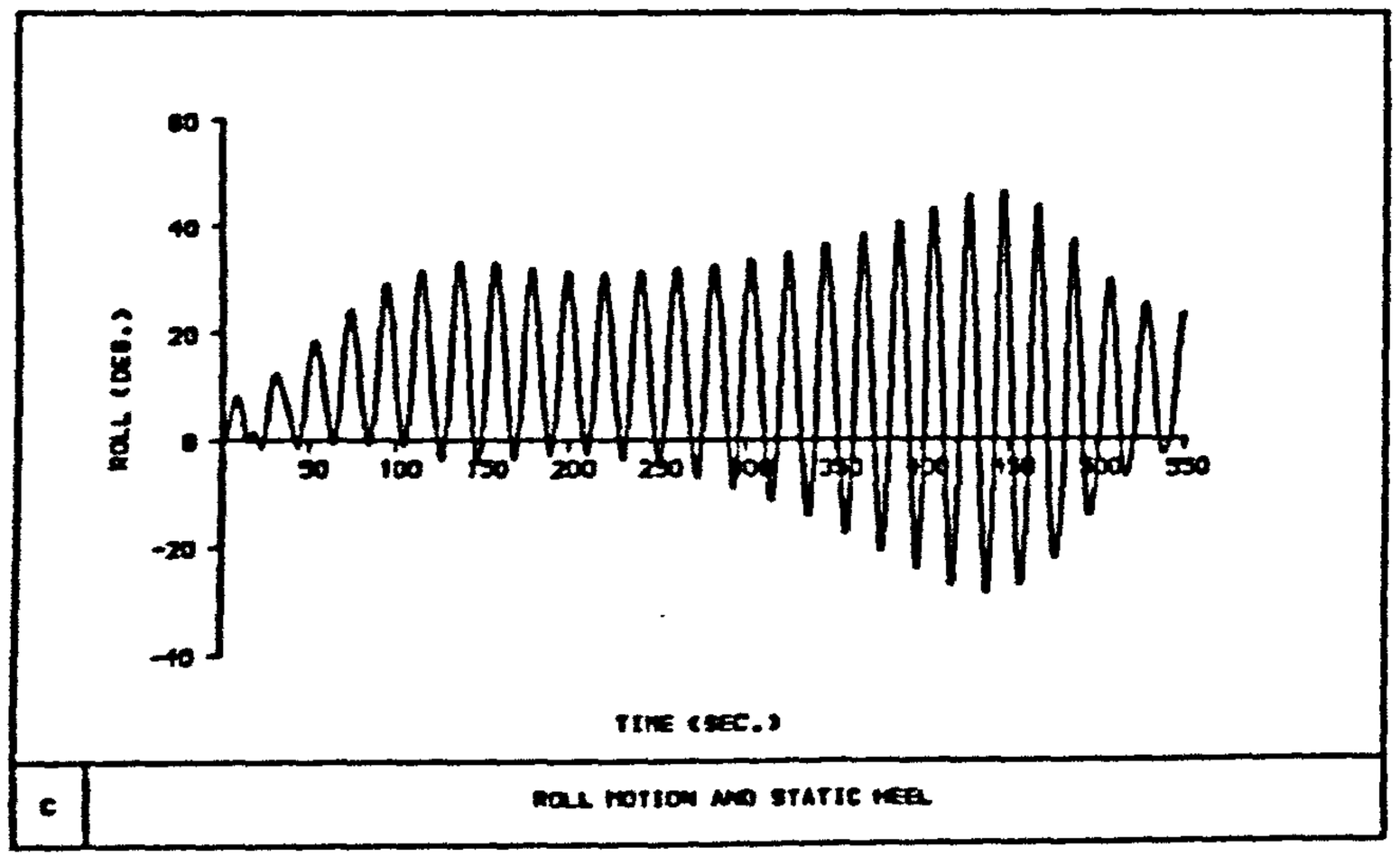

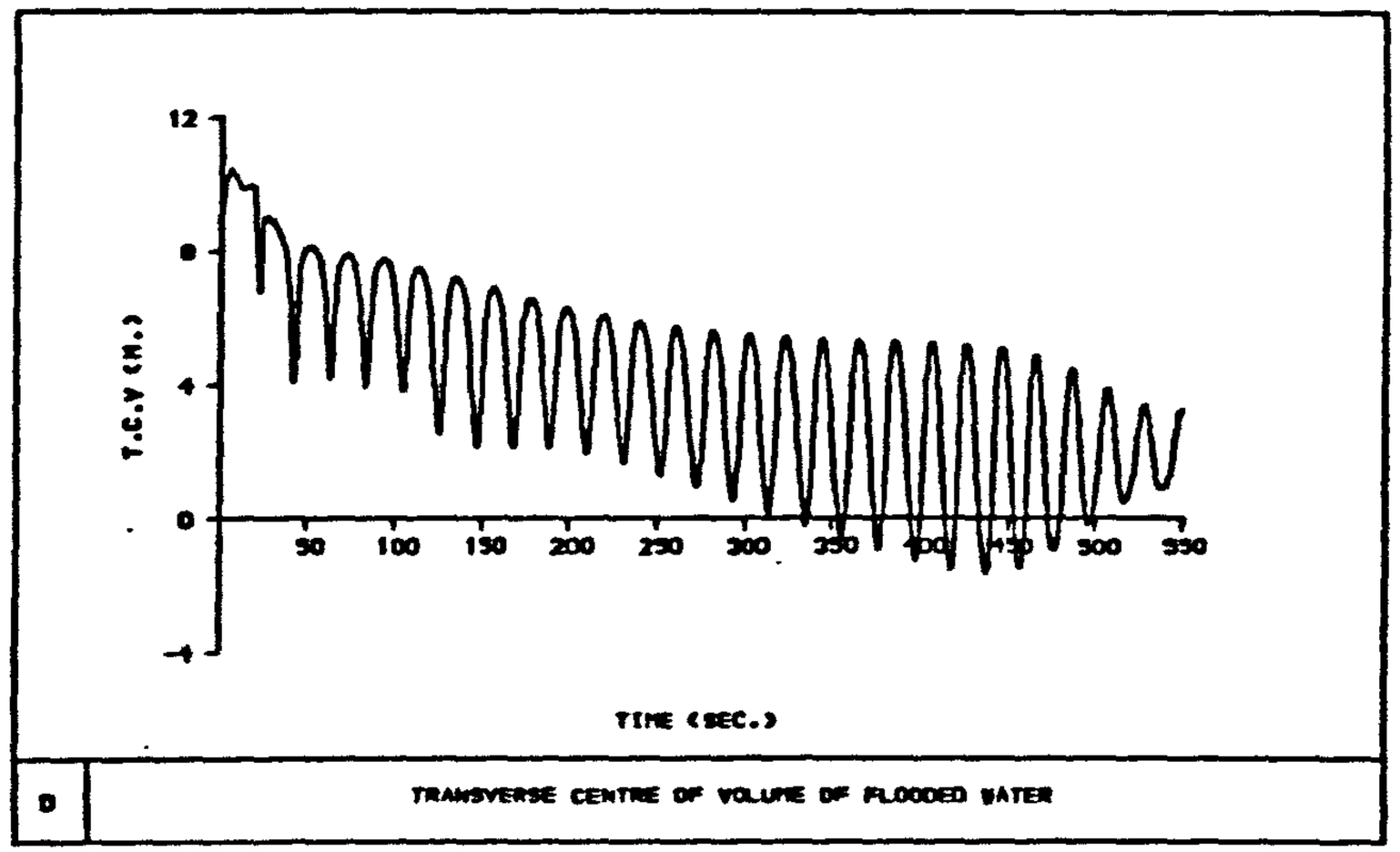

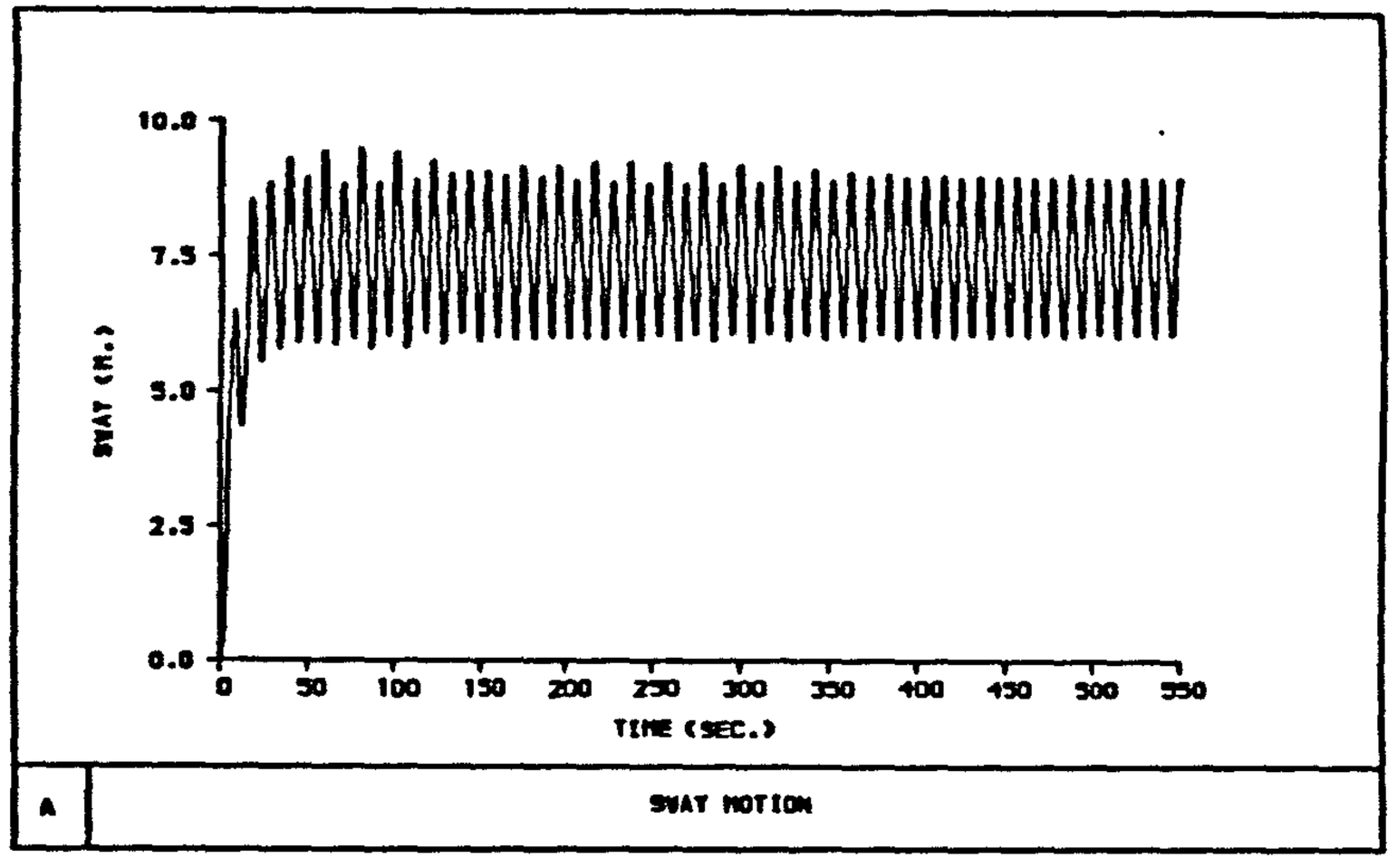

A SWAY MOTION

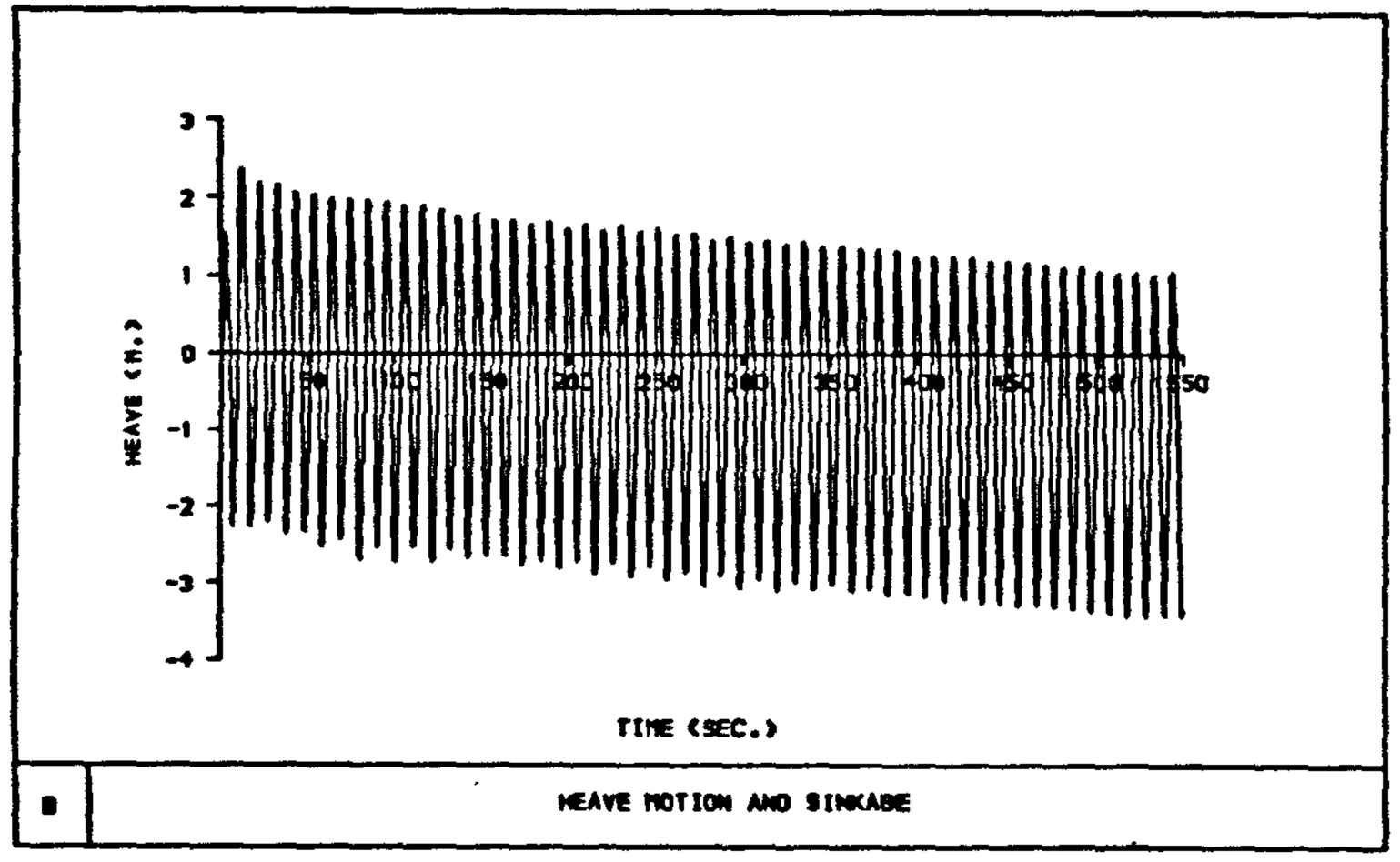

B HEAVE MOTION AND SINKAGE

Fig 7.21 Time histories of ship motions and transverse centre of gravity of water on deck during progressive flooding, KG= 11.84 m, WH= 4.0 m [DAMAGE SCENARIO 3]

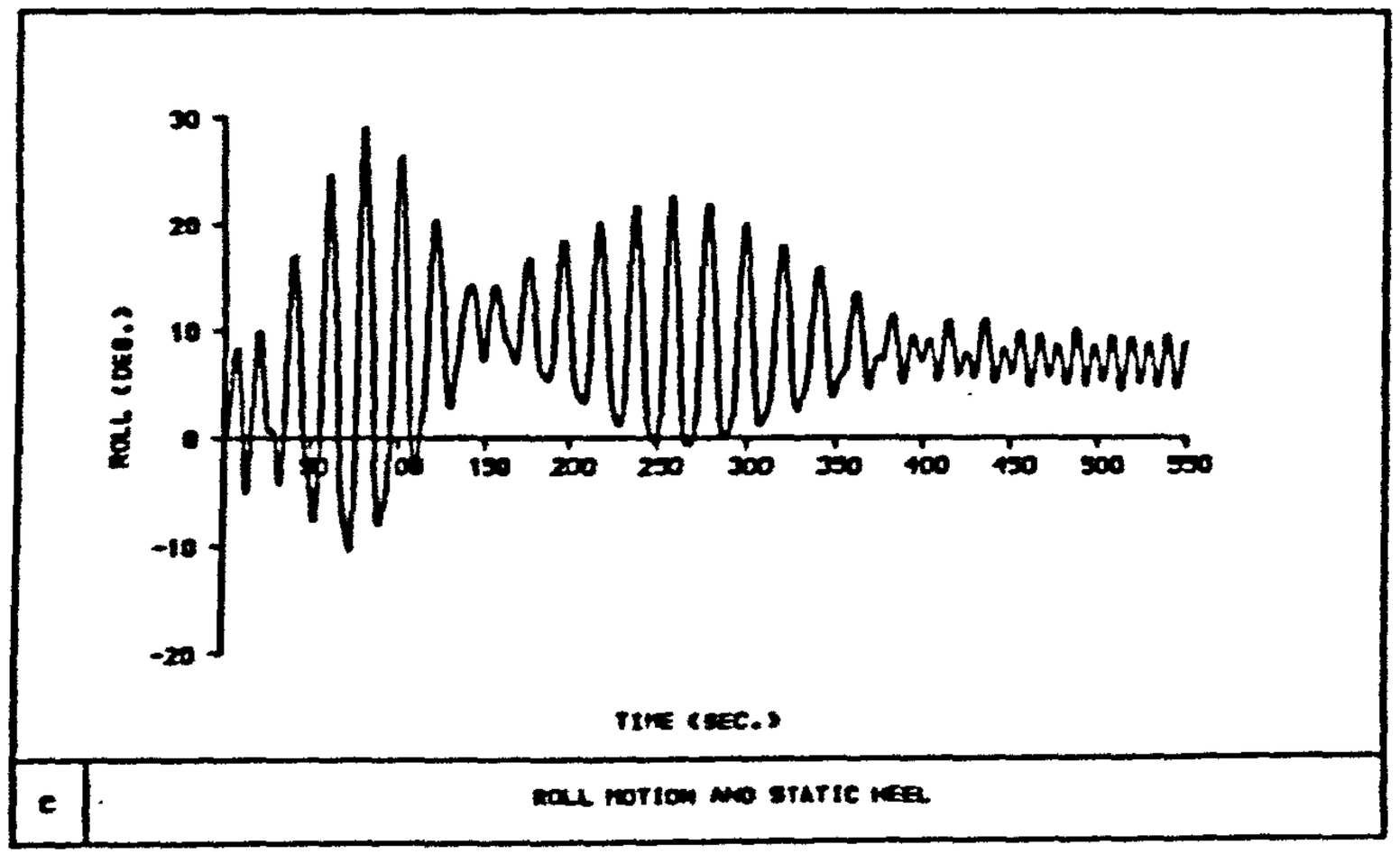

C ROLL MOTION AND STATIC HEEL

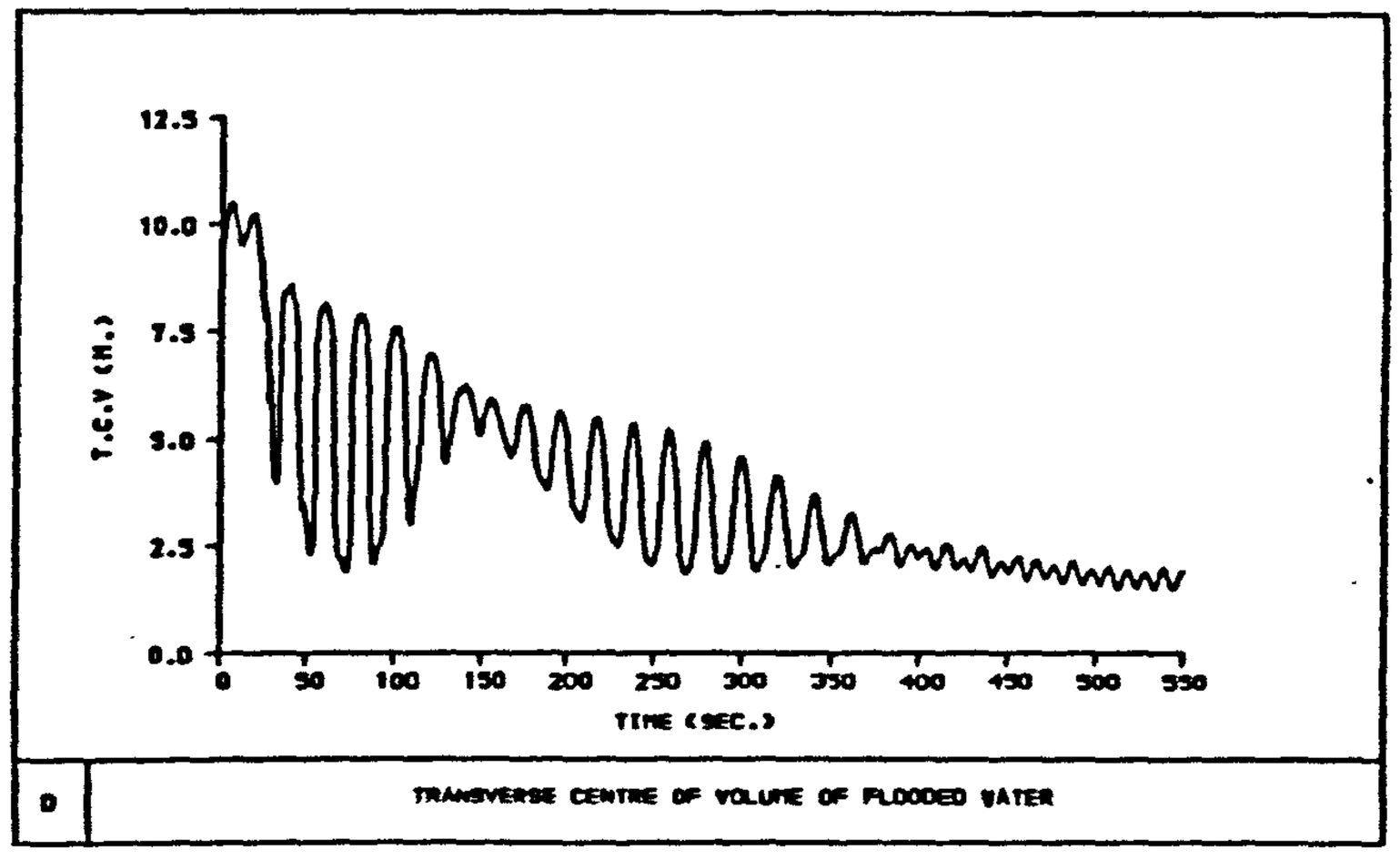

D TRANSVERSE CENTRE OF VOLUME OF FLOODED WATER

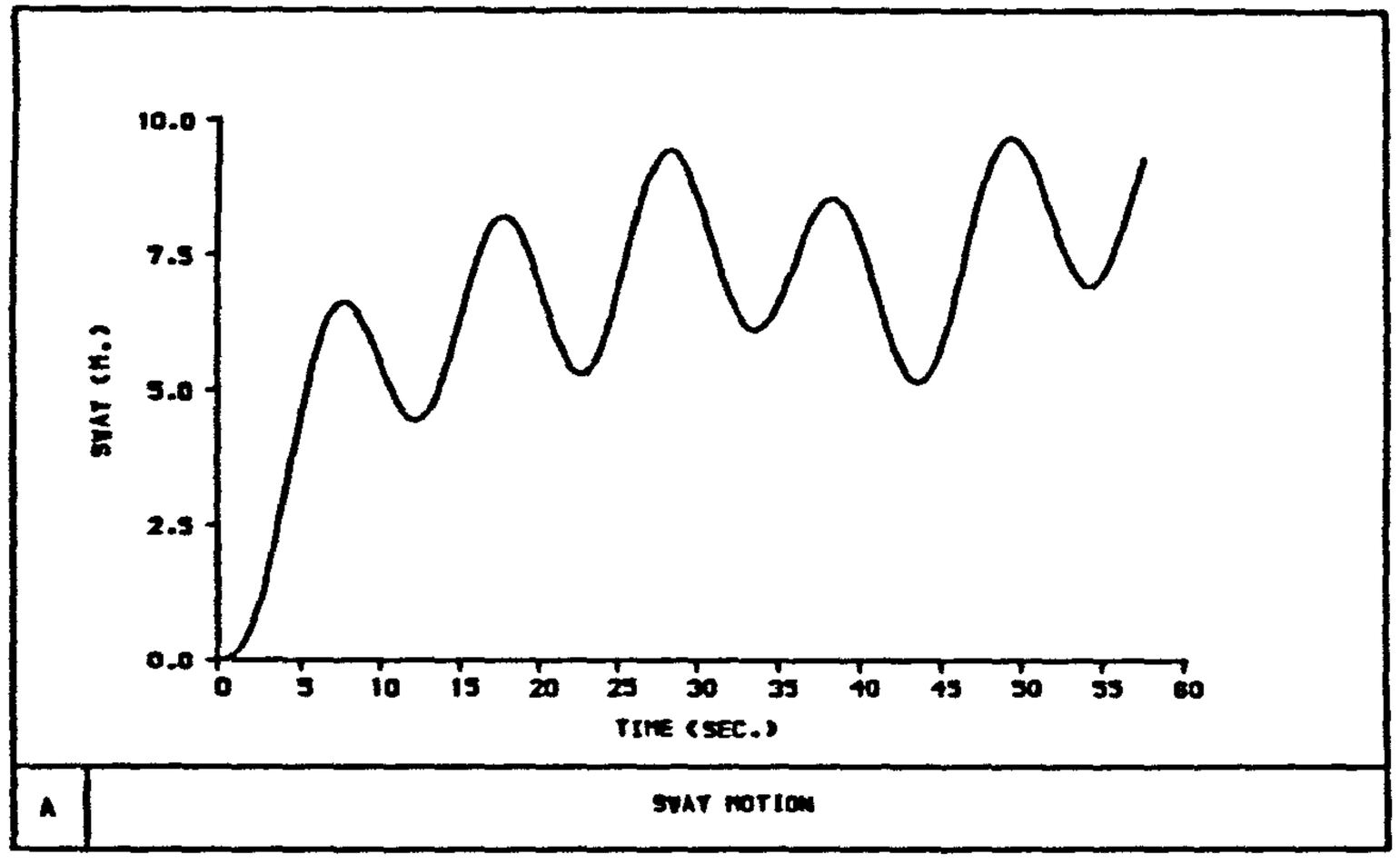

A SWAY MOTION

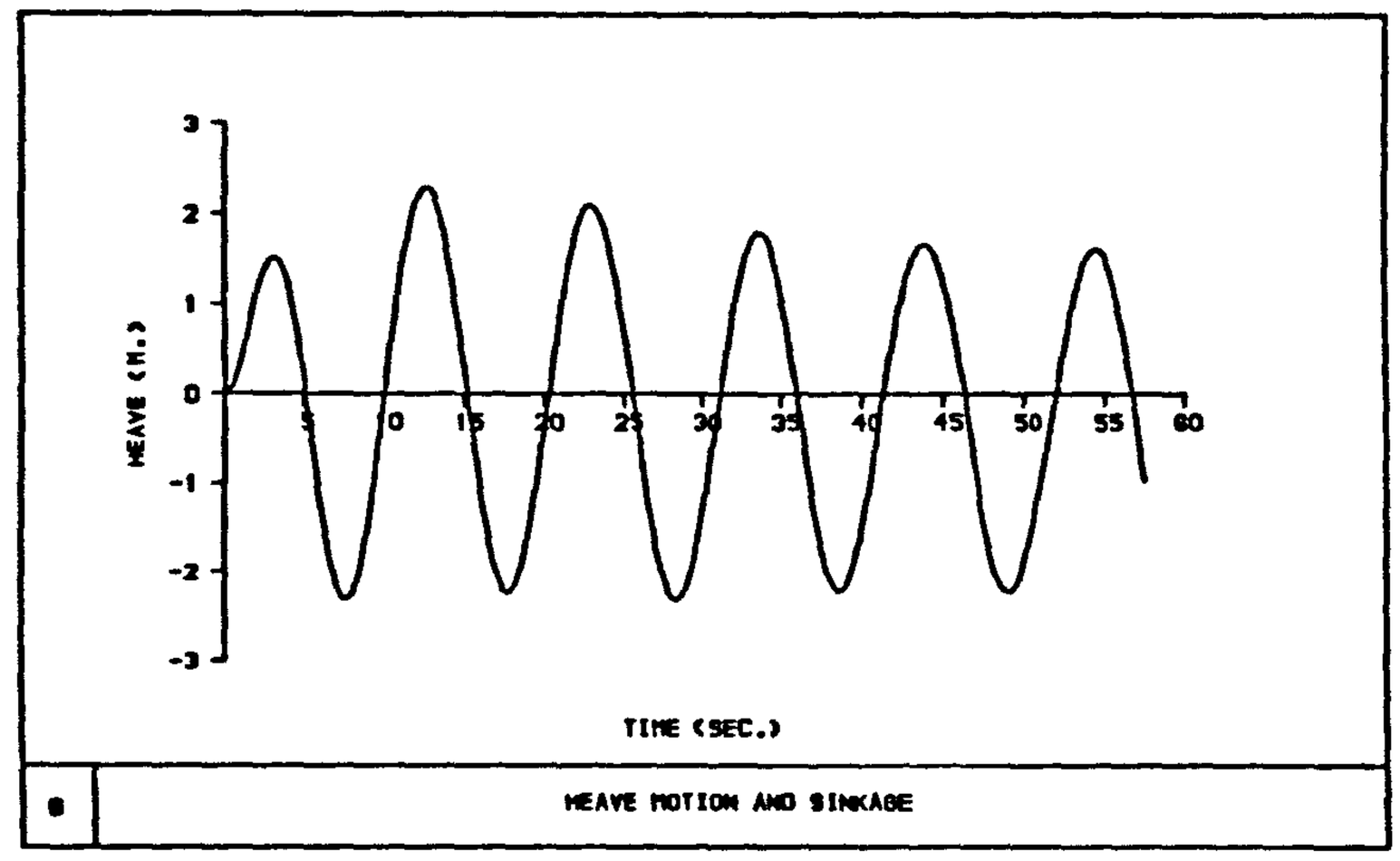

B HEAVE MOTION AND SINKAGE

Fig 7.22 Time histories of ship motions and transverse centre of gravity of water on deck during progressive flooding, KG= 12.59 m, WH= 4.0 m [DAMAGE SCENARIO 3]

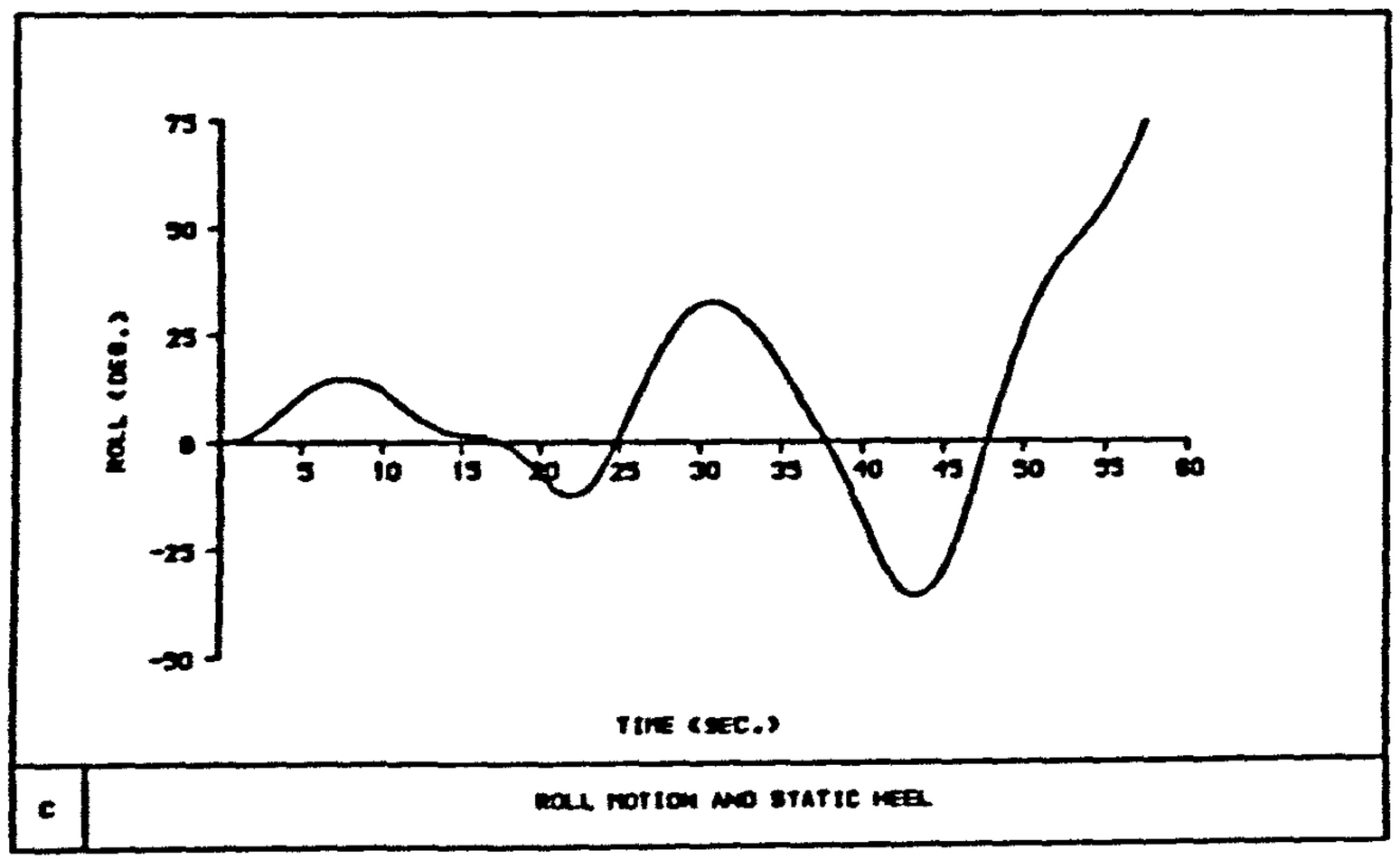

C ROLL MOTION AND STATIC HEEL

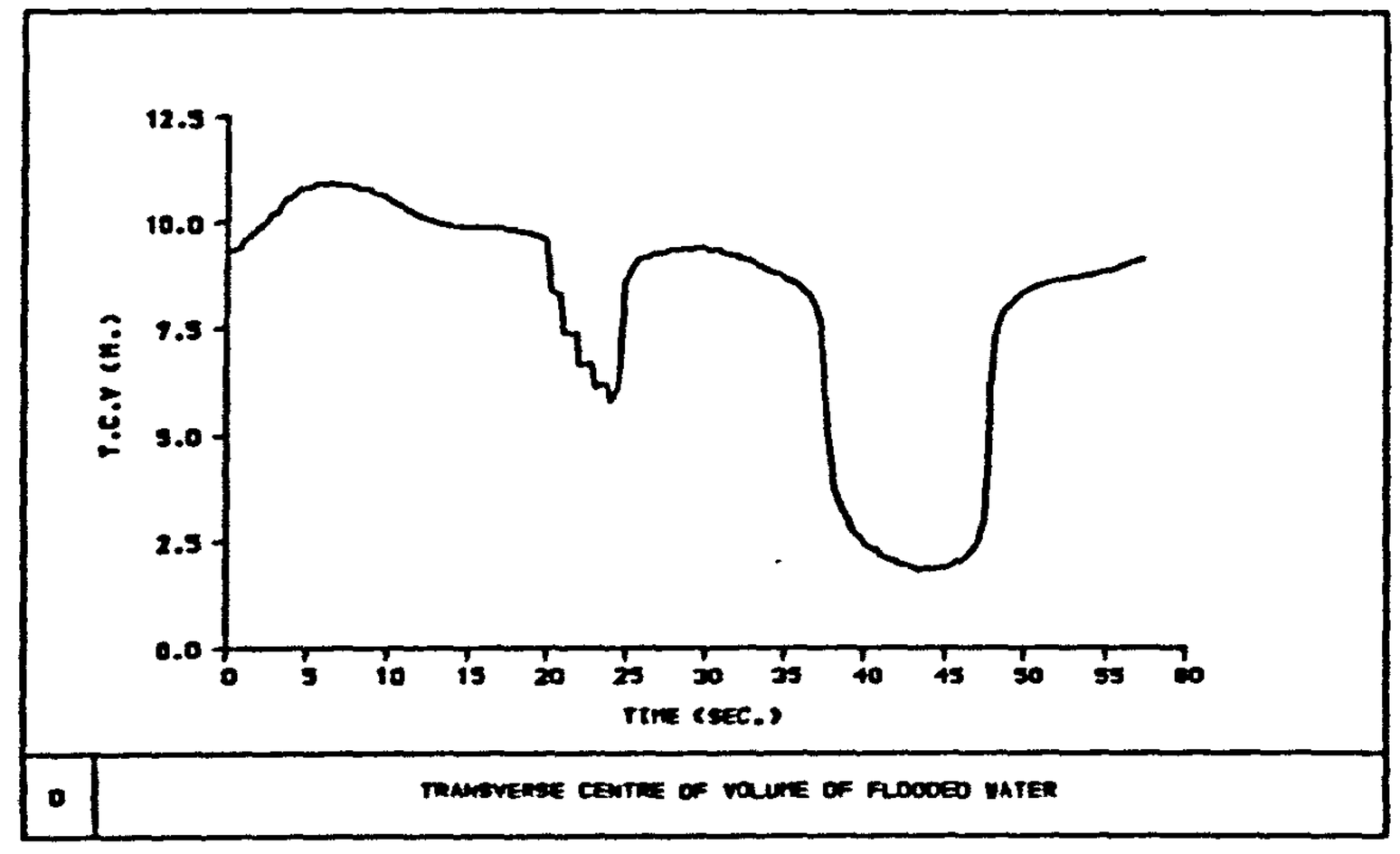

D TRANSVERSE CENTRE OF VOLUME OF FLOODED WATER

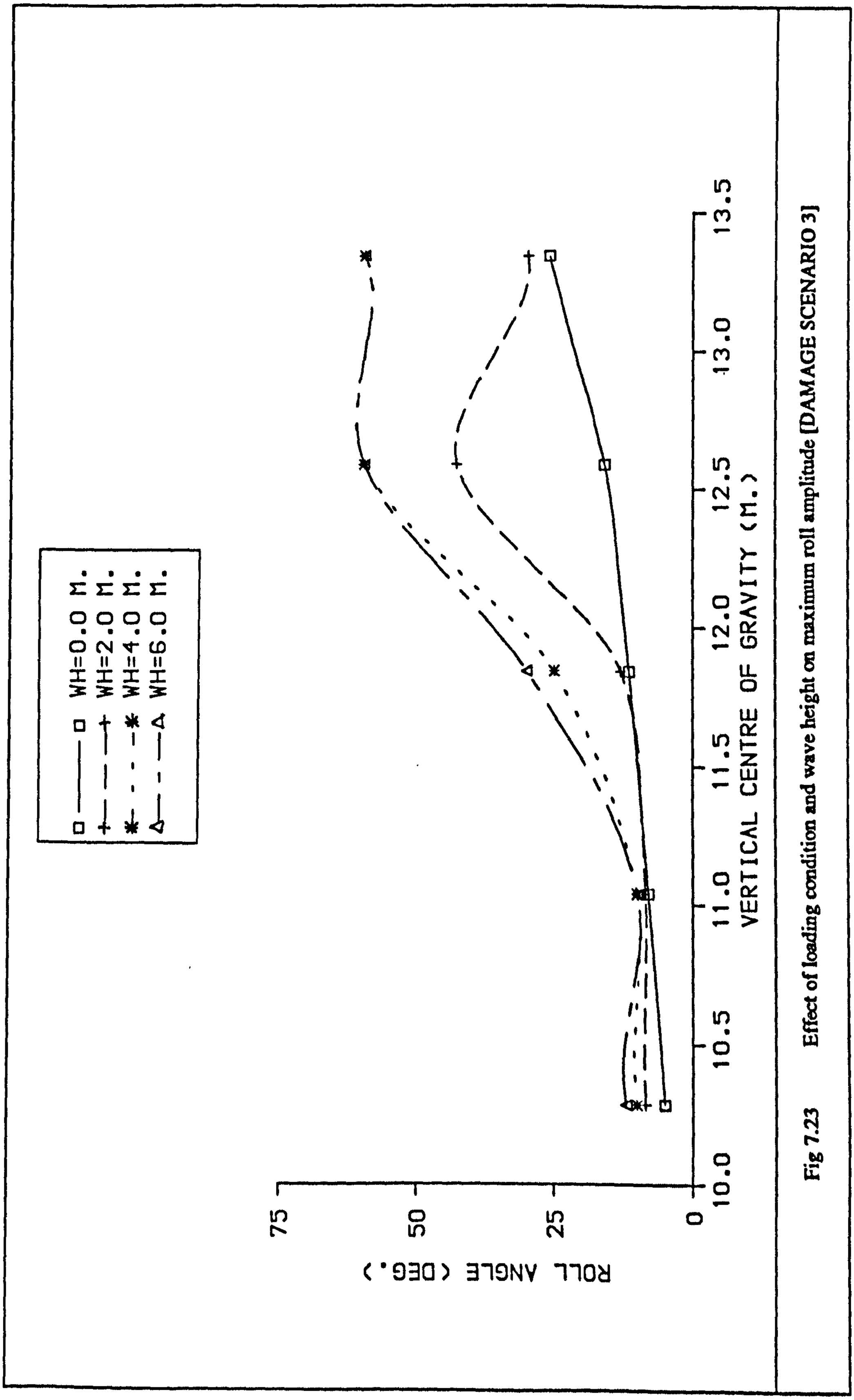

Fig 7.23 Effect of loading condition and wave height on maximum roll amplitude [DAMAGE SCENARIO 3]

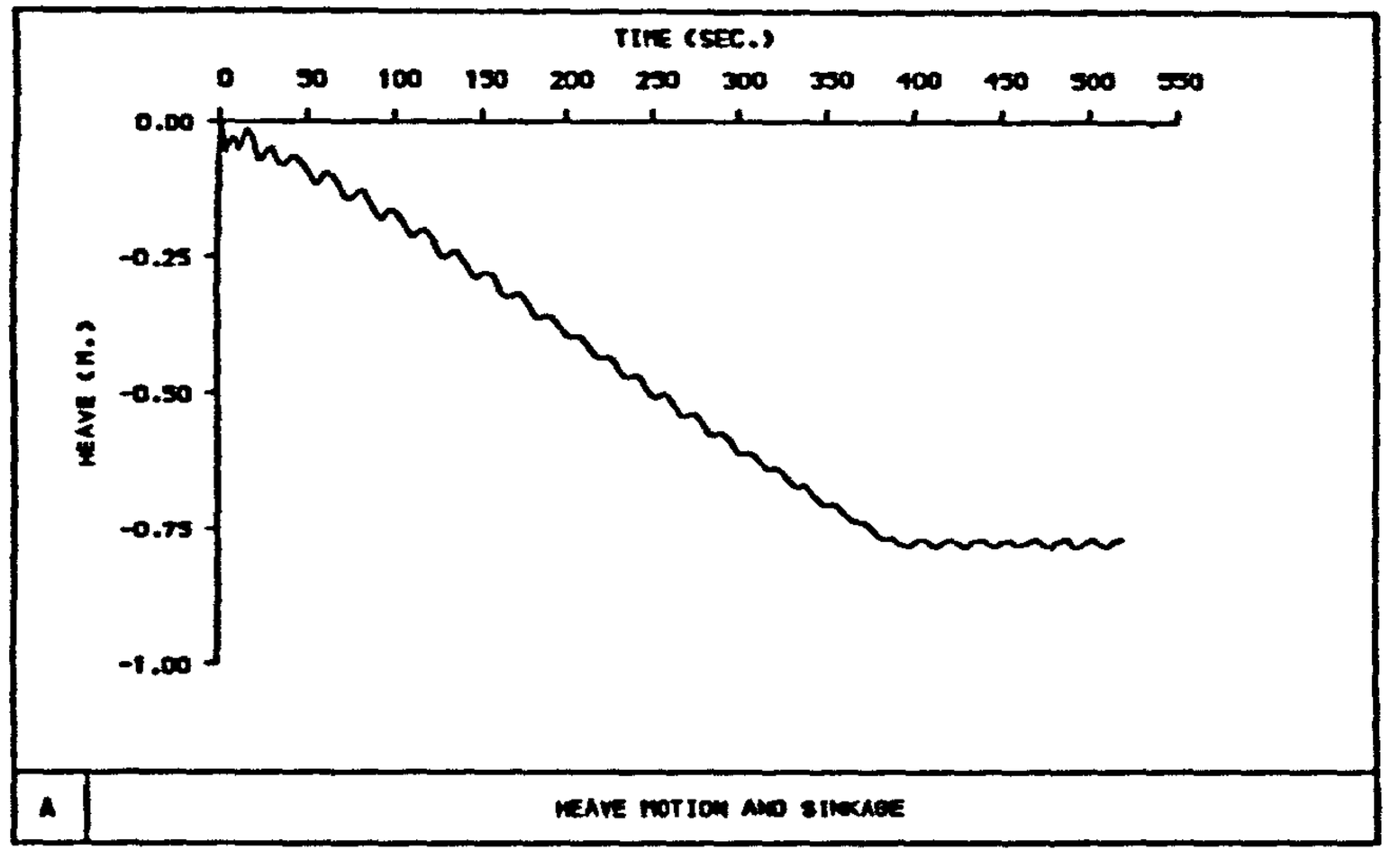

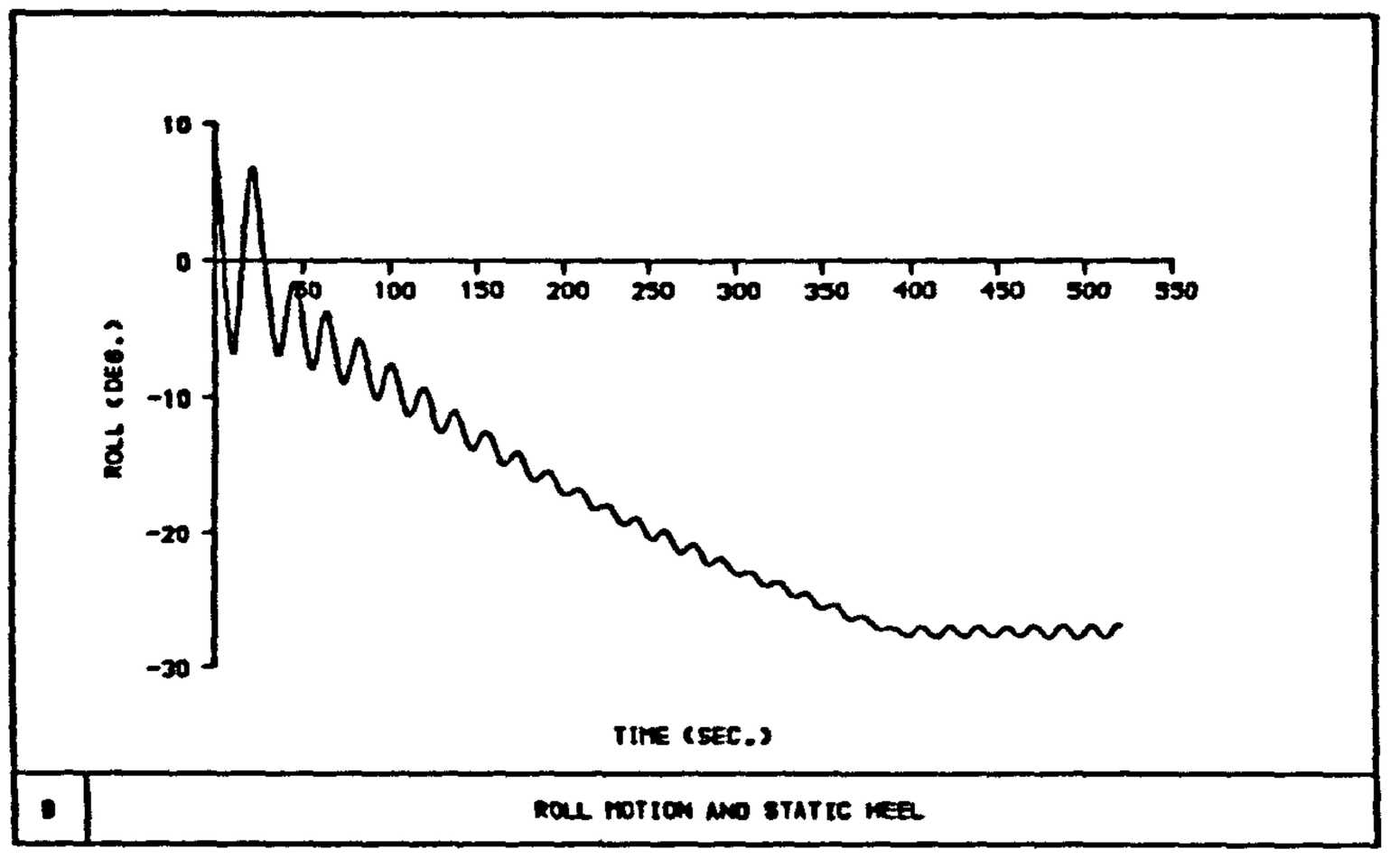

Fig 7.24 Time histories of ship motions and transverse centre of gravity of water on deck during progressive flooding, KG= 11.84 m, calm water [DAMAGE SCENARIO 4]

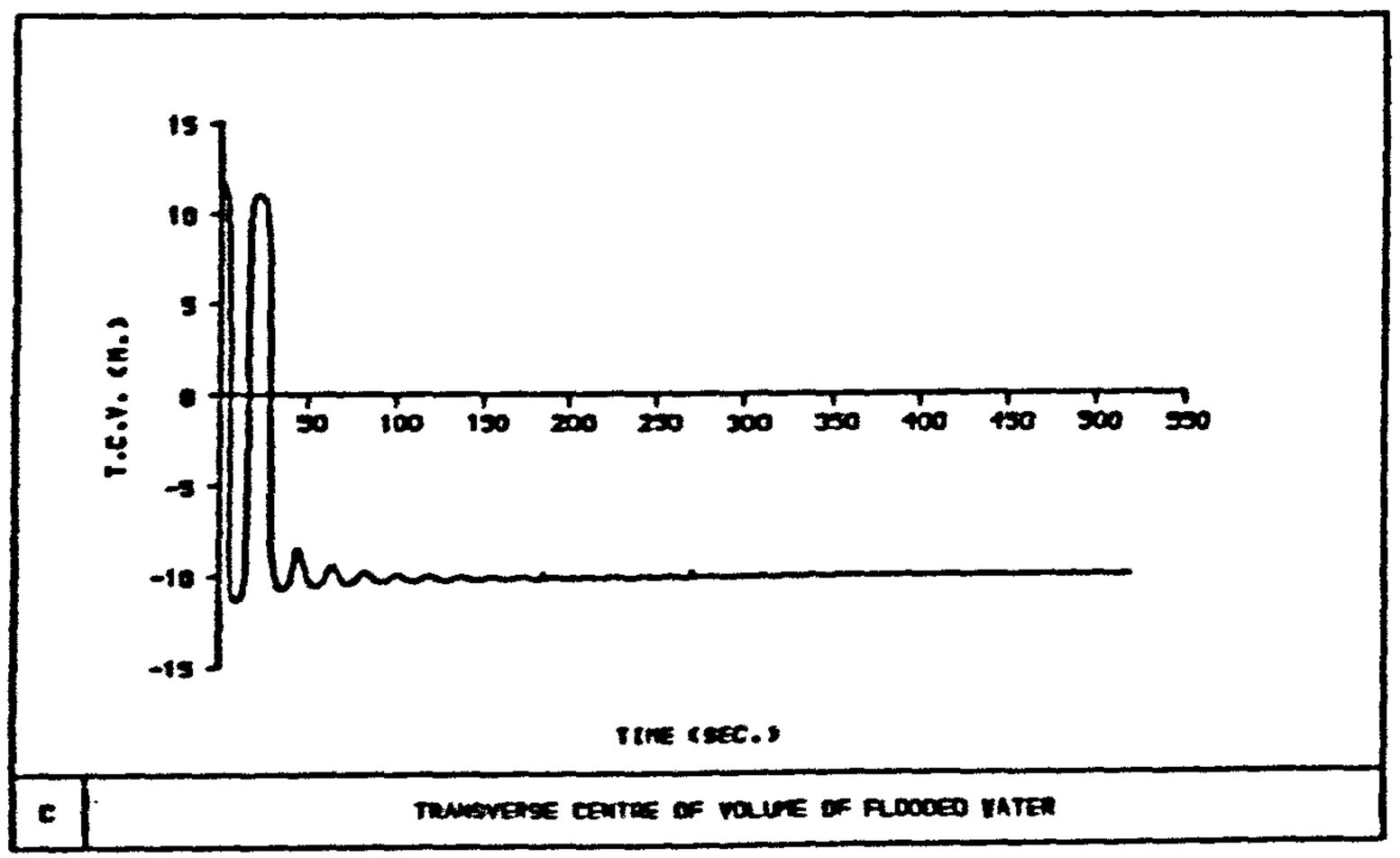

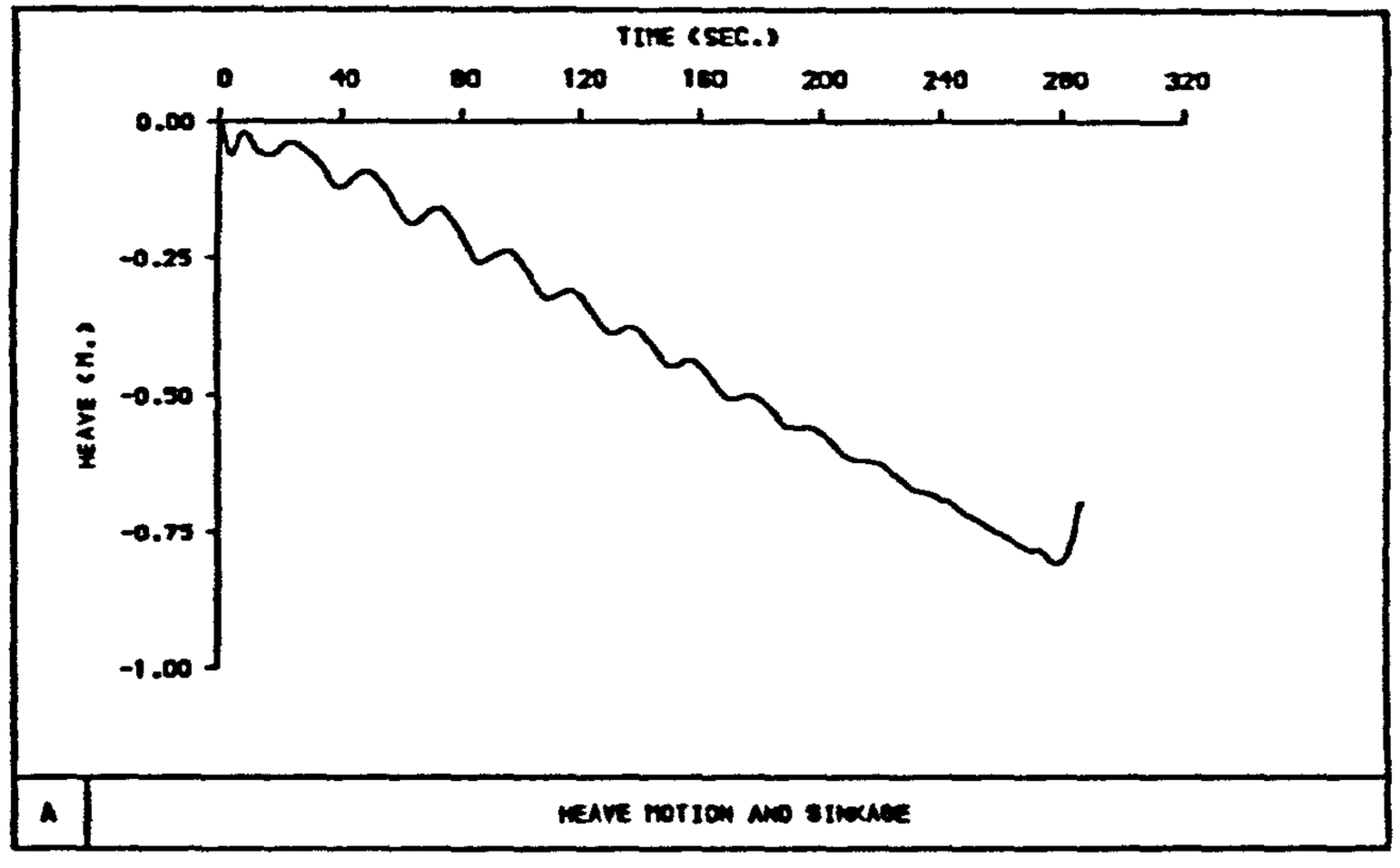

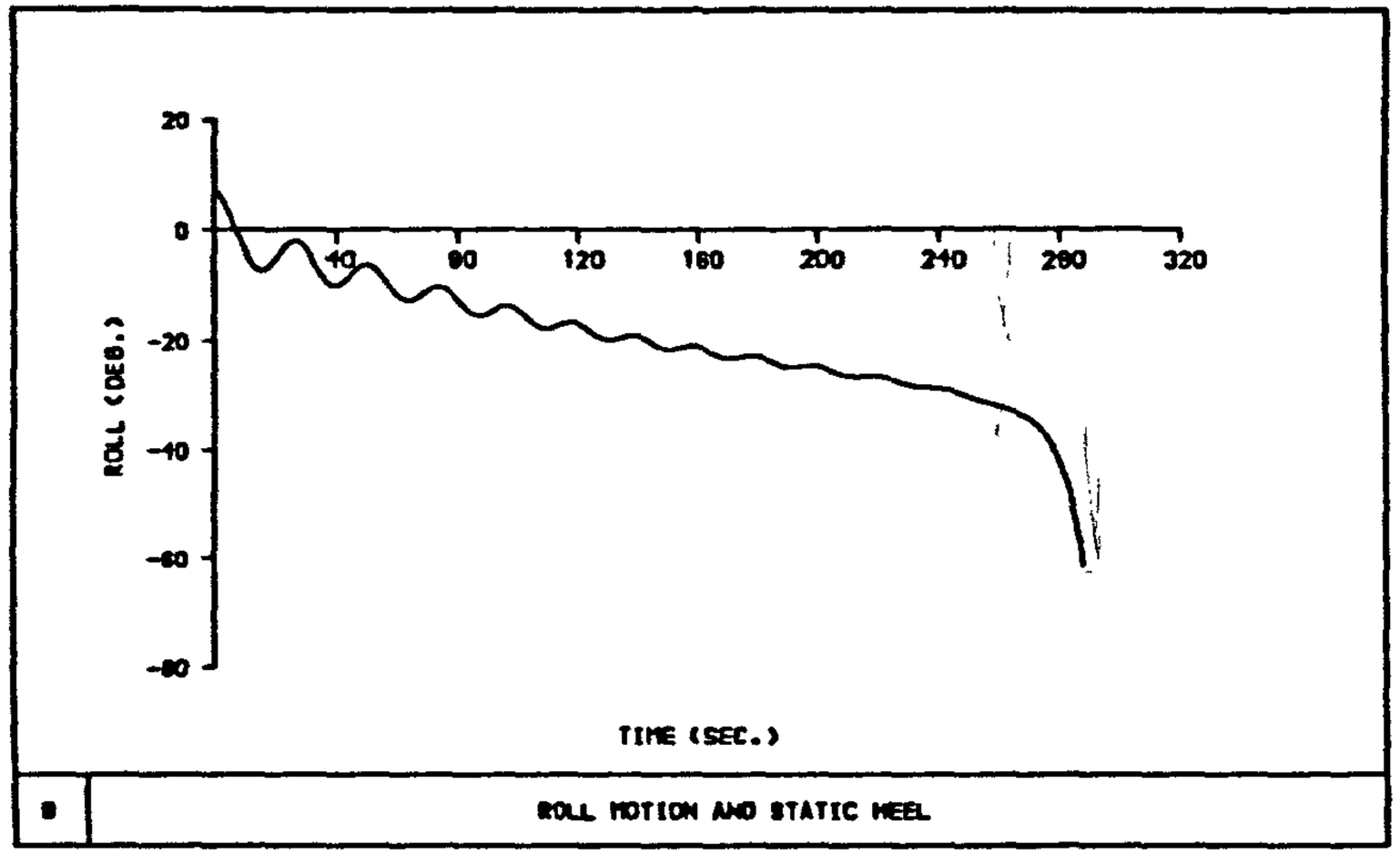

Fig 7.25 Time histories of ship motions and transverse centre of gravity of water on deck during progressive flooding, KG= 12.59 m, calm water [DAMAGE SCENARIO 4]

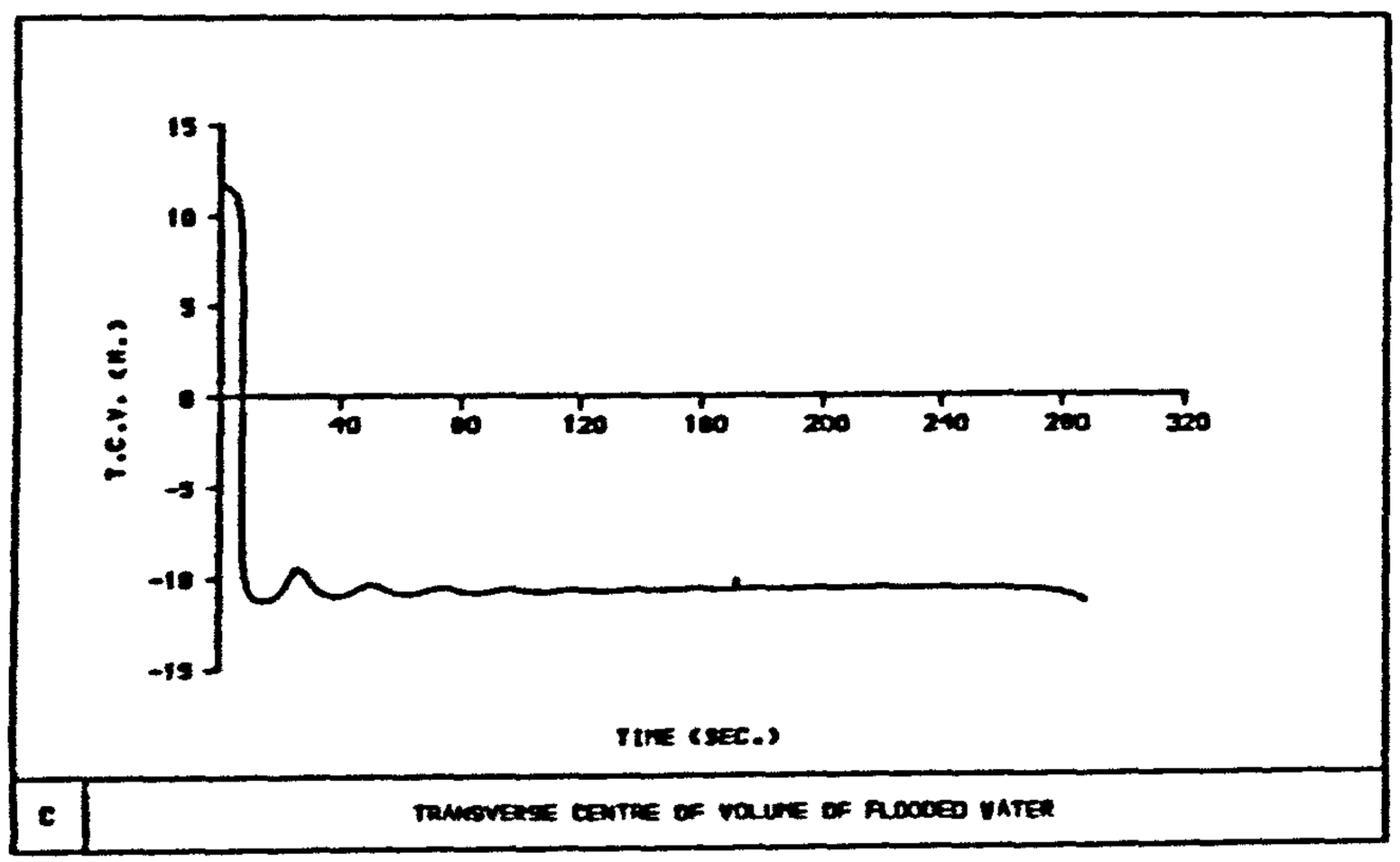

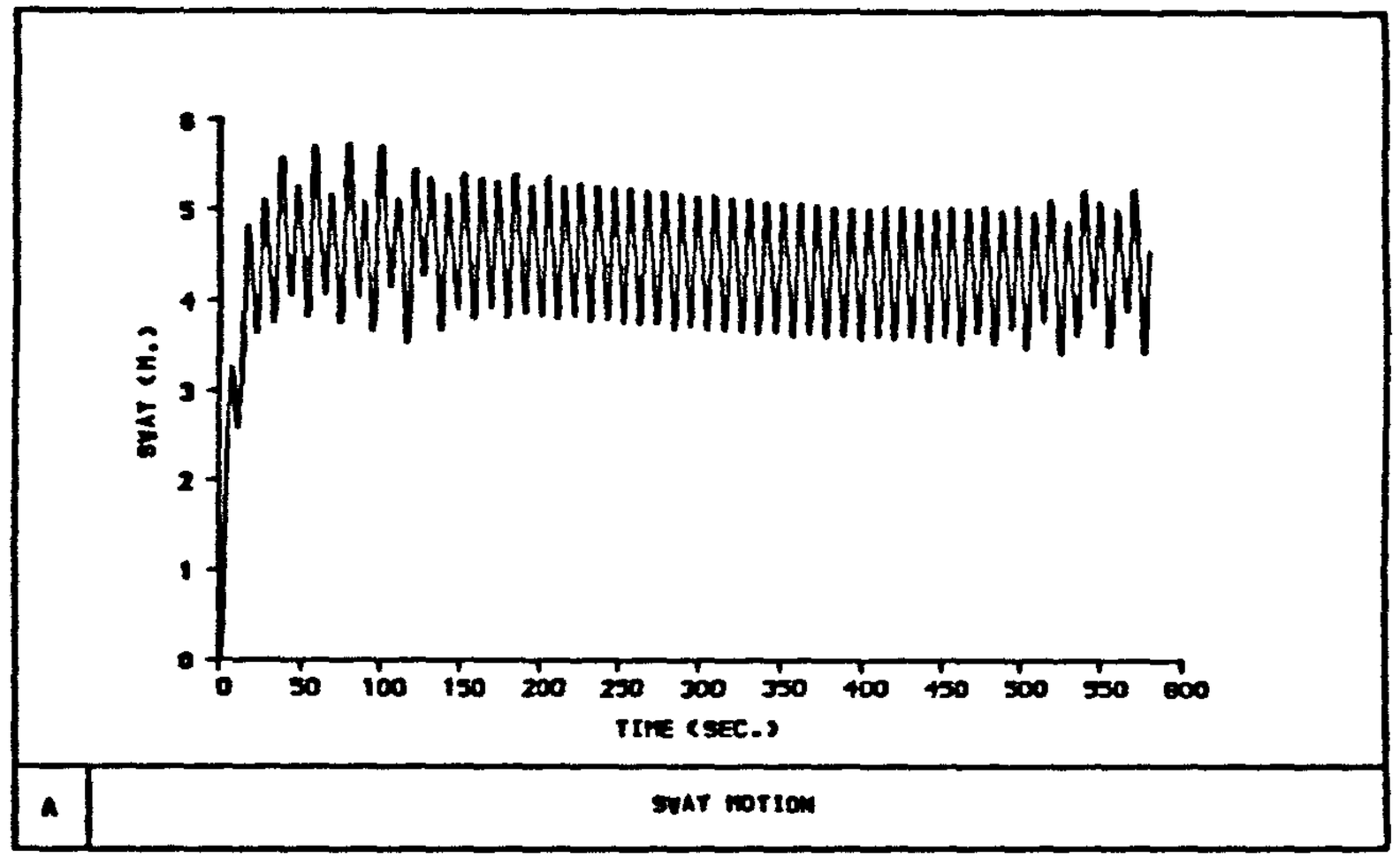

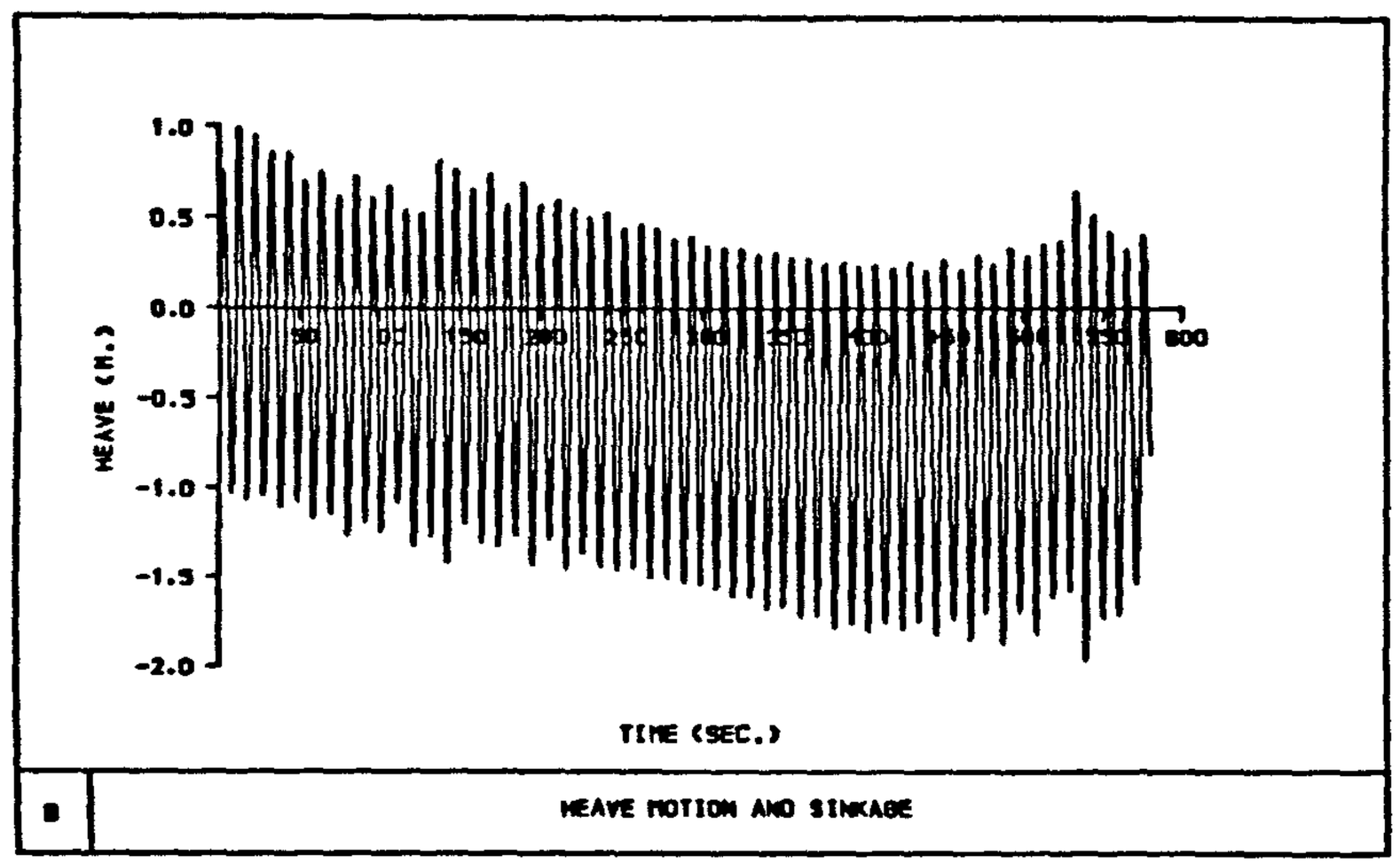

Fig 7.26 Time histories of ship motions and transverse centre of gravity of water on deck during progressive flooding, KG= 11.84 m, WH= 2.0 m [DAMAGE SCENARIO 4]

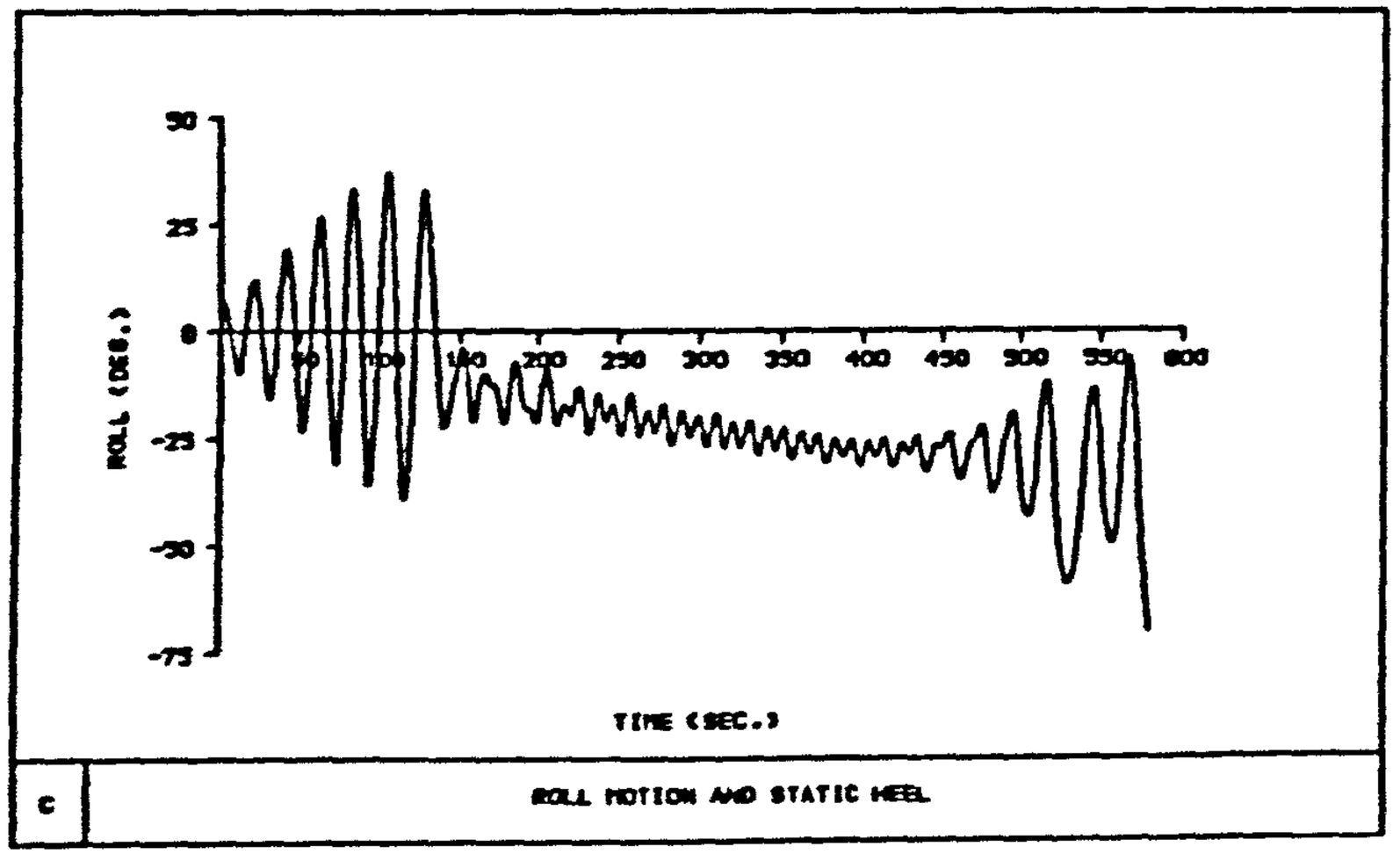

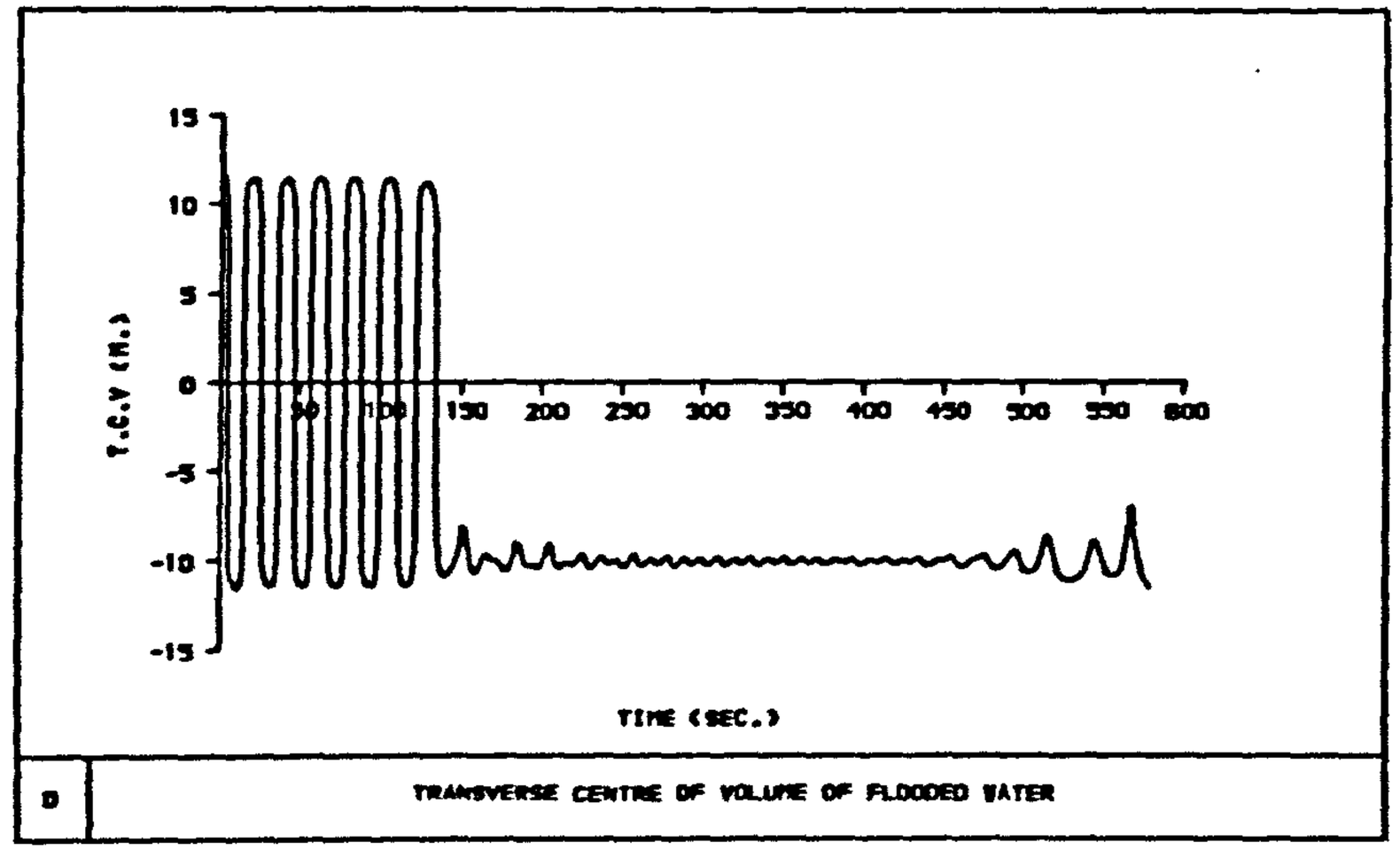

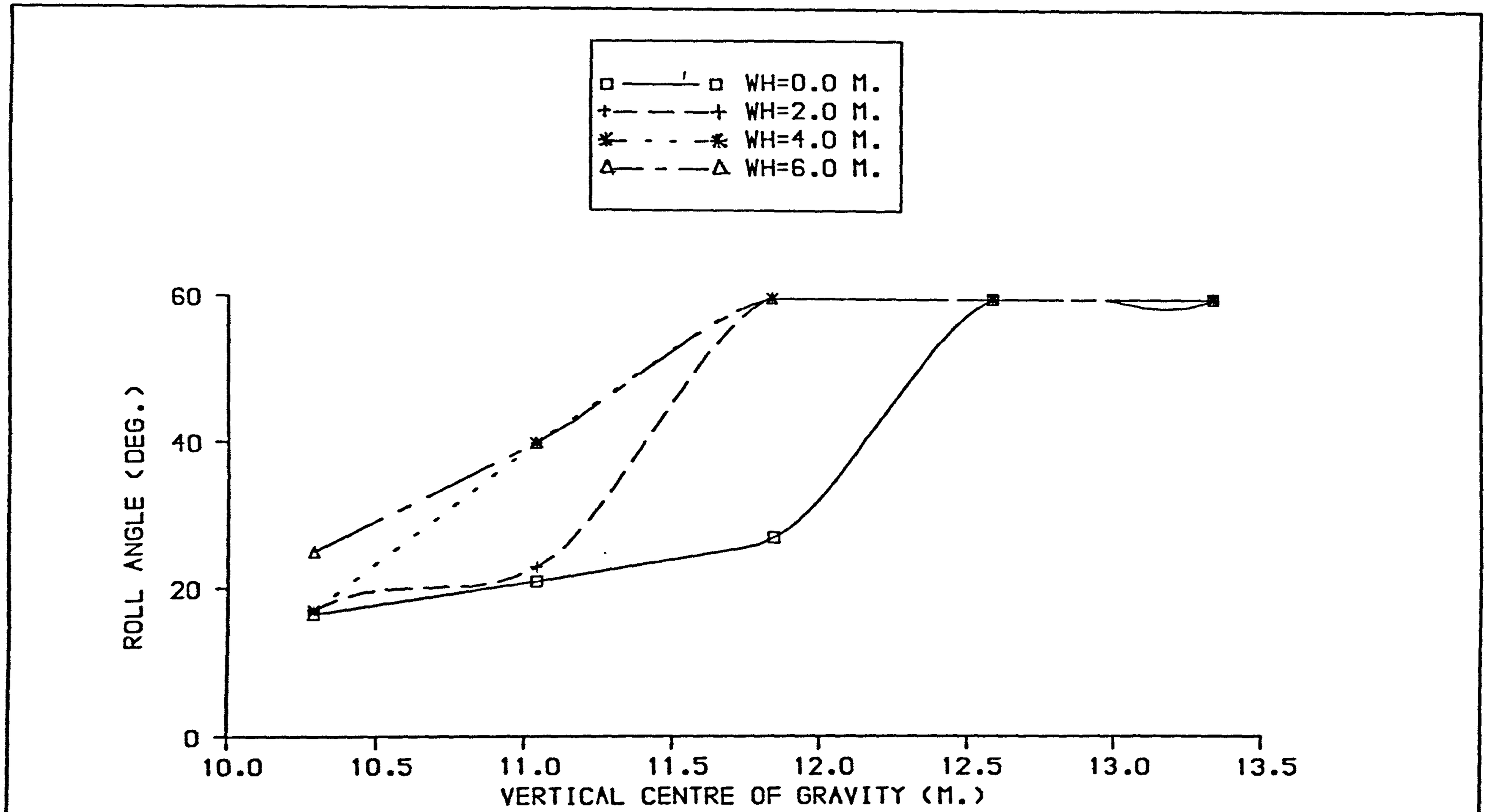

Fig 7.27 Effect of loading condition and wave height on maximum roll amplitude [DAMAGE SCENARIO 4]

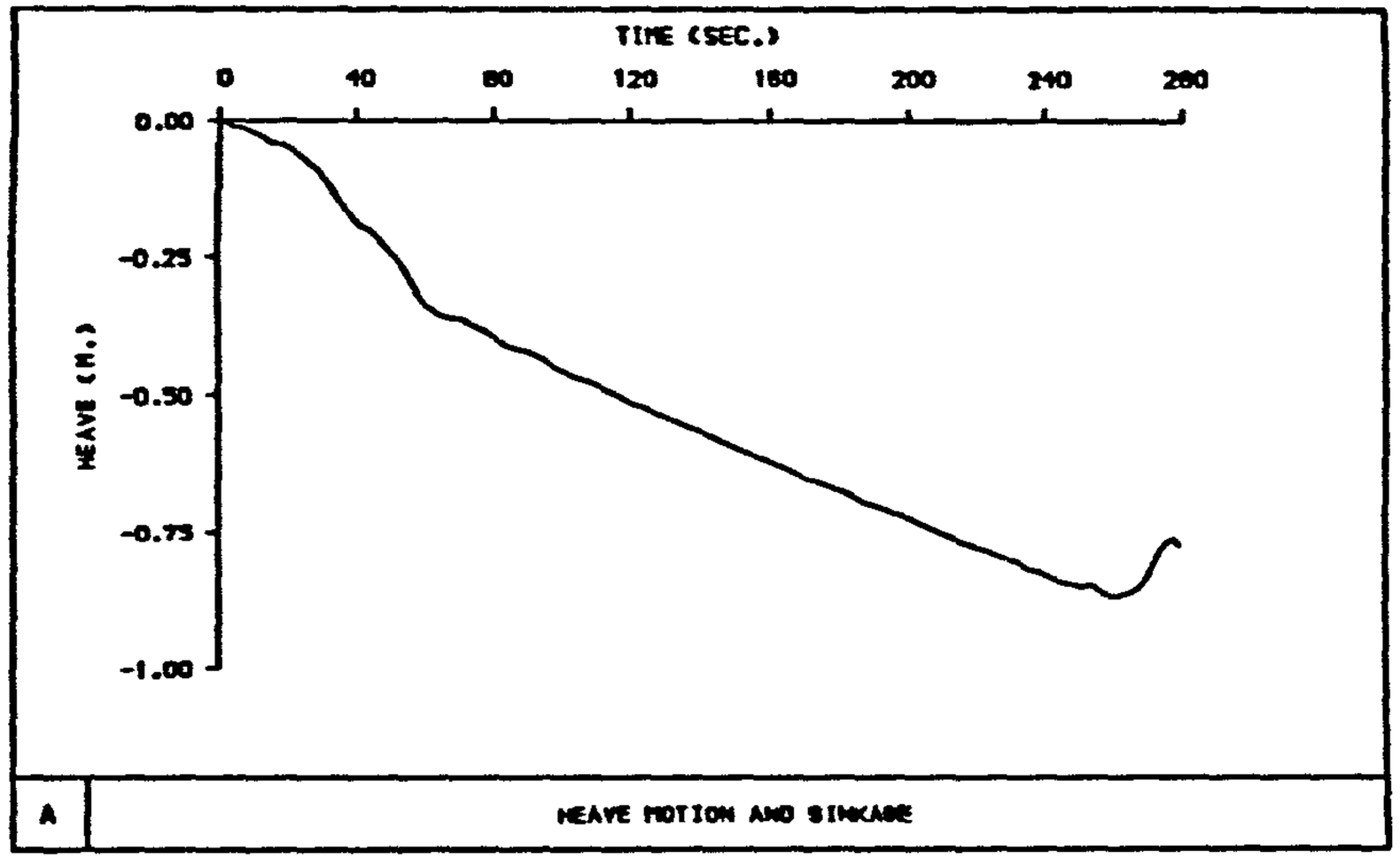

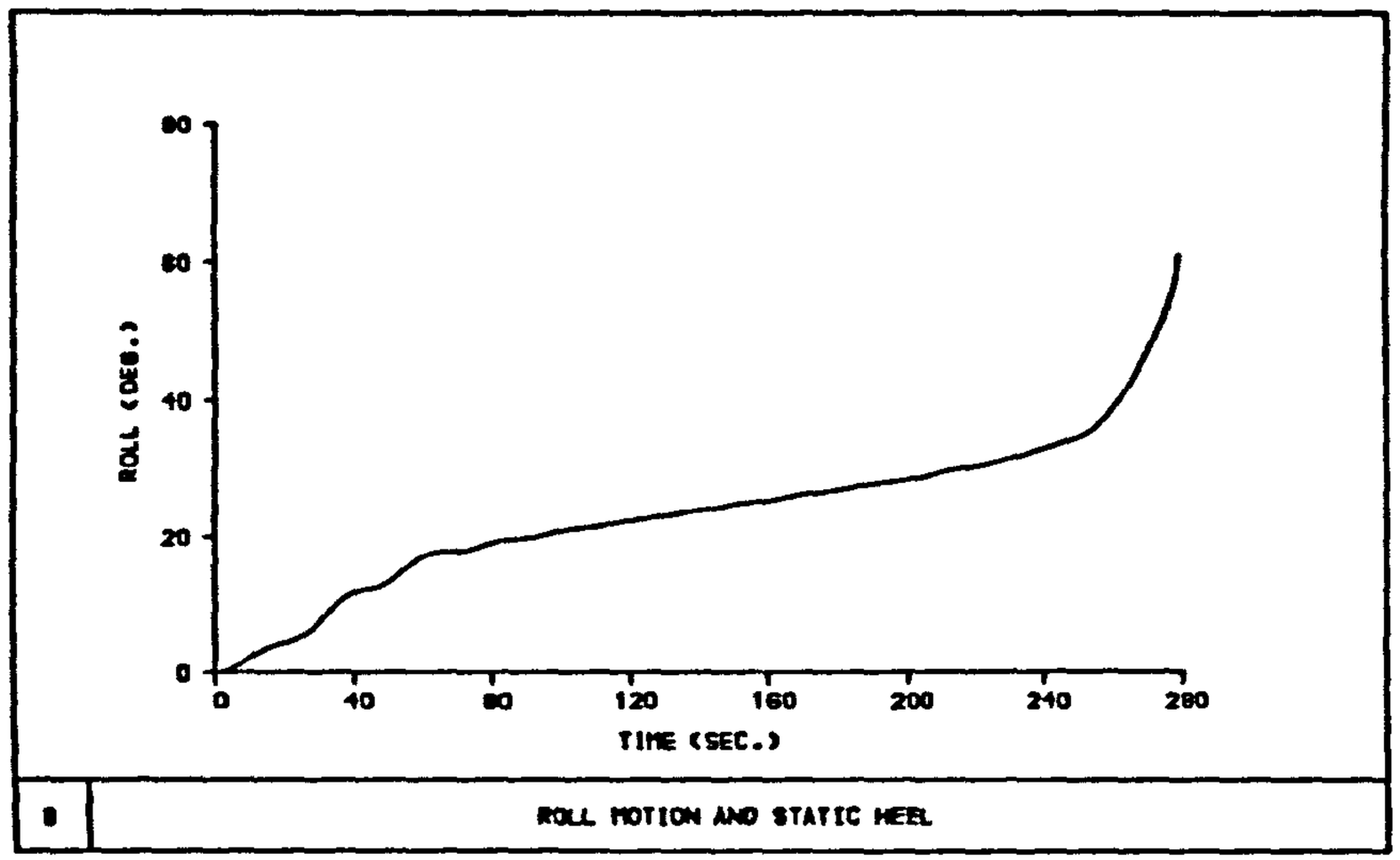

Fig 7.28 Time histories of ship motions and transverse centre of gravity of water on deck during progressive flooding, KG= 12.59 m, calm water [DAMAGE SCENARIO 5]

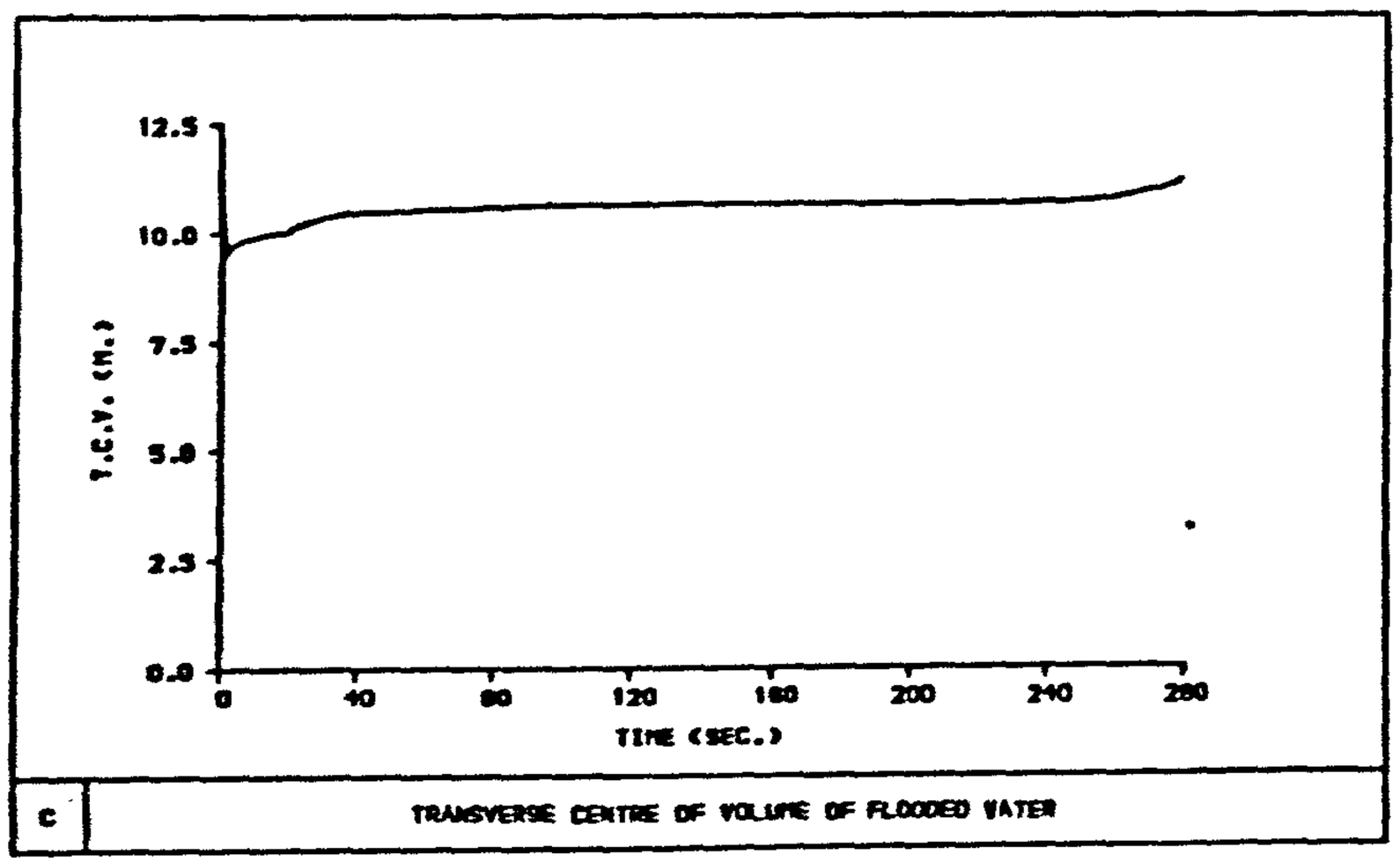

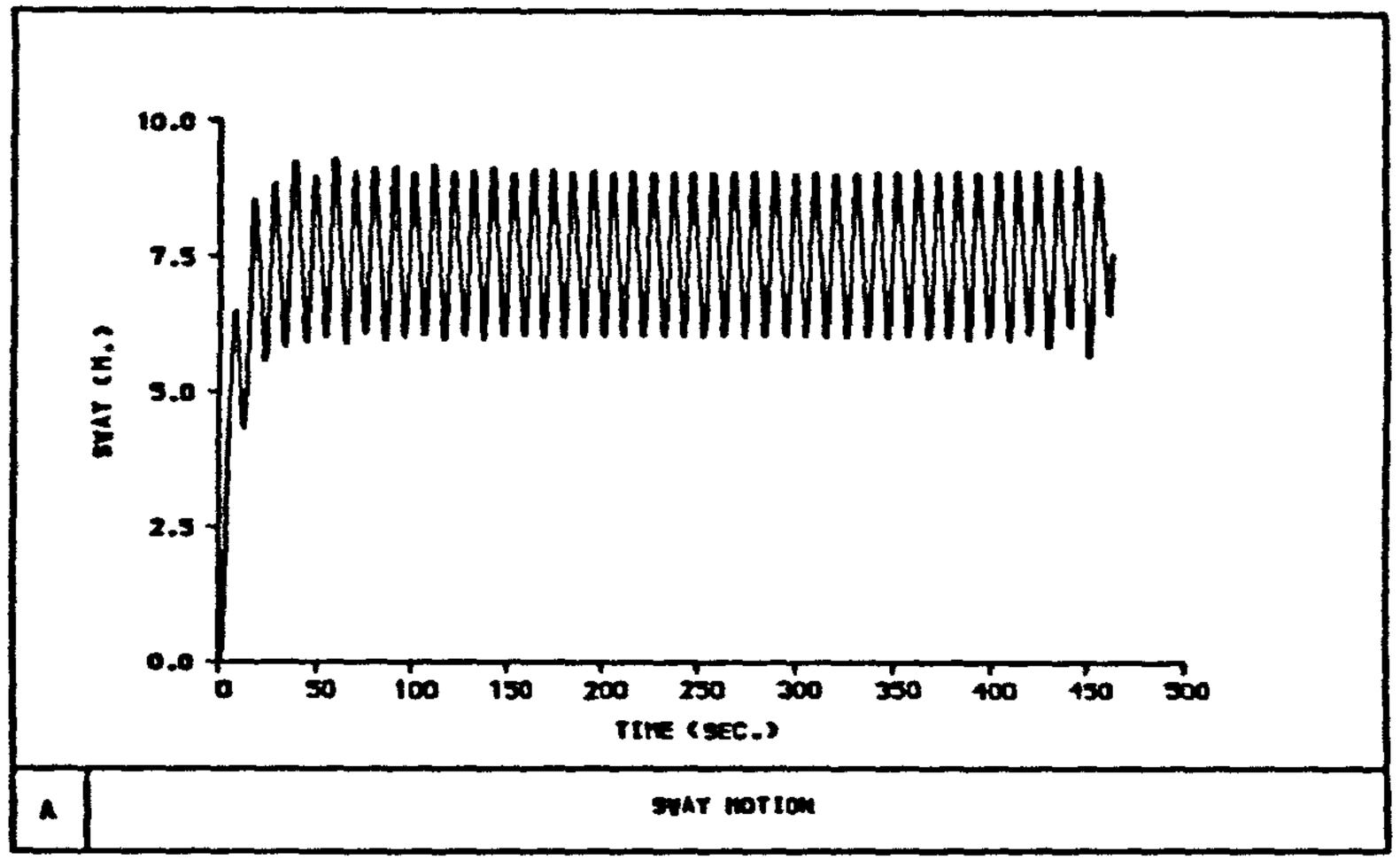

A SWAY MOTION

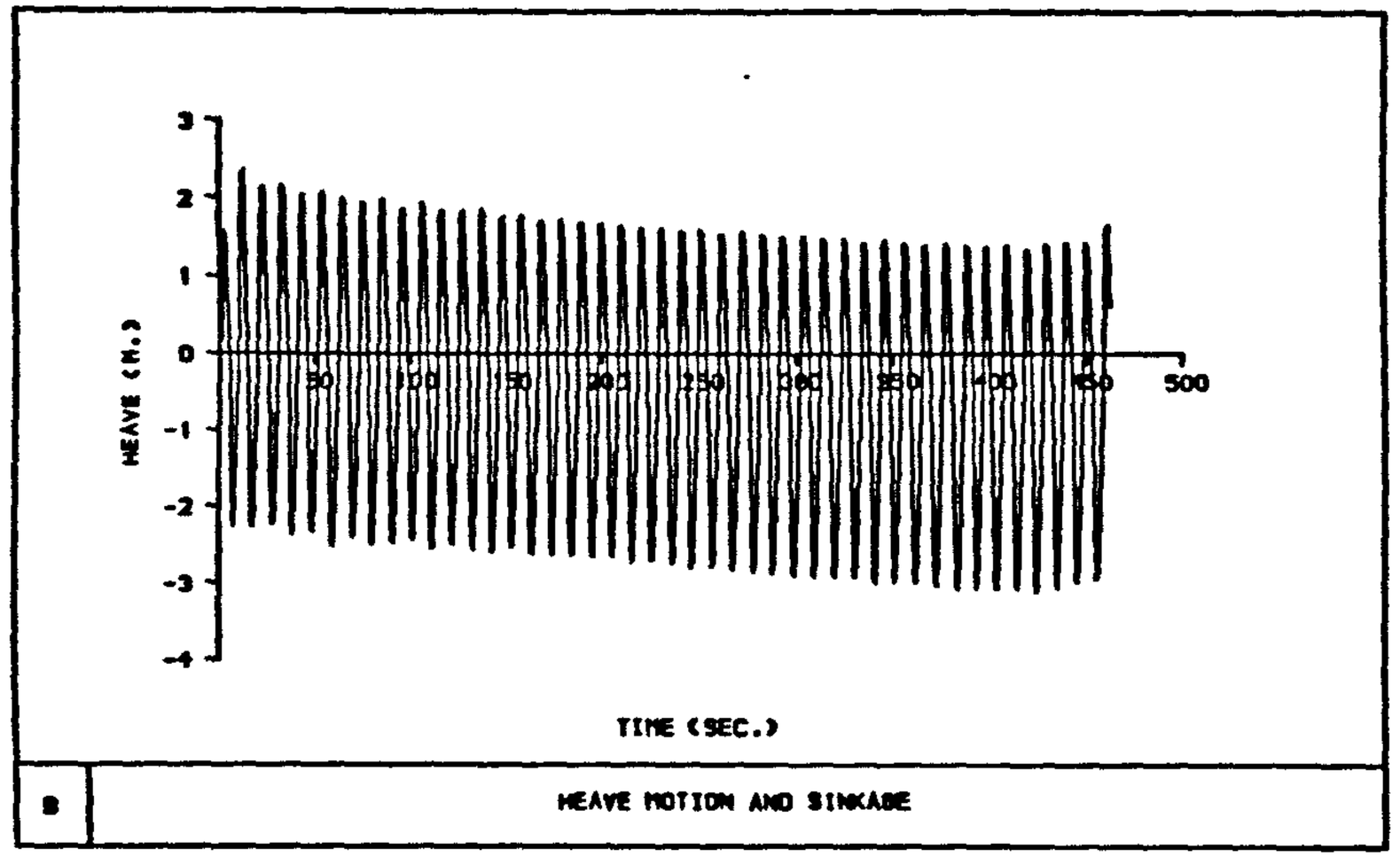

B HEAVE MOTION AND SINKAGE

Fig 7.29 Time histories of ship motions and transverse centre of gravity of water on deck during progressive flooding, KG= 11.84 m, WH= 4.0 m [DAMAGE SCENARIO 5]

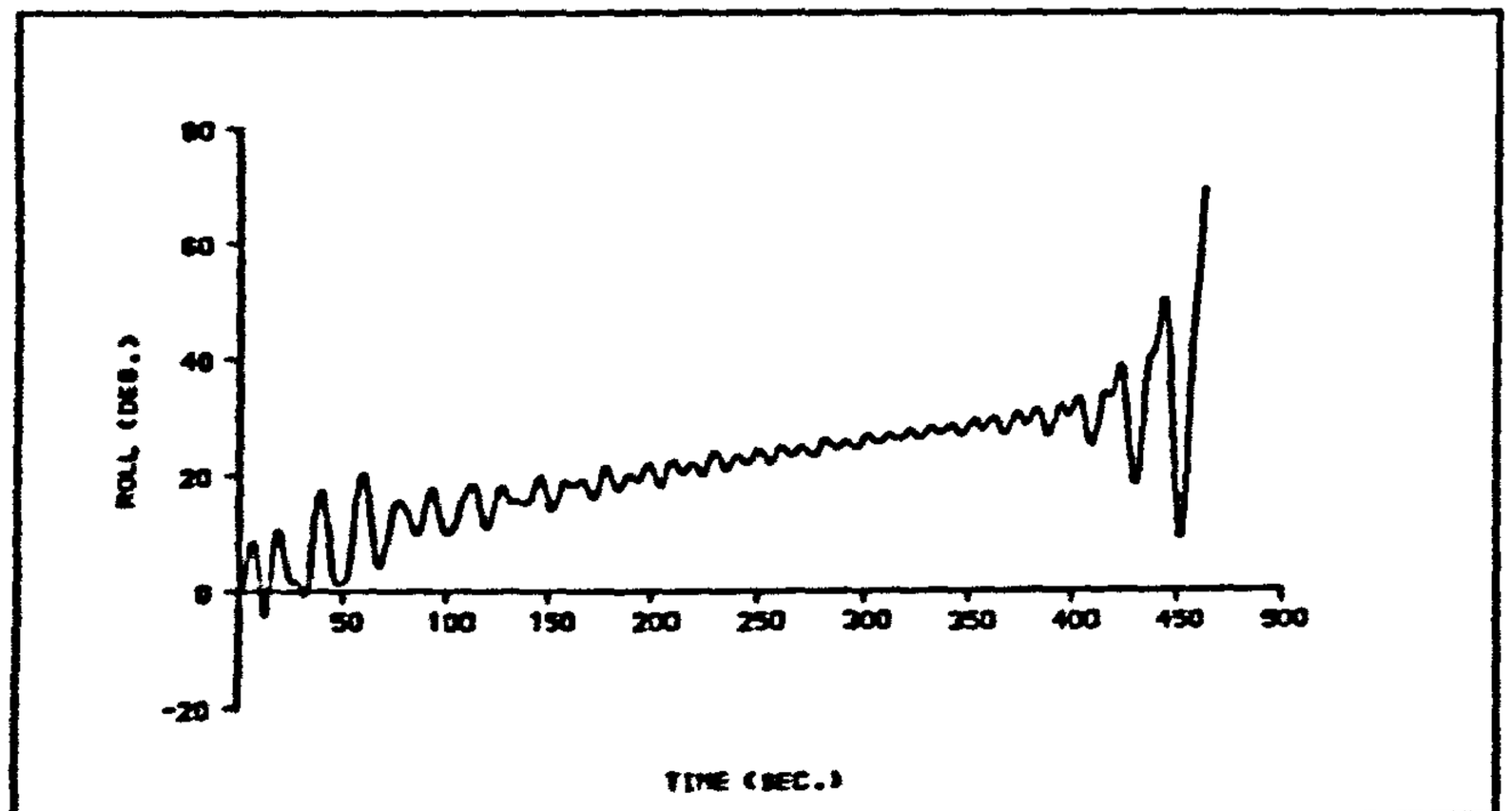

C ROLL MOTION AND STATIC HEEL

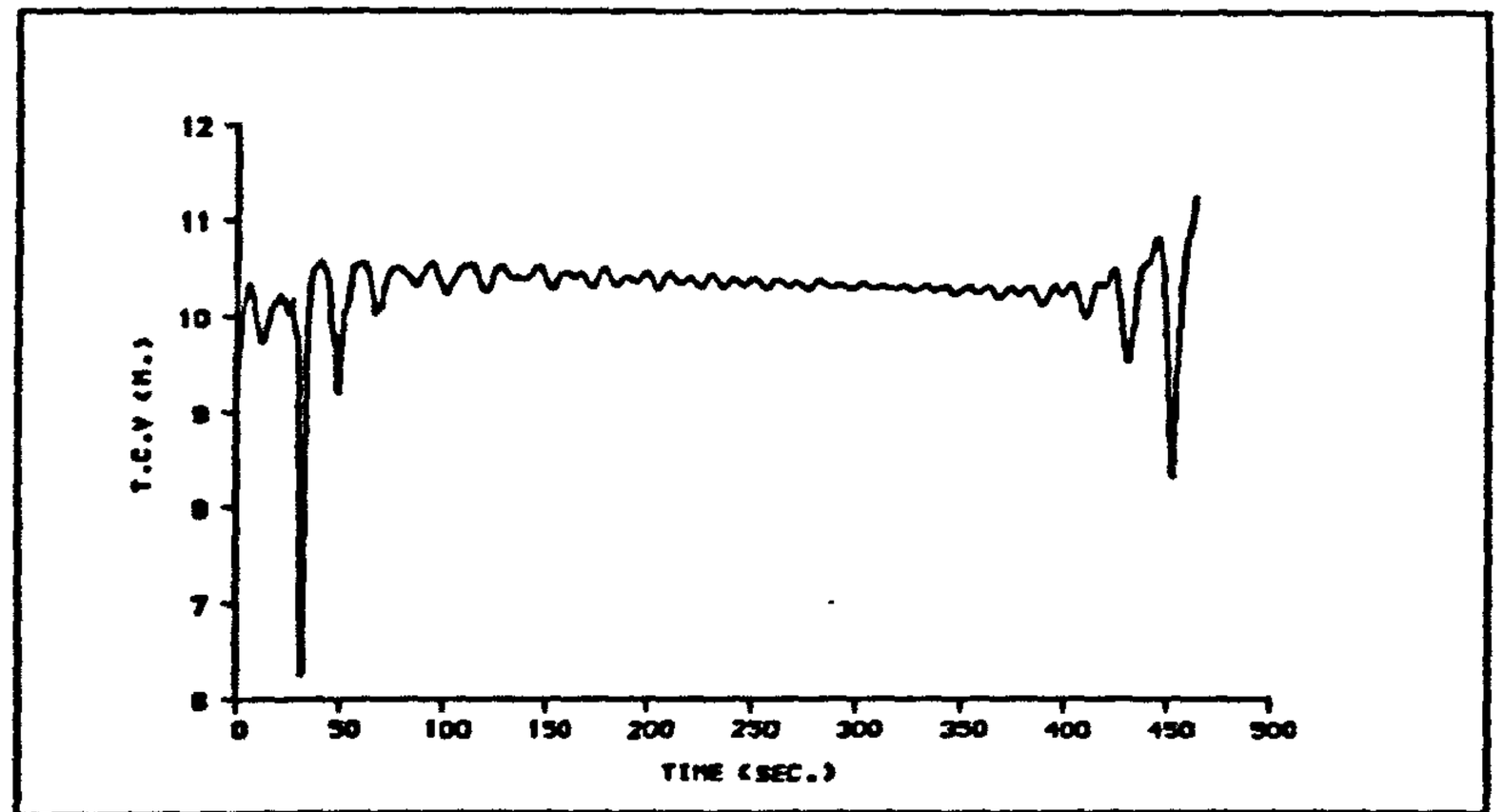

D TRANSVERSE CENTRE OF VOLUME OF FLOODED WATER

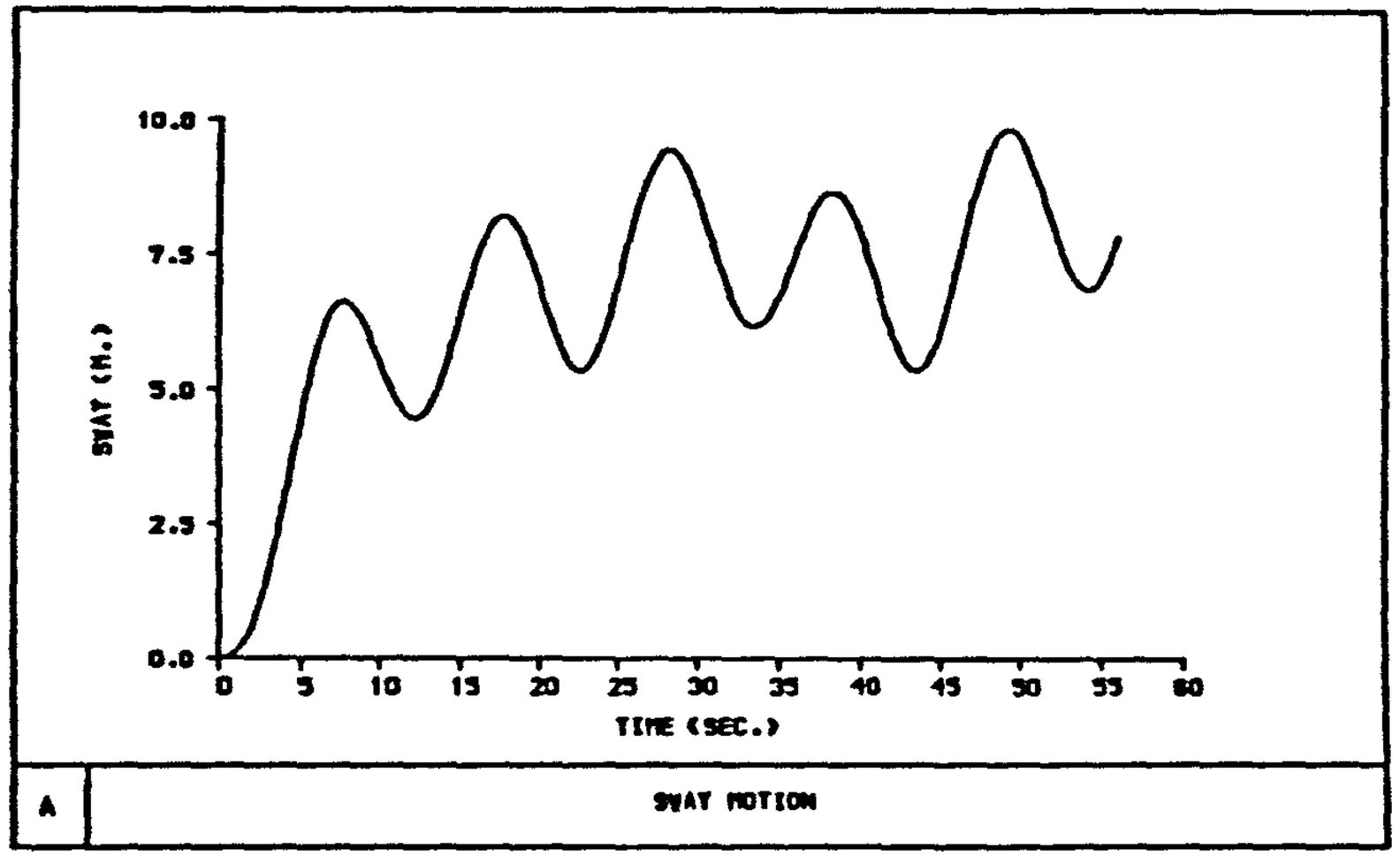

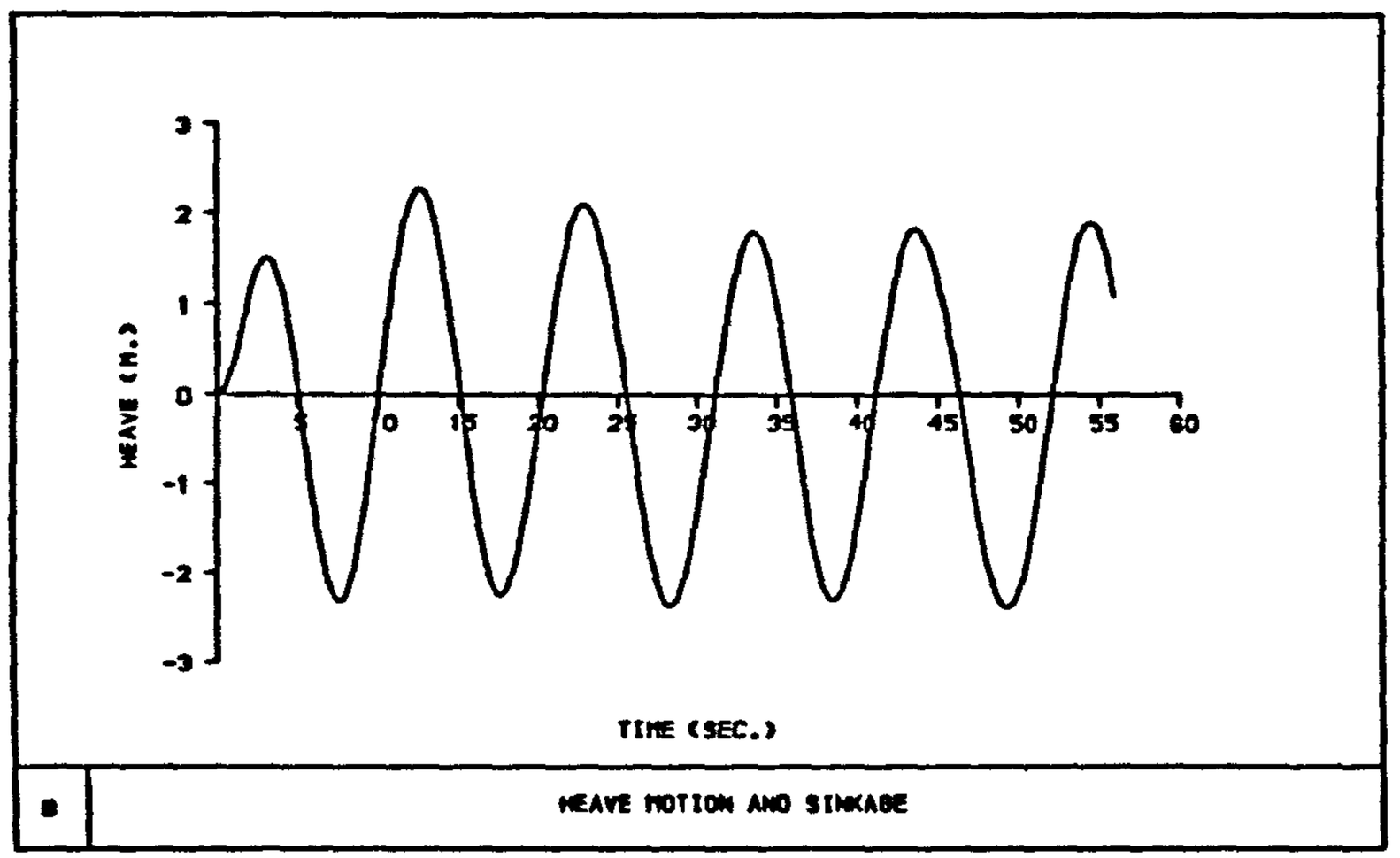

Fig 7.30 Time histories of ship motions and transverse centre of gravity of water on deck during progressive flooding, KG= 12.59 m, WH= 4.0 m [DAMAGE SCENARIO 5]

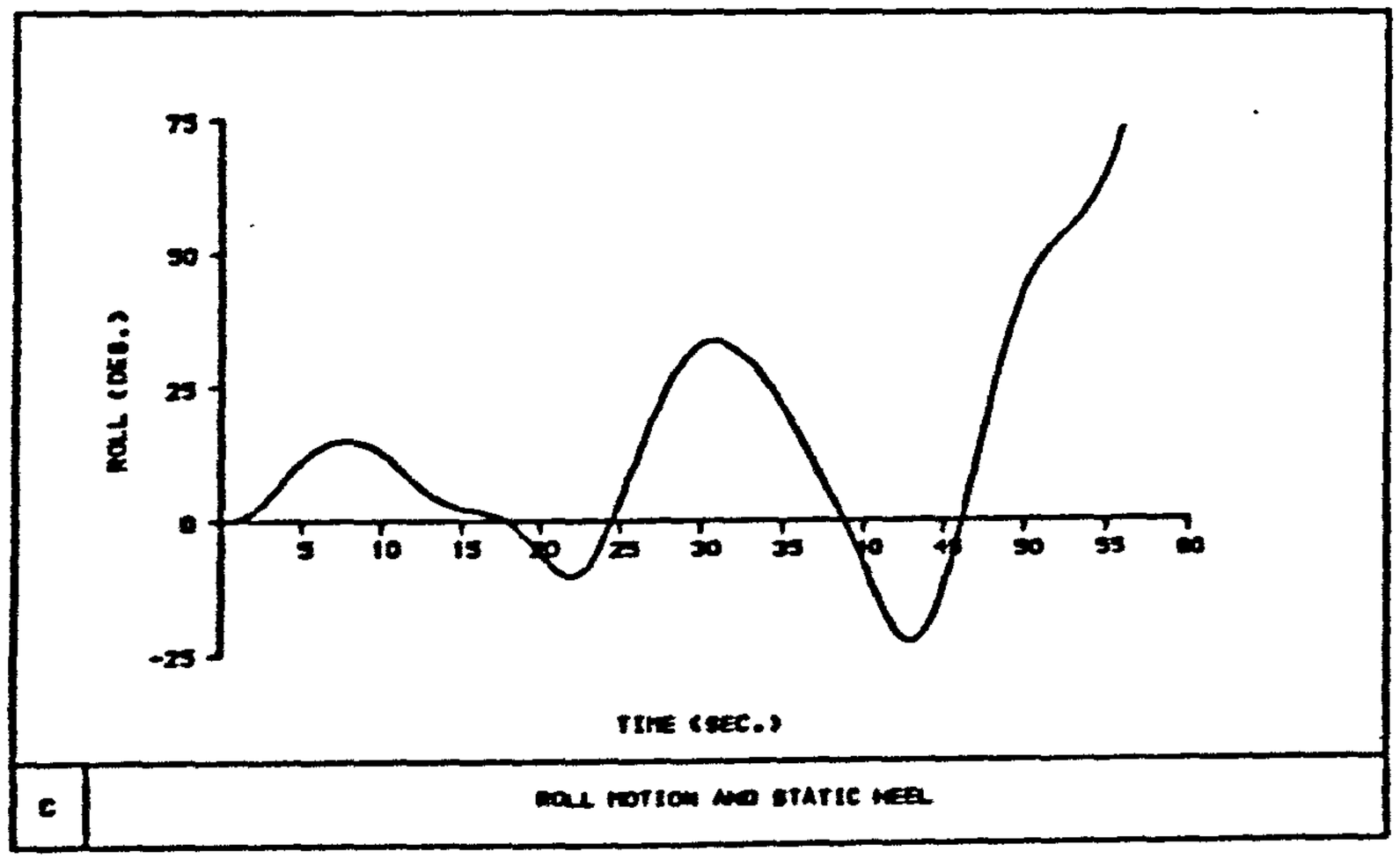

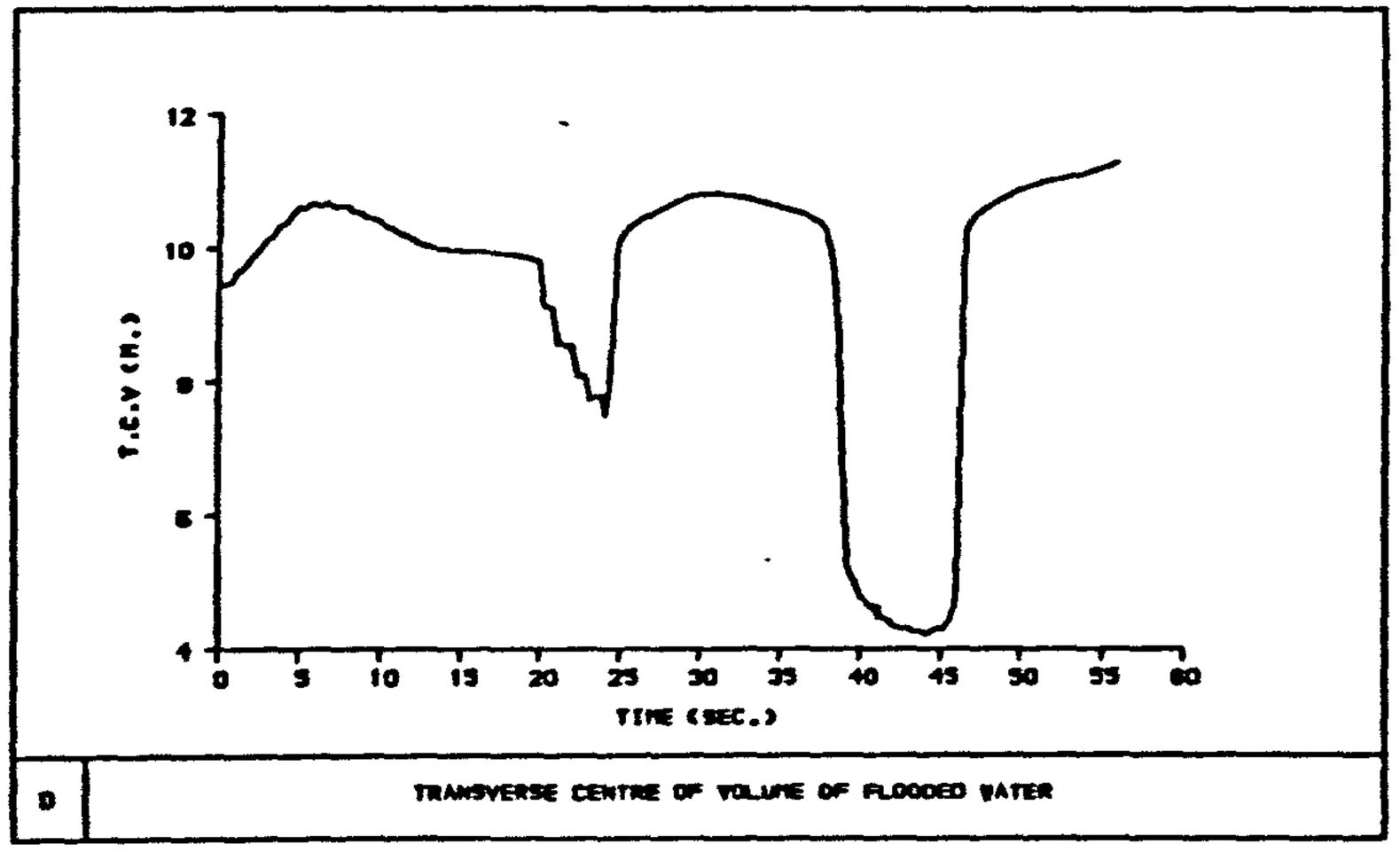

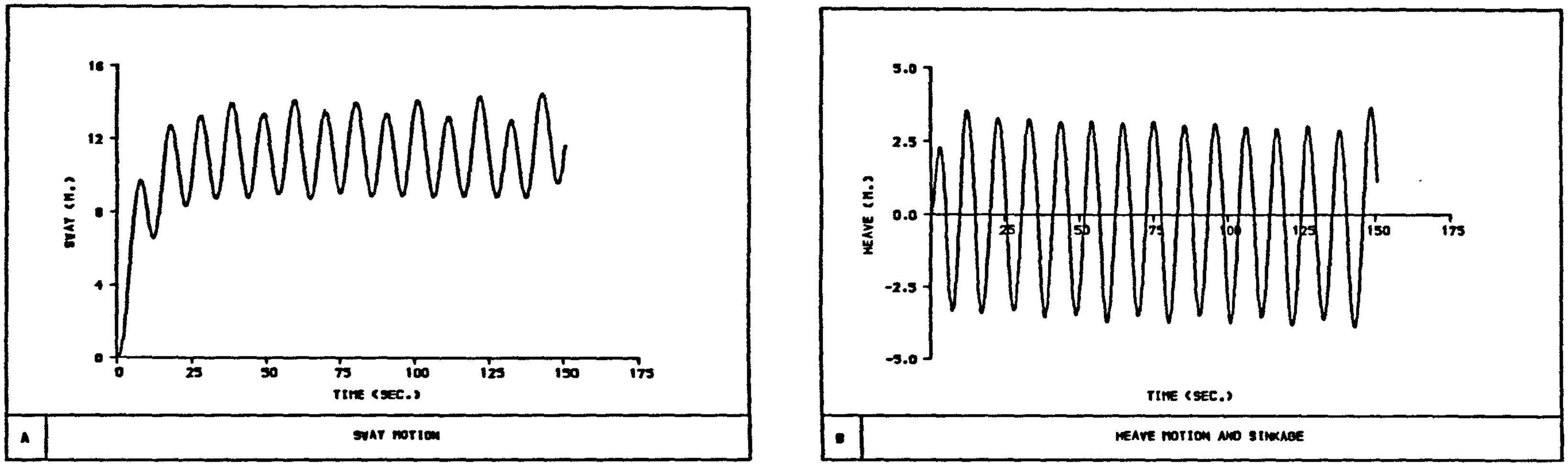

Fig 7.31 Time histories of ship motions and transverse centre of gravity of water on deck during progressive flooding, KG= 11.84 m, WH= 6.0 m [DAMAGE SCENARIO 5]

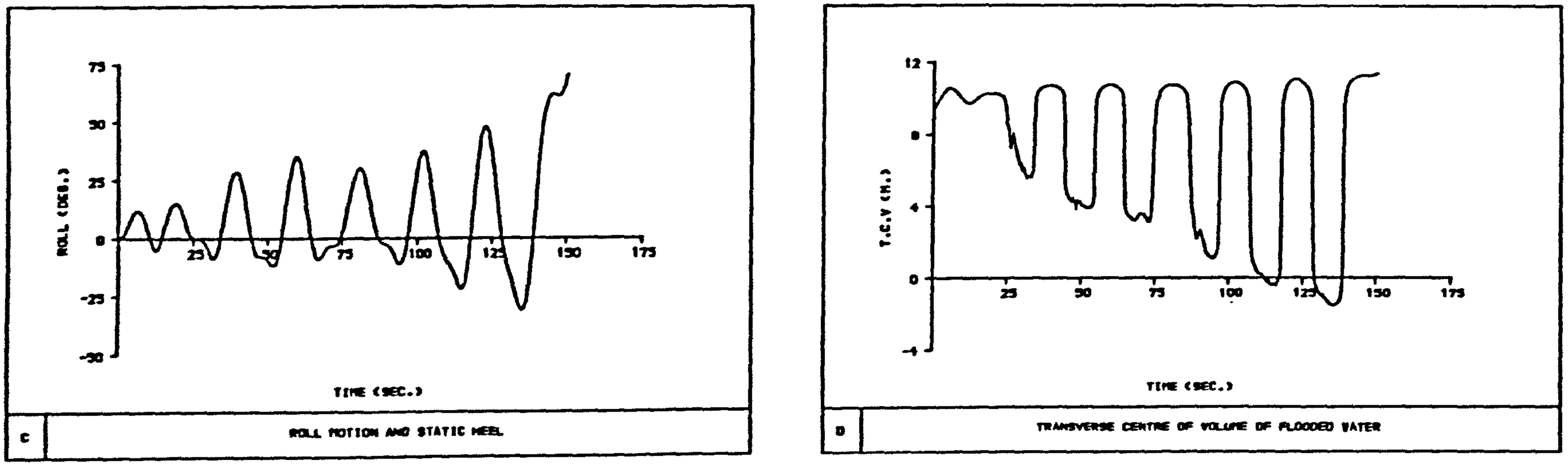

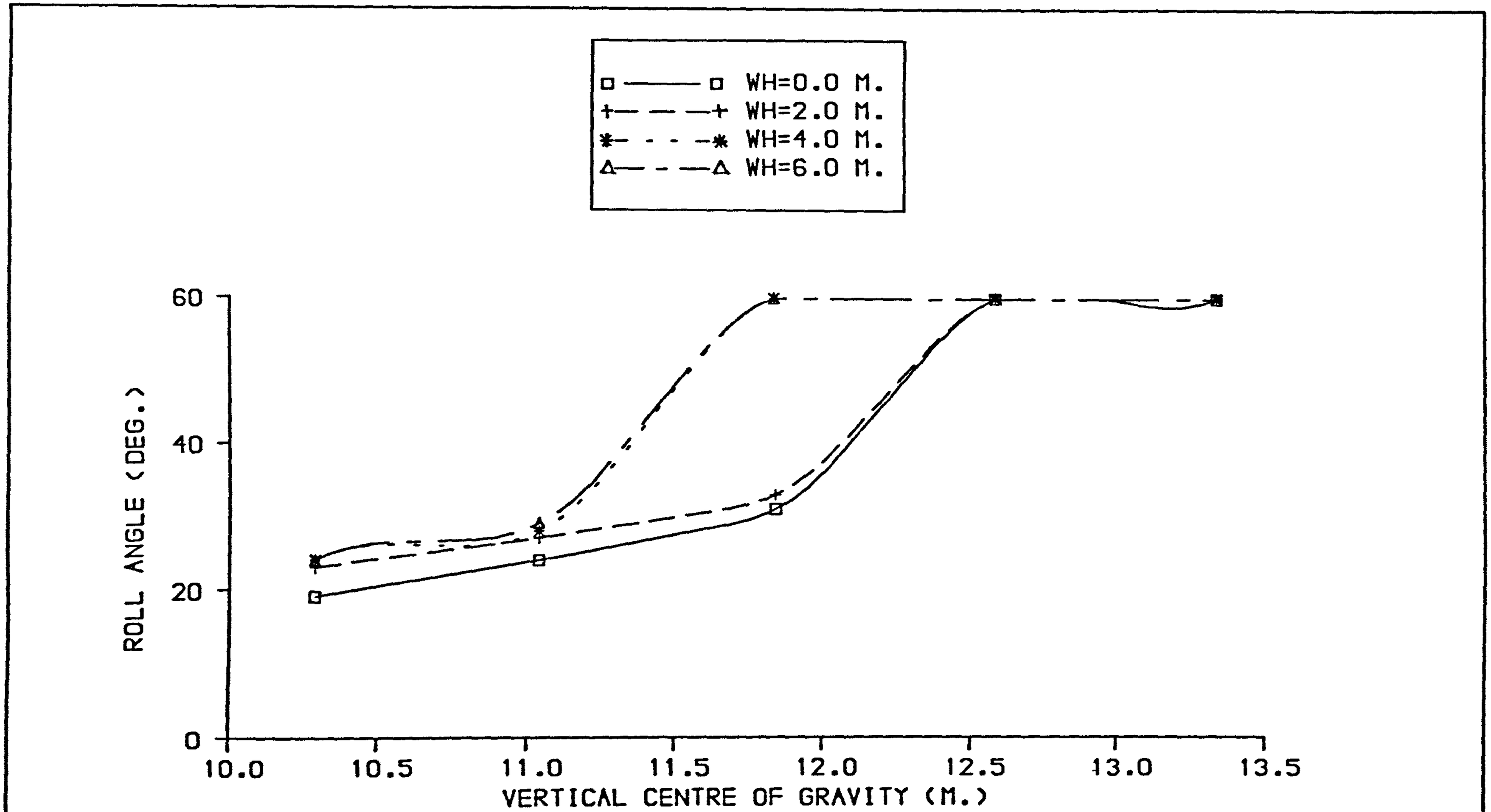

Fig 7.32 Effect of loading condition and wave height on maximum roll amplitude [DAMAGE SCENARIO 5]

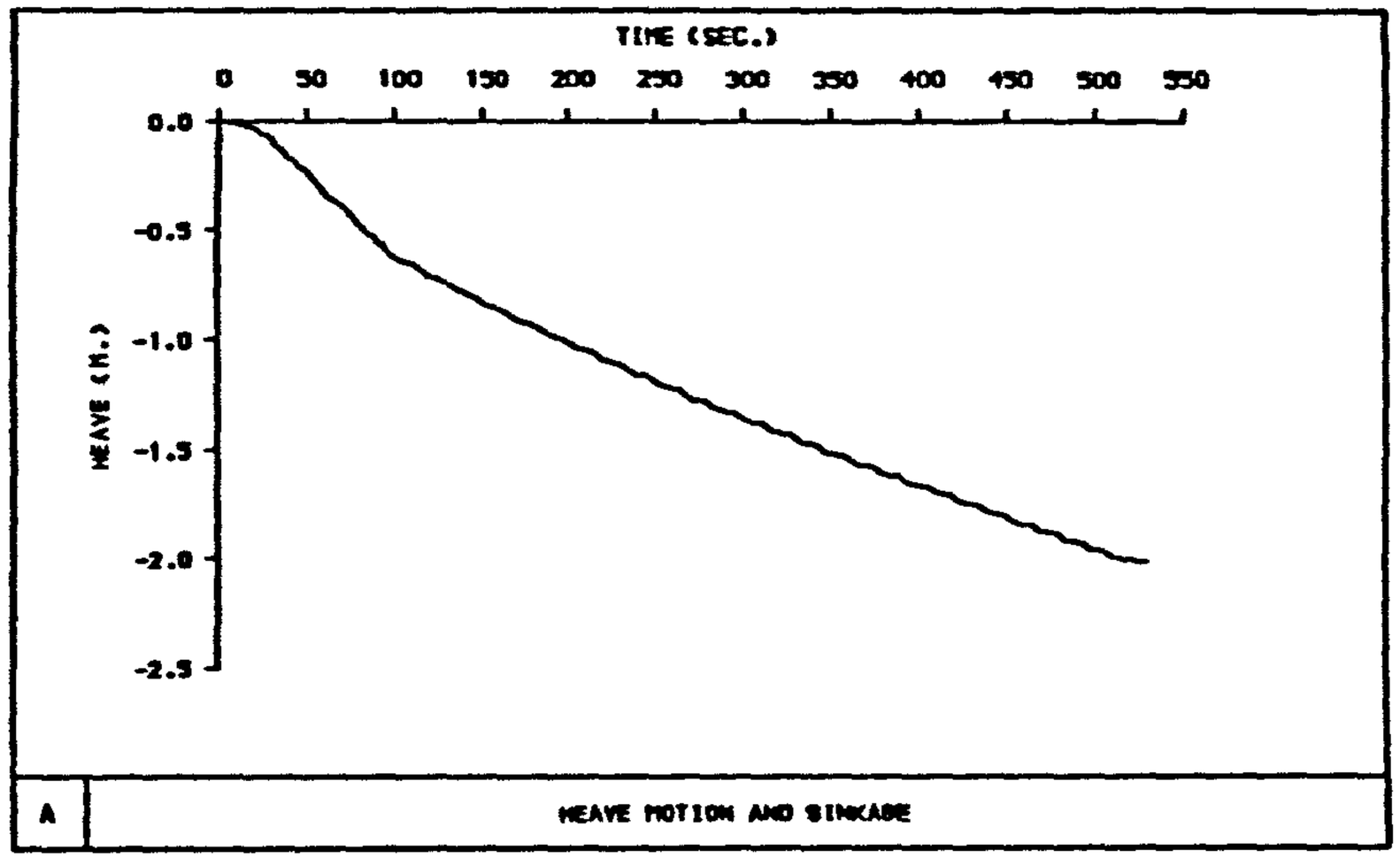

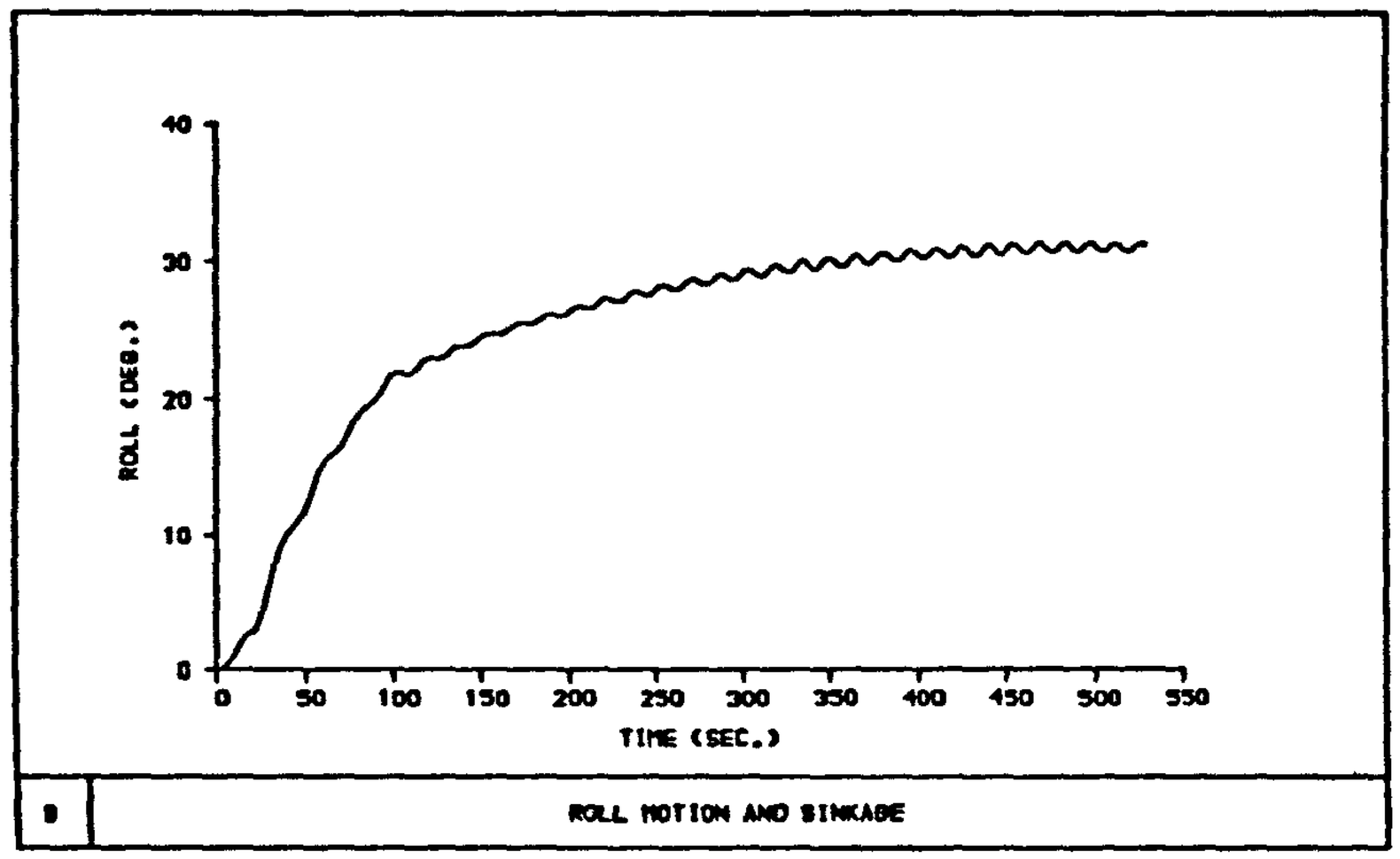

Fig 7.33 Time histories of ship motions and transverse centre of gravity of water on deck during progressive flooding, KG= 12.59 m, calm water [DAMAGE SCENARIO 6]

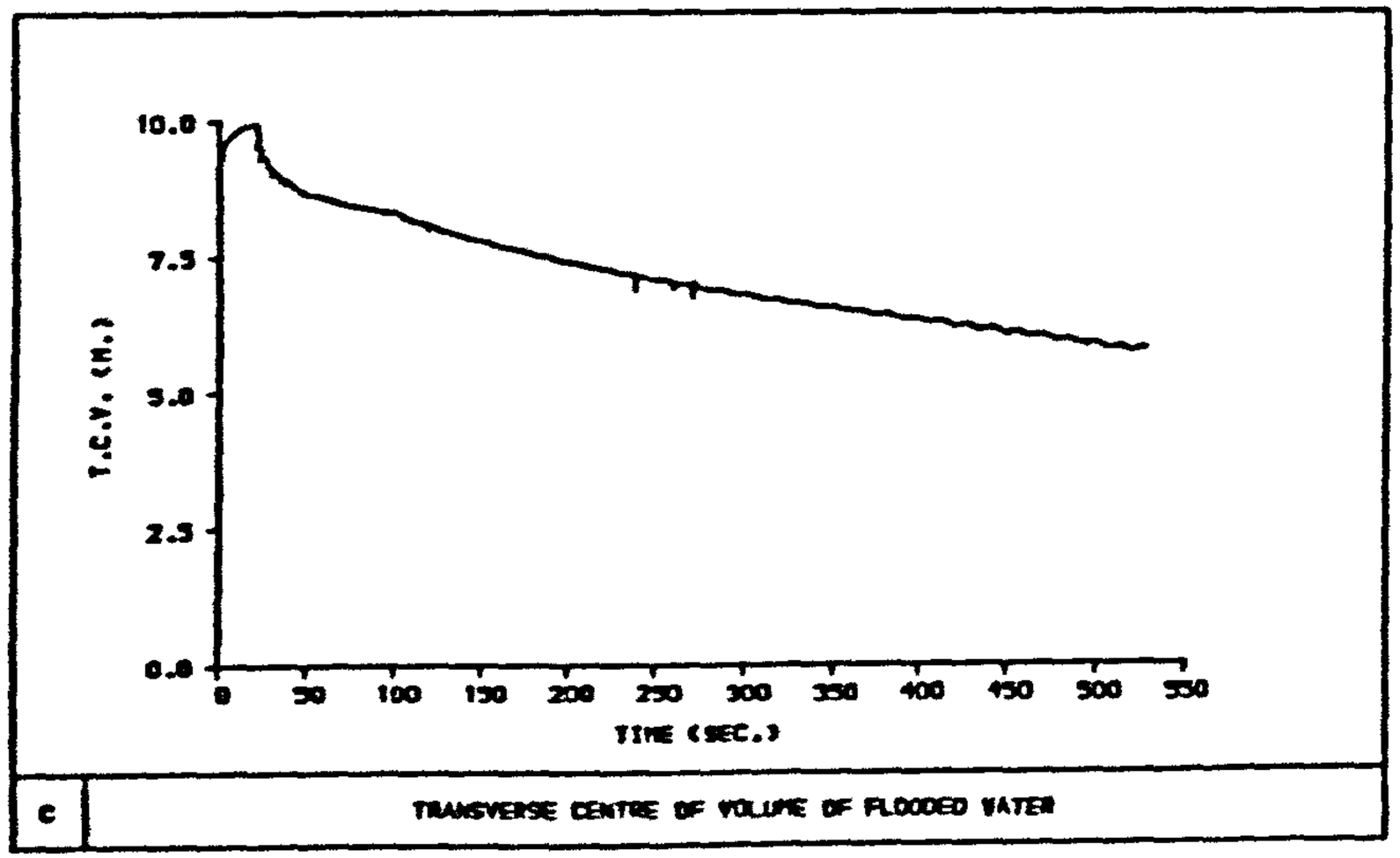

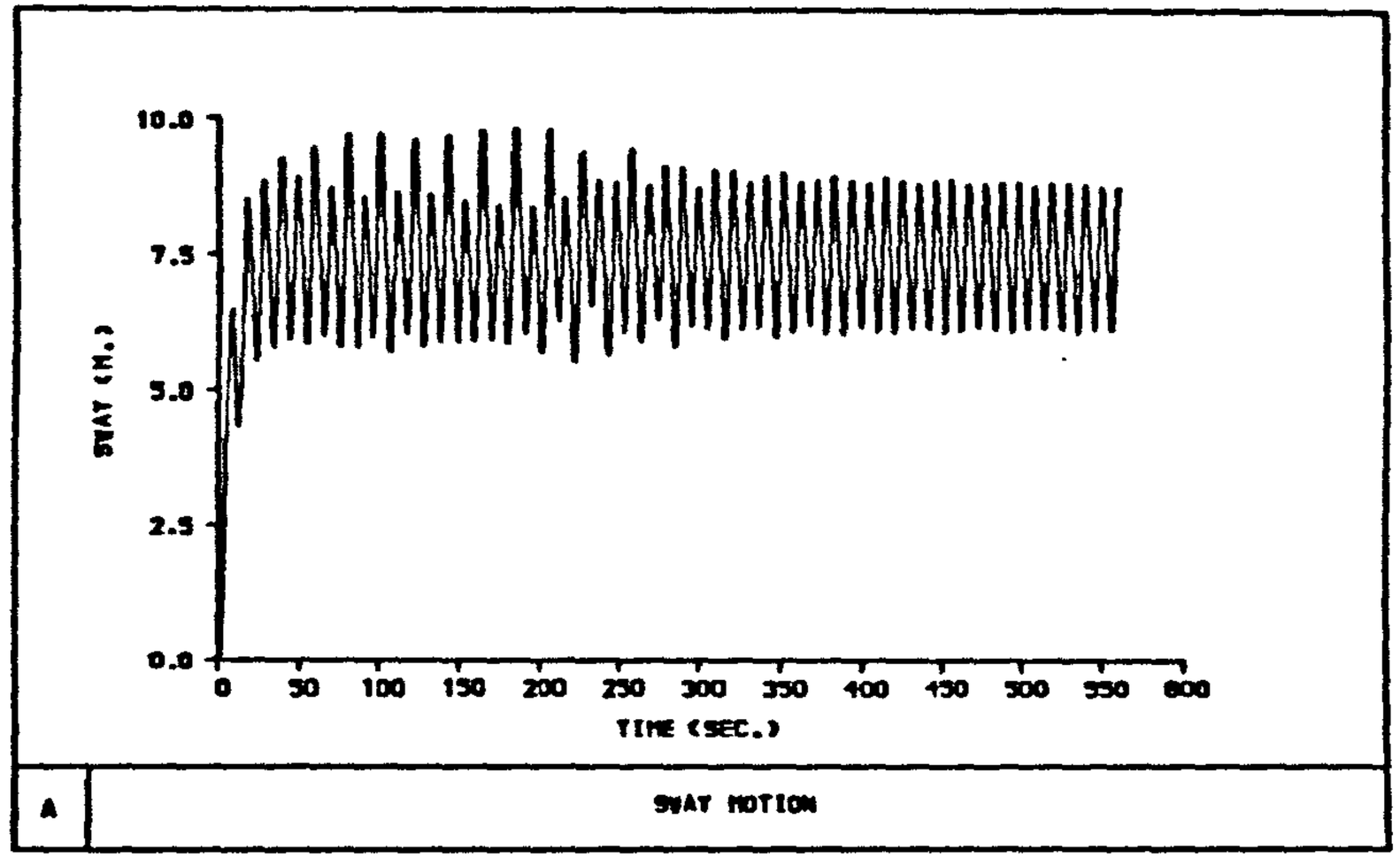

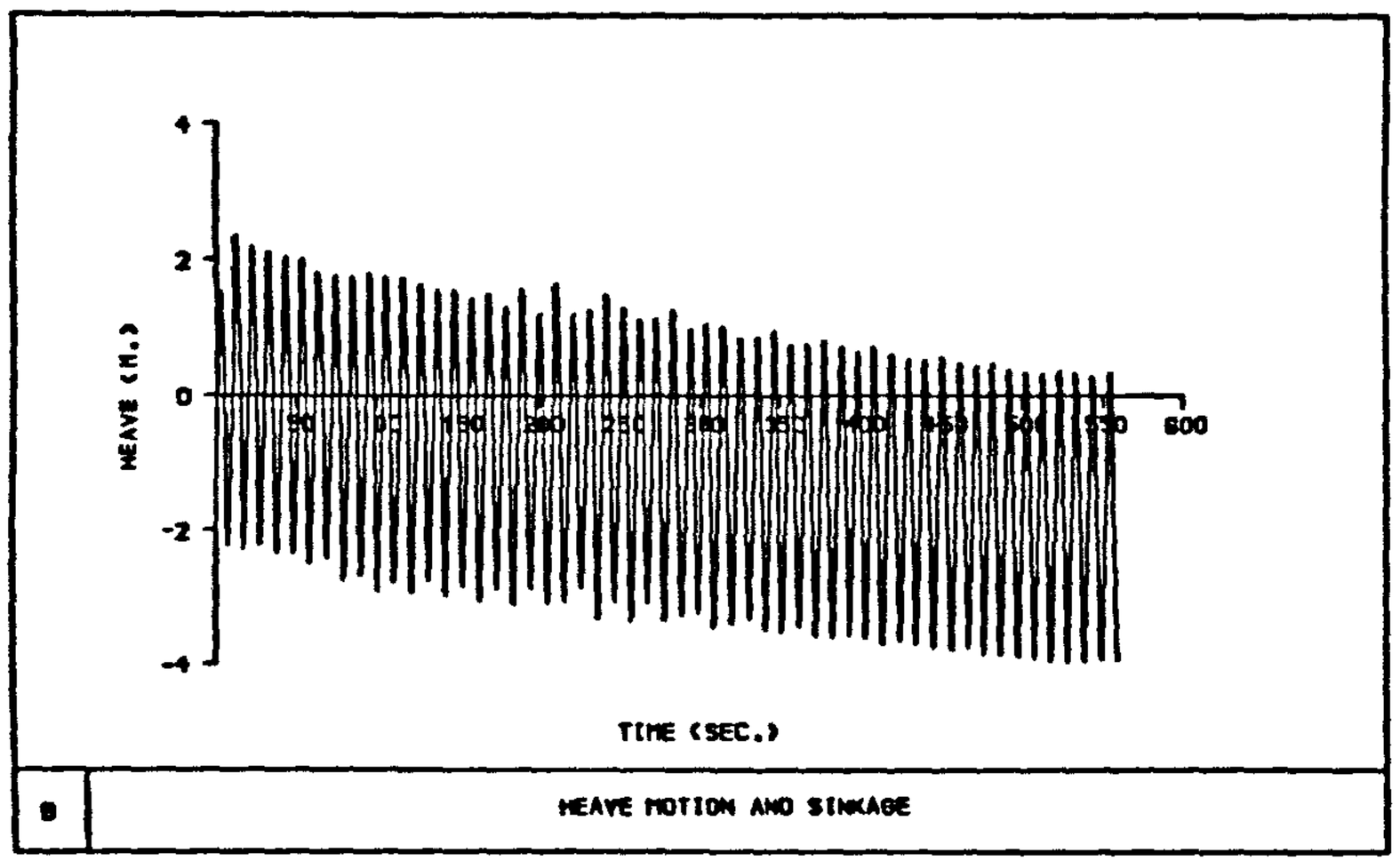

Fig 7.34 Time histories of ship motions and transverse centre of gravity of water on deck during progressive flooding, KG= 11.84 m, WH= 4.0 m [DAMAGE SCENARIO 6]

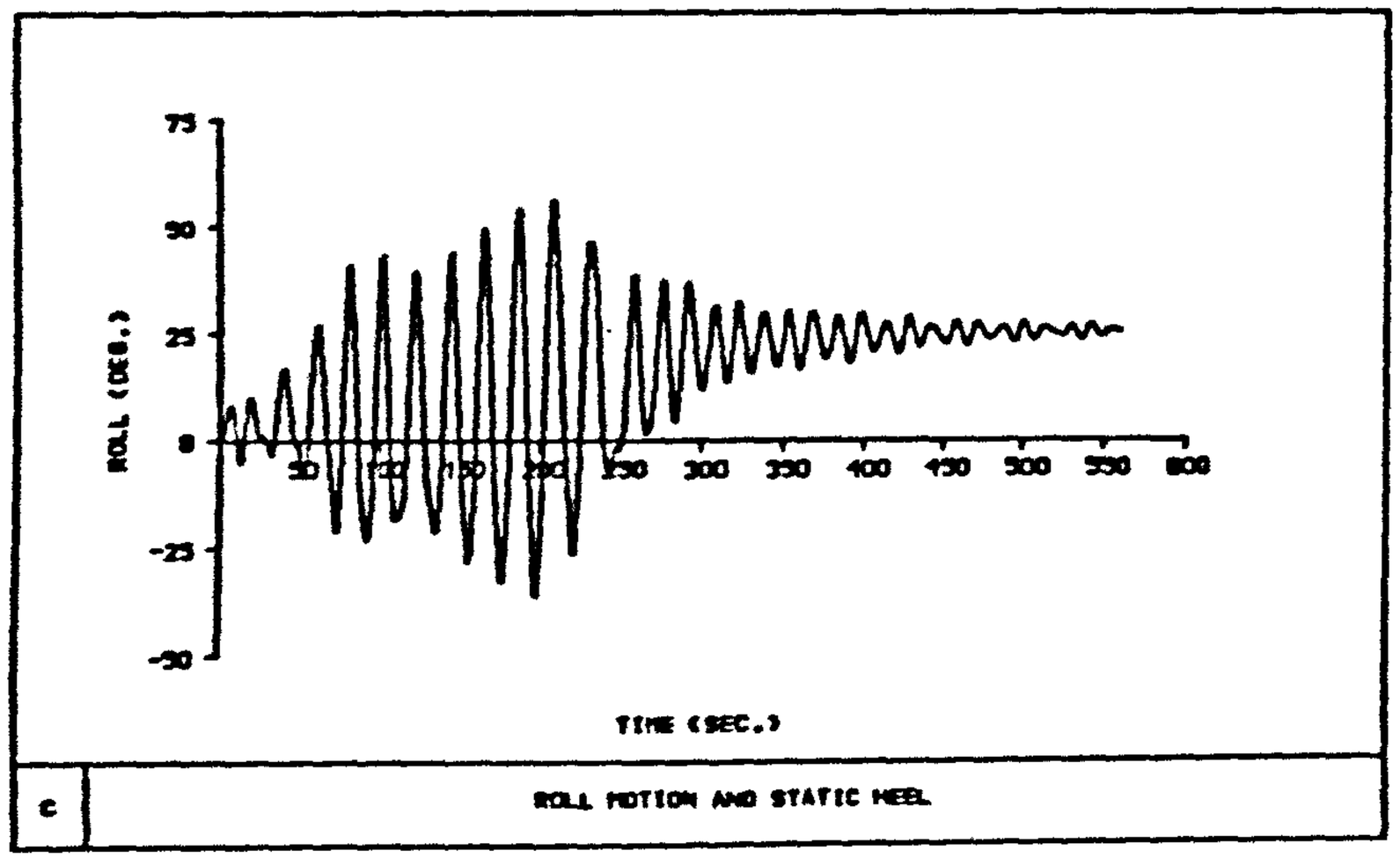

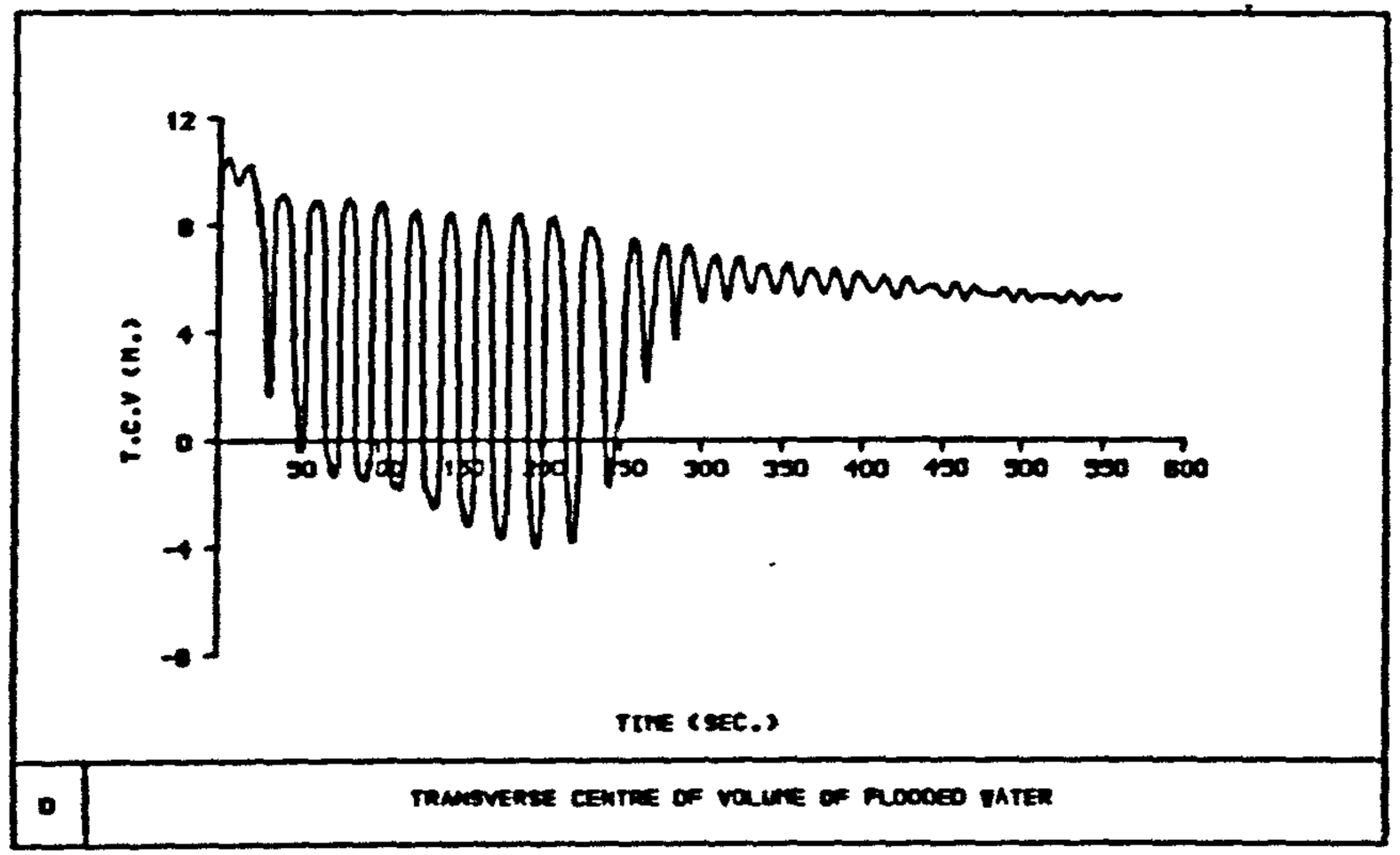

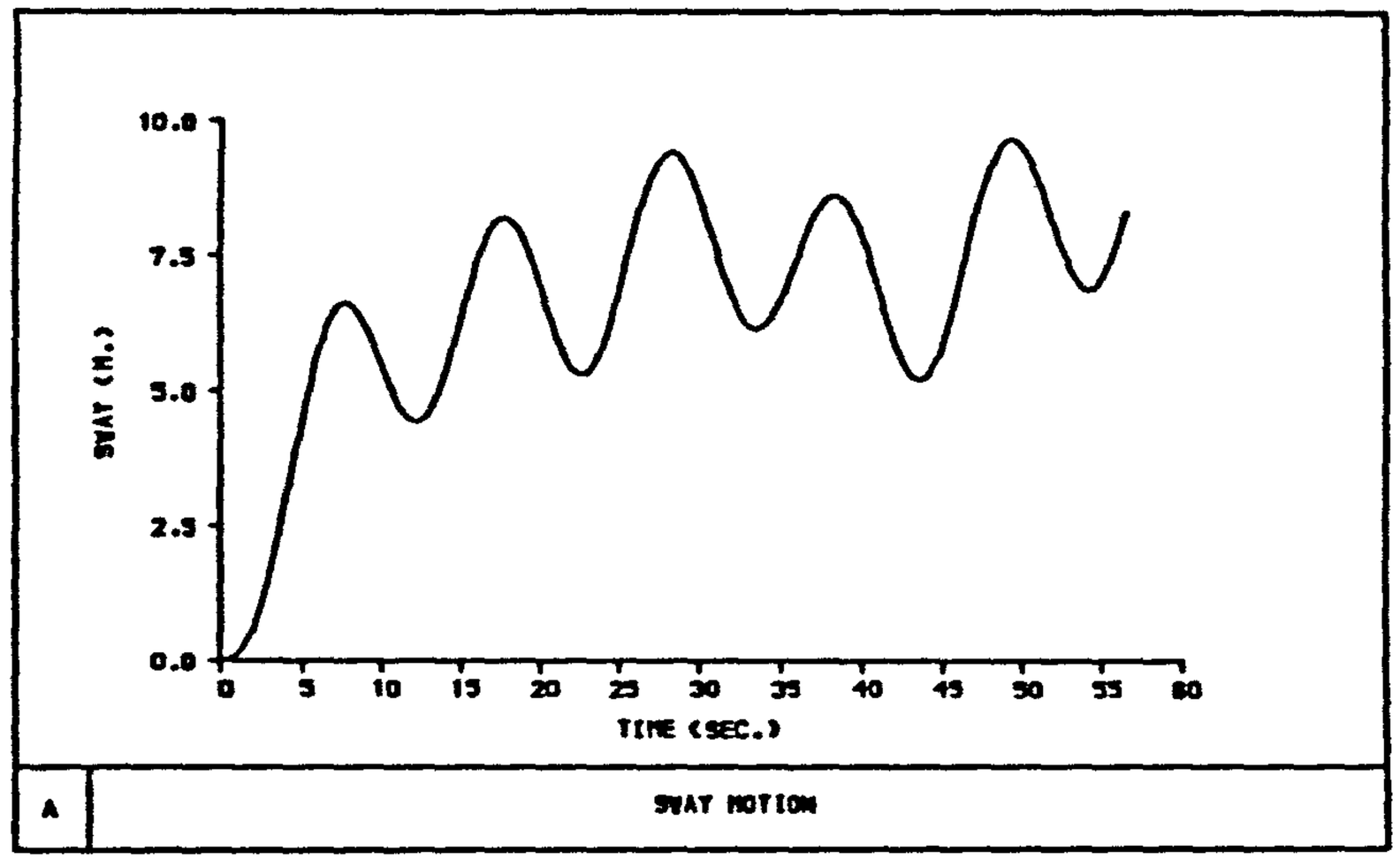

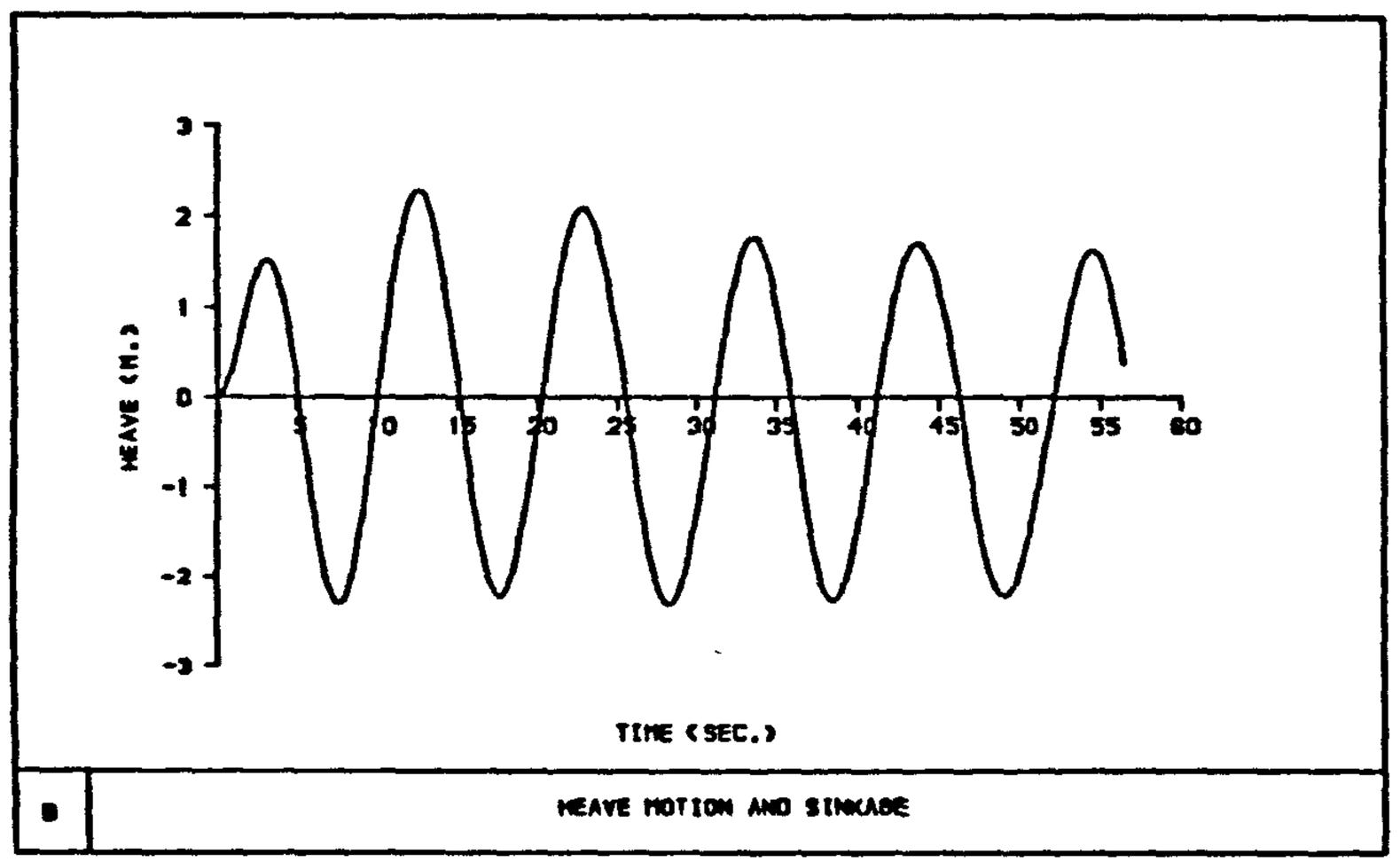

Fig 7.35 Time histories of ship motions and transverse centre of gravity of water on deck during progressive flooding, KG= 12.59 m, WH= 4.0 m [DAMAGE SCENARIO 6]

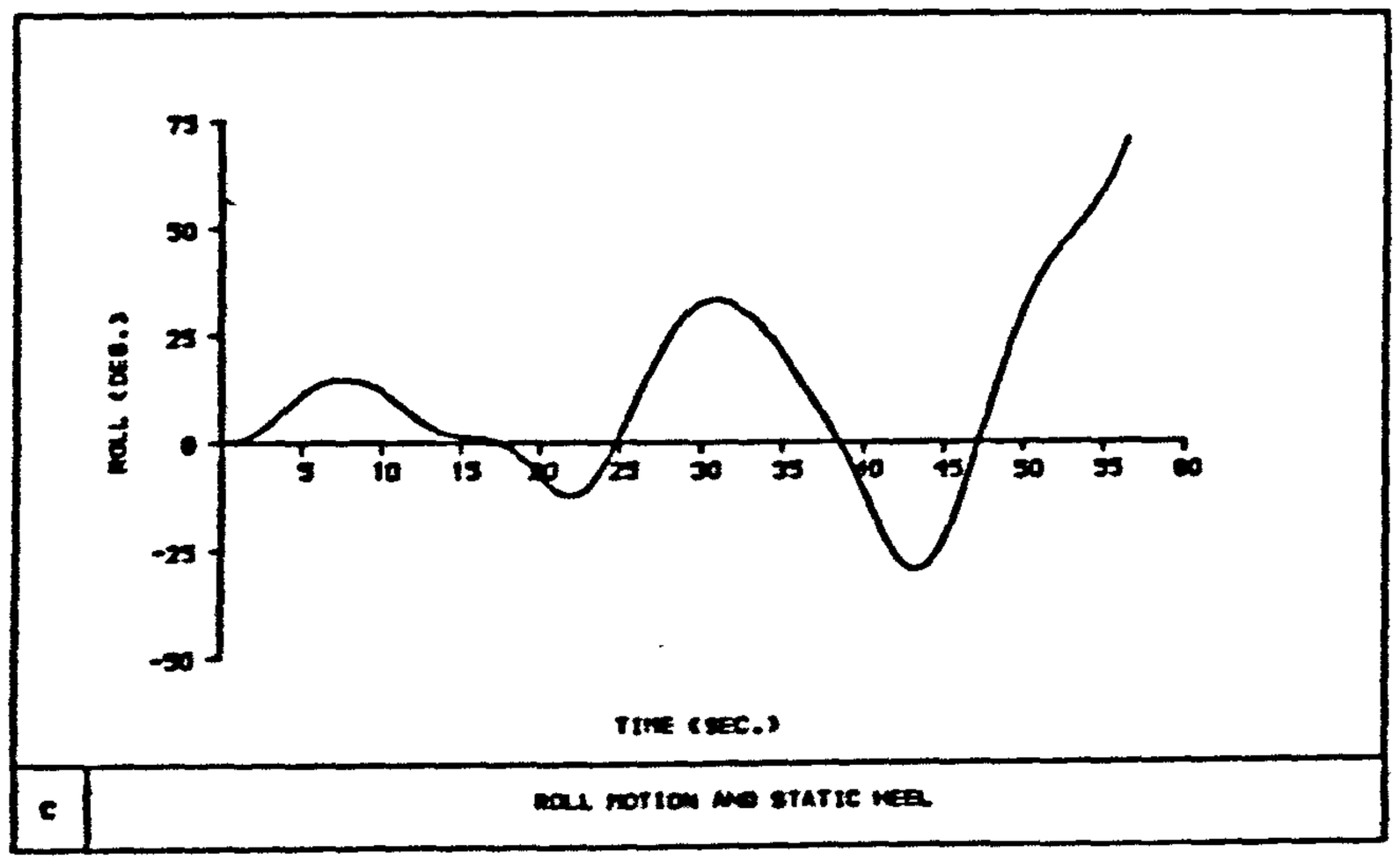

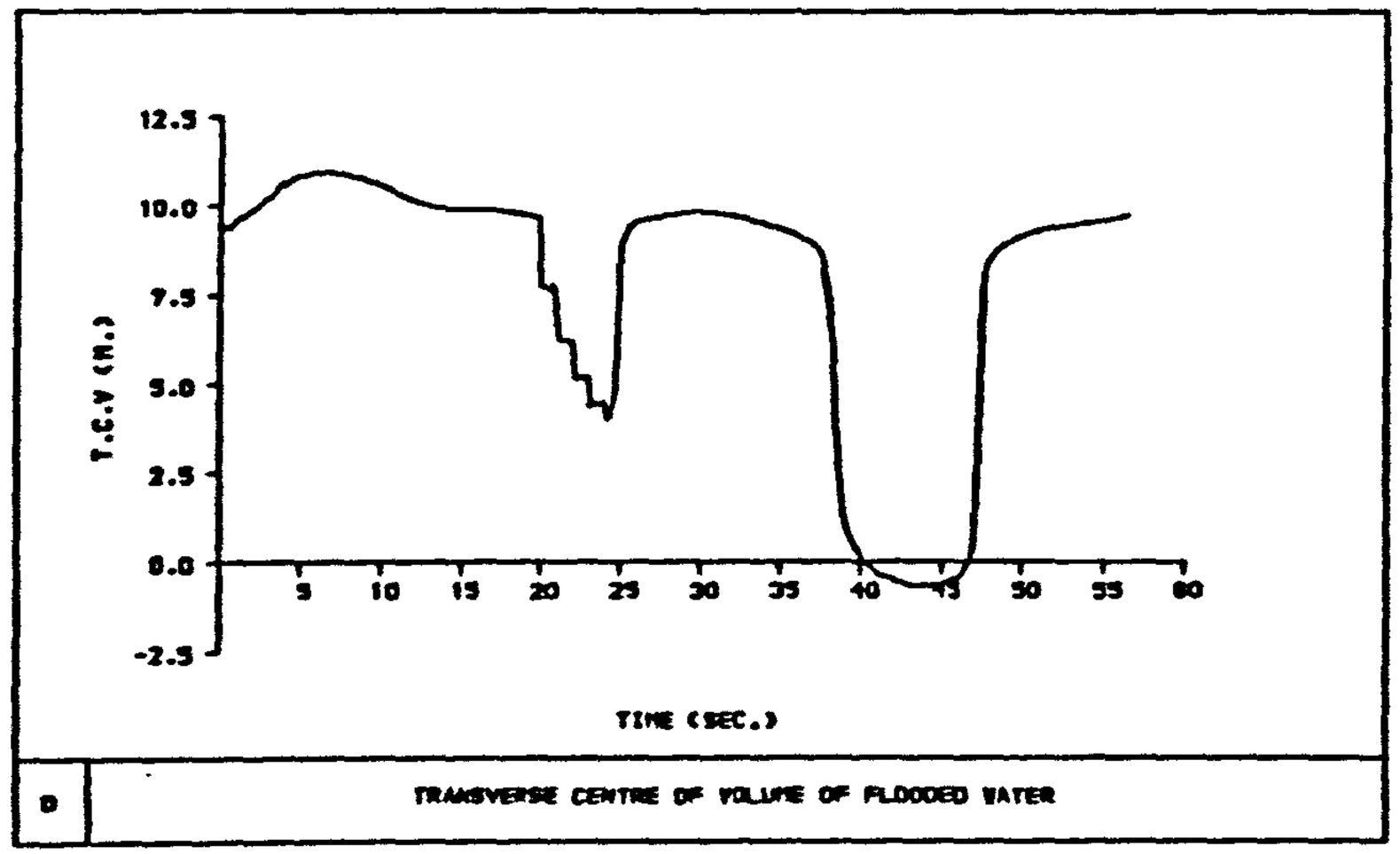

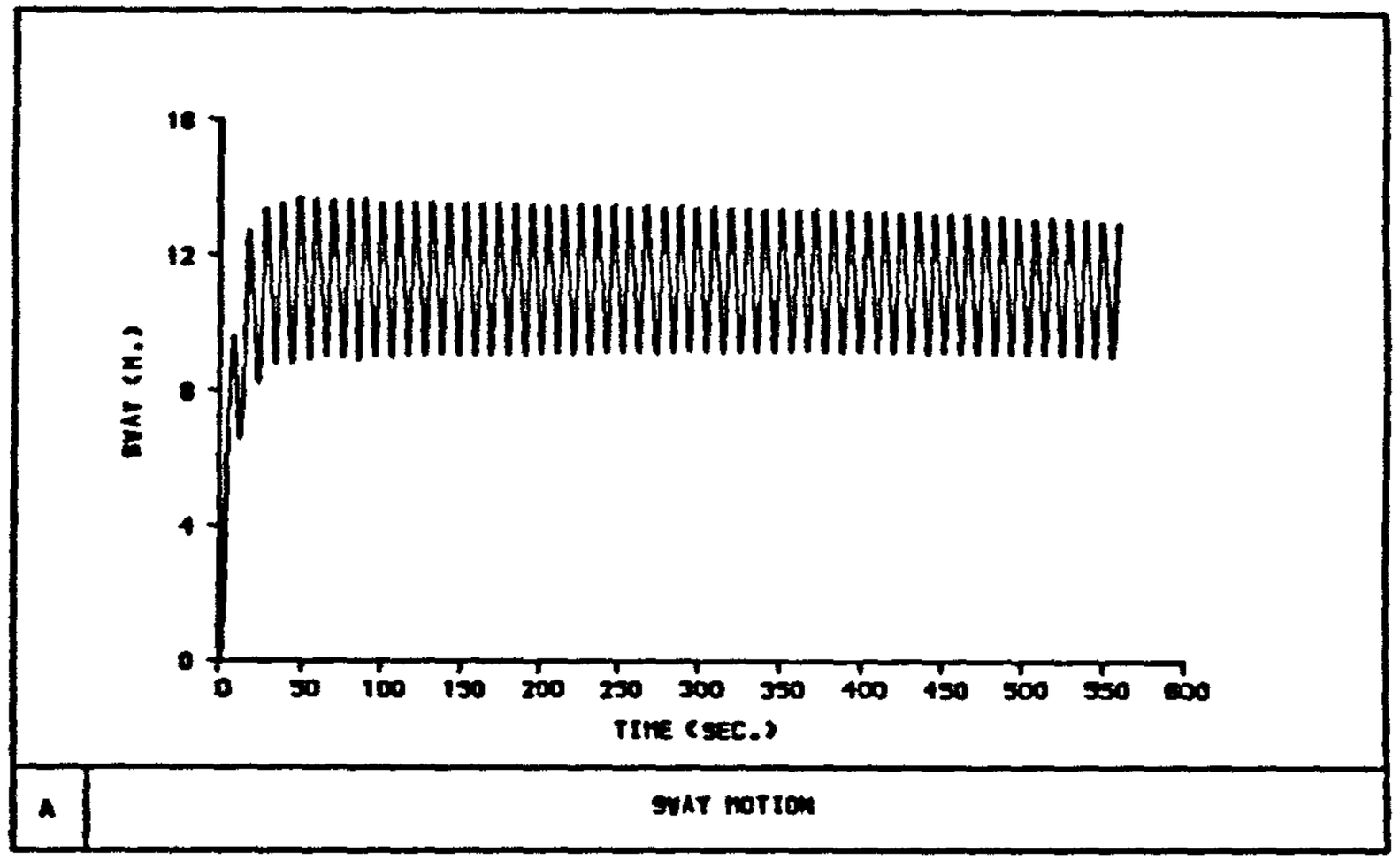

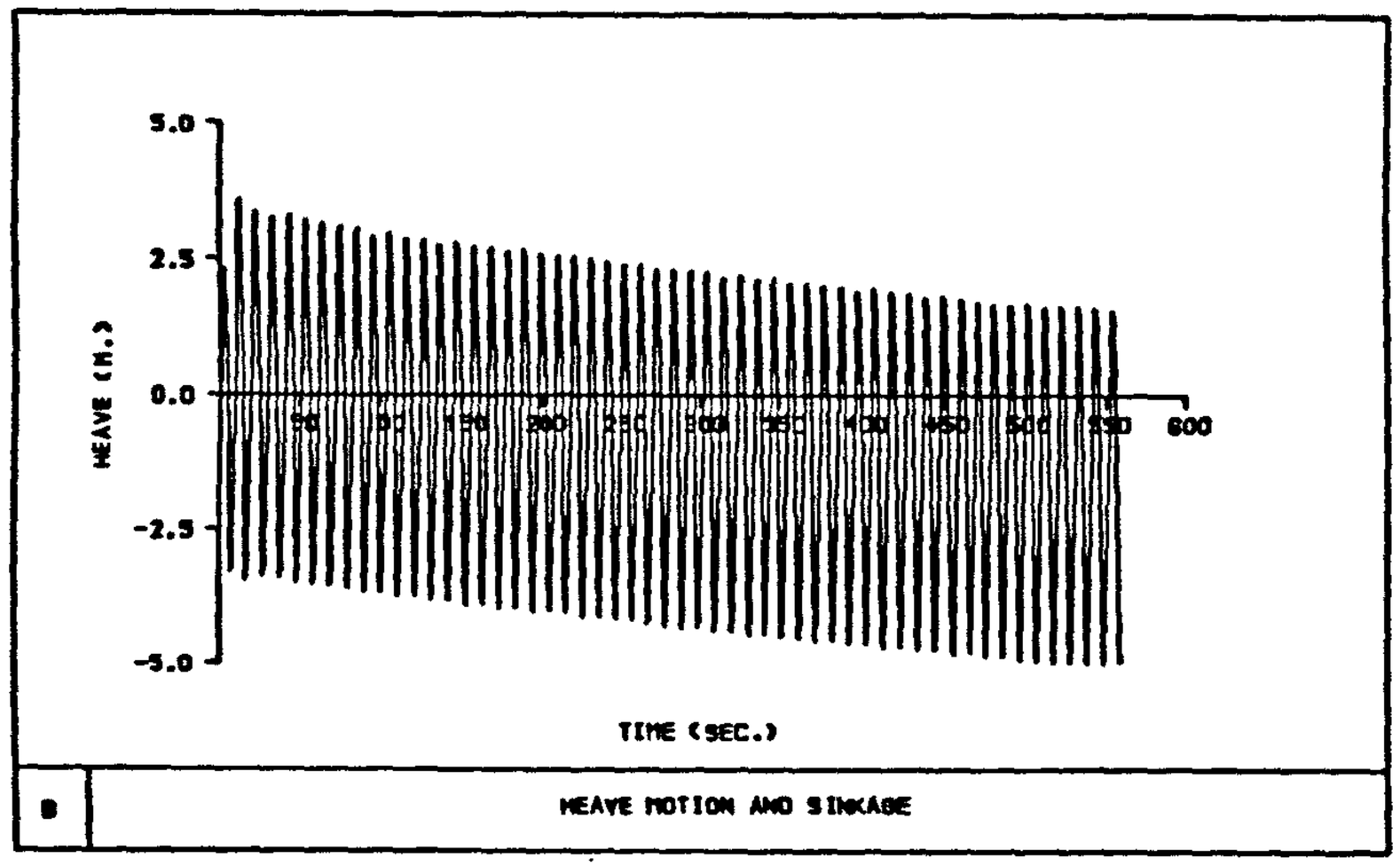

Fig 7.36 Time histories of ship motions and transverse centre of gravity of water on deck during progressive flooding, KG= 11.04 m, WH= 6.0 m [DAMAGE SCENARIO 6]

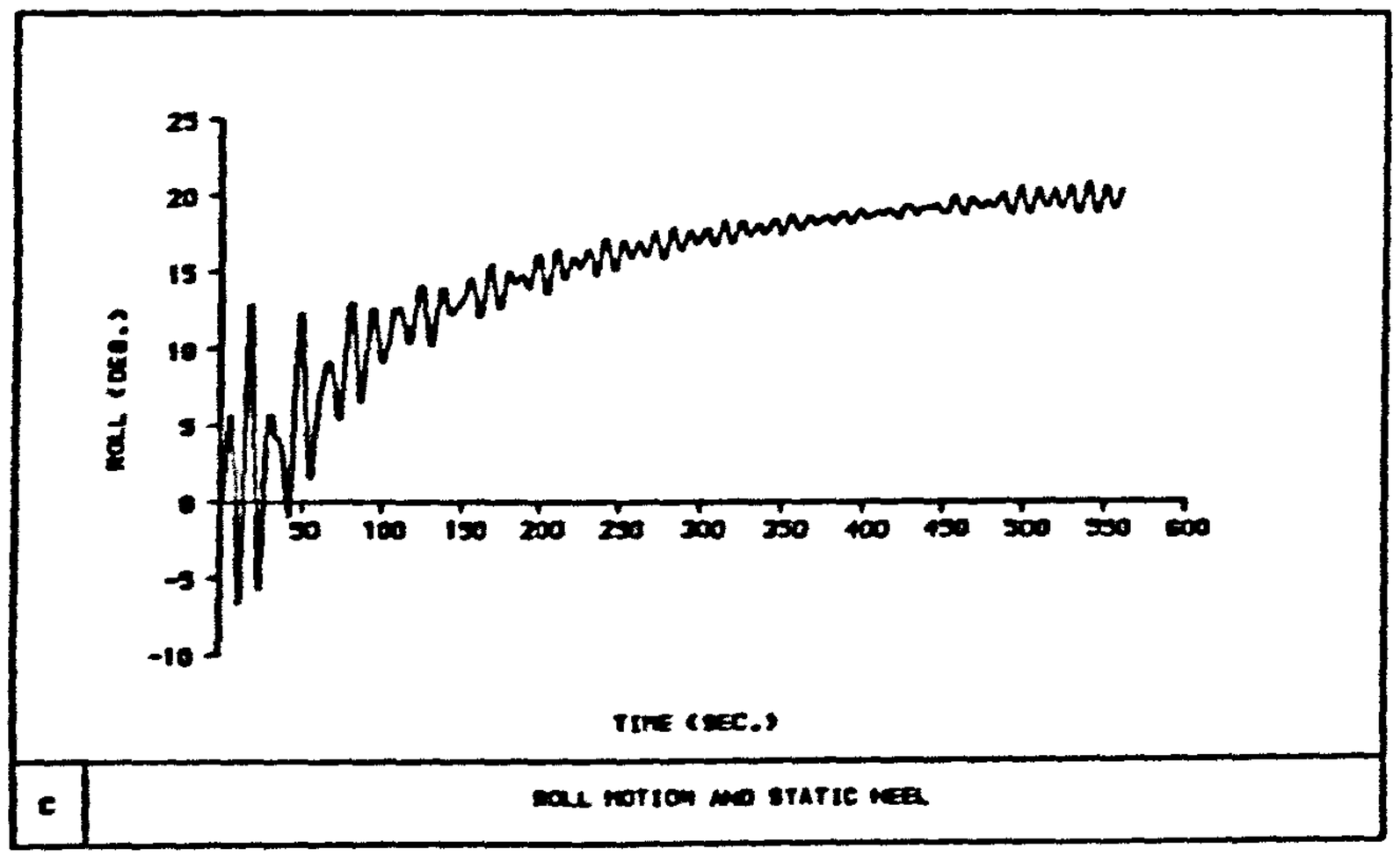

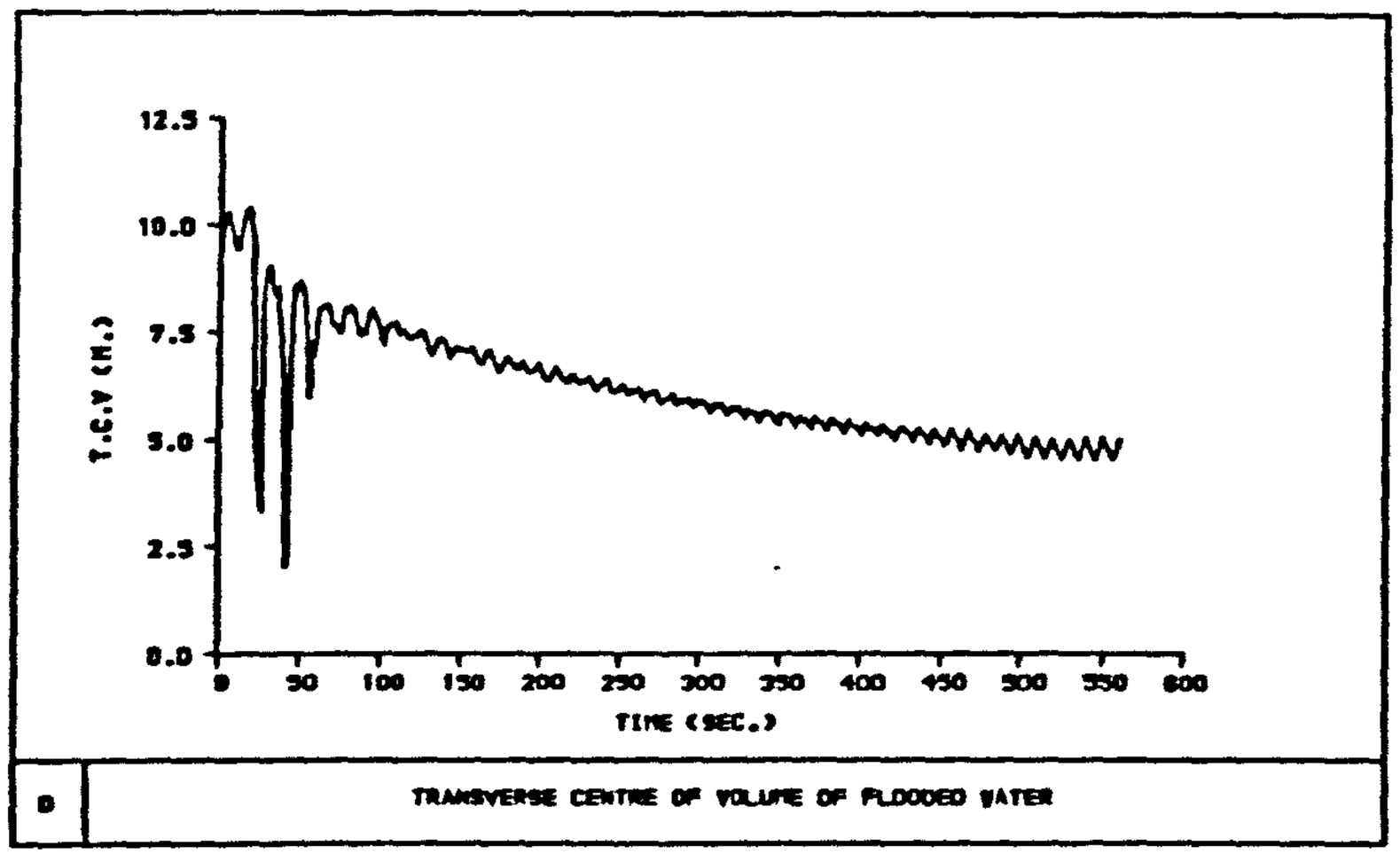

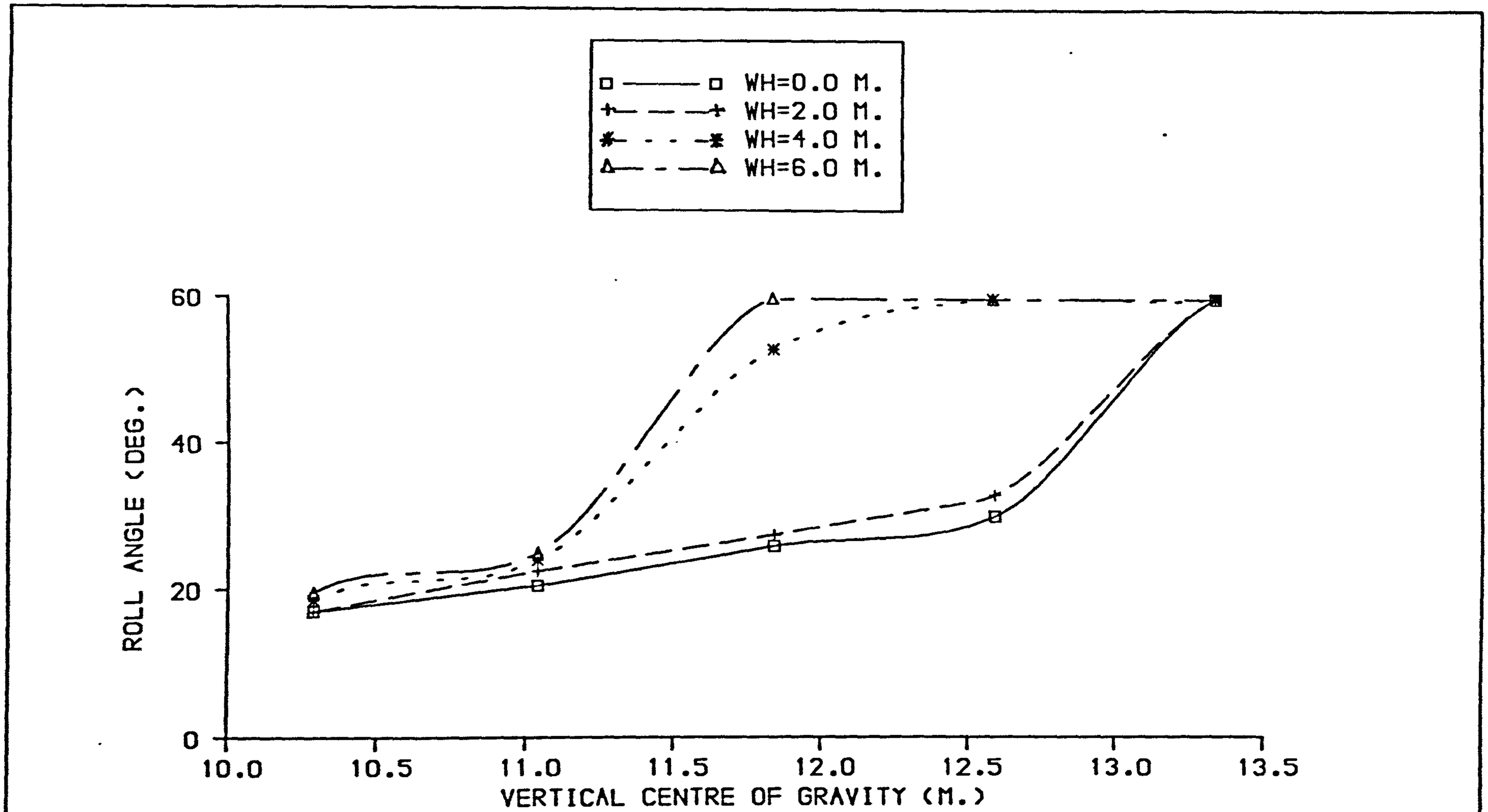

Fig 7.37 Effect of loading condition and wave height on maximum roll amplitude [DAMAGE SCENARIO 6]

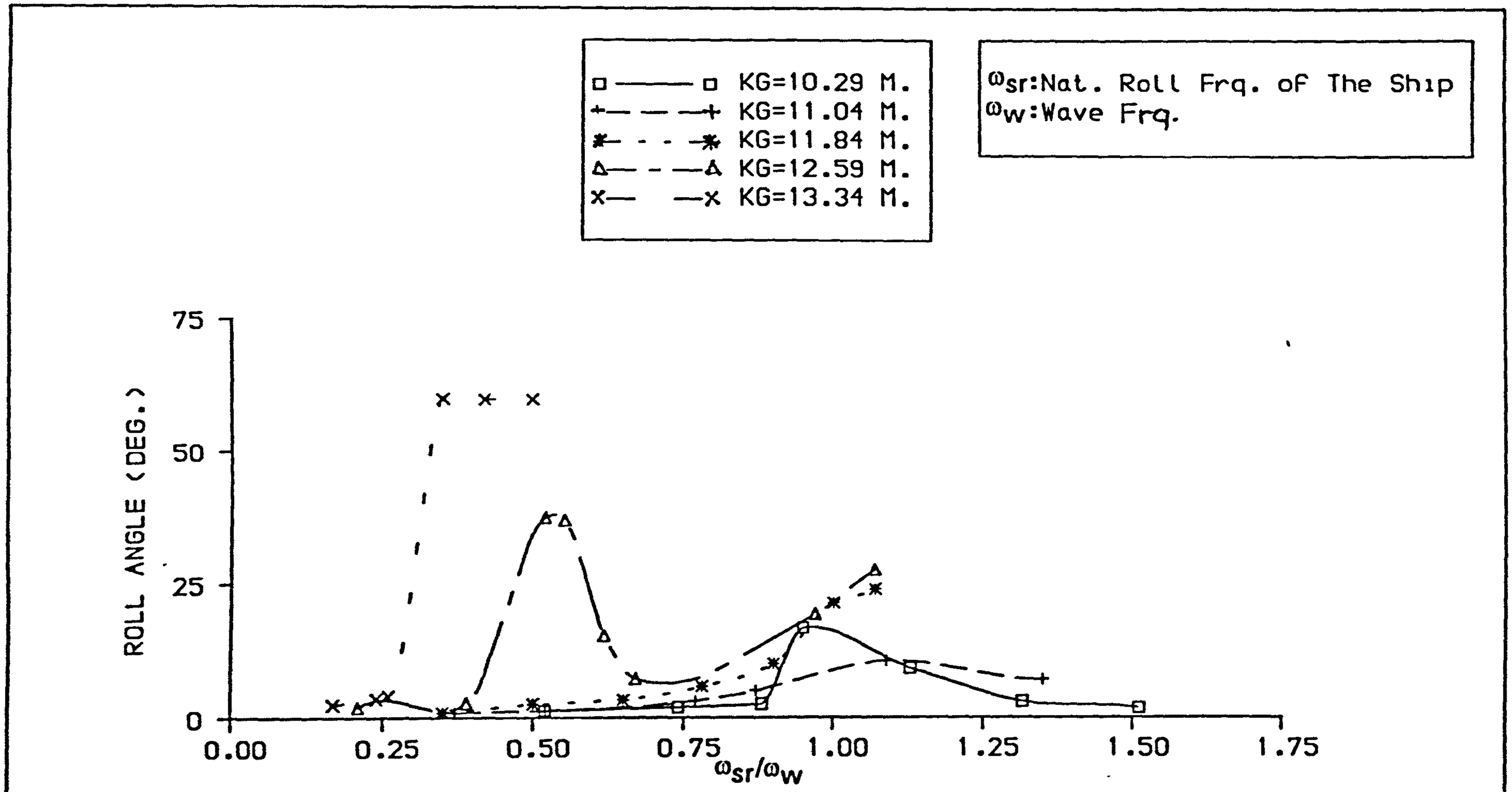

Fig 7.38 EFFECT OF DIFFERENT FREQUENCIES AND LOADING CONDITIONS ON SHIP ROLL MOTION. WH=2.0 M., RANGE OF WAVE LENGTH=40-750 M. [DAMAGE SCENARIO 3]

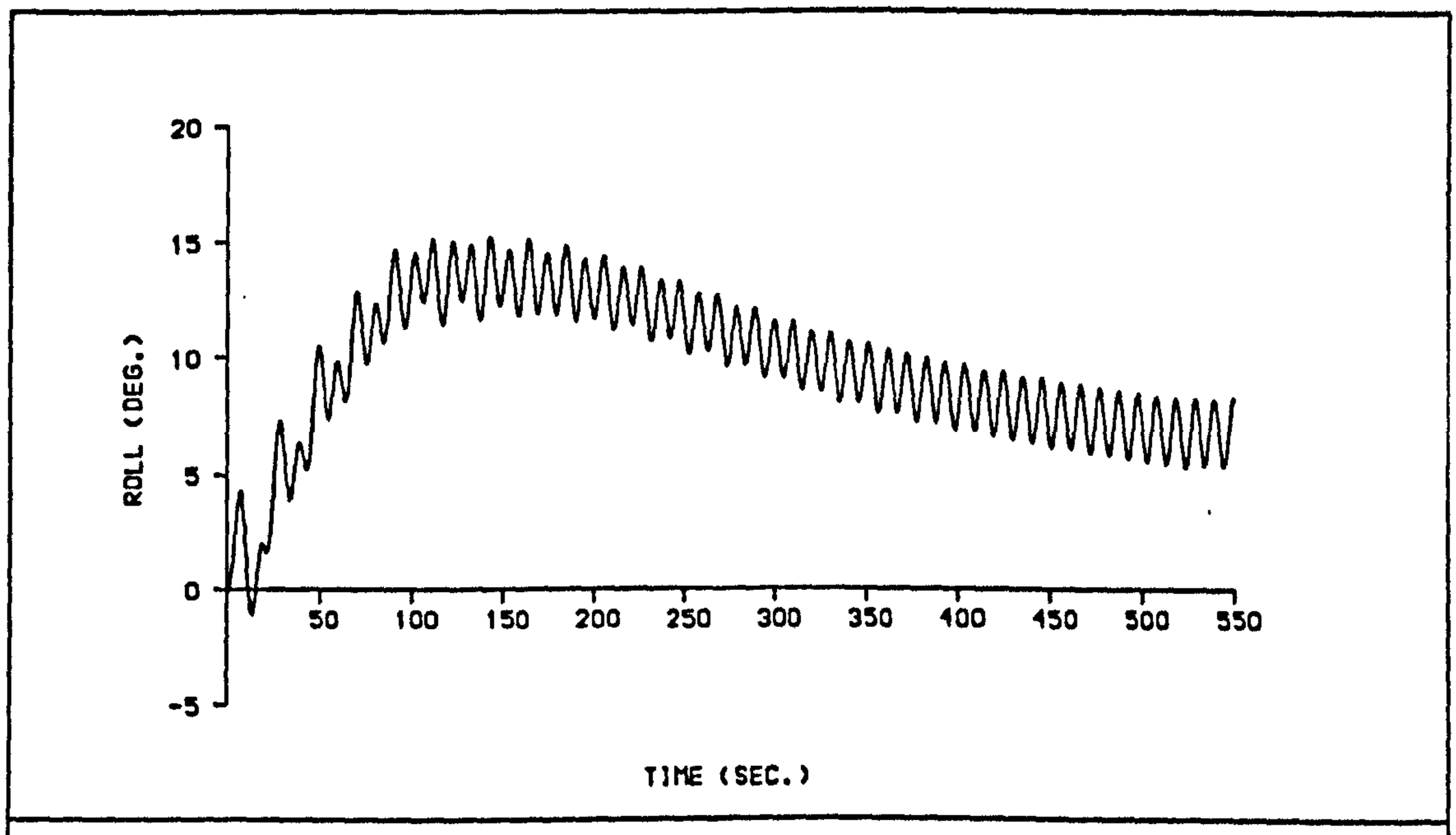

A SINGLE DEGREE ROLL MOTION, KG = 12.59 M, WH = 2.0 M [DAMAGE SCENARIO 3]

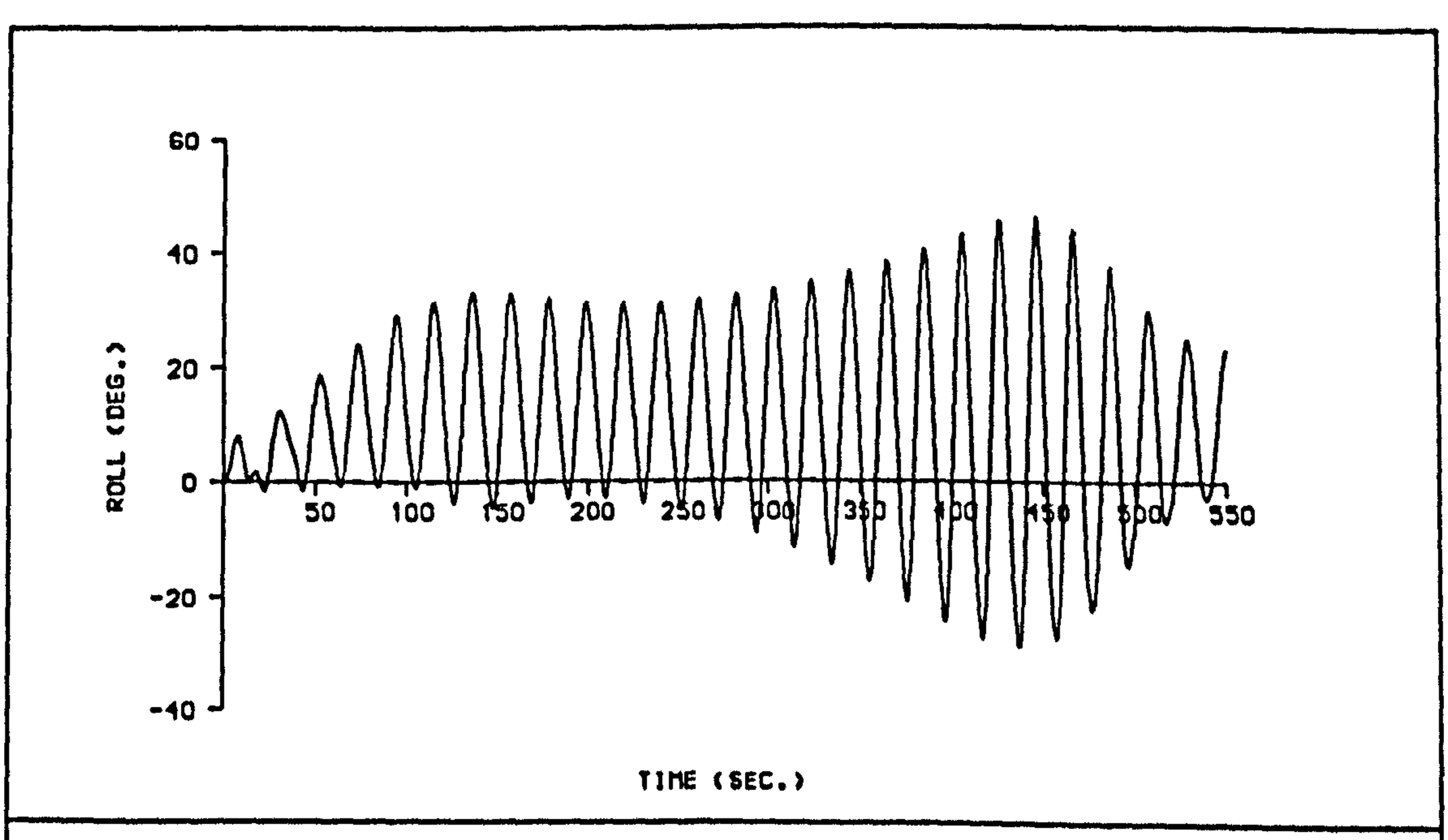

B ROLL MOTION COUPLED WITH SWAY AND HEAVE, KG = 12.59 M, WH = 2.0 M [DAMAGE SCENARIO 3]

Fig 7.39 Coupling effect of heave and sway on roll motion, WL = 170 m, beam seas [DAMAGE SCENARIO 3]

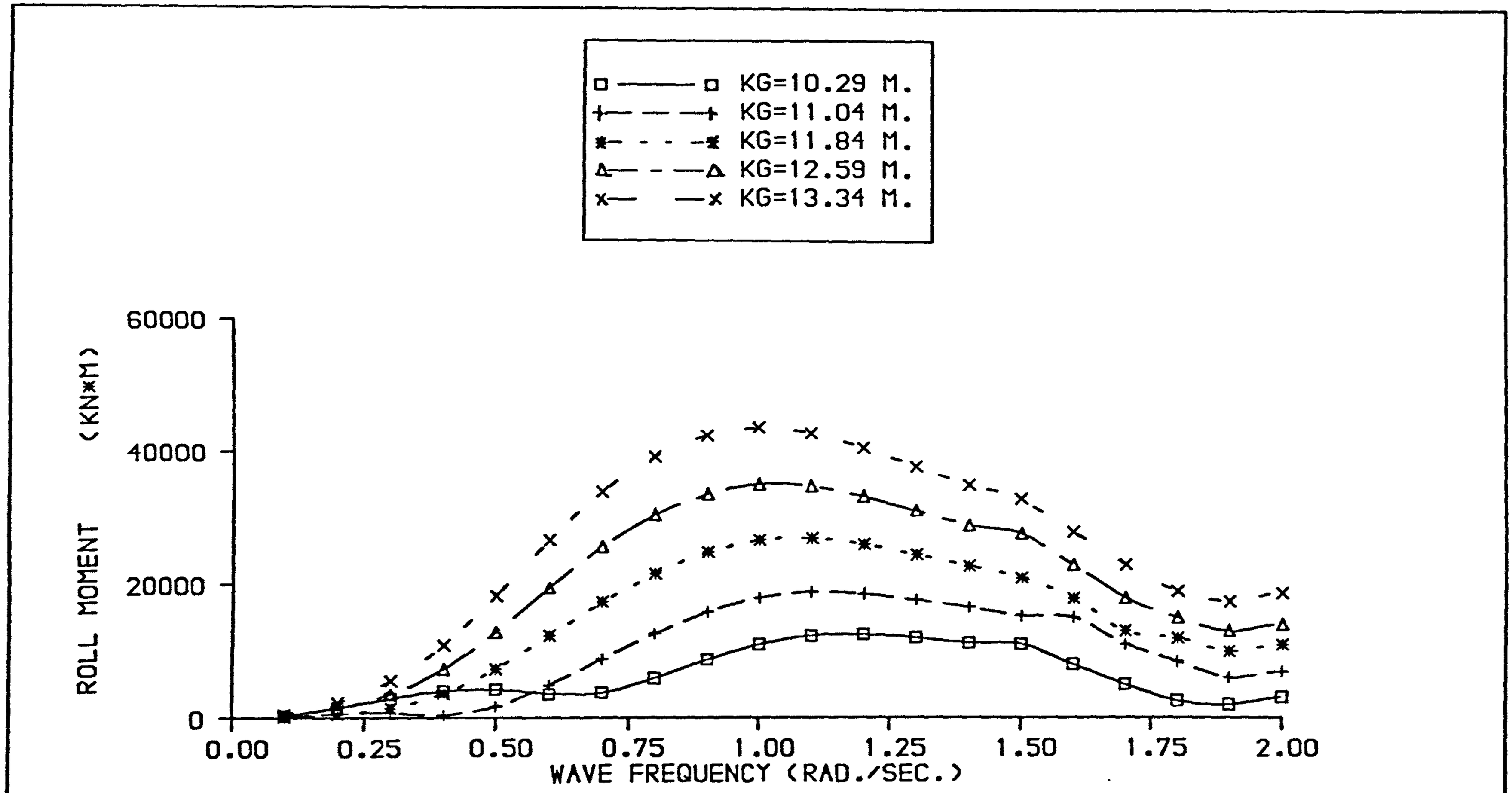

Fig 7.40 ROLL EXCITATION MOMENT FOR DIFFERENT LOADING CONDITIONS
WAVE HEIGHT=2.0 M., CONDITION: UPRIGHT, DRAUGHT= 6.08 M

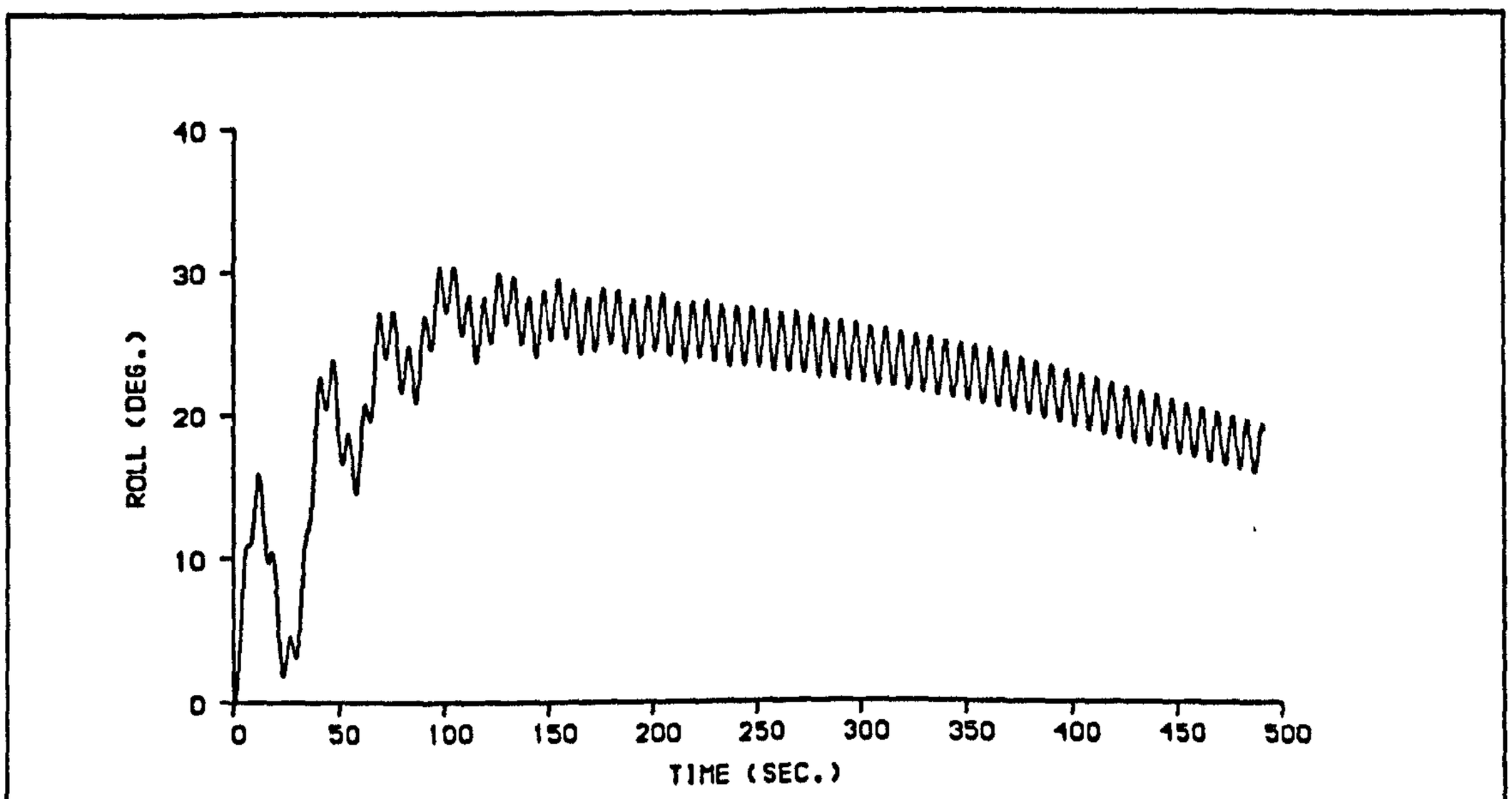

A COUPLED ROLL MOTION, KG=13.34 M., WH=2.0 M., WAVE FRQ.= 0.89 RAD/SEC
(DAMAGE SCENARIO 3)

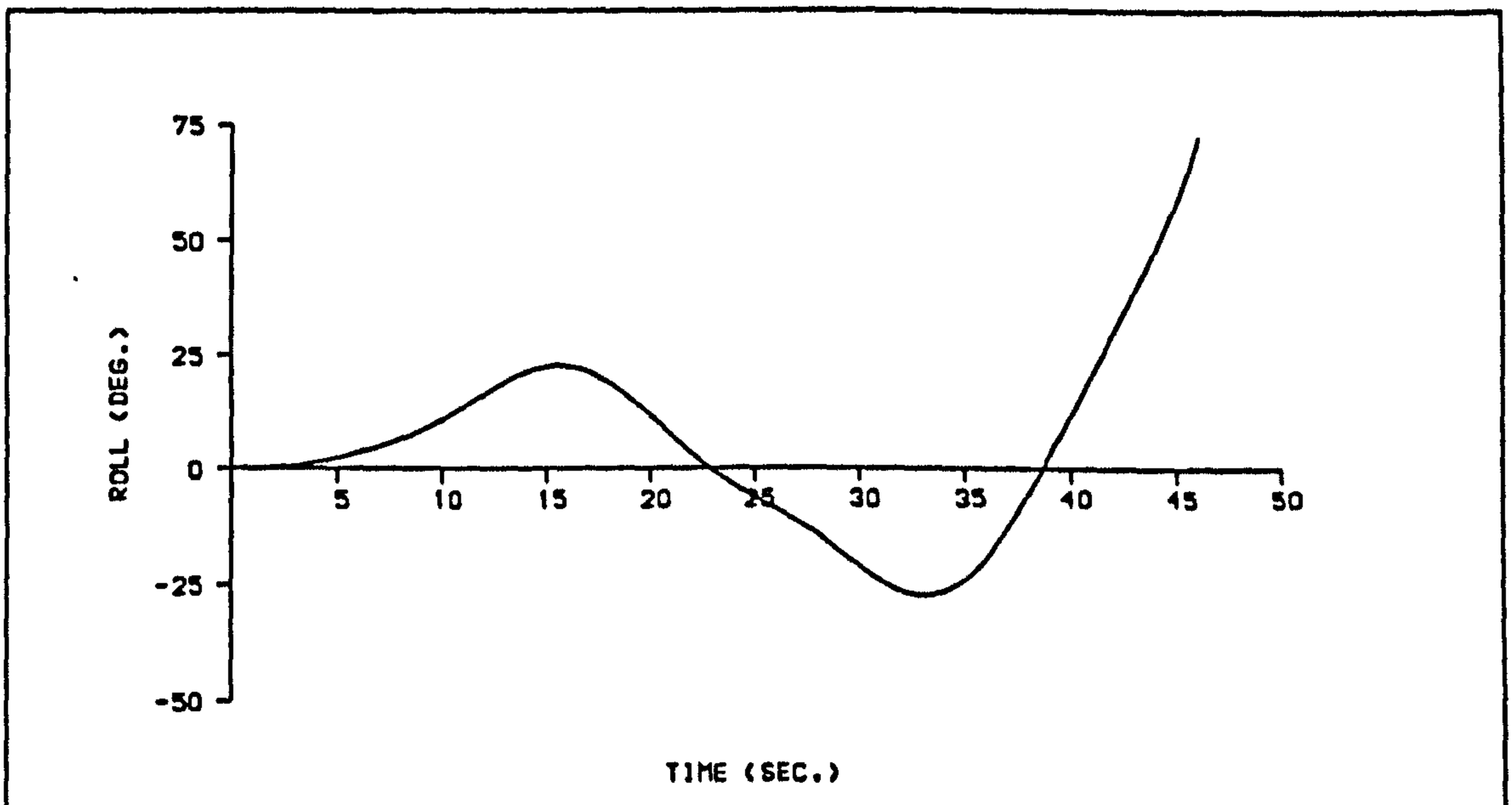

B COUPLED ROLL MOTION, KG=13.34 M., WH=2.0 M., WAVE FRQ.= 0.37 RAD/SEC
(DAMAGE SCENARIO 3)

Fig 7.41 Effect of wave frequency(wave length) on roll motion

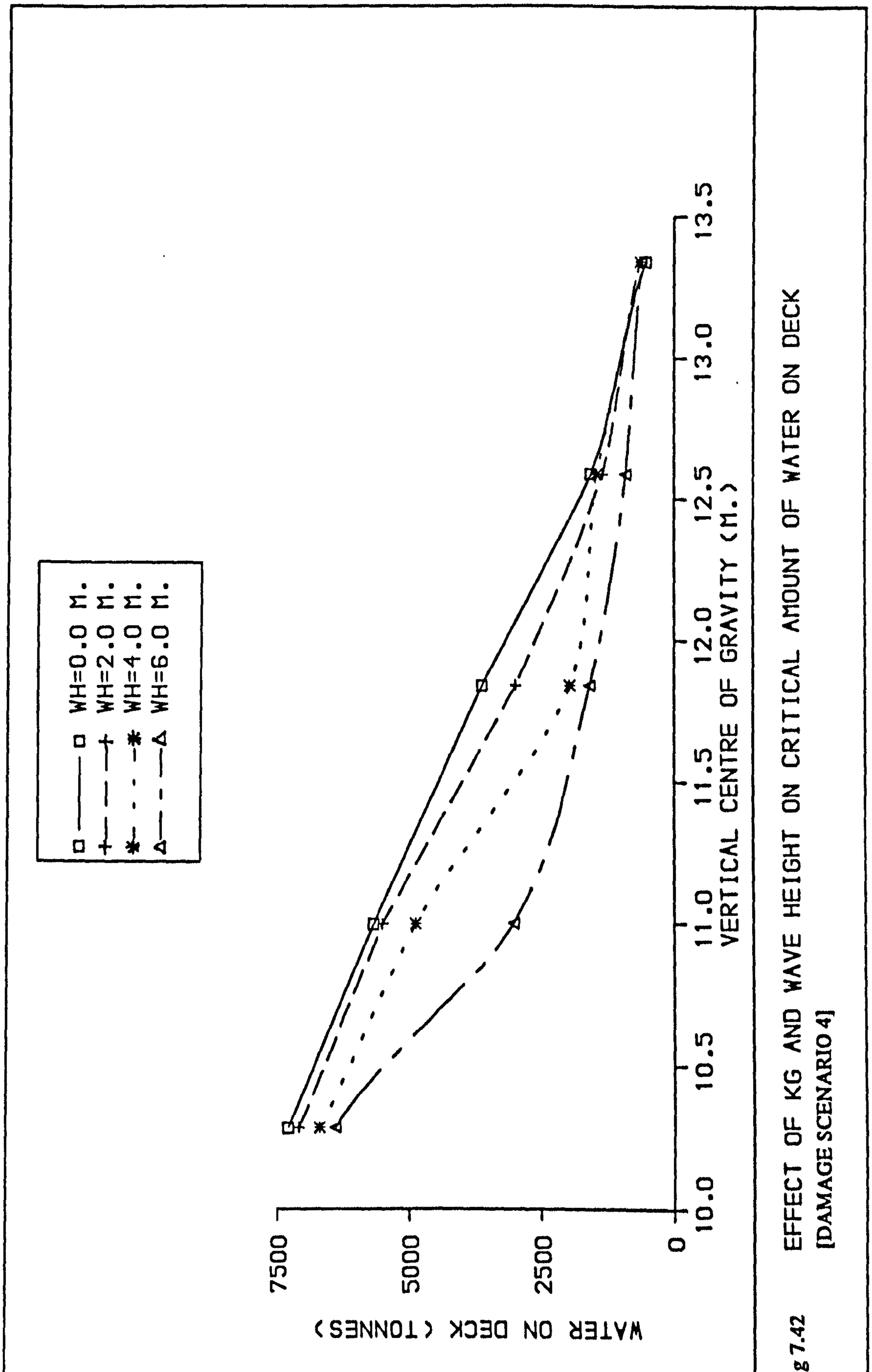
EFFECT OF KG AND WAVE HEIGHT ON CRITICAL AMOUNT OF WATER ON DECK
(DAMAGE SCENARIO 4)
WATER ON DECK (TONNES)
750
500
250
0
10.0
10.5
11.0
11.5
VERTICAL CENTRE OF GRAVITY (M.)
12.0
12.5
13.0
13.5
DECK
WH=0.0 M.
WH=2.0 M.
WH=4.0 M.
WH=6.0 M.

Fig 7.42

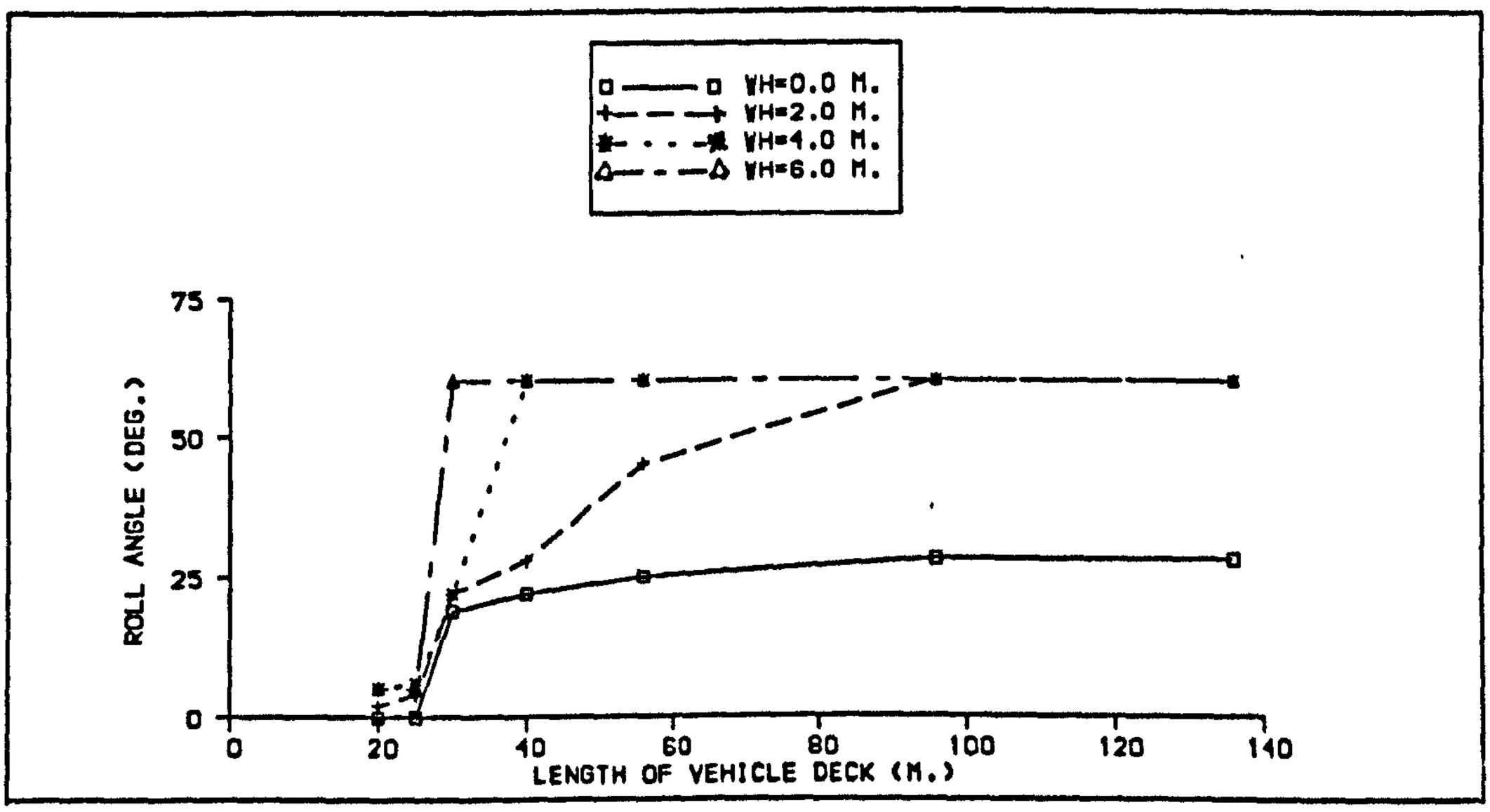

Fig 7.43A Effect of compartment length on roll motion, KG=11.84 m [DAMAGE SCENARIO 4]

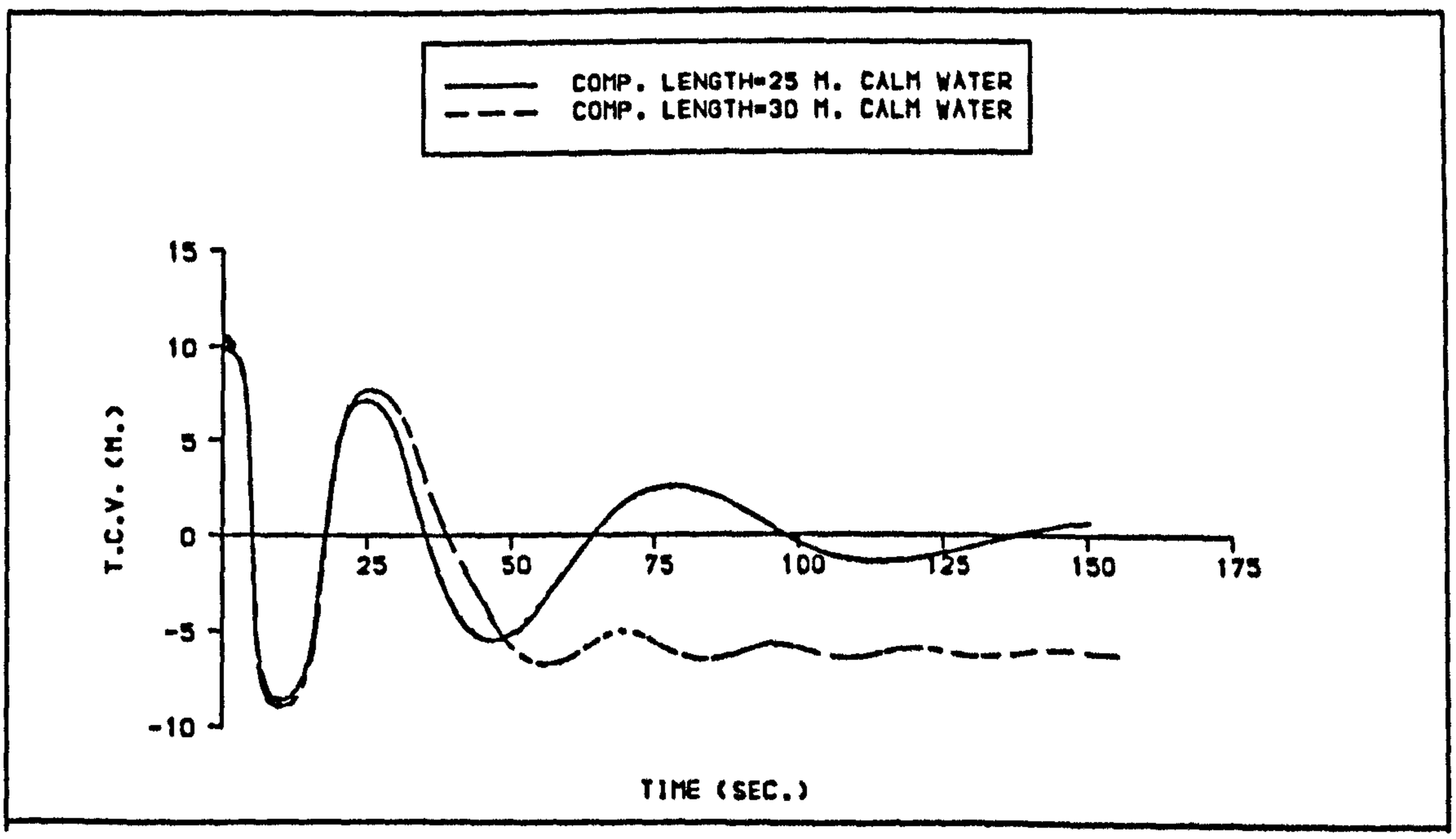

Fig 7.43B Effect of compartment length on the transverse centre of gravity of water on deck during progressive flooding [DAMAGE SCENARIO 4]

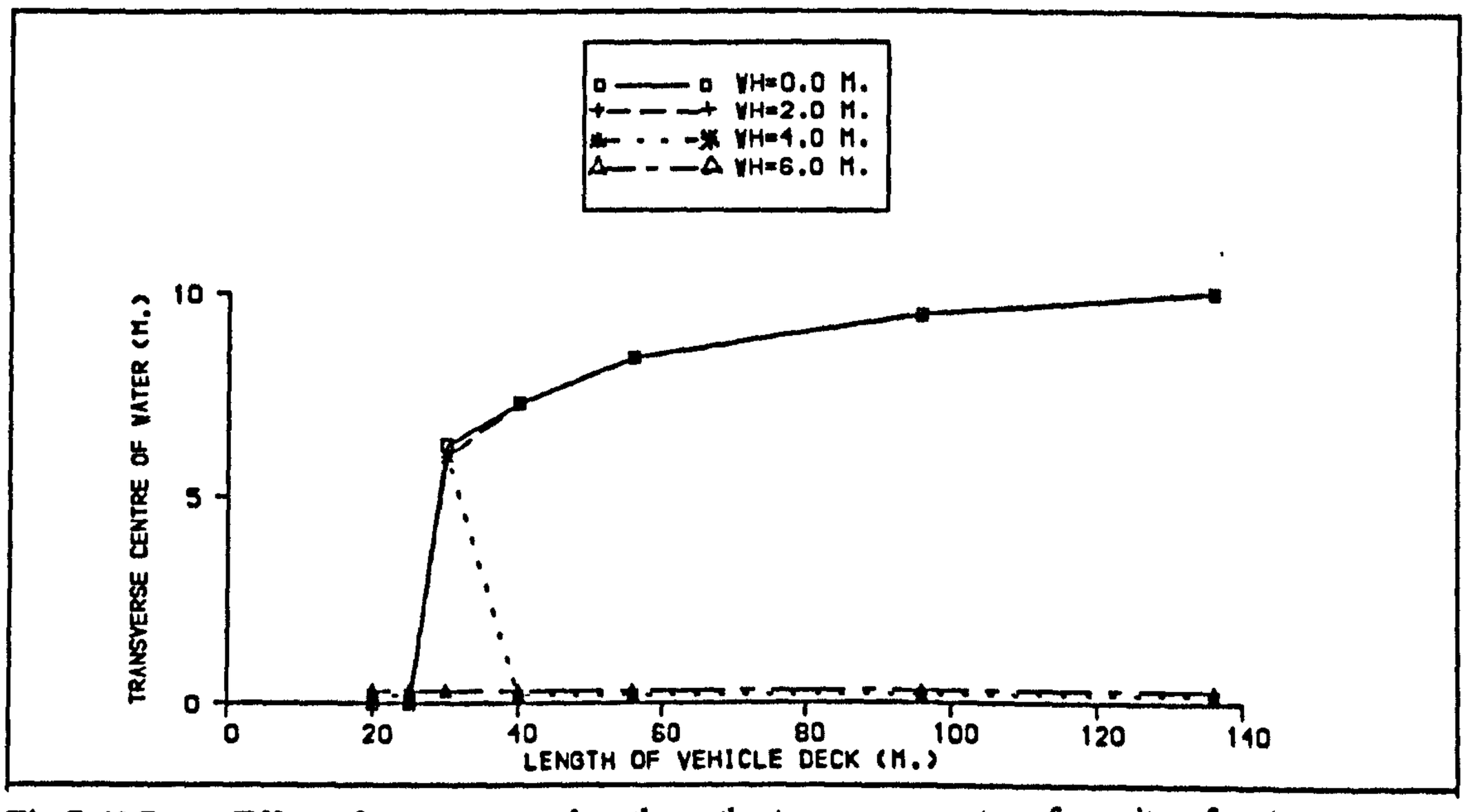

Fig 7.43C Effect of compartment length on the transverse centre of gravity of water on deck for different wave heights, KG=11.84 m [DAMAGE SCENARIO 4]

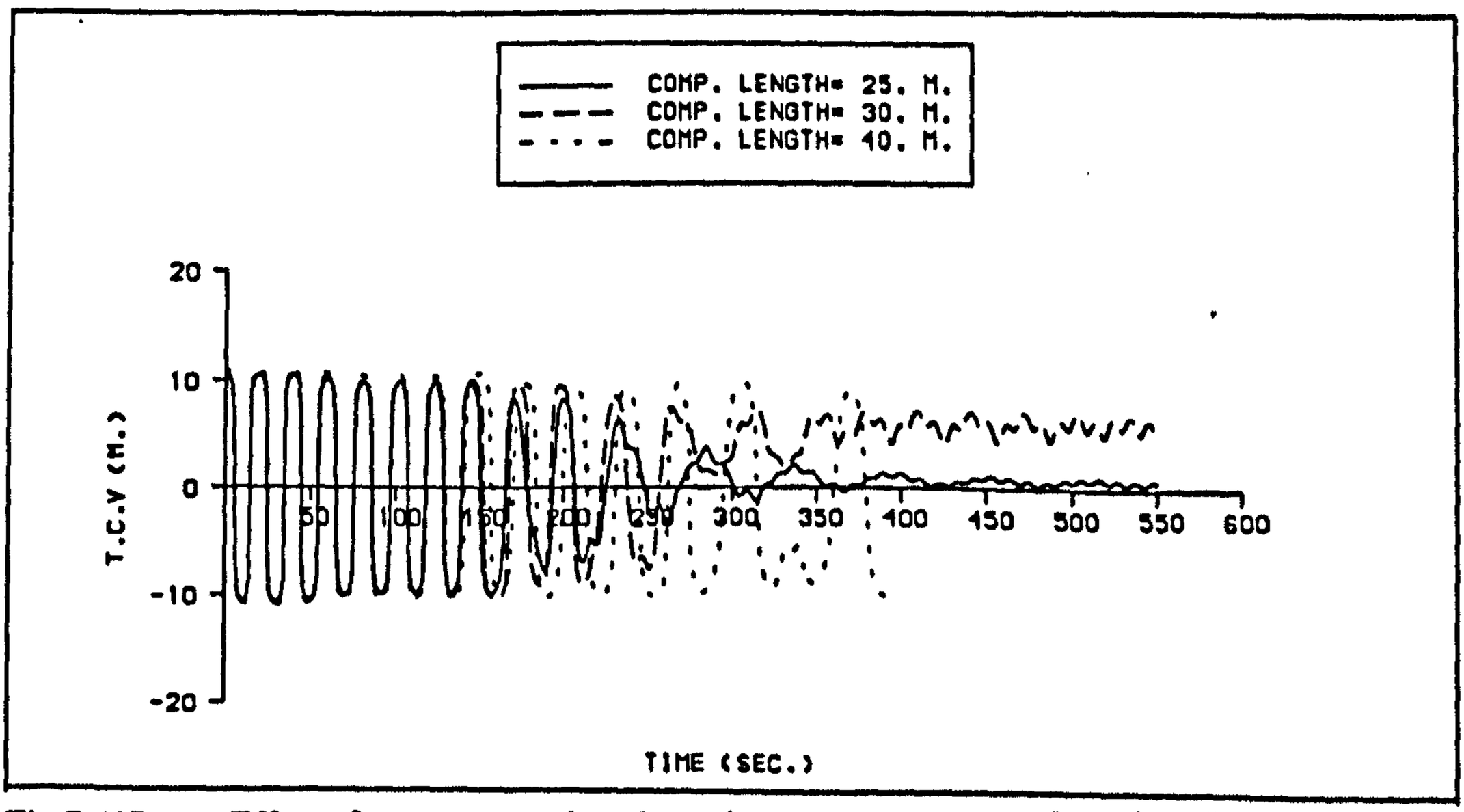

Fig 7.43D Effect of compartment length on the transverse centre of gravity of water on deck during progressive flooding KG=11.84 m, WH=4.0 m [DAMAGE SCENARIO 4]

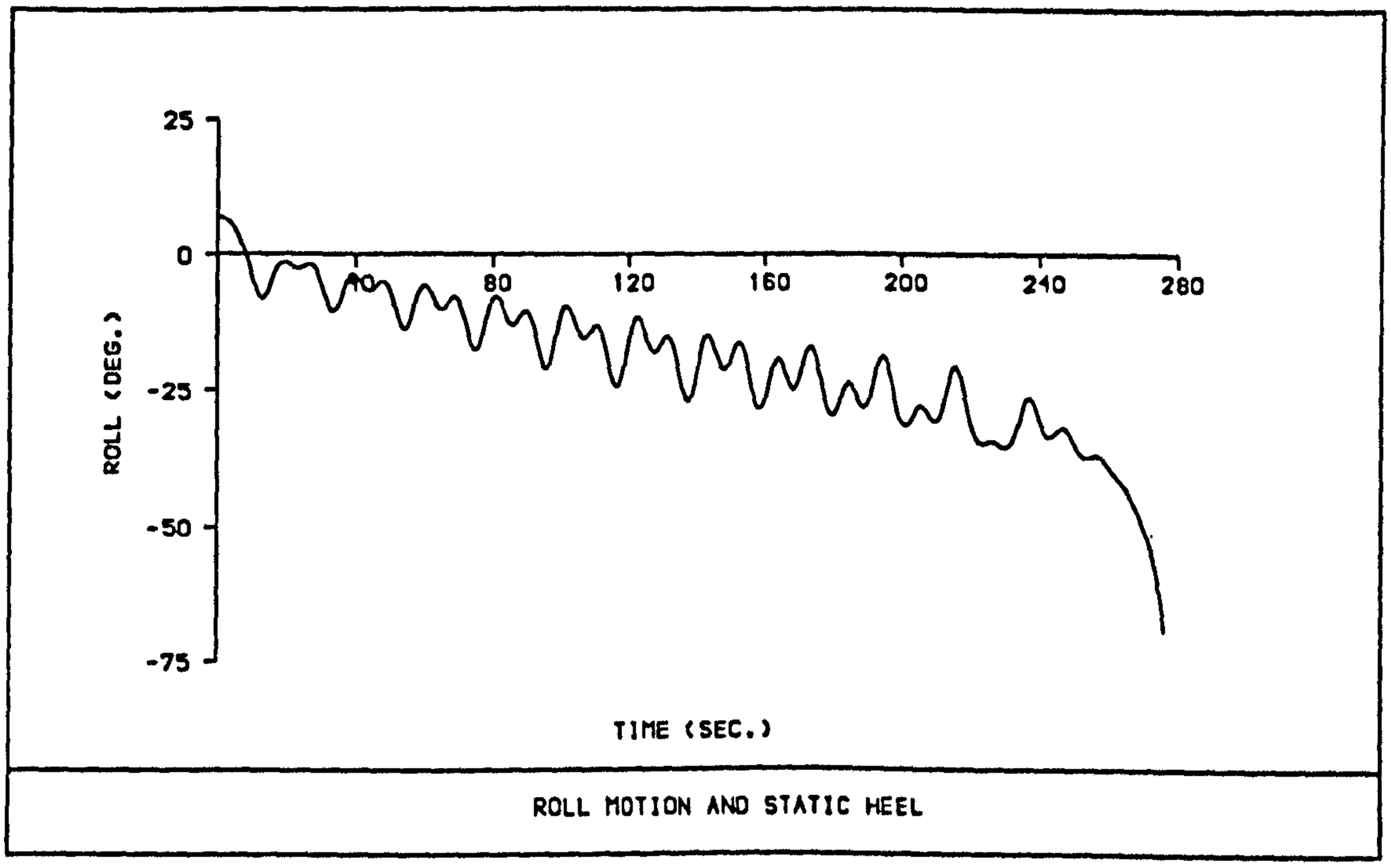

Fig 7.44A Capsizing mode A: effect of water on deck is dominant KG = 12.59 m, WH = 2.0 m [DAMAGE SCENARIO 4]

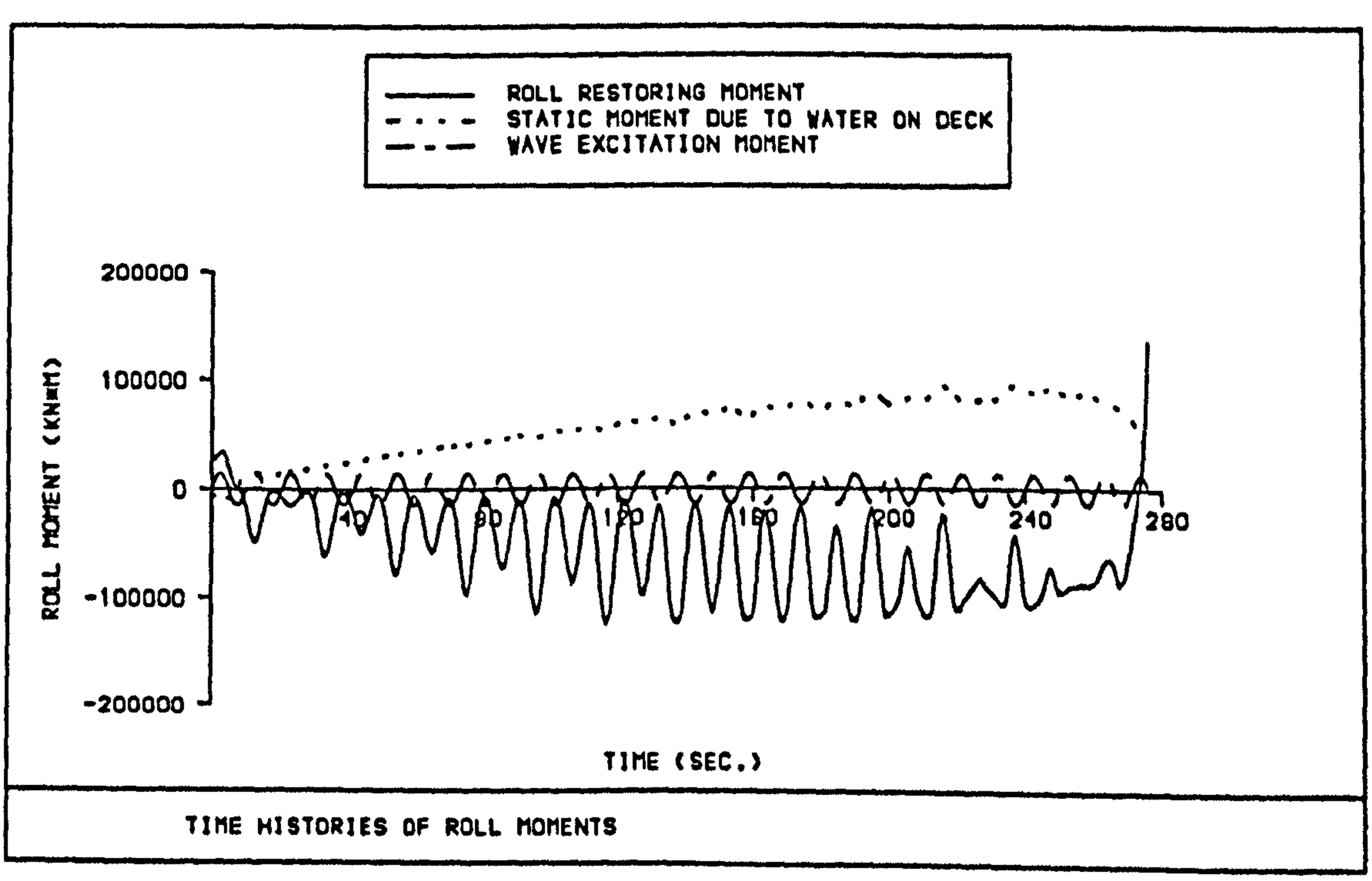

Fig 7.44B Analysis of forces acting on the ship [Capsizing mode A], KG = 12.59 m, WH = 2.0 m, [DAMAGE SCENARIO 4]

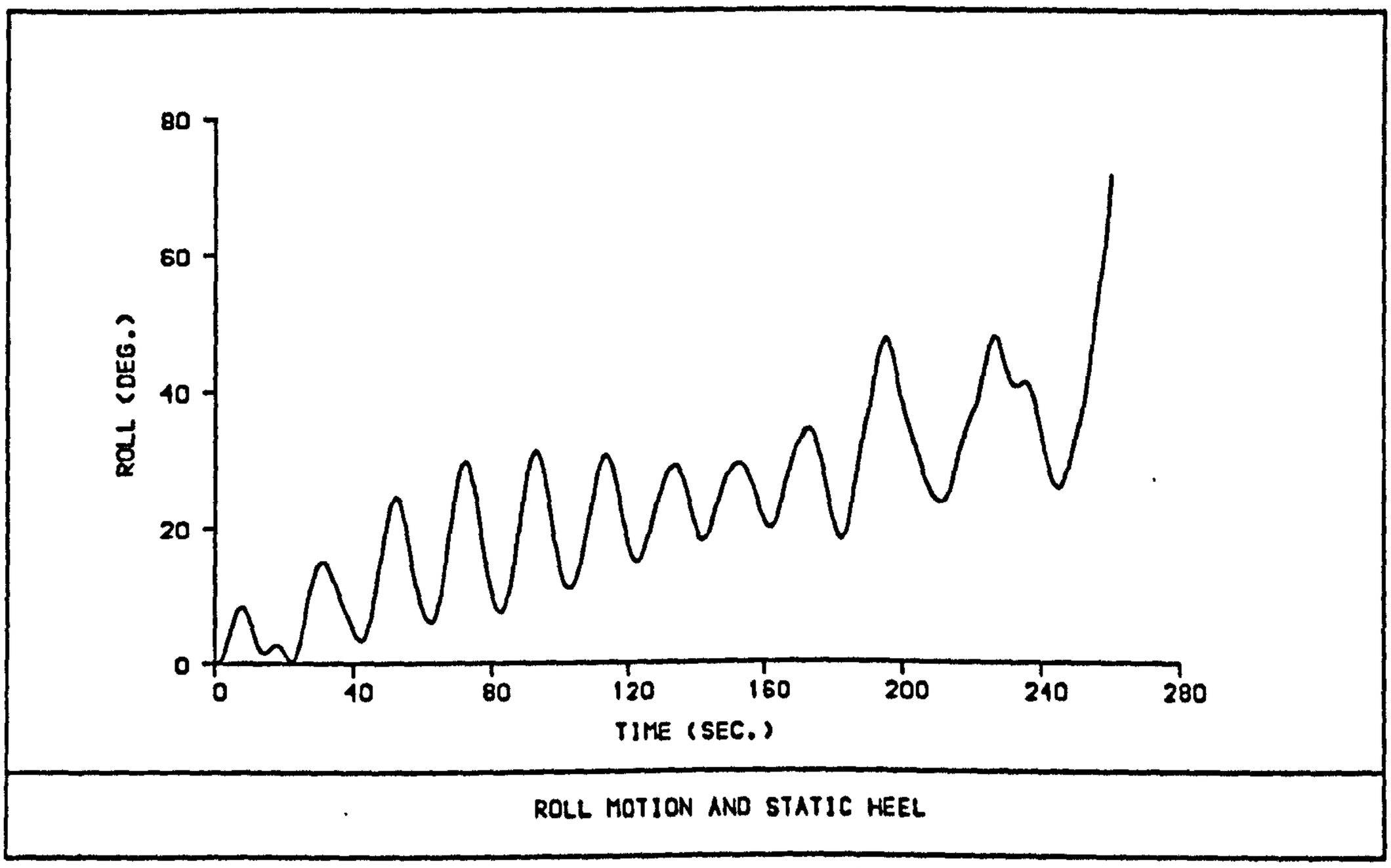

ROLL MOTION AND STATIC HEEL

Fig 7.45A Capsizing mode B: Both effects of wave and water on deck are dominant KG=12.59 m, WH= 2.0 m [DAMAGE SCENARIO 5]

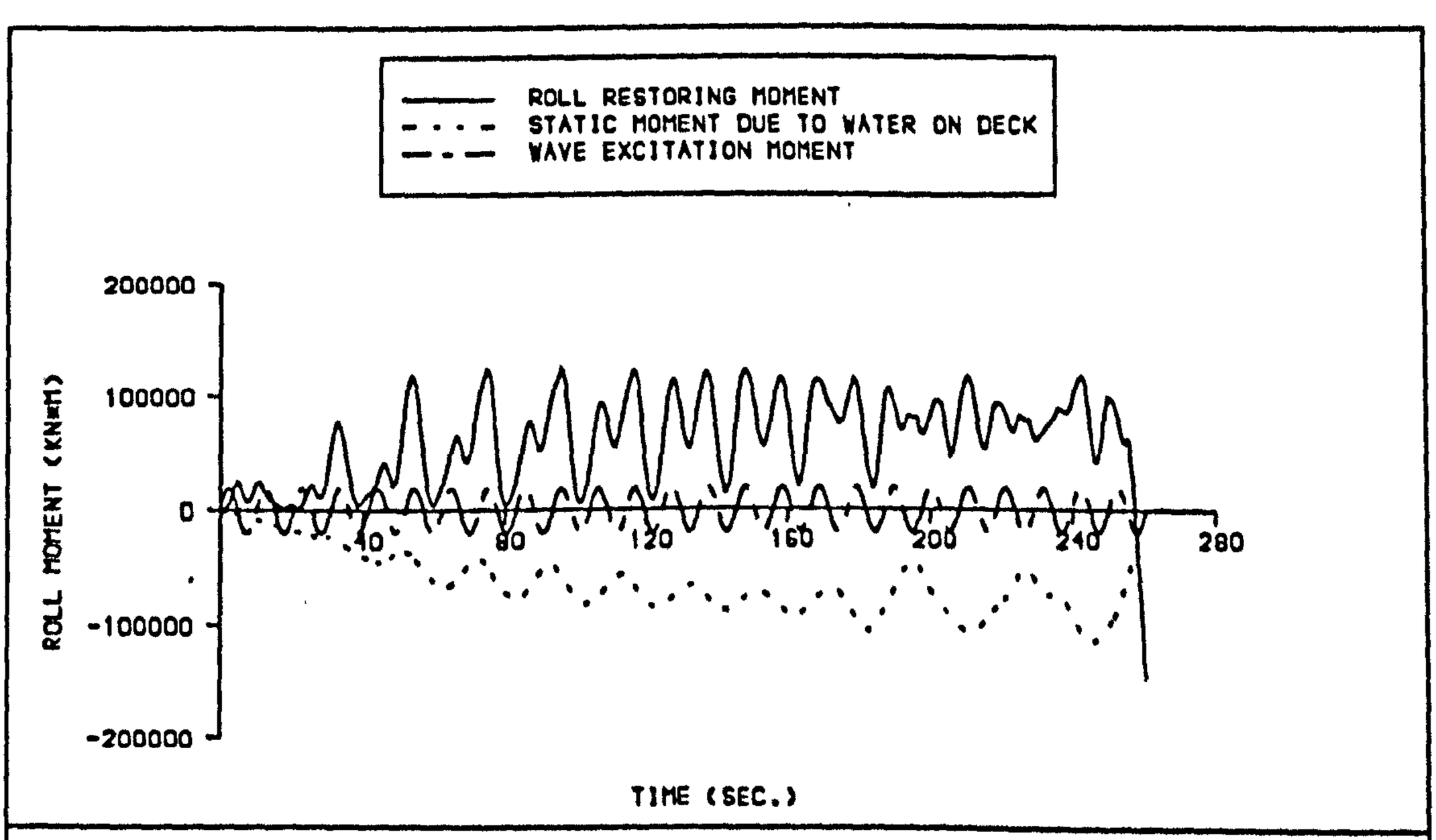

TIME HISTORIES OF ROLL MOMENTS

Fig 7.45B Analysis of the forces acting on the ship [Capsizing mode B], KG=12.59 m, WH= 2.0 m [DAMAGE SCENARIO 5]

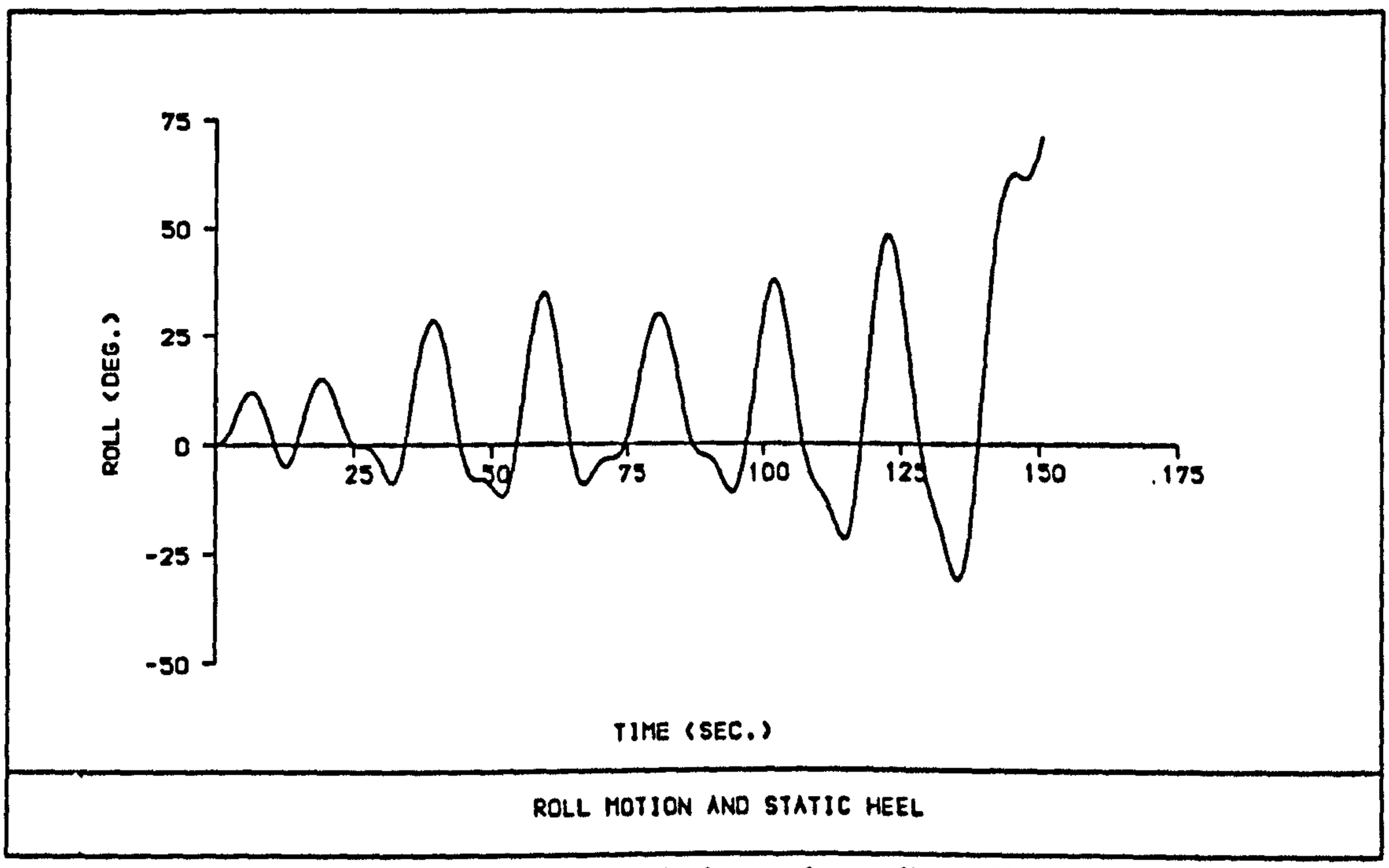

Fig 7.46A Capsizing mode C: Wave excitation and coupling effects are dominant, KG=11.84 m, WH= 6.0 m [DAMAGE SCENARIO 5]

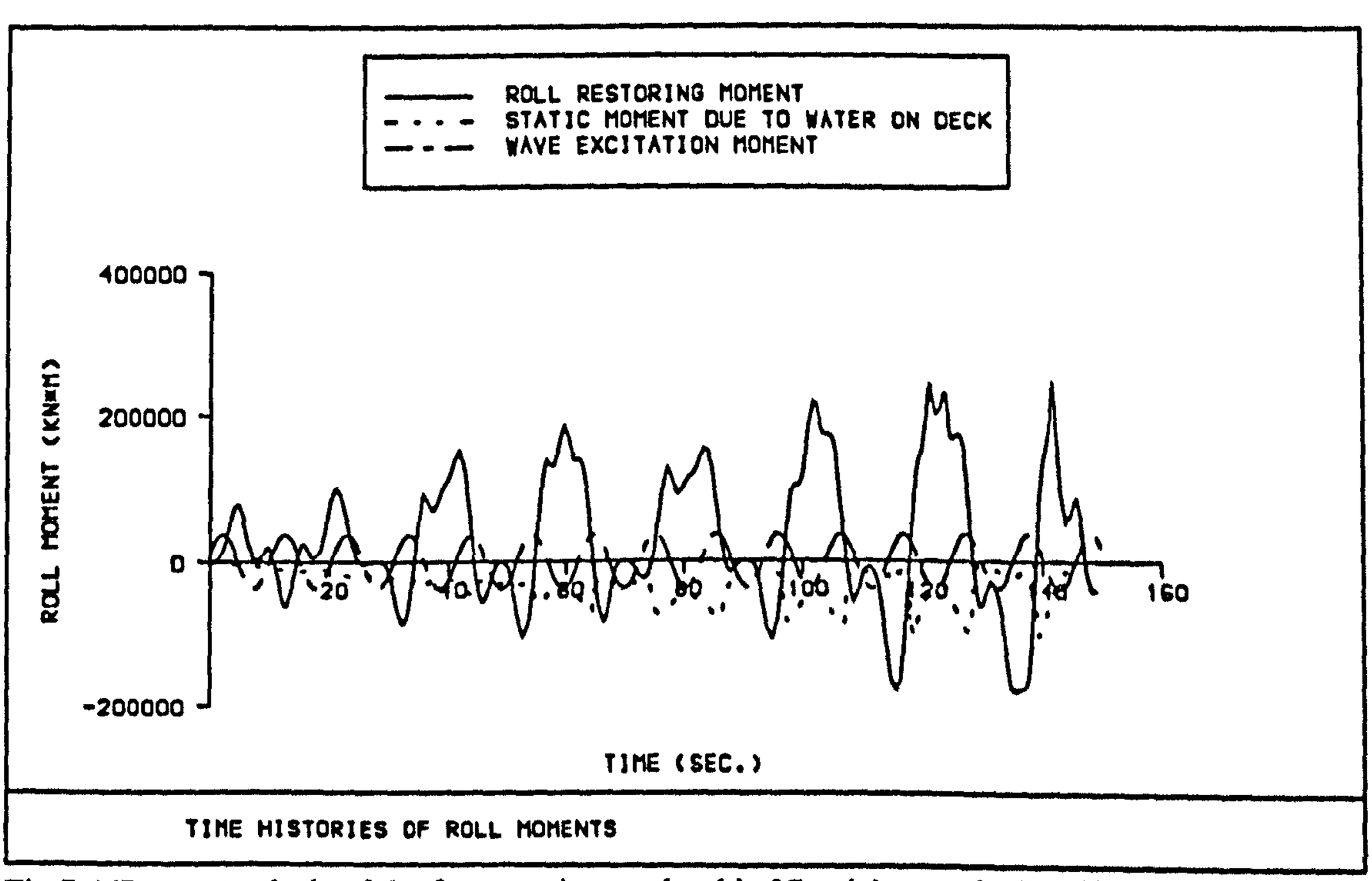

Fig 7.46B Analysis of the forces acting on the ship [Capsizing mode C], KG=11.84 m, WH=6.0 m [DAMAGE SCENARIO 5]

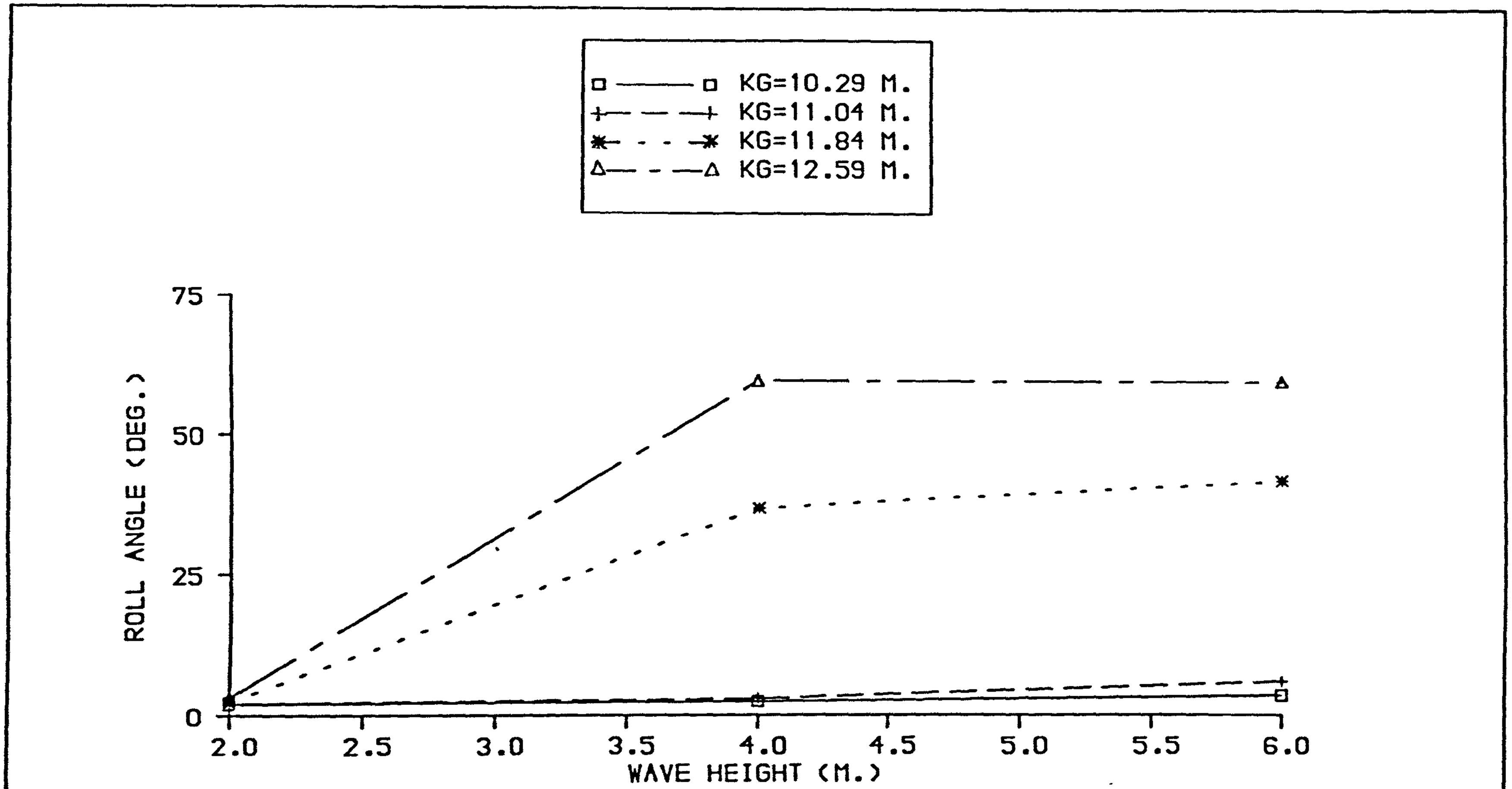

Fig 7.47 EFFECT OF WAVE HEIGHT AND LOADING CONDITIONS ON THE AMPLITUDE OF ROLL OSCILLATION, [DAMAGE SCENARIO 6]

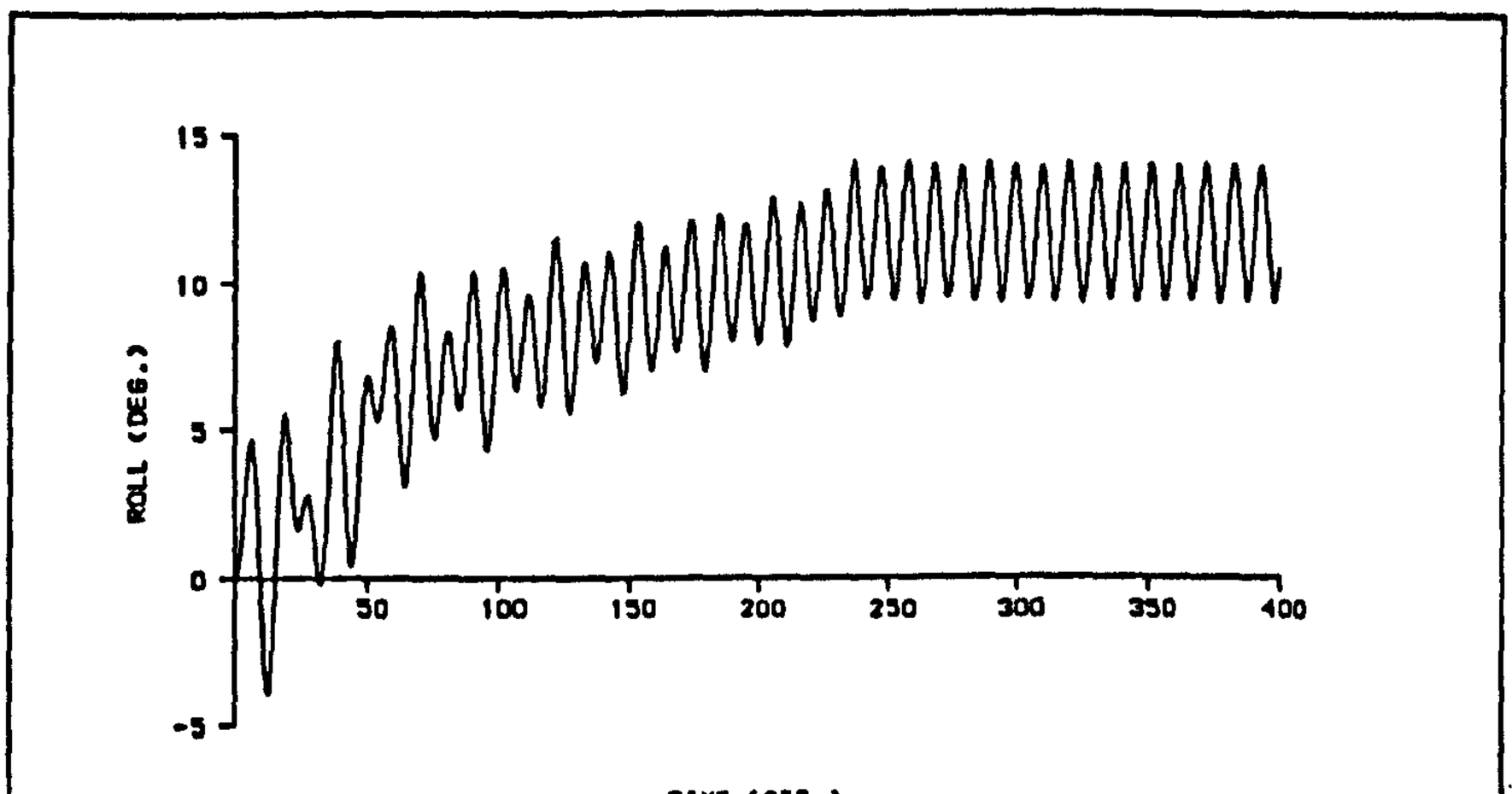

A — SINGLE DEGREE ROLL MOTION KG=11.84 M., WH=4.0 M.,[DAMAGE SCENARIO 2]

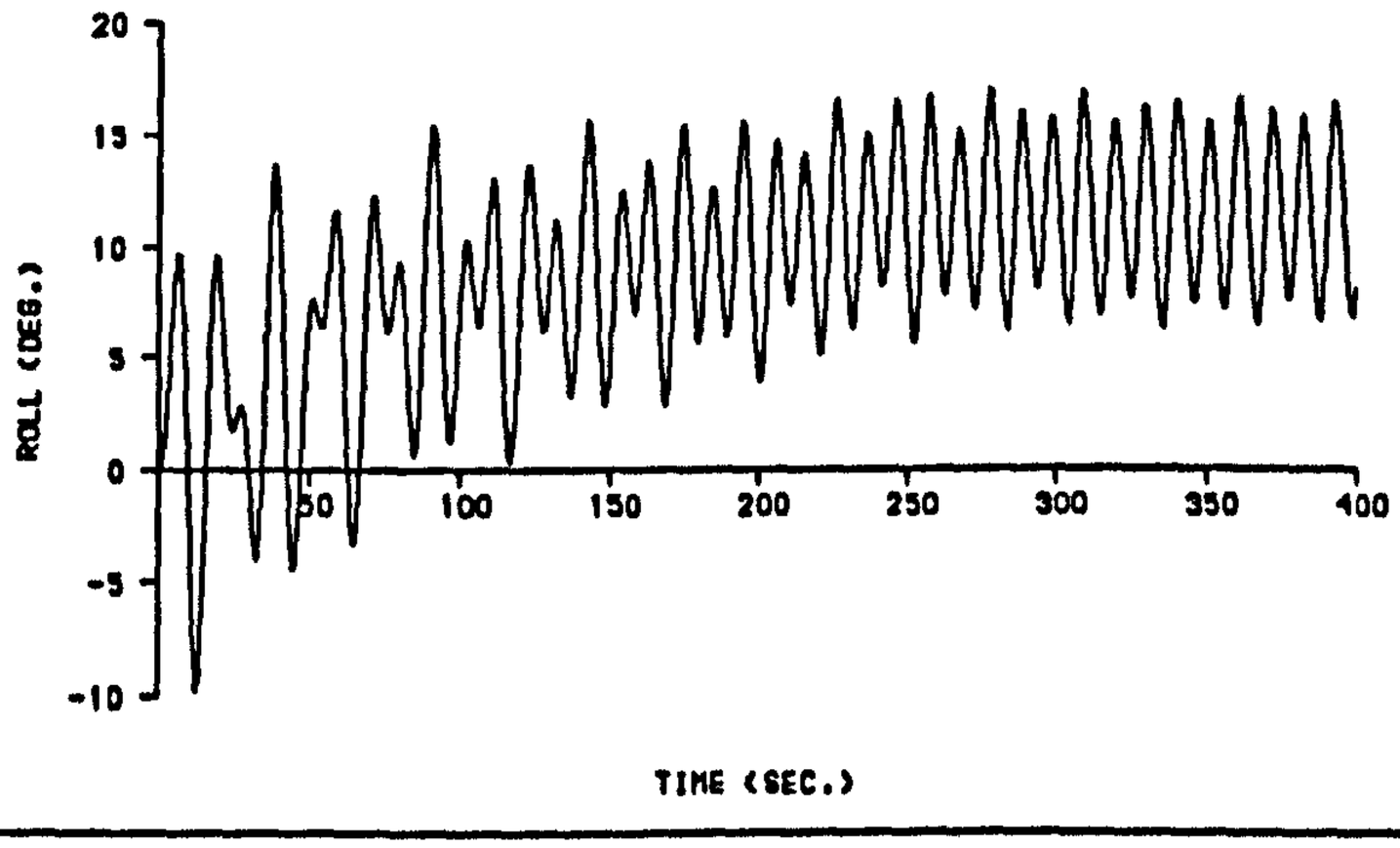

B — ROLL MOTION COUPLED WITH SWAY KG=11.84 M., WH=4.0 M., [DAMAGE SCENARIO 2]

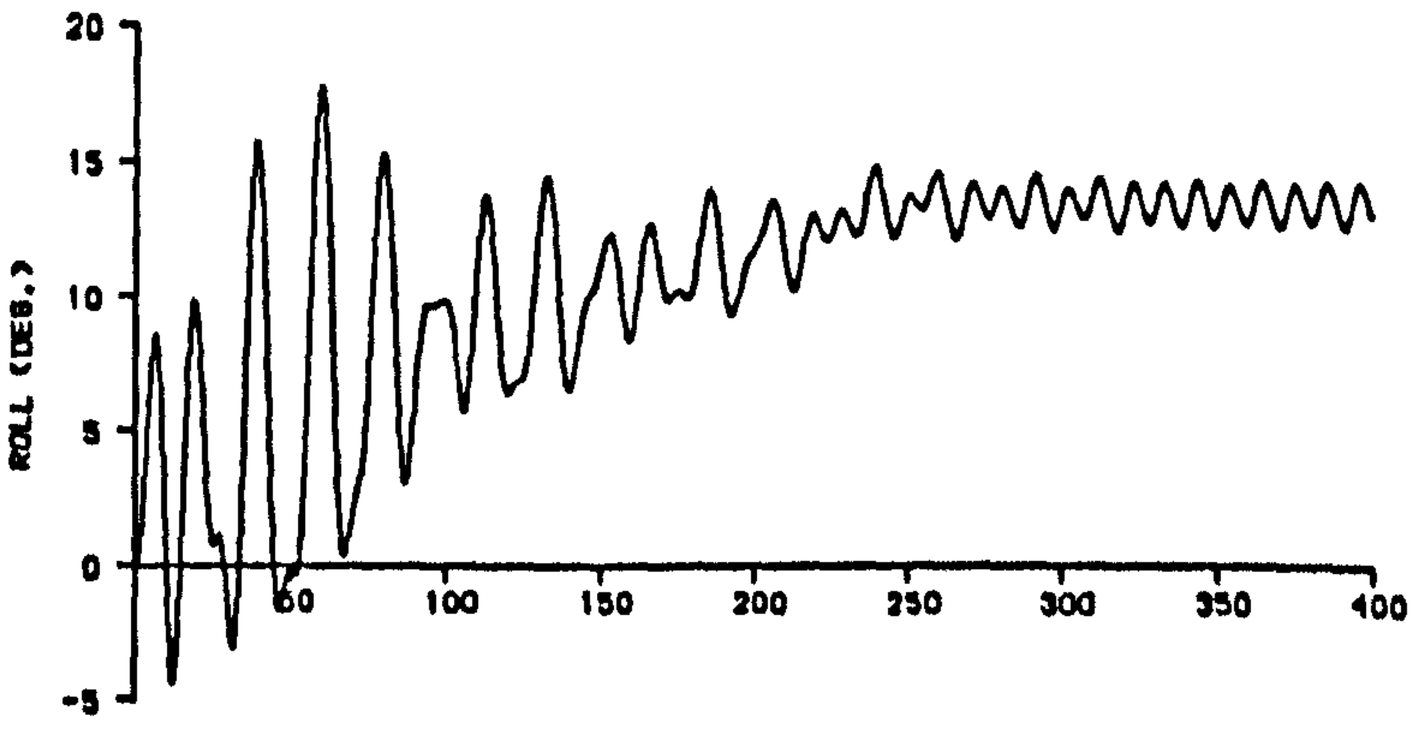

C — ROLL MOTION COUPLED WITH SWAY AND HEAVE KG=11.84 M., WH=4.0 M., [DAMAGE SCENARIO 2]

Fig 7.48 Effect of heave and sway coupling on roll motion

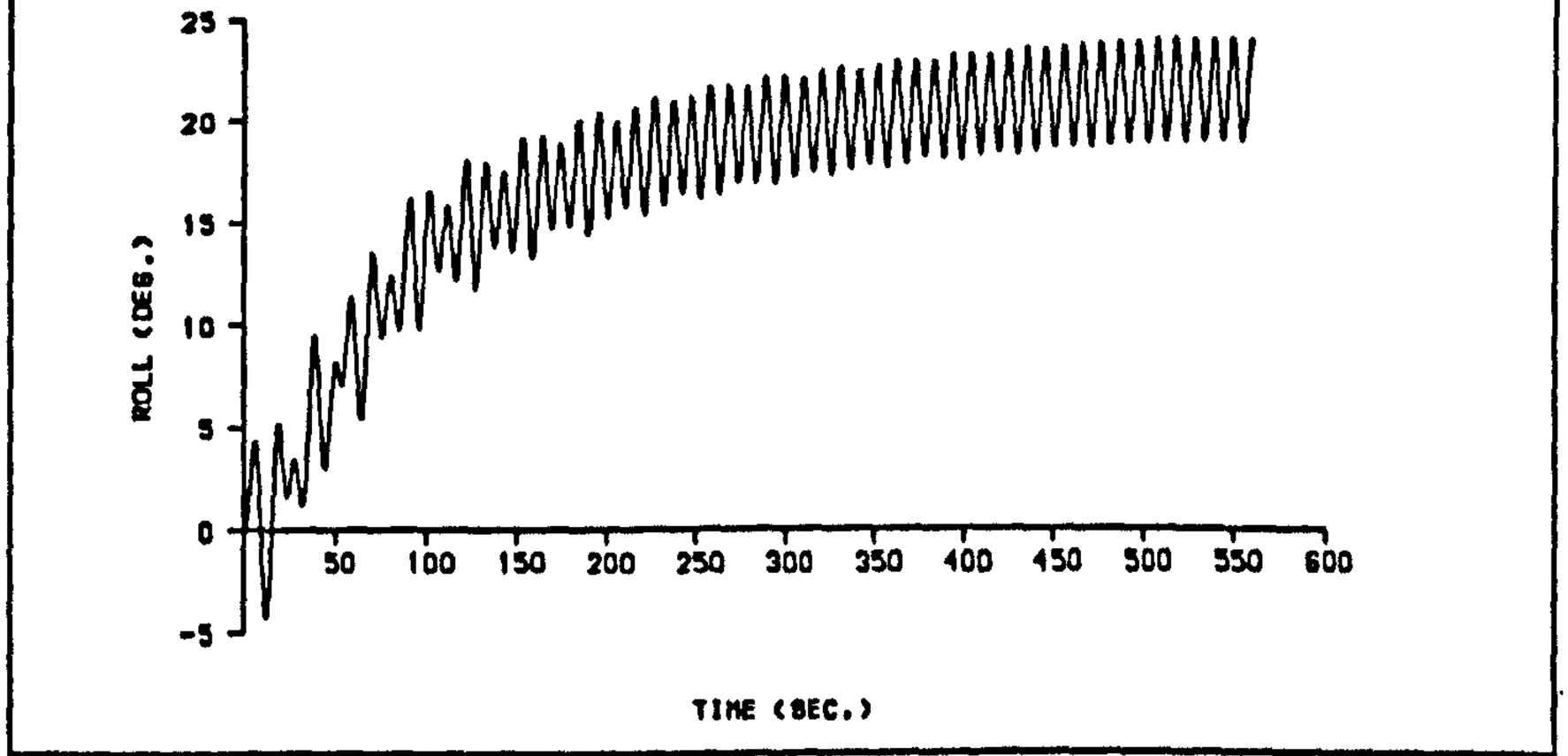

A — SINGLE DEGREE ROLL MOTION KG=11.84 M., WH=4.0 M., [DAMAGE SCENARIO 6]

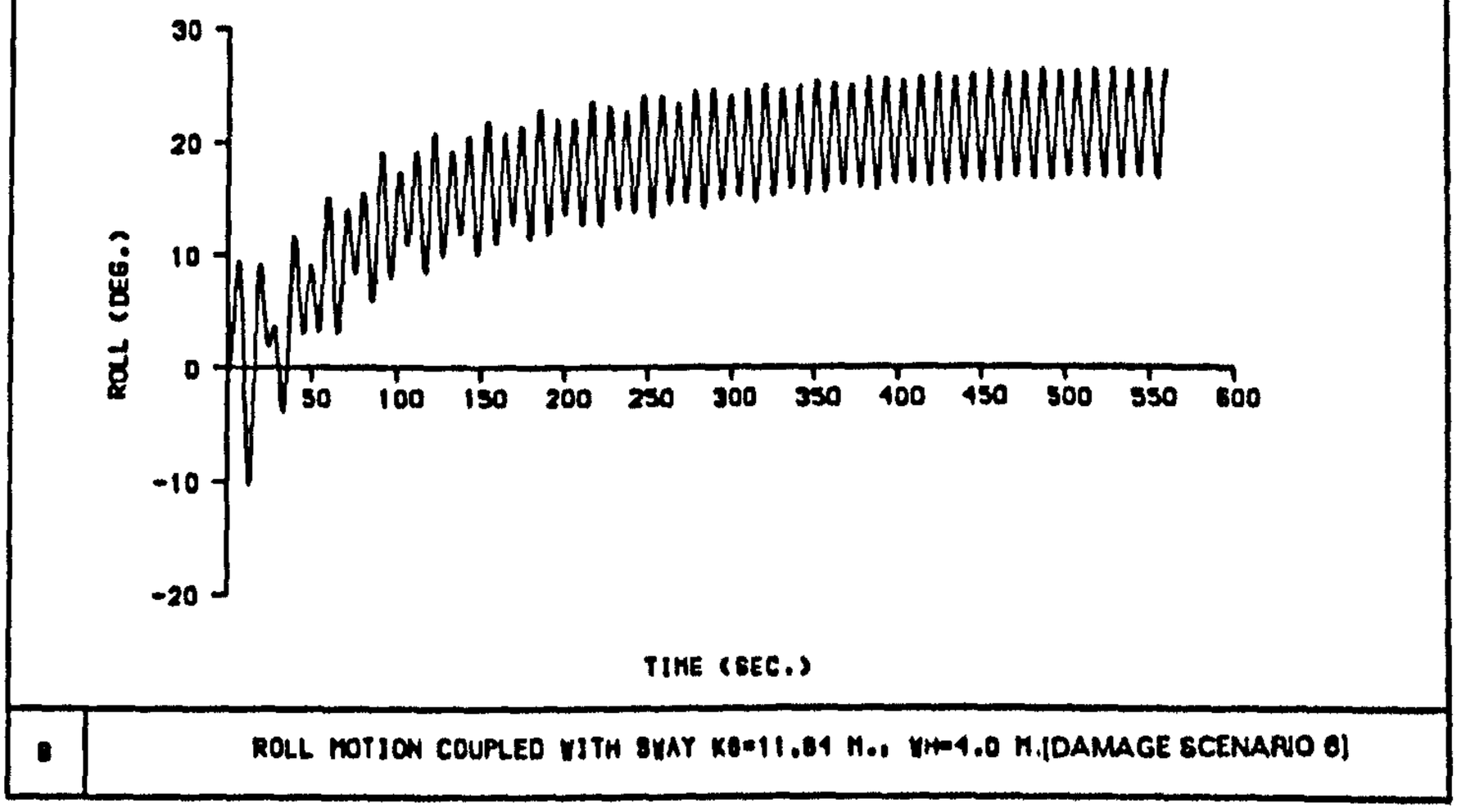

B — ROLL MOTION COUPLED WITH SWAY KG=11.84 M., WH=4.0 M.[DAMAGE SCENARIO 6]

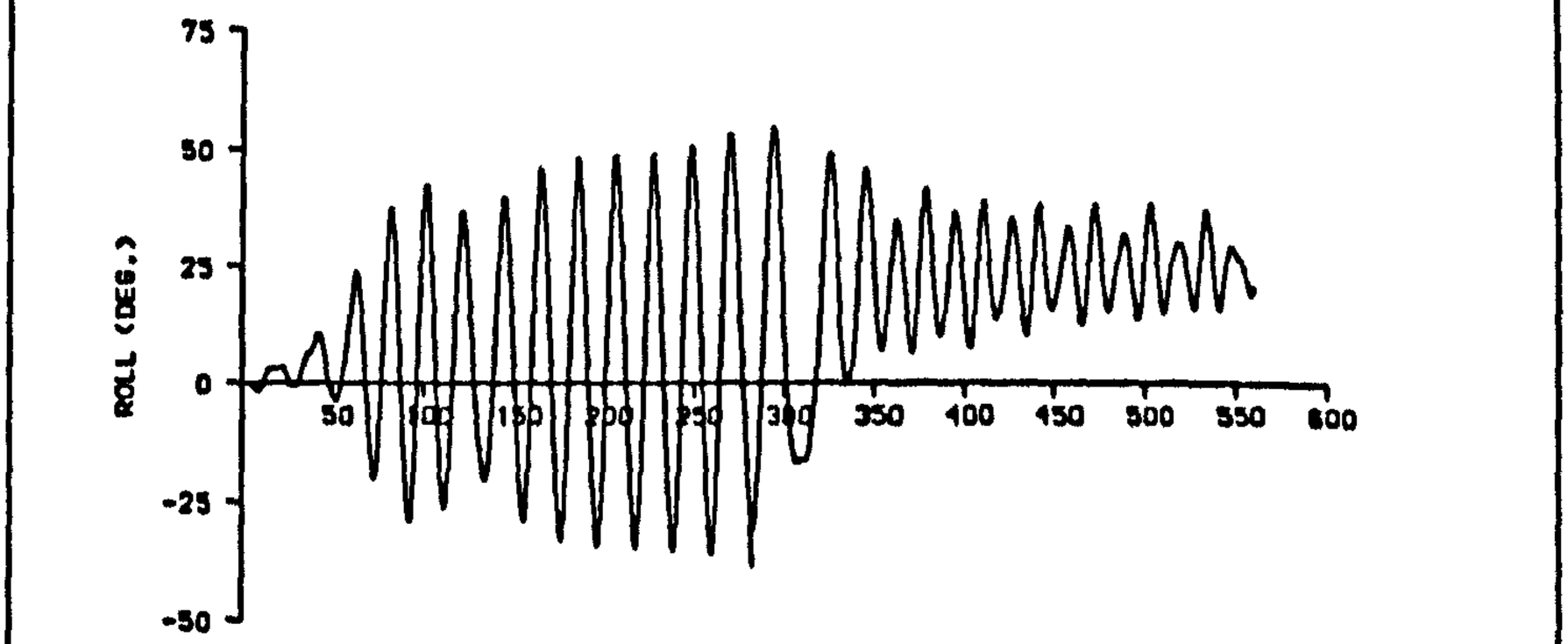

ROLL MOTION COUPLED WITH SWAY AND HEAVE KG=11.84 M., WH=4.0 M.
[DAMAGE SCENARIO 6]

Fig 7.49 Effect of heave and sway coupling on roll motion

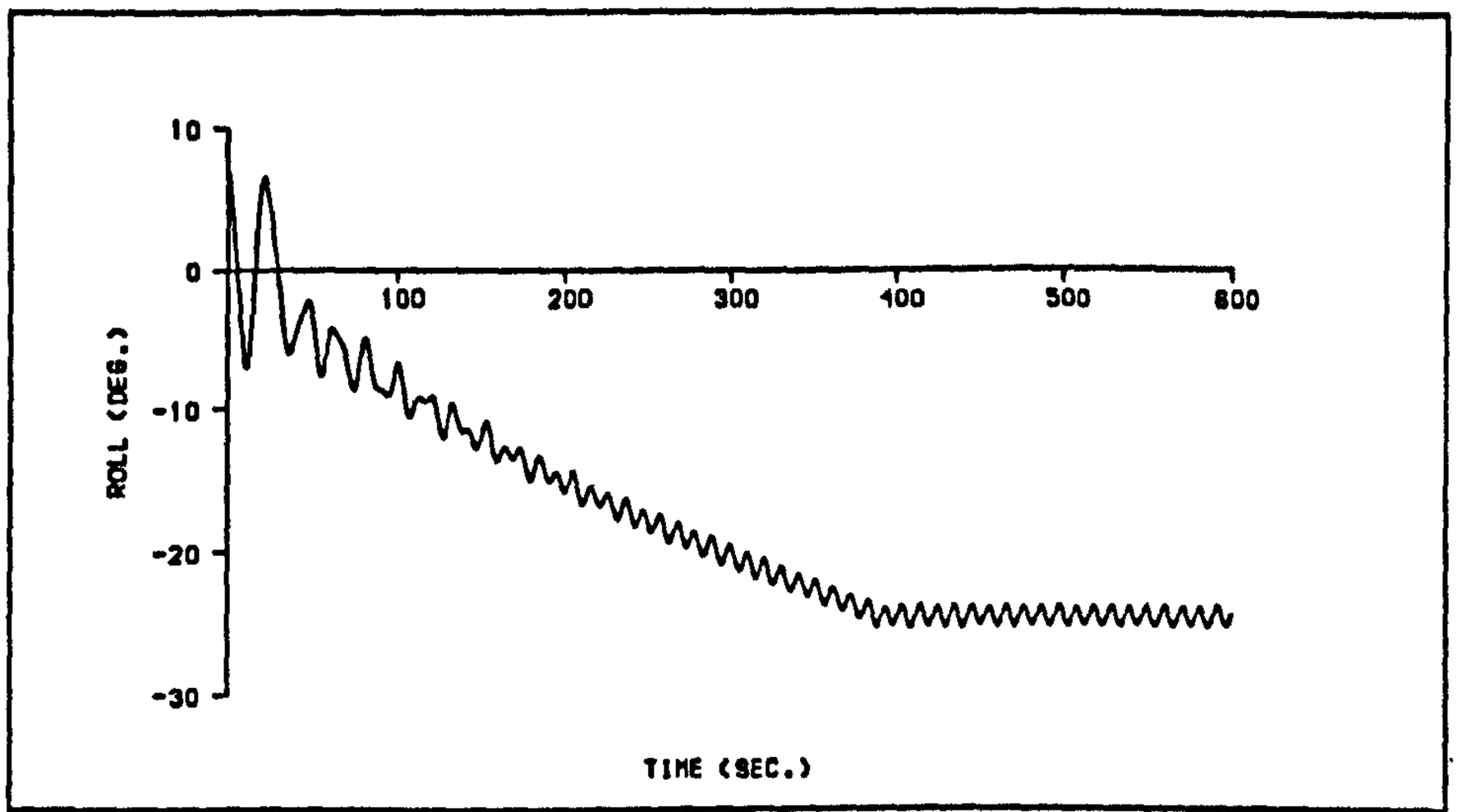

A — SINGLE DEGREE ROLL MOTION KG=11.84 M., WH=2.0 M., (DAMAGE SCENARIO 4)

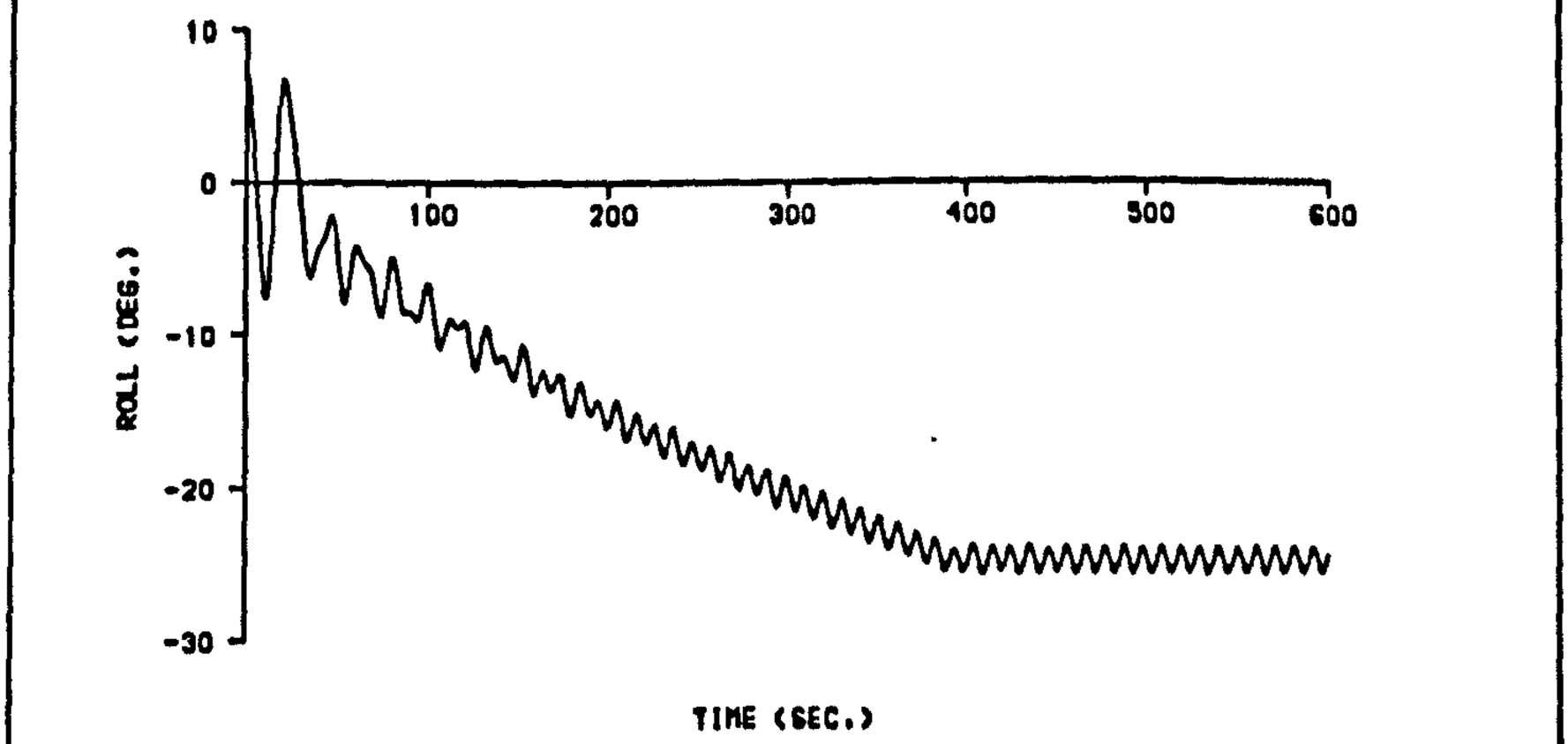

B — ROLL MOTION COUPLED WITH SWAY KG=11.84 M., WH=2.0 M., (DAMAGE SCENARIO 4)

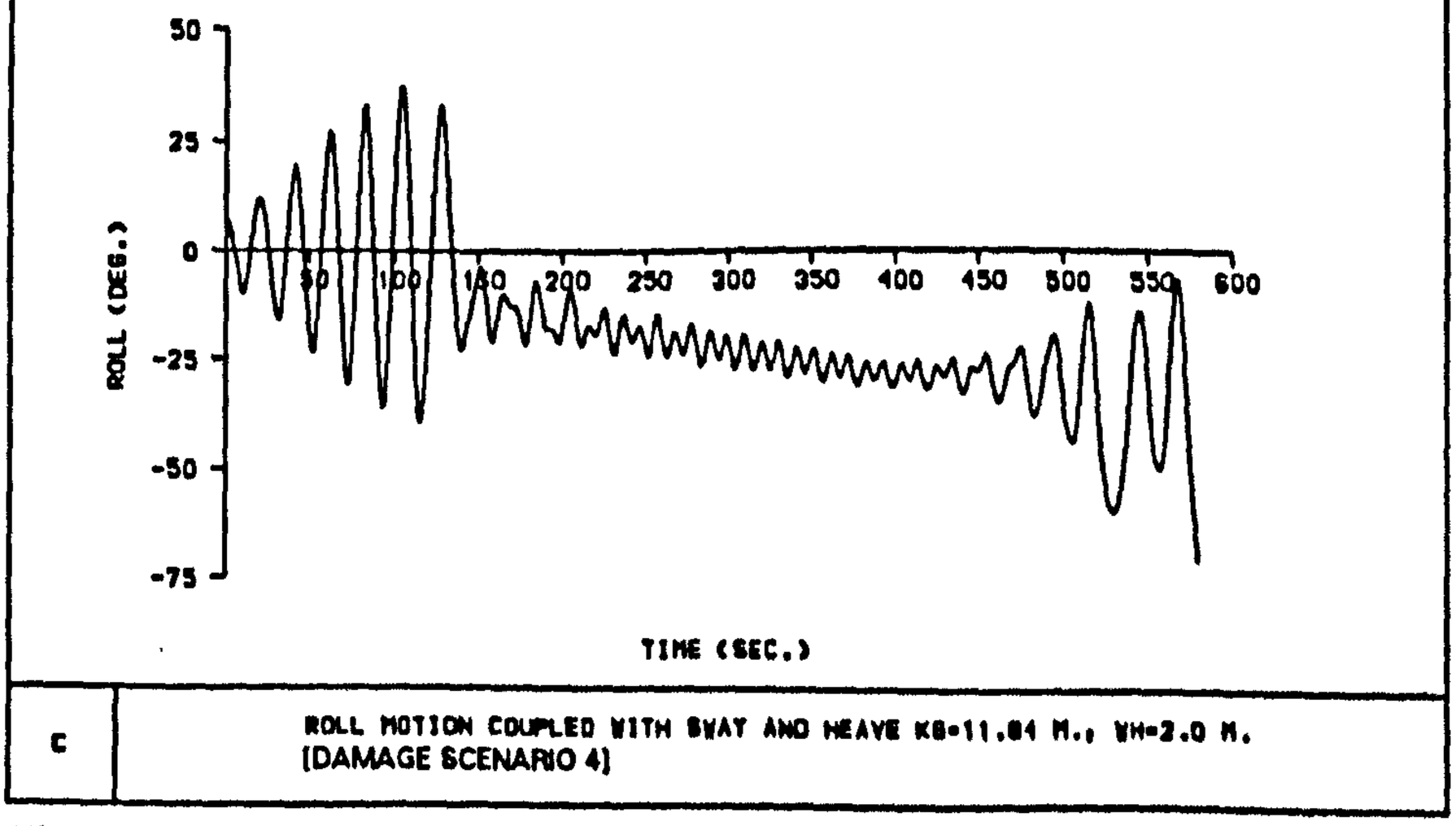

C — ROLL MOTION COUPLED WITH SWAY AND HEAVE KG=11.84 M., WH=2.0 M. (DAMAGE SCENARIO 4)

Fig 7.50 Effect of heave and sway coupling on roll motion

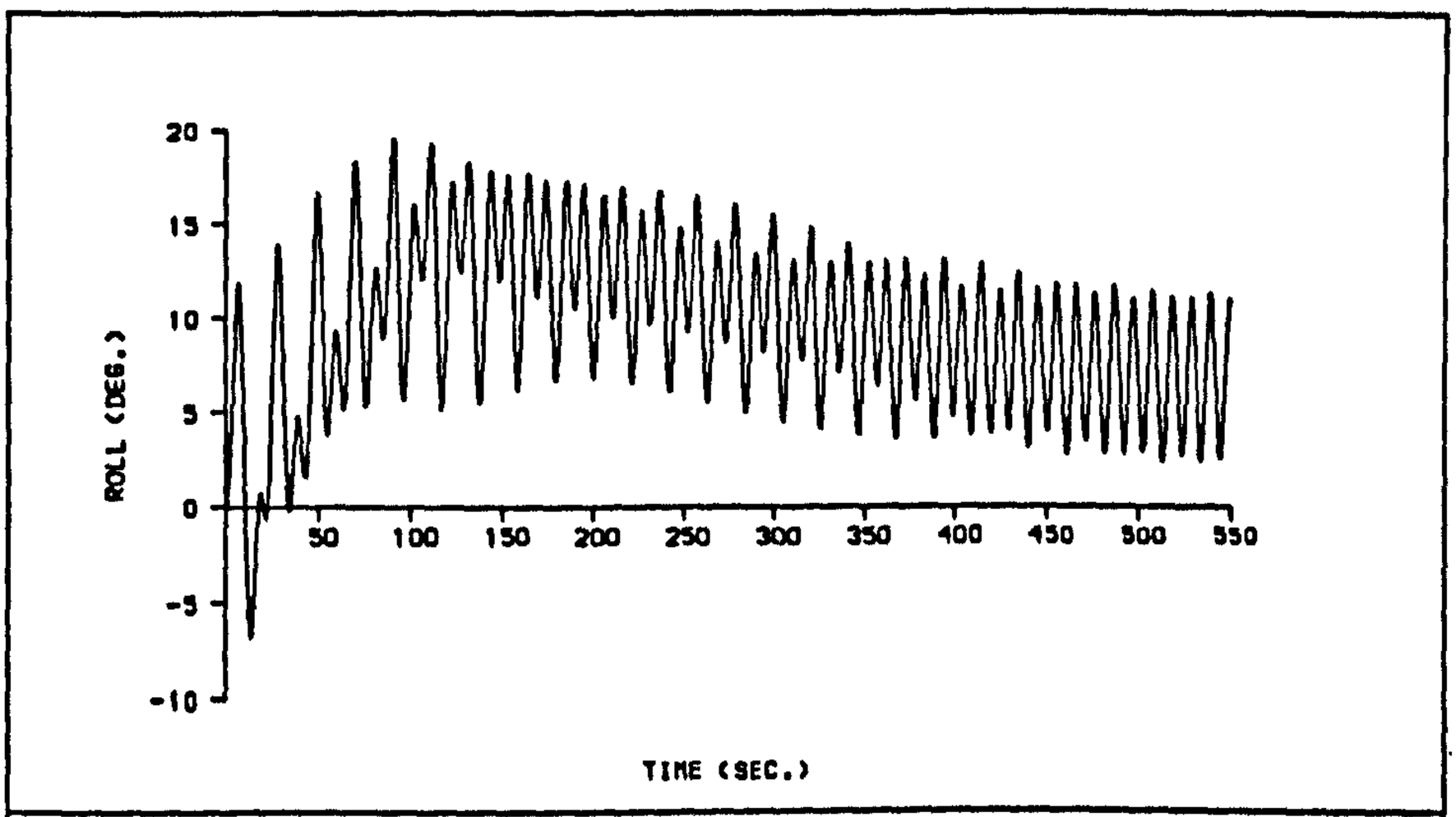

A — SINGLE DEGREE ROLL MOTION KG=12.59 M., WH=6.0 M., (DAMAGE SCENARIO 3)

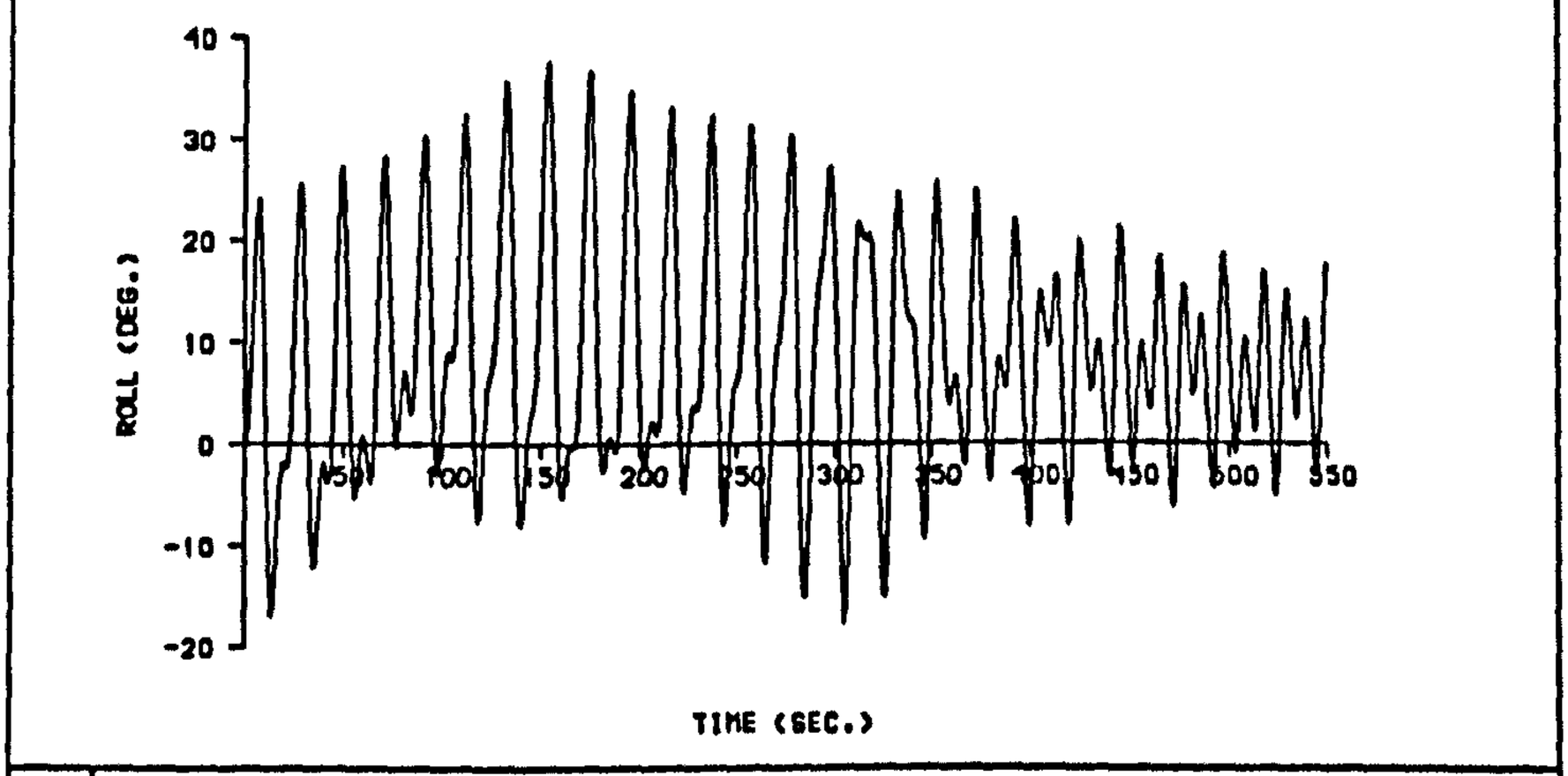

B — ROLL MOTION COUPLED WITH SWAY KG=12.59 M., WH=6.0 M., (DAMAGE SCENARIO 3)

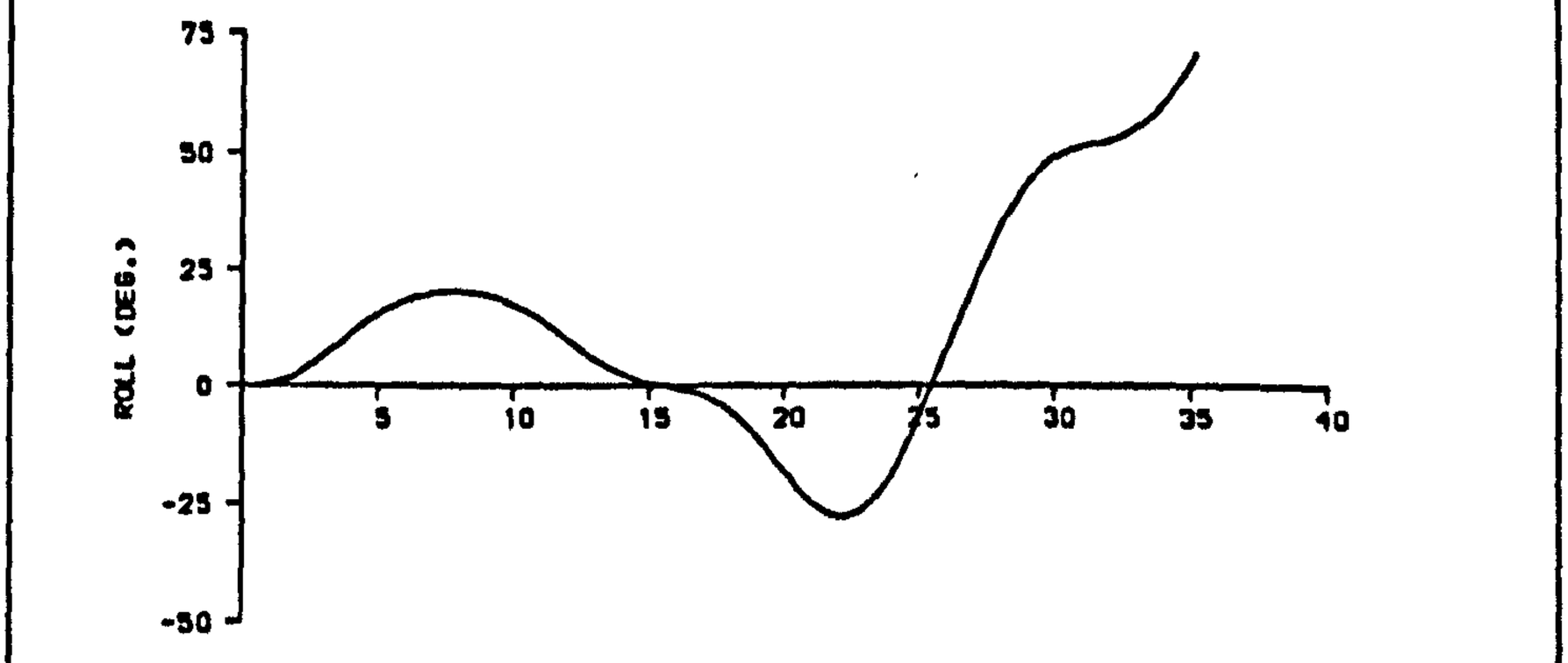

C — ROLL MOTION COUPLED WITH SWAY AND HEAVE KG=12.59 M., WH=6.0 M. (DAMAGE SCENARIO 3)

Fig 7.51 Effect of heave and sway coupling on roll motion

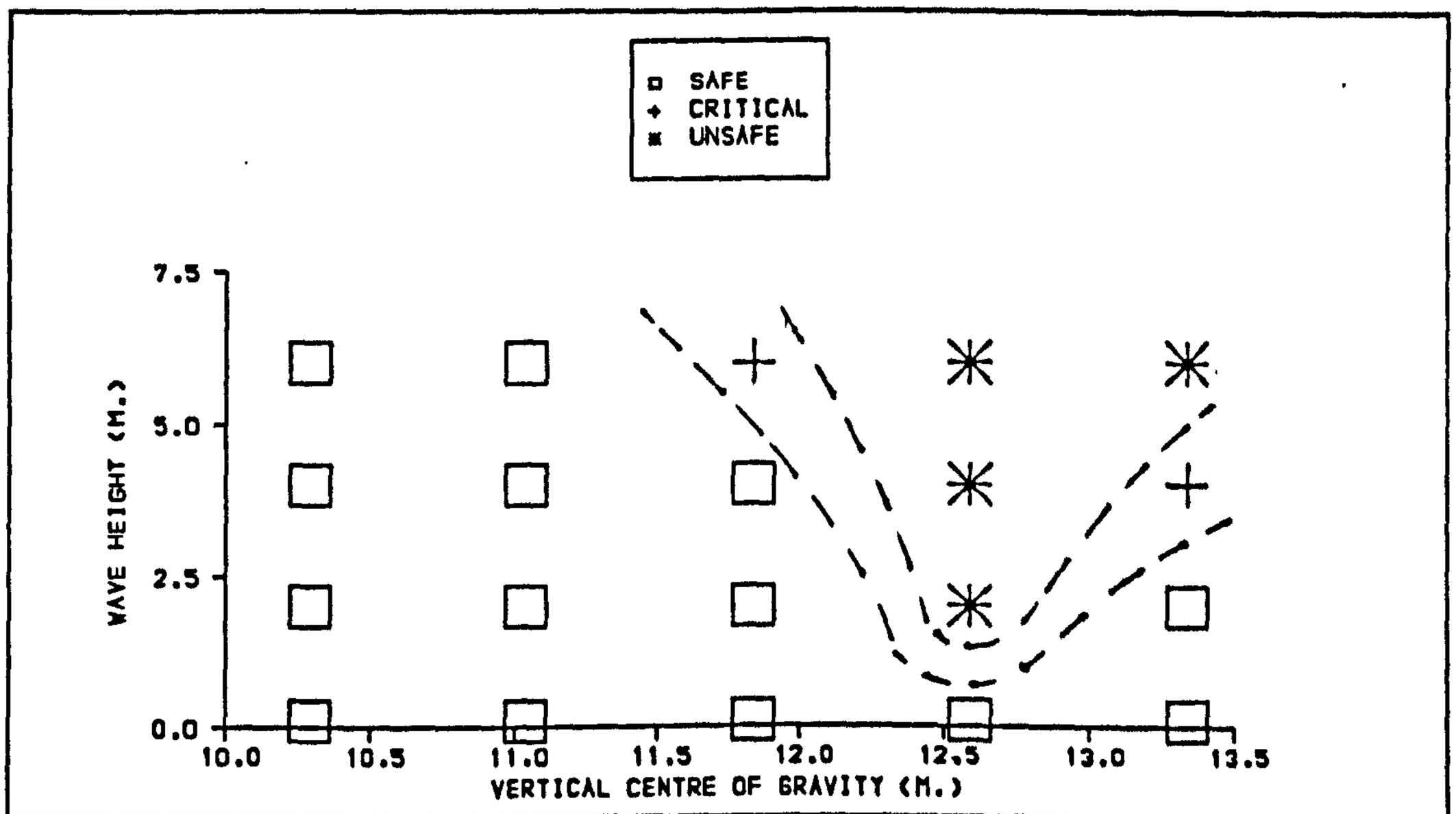

Fig 7.52 Boundary stability curves [DAMAGE SCENARIO 1]

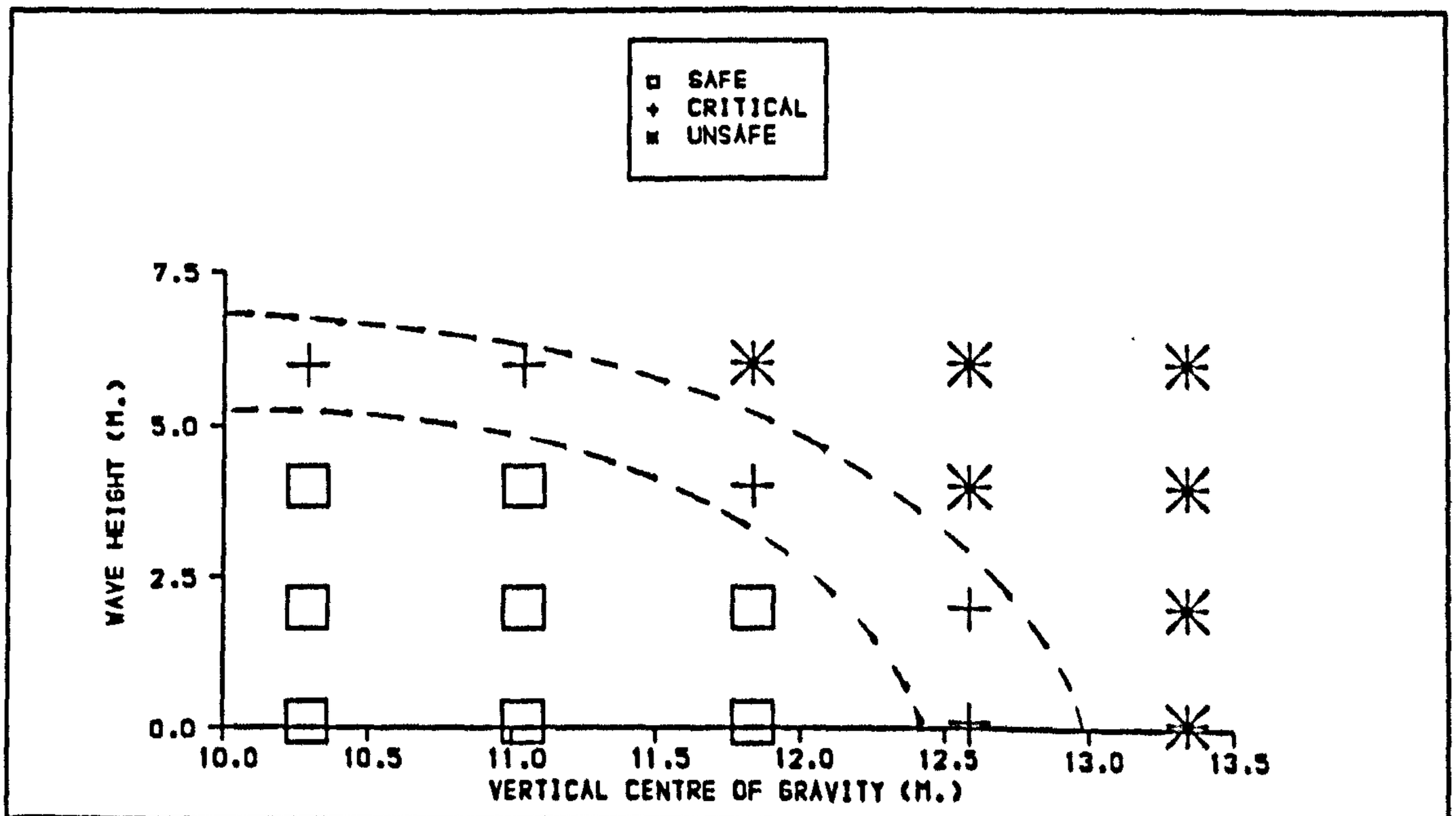

Fig 7.53 Boundary stability curves [DAMAGE SCENARIO 2]

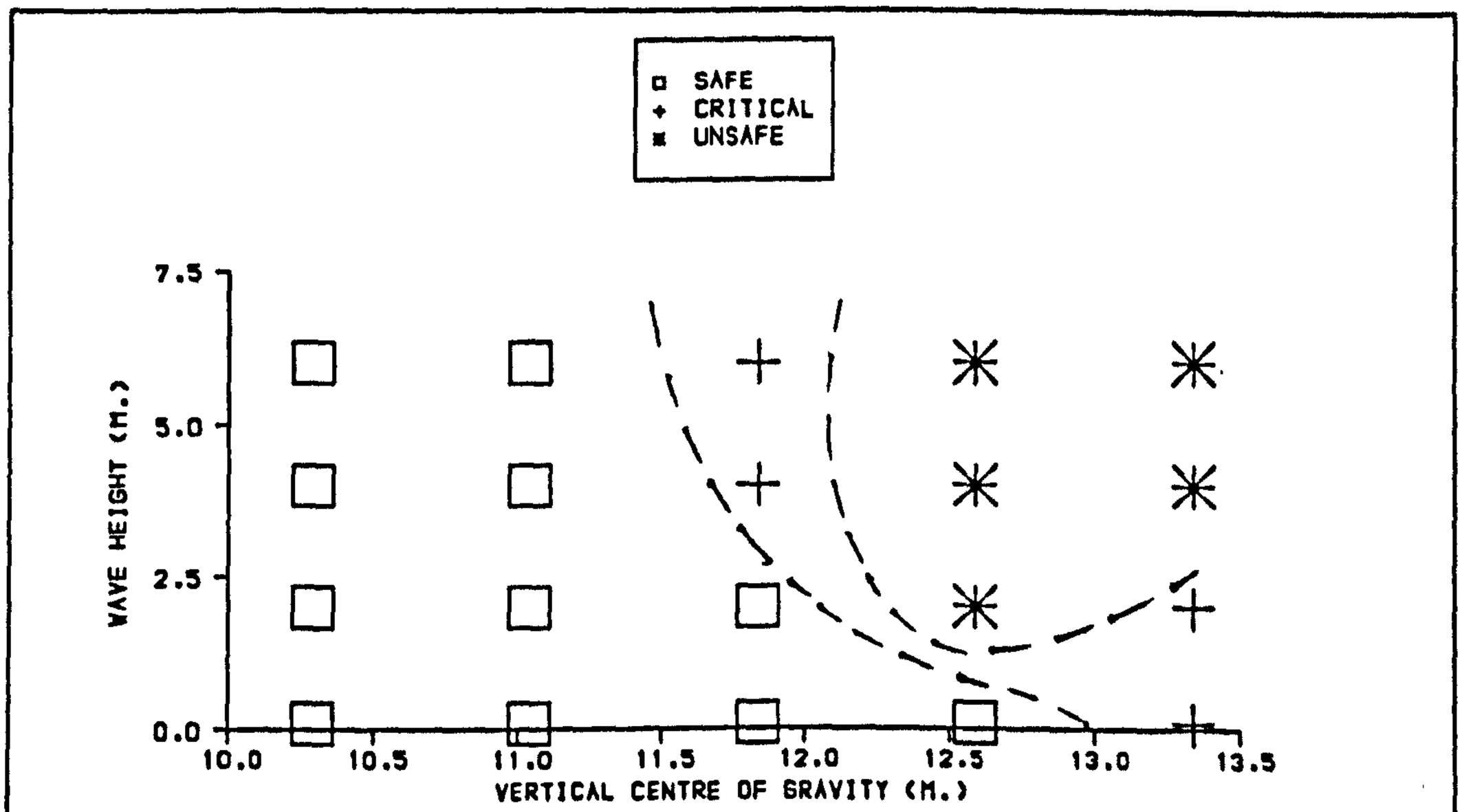

Fig 7.54 Boundary stability curves [DAMAGE SCENARIO 3]

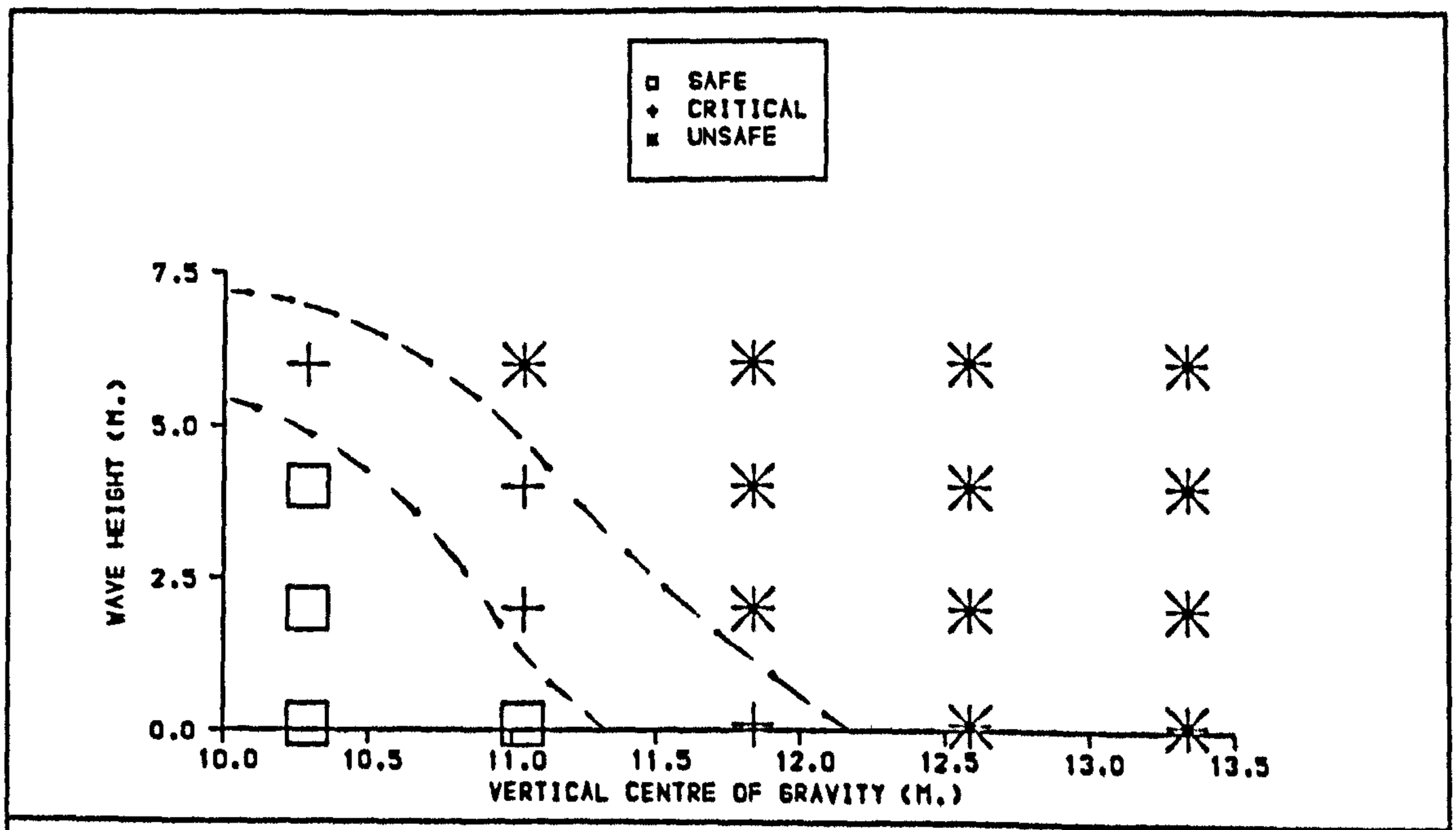

Fig 7.55 Boundary stability curves [DAMAGE SCENARIO 4]

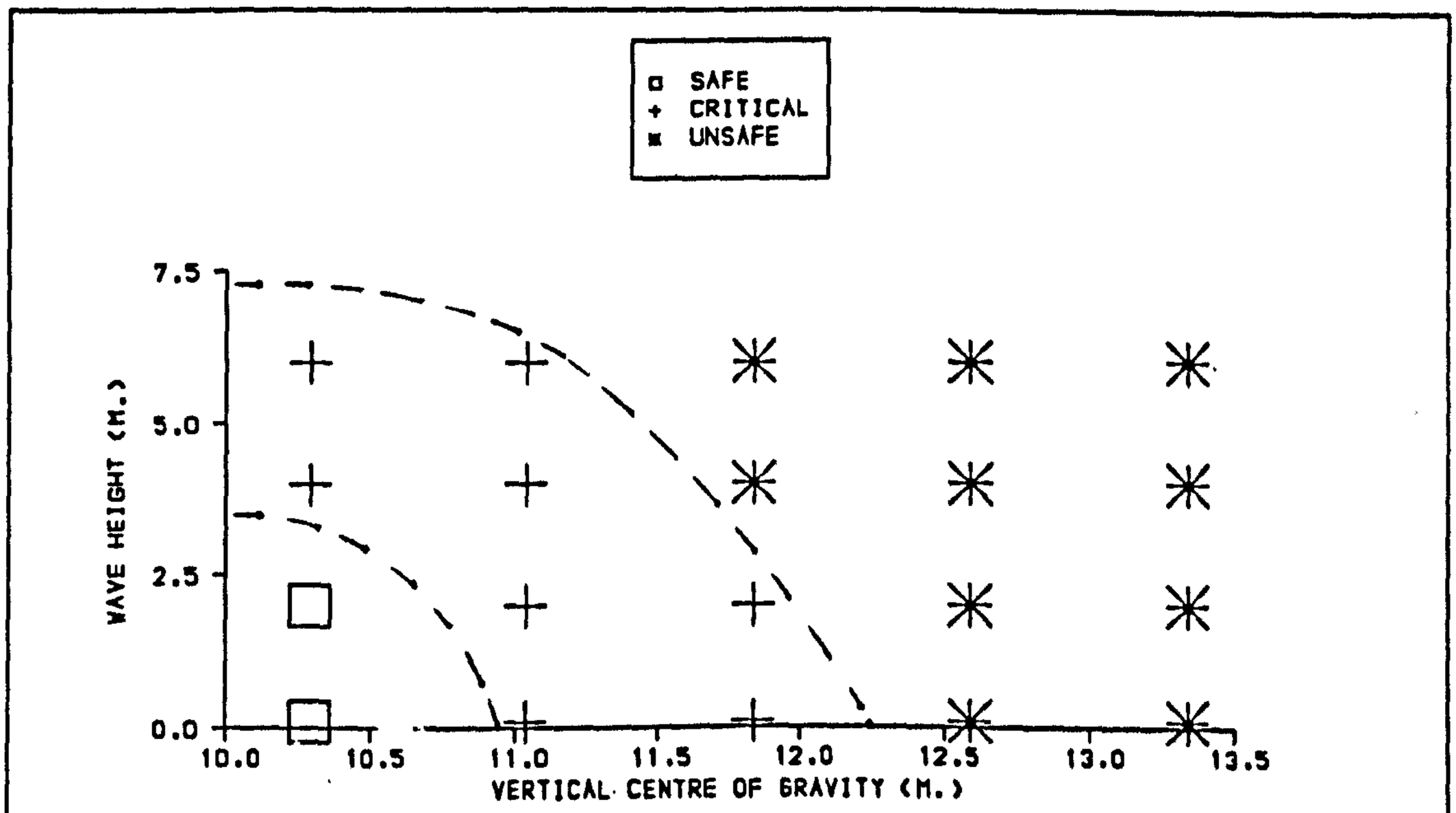

Fig 7.56 Boundary stability curves [DAMAGE SCENARIO 5]

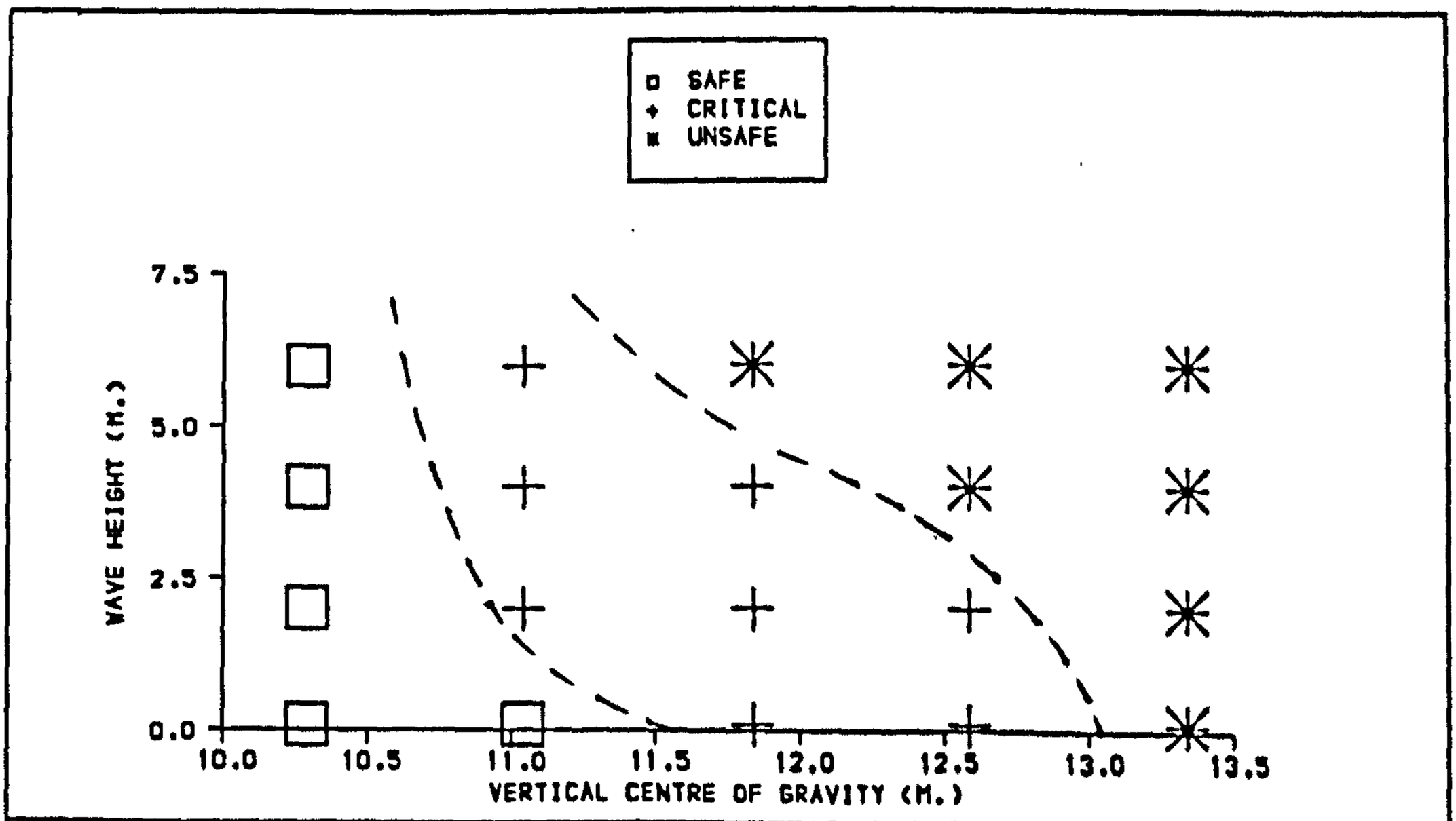

Fig 7.57 Boundary stability curves [DAMAGE SCENARIO 6]

CHAPTER 8: DISCUSSION

8.1 GENERAL

The recent accidents (European Gateway and Herald of Free Enterprise) provided strong evidence that existing rules are insufficient, and that flooding of compartments above the bulkhead deck as well as ship dynamics must be taken into consideration in assessing damage survivability.

Unfortunately safety and commercial gain conflict, and as a result even if new rules are introduced, it would take a very long time to implement them fully, therefore achieving solid progress becomes difficult. As mentioned in Chapter 3, in 1990 IMO introduced new amendments for assessing the damage stability of a ship in relation to residual restoring ability and progressive flooding, which became effective in the beginning of 1992 and will be applied in the building of all new ships. However, for existing passenger ships, IMO introduced a percentage system and a time table, and according to this system ships must comply with a certain percentage of the rules by the preset date. This strange percentage system is also disappointing, since it allows the ship to comply with 100% of the rules by the year 2010, rules whose reliability has already been questioned. It can be clearly seen that this percentage arrangement lifts the restriction on the existing ships to complete their estimated life span. This example shows the all round unwillingness to improve safety standards. Under these circumstances, introducing dynamic effects in the assessment of damage stability and survivability of ships may take a very long time.

In this chapter, the new approach adopted to assess the dynamic stability of passenger ferries and proposed methodology will be discussed. The level of achievements with respect to the objectives initially set will be reviewed, whilst the problems faced, solutions adopted, as well as the remaining problems will be elaborated upon. Following this, the possible effects of the adopted approach and key findings on the stability and design fields will be emphasised. Finally the main contribution of this research will be outlined.

8.2 IDEAL STABILITY ASSESSMENT AND CRITERIA AND MEANS FOR ACHIEVING SAME

A stability assessment procedure and adopted stability standards can be seen to be successful if they produce a meaningful relation between safety, ship design, and operational and environmental conditions. The link between these three main factors can be derived by using a mathematical model, model tests or full scale trials.

The mathematical modelling route, trusted and validated within the limits of the theory was followed in the approach adopted in this thesis. The mathematical model offers a cost effective solution while having flexibility and versatility since it is suitable for systematic studies of different parameters over a wide range of limits. Moreover, an investigation of the parameters involved, which will be very difficult to examine by model tests or trials, can be undertaken.

On the other hand, the mathematical model has drawbacks due to different reasons, such as the limits of the theory used and the non-existence of solutions. However, with the use of justifiable assumptions it is still possible to obtain meaningful results.

In order to develop the right assessment and establish meaningful standards regarding the stability of damaged ships, the process is divided into three main steps, which also constitute the main aims of the thesis. They can be listed as follows:

Step one: To understand the behaviour of the damaged vessel, to identify the main problems and needs, and finally to adopt the most suitable approach to assess the dynamic stability of a damaged ship.

Step two: To carry out an extensive systematic parametric investigation, to identify the important elements and to establish relationships between them.

Step three: To set critical standards of damage stability in a meaningful

way by using the aforementioned important findings and relationships.

The following section documents the progress made at each step.

8.3 PROGRESS ACHIEVED

i- Step One

Before the approach and the level of sophistication of the mathematical model are decided, physical understanding of the damage stability of a ship must be gained and the main problems and needs must be identified. In order to achieve this, the available published studies in the stability field over the years are probably the most valuable source. However, besides identifying the problems and gaining physical understanding in the subject, the approach to combine all these effects and the solution technique are also equally important. Therefore, development in other fields such as computer technology and numerical solution techniques have to be employed in the development of a new approach.

Review of previous work emphasised that stability of the ship whether it is intact or damage, is a dynamic phenomenon, so that it has to be treated in a fully dynamic form. Investigations also revealed that the mathematical model must include progressive flooding and accumulation of water, and coupled ship motions must be solved for realistic environmental conditions. As stated in Chapter 4, to combine all the effects in the mathematical model, the time domain technique, which solves equations of coupled roll, heave and sway motions using numerical methods, was employed.

However, despite the high number of published works in intact stability, dynamic damage stability suffers from limited available information on modelling certain phenomena such as water ingress, accumulation of water, etc. In these situations, approximated or simplified approaches, as given in Chapter 5, have to be used.

For instance, water ingress was modelled by using fixed flow rate or approximated water flow coefficients as explained in Chapter 5.

Although these approximations are very useful achievements in this field, since no other information is available, and meaningful results were achieved as shown in Chapter 5 and [61], they stopped short from offering a general calculation procedure. Since water ingress is a determining factor in affecting ship survivability, a more accurate estimation of water ingress would improve the dynamic damage stability assessment. Therefore, this subject deserves careful consideration.

Water accumulation on deck is a highly non-linear problem with a lot of complexities. So far, only a limited solution has been made available. Therefore this problem is approximated by assessing the effect to be pseudo-static, and the results proved to be satisfactory when compared with experimental results [61]. However, it is desirable to include the full dynamic effect if a suitable mathematical model is developed.

Despite some approximations in the mathematical modelling, the adopted approach is the first theoretical approach ever used to treat the damage stability of a ship in a fully dynamic manner while investigating the associated phenomena extensively and realistically. In addition, an investigative structure has been developed that allows the approach to be enriched without any difficulty and without affecting other parts of the approach.

ii- Step Two

Following completion of the adopted approach, the second stage is important in identifying parameters affecting the ship's stability, and in establishing relationships between environmental and ship design parameters, and stability characteristics. Therefore, the strategy, contents and limits of the parametric investigation play an important part in how valuable the achievements are in the damage stability field.

Probably the most fundamental idea adopted for the parametric study in this thesis is that "Damage and flooding may occur at any location in the ship and could be of any extent". This idea assures that every part of the ship receives equal consideration in the assessment. Exploring this idea produced different damage scenarios which have been

experienced or are potentially dangerous and gave rise to a new approach for assessing the survivability of a damaged ship which may be termed "Damaged Scenario Analysis". This provides the basis on which critical stability standards may be devised by considering the worst realisable scenario pertaining to the vessel itself, the operating environment and the location and extent of damage.

Taking the location and extent of damage as the basis, different parameters such as wave height, loading condition, water flow etc. were investigated extensively. As a result of this investigation some key findings can be listed as follows:

- Location and extent of flooding is vital to ship's survivability

- Flooding the vehicle deck is the worst damage scenario and the amount of water on deck is a determining factor on survivability

- Waves are also important in affecting ship survivability

- Ships can be lost as a result of progressive flooding

- The ship's loading condition is one of the very important parameters affecting both the survivability of the damaged ship as well as other related parameters such as ship roll, amount of water on deck etc.

Results of this investigation helped to establish clearly the level of critical damage stability.

However, during a research project, carried out at Strathclyde University [61], by taking into account option 2 of water ingress, and irregular seas, some key findings were revealed, which were not investigated in this thesis. For instance, damaged freeboard was found to be a vital parameter in the ship's survivability, as it controls the flooding of the deck above the water level. Wave height was also identified as an important factor on water ingress. Results also revealed

that around the design loading condition, the critical ratio between wave height and damaged freeboard (WH/F_d) is as small as 2. It has to be emphasised that roll motions in irregular seas were more modest than those experienced in regular waves but even this was enough to increase the flow rate drastically. This suggests that if option 2 of water ingress had been employed for the parametric study in this thesis, results could have been much worse than presently indicated, although a derisive conclusion merits further investigation.

These additional findings are very useful and contribute towards the identification of the real reasons and in establishing more accurate relationships between the governing factors. On the other hand, these results make it clear that it is too early to establish quantitatively critical damage stability standards and suggest the need for further research.

However, the available information allows for a selection of the most important factors in damage stability and for proposing a methodology to derive survivability criteria.

iii- Step Three

As illustrated in Chapter 7 the parametric investigation in this thesis identified the most important parameters on ship survivability whilst establishing relationships between them.

Within the limits of the parametric investigation, it is believed that the survivability of a ship is represented in a most meaningful and realistic way, linking the environmental effects, loading conditions and ship design parameters through the ship motions, and can be used to define limiting stability criteria. For each damage scenario, limiting stability zones are divided into safe, critical and unsafe zones depending on the behaviour of the ship in a wind and wave environment.

In the derived boundary stability curves KG rather than GM is used to represent the loading condition of the ship. By using KG the effect of loading condition on the ship's survivability can be seen clearly.

However, this representation can be meaningful only for this particular ship, while for other ships the representation of this KG range may not be meaningful since KG can vary greatly depending on the ship type. In this case, using GM rather than KG may be more appropriate in setting the general limits on loading condition for all types of passenger ships. However, it is not definite whether the same GM value would ensure the survivability of each ship in a damaged condition, since the dynamics of the ship are involved in the assessment. This can only be clarified by carrying out further investigations on the effect of the same GM for different ships. On the other hand, it may be feasible to provide the limiting stability curves for KG and GM separately, for the benefit of the designer and the captain of the ship. In any case using the KG or GM in the curves does not effect the outcome of the results and both representations give useful information on the survivability of ships.

All the limiting stability zones provide a clear view with regard to the worst scenario and associated zones, but due care should be given when it comes to defining the critical limits quantitatively. The following reasons justify this caution.

Firstly, it is impossible to define a clear boundary between safe and unsafe zones since there is a critical zone (as shown in Chapter 7), where it cannot be predicted whether the ship will survive or not. Of course, no matter what approach is followed there will be always an uncertainty region. Therefore, the lower limit of the critical zone must be used in assessing a vessel to have adequate stability. However, the boundaries defined in stability zone graphs in this thesis are the result of a limited investigation, hence they cannot be used without further extensive investigation.

Secondly, there are some parameters which may have to be defined more accurately or need to be included, such as shifting of cargo. Unfortunately these problems cannot be solved immediately and need more research and extensive investigations.

For instance, in order to achieve higher control in assessing the various

damage scenarios and to be able to accomplish more extensive investigations, during the parametric study carried out in the thesis, option 1 of water ingress was used, assuming that water is constantly flowing in, hence the effect of freeboard was not taken into account. However freeboard, which was not included in the investigations of this thesis, was identified as a major factor affecting damage stability, since it is the determining parameter with regard to water ingress in the case of damage above the bulkhead deck. As freeboard increases/decreases the required wave height (whether it is regular or irregular) for flooding the main deck, would increase/decrease respectively. In this case, after using option 1 of water ingress modelling for extensive investigation, option 2 of water ingress modelling can then be used to define the boundary curves more accurately or quantatively. In that case, boundary curves may change considerably depending on the freeboard.

8.4 POSSIBLE EFFECTS OF THIS RESEARCH AND RESEARCH FINDINGS ON SHIP SCIENCE

The main influence of the research undertaken and the research findings would be on ship survivability and ship design areas.

First of all, it is expected that in the light of the novel approach developed and importance of the results achieved, more research studies will follow. Area of research attention may vary from more systematic investigations to specific individual factors such as water ingress, accumulation of water, shifting of cargo etc. This would help to develop more solid modelling as well as obtaining more accurate information on dynamic damage stability.

Following improvements in assessing ship survivability, the present regulations, which have already been shown to be inadequate, will have to be replaced with more realistic dynamic damage stability assessment and standards, and with more meaningful limits regarding damage location and extent.

This change will happen eventually, but the speed at which it will happen depends entirely on influencing the attitude of the government

and regulating bodies, as well as that of the international scientific community. Otherwise the initiation of this change may have to wait for more tragic sea accidents.

On the design side, fundamental changes may incur in the compartmentation of the decks above the bulkhead deck. Introduction of dynamic stability assessments of damaged ships will definitely force designers to make radical changes in ship design, especially compartmentation and loading systems. Since the possibility of subdivision on the main vehicle deck is being currently investigated, results in this thesis would provide more accurate information on the requirements on this matter and help achieve satisfactory compartmentation arrangements.

In addition, some dynamic stability assessments take into account the dynamic behaviour of the ship, any modifications in the hull form and in principal dimensions may be inevitable in order to improve the hydrodynamic performance of the hull.

8.5 CONTRIBUTIONS OF THIS RESEARCH

The main contributions of the study in this thesis in the damaged stability field can be outlined as follows.

A new approach in assessing the stability of damaged ship was introduced. In addition this novel approach includes all the key dynamic and static effects realistically and in a most meaningful way.

The important factors on damage stability and survivability were identified and relationships between those factors were established qualitatively and quantitatively. These findings also emphasised the need for more soundly based damage stability assessment as well as criteria.

A new concept for assessing effectively the damage survivability of ships has been introduced, the "Damaged Scenario Analysis", enabling the derivation of critical stability curves and hence criteria on the basis

of the worst realisable damage scenario.

More importantly, however, the research presently undertaken on damage stability provides a proof or at least strong opposition against those resisting any serious research on damage stability, on the basis that such undertaking will be unproductive in view of the complexities involved in studying this problem.

The research work presented here proves beyond doubt that the time is ripe for scientific research in the damage stability and survivability of ships, and that it holds the key for improving the safety of life and property at sea.

CHAPTER 9:

RECOMMENDATIONS FOR FUTURE RESEARCH

In the previous chapters a methodology for assesssing ship damage survivability was described and a limited parametric investigation was carried out. As a result a number of key parameters were identified and some relationships were established. However, there is no doubt that in this area, a considerable amount of research still needs to be carried out before achieving the ultimate goal, which is establishing realistic damage stability criteria. Therefore, some suggestions for further research are summarised in the following.

9.1 WATER INGRESS

As was shown, water is a very influential factor on ship stability and capsizing, especially if there is damage above the bulkhead deck. Instantaneous water ingress, which depends on wave elevation and direction and on ship motions, is presently calculated only in an approximated way. However, modelling of the instantaneous water ingress must be further improved because of the complexities involved with hydrodynamic pressure on the free surface. Water flow is affected by wave direction relative to damage as was proven by model experiments [38], as well as by wave-vessel interactions.

In order to develop an accurate model of the water ingress, systematic experiments must be carried out to establish relationships between water inflow, outflow, wave elevation and wave direction. This can be done by measuring the amount of water flowing in at different wave heights and directions, so that an inflow coefficient, which is function of wave height and direction can be derived. An outflow coefficient can be derived by measuring the amount of water flowing out and by establishing a relationship between the amount of water flowing out and roll acceleration. Measuring the net amount of water flooding the deck as a result of inflow and outflow would help to calibrate the derived coefficients.

9.2 WAVE DIRECTION

In the calculations presented here, only beam sea is considered, but the damaged ship may face waves from different directions. Although it is assumed that beam waves is the worst case for a ship without forward speed, the ship may be excited severely by waves from other directions, depending on the condition of the ship. Due to progressive flooding, the ship may have static heel and a different underwater form. In this case, the ship can be excited by waves coming from any direction, which would not excite the ship in normal circumstances (roll in following or head seas) or some other motions such as pitching which may cause more serious water ingress, depending on the damage location. In order to develop general criteria, the effect of different wave directions at different damage conditions must be investigated, so that conditions or scenarios, which must be avoided or catered for, can be identified.

9.3 HYDRODYNAMIC COEFFICIENTS

In order to estimate the ship motions accurately the revelant hydrodynamic coefficients must be determined as accurately as possible. However, large motions and continuously changing hull form, due to flooding, makes the estimation of the correct values of coefficients very difficult. As indicated earlier, in the time simulation model, hydrodynamic coefficients are calculated for the initial conditions of the ship, before simulation starts, and the same coefficients are used during the one time simulation run.

However, since there is progressive flooding, which may cause sinkage and heel, the hydrodynamic coefficients may change considerably as proven in this research as well as by other studies. These changes in hydrodynamic coefficients during the time simulation may also change the ship's behaviour especially near the roll natural frequency. It has to be investigated whether changes in hydrodynamic coefficients change the ship's behaviour or whether initially calculated hydrodynamic coefficients can be used throughout the time simulation without losing accuracy significantly. If it is necessary to use instantaneous hydrodynamic coefficients, then the most suitable procedure to include these must be developed and

validation is carried out experimentally. This recommendation is further elaborated below.

Calculating the coefficients for each instantaneous position during the time simulation can be one of the solutions, but practically it becomes impossible considering the computer time required for this. Another option can be to create a coefficient data bank which includes coefficients for different heel and trim angles as well as draughts to simply be used during simulation. However, there still remains an important decision to be made regarding the use of coefficients at instantaneous static positions due to static heeling and sinkage or at an instantaneous position during dynamic motion as suggested by Fujino [50]. A study similar to Fujino's has been carried out by Böttcher [73]. Originally coefficients are calculated for small oscillations around the equilibrium condition. Therefore, varying coefficients at instantaneous static positions caused by the flooding appear to be more justifiable. On the other hand, for large motions these coefficients may not be suitable, therefore the feasibility of the second option has to be examined and Fujino's method further explored.

A similar problem is present for motions in irregular seas where varying frequencies are present. In irregular waves, harmonic ship motions are unlikely, therefore changes in coefficients may not be as influential as in regular waves. Although present methods predict motions reasonably well, finding out whether varying wave frequencies affect the ship motions in irregular seas would improve the present modelling. This could be done using time memory effect as used by De-Kat [23], although it may not be feasible from the computing time point of view which was also indicated by Böttcher [73].

From experiments and theoretical investigations it is clear that coupling terms affect roll motion considerably, especially near the natural roll frequency. Hydrodynamic heave into roll coupling, which is observed if there is static heel, appears to be also very influential on roll motion. It is further found from experiments (by the Author

and [15]) that coupling terms calculated theoretically and determined experimentally differ considerably and this big difference may further affect the behaviour of the ship. Here, the heave into roll coupling term is believed to have been determined experimentally for the first time. However, more experiments may have to be carried out on different hull forms at inclined conditions to support the findings of these first experiments.

9.4 ACCUMULATION OF WATER

As is experienced by the author and concluded by other researchers, modelling the accumulation and sloshing of water on deck accurately is highly complex and a full solution does not exist at present. It appears that experimental studies are the only approach which can provide some solid information and therefore the behaviour of water on deck must be analysed experimentally. So far all experiments on this problem have been carried out using tanks, which oscillate around the roll axis and have a fixed water depth. However, experiments must be carried out as realistically as possible by continuously flooding the compartment of the ship oscillating in the presence of waves. From experiments, the instantaneous forces and moments, due to water accumulation, must be measured together with the phase angle between roll motion and excitation for different excitation frequencies. Comparison between experimental results and computational results should aim to identify the frequency range at which computational results and experimental results deviate and attempt to identify the reasons for it.

9.5 SHIFTING OF CARGO

As statistics show [74], almost 60% of Ro-Ro Passenger/Ferry accidents are related to the shifting of cargo. It is likely that during heavy weather or a collision, cargo shift occurs. The effect of cargo shift ranges from creating static heel and trim to penetrating the outer skin of the ship's hull. Due to a cargo shift the ship may lose its damage freeboard and start flooding, or may even capsize very easily if the cargo shift is substantial. Even during progressive flooding, if a big static heel or roll occurs and the lashing of the cargo is not strong enough, then cargo shift may occur and can make the

conditions worse or even capsize the ship. Therefore, the effect of cargo shift on ship stability as well as determining the maximum allowable roll, roll acceleration, or heel angle to avoid it must be investigated and this effect must be included in the dynamic damage stability assessments.

9.6 THE EFFECT OF SHIP DESIGN AND BILGE KEELS

In order to find the optimum ship hull form and principal dimensions, considering the dynamic damage stability, the effect of certain ship parameters on the dynamic damage stability must be examined. Probably this investigation must start from the main ship dimensions such as L/B, B/d, D/d, Cb etc. Results of this investigation can offer valuable guidance on new designs.

Since the compartmentation of the ship is part of the design, the sample parametric study in this thesis on the effect of compartment length on capsizing, must be expanded by carrying out more analyses on the compartmentation of the vehicle deck and its effect on ship cargo transportation and damaged stability.

As stated earlier, all calculations in this thesis are carried out for the naked hull. However, almost all passenger ships and ferries have some sort of roll stabilizers. The effect of bilge keel on the reduction of roll motion has been proven and bilge keels are fitted to most of the ships. Therefore their effect on the behaviour and the stability of damaged ships must be examined and included in the damage stability assessments and limiting stability curves.

9.7 PARAMETRIC STUDY

The limiting stability curves derived in this research are the result of a limited parametric study for one sample ship at certain damaged conditions. The curves are valid for this particular ship for the assumed conditions and therefore can only be demonstrative or sample curves of proposed dynamic stability assessment and criteria. In order to generalize the findings and produce general stability curves for all types of passenger ships and Ro-Ro passenger/car ferries, this assessment must be applied to a number of ships of

different size, form and capacity, and all the possible conditions must be examined. In so doing, all the results can be reflected on the more general and meaningful limiting stability curves for damaged ships.

CHAPTER 10: CONCLUSIONS

The main conclusions that can be drawn from the present research are as follows:

a- The developed mathematical model and computational procedure are suitable for investigating the stability of a damaged ship and can predict the ship's behaviour including progressive flooding with sufficient accuracy.

b- The effect of flooding depends crucially on the location and extent of damage. It is highly possible that progressive flooding can cause a ship to capsize before she reaches the final equilibrium position.

c- The most dangerous damage is flooding of the main vehicle deck. Flooding long inner compartments can also cause a big threat to ship survivability. Unfortunately the most dangerous damage scenarios that have been identified are not considered by the present stability criteria.

d- Water on the main vehicle deck is the determining factor affecting ship capsizing with the critical amount of water to capsize the ship decreasing considerably by increasing the vertical centre of gravity. However if water ingress into the vehicle deck is not stopped or restricted, the ship will be lost regardless of her loading condition (KG).

e- In order to prevent capsizing, when the main vehicle deck is flooded, subdividing the vehicle deck transversely seems to be the only solution and a safe compartment length is found to be as small as 20-25% of the total deck length.

f- Temporary and permanent static heel increase the chances of capsizing, especially if there is flooding above the bulkhead deck. It is likely, in case of flooding of the main deck, that the

possibility of asymmetric flooding is very high and in this case the behaviour of the transverse centre of gravity of water on deck becomes a very important parameter.

g- Modest wave heights do not excite a damaged ship significantly but can worsen water ingress, since the flooding of the main vehicle deck depends on the damaged freeboard, ship motions and wave height. However as wave height increases, the dynamic effect of waves on the damaged ship increases significantly and the possibility of capsizing becomes greater.

h- The proposed damage stability criteria can improve the survivability of passenger ships considerably in the case of damage, but in order to establish general limits more applications of the developed assessment procedure on different ships are necessary.

i- This thesis represents the first systematic study into the dynamic damage stability of passenger ships, succeeding in providing a strong indication of the need to address vessel safety by considering dynamic behaviour in a realistic environment. However, several areas needing careful attention still remain. These include: Effect of hull form, different wave directions, different damage location, shifting of cargo, forward speed and water ingress and sloshing

REFERENCES

1. BEYEN, IR. R., "Safety and Ship Owners- a Contradiction?", The Kummerman International Conference on RO-RO SAFETY AND VULNERABILITY- the Way Ahead, LONDON, 14-15 December 1987

2. "Regulations on Subdivision and Stability of Passenger Ships as an Equivalent to Part B of Chapter 2 of the International Convention for the Safety of Life at Sea, 1960." I.M.O. Publications. London, 1974.

3. BIRD, H., and BROWNE, R.P., "Damage Stability Model Experiments." RINA Spring Meeting, 1973.

4. MIDDLETON, E. H. and NUMATA, E., "Tests of a Damaged Stability Model in Waves", Trans. SNAME, Vol. 78, 1970

5. J.R. PAULING, J. R., OAKLEY, O. H., and WOOD, P. D., "Ship Capsizing in Heavy Seas", Proceedings of the International Conference on Stability of Ships and Ocean Vehicles, Glasgow, 1975.

6. PLAZA, F. and SEMENOV, V. Y., "Latest Work of International Maritime Organisation Related to the Stability of Ships", Proceedings of Fourth International Conference on Stability of Ships and Ocean Vehicles, NAPLES, ITALY, 1990

7. SOLAS'74. International Convention for the Safety of Life at Sea, LONDON, 1974

8. BLOCKI, W., "Probability of Non-Capsizing of a Ship as a Measure of her Safety" Proceedings of Third International Conference on Stability of Ships and Ocean Vehicles, GDANSK, POLAND, September 1986

9. **SPOUGE, J. R.**, "The Safety of Ro-Ro Passenger Ferries", Trans. RINA, Vol. 131, 1989

10. **ADEE, H. B. and PANTAZOPOULOS, M.**, "Experimental Investigation of a Vessel Response in Waves With Water Trapped on Deck", Proceedings of Third International Conference on Stability of Ships and Ocean Vehicles, GDANSK, POLAND, September 1986

11. **FALTINSEN, O. M.**, "A Non-linear Theory of Sloshing in Rectangular Tanks" Journal of Ship Research, Vol.18, No.4, pp 224-241, 1974.

12. **DILLINGHAM, J.**, "Motion Studies of a Vessel with Water on Deck." Marine Technology, Vol. 18, No. 1, pp 38 - 50, January 1981.

13. **KOBAYASHI, M.**, "Hydrodynamic Forces and Moments Acting on Two-dimensional Asymmetrical Bodies." Proceedings of the International Conference on Stability of Ships and Ocean Vehicles, Glasgow, UK, 1975

14. **GERRITSMA, J.**, "Experimental Determination of Damping, Added Mass and Added Mass Moment of Inertia of A Ship Model" Netherlands' Research Centre T.N.O. For Shipbuliding and Navigation, Report No: 255, October 1957

15. **VUGTS, J. H.**, "The Hydrodynamic Coefficients for Swaying, Heaving and Rolling", Laboratorium Voor Scheeps - Bouwkunde, Technische Hogeschool Delft, Report No: 194, 1968

16. **BEUKELMAN, W., HUIJSMANS, R. H. M., KEVNING, P. J.**, "Calculation Methods of Hydrodynamic Coefficients of Ship in Shallow Water", International Shipbuilding Progress, 1984.

17. **LEE, C. M. and KIM, K. H.**, "Prediction of Ships in Damaged Condition in Waves", Proceedings of Second International Conference on Stability of Ships and Ocean Vehicles Stability, TOKYO, JAPAN, October, 1982.

18. **BISHOP, R.E.D., PRICE, W.G. and TEMAREL, P.**, "On the Dangers of Trim by Bow ", Trans. RINA., 1989.

19. **SALVESEN, N., TUCK, E. O. and FALTINSEN, O.**, "Ship Motions and Sea Loads", Trans. SNAME, Vol. 78, 1970

20. **KIM, C. H., CHOU, F. S., TIEN, D.**, "Motions and Hydrodynamic Loads of a Ship Advancing in Oblique Waves", Trans. SNAME, Vol. 88, pp 225-256, 1980

21. **INGLIS, R. B., PRICE, W. G.**, "A Three Dimensional Ship Motion Theory: Calculation of Wave Loading and Responses With Forward Speed", Trans. RINA., Vol 124, pp 183-192, 1982

22. **INGLIS, R. B., PRICE, W. G.**, "A Three Dimensional Ship Motion Theory: Comparison Between Theoretical Predictions and Experimental Data of The Hydrodynamic Coefficients With Forward Speed", Trans. RINA, Vol 124, pp 141-157, 1982

23. **DE KAT, J. and PAULLING, J. R.**, "The Simulation of Ship motions and Capsizing in Severe Seas", THE SOCIETY OF NAVAL ARCHITECTS AND MARINE ENGINEERS, ANNUAL MEETINGS, NOVEMBER 1989

24. **HAMAMOTO, M.**, "Transverse Stability of Ships in a Quartering Sea", Proceedings of Third International Conference on Stability of Ships and Ocean Vehicles, GDANSK, POLAND, September 1986

25. **BORODAY, I. K. and MORENSCHILDT, V. A.**, "Stability and Parametric Roll of Ships in Waves", Proceedings of Third

International Conference on Stability of Ships and Ocean Vehicles, GDANSK, POLAND, September 1986

26. **FRANCESCUTTO, A. and ARMENIO, V.,** "On the Stability of Antisymmetric Motions of a Ship Equipped with Passive Antirolling Tanks", Proceedings of Fourth International Conference on Stability of Ships and Ocean Vehicles, NAPLES, ITALY, 1990

27. **BRAUN, N.,**"Damage Stability: Research for the Future"

28. **CAO, ZHEN-HAI and LI, JUN-XING,** "Model Experiments on Inclined Ships in Waves", Proceedings of Third International Conference on Stability of Ships and Ocean Vehicles, GDANSK, POLAND, September 1986

29. **HAMAMOTO, M., SHIRAI, T. and NAKIYAMA, N.,** "An Analytical Approach to Capsizing of a Ship in Following Seas. Proceedings of Fourth International Conference on Stability of Ships and Ocean Vehicles, NAPLES, ITALY, 1990

30. **VASSALOS, D.,** "A Critical Look into the Development of Ship Stability Criteria Based on Work/Energy Balance" RINA spring Meeting, 1985.

31. **BARRIE, D. A.,** "The Influence of Ship and Environmental Parameters on Stability Assessment" Ph.D. Thesis, University of Strathclyde, Department of Ship and Marine Technology, Glasgow, April, 1986.

32. **DENISE, J-P. F.,**"On the Roll Motion of Barges", Transactions of RINA, 1982

33. **SOLIMAN, MOHAMED S.,** "An Analysis of Ship Stability Based on Transient Motions", Proceedings of Fourth International Conference on Stability of Ships and Ocean Vehicles, NAPLES, ITALY, 1990

34. **THOMSON, J. M. T., RAINEY, R. C. T. and SOLIMAN, M. S.**, "Ship Stability Criteria Based on Chaotic Transients From Incursive Fractals", Phil. Trans. Royal Soc. of London, Series A, Vol. 332, July 1990

35. **UMEDA, N., YAMAKOSHI, Y. and TSUCHIYA, T.**, "Probabilistic Study on Ship Capsizing Due to Pure Loss of Stability in Irregular Quartering Seas", Proceedings of Fourth International Conference on Stability of Ships and Ocean Vehicles, NAPLES, ITALY, 1990

36. **LLYODS, C. J.**, "UK Department of Transport- Research Into Enhancing the Stability and Survivability Standards of Ro-Ro Passenger Ferries, Overview Study" BMT Report, March 1990

37. **VOSSNACK, E.**, "Buoyancy in the Wings", The Kummerman International Conference on RO-RO SAFETY AND VULNERABILITY- the Way Ahead, LONDON, 14-15 December 1987

38. **DAND, I. W.**, "Experiments with a Floodable Model of Ro-Ro Passenger Ferry", BMT Project Report, for the Department of Transport, Marine Directorate, BMT Fluid Mechanics Ltd., February 1990

39. **IKEDA, U., et al**, "A Prediction Method for Ship Roll Damping." Dept. of Naval Architecture, University of Osaka, Prefecture, 1978.

40. **FRANK, W.**, "On the Oscillations of Cylinders in or Below the Free Surface of Deep Fluids", DTNSRDC, Report no. 2375. October 1967

41. **ATLAR, M.**, "A Study of Frank Close-fit Method, Theory, Application and Comparison with Other Methods", Report No:

NAOE-HL-81-08, Department of Naval Architecture and Ocean Engineering, University of Glasgow, February 1982

42. **BEDEL, W. and LEE, C. M.**, "Numerical Calculation of Added Mass and Damping of Cylinders Oscillating in or Below a Free Surface", DTNSRDC, Report No 3551, March 1971

43. **CHAKRABARTI, S. K.**, "Hydrodynamic of Off-shore Structures", Computational Mechanics Publications, 1987

44. **SCHELTEMA DE HEERE, R. F. and BAKKER, A. R.**, "Buoyancy and Stability of Ships, Volume 1", Technical Publications H. Stam, CULEMBORG-THE NETHERLANDS, 1969

45. Annex 5: Recommendation on a 'Severe Wind and Rolling Criterion(Weather Criterion) for the Intact Stability of Passenger and Cargo Ships Over 24 m in Length, Draft Resolution A...(13)-SLF 28/13, 1983

46. **WENDEL, K.**, "Safety From Capsizing", Fishing Boats of the World - 2, Fishing News(Books) Ltd., LONDON, 1960

47. **KINOSHITA, M. and OKADA, S.**, "Heeling Moments due to the wind Pressure on Small Vessels", Proceedings, Symposium on the Behaviour of Ships in a Seaway, Wageningen, Netherlands, 1957

48. **KING, B. K.**, "A Fast Numerical Solver for Large Amplitude Ship Motions Simulations", Proceedings of Fourth International Conference on Stability of Ships and Ocean Vehicles, NAPLES, ITALY, 1990

49. **KOBYLINSKI, L.**, "On the Possibility of Establishing Rational Stability Criteria", Proceedings of Fourth International Conference on Stability of Ships and Ocean Vehicles, NAPLES, ITALY, 1990

50. **FUJINO, M. and YOON, B. S.,** " A Practical Method of Estimating Ship Motions and Wave Loads in Large Amplitude Waves", International Shipbuilding Progress, Vol. 33, No: 385, September 1986

51. **ADEE, B. H. and CAGLAYAN, I.,** "The Effects of Free Water on Deck on the Motions and Stability of Vessels." Proceedings of Second International Conference on Stability of Ships and Ocean Vehicles, TOKYO, JAPAN, October 1982.

52. **MIKELIS, N. E., MILLER, J. K., TAYLOR, K. V.,** "Sloshing in Partially Filled Liquid Tanks and Its Effect on Ship Motions: Numerical Simulation and Experimental Verification." RINA, 1984.

53. **BRIDGES, T. J.,** "A Numerical Simulation Of Large Amplitude Sloshing", 3rd International Congress on Numerical Ship Hydrodynamics, pp 269 - 284, Paris, France, June 1981

54. **FALTINSEN, O. M.,** "A Numerical Non-linear Method of Sloshing in Tanks with Two-dimensional Flow." Journal of Ship Research, Vol. 22, No. 3, pp 193 - 202, September 1978

55. **VAN DEN BOSH, J. J. and VUGTS, J. H.,** "Roll Damping by Free Surface Tanks", Report No: 134, The Netherlands Ship Research Centre Shipbuilding Laboratory, Delft, Netherland, 1966

56. **CAGLAYAN, I.,** "Water on Deck: A Theoretical and Experimental Study", SNAME, Texas, 1985

57. **WALSHAW, A. C. and JOBSON, D. A.,** "Mechanics of Fluid", Longman Group, 1979

58. ACKERS, P., WHITE, W. R., PERKINS, C. A., HARRISON, A. C. M., "Weirs and Flumes for Flow Measurements", JOHN WILEY AND SONS, 1978

59. NAG: Fortran Library Manuals Mark 10, Numerical Algorithm Group, 1983

60. KARPPINEN, T. O., "Comparison of Theoretical Seakeeping Predictions with Model Results for a Wide Beam Fishing Vessel", American Towing Tank Conference, Hoboken, NJ, USA, 2-4 August 1983

61. VASSALOS, D., TURAN, O., " Development of Survival Criteria for Ro-Ro Passenger Ships - A Theoretical Approach", Final Report on the Ro-Ro Damage Stability Programme, Phase II for the DEPARTMENT OF TRANSPORT, MARINE DIRECTORATE, University of Strathclyde, Department of Ship and Marine Technology, December 1992

62. INGLIS, R. B., PRICE, W. G., "Comparison of Ship Responses Evaluated by Two- and Three-Dimensional Theories", International Shipbuilding Progress, Vol 27, 1980

63. GERRITSMA, J. and BEUKELMAN, W., " The Distribution of The Hydrodynamic Forces on A Heaving and Pitching Ship Model with Zero Forward Speed in Still Water", Shipbuilding Laboratory, Technological University -Delft, Report No: 124, 1965.

64. GERRITSMA, J., " Distribution of Hydrodynamic Forces Along the Length of a Ship Model in Waves", Technische Hogescholl Delft, Report No: 144, 1966

65. MOTORA, S., " On the Measurement of Added Mass and Added Mass Moment of Inertia for Ship Motions, (4) & (5). "J. Zosen Kyokai, No: 107, 1960

66. **BEUKELMAN, W. and GERRITSMA, J.,** "The Distribution of the Hydrodynamic Mass and Damping of an Oscillating Shipform in Shallow Water" International Shipbuilding Progress, Vol. 29, Nr. 339, November 1982.

67. **THOMSON, W. T.,** "Vibration Theory and Applications", GEORGE ALLEN & UNWIN LTD, LONDON, 1966

68. **CARDO, A., FRANCESCUTTO, A. and NABERGOJ, R.,** "On the Maximum Amplitudes in Nonlinear Rolling", Proceedings of Second International Conference on Stability of Ships and Ocean Vehicles, TOKYO, JAPAN, October 1982

69. **CONCEICAO, C. A. L., PRICE, W. G. and TEMAREL, P.,** "The Influence of Heel on The Hydrodynamic Coefficients of Ship Like Sections and a Trawler Form", International Ship Building Progress, Vol. 31, March 1984

70. **ATLAR, M.,** "Method for Predicting First-Order Hydrodynamic Loads on Single and Twin Sections By the Frank-Close-Fit Technique", Report No: NAOE-85-41, Department of Naval Architecture and Ocean Engineering, University of Glasgow, October 1985

71. **BREBBIA, C. A. and WALKER, S.,** "Dynamic Analysis of Off-shore Structures" Newnes-butterworths, 1979

72. **SÖDING, H.,** "Simulation of Large-Amplitude Ship Motions in a Seaway", Germanifcher Lloyd Workshop on Stability, Hamburg, Germany, 24-25 May 1984

73. **BÖTTCHER, H.,** "Ship Motion Simulation in a Seaway Using Detailed Hydrodynamic Force Coefficients", Proceedings of Third International Conference on Stability of Ships and Ocean Vehicles, GDANSK, POLAND, September 1986

74. GREENFIELD, G. G., "The Future : Lessons to be learnt from the Past", The Kummermann International Conference on Ro-Ro Safety and Vulnerability, London, 1987.

75. CHOW, WEN TE, " Open Channel Hydraulics", McGRAW-HILL BOOK COMPANY, INC., 1959

76. KUO, C., VASSALOS, D. AND MARTIN, J., "SAFESHIP Project(5)-Mathematical Modelling, Part B: Stability Criteria Based on Time-varying Roll Restoring/Excitation Moments", Dept. of Ship and Marine Technology, University of Strathclyde, September 1983

77. HOOFT, J. P., "Advanced Dynamics of Marine Structures", JOHN WILEY & SONS, 1982

78. BHATTACARYA, R., "Dynamic of Marine Vehicles", JOHN WILEY & SONS, 1978

79. NIELSEN, J. K., "Capsize Safety of Jack-Up Carriers", Proceedings of Second International Conference on Stability of Ships and Ocean Vehicles, TOKYO, JAPAN, October 1982

80. MARCHAJ, C. A., "Seawothiness : the Forgotten Factor", William Collins Sons and & Ltd, 1986

81. GRAHAM, E. W. and RODRIGUEZ, A.M., "The Characteristics of Fuel Motion Which Effect Airplane Dynamics." Journal of Applied Mechanics, September,1952.

82. VERHAGEN, J.H.G and WIJNGAARDEN, L. Van, "Non-linear Oscillations of Fluid in a Container." Journal of Fluid Mechanics, Vol. 22, Part 4, pp 737-751, 1965.

83. FENWICK, J., "An Investigation into Sloshing in Moonpools: Numerical, simulation and experimental verification"

Departmental Report, Dept of Ship and Marine Technology, Strathclyde University, 1987.

84. **WELCH, J.E., HARLOW, F.H., SHANNON, J.P. and DALY, B.J.,** "The MAC Method of Computing Technique for Solving Viscow, Incompressible, Transient Fluid-Flow Problems Involving Free Surfaces." Los Alamos Scientific Lab., Report LA -425, 1965.

85. **NAVICKAS, J., PECK, J.C., BASS, R.L., BOWLES E.B., YOSHIMURA, N. and ENDO, S.,** "Sloshing of Fluids at Highfill Levels in Closed Tanks." ASME Winter Meeting, Washington D.C., pp 191 - 198, 1981.

86. **NAKAYAMA, T. and WASHIZU, K.,** "Non-linear Analysis of Liquid Motion in a Container Subjected to Forced Pitching Oscillation." International Journal For Numerical Methods in Engineering, Vol. 15, pp 1207 - 1220, 1980.

87. **PETEY, F.,** "Numerical Calculations of Forces and Moments Due to Fluid Motions in Tanks and Damaged Compartments", STAB 86 PROCEEDINGS , VOLUME1, SECTION1, GDANKS 1986.

88. **PANTAZOPOULOS, M.,** "Sloshing of Water on Deck of Small Vessels", Proceedings of Fourth International Conference on Stability of Ships and Ocean Vehicles, NAPLES, ITALY, 1990

89. **ABRAMSON, H.N.,** "The Dynamic Behaviour of Liquids in Moving Containers with Application to Space Vehicle Technology" NASA-SP-106, 1966.

90. **SCARSI, G. and BRIZZOLARA, E.,** "On The Behaviour of Liquids in A Rectangular Tank in Motion", International Shipbuilding Progress, Vol. 17, pp 316 - 325, Oct. 1982.

91. **HUNT, B. and PRIESTLEY, N.**, "Seismic Water Waves in A Storage Tank", Bulletin of The Seismological Society Of America, Vol. 68, No. 2, pp 487 - 499, April 1978.

92. **KAYA, Y.**, "Numerical and Physical Studies of The Water Motion Caused by Sudden Disturbances in Reservoirs, Etc", Ph.D. Thesis, University of Strathclyde, 1985.

93. **TASAI, F.**, "Damping Force and Added Mass of Ships Heaving and Pitching", Reports of Research Institute For Applied Mechanics, Vol. 8, No. 31, 1960.

94. **TAKAISHI, Y.**, "Consideration on the Dangerous Situations Leading to Capsize of Ships in Waves" Second International Conference on Stability of Ships and Ocean Vehicles Stability, Tokyo, October, 1982.

95. **KASTNER, S.**, "Simulation and Assessment of Roll Motion Stability", Second International Conference on Stability of Ships and Ocean Vehicles Stability, Tokyo, October, 1982.

96. **PAULLING, J.R, et al**, "Capsizing Experiments with a Model of a Fast Cargo Liner in San Fransisco Bay" Dept. of Naval Architecture, University of California, Berkeley, 1972.

97. **DAND, I. W., and BOLTWOOD, D.T.**, "Ro-Ro Survivability : Some Technical Aspects" The Kummermann International Conference on Ro-Ro Safety and Vulnerability, London, 1987.

98. **WELAYA, Y.M.A.**, "Application of Time-Dependent Restoring for Stability Assessment of Ships and Semi-Submersibles" Ph.D., University of Strathclyde, Department of Shipbuilding and Naval Architecture, Glasgow, 1979.

99. **KONSTANTOPOULOS, G.P**, "A Unified Treatment of Semisubmersible Stability" Ph.D. Thesis, University of Strathclyde, Department of Mechanical and Off-shore

Engineering, Division of Ship and Marine Technology, Glasgow, 1988.

100. **ALEXANDER, J. G. M.**, "Design Excitations for Dynamic Stability Assessment Based on Mapping Weighted Responses" PhD Thesis, University of Strathclyde, Department of Mechanical and Off-shore Engineering, Glasgow, 1987.

101. **ROBERTS, T. B.**, "Estimation of Non-Linear Ship Roll Damping From Free- Decay Data" Journal of Ship Research, Vol. 29, No. 2, pp 127 - 138, June 1985.

102. **SPOUGE, T. R.**, "Non-Linear Analysis of Large Amplitude Rolling Experiments", International Shipbuilding Progress 35., No. 403, pp. 271- 282, 1988.

103. **RAKHMANIN, N.**, "Stability of damaged Ship During Ship Motions in Waves", Proceedings of Fourth International Conference on Stability of Ships and Ocean Vehicles, NAPLES, ITALY, 1990

104. **UMEDA, N.**, "Probabilistic Study on Surf_Riding of a Ship in Irregular Seas", Proceedings of Fourth International Conference on Stability of Ships and Ocean Vehicles, NAPLES, ITALY, 1990

105. **HAMAMOTO, M. and SHIRAI, T.**, "Study on Ship Motions and Capsizing in Following Seas (2nd Report- Simulation of Capsizing)" SOCIETY OF NAVAL ARCHITECTS OF JAPAN, 1989.

106. **NAYFEH, ALI H.**, "On the Undesirable Roll Characteristics of Ships in Regular Seas", JOURNAL OF SHIP RESEARCH VOL. 32 JUNE 1988.

107. "Principles of Naval Architects." SNAME, 1977

108. VASSALOS, D. AND TURAN, O., "Damage Location and Extent: A Dynamic Analysis", RO-RO 92: The 11th International Conference and exhibition on Through Transport using Roll-on Roll of Ships, GOTHENBURG, SWEDEN, MAY 1992

109. TURAN, O. and VASSALOS, D., "Dynamic Stability Assessment of Damaged Passenger Ships", RINA spring Meeting 1993(to be presented)

APPENDIX A:

MATHEMATICAL MODELLING

A.1: HYDRODYNAMIC FORCES

As the formulation of these forces in regular waves is also the basis of the forces due to irregular waves, in the following, the formulation for the wave excitation forces will be given for the regular waves.

A.1.1 GENERAL DEFINITIONS AND ASSUMPTIONS

It is assumed that fluid is ideal, of infinite depth and that its motion is irrotational. It will be assumed that the incident wave and resulting motion response is sufficiently small in amplitude to justify a linear description, then general motion problem can be assumed to be a linear superposition of the following boundary value problems:

-The incident wave encountered by the strip section will be diffracted from it by assuming the strip section is rigidly held in its fixed position. This is called "Diffraction Problem".

-As soon as the incident waves are diffracted due to the pressure of the section, it is assumed that the motion can be represented by the oscillations of this section in initially calm water with some frequency on the waves. This is known as "the radiation problem".

Thus the total velocity potential of the fluid motion generated by the regular waves, with the stationary strip section undergoing small amplitude oscillation, can be described by the time dependent potential

$$\Phi = \Phi_I(x,y,z,t) + \Phi_D(x,y,z,t) + \Phi_R(x,y,z,t) \qquad \text{[Eq A.1.1]}$$

where:

Φ_I : The incident wave potential (Froude-Krylov potential) representing the incoming waves

Φ_D: The diffracted wave potential representing the disturbance of the incoming waves diffracted by the

section

Φ_R: The radiation potential representing the motion i nduced disturbance of the initially calm water

The nature of the linear boundary value problems imposes the following conditions which should be satisfied by the sectional velocity potential:

- The Laplace equation in the fluid domain
- The linearised free surface condition on the free surface
- The bottom condition at the sea floor
- The radiation condition at a large distance from the strip section
- The kinematic boundary condition on the section contour given by

$$\frac{\partial\phi}{\partial n}=\frac{\partial(\phi_I+\phi_D+\phi_R)}{\partial n}= V_n \qquad \text{[Eq A.1.2]}$$

Where V_n is the normal velocity component of a point on the section contour.

Within the linear analysis further decomposition of the kinematic boundary condition yields the following for the radiation problem.

$$\frac{\partial\phi_R}{\partial n} = V_n \qquad \text{[Eq A.1.3]}$$

and for the diffraction problem it is assumed that the body was rigidly held thus

$$\frac{\partial\phi_I}{\partial n} + \frac{\partial\phi_D}{\partial n} =0 \qquad \text{[Eq A.1.4]}$$

A.1.2 WAVE EXCITATION FORCES

In the beamwise strip domain, the incident wave (i.e. Froude-Krylov) and diffracted wave potential can be represented as follows [70]:

$$\Phi_I(x,y,z,t) = \phi_I(y,z)\, e^{i(\gamma x \cos(\mu - \omega t))} \qquad \text{[Eq A.1.5]}$$

$$\phi_I(y,z) = -\frac{i\, g\, a}{\omega}\, e^{\gamma z}\, e^{i(\gamma y \sin\mu)} \qquad \text{[Eq A.1.6]}$$

Where:

$\phi_I(y,z)$:Sectional incident wave potential
a :Maximum amplitude of the incident wave
ω :Wave frequency
γ :Wave number
μ :Heading angle (0.0:following, 180:head, 90 and 270:beam seas)

The diffraction potential, Φ_D is a disturbance therefore it can be represented by a distribution of wave source potential along the strip section wetted parameter with the aid of Green's formula give by [20, 41, 42] :

$$\Phi_D(x,y,z,t) = \phi_D(y,z)\, e^{i(\gamma x \cos\mu)}\, e^{-i\omega t} \qquad \text{[Eq A.1.7]}$$

$$\phi_D(y,z) = \int_s Q_d(\zeta,\eta)\, G(y,z,\zeta,\eta)\, ds \qquad \text{[Eq A.1.8]}$$

Where:

$\phi_D(y,z)$:Sectional diffracted wave potential
Q_d :Unknown source strength
G :Pulsating source potential of unit strength at a point (ζ,η) in the strip contour [40, 41]
s :Wetted contour of the strip section

The unknown source strength Q_d is found by the application of the kinematic boundary condition [Eq A.1.2] on the strip domain.

The numerical solution of the above defined velocity potential

problem is carried out by using the Frank-Close-Fit Technique [41] which is based on Green's Function Integral Equation Method [40, 42]. This method is applicable to any two dimensional simply connected shape. It has a great advantage in that it represents the fluid potential directly due to any shape of disturbance. This facility allows the computation of hydrodynamic forces on the asymmetric hull section at heeled position. According to the this procedure the strip contour (C) is approximated by a series of straight line segments with a single pulsating source at the midpoint of each segment. The strengths of the forces are assumed constant along the segment length but vary from segment to segment. Details can be found in [41].

By solving [Eq A.1.6] with the aid of the Close-Fit technique, the unknown source strength and consequently the required diffraction potential is obtained.

Having obtained the velocity potential for the incident and diffracted wave potential, the pressure distribution around cross section can be calculated from the linearised Bernoulli equation as follows:

$$p^{(i)} = p_I^{(i)} + p_D^{(i)} = -\rho \frac{\partial(\phi_I^{(i)} + \phi_D^{(i)})}{\partial t} \qquad \text{[Eq A.1.9]}$$

where:

- p : pressure
- g : gravity accelerations
- ρ : density of water
- i : Mode of motion: 2, 3 and 4 are for sway, heave and roll respectively

Sectional excitation forces ($f^{(i)}$) can be obtained by integrating the pressures as:

$$f^{(i)} = f_{FK}^{(i)} + f_D^{(i)} = \int_S (p_I^{(i)} + p_D^{(i)})\, n^i\, ds \qquad \text{[Eq A.1.10]}$$

where:

$p^{(i)}$: sectional pressure

$n^{(i)}$: directional cosines of the outward normal vector and changes depending on the mode of motion (i)

With regard to the separate components, the total force of the ship due to the Froude-Krylov ($F_{f\text{-}k}$) and Diffraction components(F_d) can be written as:

$$\begin{pmatrix} F_{f\text{-}k}^{Sway} \\ F_{f\text{-}k}^{Heave} \\ F_{f\text{-}k}^{Roll} \end{pmatrix} = \int e^{i\gamma x} \cos\mu \begin{pmatrix} i\, f_{f\text{-}k}^{Sway} \\ f_{f\text{-}k}^{Heave} \\ i\, f_{f\text{-}k}^{Roll} \end{pmatrix} \begin{pmatrix} dx \\ dx \\ dx \end{pmatrix} e^{-i\omega t} \quad \text{[EqA.1.11]}$$

Total Diffraction Force and Moments

$$\begin{pmatrix} F_d^{Sway} \\ F_d^{Heave} \\ F_d^{Roll} \end{pmatrix} = \int e^{i\gamma x} \cos\mu \begin{pmatrix} f_d^{Sway} \\ f_d^{Heave} \\ f_d^{Roll} \end{pmatrix} \begin{pmatrix} dx \\ dx \\ dx \end{pmatrix} e^{-i\omega t} \quad \text{[Eq A.1.12]}$$

Both the Froude-Krylov and Diffraction components comprise terms in phase with the acceleration (i.e. real, F_R) and velocity (i.e. imaginary, F_I) which can be transformed to the time dependent force function as:

$$F(t) = F \cos(\omega t + \varepsilon) \quad \text{[Eq A.1.13]}$$

where F is the maximum of the force given by

$$F = \sqrt{F_R^2 + F_I^2} \quad \text{[Eq A.1.14]}$$

and Phase angle between Maximum force and Maximum wave is calculated as

$$\varepsilon = \text{Atan}\left(\frac{F_R}{F_I}\right) \quad \text{[Eq A.1.15]}$$

A.1.3 HYDRODYNAMIC COEFFICIENTS

In order to obtain the motion-induced coefficients (i.e. added mass and damping), the velocity potential for the radiation problem is solved similar to the previously solved diffraction problem with the different kinematic boundary condition which is given by [Eq A.1.2]. That is the radiation potential is represented as:

$$\phi_R{}^i = \int_S Q_R{}^i(\zeta,\eta)\ G(y,z,\zeta,\eta)\ ds \qquad \text{[Eq A.1.16]}$$

Where $Q_R{}^i$ is the unknown source strength which will be found with the aid of the Frank-Close-Fit technique.

By solving the unknown source strength the radiation potential is evaluated for each section. The resulting potential consists of components in phase with the acceleration (i.e. real component) and velocity (i.e. imaginary component). The hydrodynamic pressure along the strip contour is obtained from this potential expression using the linearised Bernoulli equation. Integrals of the pressure along the contour yield the corresponding sectional added mass/inertia in phase with the acceleration and the wave damping in phase with the velocity (See [41] for details).

Finally the sectional added mass and damping are integrated along the ship to obtain the total coefficients of a vessel.
Sectional added mass;

$$a_{ij} = \rho \int_S \Phi_{RR}{}^{(j)}\ \mathrm{Cos}(n,j)\ ds \qquad \text{[Eq A.1.17]}$$

Sectional damping;

$$b_{ij} = \rho\omega \int_S \Phi_{RI}{}^{(j)}\ \mathrm{Cos}(n,j)\ ds \qquad \text{[Eq A.1.16]}$$

Where:

Φ_{RR} : Real part of radiated velocity potential

Φ_{RI} : Imaginary part of radiated velocity potential

Cos(n,j) : Cosines directions

i, j : 2 for Sway, 3 for Heave, 4 for Roll

A.2:
ACCUMULATION AND SLOSHING OF WATER IN THE DAMAGED COMPARTMENT

A.2.1 INTRODUCTION

Stability of intact or damaged ships depends on different ship and environmental parameters. In the past, stability of ships has been assessed on static grounds. However, since experience has been gained, from the application of these assessments, and drawbacks have been observed, more dynamic parameters are now considered. Unfortunately, damage stability rules remained static and very little has been done on dynamic grounds. The accidents caused by dynamic effects forced researchers to look more into this field. One of these effects is the sloshing forces in the damaged compartment caused by the external forces such as wave and wind.

Ro-Ro ships and ferries with large open decks can lose their stability when there is flooding on the decks or compartments. The Herald of Free Enterprise disaster is the prime example of this problem and therefore this must be considered in the damaged stability calculations.

A.2.2 PROBLEMS WITH MODELLING WATER ON DECK

Modelling the physical problem of water on deck is not easy from a mathematical point of view. There are obvious non-linearities that limit the full analytical or numerical solutions. For instance, definition of the free surface, viscosity of the fluid, large motions and limited boundary conditions are some of the non-linearities. Problems however become more severe in the case of shallow water or breaking waves.

Most of the work carried out in this field is simplified by accepting partly or fully linearised mathematical models. Today most of the assumptions still stand. Although the improvements in numerical methods and in computers make the solutions easier , there is still a long way to go before this problem is solved completely.

Using finite element or finite difference numerical methods in the solutions is the normal method. Developing this kind of model in 2-D or 3-D has become very popular, but in order to develop such a method generally takes a long time and some solutions are not feasible even with the fastest computers. The main aims are:

- To understand the problem, and solve it with the most feasible assumptions for the purpose and develop a computer code.

- To link this problem and solution with the damage stability study and incorporate the sloshing code into the time simulation program developed for motions and stability of damaged ferries.

A.2.3 REVIEW OF LITERATURE ON SLOSHING

Sloshing studies have focused mainly on the following areas :

a) In fuel tanks of aircraft and space craft.

b) In dams and storage tanks based on the ground, and sloshing caused by earthquakes.

c) In ships
   - liquid cargo tanks
   - on the deck of fishing vessels
   - in the damaged compartments or on the flooded vehicle deck of ferries.

Generally, studies on sloshing started by using linear theory, then continued with non-linear theories, and recently numerical techniques have been developed and are still at the developing stage.

The main studies on sloshing in fuel tanks in aircraft have taken place in the 1950's and 1960's in order to solve the sloshing problem found in spacecrafts [89]. In 1952 the linear study of Graham and Rodriguez [81] was concerned purely with the fuel response, in connection with the effect on the dynamics of the aircraft. Their

study was based on potential theory and has been taken as an important reference for later detailed studies.

In the 1960's Abramson[89] and some others worked on the sloshing problem with relation to the liquid propellants for rockets or space vehicles.

The development of computers helped to improve prediction techniques and to progress the solution of this problem, and similar studies have taken place in the marine field since the production of larger oil carriers and Liquid Natural Gas (LNG) tankers. Liquid cargo vessels would avoid the problem by reducing the free surface by operating with completely full or empty tanks. However several factors make slosh loads more important with regard to LNG ship design, since the need for continued evaporation to maintain low temperatures results in LNG tanks being partially full. This means that higher impact forces on LNG tank design place special attention on the support structure design.

Sloshing in the tank has been examined by many researchers using non-linear theories. Generally a vast improvement has been achieved by employing non-linear solutions. Although, viscous effects are ignored in order to simplify the equations of motion, these effects have been considered recently by some researchers[52, 53] using Navier-Stokes equations and numerical solution techniques.

More importantly, using potential theory, the shallow water case was studied by Verhagen and Wijngaarden [82]. They used the shallow water wave theory to examine hydraulic jumps. Faltinsen [11] proposed a non-linear perturbation procedure for two dimensional rigid tank shapes, subject to forced roll and sway oscillations. Faltinsen's approach is valid for certain tank/depth ratios. He obtained good results for h/d=0.5 and compared his results with Olsen's experiments for roll. Faltinsen's theory does not include viscous effects. At Strathclyde University experiments [83] were carried out and some trends were found to be similar to those in Olsen's experiments.

Accumulation of water in the tank has also been used as passive tank stabilizers to reduce ship rolling, since water in the free surface tank acts as a damping mechanism under certain circumstances. The water transfer from one side to another with a certain phase lag, with respect to the rolling motion of the vessel, is used as a means to provide counteracting moments. It was revealed by Bosh and Vugts[55] that, the most important parameters are the amount of water in the tank, characterised by the water depth (D) and the frequency of the rolling motion. In addition, there are other parameters such as breadth of the tank (L), amplitude of the motion, location of the rotational axis etc, which are effective on the influence of the water accumulation. The findings of Bosh and Vugts from experimental studies can be highlighted as follows:

-Accumulation of water on deck is most effective as a damping mechanism when the natural frequency of water in the tank is close to the frequency of rolling motion, since if these frequencies are close the phase lag is around 90 degrees.

-The moment due to the accumulation of water in the tank can be divided into two parts. The first part is the roll moment which is in phase with roll motion and the second is the moment, which is in phase with roll velocity.

-The ratio between the breadth of the tank and the depth of water (D/L) is very effective on the natural frequency of water and the amplitude of the moment created by water accumulation. The natural frequency of the water in the tank can be calculated as:

$$\omega_t = \frac{\pi}{L}\sqrt{g\ D}$$

where L is the breadth of the tank and D is the water depth in the tank.

-The damping effect of water in the tank decreases with increasing

amplitude of roll motion.

-The position of the tank with respect to the axis of rotation is very important. Its position and distance affect the direction and amplitude of the centrifugal moment. It was found that the amplitude of the moment becomes larger when the tank is situated above the rotational axis.

The numerical solution of the problem is probably the best method to use since most of the restrictions made in nonlinear theory can be relaxed by using numerical techniques and large amplitude and non-linear boundary conditions can be satisfied. Faltinsen [54] formulated a numerical method of sloshing in the tank with a two dimensional flow based on a boundary integral technique. He used the source distribution method and included artificial damping to represent the viscous effect (these results are compared with those of the author in this Appendix).

One of the best known techniques for solving time dependent incompressible fluid problems is the MARKER and CELL method (MAC) developed by Harlow and Welch [84]. It is based on the finite difference method and essentially, the Navier-Stokes equations are solved for each cell of the computational mesh in conjunction with the appropriate boundary conditions. The solution is advanced through time using a 'snapshot' principle and enables viscous transient fluid problems to be treated [52].

MAC technique has been improved over the years to tackle all problems. Hirt and Nichols improved the simplified Solution algorithm (SOLA) by using a versatile surface tracking algorithm. MAC system was applied to sloshing problem. One of these applications is the SOLA-VOF code, which used a volume of fluid technique based on a function, whose volume was unity at any point occupied by fluid and zero elsewhere [53]. Navickas et al [85] has used the SOLA-SURF variation of the MAC method to model sloshing in two-dimensional prismatic tank with ceiling. Mikelis et al [52] has extended Navickas's SOLA-SURF model to cope with different tank

shapes. He applied it to sloshing in partially filled liquid tanks, and has tried to combine it with ship motions. Nakayama [86] uses the finite element method to represent the fluid. A moving reference frame is employed to allow large amplitude excitation. The nonlinear free surface boundary conditions are addressed using an incremental procedure.

All these studies mentioned above are for rigid containers and the dimensions are very small compared to the size of the deck on the ship. Water on deck has created a lot of interest since this phenomenon causes a lot of problems for fishing vessels. Also a number of capsizing incidents, due to trapped water on deck creating instabilities and eventually causing capsizing, have been reported.

Jeff Dillingham [12] studied the water on deck problem of fishing vessels. He formulated sway and roll in the time domain, using the impulse response technique. For the formulation of the problem he used Glimm's random choice method. This model is suitable for shallow water theory and helps in the modelling of hydraulic jumps. He found that a small amount of water acts as a damping mechanism, however as the amount of water increases, the effectiveness of water as a damping mechanism decreases and this creates excitation. Adee and Çaglayan [51] carried out experimental work on the behaviour of water in the tank and used Dillingham's theoretical method for comparison reasons. In their paper the effect of water on ship motion and stability is not included. They found that over a wide range of frequencies, the theory agrees with the experimental results but that the theory fails around the resonance frequency. They also found that the theory is not sensitive to water depth.

Çaglayan [56] also suggested that the dominant dynamics of the water on deck problem can be approximated by taking the pseudo-static heel angle(or moment) caused by water on deck. Similarly, Adee and Pantazopoulos [10] carried out experiments to investigate the vessel response with water trapped on deck. They confirmed that the resulting effect of the phenomenon can be described as a pseudo-static angle of heel and each of the capsizing experiments which

ended in capsizing was related to the pseudo-static angle of heel. It also indicated that at certain frequencies sloshing becomes effective on fishing vessels when the water depth is very low and metacentric height is very high. However, at low and medium GMs the 'water on deck' effect becomes pseudo-static and the ship rolls at larger amplitudes, compared to the situation of 'no water on deck'.

Petey's study [87], which is based on Glimm's random choice method revealed that as the water depth in the tank increases, the possibility that the natural frequency of water and rolling frequency of ship are close, is considerably small unless the ship is also very small such as a fishing vessel. In that case only gravitational forces are expected to play an important role. Pantazopulos [88], who also used the Glimm's random choice method, confirmed the findings of Bosh and Vugts [55], and Faltinsen[11, 54] with regard to the effect of the location of the tank or deck, relative to the axis of rotation. The amplitude of sloshing moment increases as the location of the centre of rotation increases further below the undisturbed free surface and the amplitude of sloshing moment decreases considerably when the location of the rotation above the free surface increases.

The above review of the research in this field, reveals the following points :

- All the existing mathematical approaches, to model the sloshing and accumulation of water, provide limited solutions for limited conditions. These models cannot provide accurate solutions over a wide range of important parameters.

- The best suitable theoretical method for modelling the behaviour of water on deck appears to be Glimm's random choice method in connection with the dam-breaking problem. Recent theoretical studies concentrate on the improvement of this method.

- Solutions are based on a single degree of freedom motion, therefore the behaviour of the water on deck in the case of more than one degree of freedom has not yet been investigated.

- Almost all theoretical and experimental studies are based on the behaviour of the water in the tank, which is forced harmonically. Very limited information is available [10 (experimental)] with regard to the effect of water accumulation and of sloshing on the deck on the behaviour of the ship moving under wave excitation. Although suggestions have been put forward on how to include the effect of sloshing in the ship motion equations, so far no one has presented any results with respect to how water on deck affects ship motions.

A.2.4 MATHEMATICAL MODELLING OF SLOSHING

Since one of the main aims of this study is to include the effect of water accumulating or sloshing on the deck in the mathematical model of the motions of a damaged ship, it is essential to gain better understanding of this phenomenon and its effect on the ship. Therefore, a computer program is developed based on the velocity potential of 2 – dimensional flow with non-linear surface definitions[11, 54]. The motions of the deck or tank is assumed to be small and the wave created inside the tank is assumed to be a standing wave. The solution is carried out by using power series, while numerical routines are used to compute the final equations.

By using this model, a small parametric study can be carried out to identify dominant effects and relations and to seek ways for incorporating sloshing effects in the ship motion equations.

In the following, the modelling of sloshing due to sway and roll motions is given and comparisons with other published results are presented. Results of a small parametric study are included together with discussion on the problems and drawbacks of this approach.

A.2.4.1 Co-ordinate systems

-Co-ordinate system for sway:

O'X'Z' is the inertial co-ordinate system and Oxz is the moving co-ordinate system fixed to the tank whose origin is on the mean level of the water surface at the middle of the tank breadth (Fig A.2.1). The

governing equation for the liquid motion is formulated as a non-linear initial boundary value problem, with reference to the co-ordinate system fixed to the container, assuming the liquid motion is irrotational. Therefore accelerated system's velocity potential in inertial co-ordinate system f(X',Z',t) can be written in the co-ordinate system fixed to the tank as;

$$\Phi(X',Z',t) = \Phi(x,z,t) = \Phi_1(x,z,t) + \Phi_2(x,t) \quad \text{[Eq A.2.1]}$$

-Co-ordinate System For Roll

O'X'Z' is the inertial system, oxz is the co-ordinate system fixed to the body and GX^*Z^* is the rotation axis of the tank [Fig A.2.2]. Again equations for the liquid motion are formulated as a non-linear boundary value problem with reference to the co-ordinate system fixed to the tank. The velocity potential $\Phi_T(X^*,Z^*,t)$ can be written in the fixed co-ordinate system (to the tank) as:

$$\Phi(X^*,Z^*,t) = \Phi_T(x,z,t) = \Phi(x,z,t) + \Phi_C(x,z,Z^*,t) \quad \text{[Eq A.2.2]}$$

A.2.4.1 Modelling of Sloshing due to Sway

The velocity potential of the fluid is taken initially as:

$$\Phi_1 = \sum_{n=0} F_n(t)\ \mathrm{Sin}(\alpha_n x)\ \frac{\cosh(\alpha_n(z+D))}{\mathrm{Cosh}(\alpha_n D)} \quad \text{[Eq A.2.3]}$$

where:

$F_n(t)$: An arbitrary function of time

D : Depth of the water

z : Water elevation

$$\alpha_n = \frac{(2n+1)\ \pi}{L}$$

It is assumed that the tank is accelerated in the x direction, in which case:

$$\Phi_2 = x\ \ U(t) \quad \text{[Eq A.2.4]}$$

where

$U(t) = A\ \omega\ \cos(\omega t)$

The sway motion of the ship:

$S(t) = A\ \sin(\omega t)$

Hence, the total velocity potential of the system is:

$$\Phi = \Phi_1 + \Phi_2$$

$$\Phi = \sum_{n=0} F_n(t)\ \mathrm{Sin}(\alpha_n x)\ \frac{\cosh(\alpha_n(z+D))}{\mathrm{Cosh}(\alpha_n D)} + x\ U(t) \quad \text{[Eq A.2.5]}$$

Potential must exist only for an irrotational flow and must provide continuity:

$$\nabla^2\Phi = \frac{\partial^2\Phi}{\partial x^2} + \frac{\partial^2\Phi}{\partial z^2} = 0 \quad \text{[Eq A.2.6]}$$

$$\frac{\partial\Phi}{\partial n} = V_n \qquad \text{on the surface} \quad \text{[Eq A.2.7]}$$

$$\frac{\partial\Phi}{\partial n} = 0 \qquad \text{at the bottom of the tank} \quad \text{[Eq A.2.8]}$$

In the case of a free surface, as on a water wave, kinematic and dynamic boundary conditions are needed. The kinematic condition states that any particle which lies on the free surface at any instant will never leave it. This leads to

$$\frac{\partial\eta}{\partial t} - \frac{\partial\Phi}{\partial z} + \frac{\partial\Phi}{\partial x}\ \frac{\partial\eta}{\partial x} = 0 \quad \text{at} \quad z = \eta(x,t) \quad \text{[Eq A.2.9]}$$

When the free surface is uncontaminated, the free surface tension can be taken as zero, when the flow is rotational. The Bernoulli equation can be written as dynamic free surface condition, i.e.

$$g\,\eta + \frac{\partial \Phi}{\partial t} + \frac{1}{2}\left(\left(\frac{\partial \Phi}{\partial x} \right)^2 + \left(\frac{\partial \Phi}{\partial z} \right)^2 \right) = 0 \qquad \text{[Eq A.2.10]}$$

The velocity potential is written in power series. Boundary conditions are also written in power series. System of equations, which includes velocity potential and boundary conditions are solved up to a power where the solutions of the system of equations converge.

In order to solve the problem, first the arbitrary function $F_n(t)$ must be obtained and solved for the potential and free surface shape. For the solutions of the velocity potential the motion amplitude of the tank is assumed to be small.

In order to solve the function $F_n(t)$ first, the modified version of [Eq A.2.10] is written as follows

$$\eta = -\frac{1}{g}\left(\frac{\partial \Phi}{\partial t} + \frac{1}{2}\left(\left(\frac{\partial \Phi}{\partial x} \right)^2 + \left(\frac{\partial \Phi}{\partial z} \right)^2 \right) \right)$$

η is then substituted into kinematic free surface condition [Eq A.2.9], yielding:

$$\frac{\partial \eta}{\partial t} - \frac{\partial \Phi}{\partial z} - \frac{\partial \Phi}{\partial x}\,\frac{\partial \eta}{\partial x} = 0$$

If the partial derivatives in Eq A.2.9 are employed, resultant kinematic free surface condition, which is very lengthy expression, can be written as follows;

$$f(F_n''(t),\ F_n'(t),\ F_n(t),\ U''(t),\ U'(t),\ U(t),\ \eta,\ D,..)=0$$

For the computation purposes the above expression can be re-written in a final form as follows:

$$F_n''(t) = f(F_n'(t), F_n(t), U''(t), U'(t), U(t), \eta, D,..) \qquad \text{[Eq A.2.11]}$$

Pressure

Using Bernoulli's equation [Eq A.2.10], gives:

$$\frac{p}{\rho} + g\,z + \frac{\partial \Phi}{\partial t} + \frac{1}{2}\left(\left(\frac{\partial \Phi}{\partial x} \right)^2 + \left(\frac{\partial \Phi}{\partial z} \right)^2 \right) = 0$$

This can be rearranged to give

$$p = -\rho \left(g\,z + \frac{\partial \Phi}{\partial t} + \frac{1}{2}\left(\left(\frac{\partial \Phi}{\partial x} \right)^2 + \left(\frac{\partial \Phi}{\partial z} \right)^2 \right) \right) \quad \text{[Eq A.2.12]}$$

Force

The force acting on the bottom and side walls of the tank can be found as follows.

$F = F_1 + F_2$

F_1: The force acting on the side walls

F_2: The force acting on the bottom of the tank

$$F = 0.5\,\rho \int_{-D}^{\eta} p\,dz + 0.5\,\rho \int_{-L/2}^{L/2} p\,dx \quad \text{[Eq A.2.13]}$$

Moment

As with the force the moment can be calculated as follows.

$M = M_1 + M_2$

M_1: Moment on the side walls

M_2: Moment on the bottom of the tank

$$M = 0.5\,\rho \int_{-D}^{\eta} p\,z\,dz + 0.5\,\rho \int_{-L/2}^{L/2} p\,x\,dx \quad \text{[Eq A.2.14]}$$

A.2.4.3 Modelling of Sloshing due to Roll

In order to evaluate the sloshing due to the roll same procedure as in sway is followed. The velocity potential is then written as

$$\Phi_T = \Phi + \Phi_c$$

Φ : Velocity potential of the fluid

Φ_c : Velocity potential of the tank according to the earth co-ordinate system but written in the tank co-ordinate system

Φ can be written as:

$$\Phi = \sum_{n=0} F_n(t)\ \mathrm{Sin}(\alpha_n x)\ \frac{\cosh(\alpha_n(z+D))}{\mathrm{Cosh}(\alpha_n D)} \qquad \text{[Eq A.2.15]}$$

Where $F_n(t)$ is an arbitrary function of time in velocity potential.

The fluid is irrotational, hence:

$$\nabla^2\Phi_T = 0 \qquad \text{[Eq A.2.16]}$$

Boundary conditions:

$$\frac{\partial\Phi}{\partial z} = 0 \qquad \text{at } x = \pm \frac{L}{2} \qquad \text{[Eq A.2.17]}$$

$$\frac{\partial\Phi}{\partial z} = 0 \qquad \text{at } z = -D \qquad \text{[Eq A.2.18]}$$

$$\frac{\partial\Phi_T}{\partial x} = U(t)\ (z-z_0) \qquad \text{at } x = \pm \frac{L}{2} \qquad \text{[Eq A.2.19]}$$

$$\frac{\partial\Phi_T}{\partial z} = -U(t)\ x \qquad \text{at } z = -D \qquad \text{[Eq A.2.20]}$$

U(t): Angular velocity of the tank.

Φ_c satisfies the inhomogeneous body boundary conditions [11]. Φ_c can be written as in Graham and Rodriques [81].

$$\Phi_c = -U(t) \sum_{n=0} \frac{(-1)^n\ 4}{\pi^3\ (2n+1)^3} \left(\frac{D^2\ \mathrm{Sin}(\beta_n(z+D/2))\ \mathrm{Sinh}(\beta_n x)}{\mathrm{Cosh}(\beta_n L/2)} \right)$$

$$+ \left(\frac{L^2\ \mathrm{Sin}(\alpha_n x)\ \mathrm{Cosh}(\alpha_n z)}{\mathrm{Sinh}(\alpha_n L/2)} \right) - U(t)\ (z_1 + D/2)\ x \quad \text{[Eq A.2.21]}$$

where:

z_1: The distance between rotating axis and tank axis

$$\beta_n = \frac{(2n+1)\ \pi}{D} \qquad \text{[Eq A.2.22]}$$

$$\alpha_n = \frac{(2n+1)\ \pi}{L} \qquad \text{[Eq A.2.23]}$$

The fluid is subjected to kinematic and dynamic boundary conditions on the free surface. Bernoulli's equation can be written as a dynamic free surface condition, i.e.[Eq A.2.24]:

$$g\ \eta + \frac{\partial \Phi_T}{\partial t} + \frac{1}{2}\left(\left(\frac{\partial \Phi_T}{\partial x} \right)^2 + \left(\frac{\partial \Phi_T}{\partial z} \right)^2 \right) = 0 \qquad z = \eta(x, t)$$

η: Water surface elevation

The kinematic boundary condition can be written as,

$$\frac{\partial \eta}{\partial t} - \frac{\partial \Phi_T}{\partial z} + \frac{\partial \Phi_T}{\partial x}\ \frac{\partial \eta}{\partial x} = 0 \quad \text{at} \quad z = \eta(x,t) \qquad \text{[Eq A.2.25]}$$

Calculation of Water Elevation and Function $F_n(t)$

In order to solve the problem we have to calculate the function $F_n(t)$ inside the velocity potential. The solution is achieved by using kinematic and dynamic boundary conditions as explained in sway

section.

The water elevation can be found from the following expression [Eq A.2.26]:

$$\eta = -\frac{1}{g}\left(\frac{\partial \Phi_T}{\partial t} + \frac{1}{2}\left(\left(\frac{\partial \Phi_T}{\partial x}\right)^2 + \left(\frac{\partial \Phi_T}{\partial z}\right)^2\right)\right) \qquad z = \eta(x, t)$$

Force

The force on the side wall and on the bottom of the tank can be evaluated as follows:

$$F = 0.5\,\rho \int_{-D}^{\eta} p\,dz + 0.5\,\rho \int_{-L/2}^{L/2} p\,dx \qquad \text{[Eq A.2.27]}$$

Moment

The moment acting on the side wall and on the bottom of the tank is calculated as shown:

$$M = 0.5\,\rho \int_{-D}^{\eta} p\,z\,dz + 0.5\,\rho \int_{-L/2}^{L/2} p\,x\,dx \qquad \text{[Eq A.2.28]}$$

A.2.5 COMPARISON OF THE RESULTS

In order to validate the computer program comparisons are carried out as explained next.

A.2.5.1 Comparison for Sway Motion

In order to compare the results of this research for sway excitation, Faltinsen's analytical and numerical results are taken into account [11,54]. Since Faltinsen had introduced artificial viscous damping the same method is followed for comparison purposes. Results were obtained for the tank and conditions, the details being as follows:

Breadth of the tank = 1.0 m
Depth of the water = 0.5 m

Amplitude of forced sway oscillations = 0.025 m

The behaviour of the water, due to harmonic sway oscillations at different frequencies, is examined, and water elevation results at a 0.05 m distance from the side of the tank are obtained. These results are in good agreement with the results obtained by Faltinsen [54]. As Fig. A.2.3 shows, Faltinsen's analytical solution and the non-linear solution of this research agree very well.

The behaviour of the water in the tank for the same condition is examined in the time domain, and results are again compared with Faltinsen's non-linear numerical solution, which is based on boundary integral techniques, as shown in Fig A.2.4. A small difference can be observed in the two sets of results and this is probably due to the different solution techniques employed. However, overall, it can be said that the computer program developed for this study gives good results, compared to other published results.

At a certain range of frequencies near the natural frequency of the water in the tank, a solution cannot not be obtained since the mathematical(computational) approach failed to reach any solution since solution became unstable. This can be due to the incorrect estimation of artificial viscous damping or the non-existence of viscous damping of the water or some other non-linearities which cannot be included in the present model. Faltinsen and some other researchers encountered a similar problem, which is also experienced in numerical solution techniques. It appears that near the natural frequency it is difficult to reach a reasonable estimation of water behaviour, unless viscous damping or other non-linearities are correctly modelled.

A.2.5.2 Comparisons for Rotational Motions

The behaviour of water in the compartment, due to angular motion(Roll or Pitch), is analysed and results were compared with the results of Nakayama and Washizu [86]. His study is based on a two-dimensional velocity potential and large amplitudes, while solutions are based on a finite element numerical solution technique.

Comparisons are carried out for two different tanks and conditions.

Comparison 1

Breadth of tank : 1.0 m
Depth of water : 0.35 m
Amplitude of pitch : 5 degrees
Frequency : 4.19 rad/sec
Axis of rotation : 0.1 m below the water surface

As Fig A.2.5 shows, although the results of pressure at point P are in reasonable agreement, the numerical solution of Nakayama predicts larger pressure compared to the result of this study, which is closer to the result of linear theory. This is obviously due to the different solution techniques. Furthermore, the results of Nakayama are based on the initial condition of 5 degrees inclination, while results of this research had a zero initial heel angle. This different initial condition may have some effect on the results as well.

Comparison 2

Breadth of tank : 0.9 m
Depth of water : 0.6 m
Amplitude of pitch : 0.8 Degrees
Frequency : 5.5 rad/sec
Axis of rotation : at the water surface

As Fig A.2.6 shows, in general, results are in good agreement. The non-linear solution adopted in this study estimates the water elevation to be slightly larger. However, as mentioned in comparison 1, this small difference could be due to the different solution techniques.

However, within the limits of the approach adopted here, this small difference is not believed to influence to a great extent the overall effect (static and dynamic) of water accumulation on the motions of the ship. As the limitations are decreased for more general solutions of this problem, using numerical solution techniques such as finite elements, finite difference etc, are more versatile and accurate as they can accommodate large amplitude motions and shallow water and

hence a partial dry deck condition. Of course, computationally it is more complex and takes much longer time to obtain results.

Again, due to the lack of viscous effects, results at a certain range of frequencies, cannot be obtained.

A.2.5.3 Parametric Investigation

As mentioned before, water accumulating on deck can have two different effects on the behaviour of a ship, namely, a static effect, which is due to the water mass, and a dynamic effect due to the motion of the water. Therefore, it was decided to carry out a limited parametric study to see the magnitude of these effects and how dependent they are on different parameters.

For this purpose, a tank with a breadth of 8 m is taken, filled with water, which is 3 m deep. The rotation of axis is located above the tank, which is the case for ferries. Two different distances of the axis of rotation are used; the first is 4.5 m above the tank bottom and the second 10 m. By taking these two distances, the water accumulation on the vehicle deck and in a compartment below the vehicle deck are examined. The investigation is carried out for different frequencies up to a limit at which no solution can be obtained. The investigation is based on the maximum pressure at the bottom corner of the tank. The hydrostatic pressure is obtained by inclining the tank and measuring the static pressure at the bottom corner. The dynamic pressure is obtained for different frequencies and added to the hydrostatic pressure for better comparison (Fig A.2.7). As results show, for the 4.5 m axis of rotation the dynamic pressure is very small compared to the hydrostatic pressure throughout the frequency range used. When the axis of rotation is increased to 10 m, the dynamic pressure is again small for a large range of frequencies, but the dynamic pressure starts increasing when the frequency is approaching the natural frequency of the water in the tank (natural frequency of the water in the tank in a non-dimensional form is approximately 1.36). However, this is again small compared to the hydrostatic pressure. It should also be considered that the viscous damping of water is not included.

Actually, due to the position of the axis of rotation this dynamic pressure would have an opposite effect to hydrostatic pressure and would reduce heeling.

It can be said that since ferries are big ships and generally oscillate at low frequencies, the dynamic effect, which is smaller compared to the hydrostatic effect, may not influence the overall results significantly. The damage stability experiments, carried out by DMI and results of DMI and BMT show similar trends, as gross accumulation of water was observed to be the dominant effect. However, the parametric study in this Appendix is a very limited one while experiments addressed a particular ship and conditions, therefore, these suggestions cannot be generalised for all conditions and ships.

Overall, it can be said that, the effect of accumulation of water can be approximated by taking the quasi-static effect of water on deck for certain ships and conditions. However, it is essential to develop a theoretical approach, to estimate both dynamic and static effects as realistically as possible which can be applied to all types of ships and conditions. For this purpose the following points must be considered:

- The developed application must be suitable for shallow water and large amplitude motions

- The approach must be flexible in order to consider different shapes of tanks and conditions such as static heel, partially dry deck etc. The approach must be used for extensive parametric investigations to derive the relation between accumulation of water and ship motions for all possible conditions

- By taking into account findings from the above, the adopted approach for water accumulation must be easily and meaningfully included in the system of equations of ship motions and employed in conjunction with the computation ship motions in the time simulation,so that effect of ship motions on accumulation of water

in the tank and vice versa can be estimated at each time step.

According to the published research, Glimm's random choice method with the dam breaking problem is a suitable approach, considering shallow water and large amplitudes. However, it is necessary to combine this method with ship motions to complete the solution, so that some investigations can be carried out, and the method can be validated by carrying out experiments, and corrected if necessary. These experiments must combine ship motions, water in the tank and wave excitation as used by Adee and Pantazoupolos [10] but in more extensive form.

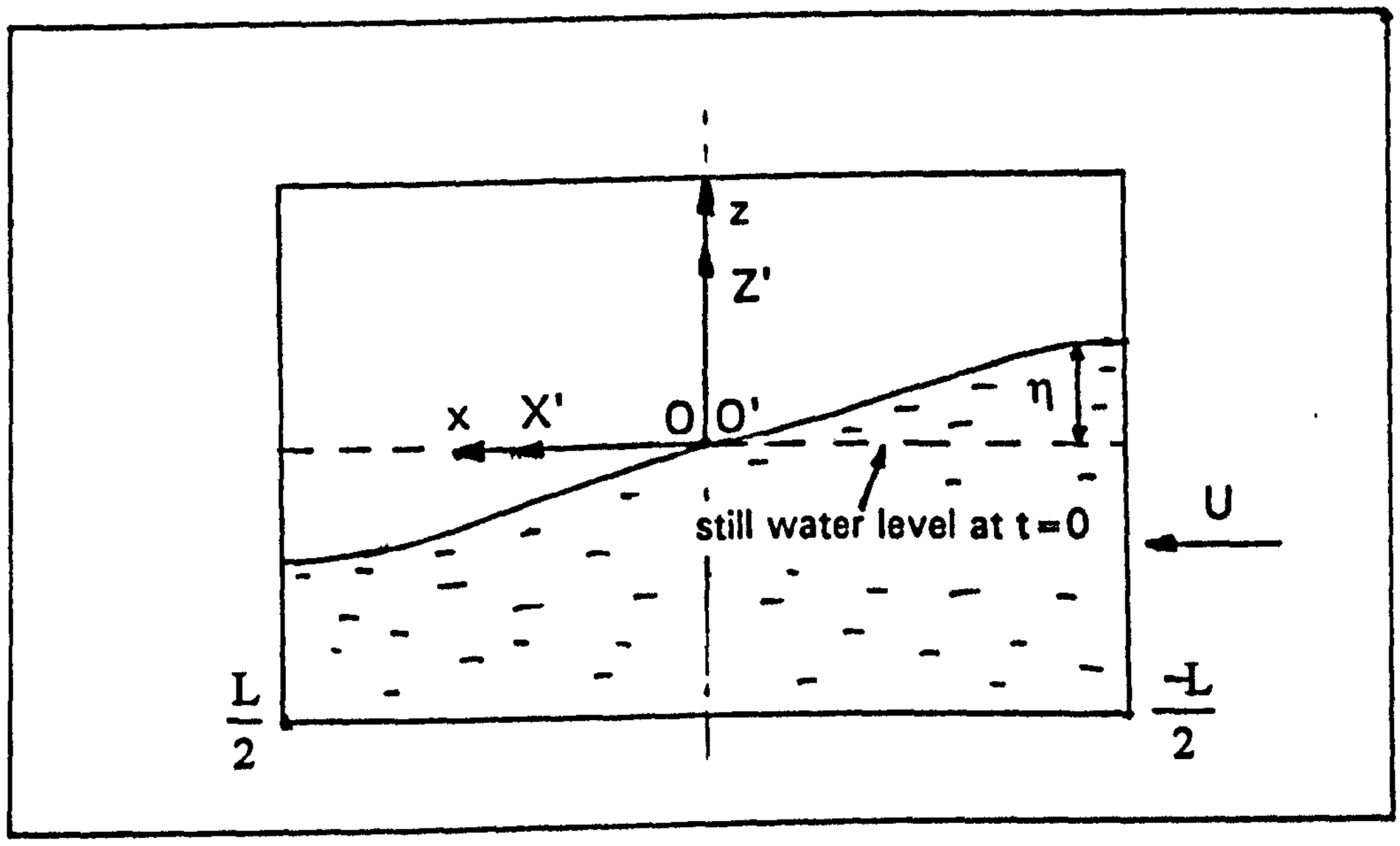

Fig A.2.1 Co-ordinate system for sloshing due to sway

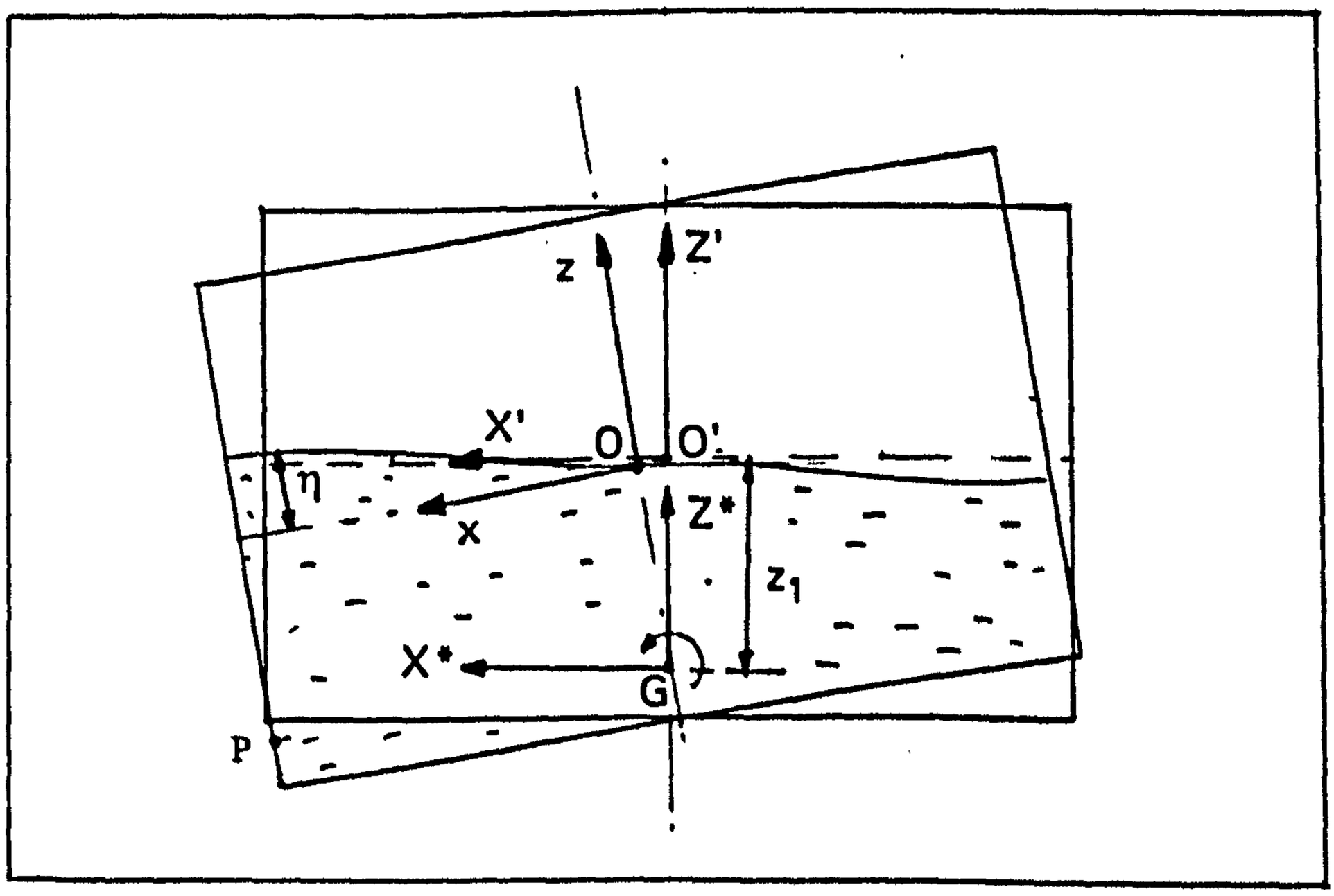

Fig A.2.2 Co-ordinate system for sloshing due to roll

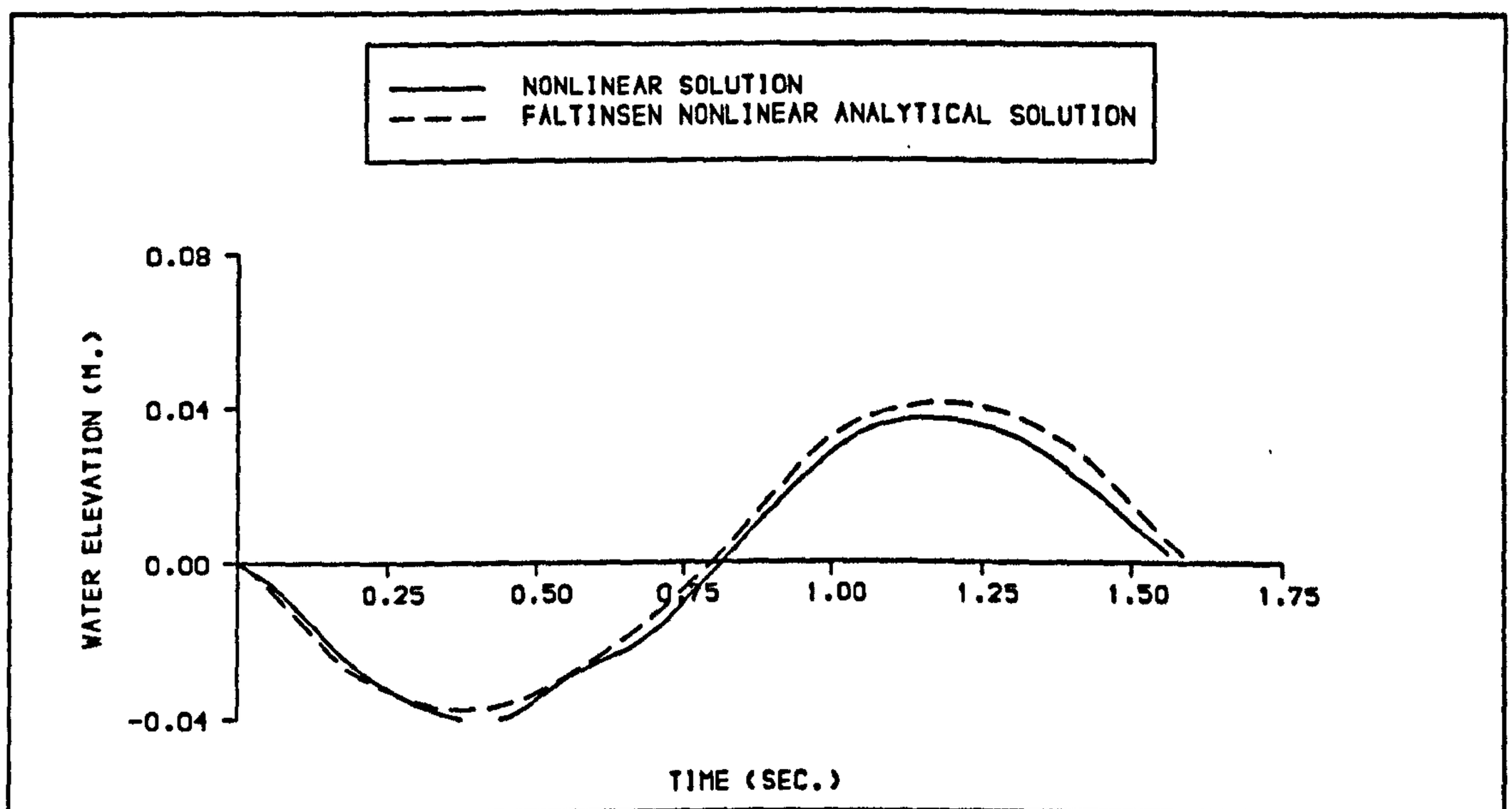

Fig A.2.3 COMPARISON OF DIFFERENT SOLUTIONS ,SWAY MOTION, W=3.926 RAD/SEC. AMP=0.025 M., DAMPING COEFF.=0.05

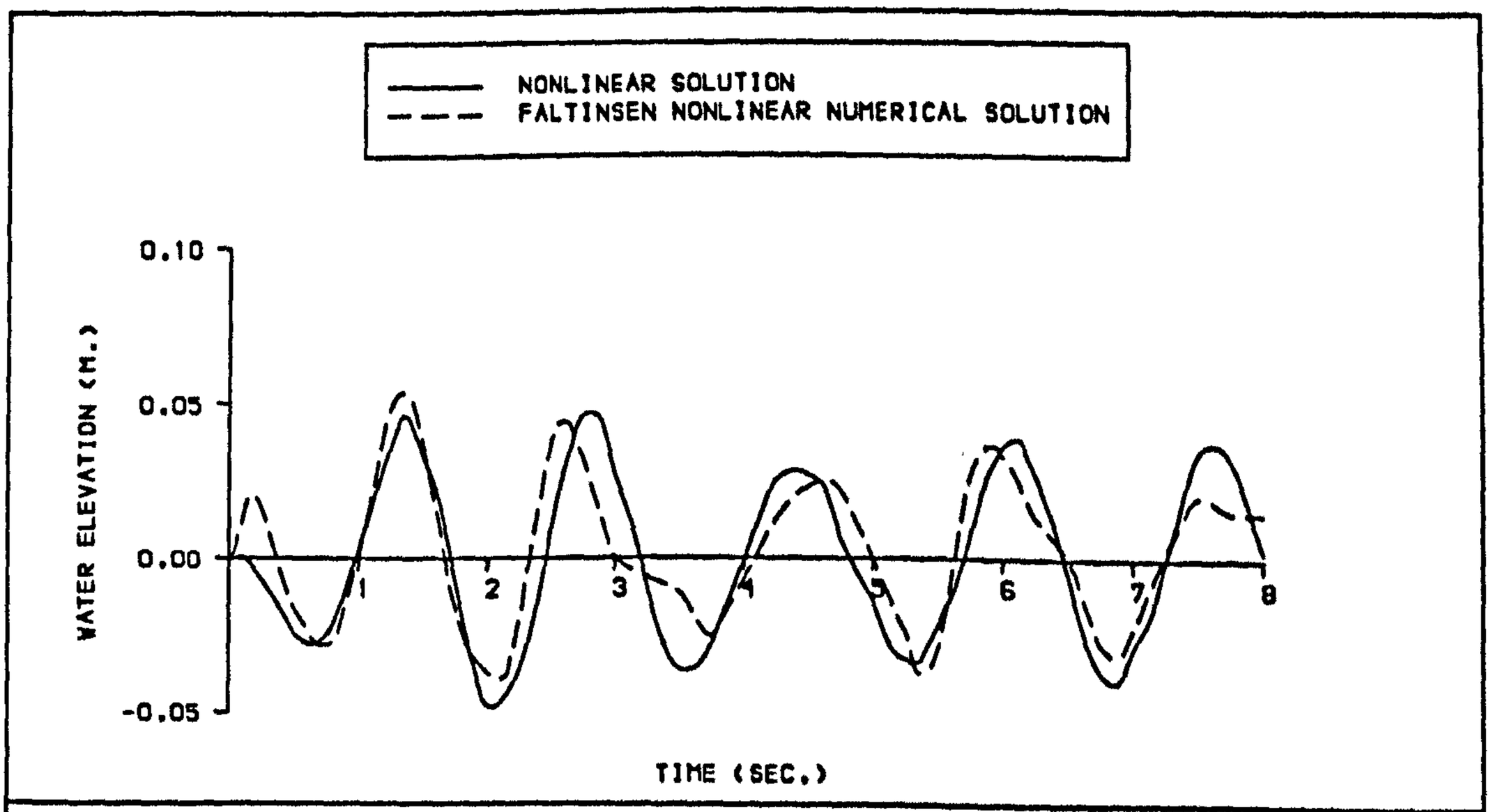

Fig A.2.4 COMPARISON OF DIFFERENT SOLUTIONS ,SWAY MOTION, W=3.926 RAD/SEC. AMP=0.025 M., DAMPING COEFF.=0.05

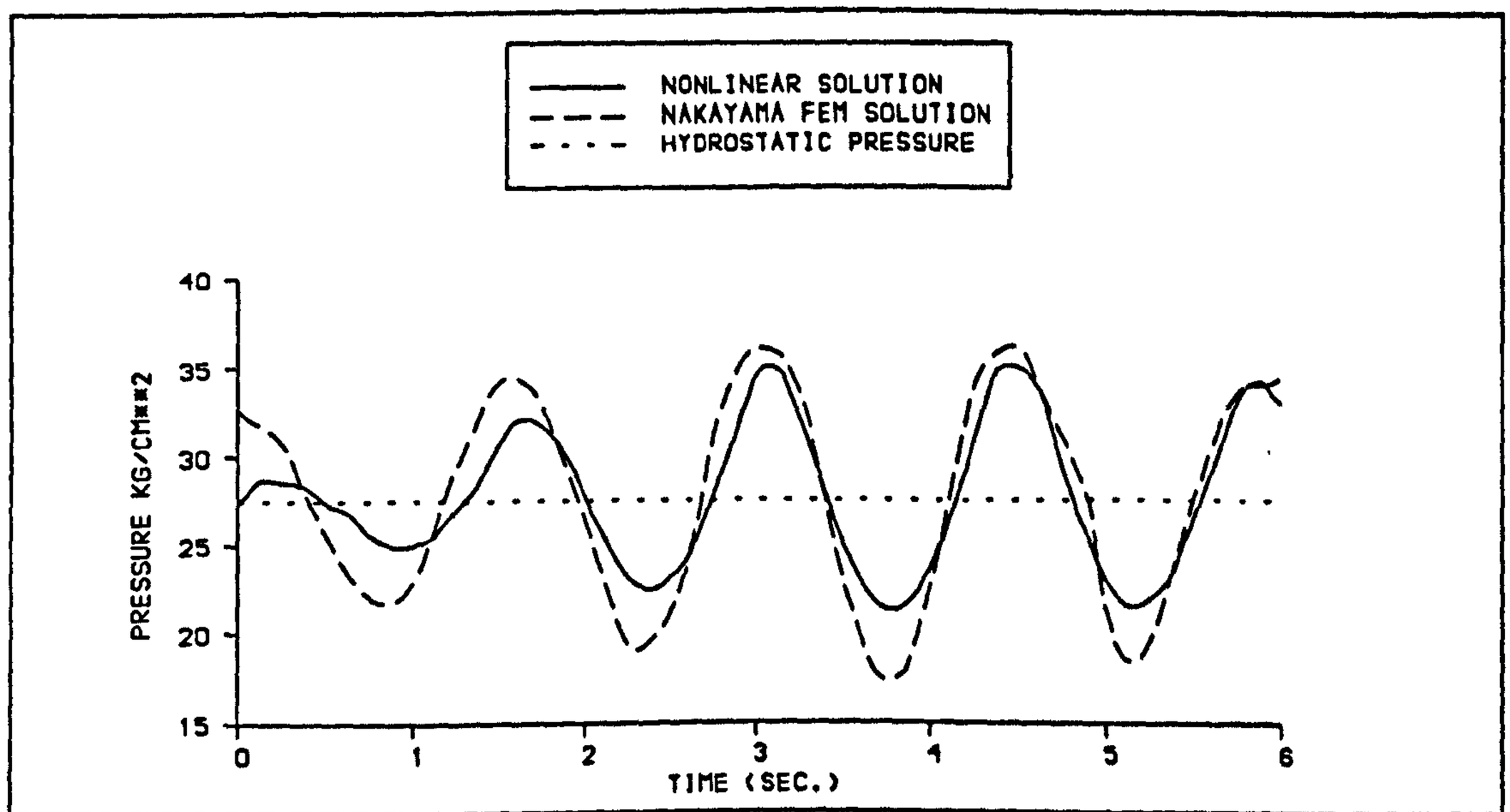

Fig A.2.5 COMPARISON OF DIFFERENT SOLUTIONS, PITCH MOTION, W=4.19 RAD/SEC., AMP= 5.0 DEGREES

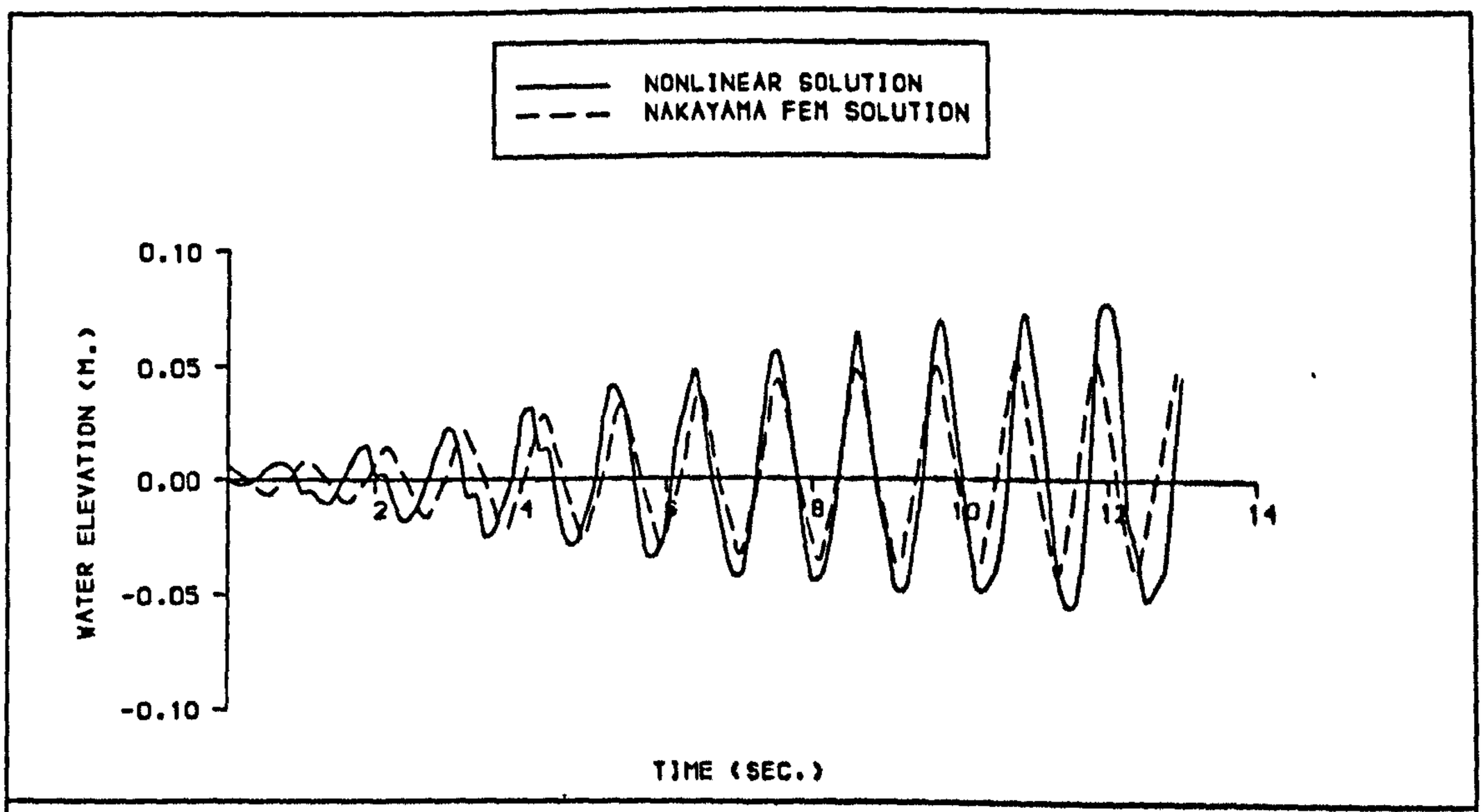

Fig A.2.6 COMPARISON OF DIFFERENT SOLUTIONS, PITCH MOTION, W=5.5 RAD/SEC., AMP= 0.8 DEGREES

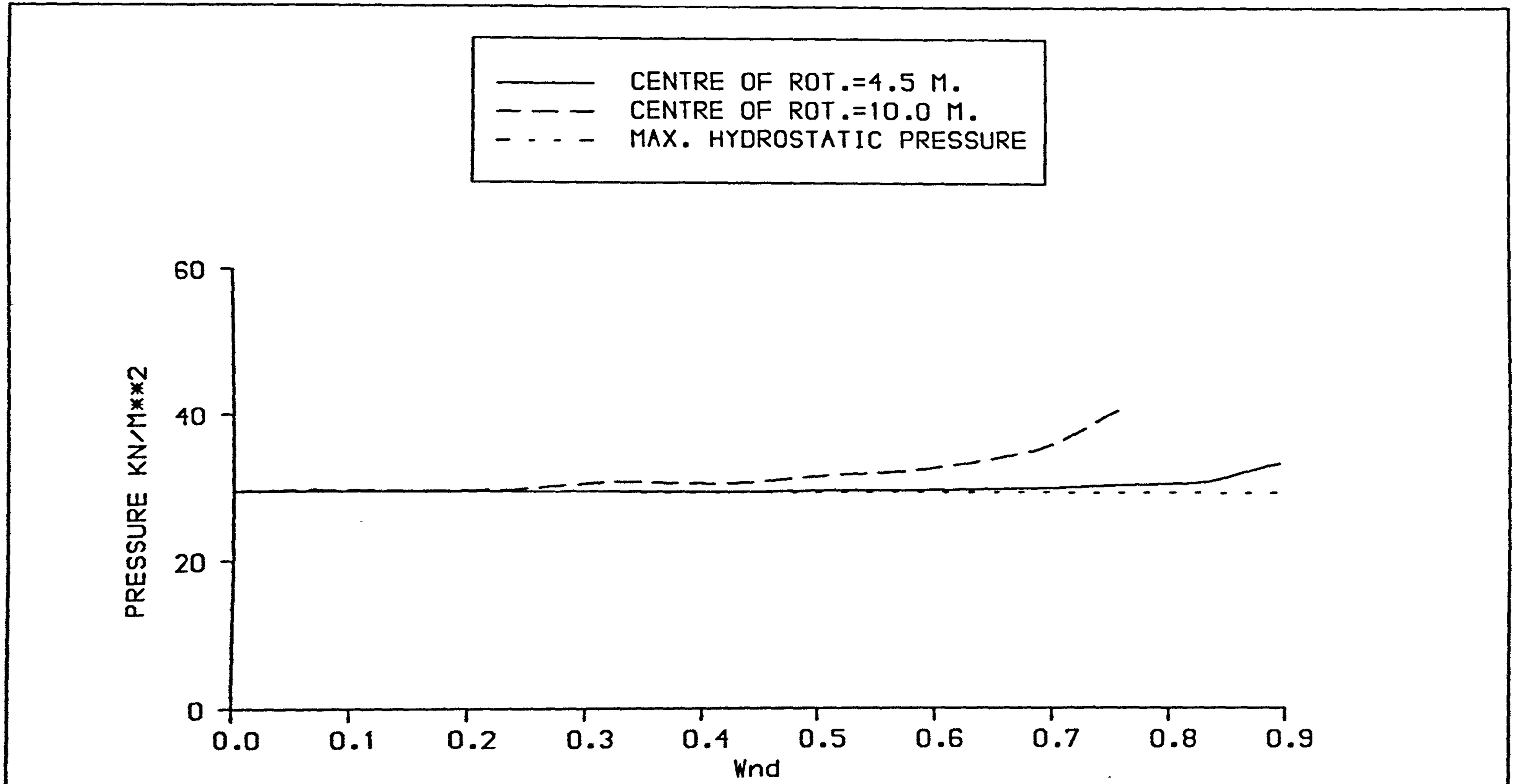

Fig A.2.7 EFFECT OF THE PLACE OF THE CENTRE OF ROTATION ON PRESSURE
AMP= 5. DEG, DEPTH/BREADTH=0.375, [ROLL MOTION]

A.3: WATER INGRESS

A.3.1 WATER FLOW THROUGH ORIFICE TYPE OF OPENINGS

Water flow into the damaged compartments has been always dealt with by using the existing hydraulic theories in civil engineering application. The hydraulic principal is based on the Bernoulli equation and is applied to the steady motion of an ideal fluid along the framed system. This equation is probably more widely used in hydraulics than any other and is capable of explaining at least qualitatively, many of the phenomena that are encountered in fluid mechanics. It suggests that the height, pressure and velocity cannot increase simultaneously in a system.

The Bernoulli principal, which assumes that ideally energy in the fluid system remains constant, which can be denoted as total hydraulic head, can be written as follows:

$$\frac{p}{\rho\gamma} + z + \frac{u^2}{2g} = H \qquad \text{[Eq A.3.1]}$$

If two points are assumed, one is point A at the water surface of the tank (indices o) and other is point B, which is at the exit of the orifice (indices 1, Fig A.3.1).

$$\frac{p_o}{\rho\gamma} + z_o + \frac{U_o^2}{2g} = \frac{p_1}{\rho\gamma} + z_1 + \frac{u_1^2}{2g} = H \qquad \text{[Eq A.3.2]}$$

However at the tank surface and the exit of the orifice, pressures P_o and P_1 are zero since the fluid is open to the atmosphere. Furthermore, velocity of the water at the water surface is assumed to be zero since the water level is kept constant. In this case the above equation can be written as follows:

$$0 + H + 0 = 0 + 0 + \frac{u_1^2}{2g} = H \qquad \text{[Eq A.3.3]}$$

or more generally the total pressure head at point B is:

$$H = \frac{U^2}{2\,g} \qquad \text{[Eq A.3.4]}$$

$$U = \sqrt{2\,g\,H} \qquad \text{[Eq A.3.5]}$$

and flow rate,

$$Q = U\ A_{op} \qquad \text{[Eq A.3.6]}$$

where:

U : Velocity of the water

H : The head between the water level and the centre of damaged hole

A_{op} : Area of the damaged hole or opening

However, in practice, there are frictions, losses, sudden discontinues of the section and shape of the orifice. Due to all these effects the real flow decreases. In hydraulic engineering these effects are considered by introducing some coefficients.

One of the coefficients is called the contraction coefficient, which is related to the edge of the orifice. For a perfectly sharp edge the contraction coefficient (C_c) is around 0.6 and this increases progressively with the lip radius until it finally approaches the value 1 for a "bell mouthed" opening which flows full [57].

In practice there is a slight energy loss due to contraction, and conditions may not be uniform across the orifice. These effects reduce the effective mean velocity and are included in the equation as coefficient of velocity (C_v), which generally changes between 0.95 and 0.99. In hydraulic applications all these coefficients are represented in one coefficient which is called discharge or flow coefficient (K):

$$K = C_v\ C_c \qquad \text{[Eq A.3.7]}$$

In practice flow coefficient is determined directly from experimental measurements for a constant head H. This coefficient also includes the corrections due to the approximations in formulations. Therefore in reality, flow rate through an opening below the water surface can be determined using the following formula:

$$Q = K\ U\ A_{op} \qquad \text{[Eq A.3.8]}$$

A.3.2 FLOW THROUGH AN OPENING ABOVE THE WATER SURFACE

Existing estimations are based on open channel hydraulics, which must have a free surface, which is subject to the atmospheric pressure. In general this is defined as flow over a weir or notch. The characteristics of flow over a weir were recognised early in hydraulics as the basis for overflow spillways. It is assumed that the horizontal velocity component of the flow is constant or does not exist and only force acting on a free flow is the gravity [57, 58, 75].

Assuming that the above and below nappe is ventilated, which means atmospheric pressure must exist at all points within it. Weisbach [58] suggested that the velocity U at a point at elevation z above the crest would be given by equating the velocity head plus potential head to the total head just upstream of the weir (Fig A.3.2):

$$H_t = z + \frac{U^2}{2\ g} \qquad \text{[Eq A.3.8]}$$

In that case, velocity would be a function of the elevation (z):

$$U = \sqrt{2\ g\ (H_t - z)} \qquad \text{[Eq A.3.9]}$$

The flow rate for per unit width passing through an element on height Δz at elevation z is:

$$\Delta q = U\ \Delta z$$

and if integration is done between sill level and the surface level:

$$q = \int_0^H U\, dz = \int_0^H \sqrt{(H_t - z)}\, dz \qquad \text{[Eq A.3.10]}$$

$$q = \frac{2}{3}\sqrt{2\ g}\left(\sqrt[3]{(H_t)^2} - \sqrt[3]{(H_t - H)^2}\right) \qquad \text{[Eq A.3.11]}$$

However as some of the parts of this formula have no fundamental significance [58], the formula for flow rate for per unit width can be simplified and the flow coefficient included as follows:

$$q = K\sqrt{g}\left(\sqrt[3]{H^2}\right) \qquad \text{[Eq A.3.12]}$$

Although H_t represents the total energy relative to crest elevation, H is easier to use since it can be measured directly whereas H_t cannot. However the difference is included in the equation via flow coefficient K [58].

This formula can be more generalised to calculate the volumetric flow for full width of any geometry such as rectangular weir triangular notch.

$$Q = K\ A_{op}\sqrt{g\ H} \qquad \text{[Eq A.3.13]}$$

Most of the flow coefficients (discharge coefficient) for different shapes and flow depths are available [75] and they have been determined experimentally. Although flow coefficient can change depending on the shape, for free flow in general they vary between 0.5 and 0.6. However, for triangular notches this may go down to 0.45 [57].

As suggested above, for different shapes, edges and conditions flow coefficients must be estimated experimentally. At present, due to lack of research and data about the water inflow/outflow into/from

damaged compartment, the existing formulas and coefficients for hydraulic engineering must be used. However, in the case of water ingress into damage compartments, the shapes of the damage holes or the conditions of the edges can change considerably while effect of wave on water ingress must be included in the estimation of flow coefficient. Therefore it is necessary to determine specific flow coefficients for water flow through a damaged hole in a ship in wave environment.

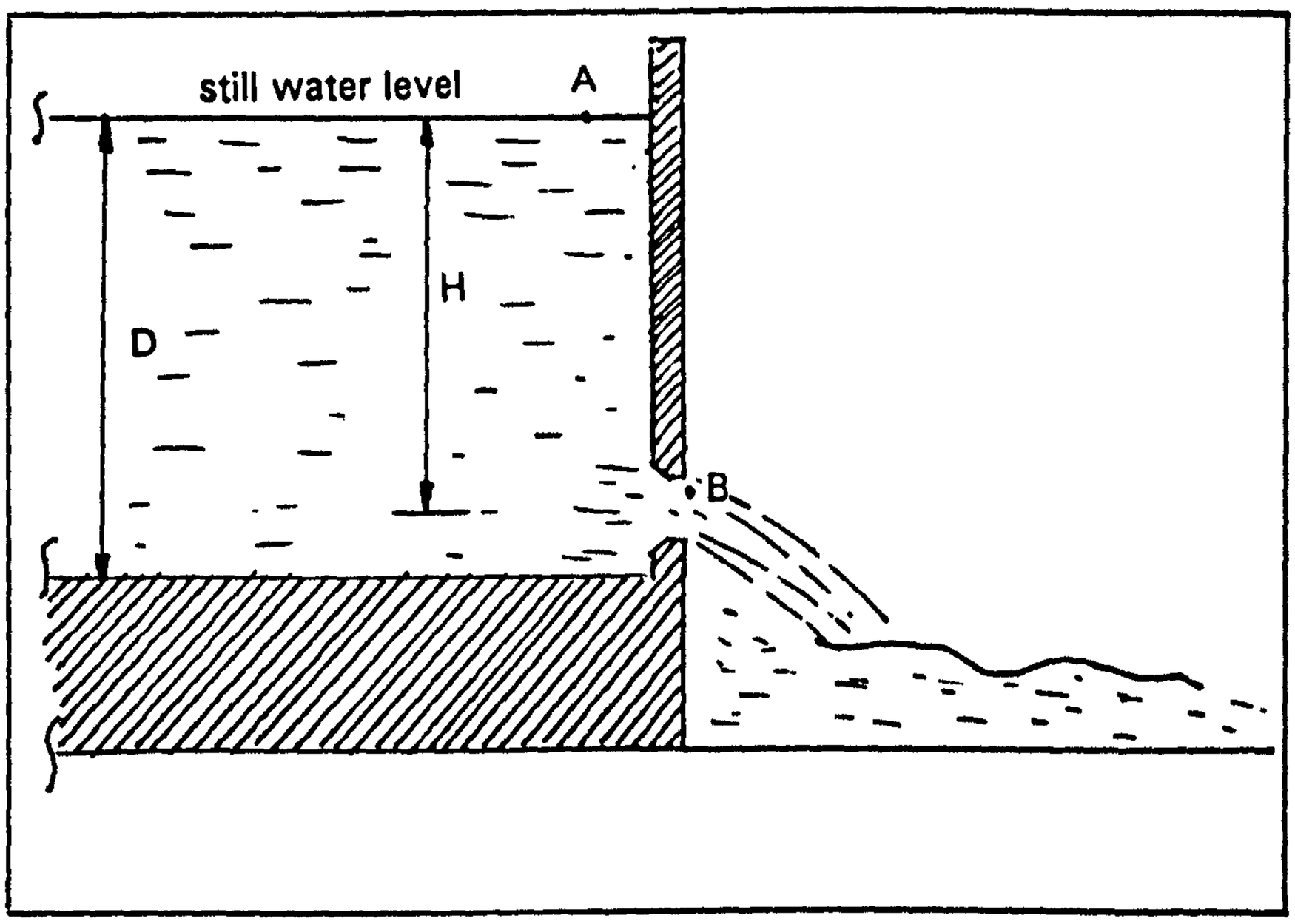

Fig A.3.1 Flow through an orifice

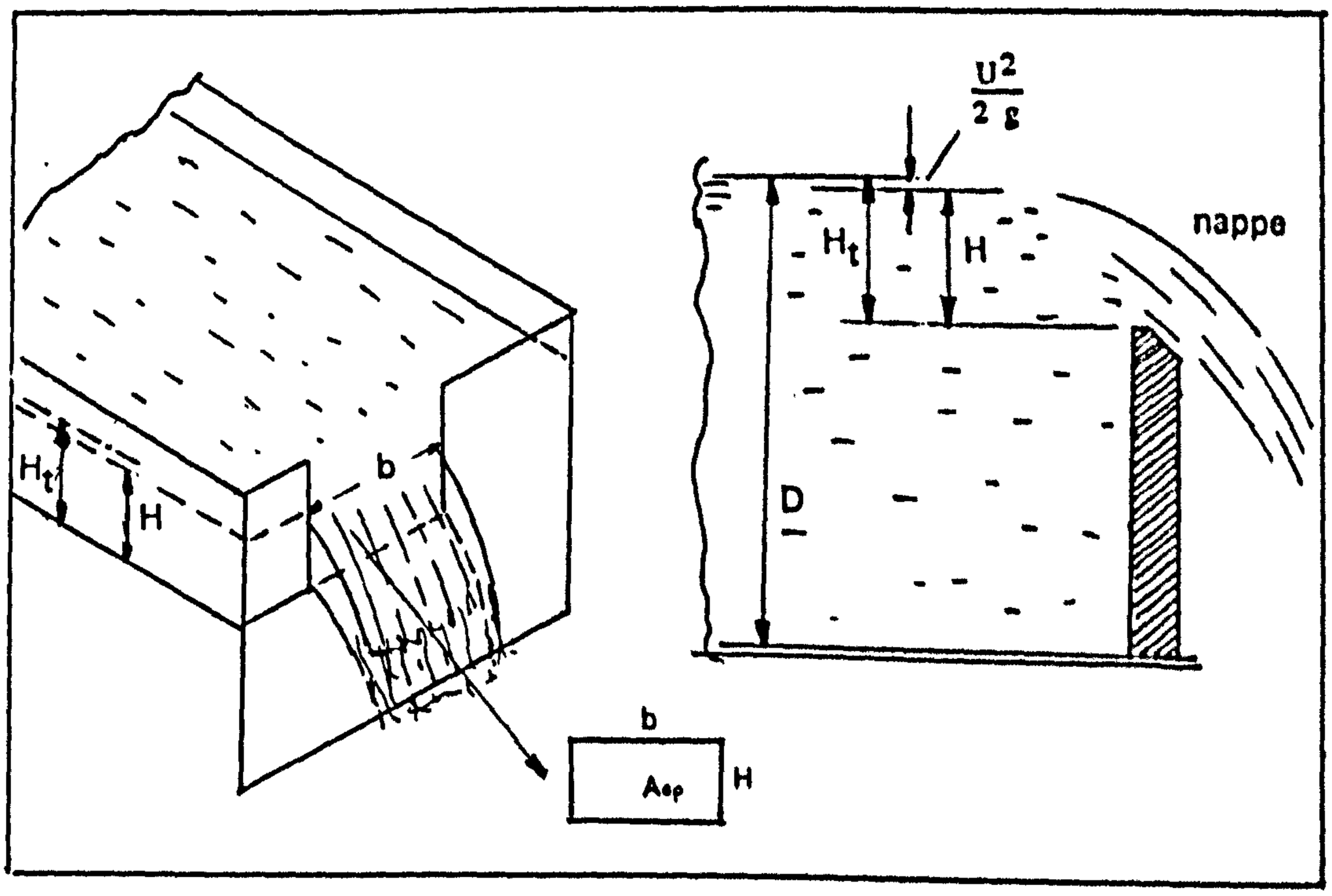

Fig A.3.2 Flow over a weir

A.4:

NUMERICAL SOLUTION OF THE EQUATION OF MOTIONS

First, the original equations can be written as follows:

Subscript i and j(X_{ij}) shows the type of motion. i,j=2 shows sway motion, i,j=3 shows the heave motion, and i,j=4 shows the roll motion.

Eq A.4.1:

$$(M + A_{22})\, X_2'' + B_{22}\, X_2' + A_{23}\, X_3'' + B_{23}\, X_3' + A_{24}\, X_4'' + B_{24}\, X_4' = F_{2wind} + F_{2wave}$$

$$(M + A_{33})\, X_3'' + B_{33}\, X_3' + RES_3(t,X_3,\theta,X_4) + A_{32}\, X_2'' + B_{32}\, X_2' + A_{34}\, X_4'' + B_{34}\, X_4' = F_{3wave} + F_{3wod}$$

$$(I_{44} + A_{44})\, X_4'' + B_{44}\, X_4' + RES_4(t,X_3,\theta,X_4) + A_{42}\, X_2'' + B_{42}\, X_2' + A_{43}\, X_3'' + B_{43}\, X_3' = M_{4wind} + M_{4wave} + M_{4wod}$$

X_2 : SWAY
X_3 : HEAVE
X_4 : ROLL

Forces can be rewritten as;

$$F_2 = F_{2wind} + F_{2wave}$$
$$F_3 = F_{3wave} + F_{3wod}$$
$$F_4 = M_{4wind} + M_{4wave} + M_{4wod}$$

For the computational solution, these equations can be arranged as follows [Eq A.4.2]:

$$X_2'' = \left(\frac{1}{(M_{22}+A_{22})}\right)[F_2 - [B_{22}\,X_2' + A_{23}\,X_3'' + B_{23}\,X_3' + A_{24}\,X_4'' + B_{24}\,X_4']]$$

$$X_3'' = \left(\frac{1}{(M_{33}+A_{33})}\right)[F_3 - [A_{32}\,X_2'' + B_{32}\,X_2' + B_{33}'\,X_3' + \mathrm{RES}_3(t,X_3,\theta,X_4) + A_{34}\,X_4'' + B_{34}\,X_4']]$$

$$X_4'' = \left(\frac{1}{(I_{44}+A_{44})}\right)[M_4 - [A_{42}\,X_2'' + B_{42}\,X_2' + A_{43}\,X_3'' + B_{43}\,X_3' + B_{44}\,X_4' + \mathrm{RES}_4(t,X_3,\theta,X_4)]]$$

Here X", X', X show acceleration, velocity and displacement respectively.

This system of second order non-linear differential equations given above are solved in the time domain using the Runge-Kutta numerical integration technique. The NAG library routines [59] provide several different numerical methods for solving non-linear equations. In order to solve a non-linear second order (or higher order) ordinary differential equation system, a system of ordinary differential equations has to be written in first form. This can be done by using the following changes:

For Sway (S)

$$X_2 = S_1$$
$$X_2' = S_1' = S_2$$
$$X_2'' = S_2'$$

For Heave (H)

$$X_3 = H_1$$

$$X_3' = H_1' = H_2$$

$$X_3'' = H_2''$$

For Roll (R)

$$X_4 = R_1$$

$$X_4' = R_1' = R_2$$

$$X_4'' = R_2''$$

In that case total number of the equation will be doubled for the computational solution and can be written in the new form as follows [Eq A.4.3]:

Sway

$$S1' = S2$$

$$S_2' = \left(\frac{1}{(M_{22}+A_{22})}\right)[F_2 - [B_{22}\, S_2 + A_{23}\, H_2' + B_{23}\, H_2 + A_{24}\, R_2' + B_{24}\, R_2]]$$

Heave

$$H1' = H2$$

$$H_2' = \left(\frac{1}{(M_{33}+A_{33})}\right)[F_3 - [A_{32}\, S_2' + B_{32}\, S_2 + B_{33}\, H_2 + RES_3(t,H_1,\theta,R_1) + A_{34}\, R_2' + B_{34}\, R_2]]$$

Roll

$$R1' = R2$$

$$R_2' = \left(\frac{1}{(I_{44}+A_{44})}\right)[M_4 - [A_{42}\, S_2' + B_{42}\, S_2 + A_{43}\, H_2' + B_{43}\, H_2 + B_{44}\, R_2 + RES_4(t,H_1,\theta,R_1)]]$$

In order to solve the above equations a number of boundary conditions which is equal to the number of equations in the system is required. This is so called an initial value problem because these boundary conditions are specified values at certain points such as the ones given below. These initial values are the initial displacements and velocities of the ship motions.

$$S_1 = S_{1o} \quad \text{at} \quad \text{time} = t_o$$
$$S_2 = S_{2o} \quad \text{at} \quad \text{time} = t_o$$

$$H_1 = H_{1o} \quad \text{at} \quad \text{time} = t_o$$
$$H_2 = H_{2o} \quad \text{at} \quad \text{time} = t_o$$

$$R_1 = R_{1o} \quad \text{at} \quad \text{time} = t_o$$
$$R_2 = R_{2o} \quad \text{at} \quad \text{time} = t_o$$

These initial conditions would enable the solution technique to integrate the equations numerically from the point t=to to specified end-time. For this integration the Nag routine named as D02BBF is used.

APPENDIX B:

MODEL EXPERIMENTS

B.1:

EXPERIMENTALLY AND THEORETICALLY CALCULATED MOMENT CREATED BY ROLL MOMENT MECHANISM

B.1.1 THEORETICAL CALCULATION METHOD

For two equal weights, each at one arm, rotating about point O (Fig B.1.1), the coupled moment acting can be calculated as:

$$M_e = F\ 2\ l \quad (N\text{-}m) \qquad \text{[Eq B.1.1]}$$

$$F = m\ \omega^2\ r \quad (N) \qquad \text{[Eq B.1.2]}$$

so,

$$M_e = m\ \omega^2\ r\ 2\ l\ (N\text{-}m) \qquad \text{[Eq B.1.3]}$$

B.1.2 EXPERIMENTAL CALCULATION PROCEDURE

- Calibration of roll mechanism

The roll mechanism is connected to the middle of a metal plate while two load cells are attached to both ends of the plate. The plate is clamped to the desk (Fig B.1.1). The roll mechanism has a control box and has rotation levels which have to be calibrated to find the equivalent frequency of each level. The roll mechanism also has to be calibrated for excitation moment and be compared to the theory. For this purpose the roll mechanism has been rotated at different levels and the forces were recorded on a chart recorder. From the chart recorder we can calculate amplitude of forces and the frequency of oscillation.

-Static Loading for Calibration of the Load Cell

Roll mechanism is attached to the beam both of whose edges are connected to the load cells (Fig B.1.1). Different weights are put directly above one of the load cells and voltage is read from the volt-meter. The static load is related to the equivalent coupled moment as follows:

$$M_{eq} = W\ G\ b\ z \quad (N\text{-}m) \qquad \text{[Eq B.1.4]}$$

$$M_{eq} = M_e = m\,\omega^2\,r\,z \text{ (N-m)} \qquad \text{[Eq B.1.5]}$$

where:

W: Static weight

ω : Frequency rad/sec

-Dynamic Loading

Same system in Fig B.1.1 was used and instead of static weights, the motor was used. The motor was put on at different levels of rotation speed and created force was measured by using load cell. These readings were recorded on a chart recorder. This procedure was repeated up to the maximum rotating speed. From the chart recorder the amplitude of voltage and frequency can be obtained. For the recorded voltages the equivalent moment can be obtained from the graph (voltage vs eq. moment). Dynamic moment can also be calculated theoretically if the weight and frequency are known [Eq B.1.5]. Calibration results can be seen in Table B.1.1. As seen in Fig B.1.2, theoretical and experimental results which are plotted as Moment vs Frequency, are very similar.

DIAL	FREQ [HERTZ]	AMPLITUDE [VOLTS]
2.0	0.208	0.005
2.5	0.265	
3.0	0.321	0.011
3.5	0.383	
4.0	0.463	0.022
5.0	0.613	0.039
6.0	0.775	0.061
7.0	1.010	0.106
8.0	1.234	0.15
9.0	1.522	0.226
10.0	1.572	0.228

Table B.1.1

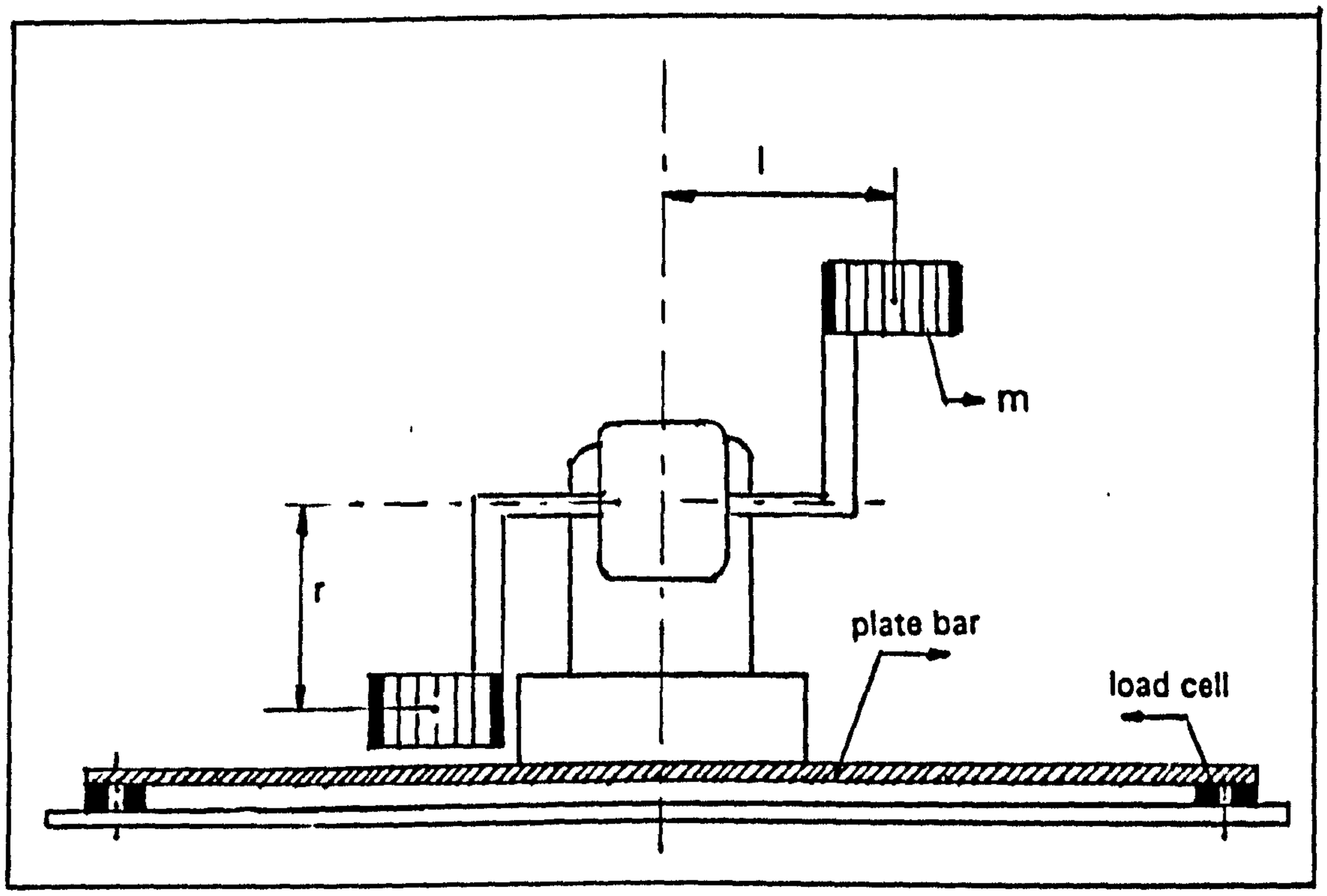

Fig B.1.1 Experimental set up to calibrate the roll moment mechanism

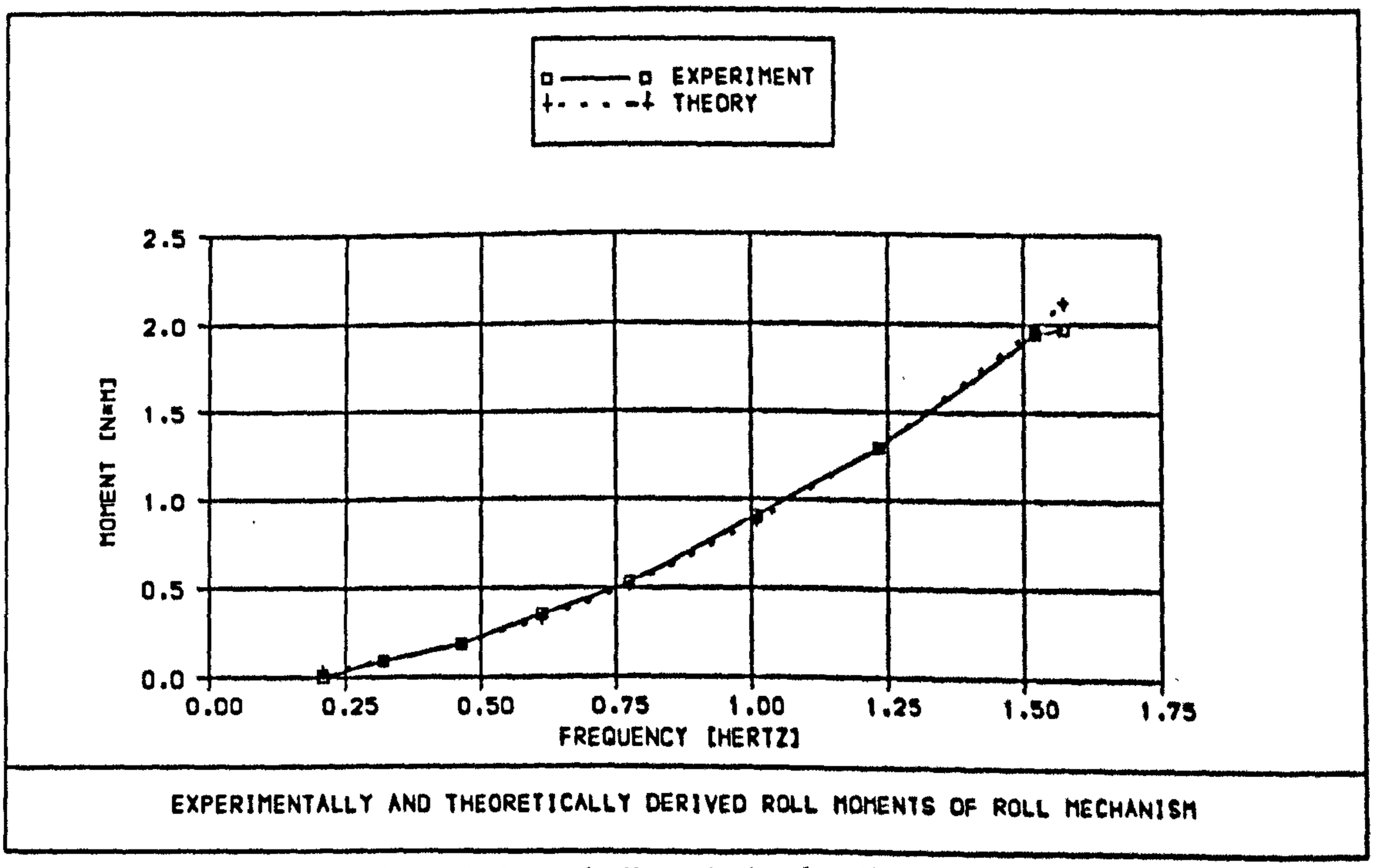

Fig B.1.2 Experimentally and theoretically calculated roll moments created by the roll moment mechanism

B.2:

DETERMINATION OF ROLL MASS MOMENT OF INERTIA FOR EXPERIMENTS

Mass moment of inertia of the ship can be estimated by using the following formula:

$$I = \frac{K}{\omega_n{}^2} \qquad \text{[Eq B.2.1]}$$

In order to reduce the error in measuring the roll period (Roll frequency) as explained in Chapter 6, as many cycles as possible must be recorded (in our case we measured 30 cycles). The following formulation is used to determine the mass moment of inertia of roll:

$$\omega_{sr} = \sqrt{\frac{K_{sr}}{I_{sr}}} \qquad \text{[Eq B.2.2]}$$

where:

ω_{sr} : Natural roll frequency of the system Rad/sec

$\omega_n = \frac{2\pi}{T_{sr}}$

K_{sr} : Stiffness of the system

I_{sr} : Mass moment of inertia of the system

$I_{sr} = \frac{K_{sr}}{\omega_{sr}{}^2}$

T_{sr} : Roll period of the system

T_{sr} = Total oscillating time/Total roll cycles

In the system there are two extra items, the steel bar and clamp which have to be taken into account for calculating the Ixx for the ship.

$$K_{sr} = K_{model} + K_{bar} + K_{clamp} \qquad \text{[Eq B.2.3]}$$

Stiffness is calculated simply by multiplying the mass of element, by

distance from rotation centre to centre of gravity of element.

Eq B.2.3:

$$K_{sr}=(M_{model}\ h_{model} + m_{bar}\ h_{bar} + m_{clamp}\ h_{clamp}) \times g$$

After finding the Is we have to substract the mass moment of inertia of bar and clamp which can be calculated by carrying out experiments. It can be done simply by detaching the ship from the whole mechanism. These values can be calculated theoretically as well.

The roll mass moment of inertia of model is then determined as:

$$I_M = I_{sr} - I_{bar} - I_{clamp} \qquad \text{[Eq B.2.4]}$$

B.2.1 CALIBRATIONS AND CALCULATIONS

Before mass moment of inertia of the system in Fig 6.A is calculated, calibration of the measuring system is carried out.

Weights

1-Bar	=	2.032 kg
2-Clamp	=	1.05 kg
2-Hook	=	0.454 kg
4-Weight	=	20.0 kg

-Mass Moment of inertia about pivot (theory)

$$I_{pivot} = I_{CG} + m\ h^2$$

For bar:

$$I_{pivot} = \frac{m\ l^2}{12} + m\ h^2$$

For weight and hook:

$$I_{pivot} = \frac{m\ l^2}{3} + m\ h^2$$

For clamp:

$$I_{pivot} = m\,k^2 + m\,h^2$$

Total I_{pivot}

$$I_p = 6.0344 \text{ kg } m^2$$

Where:

h : Distance between pivot and centre of gravity of each item

m : Weight of each item

l : Length of each item

-Mass Moment of Inertia About Pivot (Experiment)

Stiffness:

$$K = (m\,g\,h)_{bar} + (m\,g\,h)_{weight} + (m\,g\,h)_{clamp}$$

$$K = 113.442 \text{ N*m/rad}$$

From experiments, the period of the system obtained as:

$$T = 1.466 \text{ sec.} \quad (30 \text{ cycles in } 43.90 \text{ seconds})$$

$$I_{sr} = \frac{K_{sr}}{(2\,\pi\,/\,T_{sr})^2}$$

$$= 6.1756 \text{ kg } m^2$$

There is 2.34% difference between experiment and theory.

Comparison of Mass Moment of Inertia About Weight's Own CG Axis.

$$I_{CG(weight)} = I_p - (I_{CG})_{bar+clamp}\,[(m\,h^2)_{bar} + (m\,h^2)_{weight} + (m\,h^2)_{clamp}]$$

= 0.2253 (theory)
= 0.21990 (experiment)

The difference is 4.12%.

B.2.2 MEASUREMENTS AND DETERMINATION OF THE MASS MOMENT OF INERTIA

First we have to measure the mass moment of inertia of the bar and clamp;

T=1.12 sec. (from experiments ;12.32 sec. for 11 cycles)

stiffness of bar and clamp;

K= 7.2963 N m /rad

I_{pivot} of bar and clamp;

I_p=0.23183 kg m^2

Measurements and calculations were carried out for following conditions.

A-Roll

Mass of model = 45.17 kg
Oscillation = 38.87 sec. for 30 cycles
T_{sr} = 1.296 sec
K_{sr} = 151.753 N m/rad

Mass moment of inertia of the system about the pivot

I_{sp} = 6.45636 kg m^2

Mass moment of ineria of the model about pivot

$I_{pivot(model)}$ = I_{sp} - $I_{p(clamp+bar)}$
=6.22453 kg m^2

$I_{CG(model)}$ = $I_{pivot(model)}$ - $(m\ h^2)_{model}$

$= 1.42404 \text{ kg m}^2$

B- Heave-Roll

Mass of model = 44.63 kg
Oscillation = 38.73 sec for 30 cycles
T_{sr} = 1.294 sec
K_{sr} = 150.026 N m/rad

Mass moment of inertia of the system about pivot

I_{sp} = 6.3632 kg m^2
$I_{pivot(model)}$ = 6.13137 kg m^2
$I_{CG(model)}$ = 1.3883 kg m^2

C-Sway-Roll

Mass of model = 44.81 kg
Oscillation = 39 sec. for 30 cycles
T_{sr} = 1.3 sec
K_{sr} = 150.6014 N m/rad
I_{sp} = 6.44697 kg m^2
$I_{pivot(model)}$ = 6.21514 kg m^2
$I_{CG(model)}$ = 1.4529 kg m^2

If we deduct the mass moment of inertia of the heave bar:

$I_{CG(model)}$ = 1.4529-0.08778
= 1.3651 kg m^2

B.3: CALIBRATIONS

B.3.1 CALIBRATION OF LOAD CELL

The load cell is calibrated using different weights. The load cell is attached to the bar and a hook, and is suspended by clamping the bar. Different weights are attached to the hook and the voltage is recorded for each weight. Results are shown in the Fig B.3.1.

It is found that calibration of load cell is 20.223 kg/volt (1 volt is equal to 20.223 kg).

B.3.2 CALIBRATION OF LVDT

The LVDt is connected to the milling machine which has a very precise ruler. Lvdt bar is pulled by turning the mill wheel for different lengths and the voltage is measured. Results are shown in Fig B.3.2.

Calibration value is 0.5 volt/cm (0.5 volt shows the 1 cm amp).

6.3.3 CALIBRATION OF POTENTIOMETER

It is calibrated when it is attached to the rolling mechanism in the ship. An inclinometer is set to zero angle when the ship is at upright condition. Then different weights are shifted to one side, and heel angles and voltage are measured for each weight. Results of calibration are shown in Fig B.3.3.

Calibration is 34.52 deg/volt (1 volt is equal to the 34.52 deg.).

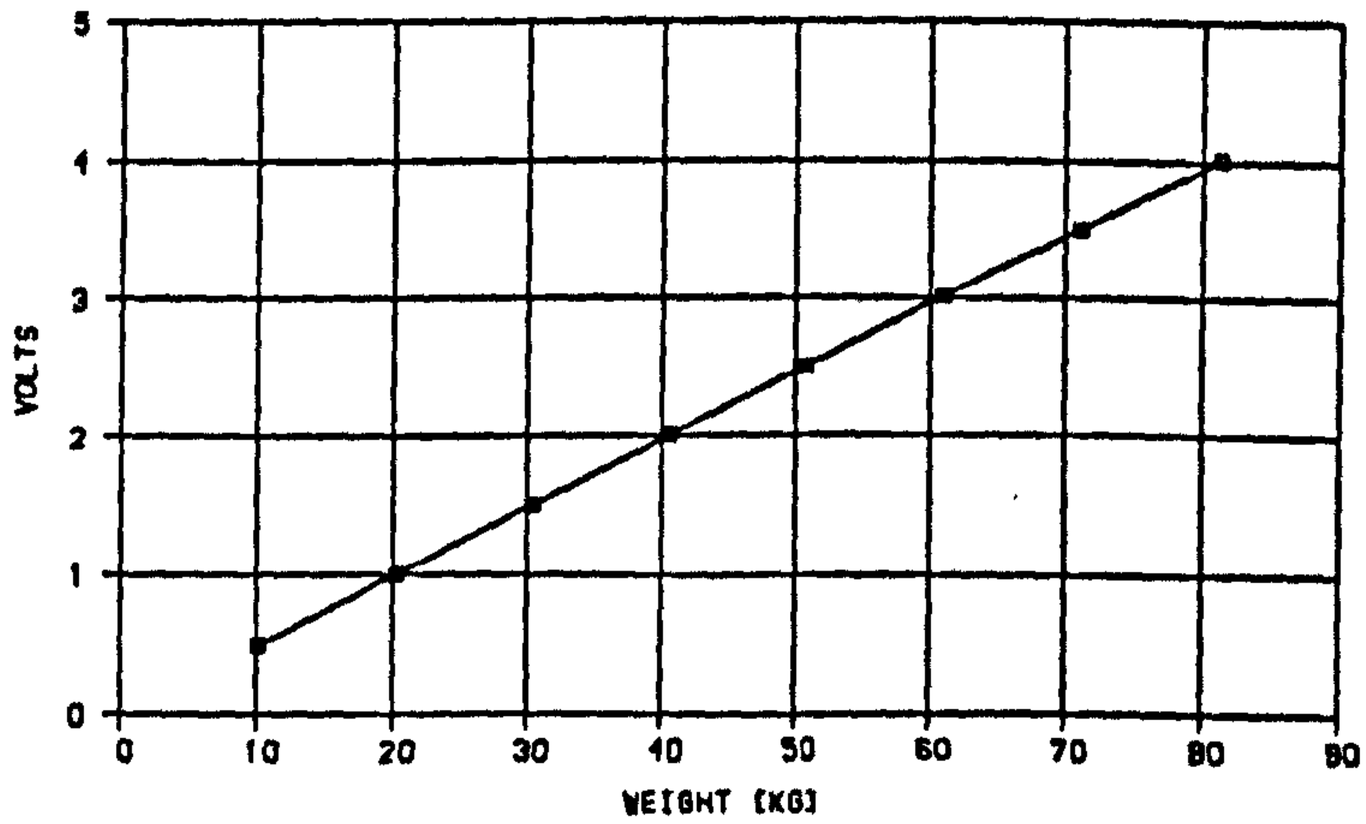

Fig B.3.1 CALIBRATION OF LOAD CELL (1 VOLT=20.223 KG)

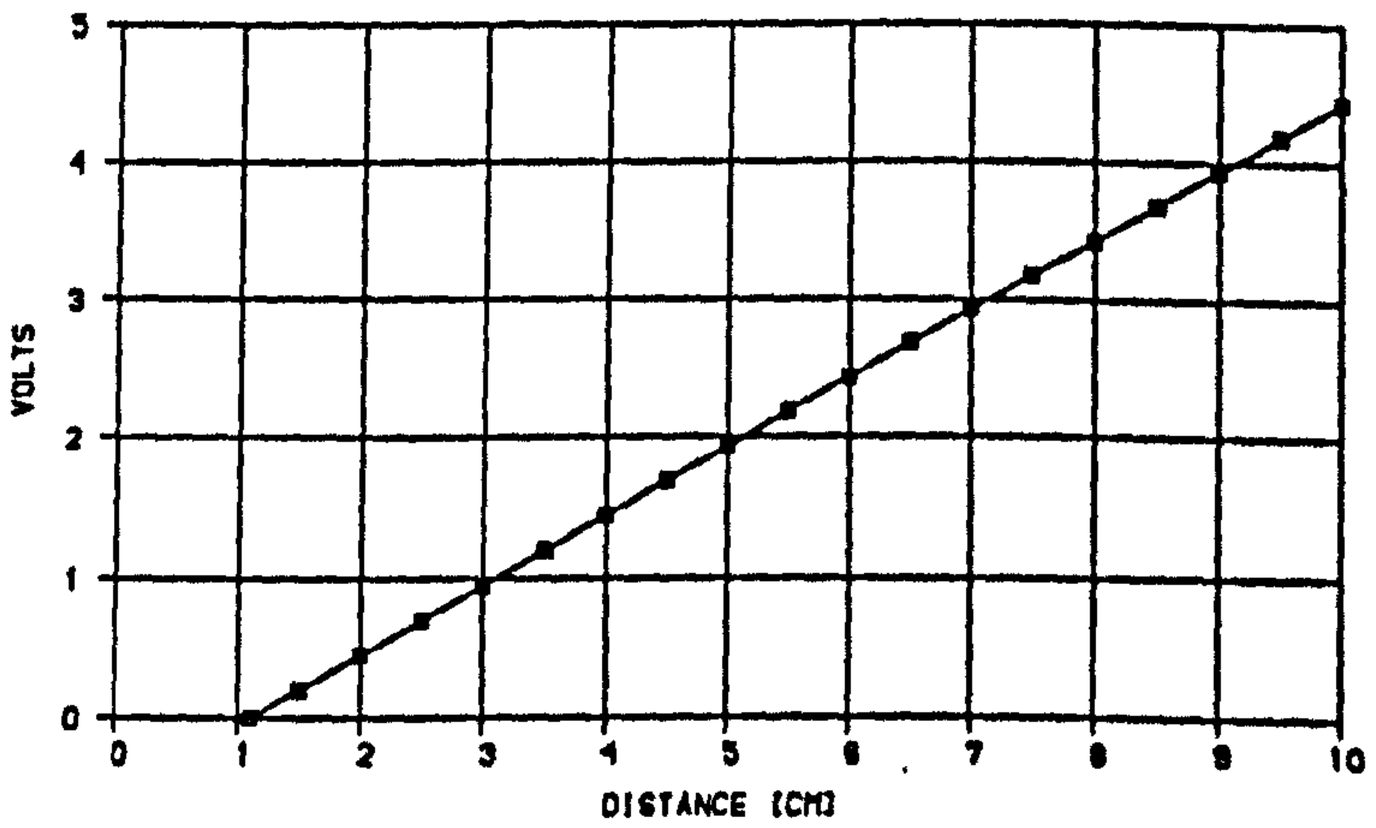

Fig B.3.2 CALIBRATION OF LVDT (0.5 VOLT=1 CM)

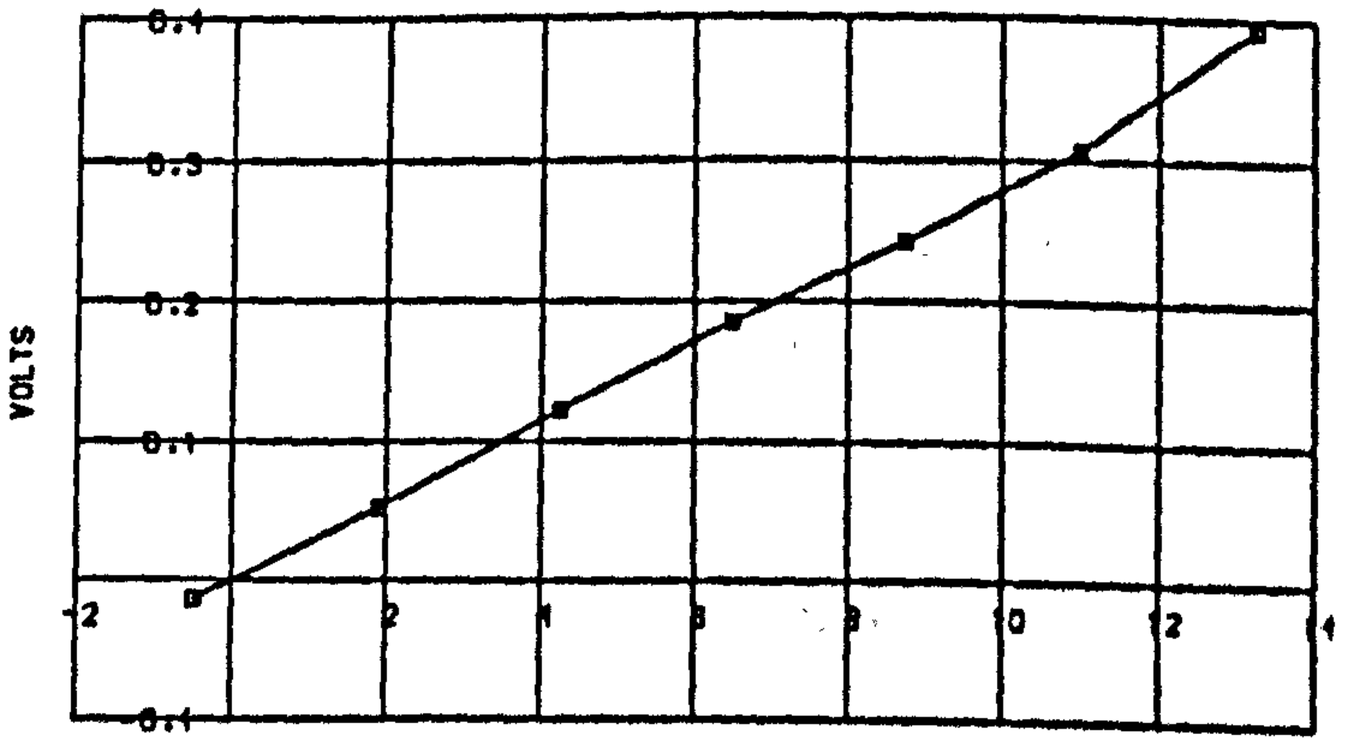

Fig B.3.3 CALIBRATION OF POTENTIOMETER (1 VOLT=34.32 DEG)

B.4: DETERMINATION OF STIFFNESS VALUES

B.4.1 ROLL STIFFNESS

Roll stiffness value for each angle of inclination is calculated experimentally. Roll stiffness is measured by adding weight statically and measuring the static angle. Roll stiffness values obtained for each angle are integrated up to the particular angle and divided by the angle to find the equivalent stiffness coefficient (K). This is done up to 25 degrees of inclination, and the stiffness is calculated for each angle by the following formulas:

$$RES_{R\phi i} = \frac{m\ d\ g\ Cos\phi_i}{\phi_i} \quad \text{(per unit amplitude)} \qquad \text{[Eq B.4.1]}$$

$$K_R(\phi_n) = \frac{\sum_{i=1}^{n} RES_{\phi i}}{\phi_n} \qquad \text{[Eq B.4.2]}$$

Where:

$RES_{\phi i}$: Roll stiffness for particular roll angle, per unit amplitude

K_R : Equivalent linearised roll stiffness for particular roll angle, per unit amplitude

m : Weight shifted

d : Distance between centre of rotation and centre of mass added (0.255 m)

ϕ_i : Heel angle for this particular weight (rad)

ϕ_n : Roll angle for which K_R is calculated

This experiment is carried out for upright condition as well as 6 and 10 degrees inclined conditions. Fig B.4.1, B.4.2 and B.4.3 show the roll stiffness and equivalent roll stiffness values for upright, 6 degrees static heel and 10 degrees static heel respectively.

B.4.2 HEAVE STIFFNESS (Experiments)

For each ballast condition and for each amplitude, values are calculated by using load cell. The ship at a particular condition, is first pushed into the water by turning the disk to the lowest position and then the static force is measured. Then the ship is lifted up by turning the disk to the highest point and static force is measured. The

average of these two values is taken and converted to the heave stiffness coefficient.

$$H_s = \frac{F\ G}{Z_0} \qquad \text{[Eq B.4.3]}$$

Where:

F : Static force measured, (N)

Z_0: Heave amplitude

Results are as follows:

Amplitude	Static Heel	Heave Stiffness
(m)	(Deg)	N/m
0.02	0.0	6854.0
0.04	0.0	6934.0
0.02	6.0	6656.0
0.02	12.0	6696.0

B.4.3 HEAVE INTO ROLL COUPLED STIFFNESS (Experiments)

These values are also calculated by experiments. For particular asymmetrical condition the ship is pushed into the water and lifted for a particular amplitude. The change in static heel between maximum and minimum position of heave amplitude is measured and the average value of these two values is taken. The difference in static heel between the rest condition, and average heel due to heave, is calculated. Then the heave into roll stiffness value is calculated using the following formula:

$$K_{hr} = \frac{RES_R\ \Delta\phi}{Z_0} \qquad \text{[Eq B.4.4]}$$

RES_R : Roll stiffnes value at given angle

$\Delta\phi$: Change in static heel

Z_0 : Heave amplitude

Results are as follows:

Static Heel	Heave Amplitude	Change in Heel	Roll stiffness	Heave-Roll Stiffness
(Deg)	(metre)	(Deg)	N m/rad	N
10.3	0.04	1.9	25.58	22.03
10.3	0.02	1.8	25.581	11.03
6.0	0.02	1.9	26.607	22.05

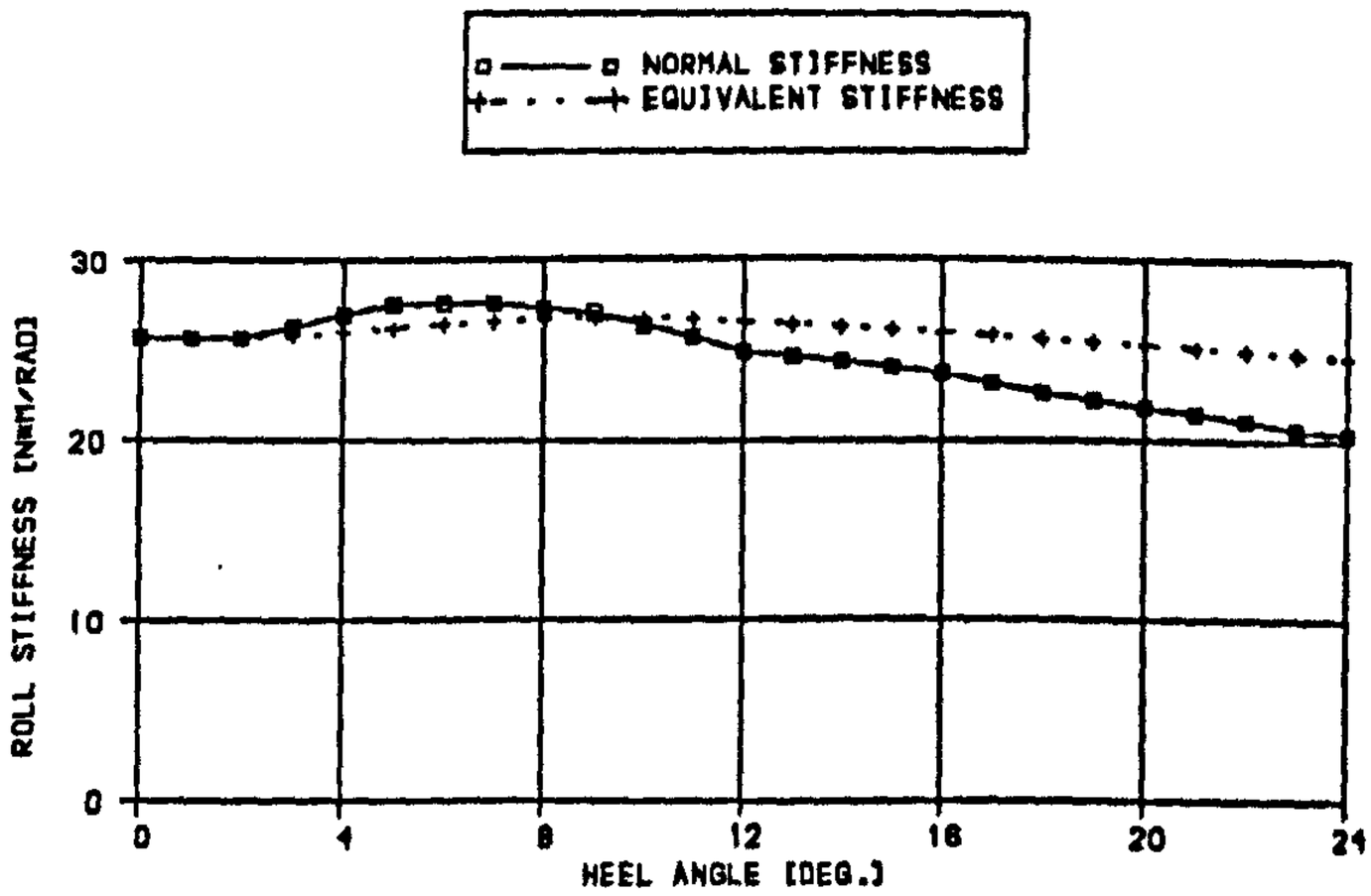

Fig B.4.1 COMPARISON BETWEEN NORMAL AND EQUIVALENT ROLL STIFFNESS VALUES UPRIGHT CONDITION

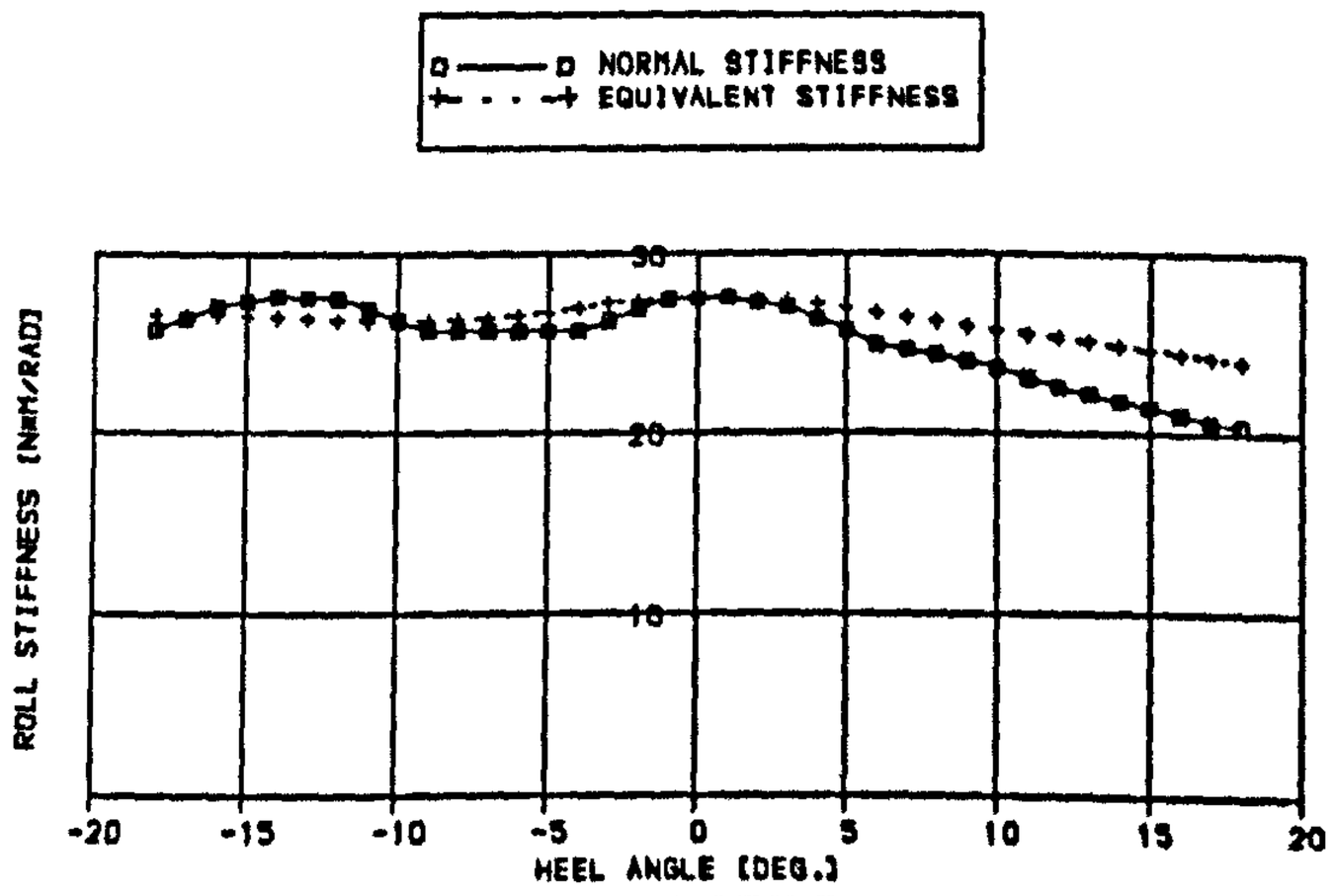

Fig B.4.2 COMPARISON BETWEEN NORMAL AND EQUIVALENT ROLL STIFFNESS VALUES INCLINED CONDITION, STATIC HEEL=6 DEG [0 deg in Fig refers to 6 deg]

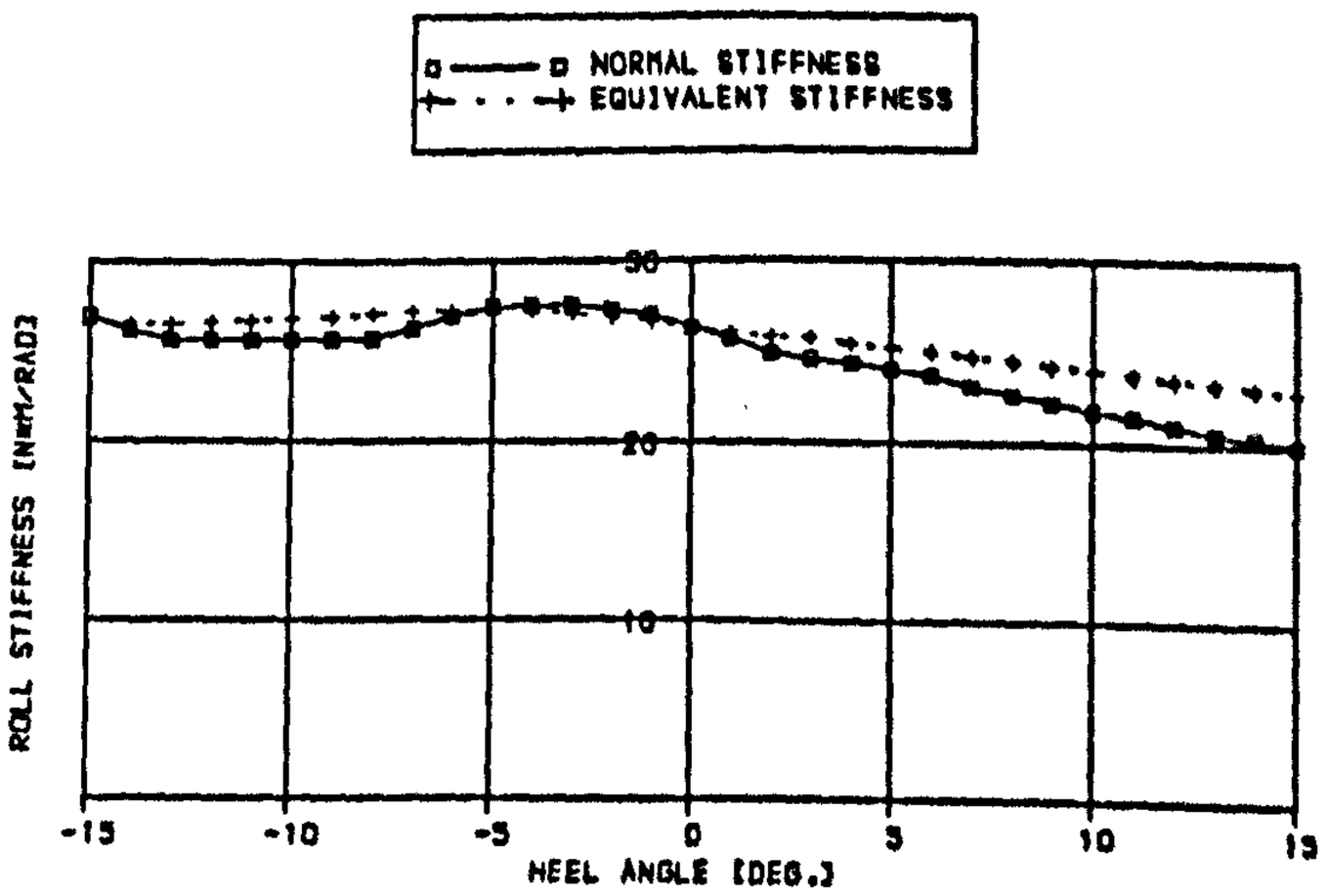

Fig B.4.3 COMPARISON BETWEEN NORMAL AND EQUIVALENT ROLL STIFFNESS VALUES INCLINED CONDITION STATIC HEEL=10.3 DEG [0 deg in Fig refers to 10.3 deg]

B.5:

DERIVING THE MATHEMATICAL EQUATIONS FOR HYDRODYNAMIC COEFFICIENTS

The equations to calculate added mass and damping coefficients, as well as coupling coefficients are derived by using motion equations as follows.

B.5.1 SINGLE DEGREE OF FREEDOM

$$(M_j+A_{jj})X_j''+ B_{jj} X_j' + K_{jj} X_j= F_j \qquad \text{[Eq B.5.1]}$$

$$X_j = X_{j0} \cos(\omega_o t-\varepsilon_j) \qquad \text{[Eq B.5.2]}$$

$$X_j' = -X_{j0} \omega_o \sin(\omega_o t-\varepsilon_j) \qquad \text{[Eq B.5.3]}$$

$$X_j'' = -X_{j0} \omega_o^2 \cos(\omega_o t-\varepsilon_j) \qquad \text{[Eq B.5.4]}$$

$$F_n = F_{j0} \cos(\omega_e t) \qquad \text{[Eq B.5.5]}$$

If the following changes are done and the equation is separated:

$$\cos(\omega_o t-\varepsilon)= \cos\omega_o t \sin\varepsilon + \sin\omega_o t \sin\varepsilon \qquad \text{[Eq B.5.6]}$$

$$\sin(\omega_o t-\varepsilon)= \sin\omega_o t \cos\varepsilon - \cos\omega_o t \sin\varepsilon \qquad \text{[Eq B.5.7]}$$

We can have 2 equations as:

$$-(I+A_{jj}) X_{j0} \omega_o^2 \cos\omega_o t \cos\varepsilon_j + B_{jj} X_{j0} \omega_o \cos\omega_o t \sin\varepsilon_j + K_{jj} X_{j0} \cos\omega_o t \cos\varepsilon_n= F_0 \cos\omega_e t \qquad \text{[Eq B.5.8]}$$

$$-(I+A_{jj}) X_{j0} \omega_o^2 \sin\omega_o t \sin\varepsilon_j - B_{jj} X_{j0} \omega_o \sin\omega_o t \cos\varepsilon_j + K_{jj} X_{j0} \sin\omega_o t \sin\varepsilon_j= 0 \qquad \text{[Eq B.5.9]}$$

For the experiments excitation frequency and response frequency are the same frequency ($\omega_o=\omega_e$), hence we denote the frequency as ω_c. If

we solve these equations we obtain the pure added mass and damping coefficients as follows:

$$A_{jj} = \frac{1}{\omega_e^2}\left(K_{jj} - \frac{F_{j0}\cos\varepsilon_j}{X_{j0}} \right) - M_{jo} \qquad \text{[Eq B.5.10]}$$

$$B_{jj} = \frac{F_{j0}\sin\varepsilon_j}{X_{j0}\,\omega_e} \qquad \text{[Eq B.5.11]}$$

Where:

B_{jj}: Damping coefficient
K_{jj} : Stiffness
M_j : Mass
I_{jj} : Mass moment of inertia
ε_j : Phase angle
ω_e : Frequency (rad/sec)

B.5.2 TWO DEGREE OF FREEDOM

After finding all the pure added mass and damping coefficients for each motion, coupled motion is solved to derive the coupling coefficients.

We can show the equation of the motion forced as:

$$(M_j + A_{jj})\, X_j'' + B_{jj}\, X_j' + K_{jj}\, X_j = F_j \qquad \text{[Eq B.5.12]}$$

and the equation of motion coupled due to the forced motion, as [Eq B.5.13]:

$$(M_i + A_{ii})\, X_i'' + B_{ii}\, X_i' + K_{ii}\, X_i\, A_{ij}\, X_j'' + B_{ij}\, X_j' + K_{ij}\, X_j = 0$$

Where:

A_{ii}, A_{jj} : Pure added mass coefficients determined from single degree of freedom motion
B_{ii},B_{jj} : Pure damping coefficients
A_{ij} : Coupled added mass coefficient (N into M)
B_{ij} : ,, damping ,, ,, ,, ,,
K_{ij} : ,, stiffness ,, ,, ,, ,,

If we solve the second equation by the same method used in single degree solution, coupled coefficients can be derived as follows:

[Eq B.5.14]:

$$A_{ij}=\left(\frac{-(M_i+A_{ii})\,X_{i0}\,\omega_e{}^2\cos(\varepsilon_i-\varepsilon_j)+B_{ii}\,X_{i0}\,\omega_e\sin(\varepsilon_i-\varepsilon_j)+K_{ii}\,X_{i0}\cos(\varepsilon_i-\varepsilon_j)+K_{ij}\,X_{j0}}{X_{j0}\,\omega_e{}^2}\right)$$

[Eq B.5.15]:

$$B_{ij}=\left(\frac{(M_i+A_{ii})+X_{i0}\,\omega_e{}^2\,\mathrm{Cos}\varepsilon_i-B_{ii}\,X_{i0}\,\omega_e\,\mathrm{Sin}\varepsilon_i-K_{ii}\,X_{i0}\,\mathrm{Cos}\varepsilon_i+A_{ij}\,X_{j0}\,\omega_e{}^2\cos\varepsilon_j-K_{ij}\,X_{j0}\cos\varepsilon_j}{X_{j0}\,\omega_e\,\mathrm{Sin}\varepsilon_j}\right)$$

B.6: RESULTS OF THE MODEL EXPERIMENTS

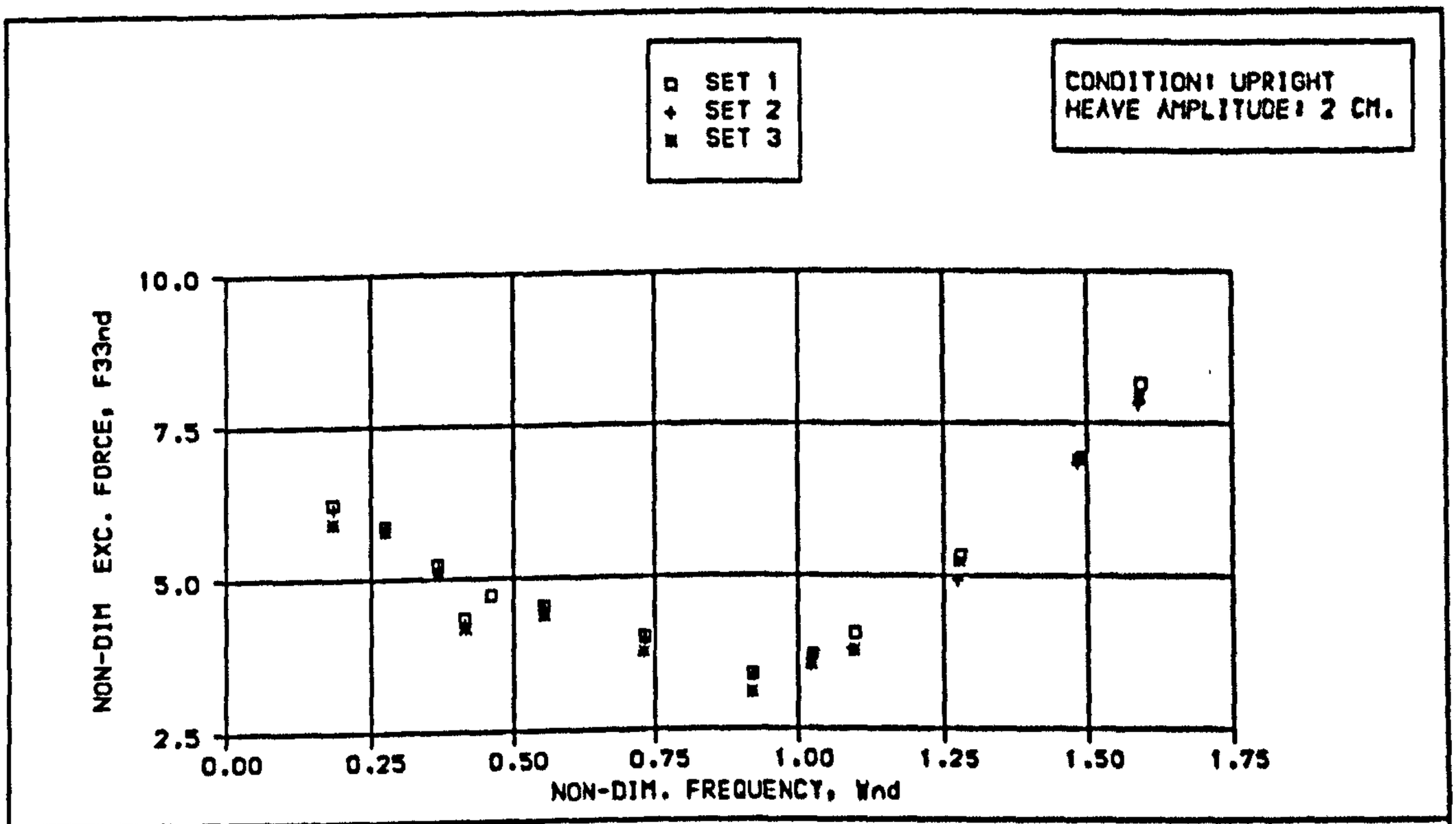

Fig B.6.1A REPETITION OF EXPERIMENTS FOR HEAVE MOTION (FORCE)

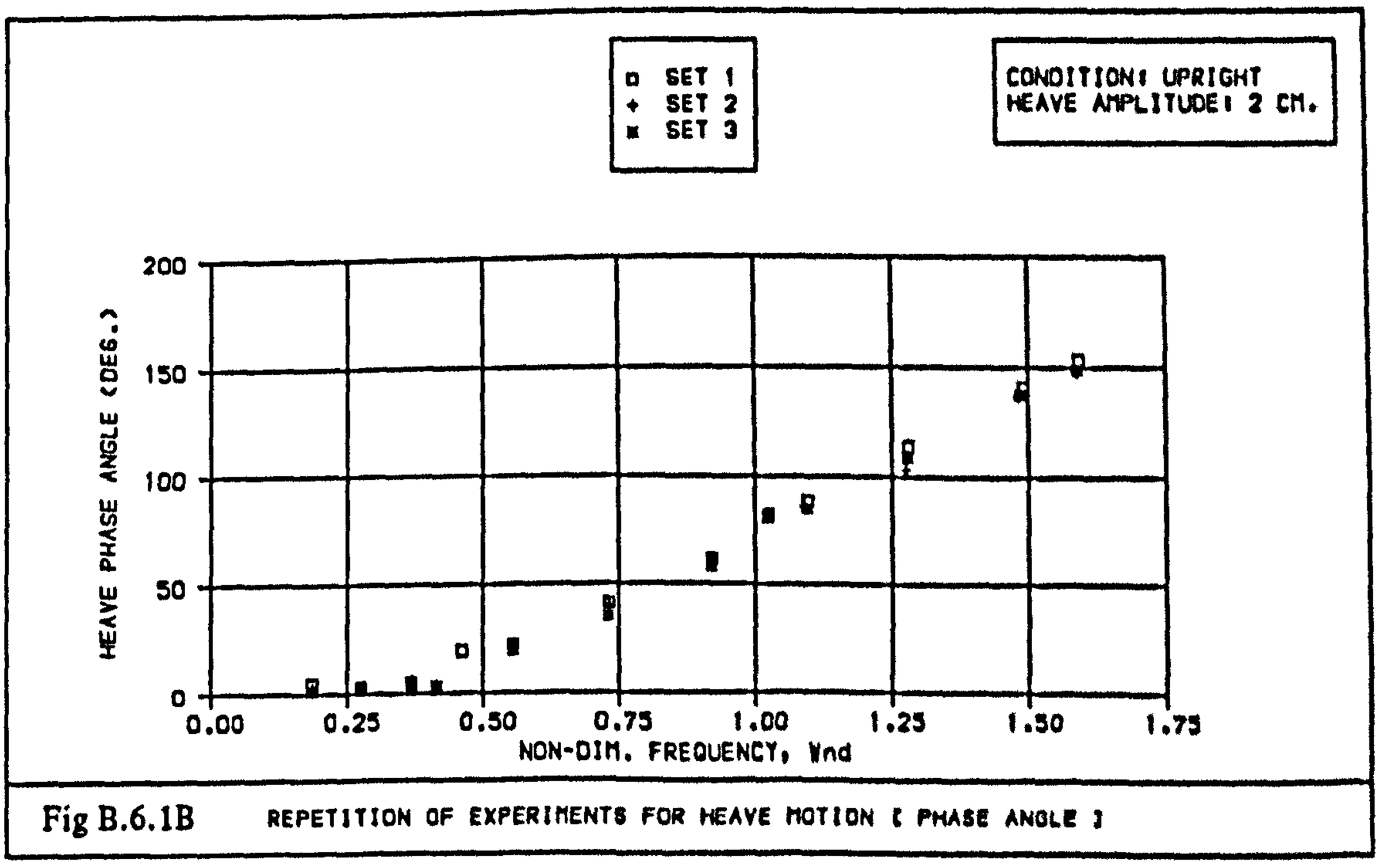

Fig B.6.1B REPETITION OF EXPERIMENTS FOR HEAVE MOTION (PHASE ANGLE)

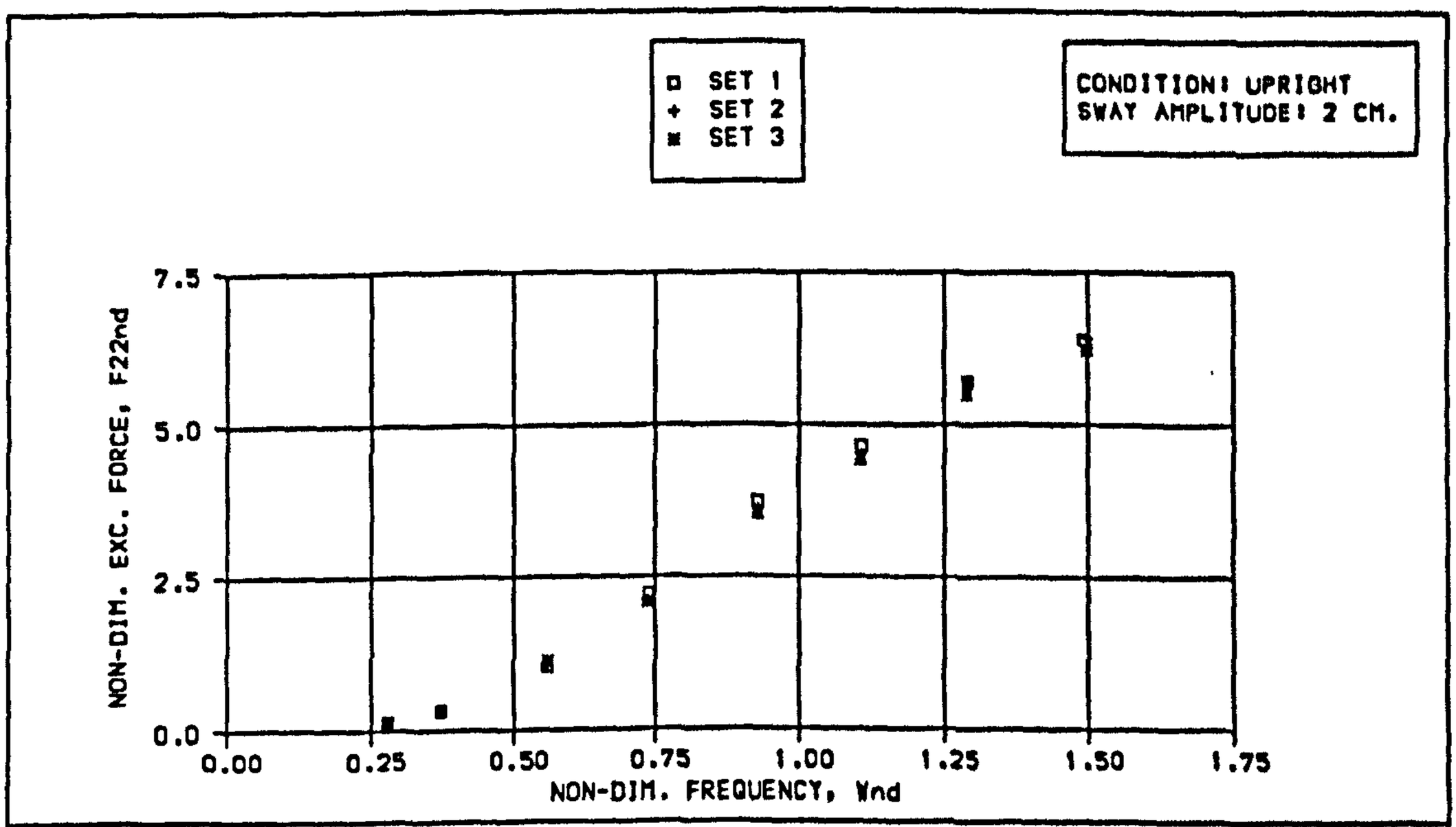

Fig B.6.2A REPETITION OF EXPERIMENTS FOR SWAY MOTION [EXC. FORCE]

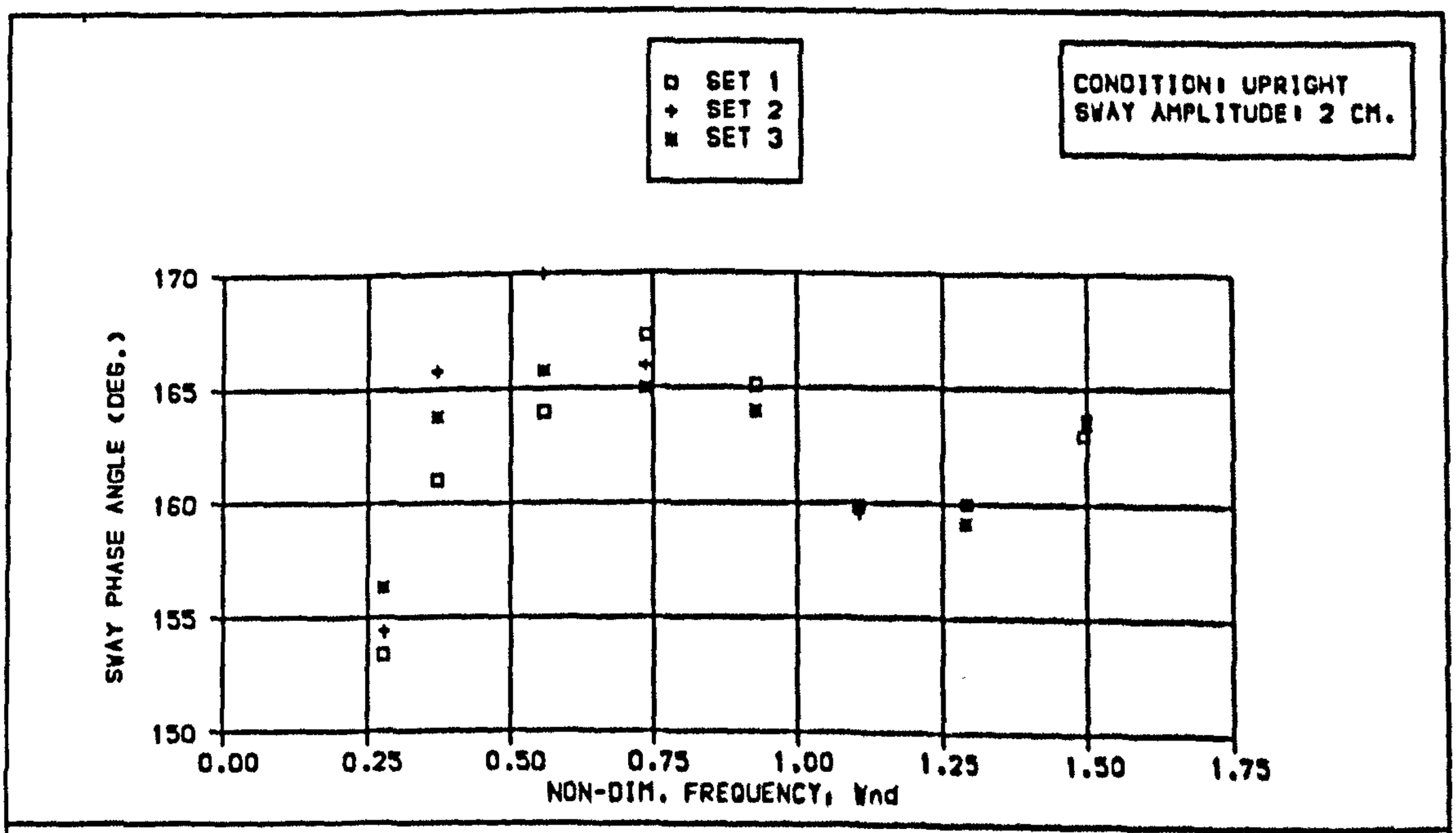

Fig B.6.2B REPETITION OF EXPERIMENTS FOR SWAY MOTION [PHASE ANGLE]

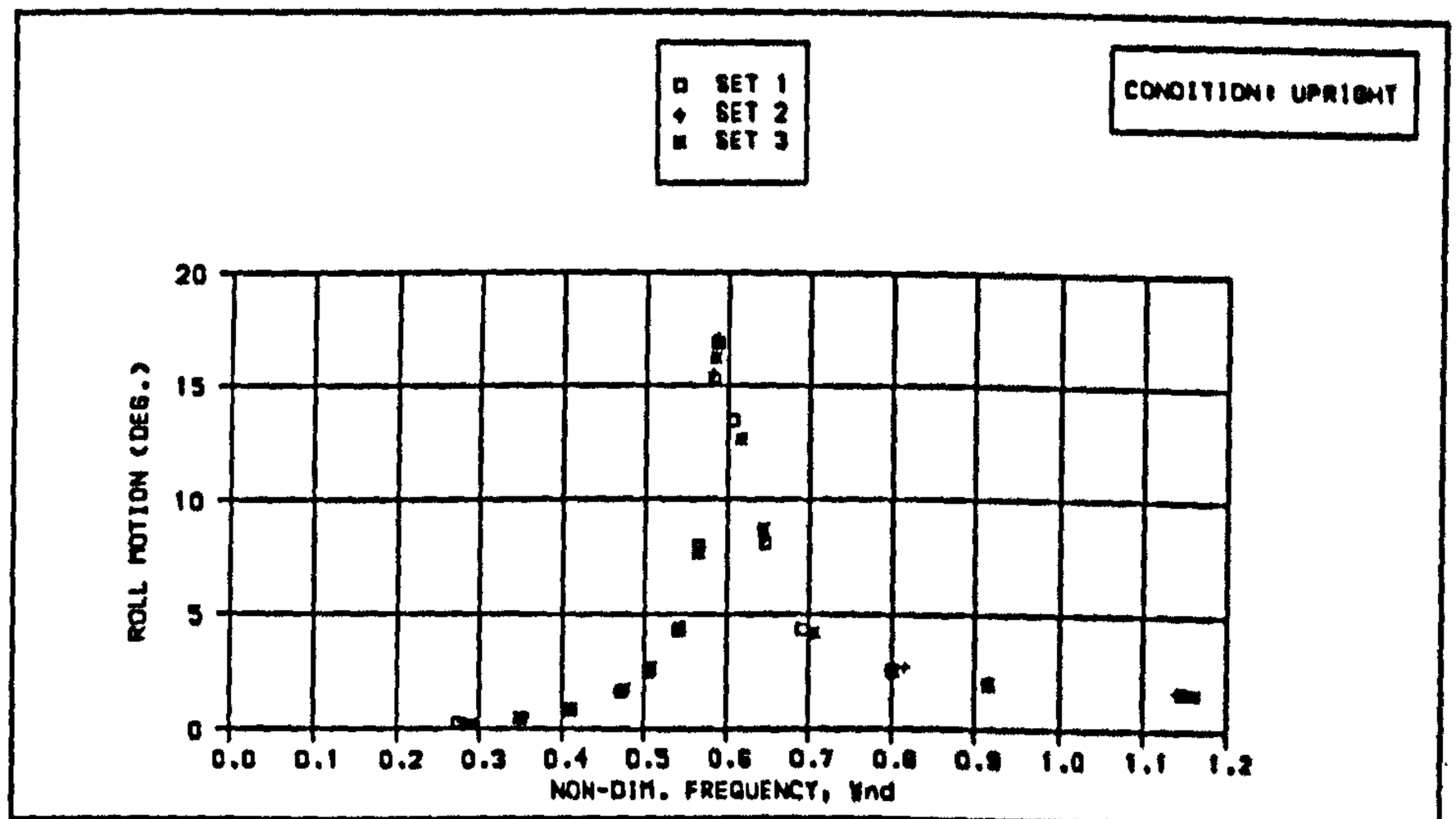

Fig B.6.3A REPETITION OF EXPERIMENTS FOR ROLL MOTION (ROLL RESPONSE)

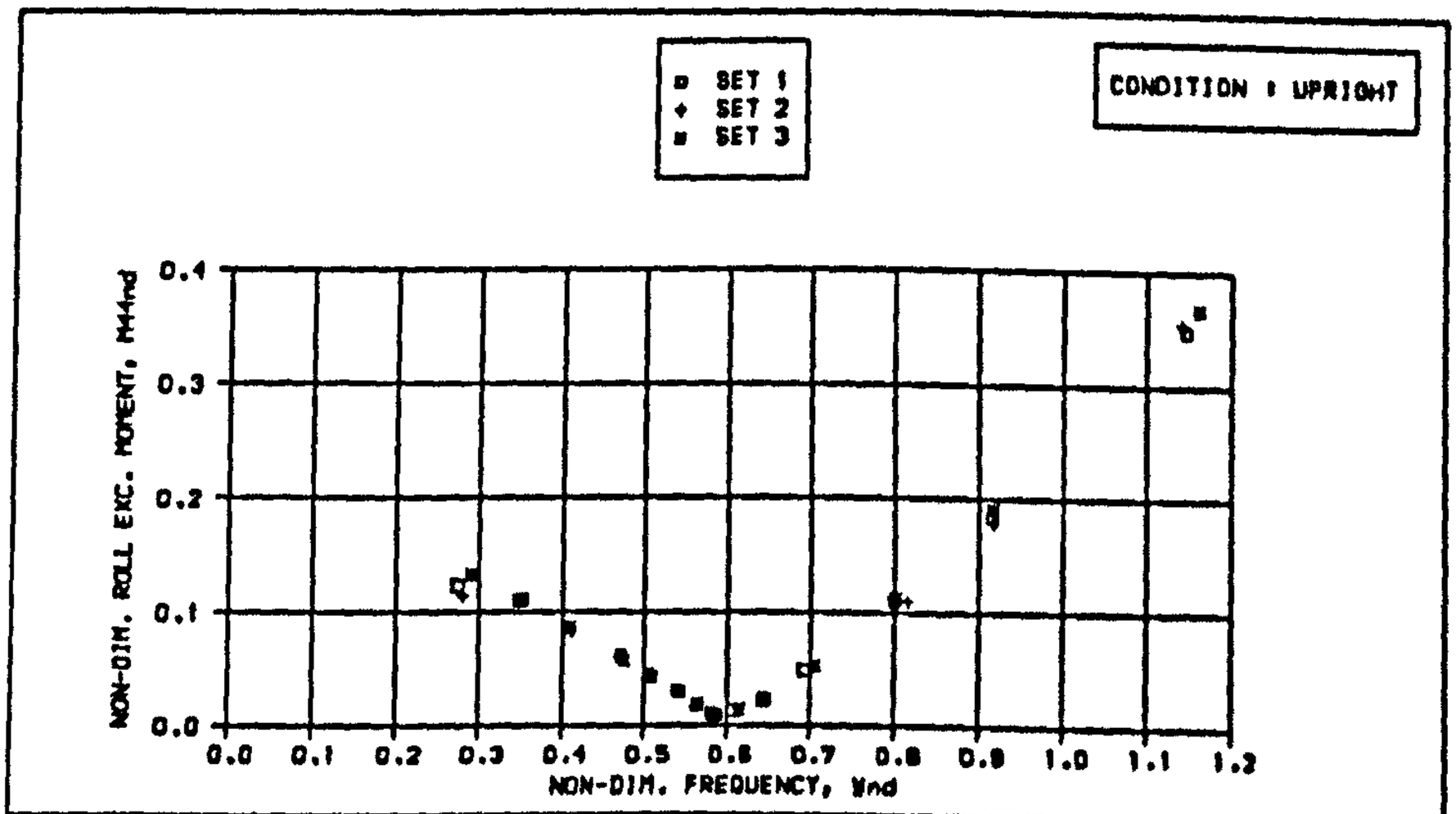

Fig B.6.3B REPETITION OF EXPERIMENTS FOR ROLL MOTION (EXC. MOMENT)

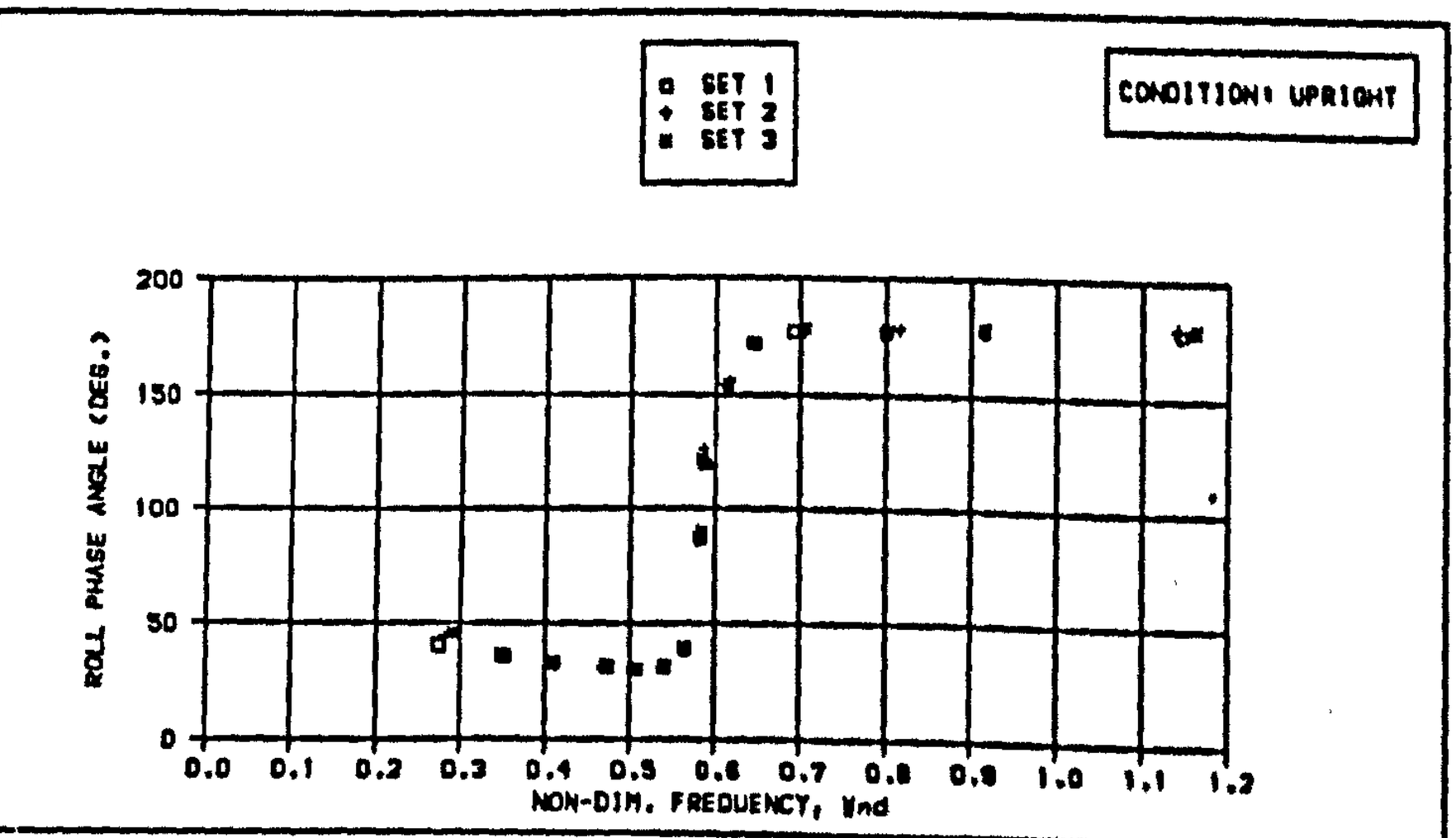

Fig B.6.3C REPETITION OF EXPERIMENTS FOR ROLL MOTION (PHASE ANGLE)

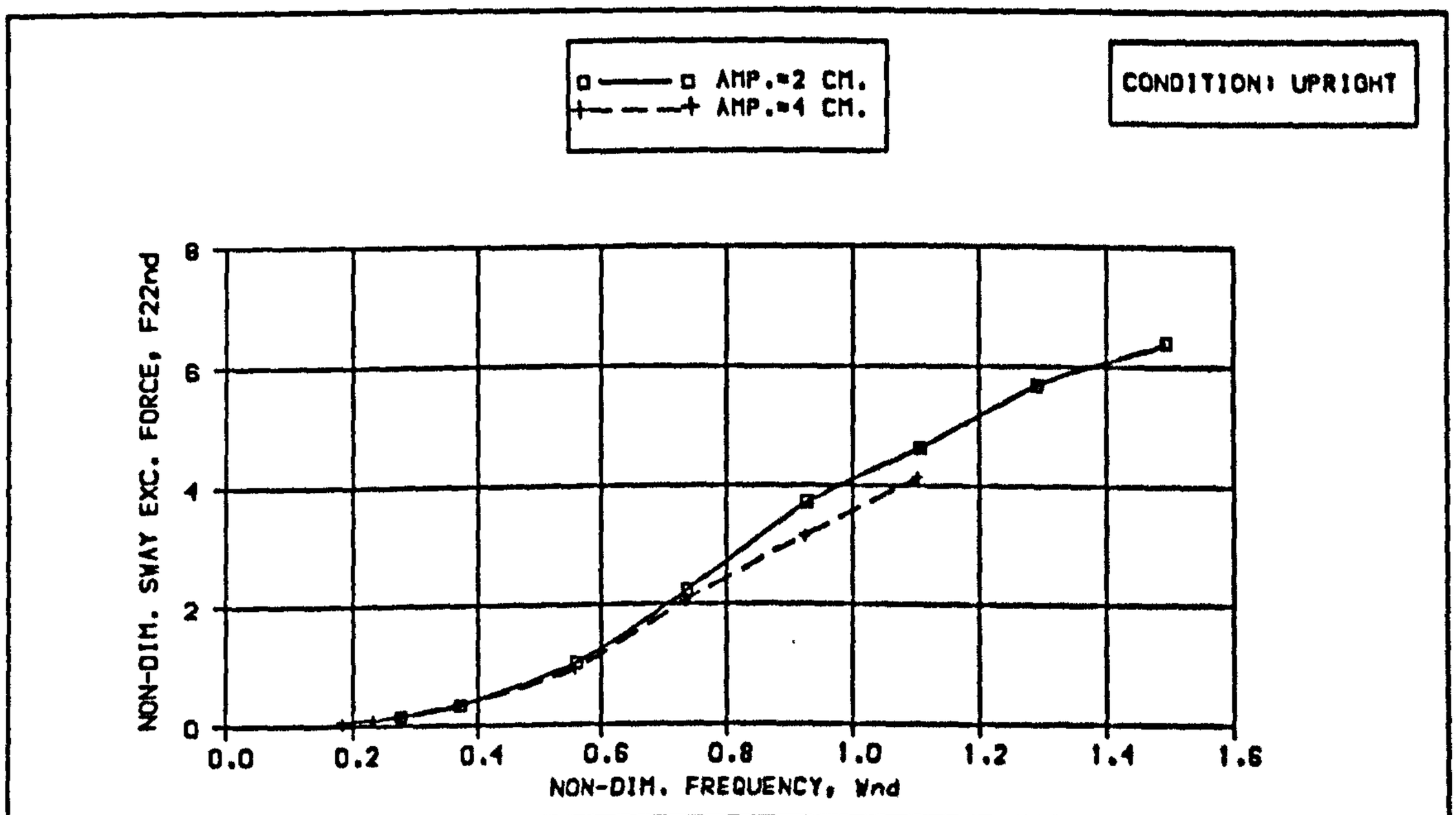

Fig B.6.4A EFFECT OF AMPLITUDE ON SWAY EXCITATION FORCE

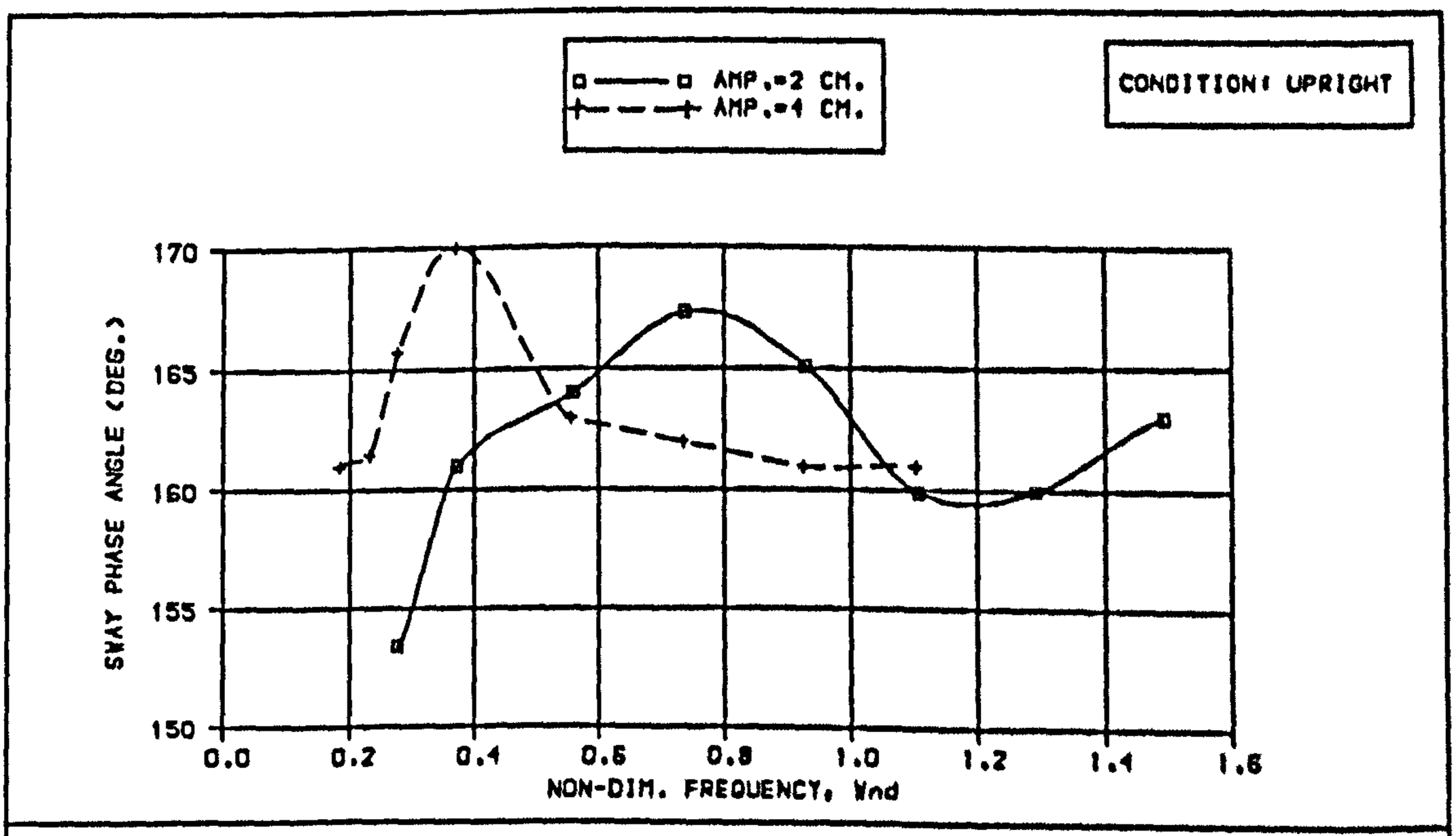

Fig B.6.4B EFFECT OF AMPLITUDE ON SWAY PHASE ANGLE

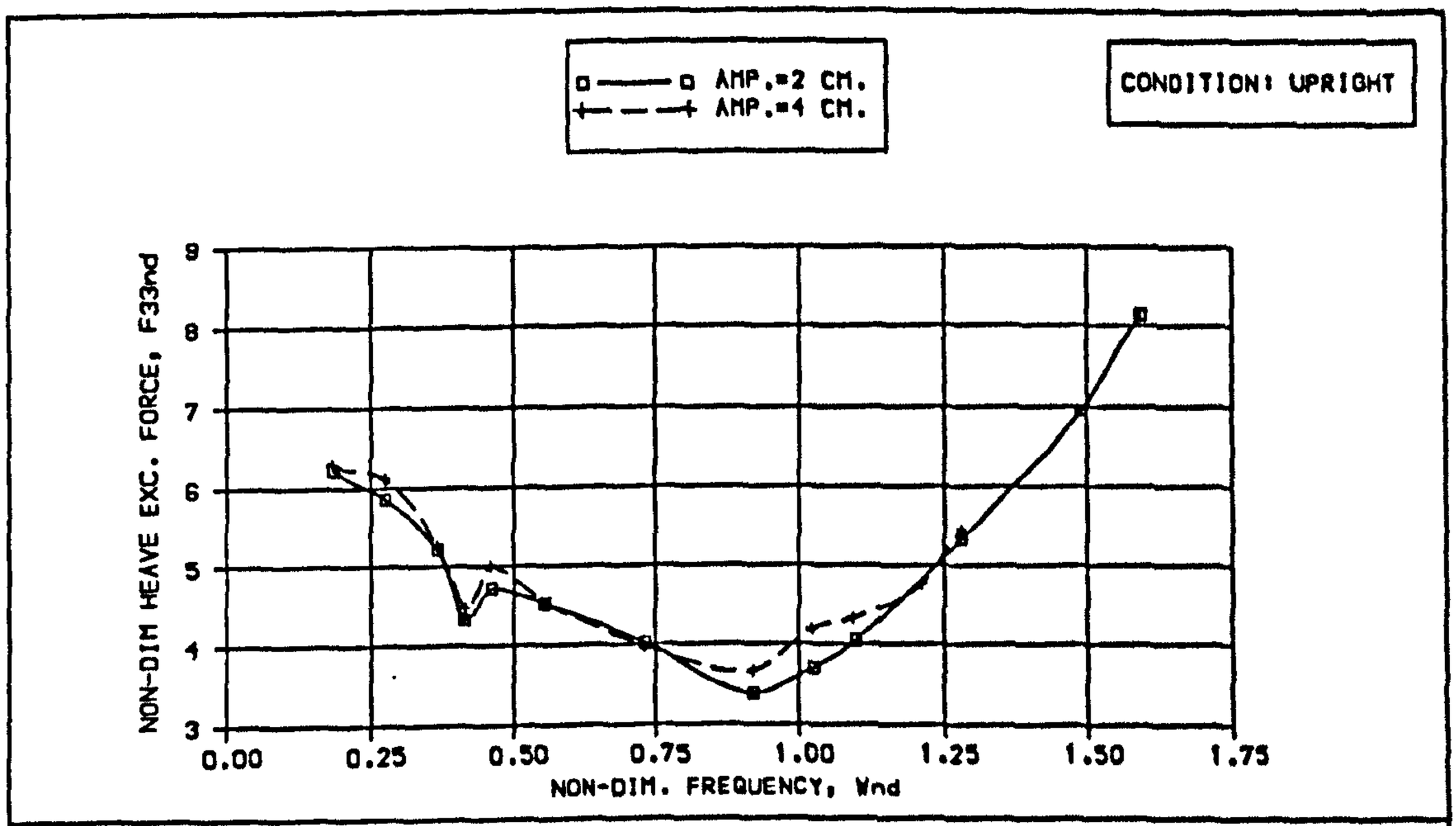

Fig B.6.5A EFFECT OF AMPLITUDE ON HEAVE EXC. FORCE

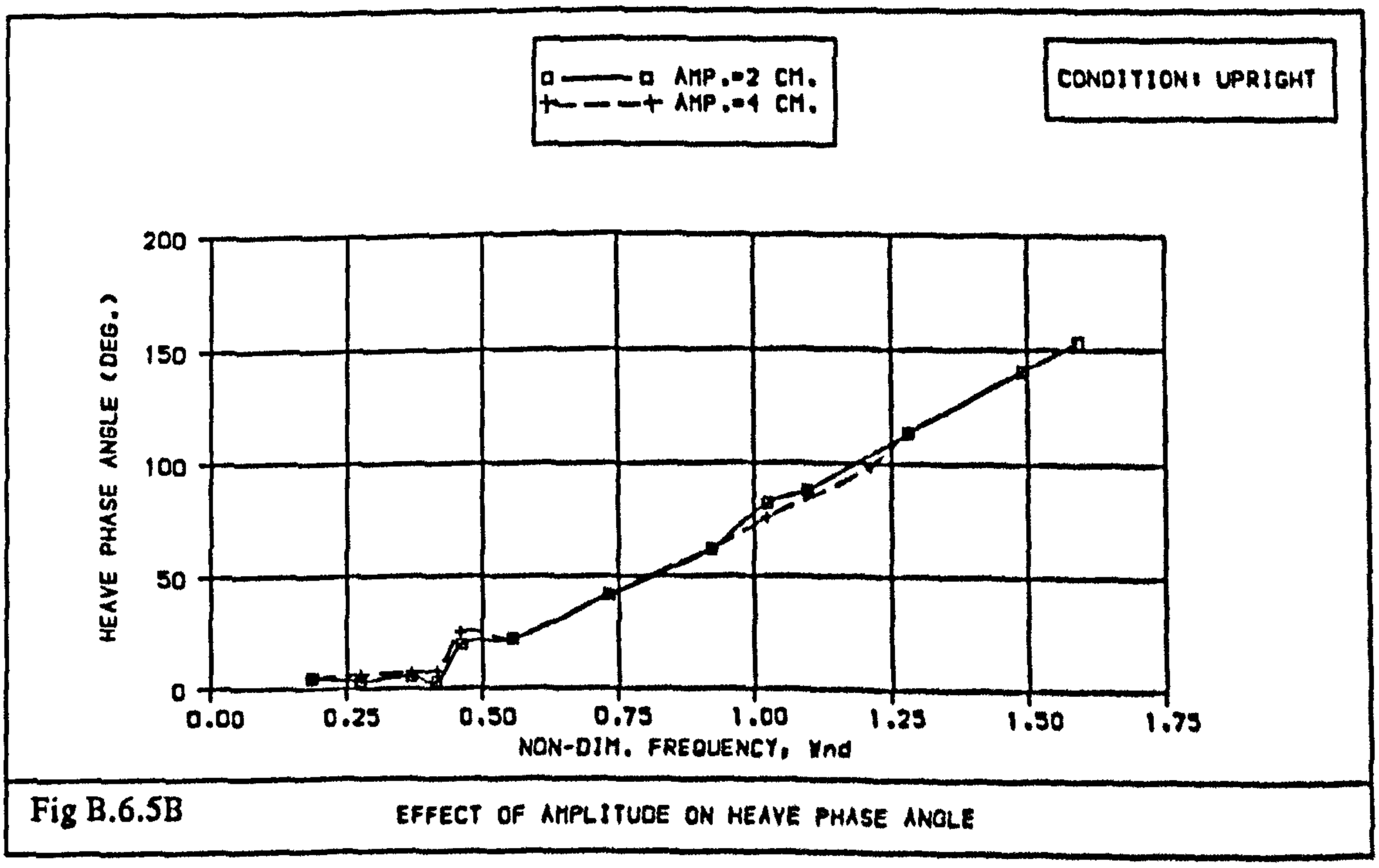

Fig B.6.5B EFFECT OF AMPLITUDE ON HEAVE PHASE ANGLE

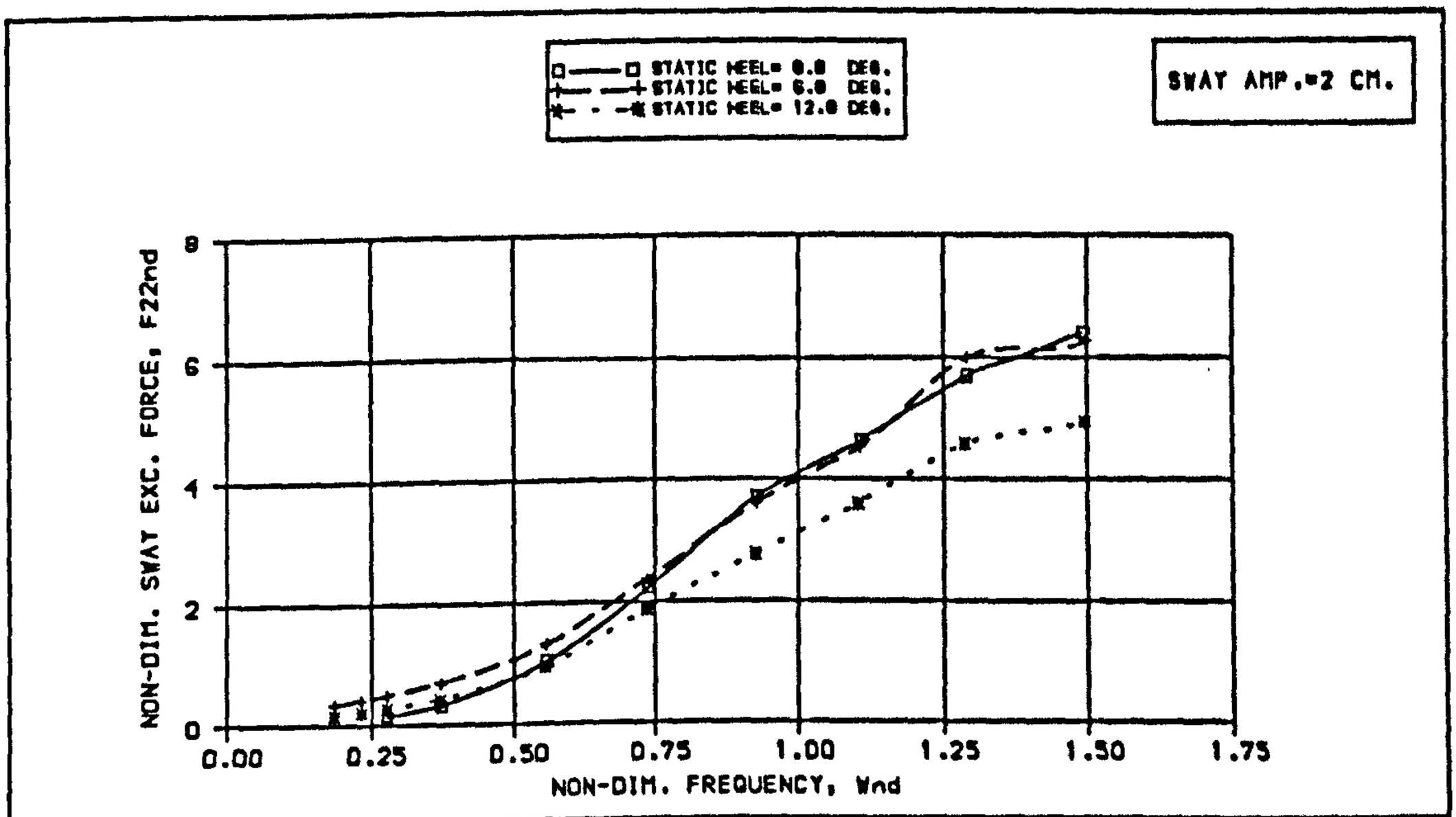

Fig B.6.6A EFFECT OF STATIC HEEL ON SWAY EXCITATION FORCE

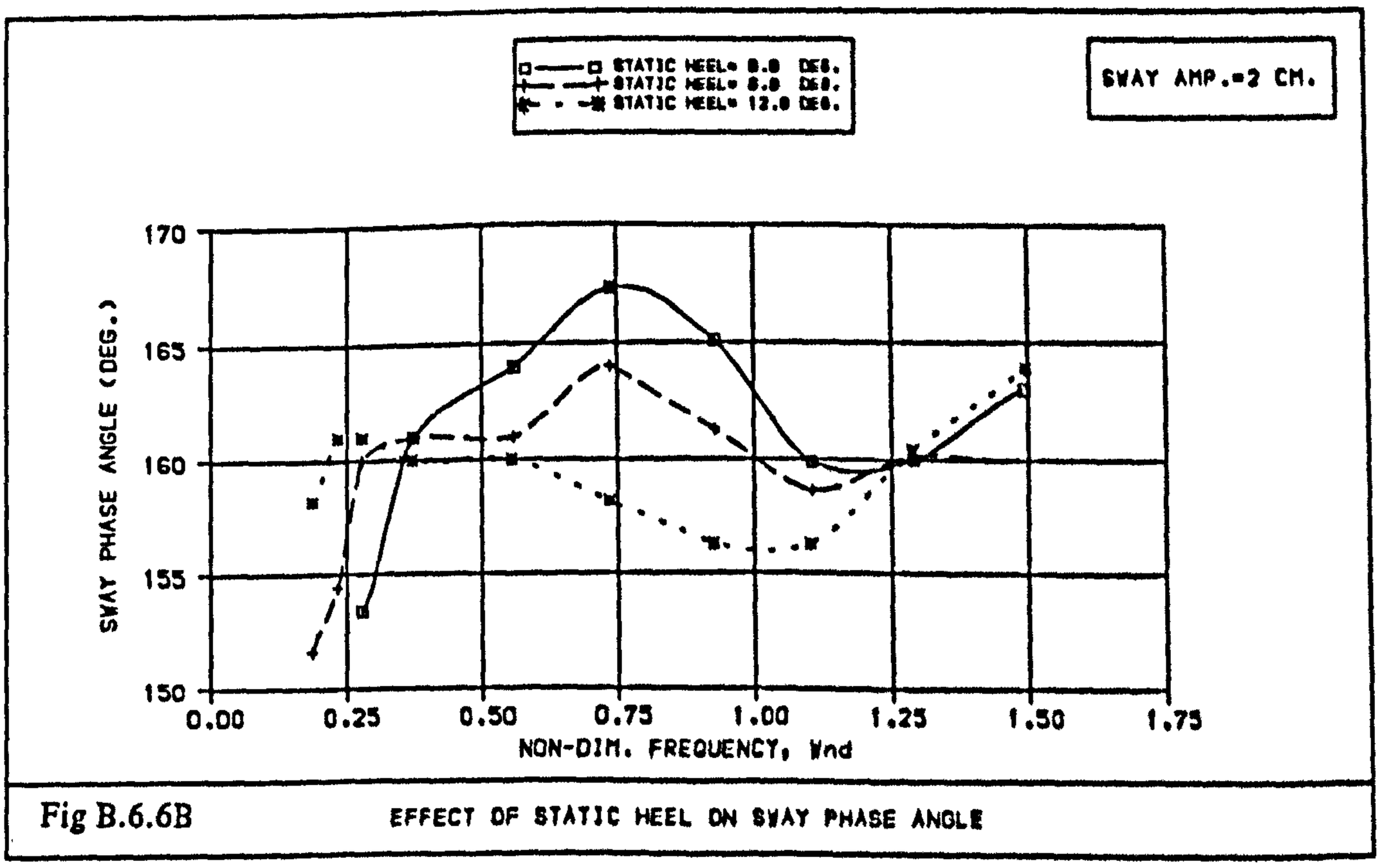

Fig B.6.6B EFFECT OF STATIC HEEL ON SWAY PHASE ANGLE

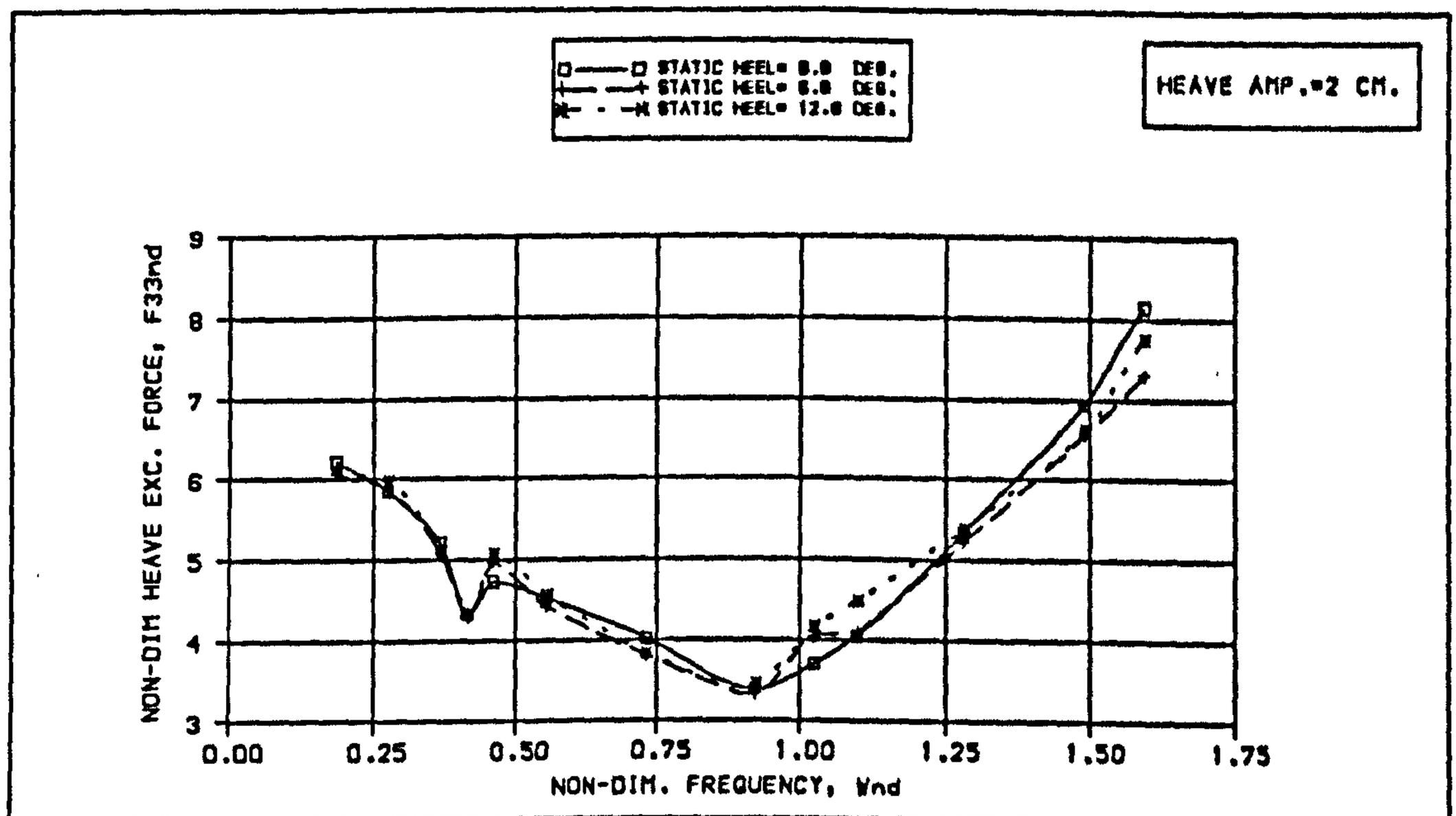

Fig B.6.7A EFFECT OF STATIC HEEL ON HEAVE EXCITATION FORCE

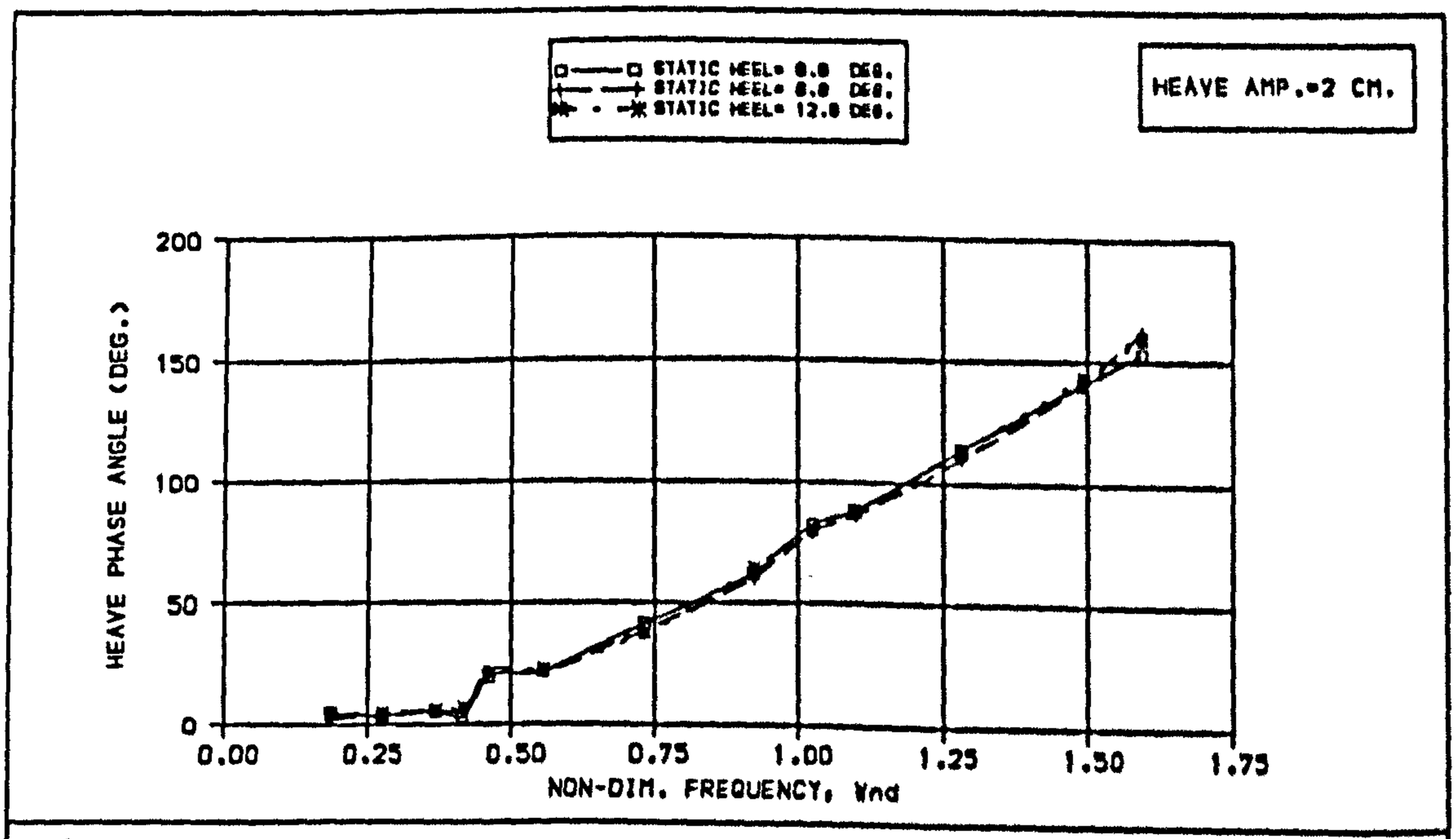

Fig B.6.7B EFFECT OF STATIC HEEL ON HEAVE PHASE ANGLE

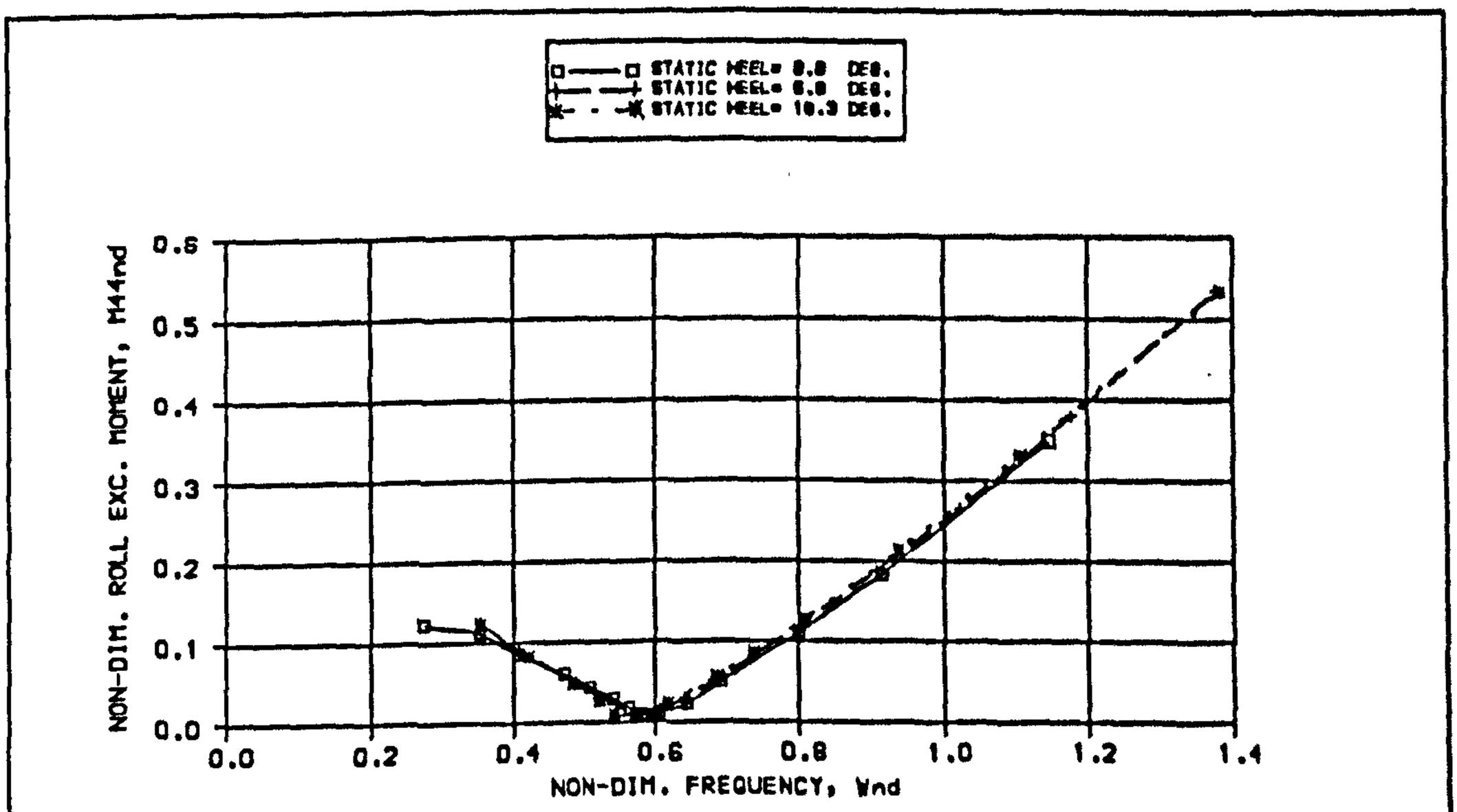

Fig B.6.8A EFFECT OF STATIC HEEL ON ROLL EXC. MOMENT

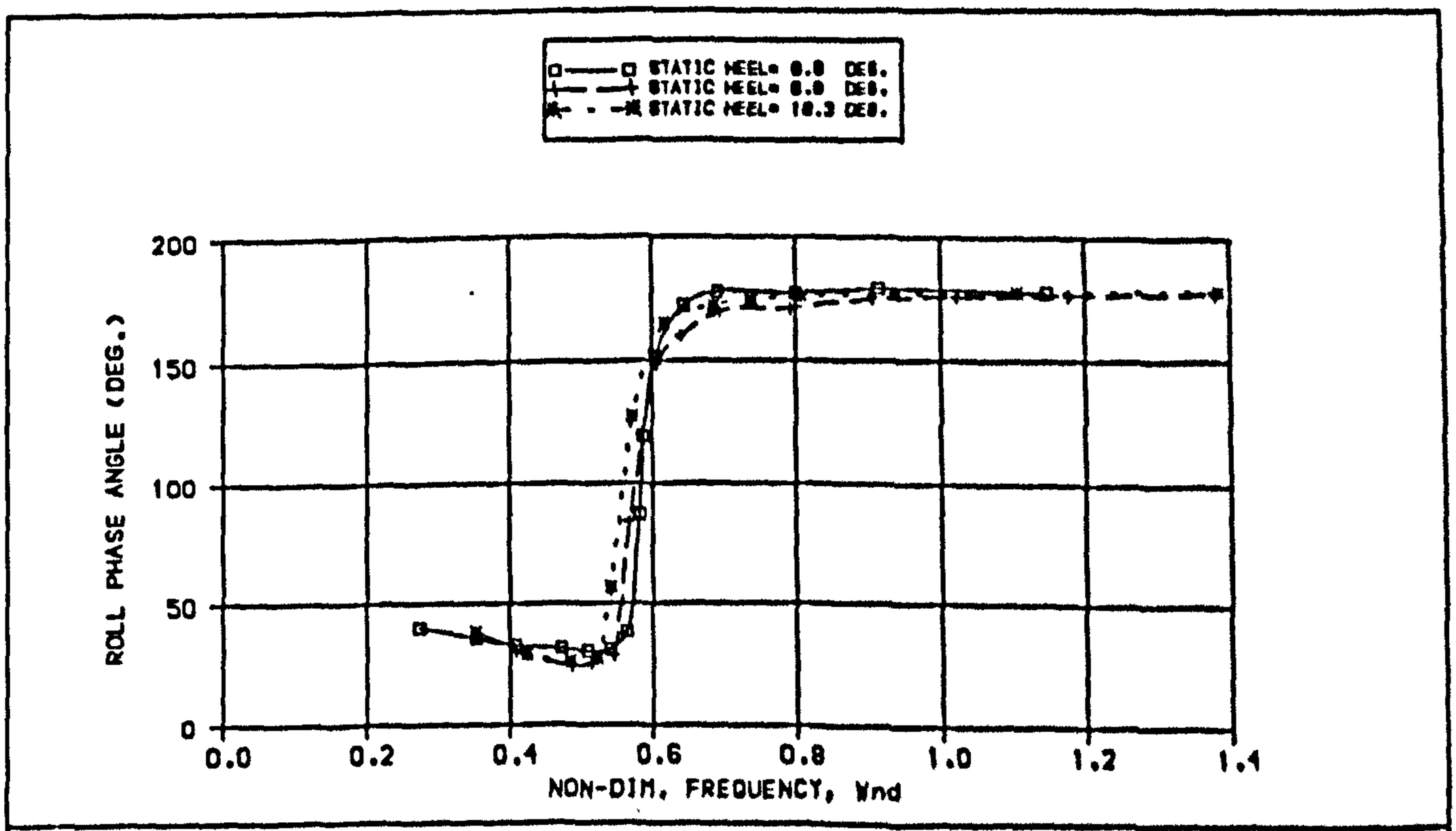

Fig B.6.8B EFFECT OF STATIC HEEL ON ROLL PHASE ANGLE

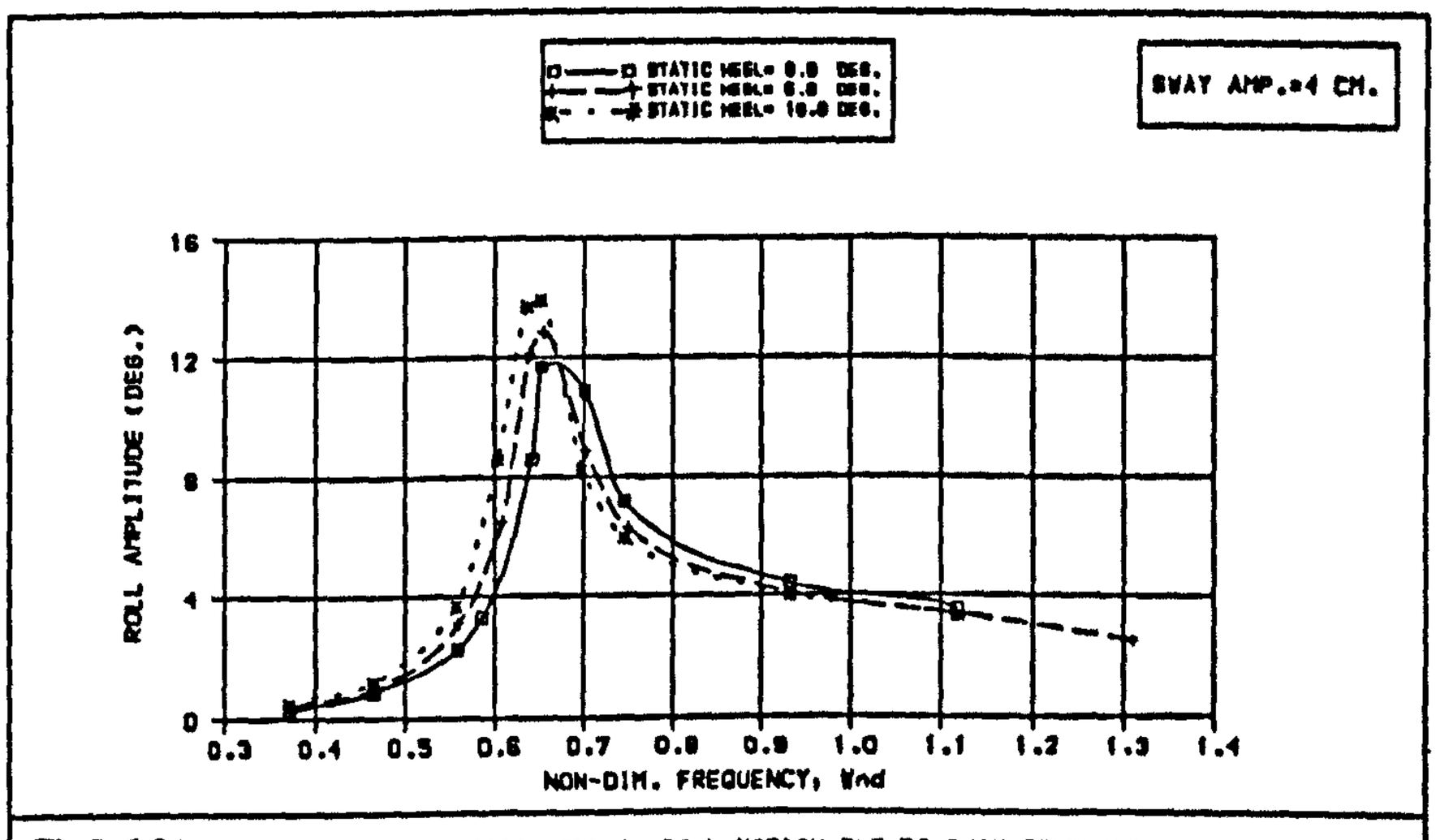

Fig B.6.9A EFFECT OF STATIC HEEL ON ROLL MOTION DUE TO SWAY COUPLING

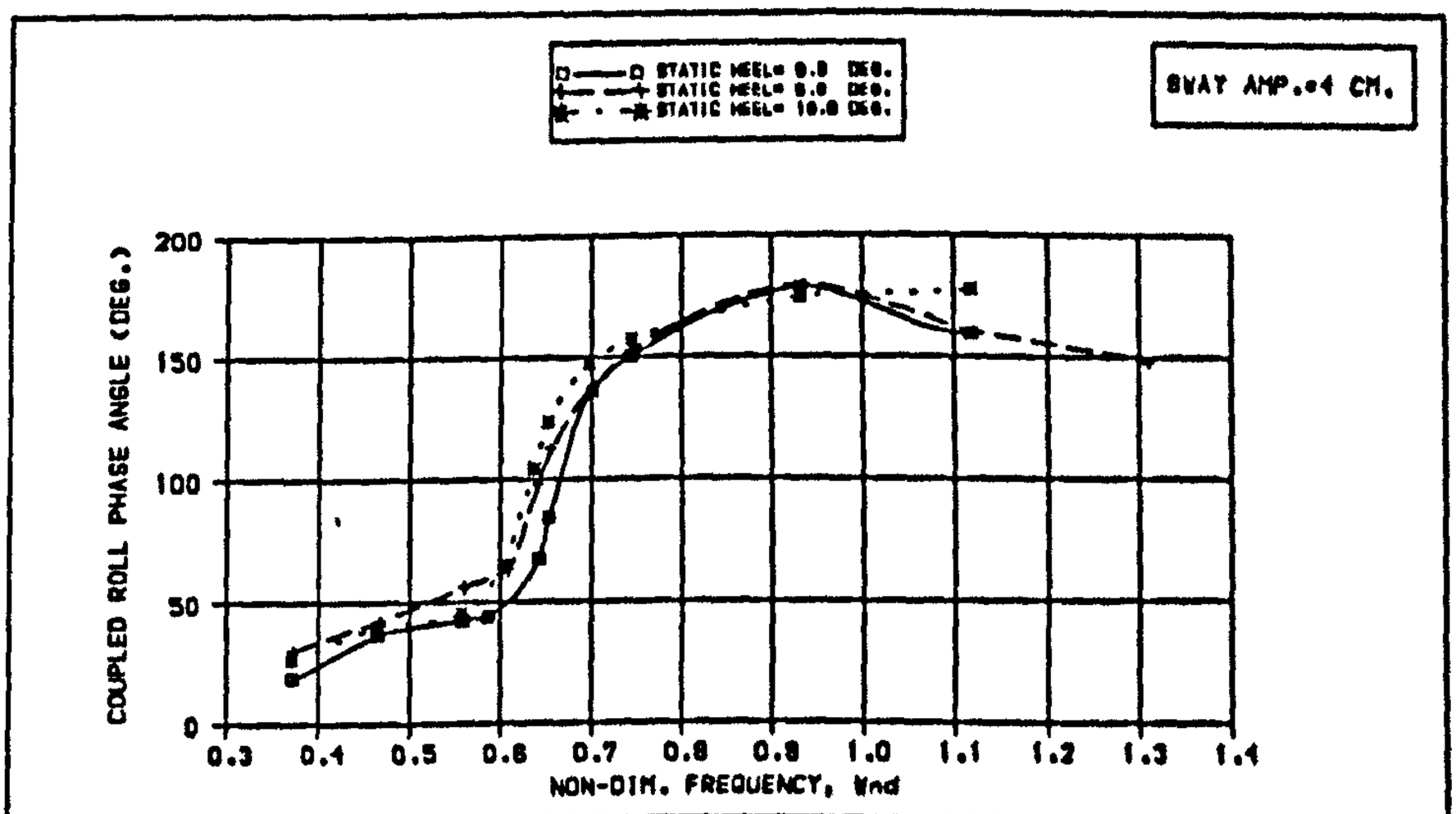

Fig B.6.9B EFFECT OF STATIC HEEL ON ROLL PHASE ANGLE DUE TO SWAY COUPLING

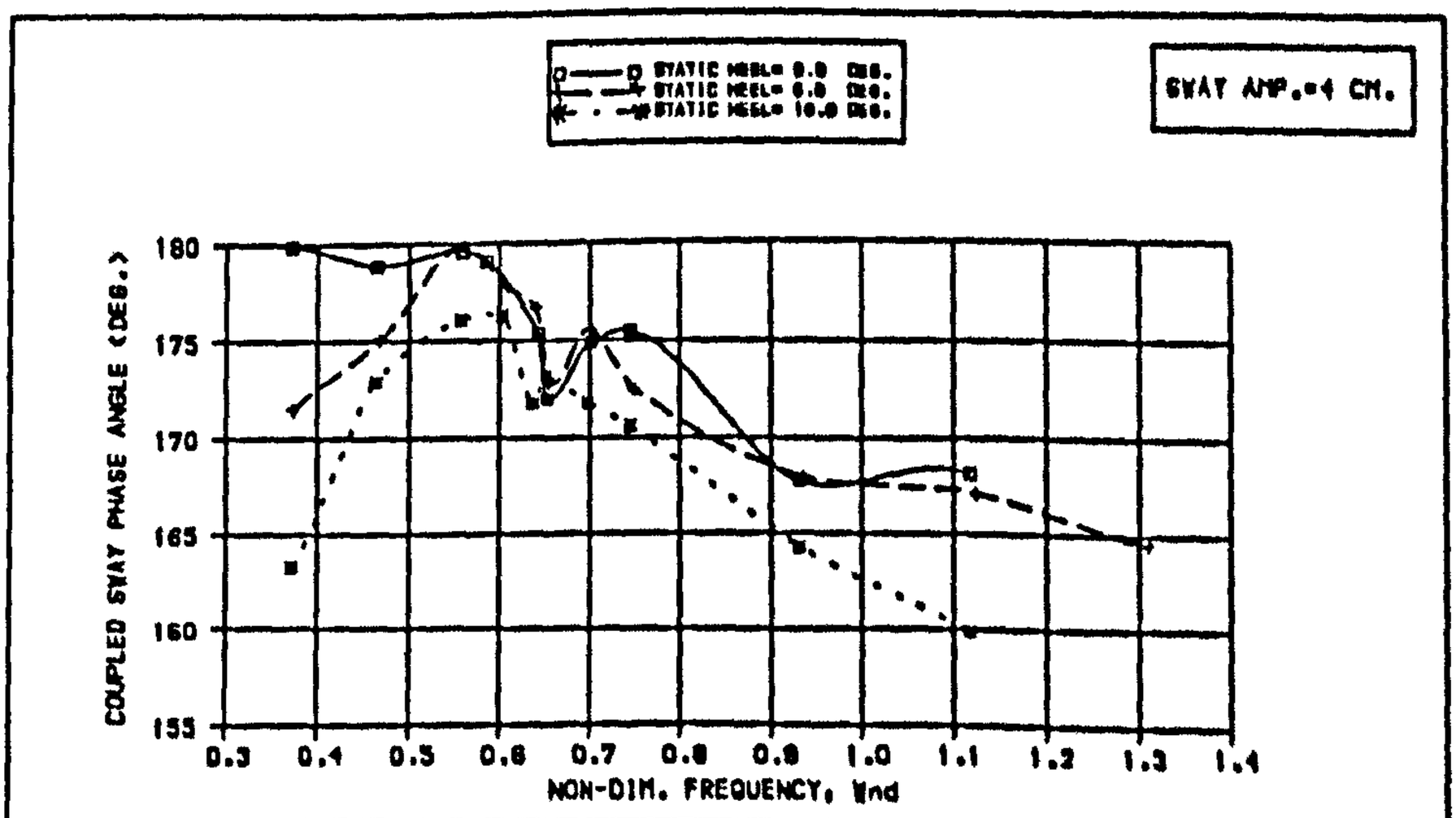

Fig B.6.9C EFFECT OF STATIC HEEL ON COUPLED SWAY PHASE ANGLE (ROLL COUPLING)

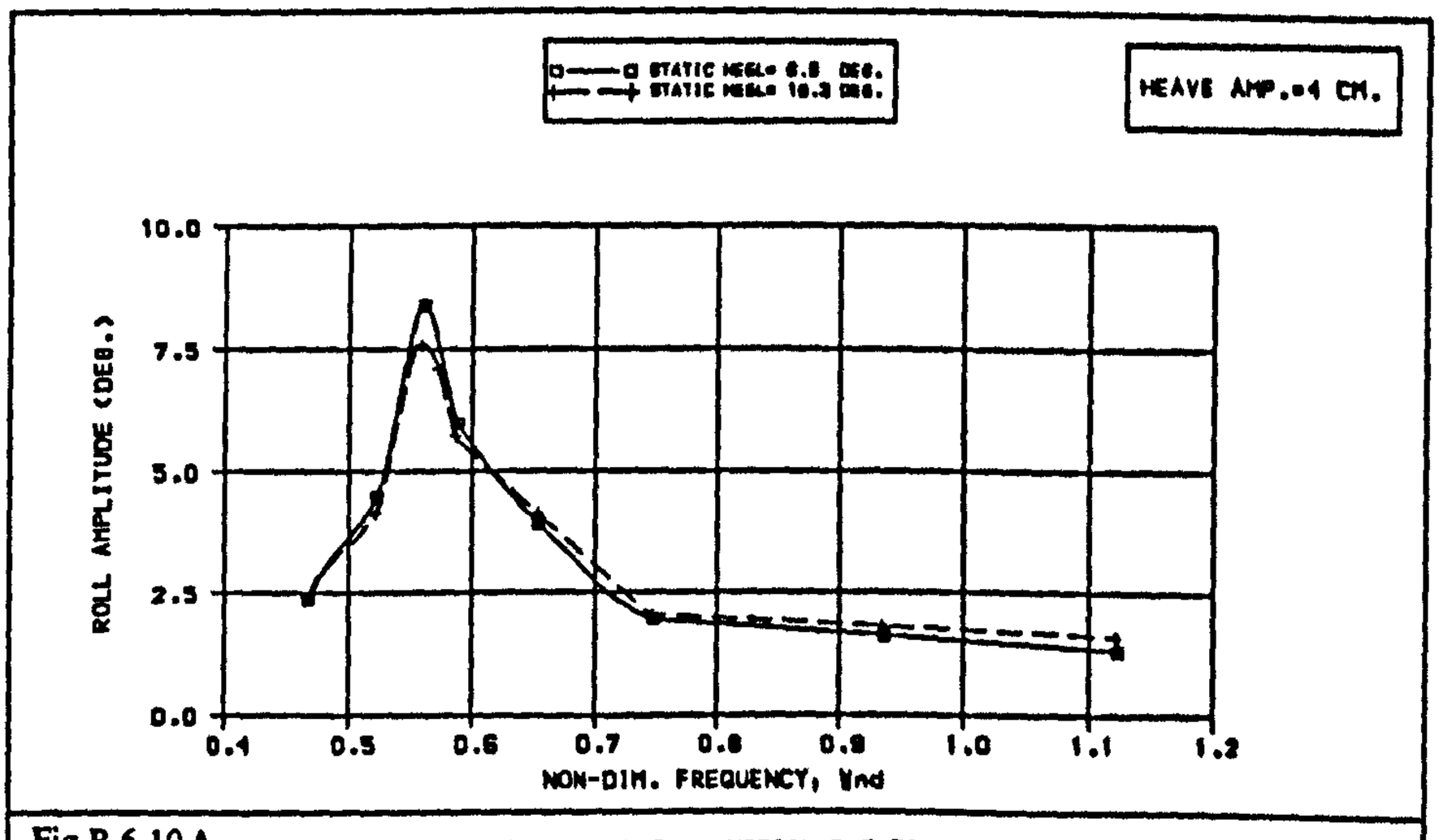

Fig B.6.10A EFFECT OF STATIC HEEL ON ROLL MOTION DUE TO HEAVE COUPLING

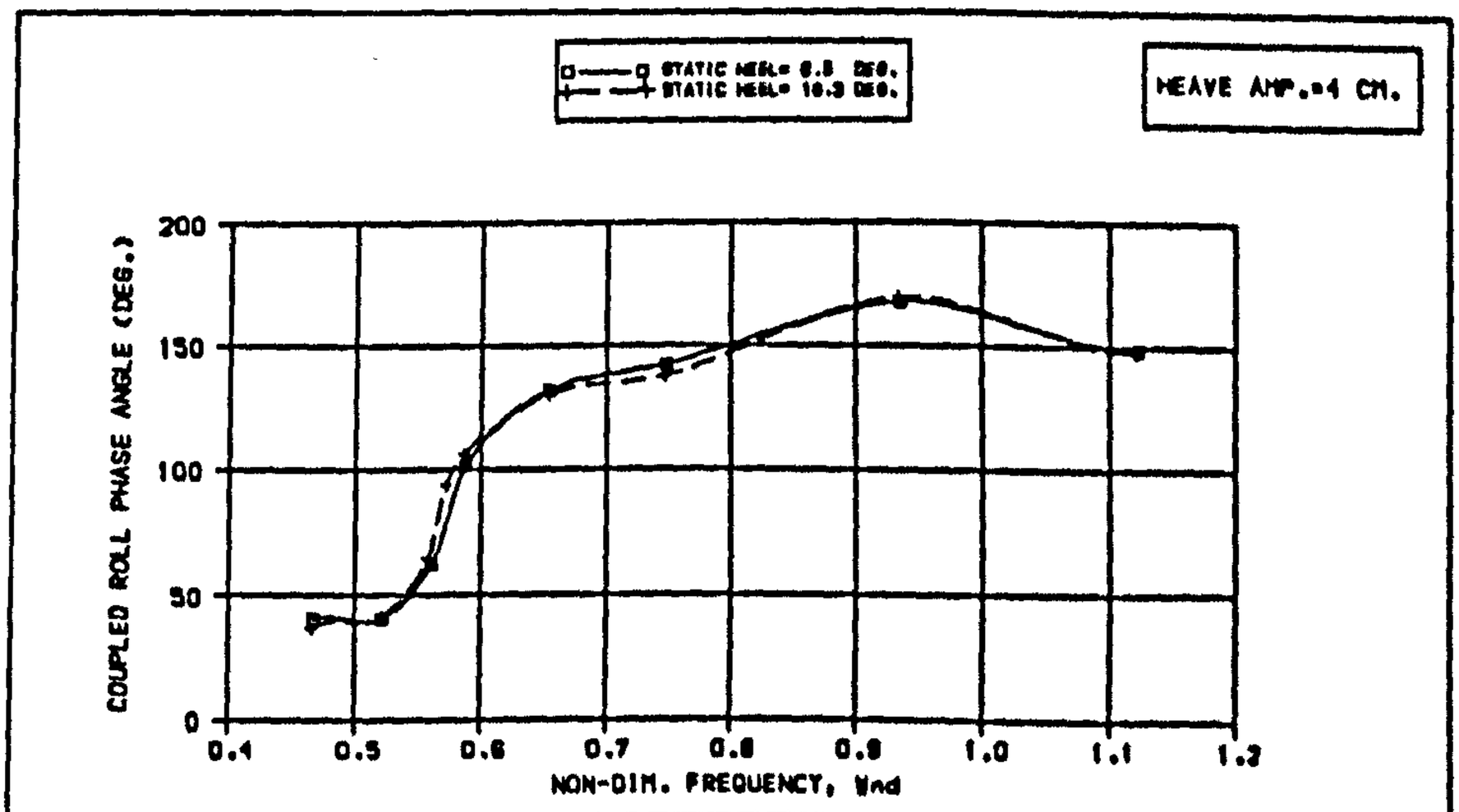

Fig B.6.10B EFFECT OF STATIC HEEL ON ROLL PHASE ANGLE DUE TO HEAVE COUPLING

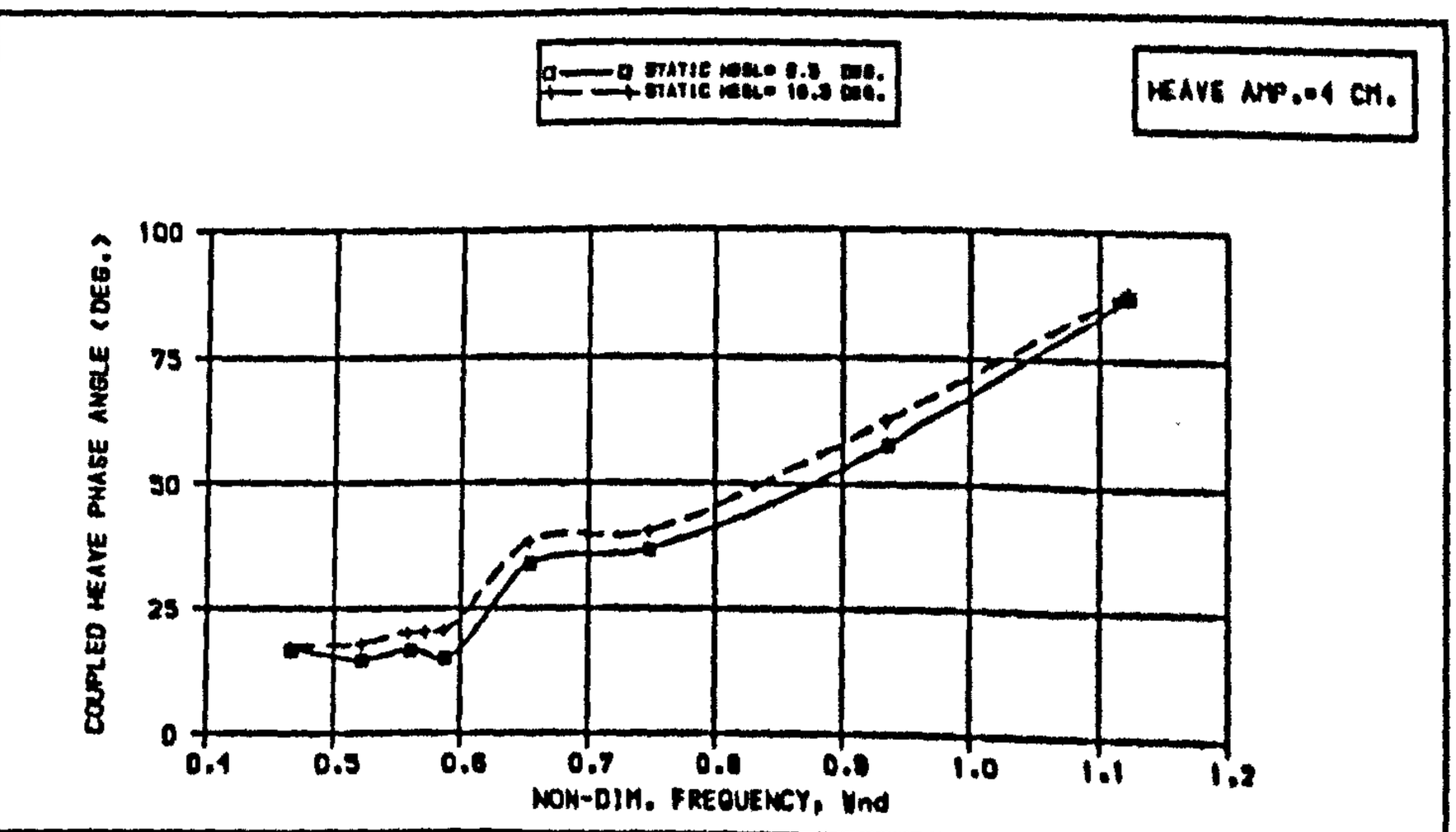

Fig B.6.10C EFFECT OF STATIC HEEL ON COUPLED HEAVE PHASE ANGLE

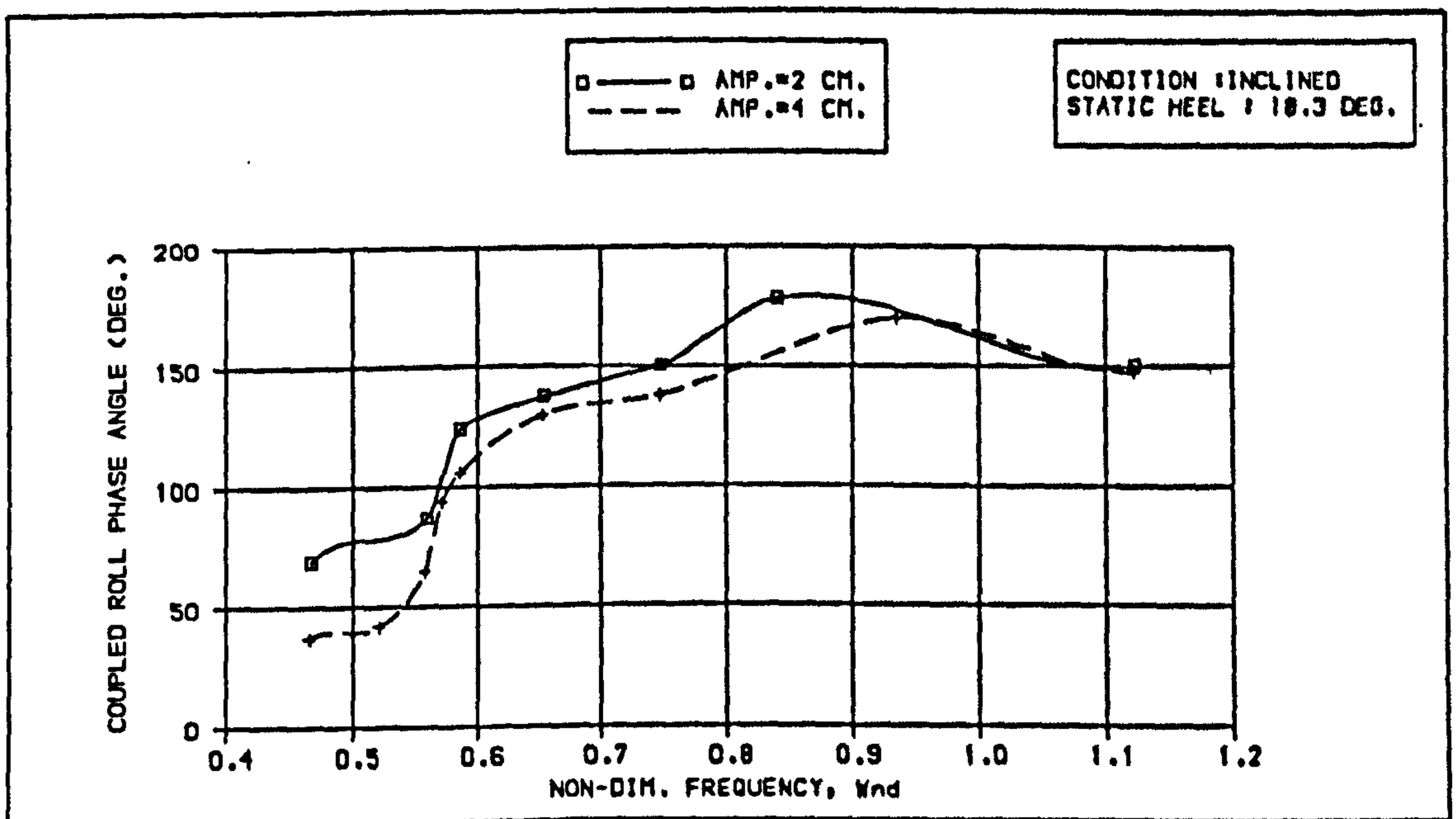

Fig B.6.11A EFFECT OF HEAVE AMPLITUDE ON ROLL PHASE ANGLE DUE TO COUPLING

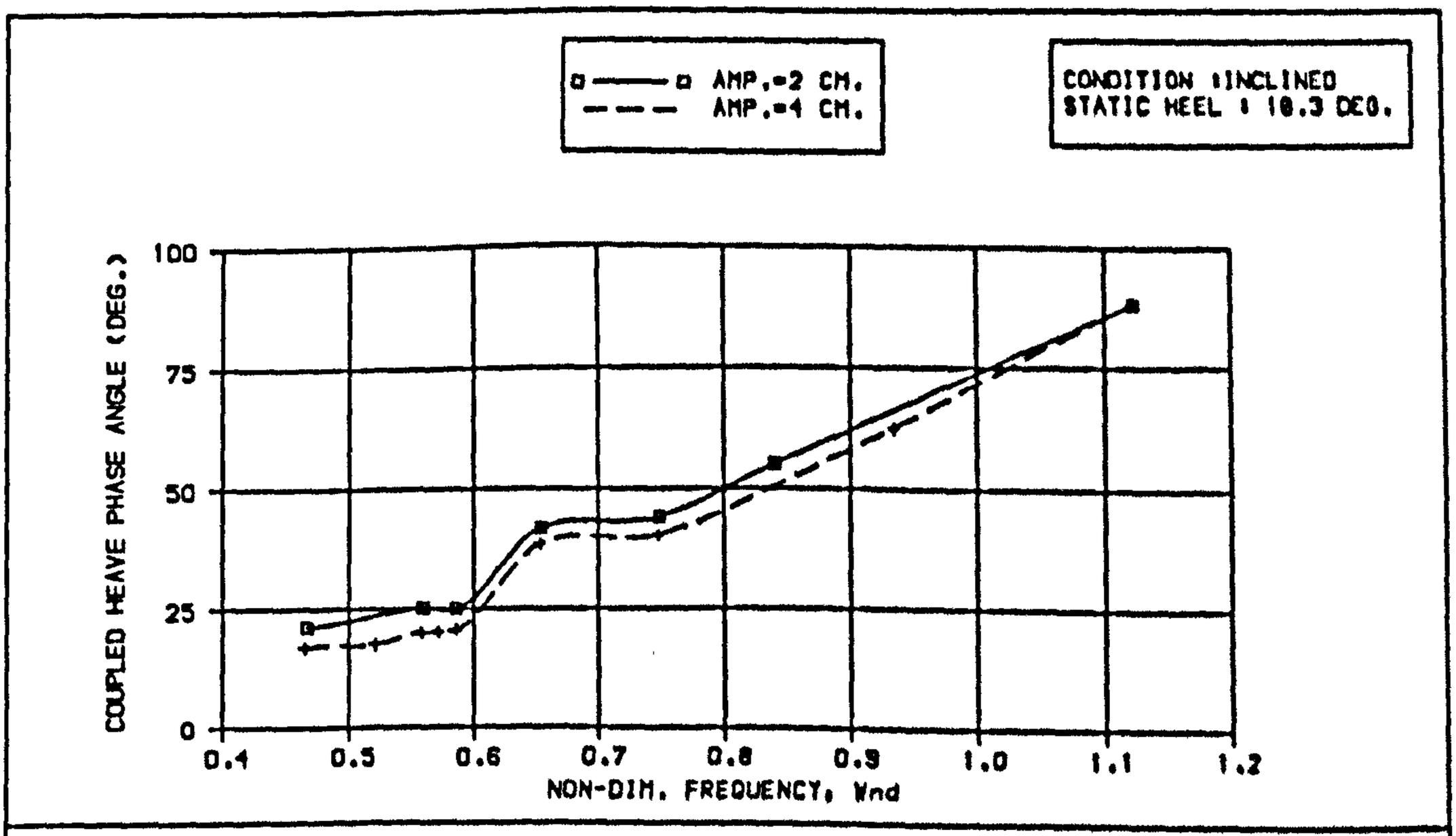

Fig B.6.11B EFFECT OF HEAVE AMPLITUDE ON COUPLED HEAVE PHASE ANGLE

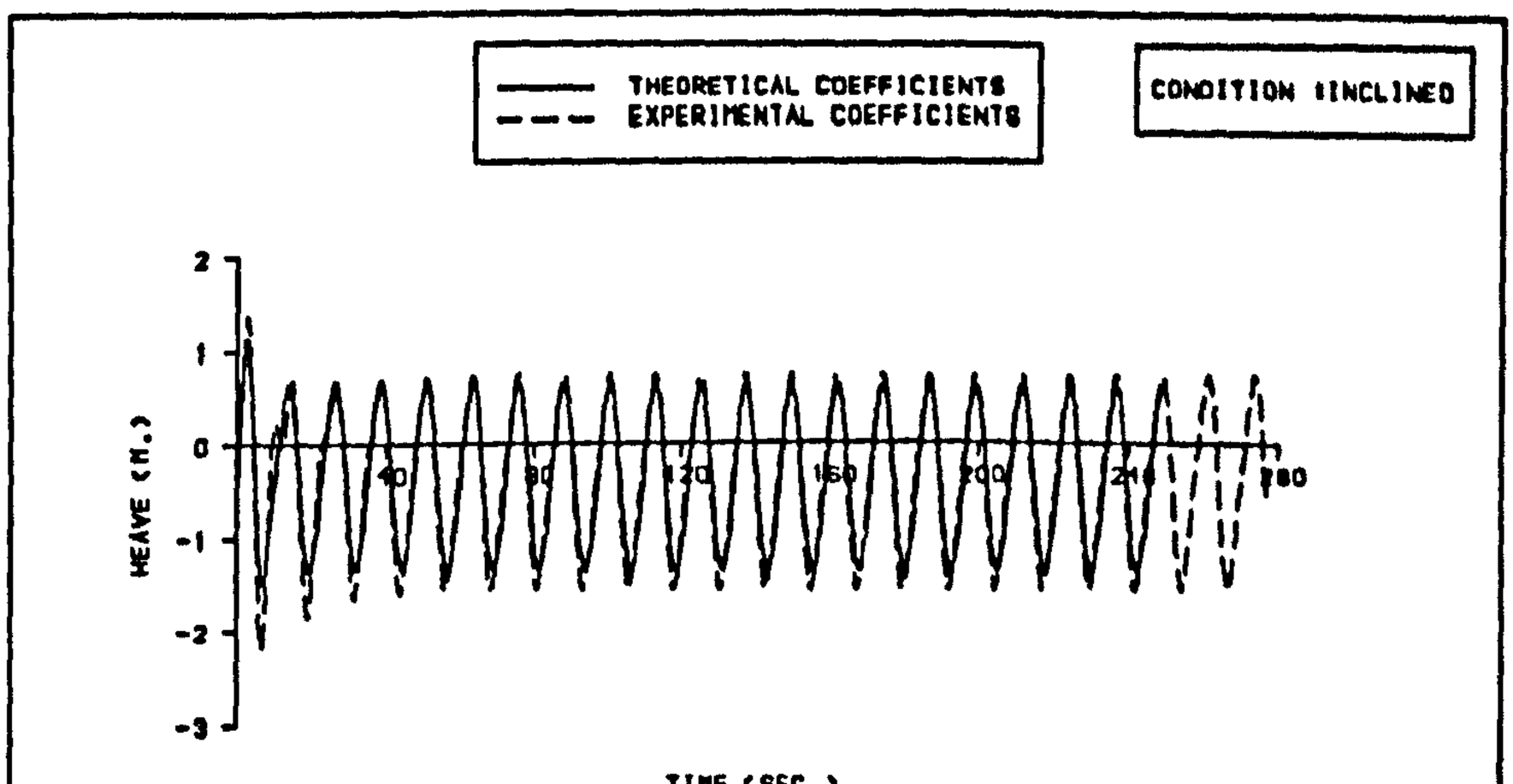

A EFFECT OF THEORETICAL AND EXPERIMENTAL COEFFICIENTS ON THE SHIP RESPONSE
(HEAVE) WH=2.0 M., FREQUENCY=0.506 RAD/SEC., WAVE DIR.=90. DEG.

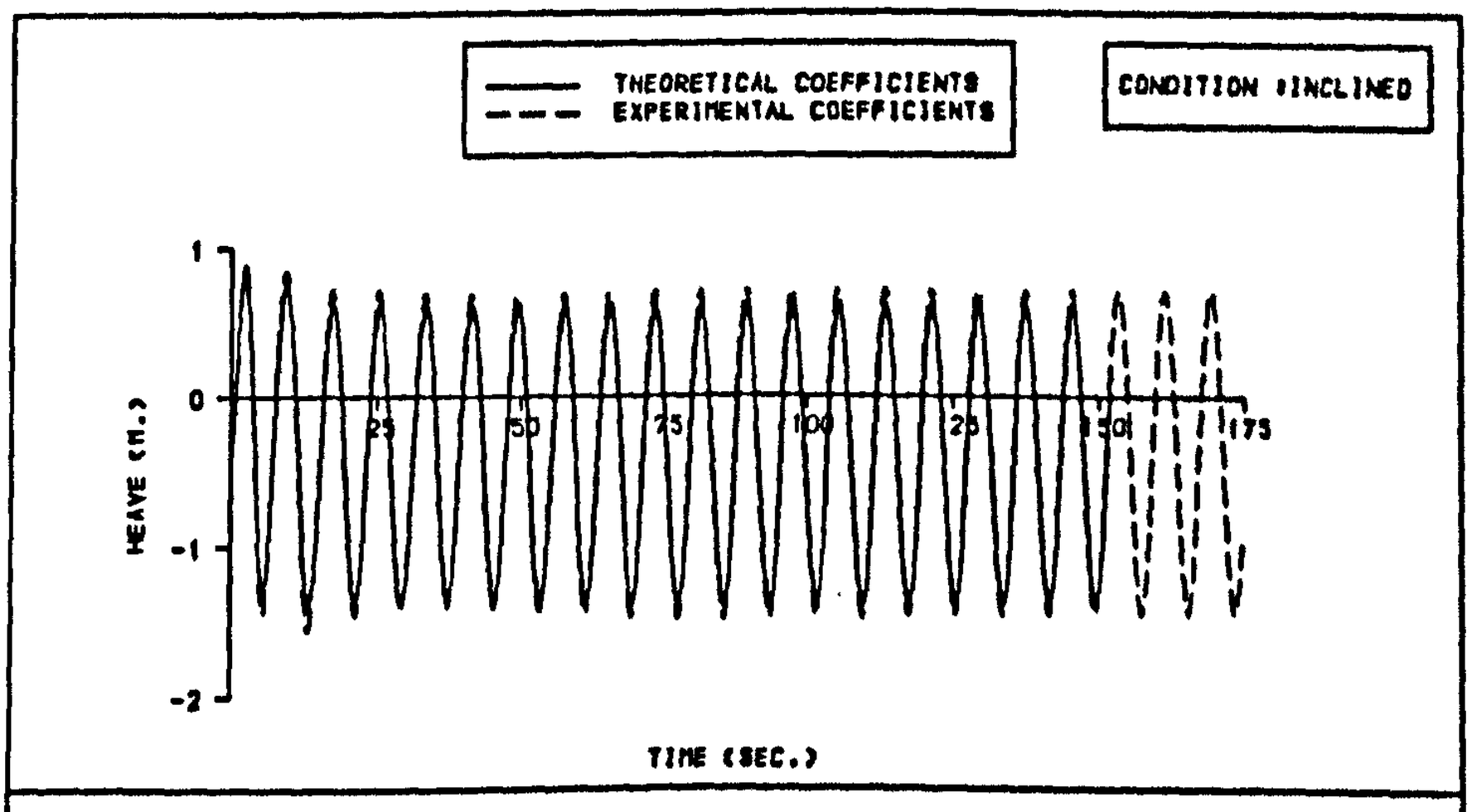

B EFFECT OF THEORETICAL AND EXPERIMENTAL COEFFICIENTS ON THE SHIP RESPONSE
(HEAVE) WH=2.0 M., FREQUENCY=0.785 RAD/SEC., WAVE DIR.=90. DEG.

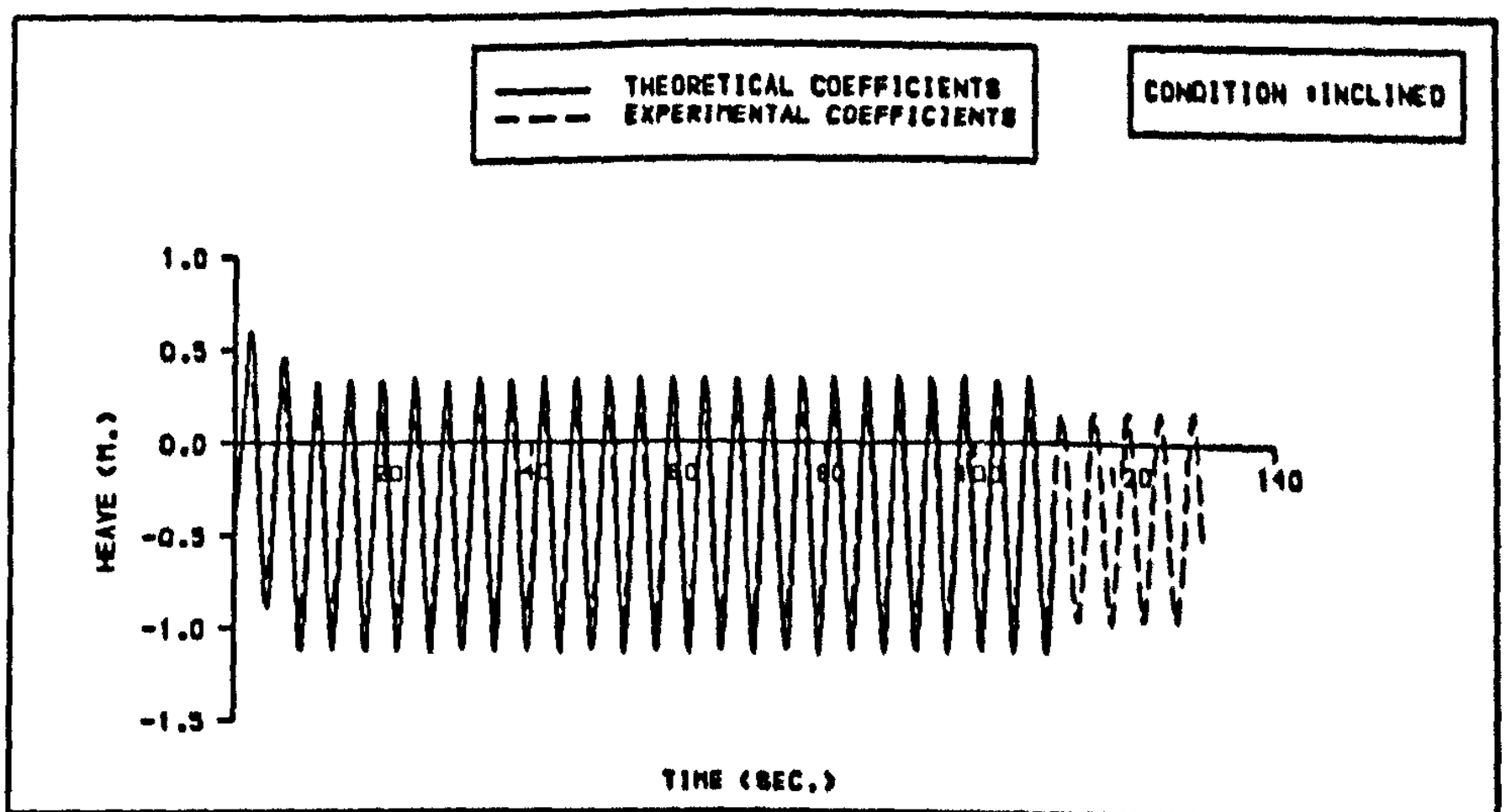

C EFFECT OF THEORETICAL AND EXPERIMENTAL COEFFICIENTS ON THE SHIP RESPONSE
(HEAVE) WH=2.0 M., FREQUENCY=1.438 RAD/SEC., WAVE DIR.=90. DEG.

Fig B.6.12 Comparison between the effect of experimentally and theoretically derived coefficients on HEAVE motion [UPRIGHT CONDITION]

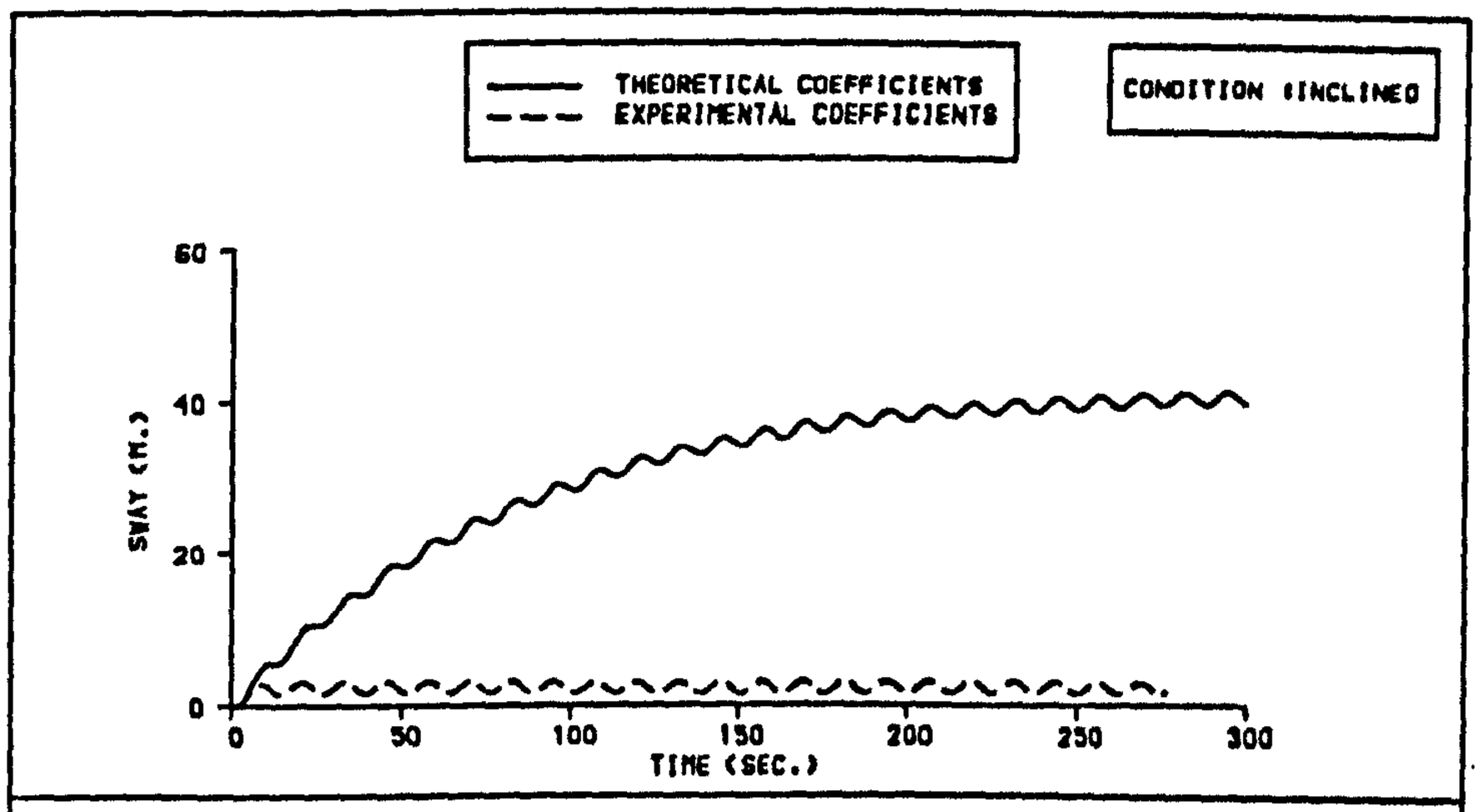

A EFFECT OF THEORETICAL AND EXPERIMENTAL COEFFICIENTS ON THE SHIP RESPONSE
[SWAY] WH=2.0 M., FREQUENCY=0.506 RAD/SEC., WAVE DIR.=90. DEG.

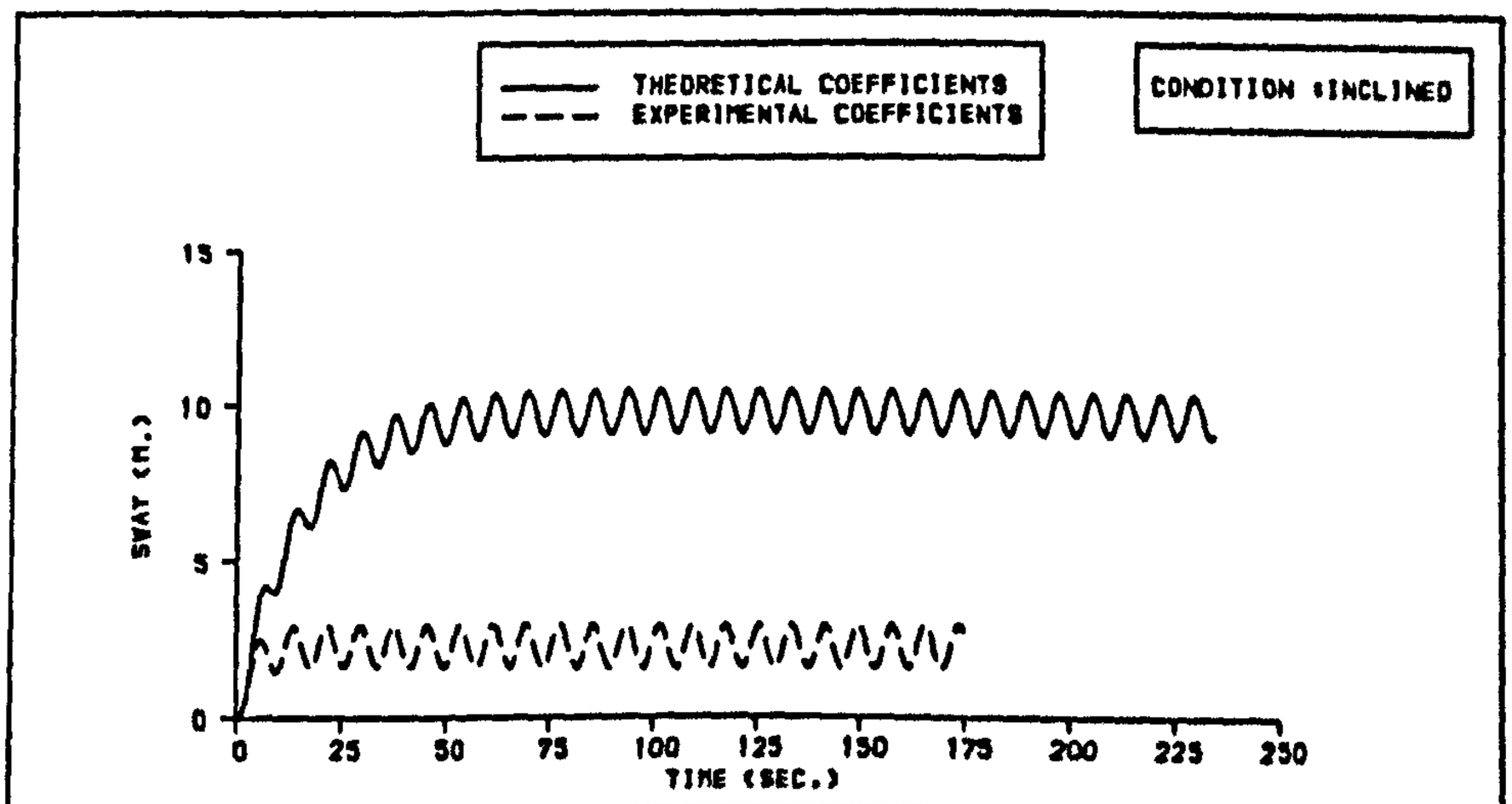

B EFFECT OF THEORETICAL AND EXPERIMENTAL COEFFICIENTS ON THE SHIP RESPONSE
[SWAY] WH=2.0 M., FREQUENCY=0.785 RAD/SEC., WAVE DIR.=90. DEG.

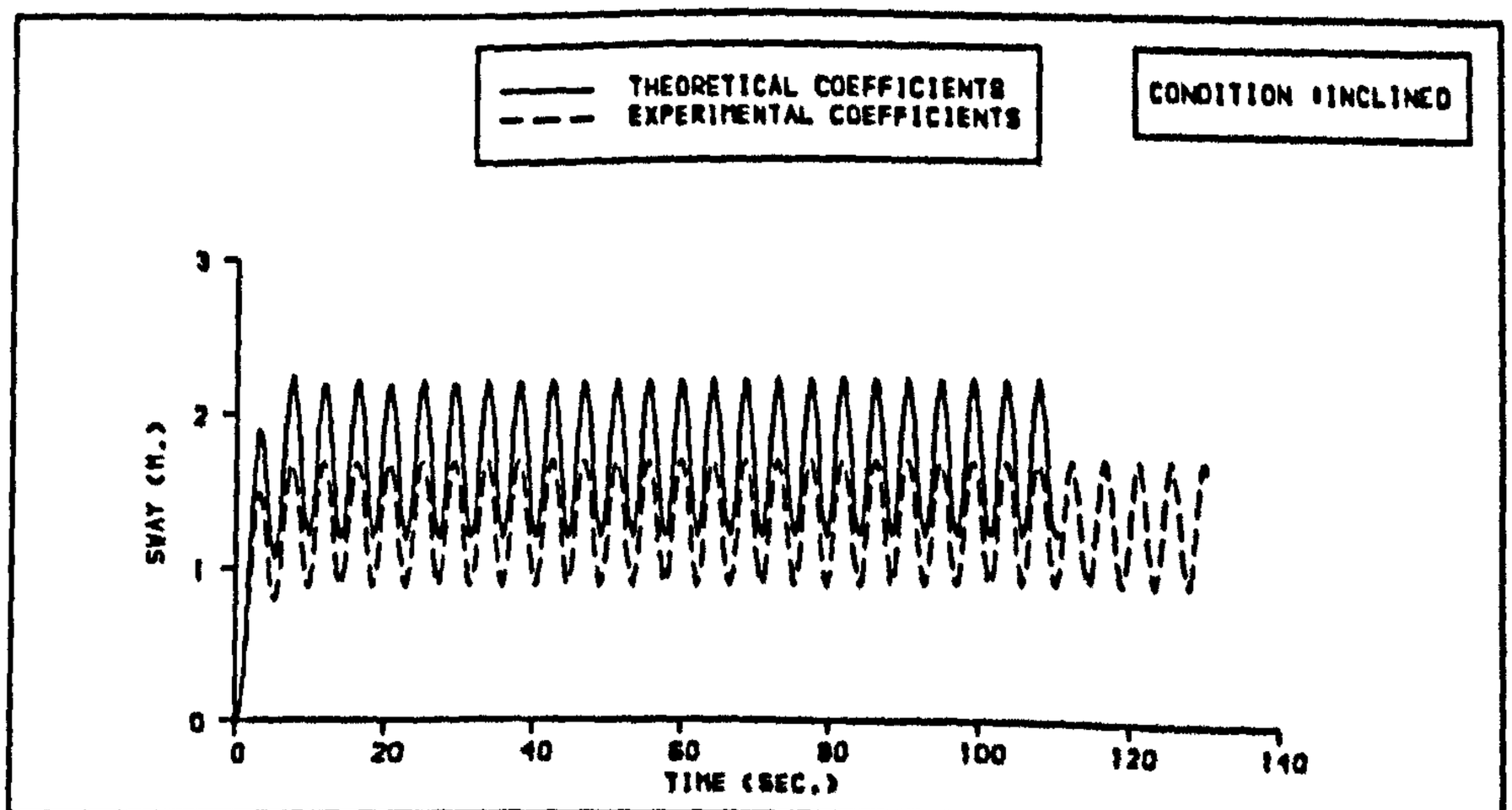

C EFFECT OF THEORETICAL AND EXPERIMENTAL COEFFICIENTS ON THE SHIP RESPONSE
[SWAY] WH=2.0 M., FREQUENCY=1.430 RAD/SEC., WAVE DIR.=90. DEG.

Fig B.6.13 Comparison between the effect of experimentally and theoretically derived coefficients on SWAY motion [UPRIGHT CONDITION]

APPENDIX C:

PARAMETRIC STUDY

C:
MAIN PARAMETERS OF THE SHIPS USED FOR THE PARAMETRIC INVESTIGATION

SHIP 1

LENGTH (L)	: 126.1	m
BREADTH (B)	: 22.7	m
DEPTH(Bulkhead deck, D_{bhk})	: 7.3	m
DRAFT(Intact, d_{in})	: 5.51	m
DRAFT(Symm. Damage, d_{sym})	: 7.21	m
DRAFT(Asymm. Damage, d_{asym})	: 6.82	m
DISPLACEMENT (Δ)	: 8556.	tonnes
VER. CENTRE OF GRAVITY (KG)	: 10.12	m
GM (Intact)	: 1.71	m
GM (Symm. Damage ,GM_{sym})	: 2.21	m
GM (Asymm. Damage,GM_{asym})	: 3.729	m
TRIM (Intact)	: 0.17	aft deg.
TRIM(Symm. Damage)	: 0.18	aft deg.
TRIM(Asymm. Damage)	: 0.185	aft deg.

SHIP 2

LENGTH (L)	: 169.5	m
BREADTH (B)	: 25.05	m
DEPTH(Bulkhead deck, D_{bhk})	: 7.805	m
DRAFT(Intact, d_{in})	: 6.08	m
DRAFT(Symm. Damage, d_{sym})	: 6.40	m
DRAFT(Asymm. Damage, d_{asym})	: 6.33	m
DISPLACEMENT (Δ)	: 18881.	tonnes
VER. CENTRE OF GRAVITY (KG)	: 11.84	m
GM (Intact)	: 1.80	m
GM (Symm. Damage ,GM_{sym})	: 1.06	m
GM (Asymm. Damage,GM_{asym})	: 2.19	m
TRIM (Intact)	: 0.07	aft deg.
TRIM(Symm. Damage)	: 0.112	aft deg.
TRIM(Asymm. Damage)	: 0.09	aft deg.

SHIP 3

LENGTH (L)	: 161.0	m	
BREADTH (B)	: 27.8	m	
DEPTH(Bulkhead deck, D_{bhk})	: 8.10	m	
DRAFT(Intact, d_{in})	: 6.12	m	
DRAFT(Symm. Damage, d_{sym})	: 7.14	m	
DRAFT(Asymm. Damage, d_{asym})	: 6.84	m	
DISPLACEMENT (Δ)	: 15205.	tonnes	
VER. CENTRE OF GRAVITY (KG)	: 11.82	m	
GM (Intact)	: 3.15	m	
GM (Symm. Damage ,GM_{sym})	: 3.18	m	
GM (Asymm. Damage,GM_{asym})	: 4.41	m	
TRIM (Intact)	: 0.14	aft	deg.
TRIM(Symm. Damage)	: 0.705	aft	deg.
TRIM(Asymm. Damage)	: 0.585	aft	deg.

SHIP 4

LENGTH (L)	: 110.2	m	
BREADTH (B)	: 19.20	m	
DEPTH(Bulkhead deck, D_{bhk})	: 6.17	m	
DRAFT(Intact, d_{in})	: 4.10	m	
DRAFT(Symm. Damage, d_{sym})	: 5.34	m	
DRAFT(Asymm. Damage, d_{asym})	: 4.96	m	
DISPLACEMENT (Δ)	: 5170.	tonnes	
VER. CENTRE OF GRAVITY (KG)	: 8.0	m	
GM (Intact)	: 1.66	m	
GM (Symm. Damage ,GM_{sym})	: 1.39	m	
GM (Asymm. Damage,GM_{asym})	: 3.05	m	
TRIM (Intact)	: 0.103	aft	deg.
TRIM(Symm. Damage)	: 1.72	aft	deg.
TRIM(Asymm. Damage)	: 1.20	aft	deg.

SHIP 5

LENGTH (L)	: 120.7	m	
BREADTH (B)	: 21.0	m	
DEPTH(Bulkhead deck, D_{bhk})	: 6.4	m	
DRAFT(Intact, d_{in})	: 5.0	m	
DRAFT(Symm. Damage, d_{sym})	: 6.10	m	
DRAFT(Asymm. Damage, d_{asym})	: 5.88	m	
DISPLACEMENT (Δ)	: 7550.	tonnes	
VER. CENTRE OF GRAVITY (KG)	: 10.05	m	
GM (Intact)	: 1.33	m	
GM (Symm. Damage ,GM_{sym})	: 0.79	m	
GM (Asymm. Damage,GM_{asym})	: 2.72	m	
TRIM (Intact)	: 0.17	aft	deg.
TRIM(Symm. Damage)	: 0.45	aft	deg.
TRIM(Asymm. Damage)	: 0.323	aft	deg.

SHIP *6*

LENGTH (L)	: 119.5	m	
BREADTH (B)	: 20.6	m	
DEPTH(Bulkhead deck, D_{bhk})	: 6.55	m	
DRAFT(Intact, d_{in})	: 4.57	m	
DRAFT(Symm. Damage, d_{sym})	: 5.95	m	
DRAFT(Asymm. Damage, d_{asym})	: 5.68	m	
DISPLACEMENT (Δ)	: 7375.	tonnes	
VER. CENTRE OF GRAVITY (KG)	: 8.87	m	
GM (Intact)	: 1.64	m	
GM (Symm. Damage ,GM_{sym})	: 0.908	m	
GM (Asymm. Damage,GM_{asym})	: 3.17	m	
TRIM (Intact)	: 0.091	aft	deg.
TRIM(Symm. Damage)	: 0.957	aft	deg.
TRIM(Asymm. Damage)	: 0.760	aft	deg.

SHIP 7

LENGTH (L)	: 78.0	m	
BREADTH (B)	: 15.8	m	
DEPTH(Bulkhead deck, D_{bhk})	: 5.0	m	
DRAFT(Intact, d_{in})	: 3.11	m	
DRAFT(Symm. Damage, d_{sym})	: 4.39	m	
DRAFT(Asymm. Damage, d_{asym})	: 4.22	m	
DISPLACEMENT (Δ)	: 2349.	tonnes	
VER. CENTRE OF GRAVITY (KG)	: 6.55	m	
GM (Intact)	: 2.26	m	
GM (Symm. Damage ,GM_{sym})	: 1.52	m	
GM (Asymm. Damage,GM_{asym})	: 2.46	m	
TRIM (Intact)	: 0.04	aft	deg.
TRIM(Symm. Damage)	: 0.24	aft	deg.
TRIM(Asymm. Damage)	: 0.21	aft	deg.

SHIP 8

LENGTH (L)	: 137.	m	
BREADTH (B)	: 17.6	m	
DEPTH(Bulkhead deck, D_{bhk})	: 5.80	m	
DRAFT(Intact, d_{in})	: 4.60	m	
DRAFT(Symm. Damage, d_{sym})	: 5.23	m	
DRAFT(Asymm. Damage, d_{asym})	: 5.10	m	
DISPLACEMENT (Δ)	: 8189.7	tonnes	
VER. CENTRE OF GRAVITY (KG)	: 7.15	m	
GM (Intact)	: 1.71	m	
GM (Symm. Damage ,GM_{sym})	: 1.452	m	
GM (Asymm. Damage,GM_{asym})	: 2.112	m	
TRIM (Intact)	: 0.07	aft	deg.
TRIM(Symm. Damage)	: 0.36	aft	deg.
TRIM(Asymm. Damage)	: 0.25	aft	deg.

SHIP 9

LENGTH (L)	: 94.	m	
BREADTH (B)	: 18.6	m	
DEPTH(Bulkhead deck, D_{bhk})	: 6.31	m	
DRAFT(Intact, d_{in})	: 4.61	m	
DRAFT(Symm. Damage, d_{sym})	: 5.89	m	
DRAFT(Asymm. Damage, d_{asym})	: 5.63	m	
DISPLACEMENT (Δ)	: 4559.07	tonnes	
VER. CENTRE OF GRAVITY (KG)	: 7.68	m	
GM (Intact)	: 1.82	m	
GM (Symm. Damage ,GM_{sym})	: 1.824	m	
GM (Asymm. Damage,GM_{asym})	: 3.19	m	
TRIM (Intact)	: 0.025	aft	deg.
TRIM(Symm. Damage)	: 0.071	aft	deg.
TRIM(Asymm. Damage)	: 0.063	aft	deg.

SHIP 10

LENGTH (L)	: 131.0	m	
BREADTH (B)	: 26.0	m	
DEPTH(Bulkhead deck, D_{bhk})	: 7.80	m	
DRAFT(Intact, d_{in})	: 6.12	m	
DRAFT(Symm. Damage, d_{sym})	: 7.46	m	
DRAFT(Asymm. Damage, d_{asym})	: 7.22	m	
DISPLACEMENT (Δ)	: 12495.	tonnes	
VER. CENTRE OF GRAVITY (KG)	: 12.1	m	
GM (Intact)	: 1.85	m	
GM (Symm. Damage ,GM_{sym})	: 3.586	m	
GM (Asymm. Damage,GM_{asym})	: 3.49	m	
TRIM (Intact)	: 0.028	aft	deg.
TRIM(Symm. damage)	: 1.16	aft	deg.
TRIM(Asymm. Damage)	: 1.01	aft	deg.

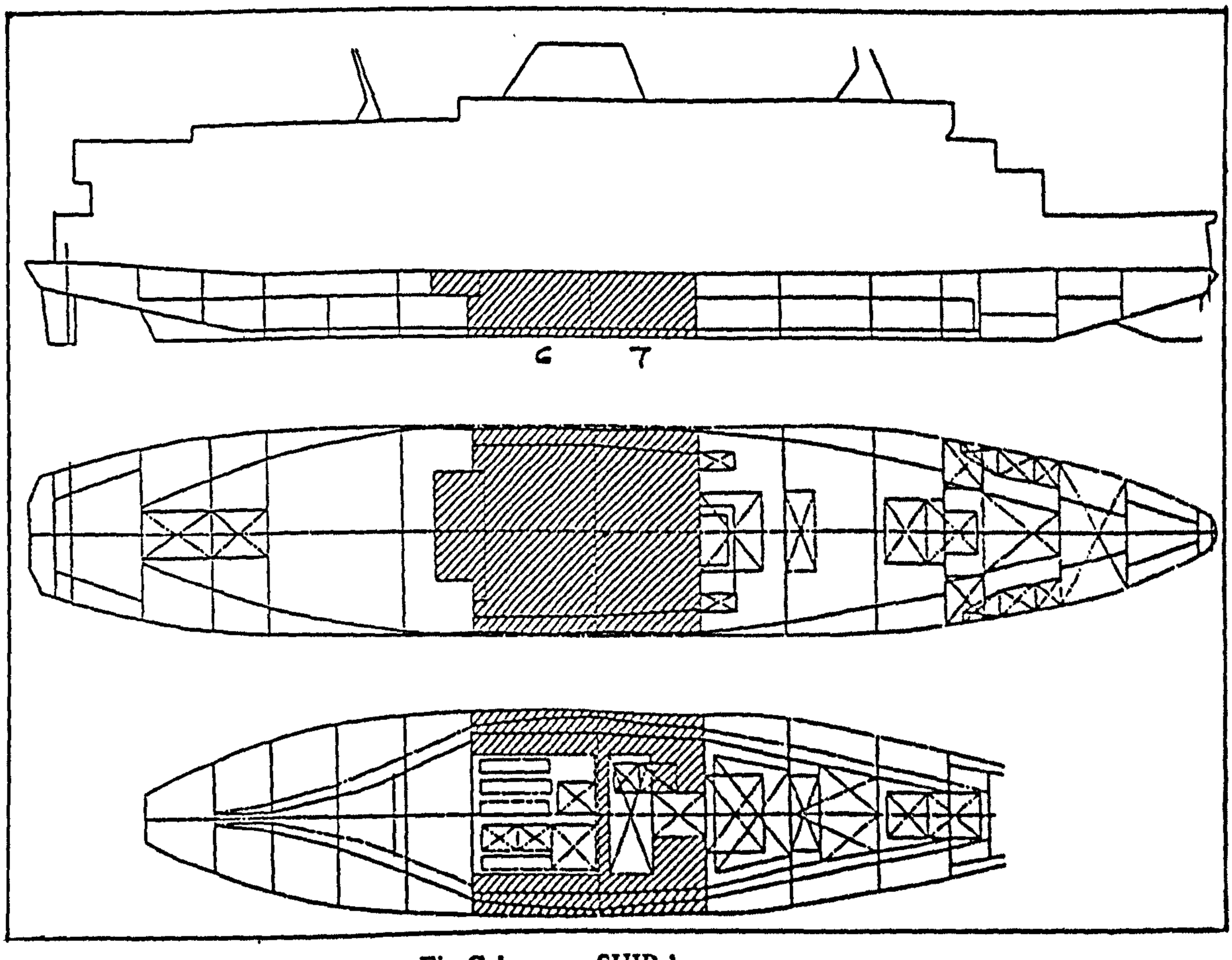

Fig C.1 SHIP 1

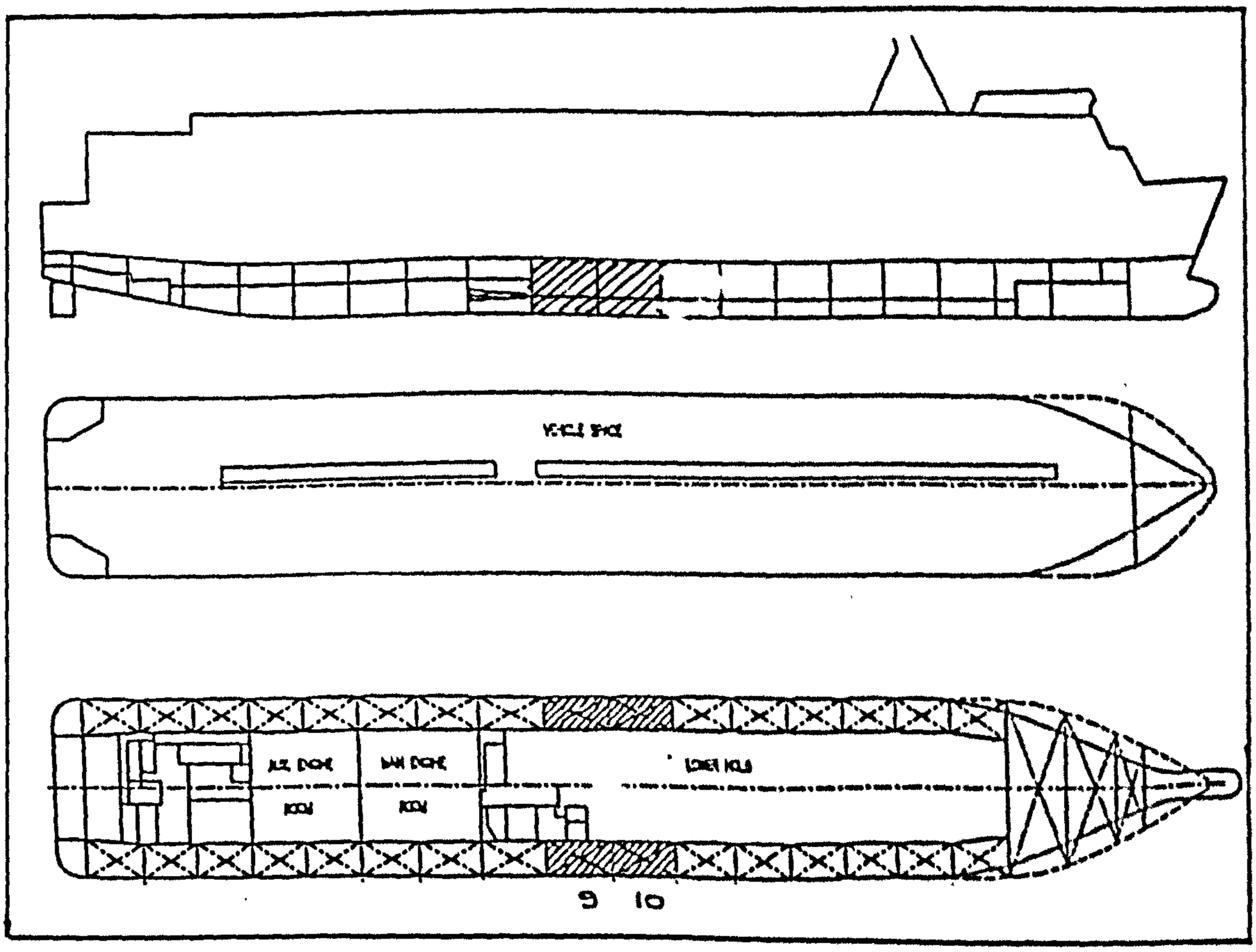

Fig C.2 SHIP 2

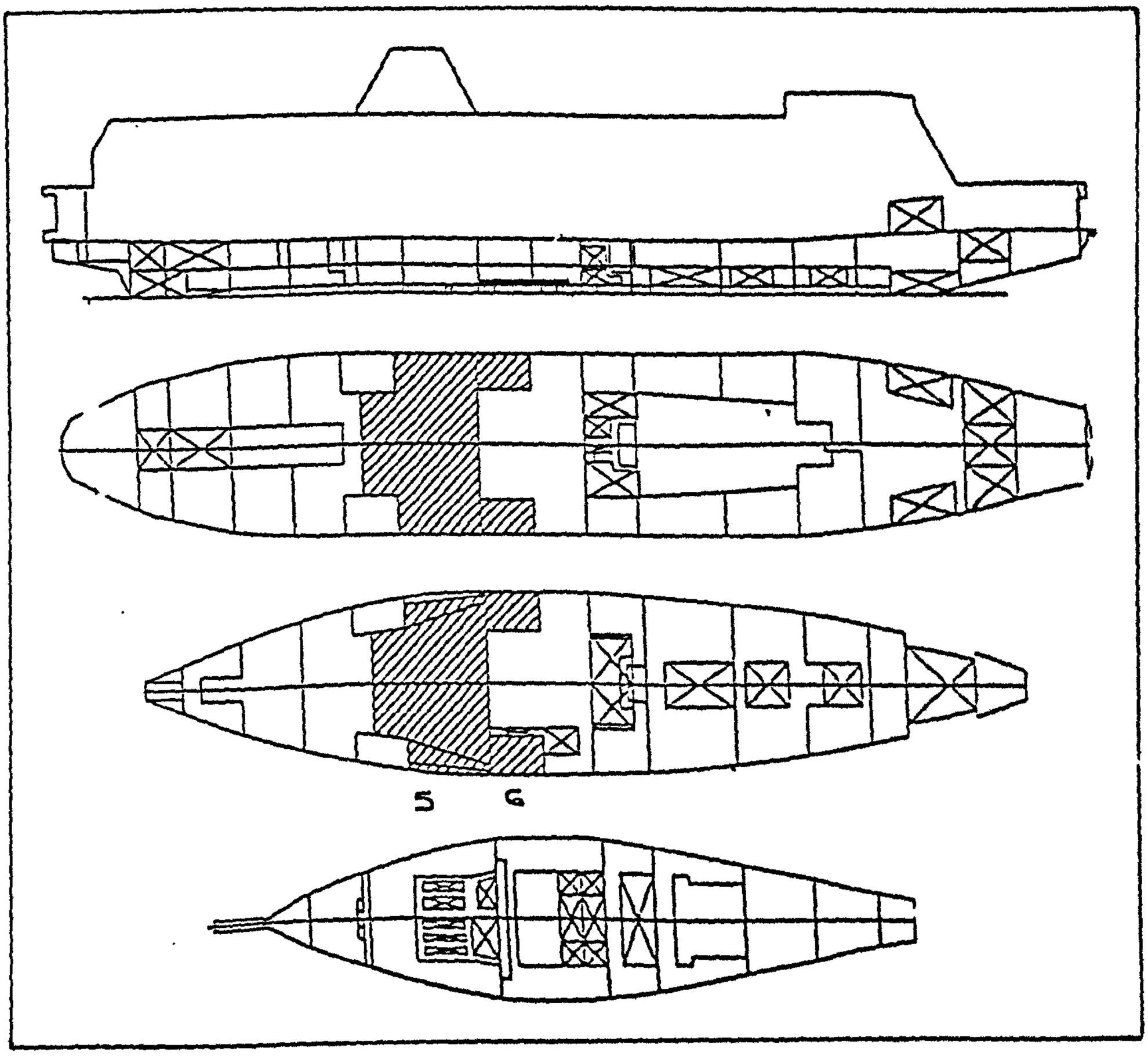

Fig C.3 SHIP 3

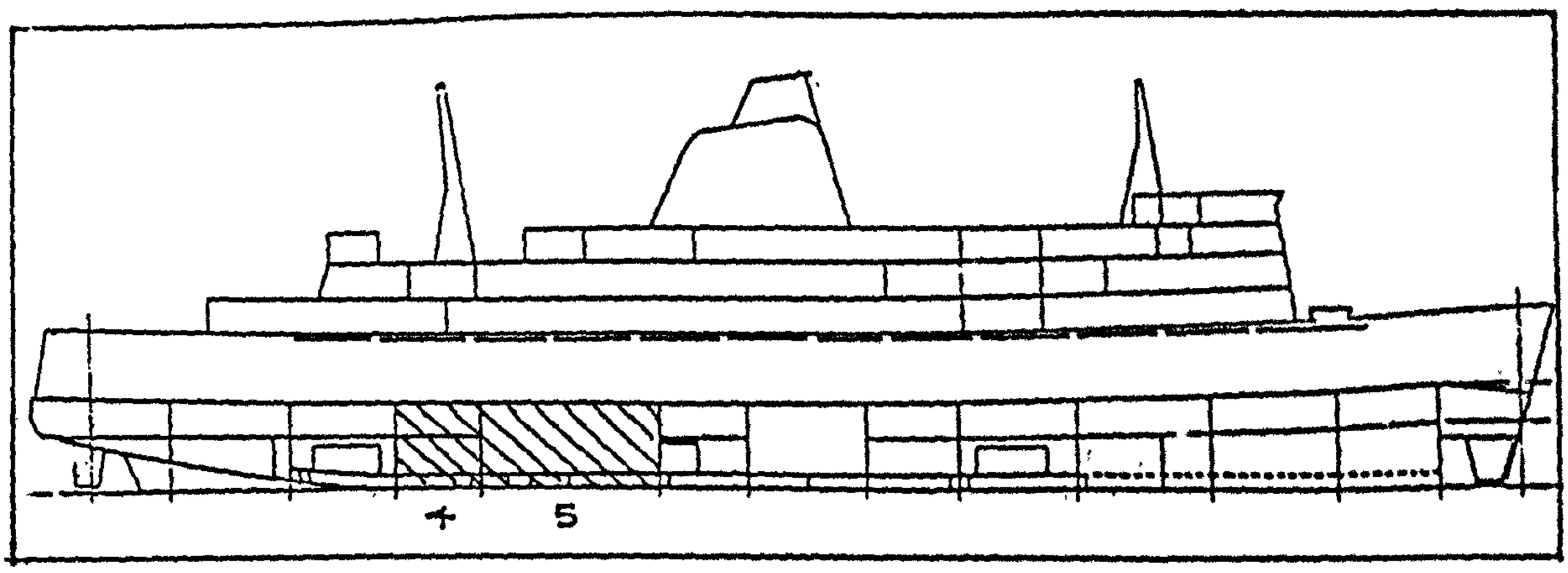

Fig C.4 SHIP 4

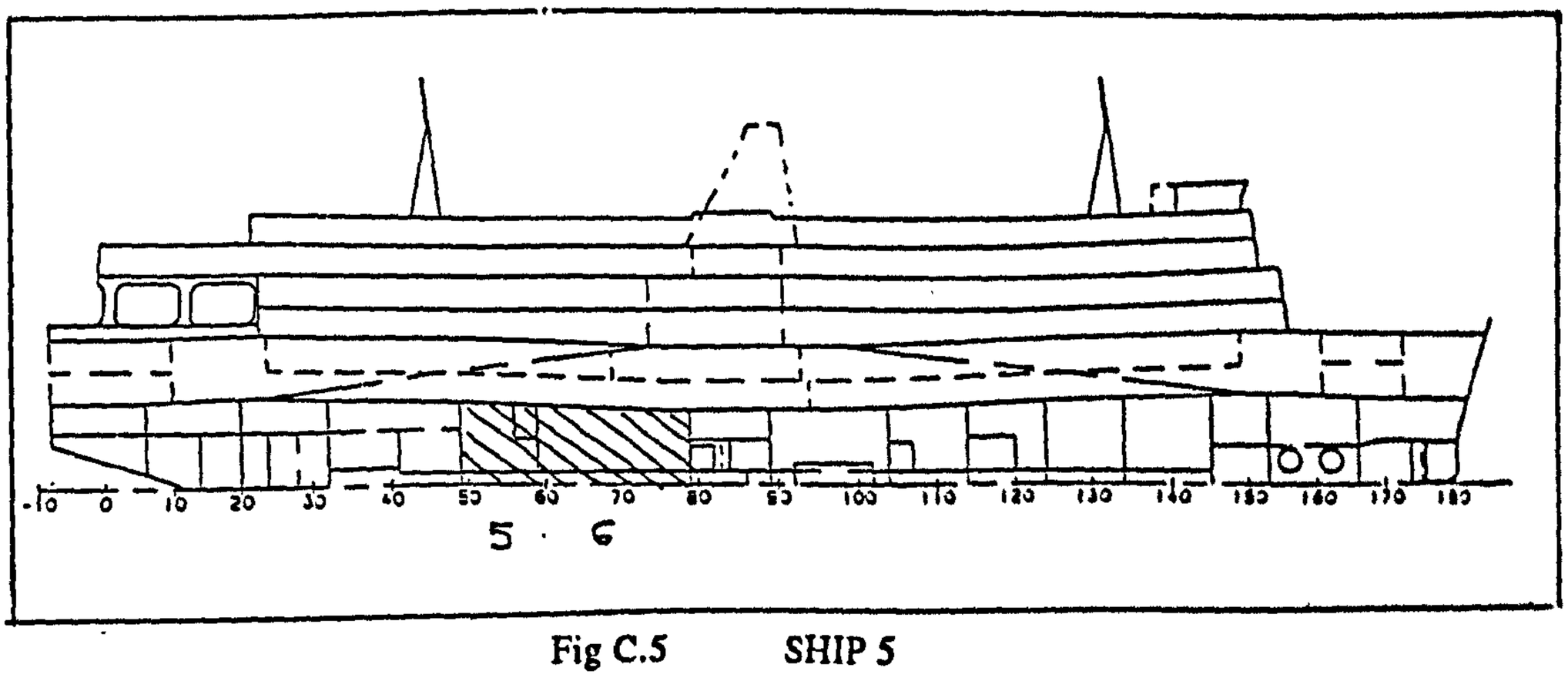

Fig C.5 SHIP 5

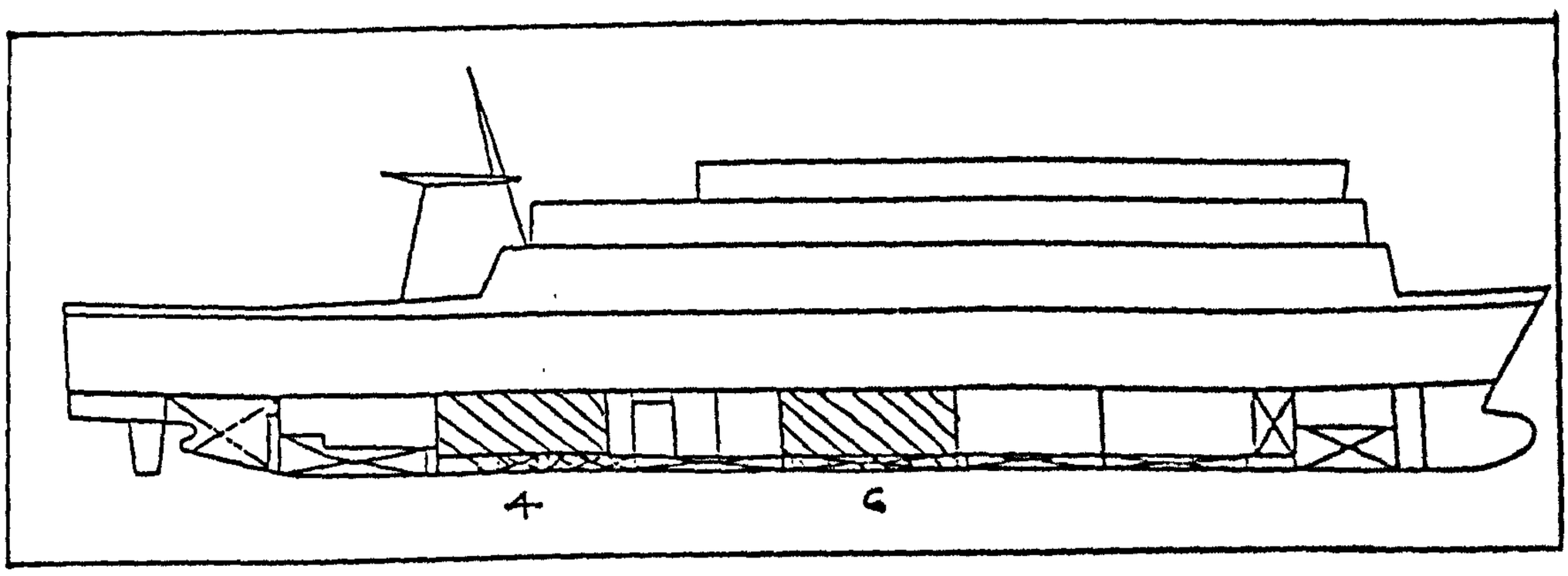

Fig C.6 SHIP 6

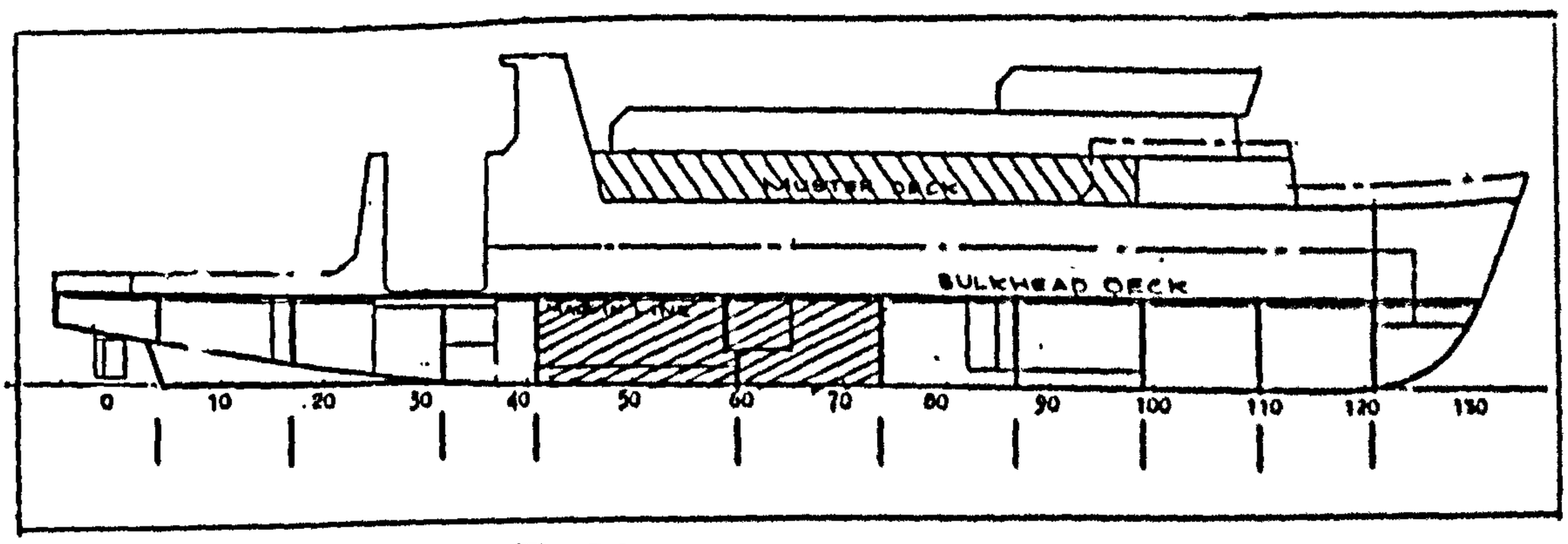

Fig C.7 SHIP 7

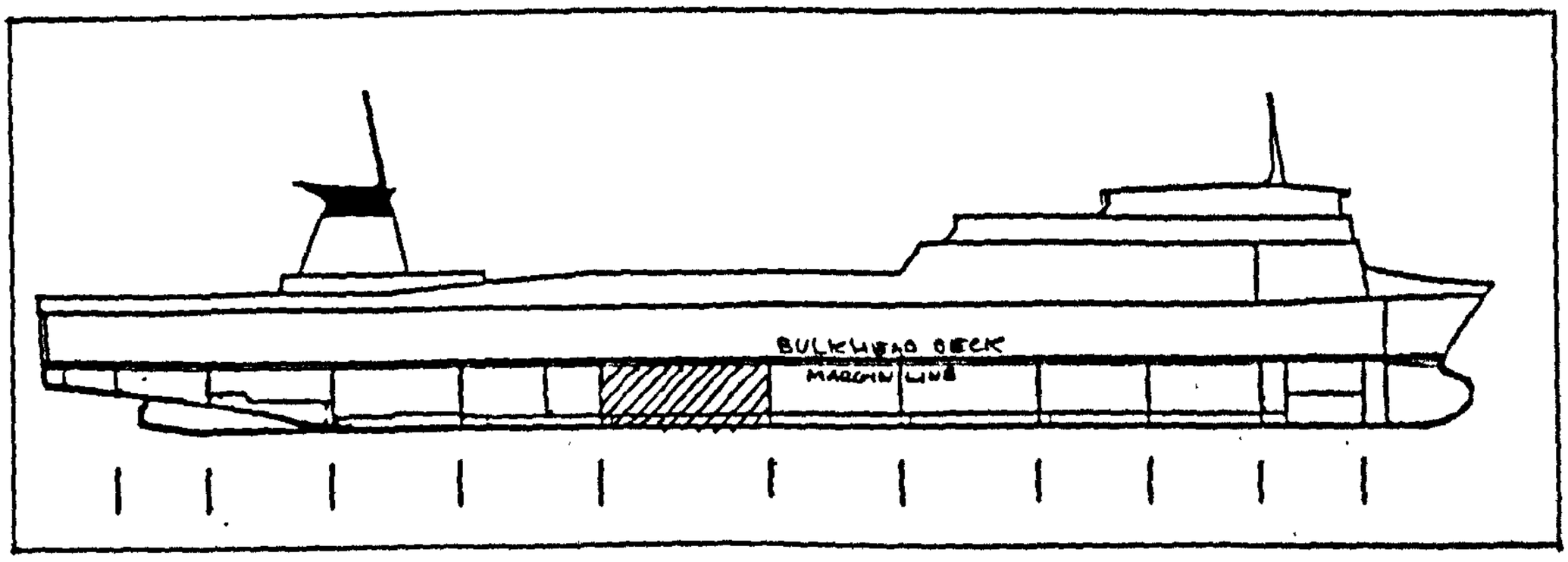

Fig C.8 SHIP 8

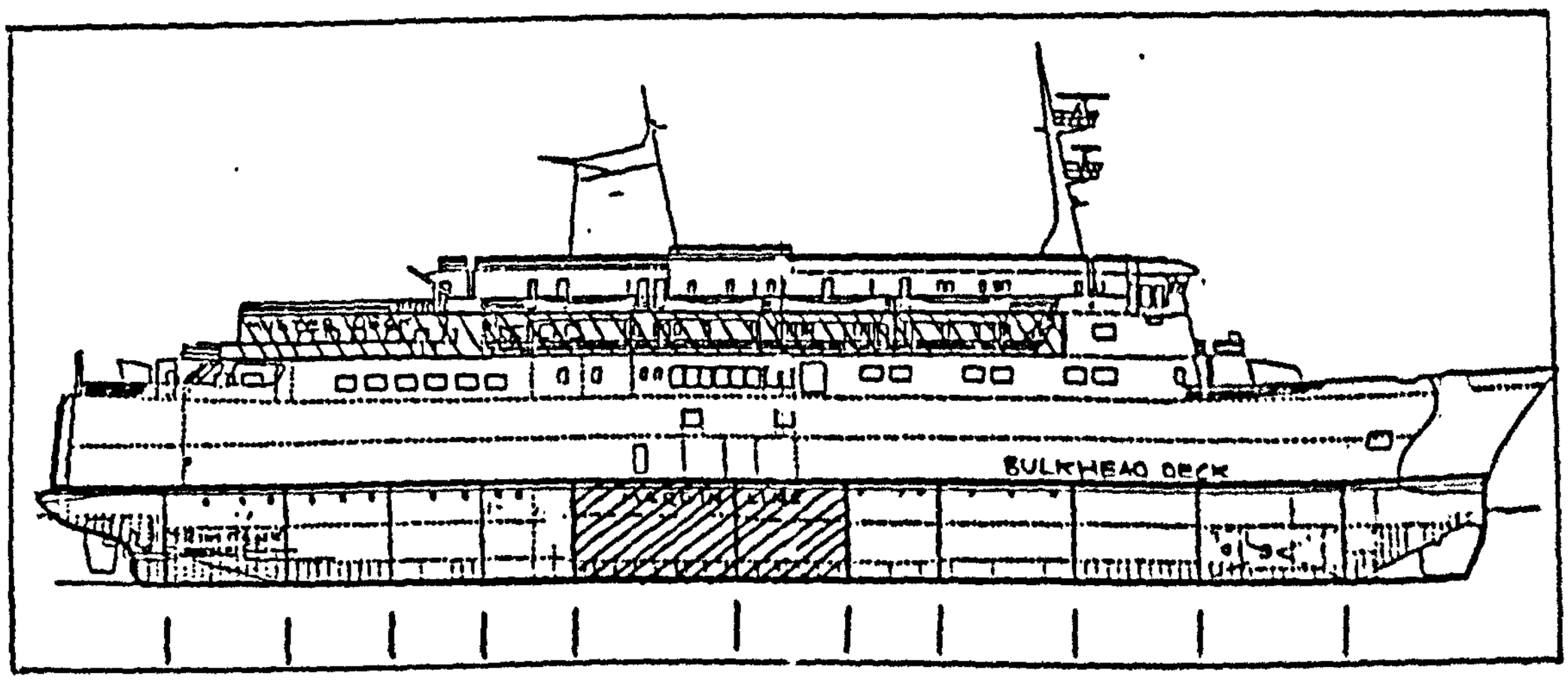

Fig C.9 SHIP 9

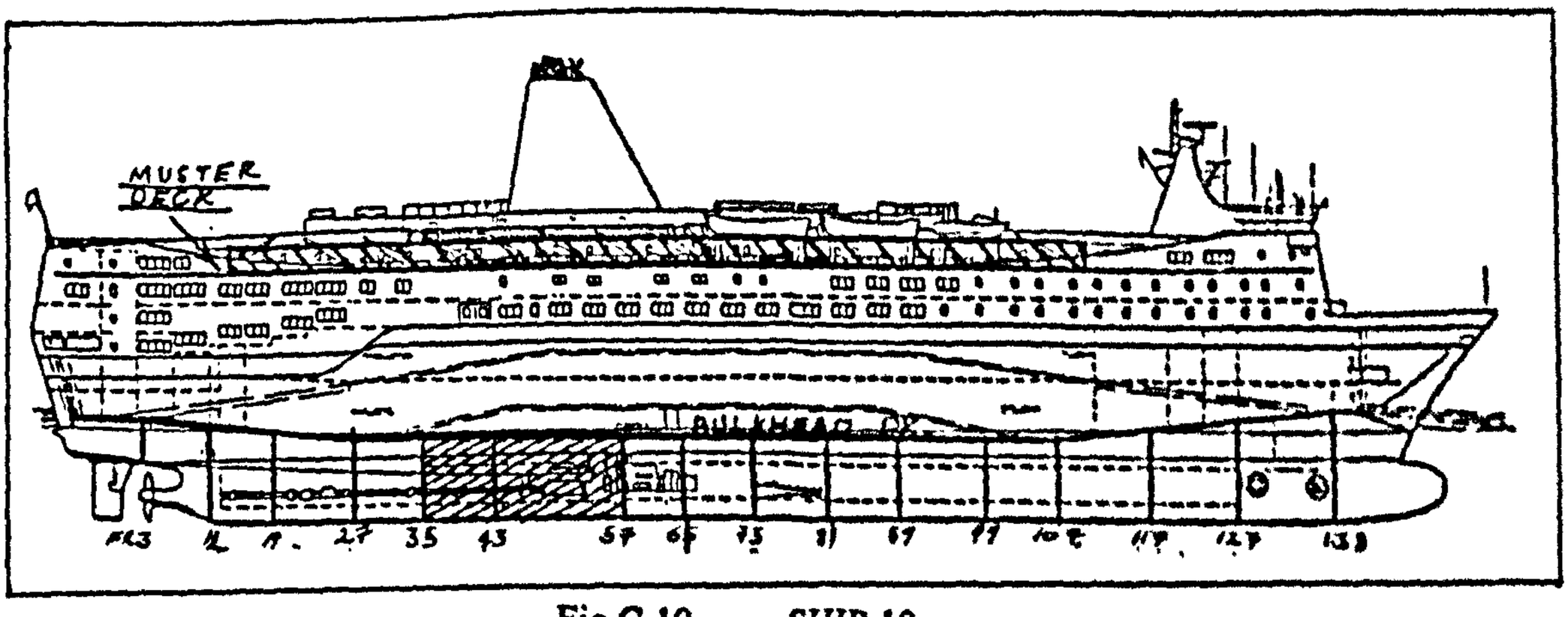

Fig C.10 SHIP 10